THE UNIVERSITY
of EDINBURGH

Mode of Action of a Novel Lymphocyte Inhibitory Factor of Attaching & Effacing *Escherichia coli*

Andrew Graham Bease

Doctor of Philosophy (Ph.D)

The University of Edinburgh

2019

Declaration

I, Andrew Graham Bease have read and understood the University of Edinburgh guidelines on plagiarism and hereby declare that this thesis is all of my own work except where indicated in the text. This work has also not been submitted for any other degree or professional qualification from any other University.

Signed… ……

Abstract

Attaching and effacing *Escherichia coli* are significant diarrhoeal pathogens that can spread between humans or via animal reservoirs. An important virulence factor produced by these bacteria is the large multifunctional protein lymphostatin (LifA), which has been reported to inhibit the mitogen- and antigen-stimulated proliferation of lymphocytes as well as mediate adherence to epithelial cells. Shiga toxin-producing *E. coli* lacking *lifA* are significantly impaired in their ability to colonise cattle. Little is known about the mode of action of LifA, however, *in silico* analysis has identified a putative glycosyltransferase domain homologous to that of large clostridial toxins and a putative cysteine protease domain homologous to that of C58 family proteases. LifA has recently been reported to bind uridine diphosphate-N-acetylglucosamine (UDP-GlcNAc) and mutation of a DXD motif within the predicted glycosyltransferase domain abolished this binding and lymphostatin activity. In this study, I sought to identify domains of LifA required for cell binding and lymphostatin activity, probe the role of the cysteine protease motif in intracellular processing and LifA activity, and to identify potential targets and interacting partners of the protein. Domains of LifA predicted by limited proteolysis were cloned, expressed and affinity purified. Robust assays for detecting interactions between LifA, or fragments thereof, and T lymphocytes were developed but none of the domains possessed lymphostatin activity alone or in combination. LifA was found to be cleaved within T cells, which by analogy with large clostridial toxins was hypothesised to be the result of autoproteolysis mediated by the cysteine protease domain. A C1480A substitution mutant of full-length LifA was constructed by site-directed mutagenesis to disrupt the predicted catalytic triad of the cysteine protease domain. The C1480A substitution resulted in a lack of intracellular processing of LifA and impaired the ability of the protein to inhibit mitogen-stimulated proliferation of bovine T cells, without obvious changes to the biophysical properties of the protein. LifA processing was also found to require endosomal acidification using the inhibitors bafilomycin A1 and chloroquine. Shotgun mass spectrometry and protein pull-downs were used to identify potential targets of LifA activity and interacting partners. Relatively few candidate proteins were identified and these were generally not consistently observed between repeated experiments. Based on analysis of signal transduction pathways perturbed by LifA, I explored if the cellular kinase Akt may be targeted by LifA directly or indirectly. Akt is known to control T cell proliferation and to be regulated by phosphorylation and GlcNAcylation. S473 phosphorylation of Akt in mitogen-stimulated T cells was inhibited by LifA in a manner dependent on the DXD and cysteine protease motifs, but O-GlcNAcylation of Akt was not detected. This inhibition only occurred in cells treated with LifA before mitogenic stimulation. Infection of T cells with an enteropathogenic *E. coli* strain inhibited Akt phosphorylation in a manner dependent on the Type III secretion system but not LifA or a homologous LifA-like protein. Taken together, this study advances our understanding of the mode of action of a key virulence factor of pathogenic *E. coli* and, in particular, identifies a key role for a cysteine protease motif in intracellular processing of the protein and lymphostatin activity.

Lay summary

Lymphostatin (LifA) is a protein that is produced by certain strains of the bacterium *Escherichia coli* that can cause severe diarrhoea. The protein is required by the bacteria to colonise the intestines of their host and is known to interfere with the replication and activity of key cells of the immune system termed T cells in response to chemical triggers. The mode of action of LifA is not fully understood, however, it is known to bind a sugar molecule (uridine diphosphate-N-acetylglucosamine; UDP-GlcNAc) and is thought to transfer the sugar onto an unidentified target in host cells. LifA is also predicted to contain a region that may be involved in self-cleavage of the protein in a way that may be required for it to reach its target within cells. In this study, I developed robust assays to detect binding of LifA to T cells and inhibitory activity. I generated various fragments of the protein, but none of these possessed lymphostatin activity alone or in combination. I found that LifA was processed into two pieces inside host cells, which required a decrease in the pH of a compartment within host cells involved in the uptake of extracellular material called the endosome. A region predicted to be involved in self-cleavage of LifA was mutated by changing a specific amino acid in the protein. This change prevented LifA from being processed inside T cells and its ability to inhibit T cell replication, but without obvious effects on the structure of the mutated protein. I attempted to identify host cell proteins onto which LifA transfers the GlcNAc sugar and proteins that may interact with LifA, however, the results were inconsistent between repeated experiments. A cellular protein called Akt was investigated as a possible target of LifA based on evidence from independent studies. LifA was found to block the activation of Akt in T cells that had been chemically stimulated to replicate and required both the ability to bind UDP-GlcNAc and be processed in order to do this. This block of Akt activation only occurred when T cells were treated with LifA before stimulation and not after. LifA did not appear to transfer sugar onto Akt. Infecting T cells with live *E. coli* before stimulating them blocked Akt activation in a manner dependent on the syringe-like bacterial secretion system but not LifA or a similar protein termed LifA-like. Taken together, the research presented in this thesis represents a significant and original contribution to our understanding of how a key virulence factor of pathogenic *E. coli* acts.

Acknowledgements

I would like to thank the following people who have supported me in some way or another throughout this project:

Professor Mark Stevens, Dr Robin Cassady-Cain and Professor Jayne Hope for supervising this project, reviewing my thesis and all the support they have given me. Your support has been greatly appreciated these last four years and I wouldn't have made this far without you. Also, the members of the Stevens and MMBP groups for the support and advice they have provided over the years.

Dr Liz Blackburn, Dr Martin Wear and Dr Matt Nowicki for the training and support they provided throughout my time at the Edinburgh Protein Production Facility. Lisa Imrie, Kinetic Parameter Facility, The University of Edinburgh, and Dr Dominic Kurian, Proteomics and Metabolomics Facility, The Roslin Institute, for the mass spectrometry analysis that they performed for me.

Professor Brendan Kenny, Newcastle University, for sharing information with us that helped lay the groundwork for Chapter 6 and for providing EPEC E2348/69 strains that were used in Chapter 6.

Irene McGuinnes and Dr Anna Raper for training me on the FACScalibur and Fortessa flow cytometers. Bob Fleming and Graeme Robertson, Bio-Imaging, The Roslin Institute, for advice and training on various microscopes.

My family and friends. My mum for always worrying about me (at least I know you care). My dad for picking me up from Roslin, even at stupid o'clock in the morning. My brother David and my friends Dave, Daniel and Graham for keeping my brain in a solid state through belly laughs and supplies for the effort. Lastly, I would like to thank my grandparents James and May Lawson, who are no longer with us. If not for you I might never have taken this path in life. I wish you were still here to see me complete my greatest achievement.

Contents

List of figures

List of tables

List of commonly used abbreviations

ABC	NH_4HCO_3 (ammonium bicarbonate)
ACN	Acetonitrile
A/E	Attaching and effacing
Akt	Protein kinase B (PKB)
Amp	Ampicillin
APCs	Antigen presenting cells
BFP	Bundle-forming pili
BSA	Bovine serum albumin
Cam	Chloramphenicol
CD	Circular dichroism
ConA	Concanavalin A
CP	Cysteine protease
DLS	Dynamic light scattering
DMEM	Dulbecco's Modified Eagle Medium
DMSO	Dimethyl sulphoxide
DNA	Deoxyribonucleic acid
DTT	Dithiothreitol
EAF	EPEC adherence factor
Efa1	EHEC factor for adherence 1
EHEC	Enterohaemorrhagic *Escherichia coli*
EPEC	Enteropathogenic *E. coli*
Esc	*E. coli* secretion components
Esp	*E. coli* secreted protein
FCS	Foetal calf serum
FITC	Fluorescein isothiocyanate
GAPDH	Glyceraldehyde 3-phosphate dehydrogenase
Glc	Glucose
GlcNAc	N-acetylglucosamine
GPx	Glutathione peroxidase
GT	Glycosyltransferase

HEPES	4-(2-hydroxyethyl)-1-piperazineethanesulphonic acid
HRP	Horseradish peroxidase
HUS	Haemolytic uraemic syndrome
IL	Interleukin
IP	Immunoprecipitation
IMAC	Ion metal affinity chromatography
INPP5E	Inositol polyphosphate-5-phosphatase E (Pharbin)
Kan	Kanamycin
LB	Lysogeny broth
LCTs	Large clostridial toxins
LDS	Lithium dodecyl sulphate
LEE	Locus of enterocyte effacement
LifA	Lymphocyte inhibitory factor A (Lymphostatin)
Nal	Nalidixic acid
Nle	Non-LEE encoded
PAGE	Polyacrylamide gel electrophoresis
PBMC	Peripheral blood mononuclear cell
PBS	Phosphate-buffered saline
PBS-T	Phosphate-buffered saline and Tween 20
PCR	Polymerase chain reaction
rLifA	Recombinant LifA with C-terminal 6 x His tag
RDEC	Rabbit diarrhoeagenic *E. coli*
RPMI	Roswell Park Memorial Institute-1640 media
RPMI-CJ	RPMI complete media for J774A.1 cells
RPMI-CT	RPMI complete media for T cells
SDS	Sodium dodecyl sulphate
SEC	Size exclusion chromatography
Str	Streptomycin
Stx	Shiga toxin
T3S	Type III secretion
T3SS	Type III secretion system
TBS	Tris-buffered saline

TBS-T	Tris-buffered saline and Tween 20
TDA	Thermal denaturation assay
Tet	Tetracyclin
Tir	Translocated intimin receptor
TRIS	Tris(hydroxymethyl)aminomethane
UDP	Uridine diphosphate
WGA	Wheat germ agglutinin
WT	Wild-type
X-gal	5-bromo-4-chloro-3-indolyl-β-D-galactopyranoside

1 Introduction

1.1 *Escherichia coli*

Escherichia coli are Gram-negative facultative anaerobes that are commonly found living in the environment (reviewed in Jang *et al*., 2017). They also exist primarily as commensals in the lower intestines of warm-blooded animals and reptiles (reviewed in Leimbach *et al*., 2013). Although. *E. coli* are the most abundant *Enterobacteriaceae* species in the human gut microbiota (Martinson *et al*., 2019), they account for less than 1 % of the total gut microbiota in healthy adults (Eckburg *et al*., 2005). The proportion of *E. coli* in the gut microbiota varies depending on multiple factors however, including age, species and host health. Their presence is usually beneficial to the host as *E. coli* are capable of synthesising vitamin K_2 (Bentley and Meganathan, 1982) and, along with the rest of the gut microbiota, exert a protective effect against pathogenic bacteria (Hudault *et al*., 2001). *E. coli* strains can be classified into serotypes based on the serological detection of distinct lipopolysaccharide (O), flagellar (H) and capsular (K) antigens (reviewed in Fratamico *et al*., 2016).

Although normally harmless to their host, *E. coli* are opportunistic pathogens that, through the acquisition of mobile genetic elements, can become serious pathogens (reviewed in Gomes *et al*., 2016). Pathogenic *E. coli* strains can be divided into two subgroups depending on the site of infection, with diarrhoeagenic *E. coli* infecting the intestines and extraintestinal *E. coli* (ExPEC) infecting sites beyond the intestines (Section 1.1.1).

1.1.1 *E. coli* pathotypes

The diarrhoeagenic *E. coli* and ExPEC subgroups can be further divided into distinct pathotypes based on their characteristics, including the possession of specific virulence factors. ExPEC consists primarily of uropathogenic *E. coli*, which infect the urinary tract, and neonatal meningitis *E. coli*, which can cross and inflame the blood-brain barrier (reviewed in Sarowska *et al*., 2019). Other pathotypes of ExPEC

exist such as septicaemia-associated *E. coli* and avian pathogenic *E. coli* although these are less well defined beyond their association with clinical outcome (reviewed in Sarowska *et al*., 2019). The main diarrhoeagenic *E. coli* pathotypes are enterotoxigenic *E. coli* (ETEC), enteroaggregative *E. coli* (EAEC), enteroinvasive *E. coli* (EIEC), diffusely-adherent *E. coli* (DAEC), enteropathogenic *E. coli* (EPEC) and enterohaemorrhagic *E. coli* (EHEC; reviewed in Gomes *et al*., 2016).

ETEC are the most common cause of traveller's diarrhoea and are also important in the farming industry, particularly as a cause of acute enteritis and colibacillosis in young pigs and calves (reviewed in Gomes *et al*., 2016; reviewed in Luppi, 2018). They are characterised by their adherence to enterocytes via colonisation factors and the secretion of heat-labile and heat-stable toxins, which cause diarrhoea (reviewed in Mirhoseini *et al*., 2018). EAEC are the second most common cause of traveller's diarrhoea and are characterised by the formation of biofilms on enterocytes using aggregative adherence fimbriae (Tzipori *et al*., 1992; Nataro *et al*., 1992). EIEC, which include bacteria of the genus *Shigella*, are characterised by their facultative intracellular lifestyle. They achieve this by passing through microfold (M) cells via transcytosis, replicating inside macrophages in the intestinal submucosa, then invading enterocytes from their basolateral side (Wassef *et al*., 1989; Sansonetti *et al*., 1996; Zychlinsky *et al*., 1992; Mounier *et al*., 1992). DAEC are characterised by forming diffuse attachments to enterocytes using fimbrial and afimbrial adhesins (Scaletsky *et al*., 1984; reviewed in Servin, 2014).

EPEC and EHEC are collectively known as attaching and effacing (A/E) *E. coli* and are described in greater detail below.

1.1.2 Attaching and effacing *E. coli*

A/E lesions are characterised by intimate bacterial attachment to the surface of enterocytes on actin-rich 'pedestals' and the destruction of microvilli, thereby disrupting the absorption of nutrients by the gut, contributing to diarrhoea (Figure 1.1; Moon *et al*., 1983; Tzipori *et al*., 1986; Knutton *et al*., 1987). The pedestals are also assembled with other cytoskeletal proteins besides actin, such as α-actinin, talin, ezrin and myosin light-chain (Finlay *et al*., 1992;

Manjarrez-Hernandez *et al*., 1992). Law *et al*. (2015) identified more than 90 proteins present in the pedestals formed by EPEC, 17 of which were in significantly higher abundance than in uninfected cells. Actin-associated proteins such as cyclophilin A may only be present due to their interactions with actin, but non-actin-associated proteins such as transgelin may have other as yet undefined roles (Law *et al*., 2015). A/E lesion formation in *E. coli* is mediated by virulence factors encoded by the locus of enterocyte effacement (LEE; Section 1.1.3.1).

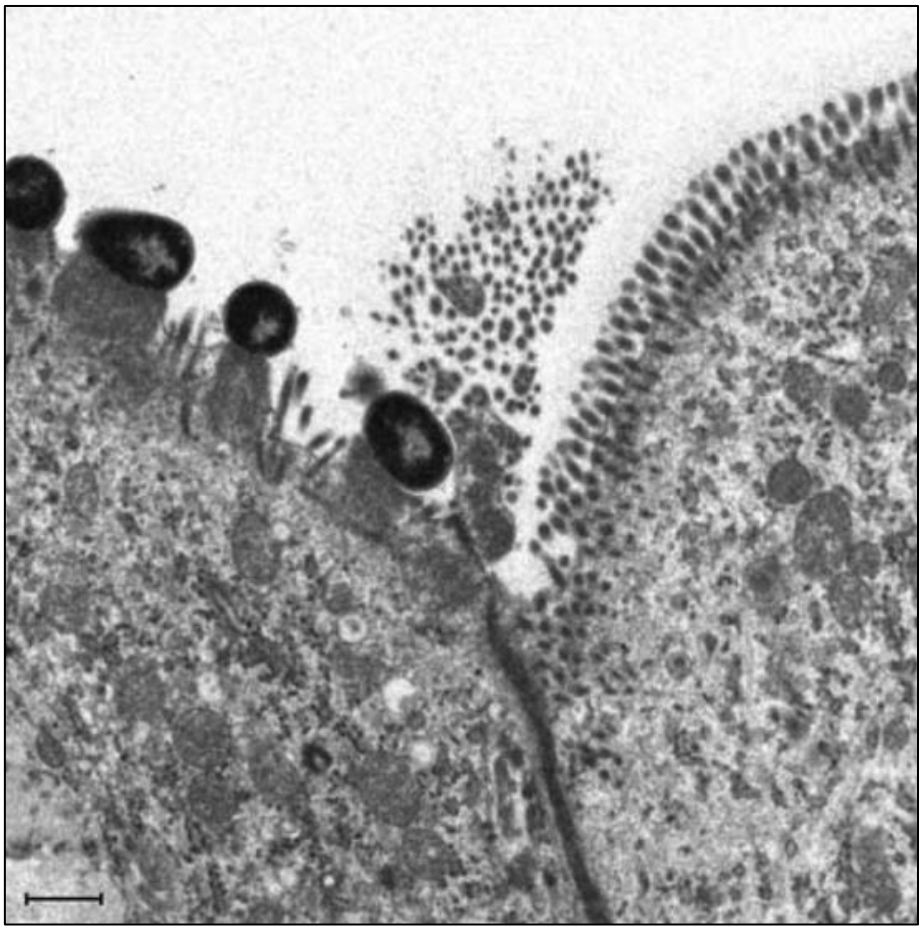

Figure 1.1. Transmission electron micrograph of EHEC O111:H- E45035N forming attaching and effacing lesions on a bovine calf colonocyte. Actin rich pedestals can be seen as electron dense regions beneath the EHEC cells. An uninfected cell to the right gives a comparison of a healthy cell surface and microvilli. Scale bar = 1 μm (from Stevens *et al*., 2002).

EPEC are a major cause of infantile diarrhoea in the developing world and cause both acute and chronic diarrhoea (reviewed in Gomes *et al*., 2016). EPEC infect the proximal small intestine (Rothbaum *et al*., 1982; Sherman *et al*., 1989) and once attached to enterocytes, they disrupt the ion balance and water absorption in the intestine by inhibiting the sodium-D-glucose co-transporter and the Na^+/H^+ exchanger NHE3, resulting in diarrhoea (Dean *et al*., 2006; Hecht *et al*., 2004). Sanger *et al*. (1996) also found that EPEC are able to use A/E pedestals as a form of motility to travel across the surface of host cells at speeds of up to 0.07 μm/second.

EPEC strains can be further divided into typical EPEC, which possess bundle-forming pili (BFP) that mediate inter-bacterial interactions and micro-colony formation on epithelial cells, and atypical EPEC, which do not (Section 1.1.3.8; reviewed in Gomes *et al*., 2016). Prevalent EPEC serotypes include O55:H6, O127:H6, O128:H2 and O142:H34 among others (Gomes *et al*., 1989; reviewed in Trabulsi *et al*., 2002; Kozub-Witkowski *et al*., 2008). The prototype EPEC strain E2348/69 was isolated in 1969 from an outbreak at a residential nursery in Taunton, UK (Taylor, 1970). It was used in this study as it can be handled at biosafety level 2 and it is the source of the *lifA* gene used to produce purified LifA, which is near identical to that from EHEC strains (Section 1.3). The genome of this prototype strain consists of an ~5 Mb circular chromosome, an ~97 kb EPEC adherence factor (EAF) plasmid, a small ~6 kb drug-resistant plasmid and a third ~5 kb plasmid encoding mobilization genes (Iguchi *et al*., 2009; Hanford *et al*., 2009; Nisa *et al*., 2013). The core genome of E2348/69 is highly conserved with laboratory strains, commensal *E. coli* and other pathotypes of *E. coli*, but is broken up by 13 prophages and eight integrative elements (Iguchi *et al*., 2009). Iguchi *et al*., (2009) also identified 424 genes that were specific to EPEC E2348/69. A nalidixic acid derivative of EPEC E2348/69 that is commonly used in laboratories was found to have several differences in its genome compared to the original strain, including three unique nonsynonymous changes (Nisa *et al*., 2013). An S83L substitution in *gyrA* confers nalidixic acid resistance (Bagel *et al*., 1999) and a nonsynonymous substitution in *ftsK* has no effect on phenotype (Nisa *et al*., 2013). The conversion of a stop codon to a tryptophan results in the fusion of the λ lysogenisation regulator *hflD* and *purB*, which compromises the growth rate and ability to invade epithelial

cells in this clone due to deficient purine biosynthesis (Kihara *et al*., 2001; Jung *et al*., 2010; Nisa *et al*., 2013). Additionally, this clone has lost the ~6 kb plasmid and is therefore no longer resistant to streptomycin (Nisa *et al*., 2013).

EHEC causes acute enteritis, that may involve haemorrhagic colitis and severe systemic sequelae, and ruminants are a key reservoir (Riley *et al*., 1983; Beutin *et al*., 1993). Outbreaks in both the developing and developed world have been caused by cattle due to faecally contaminated food or water (reviewed in Ho *et al*., 2013). EHEC primarily infect the lymphoid follicle-dense mucosa at the terminal rectum of cattle (Naylor *et al*., 2003). EHEC infection is the leading antecedent to haemolytic uraemic syndrome (HUS) in humans in many countries (reviewed in Ho *et al*., 2013). HUS is characterised by damage to vascular endothelial cells in kidney glomeruli and haemolytic anaemia and is caused by the production of one or more Shiga toxins (Stx; Karmali *et al*., 1983b; O'Brien *et al*., 1983; Johnson *et al*., 1983; Karmali *et al*., 1983a). The pathogenesis of EHEC is similar to that of EPEC with the exception of the production of Stx, which acts as a cytotoxin by depurinating 28S ribosomal RNA to arrest translation in a manner similar to ricin (Section 1.1.3.9; Endo *et al*., 1988). The dominant serotype associated with human infections in many countries is O157:H7, however, infection with non-O157 EHEC (in particular of serogroups O26, O45, O103, O111 and O121) is a significant problem that is often under-estimated by national surveillance and diagnostic laboratories (Brooks *et al*., 2005; Kozub-Witkowski *et al*., 2008). EHEC O157:H7 infection in cattle is widely reported to be asymptomatic, but Nart *et al*. (2008b) found that infection with this strain does in fact cause histopathological changes in the terminal rectal tissue of cattle and a slight but significant neutrophilic response. The chromosome of the prototype EHEC O157:H7 strain EDL933 has a similar backbone sequence to *E. coli* K-12 except for a 422 kb inversion, which spans the replication terminus (Perna *et al*., 2001). This backbone sequence is interrupted by 177 O-islands found in *E. coli* O157:H7 but not laboratory-adapted *E. coli* K-12, many of which encode known virulence proteins (Perna *et al*., 2001). There are also 18 prophages throughout the chromosome and various single nucleotide polymorphisms create proteins that are identical in size and function to *E. coli* K-12 homologues but overall only 25 % of proteins are identical (Perna *et al*., 2001). EHEC O157:H7 also contains the pO157

plasmid, which encodes various virulence factors (Burland *et al*., 1998; Makino *et al*., 1998). Numerous studies have suggested that EHEC O157:H7 has evolved from EPEC O55:H7 in a stepwise manner (Whittam *et al*., 1993; Wick *et al*., 2005; Zhou *et al*., 2010; Kyle *et al*., 2012).

1.1.3 Major virulence factors in A/E *E. coli*

EPEC and EHEC produce several key virulence factors that aid their colonisation of human and animal hosts, many of which are required for the formation of A/E lesions. Effector proteins from EPEC and EHEC were discovered before and after the genomes of prototype strains were sequenced. A variety of methods have been used to identify 'effector' proteins from A/E *E. coli* including mutagenesis, loss/gain of function mutants, sequencing and homology with known effector proteins from other bacteria.

1.1.3.1 The locus of enterocyte effacement (LEE)

The LEE is a pathogenicity island comprising over 40 contiguous genes, which encode virulence factors that aid colonisation of a host, many of which are required for attachment and effacement (reviewed in Stevens and Frankel, 2014). It is a ≥ 35 kb locus that is conserved amongst EPEC and EHEC as well as other A/E pathogens including certain strains of rabbit diarrhoeagenic *E. coli* (RDEC), *E. albertii* (previously thought to be *Hafnia alvei*) and the mouse pathogen *Citrobacter rodentium* (McDaniel *et al*., 1995; Deng *et al*., 2001; Huys *et al*., 2003). The GC content of the LEE of EPEC E2348/69 is only 38.36 % (Elliott *et al*., 1998) compared with 50.8 % across the *E. coli* K-12 genome (Blattner *et al*., 1997), which is typical of pathogenicity islands (Hacker *et al*., 1997). The LEE of E2348/69 was the first to be characterised and consists of 41 open reading frames arranged into five polycistronic operons (Figure 1.2; Elliott *et al*., 1998), three of which are involved in the production of proteins required for the assembly of a Type III secretion system (T3SS; reviewed in Gaytán *et al*., 2016) that functions in a manner akin to a molecular syringe (Section 1.1.3.2).

The LEE contains the *E. coli* secretion (*esc*)/secretion of *E. coli* proteins (*sep*) genes and genes that encode intimin, *E. coli* secreted proteins (Esps), translocated intimin receptor (Tir), as well as chaperones and regulatory genes (Elliott *et al*., 1998). The 3′ end of the LEE in EPEC is homologous to genes from *Shigella sonnei* (Donnenberg *et al*., 1997), however, the DNA sequences surrounding the LEE vary since it is inserted into different positions depending on the serotype and strain of bacteria (Ogura *et al*., 2009). These variable flanking sequences along with the low GC content suggests that *E. coli* and other A/E pathogens acquired the LEE from other species (e.g. by Hfr transfer during conjugation), or that it once existed as a mobile genetic element (Donnenberg *et al*., 1997). The LEE from EHEC O157:H7 contains 54 open reading frames, 13 of which belong to a prophage located at the *selC* end of the locus (Perna *et al*., 1998).

The regulation of the LEE is complex, with different regulatory systems specific to different operons (reviewed in Mellies and Lorenzen, 2014). The production of LEE proteins is tightly regulated by temperature and growth phase, with optimal expression occurring at 37 °C in the early logarithmic phase of growth (Rosenshine *et al*., 1996). Regulatory systems of the LEE include silencing by histone-like nucleoid-structuring protein, the LEE-encoded regulatory cascade, post-transcriptional regulation and control by phage- or plasmid-encoded regulators (reviewed in Mellies and Lorenzen, 2014). The function of each LEE-encoded gene in virulence, A/E lesion formation and T3SS activity has been systematically investigated in both EPEC E2348/69 and *C. rodentium* (Cepeda-Molero *et al*., 2017; Deng *et al*., 2004).

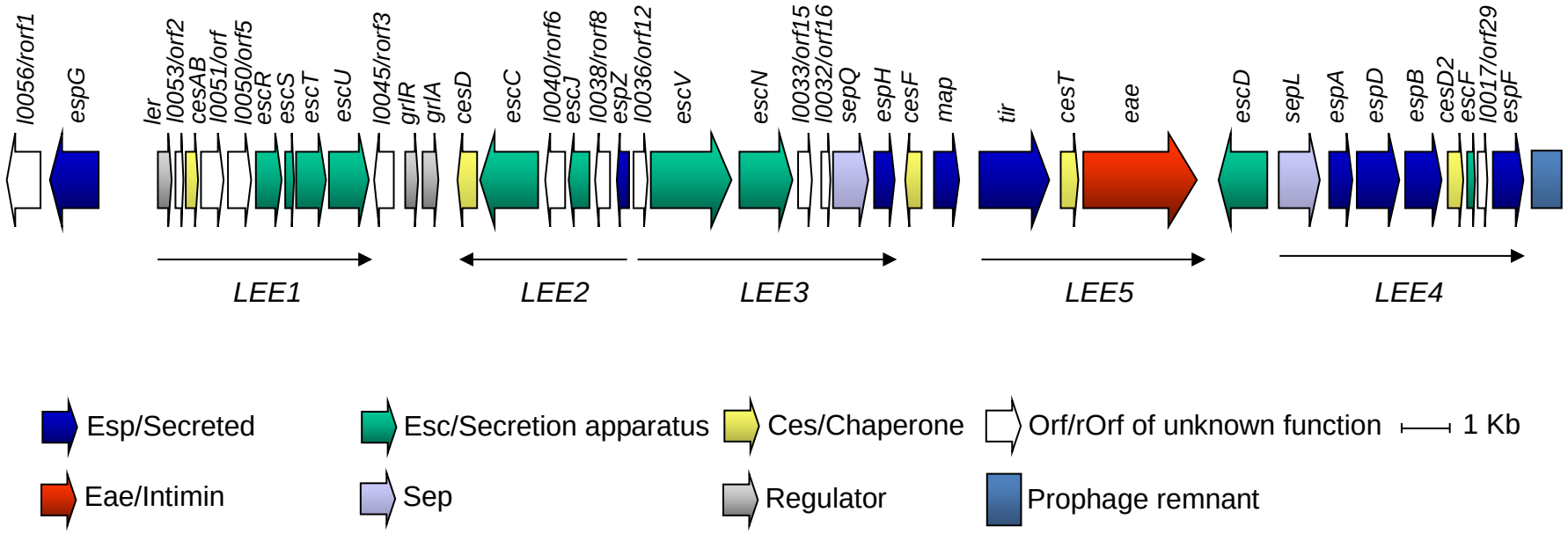

Figure 1.2. Schematic of the locus of enterocyte effacement from EHEC O157:H7 showing the five polycistronic operons and the genes encoded within them (from Stevens and Frankel, 2014).

1.1.3.2 The Type III secretion system

T3SSs are widely used by a range of Gram-negative pathogens of animals and plants (reviewed in Deng *et al*., 2017). There are at least five other well characterised secretion systems in Gram-negative bacteria (reviewed in Costa *et al*., 2015) but the T3SS is particularly important for the purpose of this study. The T3SS in A/E *E. coli* is encoded by the LEE and is composed of Esc/Sep proteins as well as EspA, B and D (Elliott *et al*., 1998). It was discovered by Jarvis *et al*. (1995), who found that certain LEE-encoded proteins exhibited homology to proteins encoding T3SSs in other bacteria. T3SSs include flagella (reviewed in Deng *et al*., 2017) but for the purpose of this study, it is the translocation-associated T3SS that is being referred to. T3SSs belonging to this category can inject effector proteins directly into a host cell (Figures 1.3 and 1.4; reviewed in Stevens and Frankel, 2014). The effector proteins can be encoded both within the LEE and elsewhere in the chromosome, and significant effort has been expended to define the full repertoire of effectors (Tobe *et al*., 2006). The LEE-encoded T3SS consists of a region that spans both membranes of the bacterial cell, which is connected via EscF to the EspA filament and the translocon, which is composed of EspB and D (reviewed in Slater *et al*., 2018; Warawa *et al*., 1999).

The proteins SepL and D regulate the order of protein secretion through the T3SS, with mutations leading to hypersecretion of effector proteins rather than translocon components (Kresse *et al*., 2000; O'Connell *et al*., 2004; Wang *et al*., 2008). EspZ halts effector translocation from inside the host cell, possibly by interacting with EspD (Berger *et al*., 2012; Creasey *et al*., 2003). The secretion of effector proteins via the T3SS is contact-dependent in some bacteria such as *Yersinia* (Rosqvist *et al*., 1994) but contact between the T3SS and host cells is not required for the secretion of effector proteins in *E. coli* (Kenny *et al*., 1997a). Various inhibitors of the T3SS have been identified, many of which are part of a family of salicylidene acylhydrazides that inhibit the transcription of T3SS encoding genes (Gauthier *et al*., 2005; Rasko *et al*., 2008; Tree *et al*., 2009). This is in contrast to T3SS inhibitors that work against *Shigella* by interfering with T3SS protein assembly (Veenendaal *et al*., 2009). Vaccines including the LEE-encoded proteins EspA, intimin and Tir as well

as the H7 flagellin have been shown to significantly reduce the shedding of EHEC O157:H7 in cattle faeces (McNeilly *et al*., 2010), consistent with a key role for this system in intestinal colonisation of cattle revealed by genome-wide and targeted mutagenesis (Dziva *et al*., 2004; Naylor *et al*., 2005; Vlisidou *et al*., 2006; Eckert *et al*. 2011).

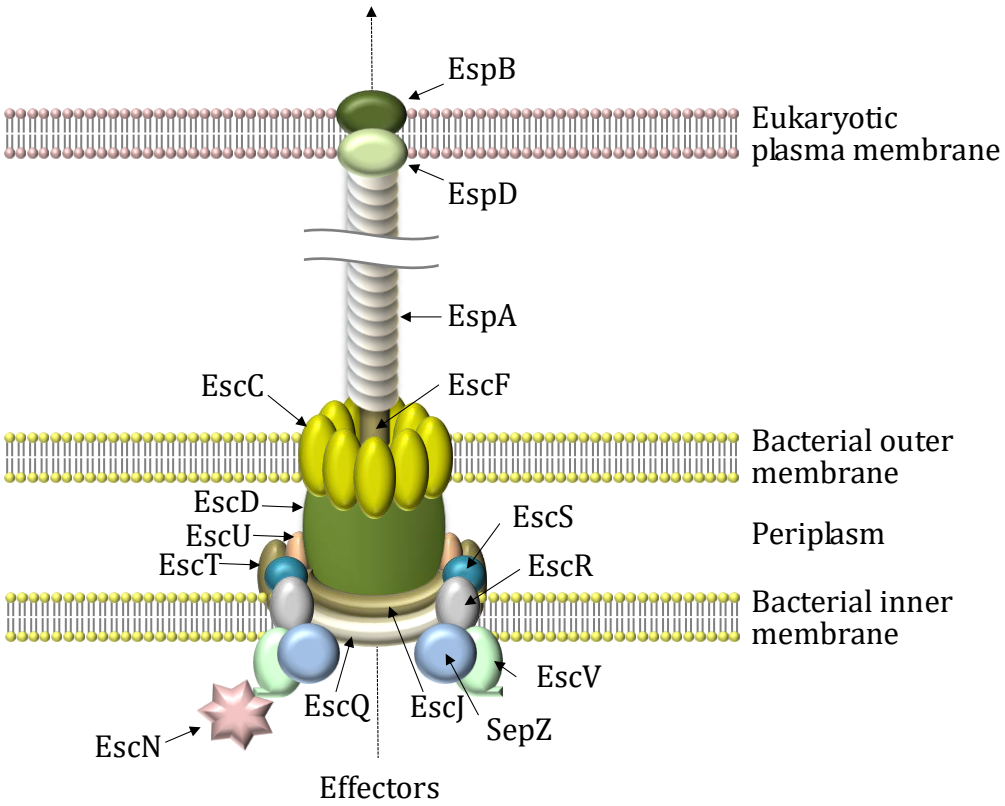

Figure 1.3. Schematic diagram of the LEE-encoded Type III secretion system showing the predicted location of proteins in attaching and effacing *E. coli*. Effector proteins are translocated through the needle complex spanning the inner and outer membranes, then through a translocon comprising the EspA filament, EspB and EspD, into the host cell cytoplasm (from Stevens and Frankel, 2014).

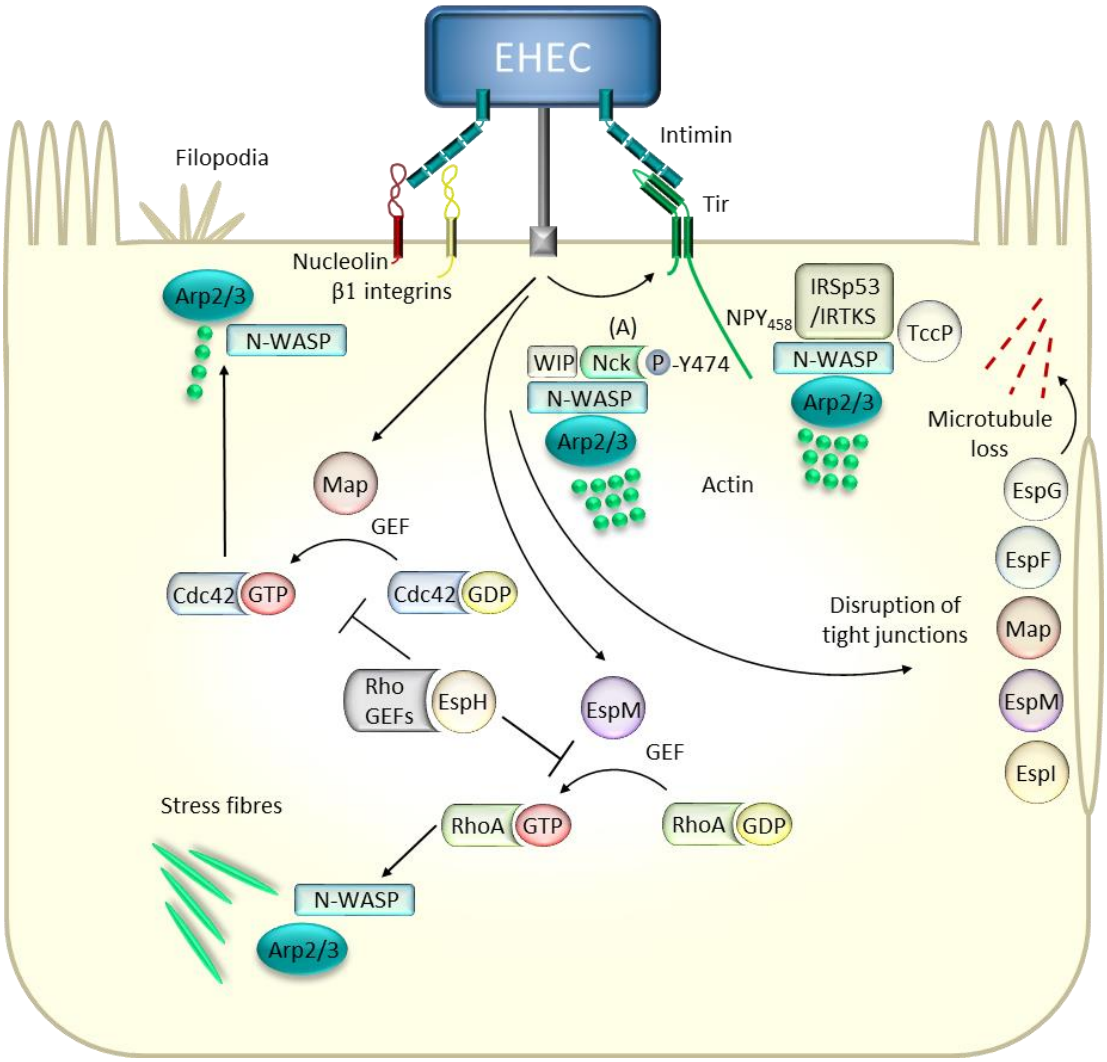

Figure 1.4. Schematic of EHEC adhering to an enterocyte and injecting various effector proteins into it via the Type III secretion system that affect the cytoskeleton. (A) The Tir:Nck pathway dependent on phosphorylation of the residue equivalent to Tyr^{474} of EPEC O127:H6 Tir, which is not present in EHEC O157:H7 (see Section 1.1.3.7; from Stevens and Frankel, 2014).

1.1.3.3 *E. coli* secretion/secretion of *E. coli* proteins

The Esc and Sep proteins are part of the same family but some Seps were renamed as Escs after Elliott *et al*. (1998) sequenced the LEE from EPEC E2348/69 in order to conform with the naming convention of homologous *Yersinia* proteins. Esc/Sep proteins comprise the *E. coli* T3SS and are essential for the translocation of

effector proteins (Jarvis *et al*., 1995; reviewed in Stevens and Frankel, 2014). EscN is the most relevant of these proteins in terms of this study as EPEC strains lacking the *escN* gene (Garmendia *et al*., 2004; Cepeda-Molero *et al*., 2017) are used as T3SS-deficient controls. EscN is an ATPase that provides the energy for the secretion of effector proteins and the energy output of the protein increases when it oligomerises (Jarvis *et al*., 1995; Andrade *et al*., 2007). Two other proteins in this family that are important for the formation of A/E lesions are SepL and SepD, which act as gatekeeper proteins (Wang *et al*., 2008). These proteins form a complex in the bacterial inner membrane and SepL binds to Tir to prevent effector proteins from being secreted before translocator proteins such as EspA (Kresse *et al*., 2000; O'Connell *et al*., 2004; Wang *et al*., 2008).

1.1.3.4 LEE-encoded effector proteins

The Esp series of proteins consists of a large number of proteins, the functions of some of which have been extensively studied (reviewed in Stevens and Frankel, 2014). EspA forms a hollow filamentous extension of the T3SS needle complex (Ebel *et al*., 1998; Knutton *et al*., 1998) that bridges the bacterial and host cells and allows the translocation of effector proteins such as Tir and EspB into the host cell (Kenny *et al*., 1997b; Wolff *et al*., 1998). EspA polymerises in a helical manner to form a channel that effector proteins can be secreted through (Daniell *et al*., 2003; Crepin *et al*., 2005). A/E *E. coli* lack these EspA filaments during intimate adhesion but the mechanism behind this is unknown (reviewed in Stevens and Frankel, 2014). EspB functions as both a component of the T3SS and an effector protein (Warawa *et al*., 1999; Taylor *et al*., 1998). It associates with EspD to form a pore in the host cell plasma membrane at the end of the EspA filament (Kresse *et al*., 1999; Warawa *et al*., 1999; Wachter *et al*., 1999) but EspB is also injected into host cells by the T3SS (Wolff *et al*., 1998). As an effector protein it binds to myosin and inhibits the interaction of myosin with actin, resulting in microvillus effacement (Iizumi *et al*., 2007).

Studies using deletion mutants and clones of the LEE established that the LEE region alone is necessary and sufficient for A/E lesion formation by EPEC

E2348/69, but not by EHEC EDL933 (McDaniel and Kaper, 1997; Pósfai *et al*., 1997). This is partly explained by the requirement for a non-LEE-encoded protein for pedestal formation by EHEC O157 termed $EspF_U$ (Campellone *et al*., 2004). Also known as Tir-cytoskeleton coupling protein (TccP), it binds to the insulin receptor tyrosine kinase substrate (IRTKS)/insulin receptor substrate p53 (IRSp53) complex and neural Wiskott-Aldrich syndrome protein (N-WASP), resulting in the formation of A/E lesions (Campellone *et al*., 2004; Garmendia *et al*., 2004; Brady *et al*., 2007; reviewed Stevens and Frankel, 2014). The homologous protein EspF has a wide range of functions including the disruption of mitochondrial function, cytoskeletal manipulation and the induction of apoptosis (Section 1.2.2.2; reviewed in Stevens and Frankel). EspG interacts with tubulin to deplete the microtubule cytoskeleton, which disrupts epithelial paracellular permeability and tight junction integrity (Matsuzawa *et al*., 2004; Shaw *et al*., 2005; Matsuzawa *et al*., 2005). It also disrupts tight junction integrity by targeting the tight junction protein tricellulin (Morampudi *et al*., 2016). EspG inhibits protein secretion by interacting with ADP-ribosylation factor, p21-activated kinases (PAKs), the Golgi matrix protein GM130 and Rab1 GTPases, which blocks endoplasmic reticulum (ER)-to-Golgi trafficking (Selyunin *et al*., 2011; Germane and Spiller, 2011; Clements *et al*., 2011; Dong *et al*., 2012). The interaction of EspG with PAKs has recently been reported to be required for pedestal formation (Singh *et al*., 2019). There are many other proteins in the Esp family but those described above are the major proteins, with the exception of EspF, that are required for A/E lesion formation. Some Esp proteins modulate innate immune responses and are described in greater detail in Section 1.2.2.2.

Mitochondrial-associated protein (Map) has a number of functions. Map targets host cell mitochondria and alters their morphology, resulting in apoptosis (Kenny and Jepson, 2000; Papatheodorou *et al*., 2006). Map also activates Cdc42, which results in the transient formation of filopodia (Kenny *et al*., 2002; Berger *et al*., 2009; Huang *et al*., 2009). Lastly, Map contributes to diarrhoea by disrupting tight junction integrity and inhibiting the sodium-D-glucose co-transporter in conjunction with EspF and Tir (Dean and Kenny, 2004; Ma *et al*., 2006; Dean *et al*., 2006).

1.1.3.5 Non-LEE-encoded (Nle) proteins

Extensive studies have been performed to map the full T3S effector repertoire of EPEC and EHEC, including the use of bioinformatics, proteomics, translocation assays and systematic knock-outs (Tobe *et al*., 2006; Iguchi *et al*., 2009; Cepeda-Molero *et al*., 2017). EPEC E2348/69 has been predicted to produce 21 effector proteins, while the EHEC O157:H7 strain RIMD 0509952 was found to produce 39 effector proteins (Iguchi *et al*., 2009; Tobe *et al*., 2006). In addition to the LEE-encoded effector proteins, the Nle proteins are also secreted effector proteins, but are encoded outwith the LEE (reviewed in Stevens and Frankel, 2014). NleA disrupts tight junction integrity between enterocytes by inhibiting protein trafficking via COPII-dependent pathways, resulting in a breakdown of the intestinal epithelial barrier and causing diarrhoea (Thanabalasuriar *et al*., 2010). NleG acts in a similar manner to RING-like E3 ubiquitin ligases from eukaryotic cells and induces the degradation of HK2, which is known to inhibit apoptosis (Wu *et al*., 2010; Valleau *et al*., 2018). Many Nle proteins, including NleA, are involved in modulating the host immune response and are described in greater detail in Section 1.2.2.1. Cell cycle inhibiting factor (Cif) is also encoded outwith the LEE but is not present or functional in all EPEC and EHEC strains (Marchès *et al*., 2003; Loukiadis *et al*., 2008). Cif causes cell cycle arrest in the G_1/S and G_2/M phases by deamidating ubiquitin or the ubiquitin-like protein NEDD8, which blocks the activation of the cell cycle (Marchès *et al*., 2003; reviewed in Taieb *et al*., 2011). Cif has also been reported to induce delayed apoptosis of IEC-6 cells, but the mechanism behind this process is unclear (Samba-Louaka *et al*., 2009).

1.1.3.6 Intimin

Intimin is a 94 kDa protein (Yu and Kaper, 1992) that is encoded by the *E. coli* attaching and effacing (*eae*) gene (Jerse *et al*., 1990) and has an 83 % amino acid homology between EPEC and EHEC strains (Yu and Kaper, 1992). The protein also has sequence homology with the invasin proteins in *Yersinia pseudotuberculosis* and *Y. enterocolitica* with the lowest homology at the N- and C-terminal ends (Jerse *et*

al., 1990; Yu and Kaper, 1992). The C-terminal end of intimin has been shown to bind to the surface of HeLa cells (Frankel *et al*., 1994; Deibel *et al*., 2001) and it has been suggested that the N-terminal end masks the C-terminus to prevent non-specific binding to host cells (Deibel *et al*., 2001).

Intimin is located in the bacterial outer membrane and primarily targets Tir, which is injected by the T3SS into host cells and located on their surface (Section 1.1.3.7; Kenny *et al*., 1997b; Rosenshine *et al*., 1992; DeVinnney *et al*., 1999). Intimin is able to bind to the surface of epithelial cells independently of Tir by binding to host cell β_1-integrins and cell surface-localised nucleolin (Frankel *et al*., 1996; Sinclair and O'Brien, 2002). Intimin binds Tir preferentially but it is possible that nucleolin acts as a target for adhesion before Tir is translocated into host cells (Sinclair and O'Brien, 2004). Intimin and Tir are both critical for intestinal colonisation by A/E pathogens, as shown for example by testing isogenic deletion mutants of *E. coli* O157:H7 in calves (Vlisidou *et al*., 2006).

1.1.3.7 Translocated intimin receptor

As mentioned above, Tir is required for intimin binding to host cells and the formation of A/E lesions (Kenny *et al*., 1997b; Rosenshine *et al*., 1992; DeVinnney *et al*., 1999). It was independently described as EspE in EHEC O26:H- strain 413/89-1 and is translocated into host cells via the T3SS (Deibel *et al*., 1998; Kenny *et al*., 1997b). In EPEC O127:H6, actin assembly requires phosphorylation of Tyr^{474} in Tir (Kenny, 1999), which results in the recruitment of the host cell proteins Nck, N-WASP and actin-related protein 2/actin-related protein 3 (Arp2/3; Gruenheid *et al*., 2001). The proteins CrkII and Grb2 are recruited in EPEC infection but not in EHEC infection (Goosney *et al*., 2001).

In EHEC O157:H7 strains, the phosphorylation of Tir is not required because these strains lack Tyr^{474} (DeVinney *et al*., 1999; DeVinney *et al*., 2001). Instead these strains utilise a 12 amino acid motif containing an Asn-Pro-Tyr sequence that recruits the proteins IRTKS, IRSp53, $EspF_U$, N-WASP and Arp2/3 in a manner independent of Nck (Brady *et al*., 2007; reviewed in Stevens and Frankel, 2014). The tyrosine in the amino acid motif can be phosphorylated in EPEC strains to initiate

Nck-independent pedestal formation but at a much lower efficiency than in EHEC (Campellone and Leong, 2005).

1.1.3.8 Type IV bundle-forming pili

Bundle-forming pili (BFP) are produced by typical EPEC and are part of the Type IV pili family, which are expressed by several bacterial pathogens (Girón *et al*., 1991; reviewed in Strom and Lory, 1993). They are encoded on an ~97 kb EAF plasmid (Girón *et al*., 1991; Nataro *et al*., 1987) by a cluster of 14 *bfp* genes, several of which are homologous to genes required for Type IV pilus production in other Gram-negative bacteria (Sohel *et al*., 1996; Stone *et al*., 1996). BfpA is the major subunit of BFP (Donnenberg *et al*., 1992) and is produced as a preprotein before being cleaved into a functional form by BfpP (Zhang *et al*., 1994). The proteins BfpD and F bind nucleotides and act as ATPases to control pilin export and assembly (Sohel *et al*., 1996; Stone *et al*., 1996).

BFP expression is controlled by the EAF plasmid-encoded regulatory proteins BfpT, V and W as well as the chromosome-encoded protein DsbA (Tobe *et al*., 1996; Zhang and Donnenberg, 1996). DsbA stabilises BFP by catalysing the formation of disulphide bonds (Zhang and Donnenberg, 1996). Environmental signals also control BFP expression, with expression occurring optimally between 35 and 37 °C during the exponential growth phase, in the presence of calcium (Puente *et al*., 1996). Puente *et al*. (1996) also found that ammonium suppresses the expression of BFP.

BFP are important virulence factors for the colonisation of hosts, including humans, by EPEC (Bieber *et al*., 1998) and are required for adhesion to epithelial cells and the formation and dispersal of micro-colonies (Girón *et al*., 1991 Knutton *et al*., 1999; Cleary *et al*., 2004). BFP bind to N-acetyllactosamine moieties on the surface of host enterocytes (Hyland *et al*., 2008) and also act in conjunction with *E. coli* common pili during micro-colony formation (Saldaña *et al*., 2009).

1.1.3.9 Shiga toxin

The Stx family of cytotoxins is composed of two major groups, Stx1 and Stx2, which are produced in various combinations by EHEC (reviewed in Krause *et al*., 2018). Stx2, however, is more common in cases of haemorrhagic colitis and HUS (Ostroff *et al*., 1989; Boerlin *et al*., 1999; Frank *et al*., 2011). Stx1 is identical to Stx from *Shigella dysenteriae* serotype I and is highly conserved whereas Stx2 exhibits sequence variation and is separated into a series of subtypes (reviewed in Lee and Tesh, 2019). The *stx* genes are encoded by lysogenic lambdoid bacteriophages, which are integrated into the bacterial chromosome (O'Brien *et al*., 1984; Johansen *et al*., 2001). Stx2 production is induced by activation of the phage lytic cycle, for example, in response to DNA damage via the bacterial SOS response (Neely and Friedman, 1998). The regulation of Stx production is complex and growth phase dependent, with many different extrinsic factors affecting gene expression including antibiotics, reactive oxygen species, iron concentration, temperature and quorum sensing (reviewed in Pacheco and Sperandio, 2012).

Stx is an AB_5 toxin consisting of an A subunit, which in turn is made from an A_1 and A_2 peptide, that is non-covalently bound to a pentameric ring of B subunits (Stein *et al*., 1992; Fraser *et al*., 1994). The Stx toxins are not secreted but are released as a result of phage-mediated lysis and via outer membrane vesicles (Toshima *et al*., 2007; Kolling and Matthews, 1999; Bielaszewska *et al*., 2017). The capacity of certain antibiotics to induce Stx production means that antibiotic use can be contraindicated in the treatment of EHEC infections as it risks increasing the severity of Stx-mediated pathology (Zhang *et al*., 2000). In humans, the B subunit pentamer binds to the Gb_3 variant of the glycolipid receptor globotriaosylceramide that is present on the surface of Paneth cells in the intestine and kidney endothelial cells (Jacewicz *et al*., 1987; Lindberg *et al*., 1987). Stx2e, which is typically associated with porcine oedema disease, uses the Gb_4 variant of this receptor (Pierard *et al*., 1991). Cattle lack the vascular Gb_3 receptor meaning that EHEC infection in cattle is largely asymptomatic (Pruimboom-Brees *et al*., 2000). There is evidence to suggest that Gb_3 can be found on crypt epithelial cells in cattle, however, Stx does not appear to be cytotoxic in these cells as it is localised in lysosomes (Hoey *et al*.,

2003). Nevertheless, differences in the Stx types expressed by EHEC may underlie strain-specific differences in colonisation and host responses in cattle (Corbishley *et al*., 2014).

Once Stx binds to its receptor, it is endocytosed by both clathrin-dependent and independent mechanisms (Sandvig *et al*., 1989; Römer *et al*., 2007), and a protease sensitive loop connecting the A_1 and A_2 subunits is cleaved by the enzyme furin (Garred *et al*., 1995; Lea *et al*., 1999). The A subunits remain connected by a disulphide bond (Lea *et al*., 1999). Stx bypasses the late endocytic pathway to undergo retrograde transportation to the trans-Golgi network and then to the ER (Sandvig *et al*., 1992; Mallard *et al*., 1998). The remaining disulphide bond is reduced in the ER and the A_1 subunit is translocated into the cytoplasm of the host cell (Tam and Lingwood, 2007). Once in the cytoplasm, the A_1 subunit exhibits N-glycosidase activity and removes an adenine nucleotide from the 28S rRNA of host cell ribosomes, resulting in the inhibition of proteins synthesis and cell death (Endo *et al*., 1988).

Stx enters human Gb_3-negative intestinal cells via macropinocytosis (Malyukova *et al*., 2009) and is translocated through the cells into the bloodstream in order to reach the kidneys (Acheson *et al*., 1996). Stx is also capable of retrograde transportation in these cells but does not inhibit protein synthesis (Schüller *et al*., 2004). Instead it modulates NF-κB activation and suppresses the host immune response (Gobert *et al*., 2007). The effects of Stx on the host immune response are described in Section 1.2.4.2.

1.2 Host immune responses to A/E *E. coli* and bacterial evasion of these responses

Bacteria in the gut interact with the host immune system at the intestinal mucosa and gut associated lymphoid tissue (Figure 1.5). A/E *E. coli* have evolved a number of strategies for subverting both the innate and adaptive immune responses, which are described in greater detail in Sections 1.2.1–1.2.4.

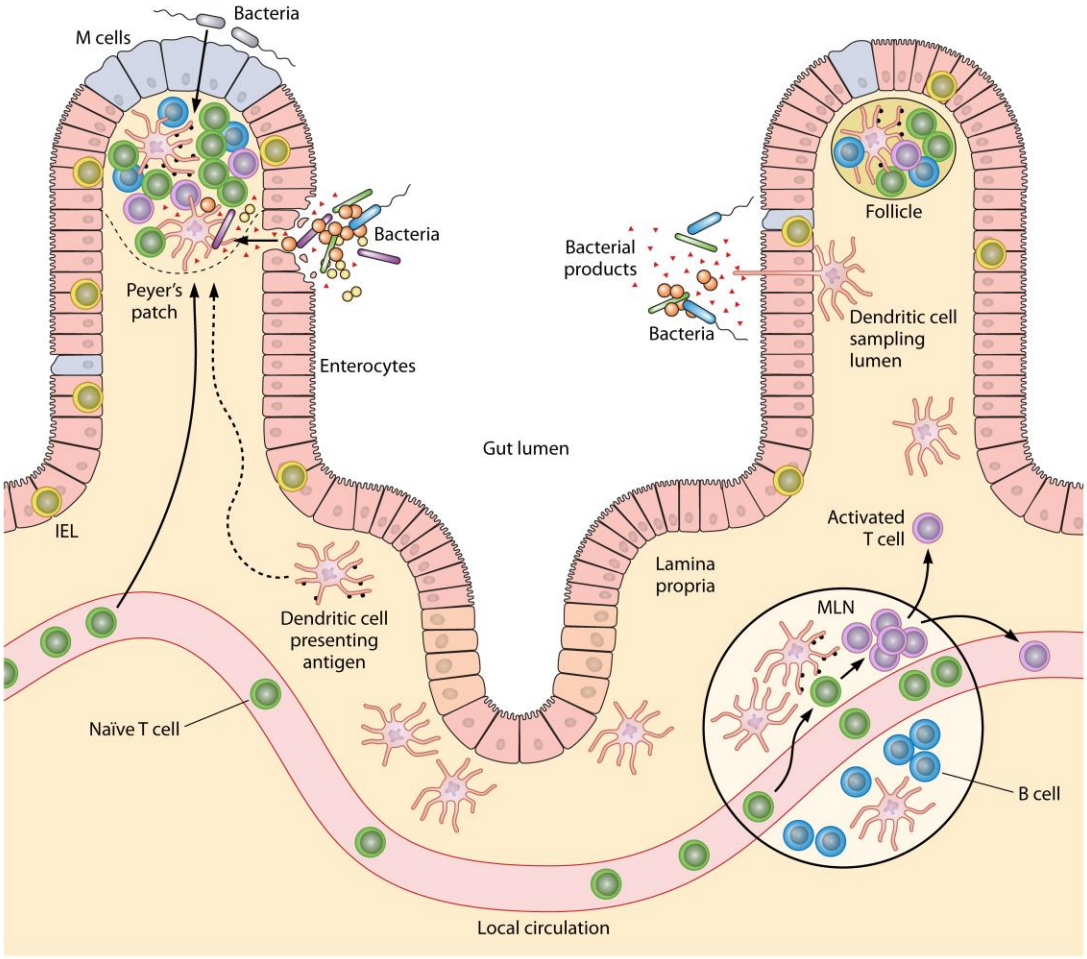

Figure 1.5. Schematic of the intestinal mucosa and gut associated lymphoid tissue, which includes Peyer's patches, mesenteric lymph nodes (MLN) and isolated lymphoid follicles. IEL – intraepithelial lymphocyte (from Cassady-Cain *et al*., 2018).

1.2.1 The innate immune response

1.2.1.1 The intestinal epithelial barrier

The innate immune response is the first line of defence against infection with A/E *E. coli* and intestinal epithelial cells play a crucial role in the innate immune responses against these bacteria. Not only do they form a protective barrier to prevent infection via the secretion of mucus and antimicrobial proteins but they also

participate in regulating both the innate and adaptive immune responses (reviewed in Peterson and Artis, 2014; reviewed in Santos and Finlay, 2015). Goblet cells secrete mucins. The most abundant of these, MUC2, forms a fixed inner mucus layer in the colon that is impenetrable to most microbes (Johansson *et al*., 2008). Goblet cells also produce factors such as intestinal trefoil factor (ITF) and resistin-like-molecule-β (RELMβ) that regulate the mucus barrier (reviewed in Peterson and Artis, 2014). ITF cross-links mucins to increase the structural stability of mucus and also promotes epithelial cell repair, migration and resistance to apoptosis (reviewed in Peterson and Artis, 2014; Dignass *et al*., 1994; Taupin *et al*., 2000). RELMβ promotes the expression of pro-inflammatory cytokines and major histocompatibility complex (MHC) class II in macrophages and regulates interferon (IFN)-γ expression in $CD4^+$ T lymphocytes, although RELMβ may only be produced in response to nematode infections (Nair *et al*., 2008; Artis *et al*., 2004). Epithelial cells in the gastrointestinal tract also have a rapid turnover rate relative to other epithelial cells, which removes cells that have been infected/colonised by pathogens (reviewed in Kim *et al*., 2010).

A plethora of antimicrobial proteins are secreted by epithelial cells in the small intestine, some of which are expressed by enterocytes, while others, such as α-defensins and lysozyme, are expressed by specialised Paneth cells (reviewed in Gallo and Hooper, 2012). Antimicrobial proteins target essential features of bacterial physiology, for example by disrupting membranes, hydrolysing peptidoglycan, and chelating metals (reviewed in Gallo and Hooper, 2012). Lipocalin 2 is an antimicrobial protein that is broadly expressed by epithelial cell types and has been shown to protect against *E. coli* infection by sequestrating iron-laden siderophores (Flo *et al*., 2004). Intestinal epithelial cells also transport and secrete IgA antibodies produced in the lamina propria (reviewed in Johansen and Kaetzel, 2012).

M cells, located at Peyer's patches and lymphoid follicles, and goblet cells are capable of transporting microbes and their products to antigen-presenting cells (APCs) in the lamina propria (reviewed in Mabbott *et al*., 2013; reviewed in McDole *et al*., 2012). Intestinal epithelial cells can themselves detect bacterial products via pattern recognition receptors (PRRs), which trigger the activation of the pro-inflammatory NF-κB and mitogen-activated protein kinase (MAPK) signalling

pathways, resulting in the expression of pro-inflammatory cytokines (reviewed in Santos and Finlay, 2015). *In vitro* studies have shown that expression of the cytokine interleukin (IL)-8, which recruits neutrophils to the site of infection to phagocytose and destroy the bacteria, is up-regulated in cells infected with EPEC and EHEC (Berin *et al*, 2002; Savkovic *et al*., 1996).

1.2.1.2 Phagocytes

Neutrophils and macrophages are drawn to the site of infection by chemoattractants, such as IL-8, where they phagocytose and destroy invading microbes (reviewed in Lim *et al*., 2017). Like epithelial cells, phagocytes detect bacterial products via PRRs, which include Toll-like and NOD-like receptors (reviewed in Brubaker *et al*., 2015; reviewed in Amarante-Mendes *et al*., 2018). PRRs recognise highly conserved bacterial features such as lipopolysaccharide (LPS), flagellin, muramyl dipeptide and the γ-D-glucose-mDAP motif of peptidoglycan (reviewed in Brubaker *et al*., 2015). Cis-phagocytosis involves the direct recognition of bacterial products, such as the recognition of LPS by macrophage class A scavenger receptors (Peiser *et al*., 2000). Trans-phagocytosis involves the detection of bacteria opsonised with the complement component iC3b or IgG antibodies, which are recognised by the CR3 complement receptor and FCγ immunoglobulin receptor respectively (Anderson *et al*., 1990; Ross *et al*., 1992).

In neutrophils, the pH of the phagosome rapidly increases during the first 5–15 minutes after engulfment as NADPH oxidase 2 (NOX2) transfers electrons from the cytosol into the lumen of phagosomes to generate superoxide, which is converted into hydrogen peroxide by superoxide dismutase (Segal *et al*., 1981; Cech and Lehrer, 1984; Gabig *et al*., 1978). The fusion of azurophil granules with the phagosome releases myeloperoxidase, which catalyses the transformation of hydrogen peroxide into various reactive oxygen species (ROS) with potent antimicrobial activity, including hypochlorous acid, hydroxyl radical and singlet oxygen (reviewed in Prokopowicz *et al*., 2012). Neutrophils also synthesise nitric oxide, which diffuses into the phagosome. Nitric oxide itself has antimicrobial properties, which are increased when it reacts with superoxide to form reactive

nitrogen species (reviewed in Manda-Handzlik and Demkow, 2015). The rise in pH also facilitates the fusion of azurophil and gelatinase granules containing proteases, antimicrobial proteins and bactericidal/permeability-increasing proteins (Reeves *et al*., 2002; reviewed in van Kessel *et al*., 2014). After the initial pH increase, the phagosome is acidified owing to the action of vacuolar proton-translocating ATPases (V-ATPases; Jankowski *et al*., 2002).

Phagocytosed bacteria are also destroyed by macrophages using a range of proteases and glycosidases delivered by lysosomes, as well as V-ATPase-induced phagosome acidification (reviewed in Hirayama *et al*., 2018). ROS production plays a less significant role in the killing of phagocytosed bacteria in macrophages than it does in neutrophils as ROS production occurs mainly at the plasma membrane in macrophages (Berton *et al*., 1982; Yamaguchi and Kaneda, 1988).

1.2.1.3 Antigen-presenting cells

Macrophages and dendritic cells can be found in the intestinal lamina propria where they receive antigens in a number of ways. Antigens can be delivered from the gut lumen via transcytosis by M cells, goblet cell-associated antigen passages and through paracellular leak, whereby antigens are permitted to the lamina propria through pores in epithelial cell tight junctions (reviewed in Knoop *et al*., 2013; reviewed in Allaire *et al*., 2018). Macrophages and dendritic cells can also directly sample the lumen using transepithelial dendrites during inflammation and acquire antigens from other macrophages (reviewed in Knoop *et al*., 2013; reviewed in Peterson and Artis, 2014; reviewed in Bekiari *et al*., 2014).

APCs phagocytose bacteria to degrade them and present antigens in the context of the major histocompatibility complex to adaptive immune cells (reviewed in Santos and Finlay, 2015). In dendritic cells, antigens are processed rather than completely degraded using various cathepsins and asparagine endopeptidase (Lennon-Duménil *et al*., 2002; Mohamadzadeh *et al*., 2004; Manoury *et al*., 1998). The degradation of antigens is controlled by protease inhibitors and low levels of NOX2 and V-ATPases maintain a neutral pH in the phagosome (Trombetta *et al*., 2003; Savina *et al*., 2006).

Processed antigens are then loaded on both MHC class I and II molecules in dendritic cells where they are presented to $CD8^+$ and $CD4^+$ T cells respectively (review in Blum *et al*., 2013). Antigens are loaded onto MHC class II molecules in the phagosome while others are exported to the cytosol, further processed by the proteasome and sent to the ER for loading onto MHC class I molecules (reviewed in Blum *et al*., 2013). Macrophages present antigens on MHC class II molecules but require stimulation with IFN-γ or RELMβ in order to express MHC class II (McCormack *et al*., 1992; Nair *et al*., 2008). IFN-γ has also been shown to upregulate the expression of cathepsin S, a protease involved in MHC class II processing, in macrophages (van's Gravesande *et al*., 2002).

1.2.1.4 Humoral innate immunity

Humoral innate immunity is comprised of the complement and contact cascades, naturally occurring antibodies and pentraxins (reviewed in Shishido *et al*., 2012). The complement system consists of blood plasma and membrane-expressed proteins and can be activated by either the classical, alternative or mannose binding lectin pathways (reviewed in Merle *et al*., 2015a). These pathways converge at the point of C3 cleavage, generating C3b, which leads to the cleavage of C5. C5b generated from the cleavage of C5 recruits complement components C6–9 to form membrane attack complexes in the membranes of pathogens, which results in direct killing by osmotic stress (reviewed in Merle *et al*., 2015b). C3b bound to the surface of a pathogen can also be cleaved into iC3b, which opsonises the pathogen and aids phagocytosis (Cunnion *et al*., 2004; Section 1.2.1.2).

The contact system consists of factor XII (FXII), plasma prekallikrein (PPK) and high molecular weight kininogen (HK) and is involved in the activation of the intrinsic coagulation pathway, the complement system, inflammation and the production of antimicrobial peptides (reviewed in Oehmcke-Hecht and Köhler, 2018). Contact factors bind to a number of molecules on the surface of pathogens including the curli fibres expressed by certain *E. coli* strains (reviewed in Oehmcke-Hecht and Köhler, 2018; Nasr *et al*., 1996; Herwald *et al*., 1998). FXII cleaves PPK into plasma kallikrein (PK), which in turn cleaves HK into bradykinin

and a variety of HK-derived antimicrobial peptides (Nordahl *et al*., 2005; Frick *et al*., 2006; Sonesson *et al*., 2011). Bradykinin and the cleavage product HKa stimulate the expression of pro-inflammatory cytokines (Tiffany and Burch, 1989; Pan *et al*., 1996; reviewed in Lalmanach *et al*., 2010; Khan *et al*., 2006) and bradykinin can also directly activate macrophages and dendritic cells as well as control neutrophil migration (Sato *et al*., 1996; Aliberti *et al*., 2003; Paegelow *et al*., 2002). FXII and PK can also trigger inflammation by inducing pro-inflammatory cytokine expression in macrophages and by causing the aggregation and degranulation of neutrophils (Vorlova *et al*., 2017; Wachtfogel *et al*., 1983; Wachtfogel *et al*., 1986). Furthermore, FXII and PK can activate the classical and alternative complement pathways respectively (Ghebrehiwet *et al*., 1981; DiScipio, 1982; Irmscher *et al*., 2018).

Naturally occurring IgM, IgA and IgG antibodies are produced by B1 B lymphocytes in the absence of antigen stimulation and recognise a variety of pathogens, but with low affinity due to restricted epitope specificity (reviewed in Shishido *et al*., 2012). Pentraxins are a family of multimeric soluble pattern recognition receptors with a conserved C-terminal domain and consist of three major members – C-reactive protein, serum-amyloid P component (SAP) and pentraxin 3 (reviewed in Ma and Garred, 2018). Like naturally occurring antibodies, pentraxins bind to multiple pathogens as well as intrinsic antigens (reviewed in Du Clos, 2013). Pentraxins act as opsonins as they are recognised by FCγ immunoglobulin receptors (Mold *et al*., 2001; Mold *et al*., 2002; Moalli *et al*., 2010). Human SAP has been shown bind to and neutralise recombinant Stx2 *in vitro* and protect mice from lethal toxicity caused by recombinant Stx2 *in vivo*, however, it is unclear why SAP does not protect humans against HUS (Kimura *et al*., 2001; Armstrong *et al*., 2006; Dettmar *et al*., 2014). Pentraxins are also capable of activating and regulating the various pathways of the complement system (reviewed in Ma and Garred, 2018).

1.2.1.5 Natural killer (NK) cells and γδ T cells

NK cells and γδ T cells are classically thought of as innate lymphoid cells but have been shown to possess a form of memory (reviewed in Pahl *et al*., 2018;

Sheridan *et al*., 2013) and therefore bridge the gap the between the innate and adaptive immune systems. Human NK cells are characterised as $CD3^-$ $CD56^+$ lymphocytes (Lanier *et al*., 1989; Zocchi *et al*., 1989; Nagler *et al*., 1989), however, bovine NK cells lack CD56 and are characterised by the expression of CD335 (Storset *et al*., 2004). Human NK cells can be subdivided into $CD56^{dim}$ cells, which account for the majority of NK cells in the peripheral blood (reviewed in Mandal and Viswanathan, 2015), and $CD56^{bright}$ cells, which are localised in secondary lymphoid tissue (Fehniger *et al*., 2003). These cell subsets are involed in cytotoxic killing and cytokine production respectively (reviewed in Mandal and Viswanathan, 2015).

NK cell function is controlled by a number of activatory and inhibitory receptors (reviewed in Mandal and Viswanathan, 2015). The recognition of self-MHC class I is a major inhibitor of NK cell activity, allowing NK cells to target infected or cancerous cells where MHC expression has been downregulated (Kärre *et al*., 1986). NK cells induce apoptosis in target cells by releasing perforin and granzyme, similar to cytotoxic T cells (Kägi *et al*., 1994; Shresta *et al*., 1995). NK cells are generally thought to protect against intracellular pathogens and cancer cells, however, they have been shown to protect mice from infection with the A/E pathogen *C. rodentium* (Hall *et al*., 2013). NK cells were shown to prevent dissemination of the bacteria to extracolonic tissues via the recruitment of other immune cells and by direct cytotoxic killing of the bacteria (Hall *et al*., 2013). Wöchtl *et al*. (2017) reported a slight increase in the number of NK cells in the blood of gnotobiotic piglets infected with EHEC O157:H7 but the relevance of these during infection was unclear.

γδ T cells differ from $CD4^+$ and $CD8^+$ T lymphocytes inthat they posses a γδ T cell receptor (TCR) rather than an αβ TCR (reviewed in Alcover *et al*., 2018). γδ T cells have a broad range of functions including the secretion of IFN-γ, cytotoxic killing and antigen presentation (reviewed in Lawand *et al*., 2017). As APCs, human and zebra fish γδ T cells have been shown to be capable of professional phagocytosis (Wu *et al*., 2009; Wan *et al*., 2017). γδ T cells are found mainly in mucosal tissues where they protect against infection and promote epithelial cell layer integrity (Mackay and Hein, 1989; Bandeira *et al*., 1990; Chen *et al*., 2002a; reviewed in McCarthy and Eberl, 2018). In cattle they also account for 60–80 % of the

circulating lymphocytes in calves, which decreases to 5–15 % with age, and are the major regulatory T cell subset in bovine peripheral blood (Mackay and Hein, 1989; Davis *et al*., 1996; Guzman *et al*., 2014). Studies in mice reported that γδ T cells produce IL-17 in response to intraperitoneal infection with laboratory adapted *E. coli*, resulting in the recruitment of neutrophils (Shibata *et al*., 2007). Schaut *et al*. (2019) also reported that the intramuscular vaccination of cattle with inactivated Stx-negative EHEC O157:H7 resulted in the proliferation of γδ T cells, which produced IFN- γ and IL-4.

1.2.2 Innate immune evasion strategies by A/E *E. coli*

Many effector proteins produced by A/E *E. coli* that modulate the innate immune system target three main functions: NF-κB signalling, to inhibit the expression of pro-inflammatory cytokines; phagocytosis, to prevent clearing of the bacteria; and apoptosis, to impede the rapid turnover of intestinal epithelial cells, which normally removes colonising bacteria. Studies of these effectors are often caveated however, as effectors are generally overexpressed, used singly and may not reflect their role during infection.

1.2.2.1 Nle proteins

Non-LEE encoded effectors modulate the immune response in intestinal epithelial cells in a number of ways (Figure 1.6). NleA prevents the de-ubiquitination of the inflammasome (protein complex involved in pro-inflammatory cytokine signalling) protein NLRP3 and therefore inhibits the secretion of IL-1β (Yen *et al*., 2015). NleB is a glycosyltransferase that targets host cell death-domain-containing proteins including FADD, TRADD and RIPK1. It has been shown to N-glycosylate Arg^{117} of FADD and Arg^{235} of TRADD, which disrupts NF-κB signalling and prevents the expression of pro-inflammatory cytokines and apoptosis (Li *et al*., 2013b; Pearson *et al*., 2013). Gao *et al*. (2013) reported that NleB O-glycosylates glyceraldehyde 3-phosphate dehydrogenase (GAPDH). This was confirmed by El

Qaidi *et al*. (2017), who found that NleB glycosylates GAPDH at residues Arg^{197} and Arg^{200}, which are required to stimulate TRAF2 ubiquitination.

NleC, E and H also interfere with NF-κB signalling in different ways. NleC is a zinc metalloprotease that degrades the NF-κB members p50, p65 and c-Rel, which results in the inhibition of IL-8 secretion (Pearson *et al*., 2011). NleC has also been shown to act synergistically with NleE (Pearson *et al*., 2011). NleE methylates conserved cysteines in the Np14 zinc finger domains of the host proteins TAB2 and 3, which prevents the downstream degradation of the NF-κB inhibitor IκB (Zhang *et al*., 2012; Nadler *et al*., 2010). NleH interferes with NF-κB signalling in multiple ways. It inhibits the phosphorylation of the NF-κB transcriptional complex ribosomal protein S3, preventing its translocation to the nucleus (Gao *et al*., 2009; Wan *et al*., 2011), and suppresses the ubiquitination and subsequent degradation of IκB (Royan *et al*., 2010). NleH also inhibits apoptosis by binding the protein Bax inhibitor-1 (Hemrajani *et al*., 2009).

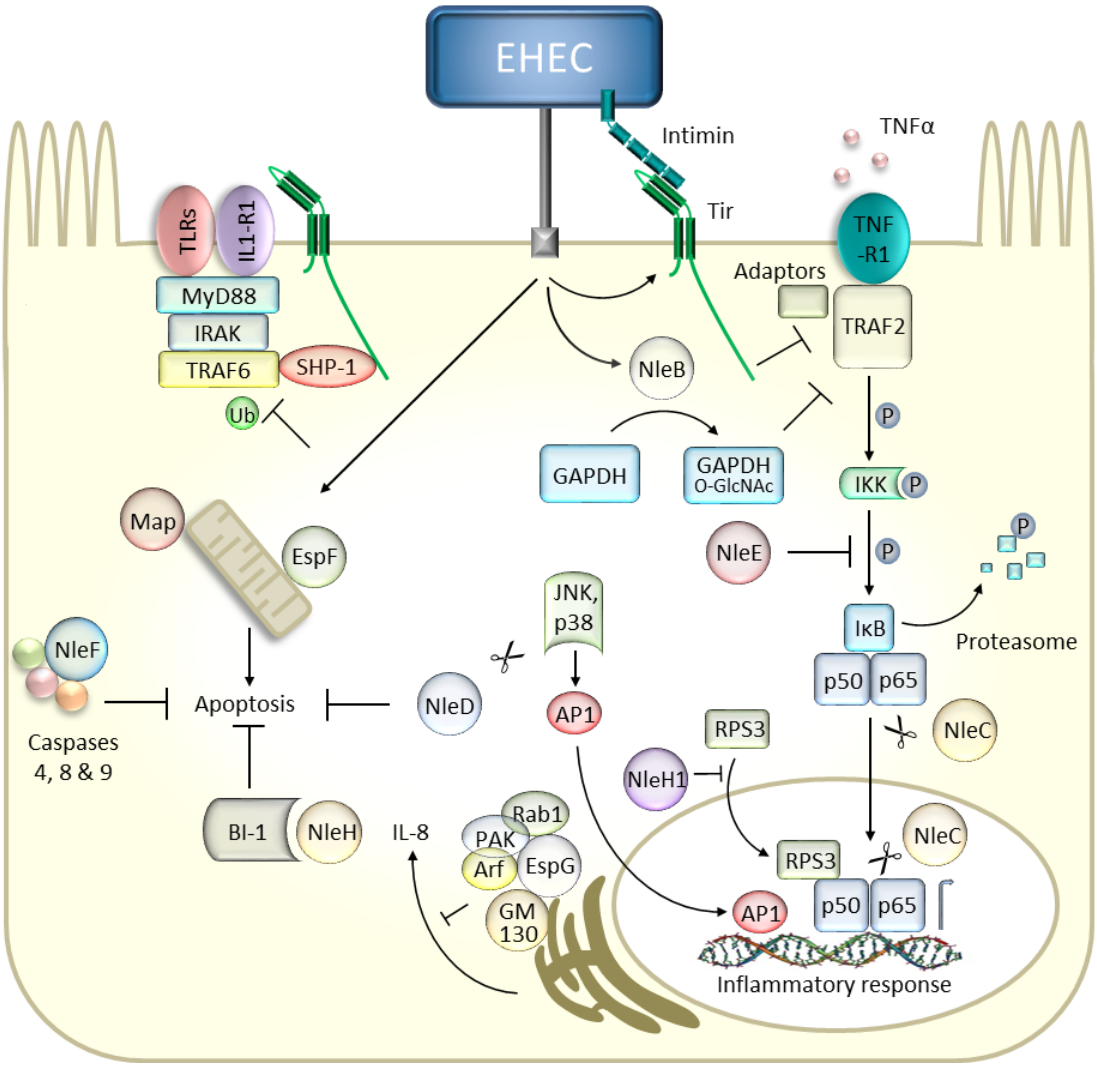

Figure 1.6. Schematic of EHEC adhering to an enterocyte and injecting various Nle proteins into it via the Type III secretion system. A number of Nle proteins inhibit the expression and secretion of pro-inflammatory cytokines. Inhibition of protein secretion by EspG also blocks cytokine secretion. NleD, F and H prevent apoptosis of the host cell induced by Map and EspF (from Stevens and Frankel, 2014).

NleD is another zinc metalloprotease that cleaves the host proteins JNK and p38 MAPK to inhibit both apoptosis and pro-inflammatory cytokine expression via activator protein 1 (AP-1) activation (Baruch *et al.*, 2011; Creuzburg *et al.*, 2017). It has been shown to differentiate between the host substrates as a conserved arginine residue is required for the cleavage of p38 but not that of JNK (Creuzburg *et al.*,

2017). NleF prevents apoptosis of infected cells by binding to caspases-4, 8 and 9, which it inhibits by inserting its C-terminus into the caspase active site (Blasche *et al*., 2013). It should be noted that the role of many of these proteins was determined using cell culture models with high multiplicity of infections, which does not reflect their relevance during infection.

1.2.2.2 Esps

As described in Section 1.1.3.4, EspB inhibits the interaction of myosin with actin, which has been shown to inhibit the phagocytosis of EPEC E2348/69 by murine bone marrow-derived macrophages (Iizumi *et al*., 2007). EspB also suppresses NF-κB activation (Hauf and Chakraborty, 2003), although it is unclear if this reflects a direct role or the requirement for EspB in injection of other effectors. EspZ inhibits apoptosis of epithelial cells early in infection by interacting with CD98, which mediates cell survival (Shames *et al*., 2010), and the translocase of inner mitochondrial membrane 17b, which prevents the release of cytochrome c from mitochondria (Shames *et al*., 2011; Roxas *et al*., 2012). EspL is a cysteine protease that cleaves within the receptor-interacting protein homotypic interaction motifs of the proteins RIPK1, RIPK3, TRIF and ZBP1/DAI to inhibit necroptosis and inflammation (Pearson *et al*., 2017).

EspF, H, and J are involved in the inhibition of phagocytosis (Stevens and Frankel, 2014). EspF has been shown to inhibit phosphoinositide 3-kinase (PI3K)-dependent phagocytosis by macrophages and translocation by M cells (Celli *et al*., 2001; Quitard *et al*., 2006; Martinez-Argudo *et al*., 2007). EspF interacts with sorting nexin 9, actin, profilin and annexin A6 (Marchès *et al*., 2006; Alto *et al*., 2007; Peralta-Ramírez *et al*., 2008; Hua *et al*., 2017), suggesting that it inhibits phagocytosis by disrupting the actin cytoskeleton. Annexin A6 has been implicated in cell survival, proliferation, migration and inflammation (Grewal *et al*., 2016), suggesting a possible wider role for EspF in modulating the host immune response. EspH competes with Rho to bind the DH-PH domain of Rho guanine nucleotide exchange factors, preventing the activation of Rho and remodelling of the actin cytoskeleton (Dong *et al*., 2010). EspJ inhibits trans-phagocytosis by simultaneously

amidating and ADP-ribosylating members of the Src kinase family (Marchès *et al*., 2008; Young *et al*., 2014; Pollard *et al*., 2018).

1.2.2.3 Secreted protease of C1 esterase inhibitor from EHEC (StcE)

StcE is a Type II secreted zinc metalloprotease encoded on the pO157 plasmid of EHEC O157:H7 (Lathem *et al*., 2002). It cleaves the serum protein C1-esterase inhibitor (C1-INH), which is an anti-inflammatory serine protease and major regulator of the classical complement pathway (Lathem *et al*., 2002; Caliezi *et al*., 2000). StcE has been shown to increase the activity of C1-INH by localising it to the surface of erythrocytes, protecting bacterial cells against complement-mediated lysis, but cleavage of C1-INH is not required for this activity (Lathem *et al*., 2004). Grys *et al*. (2006) reported that recombinant StcE did not cleave the mucins MUC2 or MUC5AC *in vitro*. However, it was subsequently found that EHEC cleaved MUC2 in human colonic biopsy samples in a StcE-dependent manner (Hews *et al*., 2017), suggesting that a co-factor is required for this cleavage. StcE also cleaves other O-glycosylated mucin-type proteins such as MUC7 and glycoprotein 340, contributing to the intimate adherence of EHEC O157:H7 to host epithelial cells (Grys *et al*., 2005 and 2006; Hews *et al*., 2017).

StcE has also been found to cleave the mucin-type glycoproteins CD43 and CD45, which are found on most haematopoietic cells (Szabady *et al*., 2009; reviewed in Rheinländer *et al*., 2018; Fukuda and Carlsson, 1986; Borche *et al*., 1987). Cleavage of CD43 and CD45 has been shown to increase the respiratory burst in neutrophils but the biological significance of this remains unknown (Szabady *et al*., 2009). CD43 has anti-adhesive properties and is relocalised to the trailing end uropod of migrating neutrophils to release them from the extracellular matrix (Seveau *et al*., 2000). The cleavage of CD43 by StcE increases adhesion at the leading edge of neutrophils, thus increasing adhesion to the extracellular matrix and impairing neutrophil migration (Szabady *et al*., 2009). Proteolytically inactive StcE was also found to increase adhesion by relocalising CD43 to the uropod and blocking its anti-adhesive function (Szabady *et al*., 2009). CD45 has also been reported to be important for cell adhesion and chemotaxis in neutrophils (Shivtiel *et al*., 2008;

Harvath *et al*., 1991), suggesting that cleavage by StcE may affect these functions (Szabady *et al*., 2009). It was also recently found that StcE cleaves CD55 on epithelial cells (Furniss *et al*., 2018). CD55 is responsible for the release of neutrophils from the apical surface of intestinal epithelial cells (Lawrence *et al*., 2003) and cleavage of CD55 by StcE resulted in increased adhesion of neutrophils to Caco-2 monolayers (Furniss *et al*., 2018). Given that StcE has also been shown to cause aggregation of human T lymphocyte cell lines (Lathem *et al*., 2002), the cleavage of CD43 and CD45 may be responsible for this. CD45 also activates Src family kinases, which is an important step in TCR signal transduction (reviewed in Rheinländer *et al*., 2018), indicating a possible role for StcE in modulating the adaptive immune response.

1.2.3 The adaptive immune response

The adaptive immune system is composed of B and T lymphocytes, which possess immunological memory (reviewed in Marshall *et al*., 2018). B cells recognise antigens directly via the B cell receptor (an immunoglobulin molecule), which drives them to differentiate into memory B cells or antibody producing plasma cells. B cells can also be driven to proliferate by cytokines and can act as APCs (reviewed in Hoffman *et al*., 2016). T cells require seconadary stimulation from APCs in addition to the recognition of MHC-antigen complexes via the TCR (reviewed in Marshall *et al*., 2018). $CD8^+$ T cells are cytotoxic and act to destroy infected or cancerous cells, in a similar manner to NK cells (reviewed in Zhang and Bevan, 2011). $CD4^+$ T cells produce cytokines and can act as APCs. $CD4^+$ T cells can be further catagorised into four main subsets: T helper (Th) 1 cells, which are involved in the elimination of intracellular pathogens; Th2 cells, which mount an immune response to extracellular parasites; Th17 cells, which mount an immune response to extracellular bacteria and fungi; and regulatory T cells, which negatively regulate immune responses (reviewed in Luckheeram *et al*., 2012).

1.2.3.1 B lymphocyte response

The production of antibodies by B cells forms one part of the adaptive immune response against A/E *E. coli*. Children infected with EPEC have been shown to produce high levels of IgG against EspA and B, intimin and BfpA, which are all important for bacterial adherence (Martinez *et al*., 1999). People infected with EHEC have also been shown to produce serum antibodies against EspA and B, intimin and Tir (Li *et al*., 2000). The production of IgA antibodies against various bacterial components including O157 LPS, H7 flagellin and the outer membrane protein OmpC was observed in the rectal mucosa of cattle infected with EHEC O157:H7 (Nart *et al*., 2008a). Such antibodies may aid clearance of infection as vaccination with the proteins EspA, intimin and Tir significantly reduced the shedding of EHEC O157:H7 in the faeces of cattle (McNeilly *et al*., 2010). Serum IgG raised by vaccinating calves with intiminC_{280}, the C-terminal fraction of intimin-γ, EspB and a fusion protein of Stx2 B subunit and *Brucella* lumazine synthase was able to neutralise Stx2 toxicity, inhibit T3SS-induced erythrocyte lysis and prevent the adherence of EHEC O157:H7 to epithelial cells *in vitro* (Martorelli *et al*., 2017). DNA vaccines against LomW and the C-terminus of EscC have also been reported to stimulate IgA and IgG responses that are associated with the protection of mice against EHEC O157:H7 infection (Tapia *et al*., 2016; García-Angulo *et al*., 2014). There have been many other vaccine studies that have assessed the antibody responses of cattle and mice to EHEC antigens, however, few studies have used passive transfer of antibodies or Ig-deficient animals to prove the role of such antibodies in protective immunity (reviewed in García-Angulo *et al*., 2013). It should also be noted that EHEC infection studies in mice should be interpreted with care as EHEC strains do not effectively form A/E lesions in mice (Mundy *et al*., 2006; Girard *et al*., 2008; Eaton *et al*., 2017).

1.2.3.2 T lymphocyte response

The T cell response against EPEC and EHEC is less well defined than that of B cells but studies have shown a role for T cells in A/E *E. coli* infection. Mice

depleted in $CD4^+$ T cells failed to eradicate the murine A/E pathogen *C. rodentium* and had a diminished IgA and IgG response to EspA (Simmons *et al*., 2003). RAG1 knock-out mice, which cannot produce T or B cells, also failed to clear *C. rodentium* infection, suggesting a role for these cell types in clearance (Vallance *et al*., 2002). Corbishley *et al*. (2014) found that T lymphocytes have a role in the bovine immune response to EHEC O157:H7. It was observed that $CD4^+$ T cells skew the immune response towards a Th1 response, which involves intracellular killing, early in the infection. This skew towards a Th1 response has also been observed in mice infected with *C. rodentium* and occurs in an intimin-dependent manner (Higgins *et al*., 1999a; Higgins *et al*., 1999b). Moreover, EPEC intimin has been reported to bind $CD4^+$ T cells via β_1-integrins and co-stimulate these cells from murine Peyer's patches, mesenteric lymph node and caecal follicles (Frankel *et al*., 1996; Gonçalves *et al*., 2003). Intimin also co-stimulated proliferation of splenic $CD4^+$ T cells but not lamina propria $CD4^+$ T cells, which did not bind to intimin as strongly as T cells from other locations (Gonçalves *et al*., 2003). Schaut *et al*. (2019) reported that bovine $CD4^+$ T cells proliferated and produced IFN-γ in response to intramuscular vaccination with inactivated EHEC O157:H7. Corbishley *et al*. (2014) also found that Type III secreted proteins triggered proliferation in $CD8^+$ and γδ T cells *ex vivo* but that these cell types had reduced numbers in terminal rectal biopsies and so the role of these cells in infection is unclear.

1.2.4 Adaptive immune evasion strategies of A/E *E. coli*

1.2.4.1 Subtilase cytotoxin (SubAB)

SubAB is an AB_5 toxin found in some A/E *E. coli*, but also LEE-negative Stx-producing strains (reviewed in Krause *et al*., 2018). The A subunit of the toxin is a serine protease that cleaves the ER chaperone BiP, activating the ER stress-induced unfolded protein response that triggers apoptosis (reviewed in Paton and Paton, 2010). Other effects of SubAB include the inhibition of protein synthesis and cell cycle arrest in the G1 phase (reviewed in Paton and Paton, 2010). The pathology caused by SubAB is similar to that caused by Stx (Wang *et al*., 2007). However,

subcytotoxic concentrations of SubAB have been reported to inhibit NF-κB activation in murine macrophages (Harama *et al*., 2009).

SubAB has been shown to bind to murine macrophages, neutrophils and lymphocytes and induce apoptosis in these cell types (Wang *et al*., 2011). The apoptosis rates of $CD4^+$ T cells and $B220^+$ B cells in murine blood were found to be significantly different from the basal rate up to 6 hours after SubAB injection (Wang *et al*., 2011). SubAB has also been shown to inhibit antibody secretion in murine B cells (Hu *et al*., 2009). BiP is required for the assembly of immunoglobulin heavy and light chains in the ER (Bole *et al*., 1986; Knittler and Haas, 1992). The SubAB-cleaved C-terminal fragment of BiP strongly binds to newly synthesised light chains and prevents their assembly with heavy chains, causing the unassembled immunoglobulins to be retained in the ER (Hu *et al*., 2009).

1.2.4.2 Stx

Stx modulates both the innate and adaptive immune responses. As described previously, Stx inhibits NF-κB activation in human Gb_3-negative epithelial cells (Gobert *et al*., 2007). Stx has also been shown to target bovine peripheral blood lymphocytes and intraepithelial lymphocytes, which display Gb_3 receptors (Menge *et al*., 1999; Menge *et al*., 2003; Menge *et al*., 2004a). It directly inhibits the proliferation of mitogen-stimulated bovine T and B cells (Menge *et al*., 1999; Stamm *et al*., 2002; Menge *et al*., 2003), as well as bovine leukemia virus infected lymphocytes (Ferens and Hovde, 2000), without inducing cell death. Menge *et al*. (2004b) also found that EHEC O103:H2 producing Stx1 significantly reduced the number of $CD8\alpha^+$ T cells in bovine ligated ileal loops within 12 hours of infection in a Stx1-dependent manner, albeit differences in proliferative capacity, natural killer cell activity or the cytokine mRNA profile of isolated cells did not differ significantly. Studies in calves demonstrated that animals infected with Stx-producing EHEC strains did not mount an effective cellular immune response after re-infection (Hoffman *et al*., 2006). Stx delays the onset of a cellular immune response rather than downregulating it (Stamm *et al*., 2002; Hoffman *et al*., 2006) and appears to target T cells in particular *in vivo* (Hoffman *et al*., 2006). As well as

inhibiting adaptive immune responses in cattle, Stx has been shown to induce the expression of pro-inflammatory cytokines in human and murine macrophages, which is thought to contribute to pathology (Tesh *et al*., 1994; Leyva-Illades *et al*., 2012; Brandelli *et al*., 2015; Lee *et al*., 2016; reviewed in Lee and Tesh, 2019). Although studies have shown that Stx is not essential for the colonisation of sheep, mice and infant rabbits, these did not consider the nature of immune responses during such infections (Ritchie *et al*., 2003; Woodward *et al*., 2003; Robinson *et al*., 2006).

1.3 Lymphostatin

1.3.1 The discovery of lymphostatin

In 1995 Klapproth *et al*. discovered that lysates of certain EPEC strains were capable of dose-dependent inhibition of cytokine expression by human peripheral blood mononuclear cells (PBMCs), but that laboratory-adapted *E. coli* K-12 strains, other *E. coli* pathotypes and whole EPEC lacked this ability. Lysates of EHEC O157:H7 strain EDL933 were found to inhibit cytokine expression but were not tested in a dose-dependent manner. Only one EPEC strain tested, O119:H6 0659-79, did not have inhibitory activity against PBMCs, which may be due to known variation in EPEC strains (Levine and Edelman, 1984). Klapproth *et al*. (1995) determined that inhibitory activity was caused by a protein or proteins encoded on the bacterial chromosome. They also found, using lysates of an *E. coli* K-12 strain transformed with an EPEC cosmid (pIV-8-A), that these lysates inhibited cytokine expression in human peripheral blood lymphocytes irrespective of the mechanism of lymphocyte activation. These cosmid clone lysates could also inhibit the mitogen-stimulated proliferation of lymphocytes. The inhibition observed in these experiments was reportedly not due to cellular toxicity.

In 1996, further experiments by Klapproth *et al*. found that lysates of *E. coli* K-12 containing the EPEC pIV-8-A cosmid clone exhibited dose-dependent inhibition of IL-2 expression against human PBMCs and lamina propria mononuclear cells (LPMCs). The inhibition of cytokine synthesis was non-selective and the inhibition of lymphocyte proliferation was not caused by the inhibition of

IL-2 receptor expression. CD25 (α-chain of the IL-2 receptor) expression, which rapidly increases after T cell activation, was not inhibited in $CD45RO^+$ cells (activated T cells) by lysates of *E. coli* K-12 containing pIV-8-A. It was found that the inhibitory effect of EPEC E2348/69 lysates was similar in mitogen-stimulated PBMCs and LPMCs. The culture supernatants of EPEC were also found to inhibit IL-2 and IL-5 expression in mitogen-stimulated PBMCs. Lastly, Klapproth *et al*. (1996) found that EPEC and cosmid clone lysates could inhibit cytokine expression in human lymphocytes activated by products of non-pathogenic *E. coli*.

Malstrom and James (1998) observed that EPEC E2348/69 lysates inhibited IL-2 expression in murine splenic cells stimulated with 12-myristate 13-acetate and phytohaemagglutinin without causing apoptosis. EPEC lysates inhibited multiple cytokines but increased the production of IL-10, which itself inhibits inflammatory cytokine expression. However, the inhibitory activity of EPEC lysates was independent of IL-10 and the regulatory cytokine TGF-β. Macrophages were also not required for the increased production of IL-10. IL-2 expression was inhibited by EPEC lysates in mitogen-stimulated Jurkat cells (an immortalised human T cell line) as well as small intestinal intraepithelial and Peyer's patches lymphocytes. Pre-exposure of murine splenic cells to EPEC lysates resulted in decreased IL-2 and increased IL-10 expression when the cells were both mitogen- and antigen-stimulated. Malstrom and James (1998) also found that lysates of EHEC EDL933, RDEC-1 and *C. rodentium* had inhibitory activity against murine splenic lymphocytes and that this activity was not related to EspB, which was examined due its requirement for signal transduction in host cells and the activation of NF-κB transcription factors (Foubister *et al*., 1994; Savkovic *et al*., 1997).

In 2000 Klapproth *et al*. discovered the protein responsible for the inhibitory activity described above, which they named lymphostatin or lymphocyte inhibitory factor A (LifA) due its ability to specifically inhibit lymphocyte proliferation and cytokine expression. DNA sequencing of the pIV-8-A cosmid revealed the *lifA* gene to be 9,669 bp encoding a predicted 365,950 Da protein – the largest protein so far described in *E. coli*. Mutation of the *lifA* gene from EPEC E2348/69 abolished the inhibitory activity of bacterial lysates against human PBMCs but did not affect the

ability of the strain to nucleate actin under sites of attachment in a fluorescent actin staining test, a proxy for A/E lesion formation (Klapproth *et al*., 2000).

1.3.2 Homologous proteins and sequences to lymphostatin

In the same year as LifA was first described, Nicholls *et al*. (2000) discovered a protein in EHEC O111:H- strain E45035 that increased the adhesion of bacteria to Chinese hamster ovary (CHO) cells *in vitro* and named it EHEC factor for adherence 1 (Efa1). Efa1 was identical in size to LifA and was predicted to be 99.9 % identical to LifA at a nucleotide level and 99 % identical at an amino acid level (Nicholls *et al*., 2000), with only a single amino acid difference between the two proteins. As such, LifA and Efa1 are considered to be the same protein and their names are used interchangeably in the literature.

LifA and homologous proteins have been found in EPEC, EHEC, RDEC, *E. albertii*, *C. rodentium* and various *Chlamydia* species (reviewed in Klapproth, 2010). An NCBI Blast search reveals that EPEC E2348/69 possesses a LifA homologue termed LifA-like protein, which is also present in EPEC O111:H- strain B171-8 and is predicted to be ~298 kDa in size. The LifA-like protein from EPEC E2348/69 shares 34 % identity and 54 % similarity with amino acids (aa) 244–716 of LifA, and 28 % identity and 48 % similarity with aa 707–2356 of LifA. The LifA-like protein from EPEC B171-8 shares 31 % identity and 51 % similarity with aa 62–716, and 27 % identity and 47 % similarity with aa 728–2555 of LifA. EPEC B171-8 LifA-like protein is also larger than the E2348/69 variant at ~339 kDa. The LifA-like protein, along with LifA, has recently been implicated in having an accessory role in the formation of actin pedestals and A/E lesions that is masked by other T3S effector proteins (Cepeda-Molero *et al*., 2017).

The prototype EHEC O157:H7 strain EDL933 does not produce LifA but rather encodes two homologous proteins termed Efa1′ and ToxB. Efa1′ is a truncated version of LifA that is encoded on open reading frames *z4332* and *z4333* on O-island 122 of the chromosome of strain EDL933 (Hayashi *et al*., 2001; Perna *et al*., 2001). Efa1′ shares 99 % identity and 99 % similarity with aa 1–433 of LifA and is identical to aa 437–711 of LifA (Hayashi *et al*., 2001; Perna *et al*., 2001). It is unclear if only

the 433 amino acid protein is made or if a 710 amino acid protein can be made via ribosome frameshifting. ToxB is of a similar predicted size to LifA and is encoded on the EHEC O157:H7 large plasmid pO157 (Burland *et al*., 1998; Makino *et al*., 1998). ToxB shares 30 % identity and 48 % similarity with aa 48–3204 of LifA (Burland *et al*., 1998; Makino *et al*., 1998). ToxB sequences have also been found in non-O157 EHEC strains and EPEC (for example, Badea *et al*., 2003; Tozzoli *et al*., 2005). Stevens *et al*. (2004) reported that the LifA homologues Efa1′ and ToxB influenced the adherence of EHEC O157:H7 to HeLa cells but were not required for the colonisation of cattle or sheep. They also reported that mutations in the *efa1′* and *toxB* genes reduced the production and secretion of proteins encoded by the LEE4 operon but did not affect the activity of the LEE1, 4 and 5 operon promoters. This is consistent with observations by Tatsuno *et al*. (2001) that suggest that ToxB affects expression and secretion of LEE-encoded proteins at a post-transcriptional level. Abu-Median *et al*. (2006) also performed experiments with *efa1′* and *toxB* mutants and reported that these proteins did not appear to confer lymphostatin-like activity against mitogen-stimulated peripheral blood lymphocytes, however, the assay relied on crude bacterial lysates and is relatively insensitive. Recent experiments by Cassady-Cain *et al*. (2017) have since shown that recombinant ToxB does inhibit the mitogen-stimulated proliferation of bovine T cells in a dose dependent manner, similar to LifA.

In *Chlamydia*, *C. psittaci* contains a single *lifA* homologue, *C. muridarum* possesses three copies and *C. trachomatis* contains a pseudogene with frameshift mutations (Xie *et al*., 2003). LifA homologues from *Chlamydia* species share ~34–37 % identity with EPEC E2348/69 LifA. Belland *et al*. (2001) have shown that LifA homologues from *C. trachomatis* act as cytotoxins and suggested that it is possible that the immunomodulatory ability of LifA homologues may allow *Chlamydia* species to cause persistent infections. The Stevens laboratory has recently shown that a LifA homologue from *C. pecorum*, which shares ~36 % identity with LifA, inhibits the mitogen-stimulated proliferation of bovine T cells in a dose-dependent manner. This involved cloning, expression and affinity purification of the protein and inhibitory activity is not the result of cytotoxicity (Stevens Laboratory unpublished data).

1.3.3 Secretion of lymphostatin

Little work has been carried out towards understanding the mechanism of secretion of LifA. Deng *et al*. (2012) reported that LifA appeared to be secreted by the LEE-encoded T3SS based on quantitative proteomic (SILAC) analysis of proteins secreted by EPEC O127:H6 strain E2348/69 and an isogenic LEE mutant. This involved mapping peptides across the protein and detecting them using mass spectrometry. Reporter assays using the N-terminal 50–100 amino acids of LifA fused to TEM-1/β-lactamase showed that this sequence of LifA was capable of directing the translocation of the TEM1 fusion protein into HeLa cells, which was detected by a change in fluorescence of a β-lactamase substrate. Due to the limitations of the cloning vector that was used, only the N-terminal 50–100 amino acids of LifA were used instead of the full-length protein. This was suitable for examining Type III secretion as Charpentier and Oswald (2004) found that as little as 20 amino acids from the N-terminus of various T3S proteins are sufficient to mediate translocation through the T3SS. LifA was detected in the culture supernatant, but only when using a hypersecreting strain (Deng *et al*., 2012). The secretion of full-length LifA via the T3SS was recently confirmed by western blots of Type III secretion-induced EPEC E2348/69 culture supernatants and polyclonal LifA-specific antiserum (Bease, 2015). Efa1 was first identified by Tn*5phoA* mutagenesis, whereby an in-frame fusion of the gene encoding alkaline phosphatase to the first 533 amino acids of Efa1 was created (Nicholls *et al*. 2000). Alkaline phosphatase is only active in the bacterial periplasm and extracellularly, and the fact that the fusion was active against the chromogenic substrate 5-Bromo-4-chloro-3-indolyl phosphate indicates that at least part of the protein is located beyond the cytoplasmic membrane (Nicholls *et al*., 2000).

The mechanism of LifA secretion is important for understanding how it acts on host cells. Studies by Klapproth *et al*. (1995, 1996 and 2000), Malstrom and James (1998) and Stevens *et al*. (2002) have all shown that bacterial lysates containing LifA have inhibitory activity against lymphocytes and mononuclear cells, indicating that injection is unlikely to be needed for lymphostatin activity. Moreover, activity can be transferred to laboratory-adapted *E. coli* K-12 containing cloned LifA

even though it lacks the T3SS. Purified recombinant LifA has also been found to inhibit the mitogen-stimulated proliferation of lymphocytes (Bease, 2015; Cassady-Cain *et al*., 2016; Cassady-Cain *et al*., 2017), suggesting that T3SS-mediated injection into host cells is not required for LifA to function. It is unclear exactly how LifA is delivered to its target cells but possible mechanisms include: direct injection via the T3SS into intraepithelial lymphocytes; secretion into the gut lumen where it endocytosed by intraepithelial lymphocytes or crosses the epithelial cell layer via transcytosis or paracellular leak to reach gut associated lymphoid tissue; delivery across the epithelial cell layer into the circulation to act on lymphocytes before they reach the site of infection; and delivery via bacterial outer membrane vesicles, similar to Stx.

1.3.4 Importance of lymphostatin as a virulence factor

LifA has been shown to be an important virulence factor in A/E pathogens (Stevens *et al*., 2002; Badea *et al*., 2003; Klapproth *et al*., 2005; Deacon *et al*., 2010). Stevens *et al*. (2002) found that deleting the *lifA* gene in EHEC O5:H- strain S102-9 caused a 19-fold reduction in adherence to HeLa cells. A reduction in adherence was not observed in EPEC E2348/69 but this may have been due to the expression of BFP and elevated expression of the T3SS in this strain. Lysates of both EPEC E2348/69 and EHEC S102-9 were found to inhibit the mitogen-stimulated proliferation of bovine PBMCs, although the inhibition caused by EHEC may have been due to other toxins such as Stx. Stx is capable of inhibiting the proliferation of lymphocytes (Menge *et al*., 1999) and deleting the *lifA* gene did not relieve the inhibitory effect of the EHEC lysate. Deleting the *lifA* gene in EHEC S102-9 and E45035N significantly reduced the magnitude of faecal excretion of the bacteria in calves and adherence of the bacteria to the intestinal epithelium. It was also found that EHEC S102-9 Δ*lifA* mutants were reduced in their ability to produce and secrete EspA and Tir, but were still able to nucleate actin at sites of attachment. This suggests that the loss of LifA could have affected gut colonisation via indirect effects on Type III secretion, which is known to be vital for colonisation of the bovine gut by EHEC O157:H7 (Dziva *et al*., 2004; Naylor *et al*., 2005; Eckert *et al*., 2011). The

presence of *lifA* in atypical EPEC strains has also been strongly associated with diarrhoea and higher bacterial loads in the faeces of humans (Afset *et al*., 2006; Narimatsu *et al*., 2010; Slinger *et al*., 2017).

Badea *et al*. (2003) reported that LifA was necessary for the *in vitro* adherence of rabbit EPEC to epithelial cells. The rabbit EPEC strain used lacked BFP, which may have masked the effects of LifA. Rabbit EPEC with mutated *lifA* had reduced adherence to CHO and HeLa cells and polyclonal antibodies against LifA also reduced adherence. The mutation of the *lifA* gene did not disrupt EspA secretion, indicating that pleotropic effects of *lifA* mutation on the expression of LEE-encoded proteins may be strain-specific. It is noteworthy that *lifA* has been reported to be encoded immediately 3′ of the *LEE4* operon in the opposite direction in some strains (Ogura *et al*., 2009).

Klapproth *et al*. (2005) found that mutating the *lifA* gene in *C. rodentium* did not reduce the ability of the bacteria to colonise the colon of mice but did result in reduced pathology and accelerated clearance of the bacteria. In these experiments Klapproth *et al*. (2005) mutated putative glycosyltransferase and cysteine protease domains within LifA as well as a domain between these two that does not encode any known activity. However, later it was discovered that the mutations created stop codons at the site of the in-frame deletions, which resulted in the truncation of the LifA protein (Deacon *et al*., 2010). This means that the results were invalid in relation to the effects of the specific domains but still showed that the protein as a whole is required for colonic hyperplasia in mice.

Deacon *et al*. (2010) also investigated the importance of the putative glycosyltransferase and cysteine protease domains by substituting specific motifs within these domains in EHEC O26:H- strain 193. The strain used was incapable of producing Stx1 in order to prevent it from masking the effects of LifA. It was found that *lifA* null mutants had significantly reduced ability to colonise cattle but mutants of the putative glycosyltransferase and cysteine protease domains did not (Deacon *et al*., 2010). No effect of the *lifA* mutation on expression of EspA was observed in EHEC O26:H-. In contrast to Stevens *et al*. (2002), this shows that LifA has a direct role in gut colonisation independently of effects on EspA. LifA was not necessary to induce enteritis in bovine ligated ileal loops (Deacon *et al*., 2010). In contrast to

previous experiments, *lifA* null and motif mutants did not have significantly reduced adherence to HeLa cells or ability to inhibit the mitogen-stimulated proliferation of bovine lymphocytes. However, when the motif substitutions were transferred to the chromosome of EPEC E2348/69 it was observed that the ability to inhibit mitogen-stimulated proliferation of lymphocytes was significantly reduced in the motif mutants compared with the parental EPEC E2348/69 strain.

Vaccines using subunits of LifA from EHEC E45035 and the *z4332* gene product generated an antibody response against these proteins but did not protect calves from infection with EHEC strains EDL933 or 193 of serogroups O157 or O26, respectively (van Diemen *et al*., 2007). However, immunisation of calves in this study with the cell binding domain of intimin subtypes β or γ also did not protect against infection despite inducing an antibody response. Subsequent studies using intimin vaccines have reported protection against infection (Martorelli *et al*., 2017), suggesting that the lack of protection observed by van Diemen *et al*. (2007) may be due to the experimental design, which involved inoculation with a high dose that may have overwhelmed immune responses. It is also possible that the LifA protein used in the vaccine was not properly folded or exposed pertinent epitopes required for an efficient response. In contrast to van Diemen *et al*. (2007), Riquelme-Neira *et al*. (2016) reported that vaccinating mice with DNA encoding Efa1′ conferred protective immunity against EHEC O157:H7 colonisation, while also generating specific serum antibodies against the protein, and increasing the proliferative response of T cells against EHEC proteins and heat-killed bacteria. The plasmid containing the *efa1′* gene was reported to express FLAG-tagged recombinant protein, however, western blots of the protein were not published and therefore it remains unclear whether Efa1′ is the product of both open reading frames *z4332* and *z4333* (Riquelme-Neira *et al*., 2016).

1.3.5 Structural motifs of lymphostatin

1.3.5.1 The glycosyltransferase domain

The N-terminal portion of LifA is ~40 % homologous over the first 470 amino acids to the catalytic domains of large clostridial toxins (LCTs), including TcdA and B from *Clostridium difficile*, the lethal and haemorrhagic toxins (TcsL and TcsH) from *C. sordellii*, α-toxin (TcnA) from *C. novyi* and TpeL from *C. perfringens* (Klapproth *et al*., 2000; Nicholls *et al*., 2000; Busch *et al*., 1998; Amimoto *et al*., 2007). This homologous region in LifA encompasses a catalytic DXD motif that is necessary for sugar binding in LCTs (Klapproth *et al*., 2000; Nicholls *et al*., 2000; Busch *et al*., 1998). The LCTs are known glycosyltransferases (Triadafilopoulos *et al*., 1987), most of which bind uridine diphosphate-glucose (UDP-Glc; Just *et al*., 1995b and 1995c; Schirmer and Aktories, 2004). TcnA and TpeL can bind UDP-Glc but their primary substrate is uridine diphosphate-N-acetylglucosamine (UDP-GlcNAc; Selzer *et al*., 1996; Schrimer and Aktories, 2004; Nagahama *et al*., 2011; Guttenberg *et al*., 2012). LCTs are known to act as cytotoxins by hydrolysing UDP-sugars and transferring the sugar moieties onto Rho GTPases, thereby inhibiting Rho GTPase activity and causing the collapse of the actin cytoskeleton (Just *et al*., 1995a, 1995b and 1995c; Selzer *et al*., 1996). However, LifA has never been shown to act in this manner or cause direct cytotoxicity, for example by assays for the release of lactate dehydrogenase or analysis of cell permeability by trypan blue exclusion (Klapproth *et al*., 1995 and 2000; Malstrom and James, 1998; Nicholls *et al*., 2000; Stevens *et al*., 2002; Bease, 2015; Cassady-Cain *et al*., 2016).

As described previously, an initial attempt to mutate the glycosyltransferase (GT) domain of LifA in *C. rodentium* by Klapproth *et al*. (2005) produced a truncated protein. Babbin *et al*. (2009) corrected the mutation and implicated the GT domain in causing the redistribution of ZO-1 and occludin from enterocyte tight junctions, compromising the intestinal epithelial cell barrier and suppressing Cdc42 activity. However, this study did not investigate claims by Klapproth *et al*. (2005) that the GT domain is required for the effective colonisation of mice by *C. rodentium*, induction of colonic hyperplasia or inhibition of lymphocyte function.

Deacon *et al*. (2010) substituted the DXD motif of LifA in EHEC 193 for a triple alanine sequence and found that it did not affect the ability of the bacteria to colonise calves or to adhere to epithelial cells. When this substitution was transferred to the chromosome of EPEC E2348/69, there was a significant reduction in the ability of bacterial lysates to inhibit mitogen-stimulated T cell proliferation.

Recently, recombinant LifA was found to bind UDP-GlcNAc but not UDP-Glc (Bease, 2015; Cassady-Cain *et al*., 2016). Purified LifA containing a DXD-AAA substitution was found to be structurally similar to the wild-type protein, but its ability to bind UDP-GlcNAc and inhibit T cell proliferation was abolished (Bease, 2015; Cassady-Cain *et al*., 2016). This suggests that LifA acts as a glycosyltransferase but the target(s) of this activity in host cells remains unknown. The GT domain was predicted to contain a Mn^{2+} ion as incubating recombinant LifA with $MnCl_2$ increased the thermal stability of the protein (Cassady-Cain *et al*., 2016). The DXD motif is absent from the truncated version of LifA found in many *E. coli* O157:H7 strains (*z4332*) and this may explain the lack of phenotype of *efa1′* deletion mutants in assays of mitogen-activated lymphocyte proliferation (Abu-Median *et al*., 2006). Given that glycoproteins modified with GlcNAc are required for cell-cell and cell-matrix interactions in *Drosophila* (Sakaidani *et al*., 2011), and that *E. coli* are known to bind mannose and N-acetyllactosamine moieites on host cell surfaces via Type I fimbriae (Ofek *et al*., 1977) and BFP (Hyland *et al*., 2008) respectively, this raises the possibility that GlcNAc binding by LifA may be linked to its reported role as an adhesin.

1.3.5.2 The cysteine protease domain

In addition to the GT domain, LifA also contains a C58 cysteine protease (CP) domain and is a member of the YopT-like cysteine protease superfamily (Shao *et al*., 2002). YopT is a virulence factor from *Yersinia* that cleaves host cell Rho GTPases, resulting in the collapse of the actin cytoskeleton (Shao *et al*., 2002). As stated above, LifA does not appear to act as a direct cytotoxin, which suggests another role for the CP domain of LifA. The CP domain of another C58 protease, AvrPphB from *Pseudomonas syringae*, cleaves the host protein PBS1 but is also

required for the autocatalytic cleavage of AvrPphB (Shao *et al*., 2002 and 2003a). Therefore, a possible role for CP domain of LifA may be to mediate autoproteolysis. Shao *et al*. (2002) found that C58 proteases require a C/H/D catalytic triad for proteolysis and this triad is also found in the sequences of LifA and ToxB. C58 proteases have little homology beyond the C/H/D catalytic triad and the sequence that most closely matches the LifA CP domain outwith the various LifA homologues is the CP domain of PaTox from *Photorhabdus asymbiotica* (Jank *et al*., 2013; Bogdanović *et al*., 2018). A predicted structural model of the LifA CP domain was produced by Dr Liz Blackburn (Edinburgh Protein Production Facility (EPPF), Centre for Translational & Chemical Biology, University of Edinburgh) by alignment of the LifA sequence with the crystal structure of a C1865A PaTox CP domain mutant (Bogdanović *et al*., 2018; Figure 1.7).

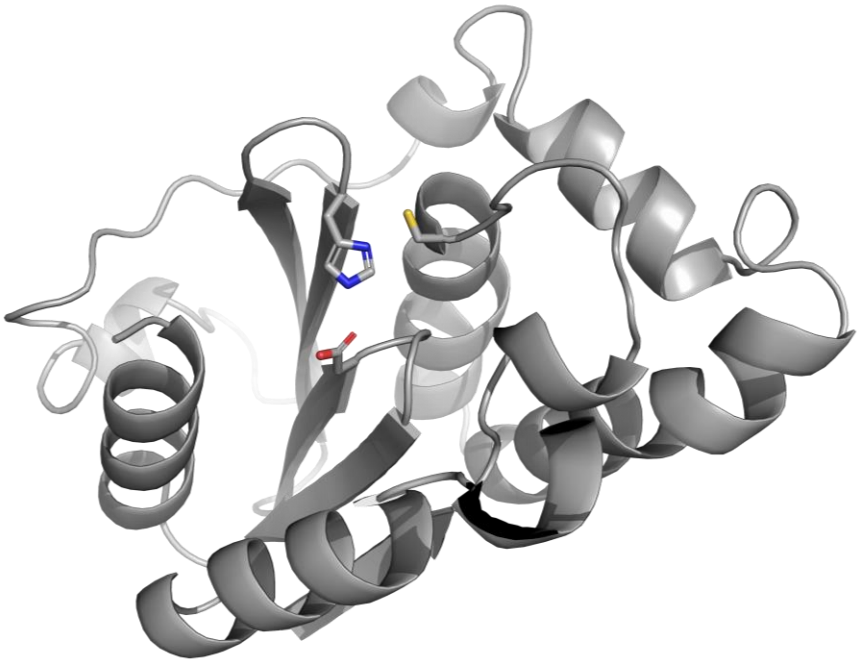

Figure 1.7. Predicted structure of the LifA cysteine protease domain based on the crystal structure of the PaTox^{C1865A} cysteine protease domain from *Photorhabdus asymbiotica*. The predicted catalytic cysteine, histidine and aspartic acid residues can be identified by their respective sulphur (yellow), nitrogen (blue) and oxygen (red) atoms (created by Dr Liz Blackburn, EPPF).

LCTs also have CP domains that, like AvrPphB, are required for autocatalytic cleavage (Pfeifer *et al*., 2003; Egerer *et al*., 2007; Guttenberg *et al*., 2011 and 2012). Although the CP domains of LCTs are not homologous to the C58 proteases, given the N-terminal homology between LifA and LCTs, this lends further weight to the hypothesis that the CP domain of LifA is required for autoproteolysis.

As with previous experiments concerning the GT domain, the first CP domain mutants made by Klapproth *et al*. (2005) were invalid. Babbin *et al*. (2009) corrected the mutation and implicated the CP domain in causing the redistribution of β-catenin and E-cadherin at enterocyte apical junctions, and the activation of RhoA, but again did not investigate its role in gut colonisation or inhibition of lymphocyte function. Deacon *et al*. (2010) deleted a 369 bp section of the EHEC O26:H- strain 193 *lifA* gene that encompassed the C/H/D motif, which was marked with a triple alanine sequence. In a similar manner to the DXD motif, the CP domain was found not to be required for the intestinal colonisation of calves by this strain but was required for lymphostatin activity in EPEC E2348/69. In contrast to Babbin *et al*. (2009), Deacon *et al*. (2010) did not detect the activation of Rho by any of the wild-type or Δ*lifA* bacterial strains. Unlike the DXD motif mutant, the CP domain mutant had over 100 amino acids removed from the sequence and so it is possible that the results observed by Deacon *et al*. (2010) are the consequence of structural abnormalities in the mutant protein rather than mutation of the specific motif.

1.3.6 Recent advances in understanding the mode of action of lymphostatin

LifA clones are unstable and under-represented in cosmid libraries (Klapproth *et al*., 2000; Janka *et al*., 2002). Nicholls *et al*. (2000) reported that they were unable to assemble the full-length *lifA/efa1* gene from cloned N- and C-terminal fragments and that the protein may be toxic to the *E. coli* cell. Recent work by Cassady-Cain *et al*. (2016) has enabled the further study of LifA. Through the use of tightly inducible expression vectors, it has been possible to create a stable plasmid encoding recombinant LifA with a 6 x His tag. This recombinant LifA has been purified and biophysically characterised. It is capable of inhibiting the concanavalin A (ConA)- and antigen-stimulated proliferation of bovine T cells and IL-4-stimulated B cells in

a dose-dependent manner (Cassady-Cain *et al*., 2016 and 2017). The recombinant protein inhibited proliferation in all major T cell subsets in bovine peripheral blood as well as the expression of IL-2, 4, 10, 17A and IFN-γ. Cassady-Cain *et al*. (2017) also found that T cell proliferation was inhibited up to 18 hours after transient exposure to LifA and that, although LifA inhibits ConA-stimulated proliferation, T cells treated with lymphostatin proliferated normally when stimulated with PMA and ionomycin. A rabbit polyclonal antibody has also been produced against this recombinant LifA, allowing for the sensitive detection of the protein by western blotting (Cassady-Cain and Bease, unpublished observations). A robust system for expression, purification and functional characterisation of LifA also allowed for the investigation of the glycosyltransferase activity of LifA (Bease, 2015; Cassady-Cain *et al*., 2016).

1.4 T lymphocyte modulation by other enteric bacteria

A number of virulence factors employed by enteric pathogens to interfere with T cell processes have now been described. These tend to act on host cells in one of three ways: modulation of lymphocyte activation and proliferation; interference in lymphocyte chemotaxis; and the induction of apoptosis (Figure 1.8; reviewed in Cassady-Cain *et al*., 2018).

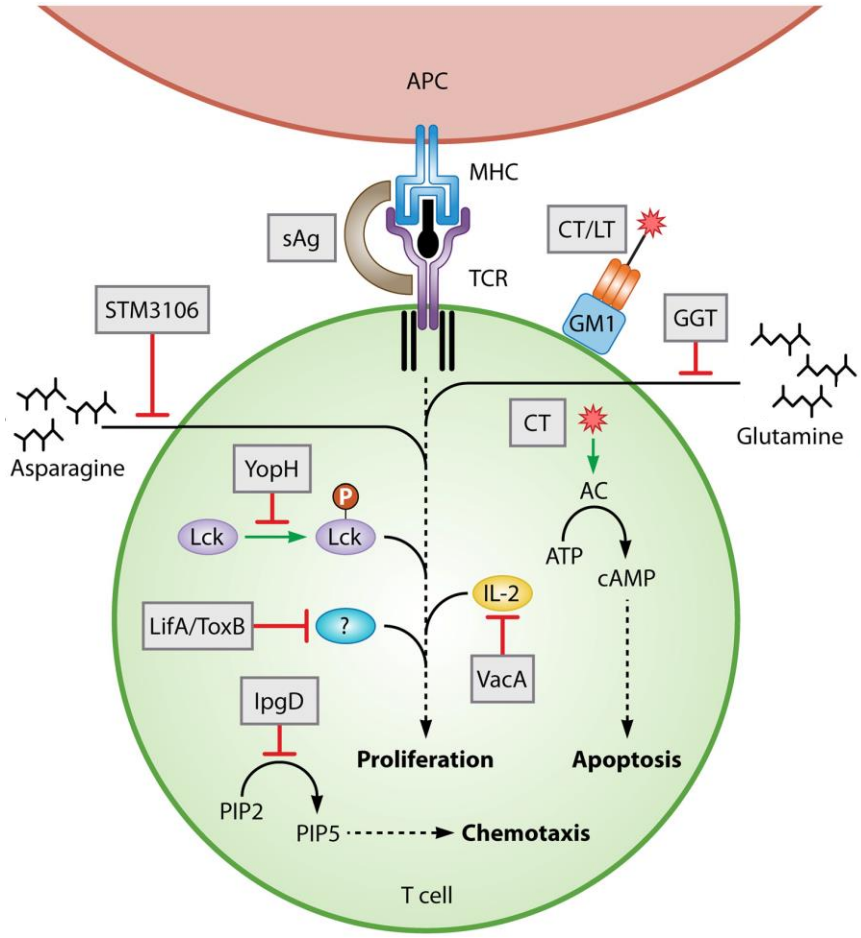

Figure 1.8. Summary of the virulence factors produced by enteric bacteria that modulate T lymphocyte functions (grey boxes) and the molecules/processes that they interfere with. sAg – superantigens; CT – cholera toxin; LT – ETEC heat labile toxin; STM3106 – *S.* Typhimurium L-asparaginase II; GGT – *Helicobacter* and *C. jejuni* γ-glutamyl transferase; YopH – *Yersinia* outer protein H; VacA – *H. pylori* vacuolating cytotoxin A; IpgD – *S. flexneri* invasion plasmid gene D (from Cassady-Cain *et al*., 2018).

1.4.1 Superantigens

Superantigens cross-link MHC class II molecules from APCs with the Vβ-chain of the TCR, resulting in non-specific T cell activation (reviewed in Krakauer, 2013). This leads to the CD95-mediated death of T cells and the residual activated T cells become functionally unresponsive, thereby suppressing an effective

T cell response (reviewed in Krakauer *et al*., 2016). Superantigens are capable of activating a large number of T cells even at low concentrations (Choi, *et al*., 1989; reviewed in Krakauer *et al*., 2016). Superantigens have been best characterised in *Staphylococcus aureus*, which produce a number of superantigens (reviewed in McKay, 2001), but are also produced by *Yersinia enterocolitica* and *Y. pseudotuberculosis* (Stuart and Goodward, 1992; Abe *et al*., 1993). The superantigen *Y. pseudotuberculosis*-derived mitogen A (YPMa) is associated with strains that cause Far Eastern scarlet-like fever and has been shown to increase the virulence of *Y. pseudotuberculosis* in mice (Fukushima *et al*., 2001; reviewed in Amphlett, 2016; Carnoy *et al*., 2000). YPMa has also been reported to cause the release of perforin and granzyme from $CD4^+$ T cells in the spleen and liver of mice, resulting in hepatotoxicity (Goubard *et al*., 2015).

1.4.2 *Helicobacter pylori* vacuolating cytotoxin A (VacA)

VacA has been shown in multiple studies to inhibit the proliferation of T cells as well as exerting effects on a variety of other cell types including epithelial cells, neutrophils and macrophages (Boncristiano *et al*., 2003; Gebert *et al*., 2003; Sundrud *et al*., 2004; reviewed in Utsch and Haas, 2016). VacA is expressed as a 140 kDa protein, which is cleaved into an 88 kDa form and secreted via the Type V secretion pathway (reviewed in Foegeding *et al*., 2016). The 88 kDa toxin is composed of two domains that are both required for cell entry (Torres *et al*., 2005). The exact mechanism of cell entry is unclear but CD18 has been identified as a receptor for VacA on T cells (Sewald *et al*., 2008). Endocytosis is mediated by protein kinase C (PKC) and requires the activation of T cells (Sewald *et al*., 2010). Once inside the host cell, VacA inhibits the activation and nuclear translocation of the transcription factor NF-AT and has also been shown to block calcium flux, which is important for T cell signalling (Boncristiano *et al*., 2003; Gebert *et al*., 2003; Kern *et al*., 2015). The inhibition of NF-AT prevents IL-2 expression in Jurkat cells but not to as great an extent in primary human $CD4^+$ T cells, suggesting that the inhibition of proliferation is IL-2 independent (Boncristiano *et al*., 2003; Gebert *et al*., 2003; Sundrud *et al*., 2004). The initial colonisation of mice was reported to be impaired in

a Δ*vacA H. pylori* mutant but the bacterial load and intestinal inflammation developed to the same level as the wild-type strain once the infection became established (Salama *et al*., 2001). However, since murine T cells do not express the appropriate receptor for VacA (Sewald *et al*., 2008), this observation was likely to be independent of the effects of VacA on lymphocyte proliferation.

1.4.3 *Yersinia* YopH, invasin and YpkA

YopH is a Type III secreted tyrosine phosphatase produced by *Yersinia* species including *Y. enterocolitica* and *Y. pseudotuberculosis* (Cornelis *et al*., 1989; Guan and Dixon, 1990; Cornelis *et al*., 1998). YopH inhibits the proliferation and expression of IL-2 by T cells and has also been shown to suppress the activation of B cells stimulated via the B cell receptor (Yao *et al*. 1999; Sauvonnet *et al*., 2002). In T cells, YopH has been shown to dephosphorylate Lck, Fyb and the p85 subunit of PI3K, as well as interact with numerous signalling proteins, which are likely used to localise YopH to the proximity of its targets (Alonso *et al*., 2004; de la Puerta *et al*., 2009). Since Lck is located upstream of most tyrosine phosphorylation events in the signalling cascade of T cells, dephosphorylation of only a few Lck molecules is predicted to have a significant impact on signalling (Alonso *et al*., 2004). How YopH inhibits B cell activation is unknown but given that Lck has been reported to be involved in B cell activation (Talab *et al*., 2013; Zhou *et al*., 2018), the mechanism may be similar to that in T cells. YopH has also been reported to cause the breakdown of mitochondria in T cells, resulting in apoptosis, but little is known about the mechanism of this activity (Bruckner *et al*., 2005). YopH-deficient *Y. enterocolitica* was previously found to have a marked reduction in its ability to colonise mice after oral infection (Trülzsch *et al*., 2004). This attenuation was confirmed for intravenous infection with *Y. enterocolitica* and intranasal infections with *Y. pseudotuberculosis* (Trülzsch *et al*., 2004; Fisher *et al*., 2007).

Much less is known about the roles of invasin and YpkA. Invasin, which is homologous to intimin from A/E pathogens, induces T cell migration and is thought to cause lymphocytes to disseminate from sites of infection (Leo *et al*., 2015; Arencibia *et al*., 1997). YpkA, also known as YopO, is thought to modulate the

cytoskeleton by interacting with actin and Rho GTPases but has also been shown to induce apoptosis in Jurkat cells via disruption of the mitochondrial membrane potential (Park *et al*., 2007).

1.4.4 *Helicobacter* and *Campylobacter jejuni* γ-glutamyl transferase (GGT)

Upon activation, T cells undergo metabolic reprogramming that requires the uptake of extracellular amino acids, one of which is glutamine (reviewed in Patel and Powell, 2017; reviewed in MacIver *et al*., 2013). GGTs are threonine N-terminal nucleophile hydrolases that degrade glutathione and related compounds (Suzuki *et al*., 1986). Bacterial and mammalian homologues are highly conserved and in particular, GGT from *Helicobacter* species and *C. jejuni* exhibit a high degree of similarity (Rossi *et al*., 2012). GGT from *H. pylori* has been shown to inhibit both the CD3/CD28- and PMA/ionomycin-stimulated proliferation of human T cells, causing G_1 cell cycle arrest and the inhibition of c-Myc and c-Raf signalling (Schmees *et al*., 2007). c-Myc and IRF4 are downregulated in T cells as GGT deprives the extracellular space of glutamine, which is required for these signalling pathways (Wüstner *et al*., 2015). GGT from *H. suis* has also been found to inhibit the proliferation of Jurkat cells as well as CD3/CD28-stimulated murine T cells and anti-IgM-stimulated B cells (Zhang *et al*., 2013a). It is also essential for the gastric colonisation of mice by *H. pylori* (Chevalier *et al*., 1999).

GGT is known to play an important role in the colonisation of the avian gut by *C. jejuni* (Barnes *et al*., 2007) but little is known about its effects on T cells. Floch *et al*. (2014), however, demonstrated that *C. jejuni* GGT inhibited the proliferation of human T cells *in vitro*, causing cell cycle arrest in the G_0/G_1 phase.

1.4.5 *Salmonella enterica* serovar Typhimurium L-asparaginase II

Another amino acid that is required for T cell metabolic reprogramming is asparagine (Torres *et al*., 2016). Originally, *S.* Typhimurium was shown to inhibit the CD3/CD8- and PMA/ionomycin-stimulated proliferation of murine T cells in a contact-dependent manner (van der Velden *et al*., 2005). Expression of the β-chain of

the TCR was also downregulated in T cells infected with *S.* Typhimurium, which was thought to explain the inhibition of proliferation (van der Velden *et al*., 2008). L-asparaginase II, encoded by the gene *STM3106* (*ansB*), was later found to be the cause of suppressed T cell proliferation and TCR-β expression, and *S.* Typhimurium Δ*ansB* mutants exhibited attenuated virulence in mice (Kullas *et al*., 2012). L-asparaginase II is an asparagine hydrolase that catabolises asparagine, depriving T cells of this amino acid and suppressing mTOR signalling, which regulates metabolic reprogramming (Torres *et al*., 2016; McLaughlin *et al*., 2016). In contrast to experiments with mice, a screen of *S.* Typhimurium transposon insertion mutants in pigs, calves and chickens did not find L-asparaginase II to be required for intestinal colonisation (Chaudhuri *et al*., 2013).

1.4.6 *Shigella flexneri* invasion plasmid gene D (IpgD)

Another strategy employed by enteric pathogens to modulate the host T cell response is to interfere with lymphocyte chemotaxis. Konradt *et al*. (2011) found that *S. flexneri* were capable of invading PMA-stimulated $CD4^+$ T cells and suppressing their response to the chemoattractant CXCL12 without affecting expression of the CXCL12 receptor CXCR4. It was found that the T3S protein IpgD, which promotes uptake into and survival within epithelial cells (reviewed in Parsot, 2009), hydrolysed intracellular phosphatidylinositol 4, 5-bisphosphate (PIP_2), causing dephosphorylation of the proteins ezrin, radixin and moesin (Konradt *et al*., 2011). This in turn prevents T cells from becoming polarised in response to chemoattractants. *In vivo* experiments confirmed that *S. flexneri* invade $CD4^+$ T cells in murine mesenteric lymph nodes and impairs their migration (Salgado-Pabón *et al*., 2013). Only activated T cells are invaded by *S. flexneri* (Konradt *et al*., 2011), however, recent studies have shown that $CD4^+$ and $CD8^+$ T cells, as well as B cells, are largely targeted by the T3SS of extracellular bacteria (Pinaud *et al*., 2017). Additionally, it was found that lamina propria lymphocytes were targeted, suggesting the bacteria affect the chemotaxis of lymphocytes responding to the infection without the prior requirement of invasion (Pinaud *et al*., 2017).

1.4.7 *Vibrio cholerae* cholera toxin (CT) and ETEC heat labile enterotoxin (LT)

CT and LT are structurally related toxins that cause diarrhoea and eliminate T cells by inducing apoptosis (Gill *et al*., 1981; reviewed in Spangler, 1992). CT and LT are Type II secreted AB_5 toxins, of which both subunits are required for toxicity (Sandkvist *et al*., 1997; Tauschek *et al*., 2002; reviewed in Spangler, 1992). The B subunit ring binds the ganglioside GM1 on epithelial cells and once inside the cell, the A subunit ADP ribosylates adenylate cyclase, leading to diarrhoea (reviewed in Baldauf *et al*., 2015). The B subunit of CT has been shown to induce apoptosis in murine T cells *in vitro* independently of the A subunit and preferentially targets the $CD8^+$ subpopulation (Yankelevich *et al*., 1996). CT-induced apoptosis of murine T cells was confirmed by Arce *et al*. (2005), but the preferential targeting of the $CD8^+$ subpopulation was not observed. In this same study, CT was found to inhibit the proliferation of $CD4^+$ T cells without inducing apoptosis.

Arce *et al*. (2005) also found that LTIIa induced apoptosis in $CD8^+$ T cells and proposed that this may be caused by the toxin cross-linking the ganglioside receptor. When injected into mice, LT caused an increase in circulating corticosterone, which in turn induced apoptosis in immature T and B cell populations (Tamayo *et al*., 2005). The route of administration of the toxin was reported to affect the induction of apoptosis and it was also found that the enzymatic function of LT was required for this process (Tamayo *et al*., 2005). Further studies revealed that LT induces apoptosis by different mechanisms in mature and immature lymphocytes (Tamayo *et al*., 2009).

1.5 Aims and objectives

A working model of lymphostatin in colonisation is illustrated in Figure 1.9, showing the three functions that have been attributed to the protein.

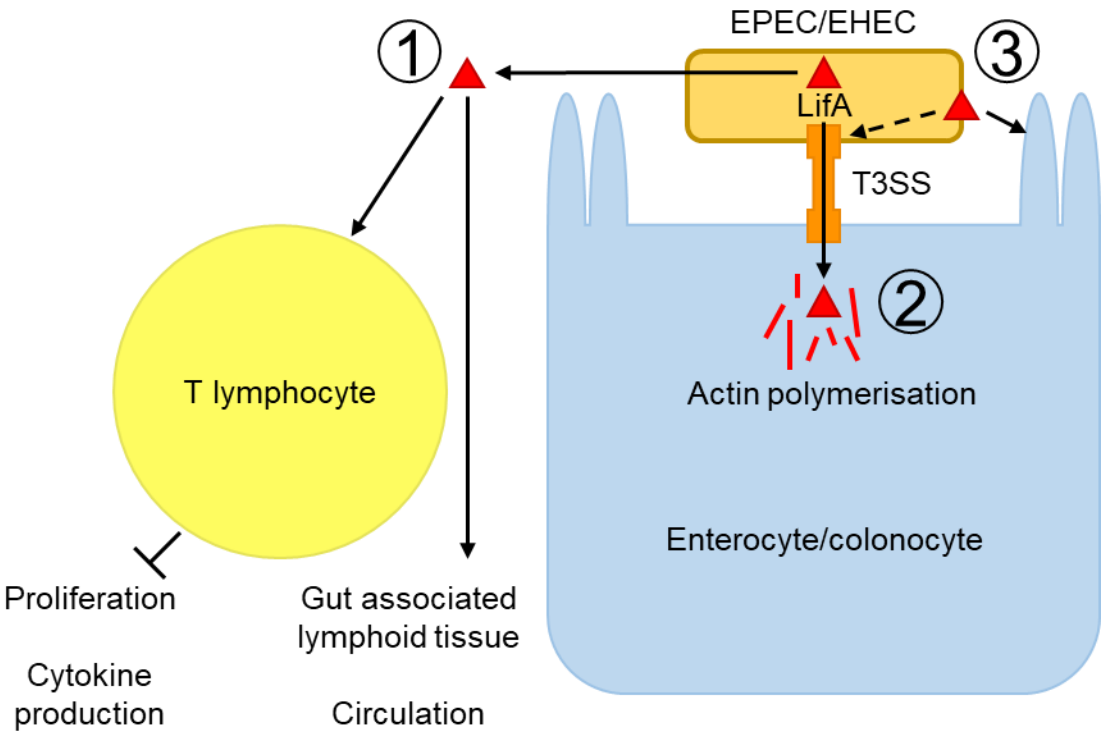

Figure 1.9. Schematic of the working model of lymphostatin (LifA) in gut colonisation by EPEC/EHEC. 1. LifA acts on T lymphocytes to inhibit proliferation and the production of pro-inflammatory cytokines (Klapproth *et al.*, 2000). It may be injected directly into intraepithelial lymphocytes or secreted into the gut lumen where it is taken up by lymphocytes or transported across the epithelium to gut associated lymphoid tissue or circulating blood. 2. LifA is injected into enterocytes/colonocytes via the Type III secretion system (T3SS) where it is reported to have an accessory role in the formation of actin pedestals (Cepeda-Molero *et al.*, 2017). 3. LifA influences bacterial adhesion either by direct binding between bacterial and host cells (normal arrow) or via indirect effects on Type III secretion (dashed arrow; Nicholls *et al.*, 2000), and has been reported to disrupt apical junction complexes (Babbin *et al.*, 2009).

There are a number of outstanding questions regarding the role of lymphostatin in colonisation, which include:

- Which domains/motifs are required for the three activites attributed to LifA?
- To what extent are these activites the cause of attenuation of *lifA* mutants?
- Is the impact of LifA on adherence direct?
- Can the role of LifA in colonisation be explained by its impact on T cells, given the time at which lymphocytes respond during an infection?

Given that little is understood about the molecular mechanisms underlying lymphostatin activity, this study sought to determine which portions of the protein are required for activity, to investigate the role of the putative cysteine protease domain and to identify possible targets of the predicted glycosyltransferase activity of LifA. The overall objectives of this study were to:

1. Identify functional domains of LifA by:
   a) Cloning and purifying recombinant fragments of LifA based on putative domains previously identified by limited tryptic proteolysis.
   b) Determining whether these fragments can inhibit mitogen-stimulated T cell proliferation.
   c) Identifying which fragments, if any, are required for T lymphocyte binding.

2. Probe the role of a predicted C/H/D motif within the putative cysteine protease domain of LifA by:
   a) Creating a C1480A mutant and purifying the mutant protein.
   b) Biophysically characterising the mutant protein and comparing it with wild-type LifA protein.
   c) Comparing the ability of the C1480A mutant LifA protein to inhibit the ConA-stimulated proliferation of bovine T lymphocytes with the wild-type protein.

d) Determining whether LifA is processed in bovine T cells and if so, whether the C/H/D motif is required for this event.

3. Identify putative interacting partners of LifA by:
    a) Using shotgun mass spectrometry to identify peptides that have increased by the mass of GlcNAc from LifA-treated T cells and are thus candidate targets of glycosylation.
    b) Using protein pull-down assays and mass spectrometry to identify proteins that may interact with LifA.
    c) Investigating the impact of LifA on post-translational modifications of the key cellular kinase Akt.

2 Materials and Methods

2.1 Preparation of bovine lymphocytes and T cell enrichment

Peripheral venous blood (50–200 mL) was collected into heparinised bags from 12–18-month old Holstein-Friesian calves in accordance with the requirements of the Animals (Scientific Procedures) Act 1986 under project licence P803DD07A. Blood was centrifuged at 1200 x g for 15 minutes with no brake and the lymphocyte interfaces were removed, pooled into two centrifuge tubes, and made up to 30 mL with phosphate-buffered saline (PBS). Each 30 mL was overlaid onto 20 mL Ficoll-Paque Plus density medium (GE Healthcare Life Sciences) and centrifuged at 1200 x g for 25 minutes with no brake. The lymphocyte cells at the interface were removed and pooled for each donor and made up to 50 mL with PBS and centrifuged at 1200 x g for 10 minutes. Where the cells were contaminated with erythrocytes, the pellet was resuspended in 1 mL of red blood cell lysis buffer (see Appendix 1) and then made up to 50 mL with RPMI-1640 medium (Gibco) with 10 % (v/v) foetal calf serum (FCS; Gibco), 20 mM HEPES (Sigma-Aldrich), 1mM sodium pyruvate (Gibco), 2 mM L-glutamine (Gibco) and 100 µg/mL penicillin/streptomycin (Sigma-Aldrich; RPMI-CT). The cells were washed twice in RPMI-CT and resuspended in 2 mL RPMI-CT. The cells were then counted by trypan blue exclusion (0.4 % (w/v) trypan blue; HyClone) using disposable haemocytometer grids (Kova International).

To enrich for T cells, nylon wool fiber columns (Polysciences Inc.) were used owing to differences in the ability of leukocytes to adhere to the nylon wool matrix, where T cells are relatively non-adherent but B cells and antigen-presenting cells are retained (Eisen *et al*., 1972; reviewed in Hathcock, 2001). Columns were conditioned by adding 10 mL RPMI-CT, tapping to remove air bubbles, and draining the medium. The column was washed twice with RPMI-CT, filled with 5 mL RPMI-CT, sealed and incubated at 37 °C, 5 % CO_2 for 1 hour. The medium was drained from the column, cells were applied at a density of 1 x 10^8 cells/mL and run into the column. The column was sealed and incubated at 37 °C, 5 % CO_2 for 1 hour. The non-adherent T cells were eluted from the column, which was then washed twice

with RPMI-CT to enhance recovery of the cells. The cells were counted as described above and the concentration was adjusted for the appropriate experiment.

2.2 Flow cytometry

Samples of 0.2 x 10^7 cells were taken before and after T cell enrichment, centrifuged at 425 x g for 10 minutes and washed in FCS buffer (PBS with 2 % (v/v) FCS). Cells were fixed by incubating them with 4 % (w/v) paraformaldehyde (PFA) on ice for 30 minutes before being resuspended in FCS buffer and stored at 4 °C until required.

Samples were split into two aliquots, one of which was incubated with 2 µg/mL monoclonal MM1A IgG1 anti-CD3 antibody specific to T cells (Monoclonal Antibody Center, Washington State University) for 1 hour on ice then washed three times with FCS buffer. Both aliquots were then incubated with 4 µg/mL monoclonal fluorescein isothiocyanate (FITC)-conjugated goat anti-mouse IgG1 (Invitrogen) for 1 hour on ice before a final three washes with FCS buffer. Cells were resuspended in 300 µL of FCS buffer and the purity of T cells in each sample was measured using FACScalibur and Fortessa X20 cytometers (both from BD Biosciences) with gates for live cells, single cells and T cells. A minimum of 10,000 events were sampled. Data was analysed using FlowJo® v10 software (FlowJo, LLC). T cells typically accounted for 50–60 % of the pre-enriched cell population and 70–90 % of the post-enriched cell population.

2.3 T lymphocyte proliferation assays

Wells of a 96 well plate were seeded in triplicate with 2 x 10^5 cells in 50 µL RPMI-CT. Proteins at the final concentrations specified in figures were added to the appropriate wells in triplicate in 25 µL. The buffers that the proteins were dissolved in (see Appendix 1) were used as controls. Concanavalin A (ConA; Sigma-Aldrich) at a stock concentration of 4 µg/mL was added to the cells in a volume of 25 µL RPMI-CT to make a final concentration of 1 µg/mL. A background control was set up using 100 µL RPMI-CT. Cells alone and cells with ConA, made up to 100 µL

with RPMI-CT, were used as negative and positive controls respectively. Empty wells were filled with PBS to reduce evaporation of the media during incubation.

The plates were incubated at 37 °C, 5 % CO_2 for 3 days and, at 16 hours before the end of the assay, 20 µL CellTitre 96 AQ_{ueous} One Solution (Promega) was added to each well. This reagent contained a tetrazolium compound and electron coupling reagent such that in the presence of proliferating cells a formazan compound was formed that could be measured by colorimetry. Absorbance was read at 492 nm using a Multiskan Ascent Spectrophotometer (Thermo Scientific). Ratios of the absorbance value for each titration against the positive control (proliferation indices) were calculated using averaged experimental (E), maximum proliferation (Mp) and background (B) absorbance values with the following formula:

$$\text{Proliferation index} = (E - B)/(Mp - B)$$

Proliferation index values were plotted against the concentration of protein or type of protein added with standard deviations using Microsoft Excel 2013. The mean of three technical replicates from each blood donor was used to calculate the mean and standard deviation from at least three independent studies. The effective dose at which 50 % inhibition of ConA-stimulated proliferation was observed (ED_{50}) for certain experiments was calculated using R with the drc package (Ritz *et al*., 2015). The standard error of the mean was calculated for each ED_{50} using Minitab 17. Mann-Whitney tests were used to determine statistically significant differences between the ED_{50} values using Minitab 17. P values ≤ 0.05 were taken to be statistically significant.

2.4 Sodium dodecyl sulphate-polyacrylamide gel electrophoresis (SDS-PAGE)

Proteins were analysed by SDS-PAGE using the Novex (Life Technologies) gel system. Where the detection of full-length LifA was required, 3–8 % Tris-Acetate gels (Novex) were used. For analysis of proteins < 100 kDa, 4–12 % Tris-Glycine gels (Novex) were used. The Tris-Acetate and Tris-Glycine gels were run with 1 x Tris-Acetate SDS running buffer (Novex), with 0.25 % (v/v) antioxidant

(Invitrogen) in the buffer that was in contact with the anode of the gel tank, and 1 x Tris-Glycine SDS running buffer (Novex) respectively. HiMark pre-stained protein standards (Invitrogen) and Precision Plus Protein pre-stained standards (Bio-Rad) were used with the Tris-Acetate and Tris-Glycine gels respectively. The gels were typically run at 180 V until the dye front had left the bottom of the gel. Gels were analysed by staining with Coomassie stain (Bio-Rad), according to the manufacturer's instructions, or by western blotting. Where the gels were stained, the images were captured using a Gel Doc EZ system (Bio-Rad).

2.5 Western blotting

Proteins were transferred to polyvinylidene fluoride (PVDF) membranes (Amersham Hybond) for western blotting. The gels were soaked in 2 x transfer buffer (Novex) with 0.04 % (w/v) SDS (Sigma-Aldrich) for 15 minutes while PVDF membranes were washed in methanol then distilled water before being soaked and gently rocked in 1 x transfer buffer with 10 % (v/v) methanol (Fisher Scientific) and 0.1 % (v/v) antioxidant (Novex) for 15 minutes. To get efficient transfer of large proteins (> 100 kDa), gels were transferred using a wet transfer at 25 V for 75 minutes, using a Mini Blot Module (Life Technologies). For enhanced chemiluminescence (ECL) detection, which relies on production of a chemiluminescent product by horseradish peroxidase (HRP)-conjugated secondary antibodies, membranes were blocked in Tris-buffered saline/0.1 % (v/v) Tween® 20 (TBS-T; VWR International) and 5 % (w/v) bovine serum albumin (BSA; Merck Millipore) for 1 hour on a rocking platform, then rinsed briefly with TBS-T and washed for 15 minutes, followed by an additional two washes of 5 minutes. For blots using fluorophore conjugated antibodies, membranes were treated as described for ECL blots but the TBS-T/5 % BSA block was replaced with Odyssey® Blocking Buffer in TBS (LI-COR Biosciences). Membranes were incubated at 4 °C overnight with antibodies as indicated at the appropriate dilutions.

ECL blots were washed with TBS-T as above but for fluorescent blots the final wash was performed with PBS/0.1 % Tween® 20 (PBS-T). Membranes were incubated at room temperature for 1 hour with secondary antibodies as indicated at

the appropriate dilutions. ECL and fluorescent blots were washed with TBS-T and PBS-T respectively as above. ECL blots were dried and developed using SuperSignal West Pico Chemiluminescent Substrate (Thermo Scientific) following the manufacturer's instructions and exposed to Amersham Hyperfilm for various times to achieve clear images. Films were developed using an SRX-101A film processor (Konica Minolta). Blots using fluorophore-conjugated antibodies were scanned using a LI-COR Odyssey blot imager and images were analysed in Image Studio Lite v5.2 (both from LI-COR Biosciences).

2.6 T lymphocyte protein association assays

Enriched T cells were serum starved at a density of 8 x 10^6 cells/mL in serum-free RPMI medium with 25 mM HEPES (Sigma-Aldrich) at 37 °C, 5 % CO_2 for 1 hour. Cells were divided into 1.5 mL aliquots in microcentrifuge tubes and proteins were added to the cells at a final equimolar concentration of 5.45 nM, equivalent to 2 µg/mL of wild-type (WT) recombinant LifA (rLifA), before the samples were incubated at 37 °C for the indicated times. Buffer treated cells were used as negative controls and protein in medium without cells was used a control to ensure that protein was not binding to the microcentrifuge tubes.

Samples were centrifuged at 17,949 x g, 4 °C for 1 minute to collect the T cells and the supernatant was discarded. Samples were centrifuged for a further 15 seconds to collect and aspirate residual supernatant. Cells were resuspended in 100 µL of ice-cold PBS and transferred to clean microcentrifuge tubes then centrifuged as described above. This process was repeated a second time. Cells were lysed with 90 µL of NP-40 lysis buffer (see Appendix 1) and incubated on ice for 30 minutes. Lysates were centrifuged at 17,949 x g, 4 °C for 10 minutes and the supernatants were transferred into clean microcentrifuge tubes for further processing. Protein samples (supernatants) were denatured by the addition of an appropriate volume of 1 x sample reducing agent and 1 x lithium dodecyl sulphate (LDS) sample buffer (both from Novex) and heated at 70 °C for 10 minutes. Samples were stored at -20 °C until analysis. Before analysis, samples were mixed and heated at 70 °C for 2 minutes then centrifuged briefly to sediment insoluble material. Western blots used

rabbit polyclonal anti-LifA antibody (Stevens Laboratory, Clone 45) at a dilution of 1/20,000, which was detected using HRP-conjugated goat anti-rabbit secondary antibody (Bio-Rad), applied at a dilution of 1/10,000 in TBS-T/2 % (w/v) skimmed milk powder (Chem Cruz).

2.7 Bacterial growth media and chemicals

Bacterial strains were cultured in suspension using lysogeny broth (LB) or on LB agar plates (Sigma-Aldrich) and supplemented with antibiotics as indicated. Antibiotics were used at the following final concentrations: Kanamycin (Kan), 30 µg/mL; Ampicillin (Amp), 25 µg/mL; Nalidixic acid (Nal), 20 µg/mL. Where indicated, cultures were supplemented with 0.5 % (w/v) D-glucose. Glycerol stocks for bacteria were prepared from fresh liquid cultures and supplemented with glycerol at a final concentration of 15 % (v/v). To induce Type III secretion, bacteria were grown in Dulbecco's Modified Eagle Medium supplemented with 4.5 g/L D-glucose, L-glutamine and sodium bicarbonate (DMEM; Sigma-Aldrich; Kenny *et al*., 1997a).

2.8 Bacterial strains, plasmids and oligonucleotides

The strains and plasmids used in this study are listed in Tables 2.1 and 2.2 respectively. The pRham-LifA-6 x His plasmid encodes the *lifA* gene, which is controlled by a rhamnose-inducible and glucose-repressible promoter (Cassady-Cain *et al*., 2016). The pRham empty vector was used as a negative control. The oligonucleotides used for cloning, site-directed mutagenesis and double-stranded sequencing are shown in Table 2.3. EPEC E2348/69 clones from Taylor (1970) and Cepeda-Molero *et al*. (2017) were provided and PCR validated by Professor Brendan Kenny, The Institute for Cell and Molecular Biosciences, Newcastle University.

Table 2.1. Strains used in this study. Properties of strains used are shown with references.

Strain	Description	Antibiotic resistance	Reference/source
E. coli E2348/69[a]	EPEC O127:H6 ΔpE2348-2 *gyrA*, *ftsK*, *φhflD-purB*.	Nal^R	Levine *et al.* (1978); Levine *et al.* (1985)
E. coli E2348/69 Δ*lifA*	E2348/69[a] with a complete deletion of *lifA*.	Nal^R	Stevens *et al.* (2002)
E. coli E2348/69 Δ*escN*::Kan^R	E2348/69[a] with a deletion of *escN*, encoding an ATPase of the LEE-encoded T3SS, and the insertion of a Kan resistance cassette.	Kan^R	Garmendia *et al.* (2004)
E. coli E2348/69[b]	Wild-type EPEC O127:H6 strain.	Str^R	Taylor (1970); Prof. Brendan Kenny
E. coli E2348/69 Δ*lifA*	Derivative of the E2348/69[b] strain from B. Kenny with a deletion of *lifA*.	Str^R	Cepeda-Molero *et al.* (2017); Prof. Brendan Kenny
E. coli E2348/69 Δ*lifA-like*	Derivative of the E2348/69[b] strain from B. Kenny with a deletion of the *lifA-like* gene.	Str^R	Cepeda-Molero *et al.* (2017); Prof. Brendan Kenny
E. coli E2348/69 Δ*lifA* Δ*lifA-like*	Derivative of the E2348/69 strain from B. Kenny with deletions of both *lifA* and *lifA-like* genes.	Str^R	Cepeda-Molero *et al.* (2017); Prof. Brendan Kenny
E. coli E2348/69 Δ*escN*	Derivative of the E2348/69[b] strain from B. Kenny with a deletion of *escN*.	Str^R	Cepeda-Molero *et al.* (2017); Prof. Brendan Kenny
E. cloni® 10G	Chemically-competent cells for transformation and protein expression. F^- *mcr*A Δ(*mrr-hsd*RMS-*mcr*BC) *end*A1 *rec*A1 φ80d*lac*ZΔM15 Δ*lac*X74 *ara*D139 Δ(*ara, leu*)7697 *gal*U *gal*K *rps*L (Str^R) *nup*G λ^- *ton*A	Str^R	Lucigen
XL 10-Gold Ultracompetent cells	Chemically-competent cells for transformation. Tet^R Δ(*mcrA*)*183* Δ(*mcrCB-hsdSMR-mrr*)*173 endA1 supE44 thi-1 recA1 gyrA96 relA1 lac* Hte [F´ *proAB* $lacI^qZ\Delta M15$ *Tn10* (Tet^R) Amy Cam^R]	Tet^R, Cam^R	Agilent Technologies

[a] is a Nal resistant clone derived from the original EPEC E2348/69 clone [b].

Table 2.2. Plasmids used in this study. Properties of plasmids used are shown with references.

Plasmid	Description	Antibiotic resistance	Reference/source
pRham-LifA-6 x His	Encodes LifA tagged at the C-terminus with 6 x His under a rhamnose-inducible promoter.	Kan^R	Cassady-Cain *et al*. (2016)
pRham empty	Re-ligated pRham vector backbone.	Kan^R	Cassady-Cain *et al*. (2016)
pRham-LifA-6 x His DXD-AAA	As pRham-LifA-6 x His but with a DXD-AAA substitution in the glycosyltransferase domain.	Kan^R	Bease (2015); Cassady-Cain *et al*. (2016)
pRham-LifA-6 x His F1	Encodes F1 fragment of LifA (aa 1–1620) with C-terminal 6 x His tag under a rhamnose-inducible promoter.	Kan^R	Made in this study
pRham-LifA-6 x His F3	Encodes F3 fragment of LifA (aa 2111–2900) with C-terminal 6 x His tag under a rhamnose-inducible promoter.	Kan^R	Made in this study
pRham-LifA-6 x His F5	Encodes F5 fragment of LifA (aa 2901–3223) with C-terminal 6 x His tag under a rhamnose-inducible promoter.	Kan^R	Made in this study
pRham-LifA-6 x His GT	Encodes GT domain of LifA (aa 221–1033) with N-terminal 6 x His tag under a rhamnose-inducible promoter.	Kan^R	Made in this study
pRham-LifA-6 x His C1480A	As pRham-LifA-6 x His but with a C1480A substitution in the cysteine protease domain.	Kan^R	Made in this study
pWhitescript	Mutagenesis control. Allows for colour screening.	Amp^R	Agilent Technologies
pUC18	Transformation control. Allows for colour screening.	Amp^R	Agilent Technologies

Table 2.3. Oligonucleotides used in this study.

Primer	Sequence (5' to 3')	Purpose	Source
LifA F1 CT forward	GAAGGAGATATACATATGAGACTGCCAGAGAAAGTTCTT	Cloning of the F1 fragment of LifA with C-terminal 6 x His tag	Sigma-Aldrich
LifA F1 CT reverse	GTGATGGTGGTGATGATGTAATTGTATCATAGCCTCAAT	As LifA F1 CT forward	Sigma-Aldrich
LifA F3 NT forward	CATCATCACCACCATCACGGGGACTGGCAAATTCGTGAG	Cloning of the F3 fragment of LifA with N-terminal 6 x His tag	Sigma-Aldrich
LifA F3 NT reverse	GTGGCGGCCGCTCTATTATCCATCTGTTTTTTTTTTCAT	As LifA F3 NT forward	Sigma-Aldrich
LifA F3 CT forward	GAAGGAGATATACATATGGGGGACTGGCAAATTCGTGAG	Cloning of the F3 fragment of LifA with C-terminal 6 x His tag	Sigma-Aldrich
LifA F3 CT reverse	GTGATGGTGGTGATGATGTCCATCTGTTTTTTTTTTCAT	As LifA F3 CT forward	Sigma-Aldrich
LifA F5 NT forward	CATCATCACCACCATCACCCATCTGTGGTAGAAGATGCC	Cloning of the F5 fragment of LifA with N-terminal 6 x His tag	Sigma-Aldrich
LifA F5 NT reverse	GTGGCGGCCGCTCTATTAGTTAAAAAGGTTGTCACCATT	As LifA F5 NT forward	Sigma-Aldrich
LifA F5 CT forward	GAAGGAGATATACATATGCCATCTGTGGTAGAAGATGCC	Cloning of the F5 fragment of LifA with C-terminal 6 x His tag	Sigma-Aldrich
LifA F5 CT reverse	GTGATGGTGGTGATGATGGTTAAAAAGGTTGTCACCATT	As LifA F5 CT forward	Sigma-Aldrich
LifA GT NT forward	CATCATCACCACCATCACTCGTTAACACCAGAAAATTTT	Cloning of the GT domain of LifA with N-terminal 6 x His tag	Sigma-Aldrich
LifA GT NT reverse	GTGGCGGCCGCTCTATTAACTAAGATGATCTTTCATTTT	As LifA GT NT forward	Sigma-Aldrich
LifA GT CT forward	GAAGGAGATATACATATGTCGTTAACACCAGAAAATTTT	Cloning of the GT domain of LifA with C-terminal 6 x His tag	Sigma-Aldrich
LifA GT CT reverse	GTGATGGTGGTGATGATGACTAAGATGATCTTTCATTTT	As LifA GT CT forward	Sigma-Aldrich

Primer (cont.)	Sequence (5' to 3')	Purpose	Source
LifA-C1480A-1	CTATTGGTAACCCAAGAAGGACGCGCAATGGGATTAGCCTTACTTTATT	For site-directed C1480A substitution	Sigma-Aldrich
LifA-C1480A-2	TAAATAAAGTAAGGCTAATCCCATTGCGCGTCCTTCTTGGGTTACCAATAG	As LifA-C1480A-1	Sigma-Aldrich
pRham forward	GAAGGAGATATACATATGAGACTGCCAGAGAAAGTTCTT	Replication of pRham plasmids and sequencing of inserts in the pRham vector	Lucigen
pETite reverse	GTGATGGTGGTGATGATGGTTAAAAAGGTTGTCACCATT	As pRham forward	Lucigen
LifA FL For1	GCAGGAAAGATAGCTGGTAAC	Forward primer for sequencing of the *lifA* genes	Sigma-Aldrich
LifA FL For2	GTTCCCCACCTGAAAGCATT	As LifA FL For1	Sigma-Aldrich
LifA FL For3	GGTGAAAACCGCATTTCAAT	As LifA FL For1	Sigma-Aldrich
LifA FL For4	CGTGGGCTCAATGGATTCATG	As LifA FL For1	Sigma-Aldrich
LifA FL For5	CCTGTTCAAAGATGTTTCAAC	As LifA FL For1	Sigma-Aldrich
LifA FL For6	GACTCCTGAAAACTGGGAAG	As LifA FL For1	Sigma-Aldrich
LifA FL For7	CGGACTAGGAATAACTGGTG	As LifA FL For1	Sigma-Aldrich
LifA FL For8	GGATTACCAACTATTGCCG	As LifA FL For1	Sigma-Aldrich
LifA FL For9	CCAACGAATCGCTACTACA	As LifA FL For1	Sigma-Aldrich
LifA FL For10	CTGTCCCGCACAGTTCTGAC	As LifA FL For1	Sigma-Aldrich
LifA FL For11	CCGAAGCAACTCTCGGCAGC	As LifA FL For1	Sigma-Aldrich
LifA FL For12	CAGTCTCCTCCTCTCTTGC	As LifA FL For1	Sigma-Aldrich
LifA FL For13	CCGGAAGAGTTTCCGCTCACC	As LifA FL For1	Sigma-Aldrich
LifA FL For14	CAGGCTGTTTATCCGGAAG	As LifA FL For1	Sigma-Aldrich
LifA FL For15	GGTCATACACCAACGGTAAAC	As LifA FL For1	Sigma-Aldrich
LifA FL For16	GAACAGCCAGGTATCGGCAG	As LifA FL For1	Sigma-Aldrich

Primer (cont.)	Sequence (5' to 3')	Purpose	Source
LifA FL For17	CTTATCCGAAATCCCTCAG	As LifA FL For1	Sigma-Aldrich
LifA FL For18	GCGGCTACCAAGTGTATTATC	As LifA FL For1	Sigma-Aldrich
LifA FL Rev1	GGAATAGAGCTCGCCCTGATG	Reverse primer for sequencing of the *lifA* genes	Sigma-Aldrich
LifA FL Rev2	GCCAGATTCAGAACGCCATC	As LifA FL Rev1	Sigma-Aldrich
LifA FL Rev3	CAGATACAGACGTGAATAGG	As LifA FL Rev1	Sigma-Aldrich
LifA FL Rev4	GCCAGTATGATTTGTGTCGG	As LifA FL Rev1	Sigma-Aldrich
LifA FL Rev5	CAAACTCAGCTCAAAGGCGAC	As LifA FL Rev1	Sigma-Aldrich
LifA FL Rev6	CTCTCAGGGGAAGTACTGTG	As LifA FL Rev1	Sigma-Aldrich
LifA FL Rev7	CAGCCATTGTGTATGCCGTTC	As LifA FL Rev1	Sigma-Aldrich
LifA FL Rev8	GTACTGTCTTCGTGCCCCTG	As LifA FL Rev1	Sigma-Aldrich
LifA FL Rev9	CATCACCGTTGAGACGCAGAG	As LifA FL Rev1	Sigma-Aldrich
LifA FL Rev10	GCGGTCTTATGTAGTAGCG	As LifA FL Rev1	Sigma-Aldrich
LifA FL Rev11	GGGTTGCATCGGCAATAGTTG	As LifA FL Rev1	Sigma-Aldrich
LifA FL Rev12	CGATCAAGAAGTCTATCGTA	As LifA FL Rev1	Sigma-Aldrich
LifA FL Rev13	CGCAAGAAAGCCTTTTATGG	As LifA FL Rev1	Sigma-Aldrich
LifA FL Rev14	CTGATATCTGGAGGGTGCTC	As LifA FL Rev1	Sigma-Aldrich
LifA FL Rev15	CCATCAGATATTGCACGACG	As LifA FL Rev1	Sigma-Aldrich
LifA FL Rev16	GTAGCATAAAGCTCTCTGAG	As LifA FL Rev1	Sigma-Aldrich

2.9 Plasmid DNA purification

Plasmid DNA was prepared from small-scale stationary phase bacterial cultures (5–10 mL; Miniprep) or larger-scale cultures (50–100 mL; Midiprep) using alkaline lysis followed by affinity purification of plasmid DNA. To perform a

Miniprep, 3 mL from overnight cultures were each added to two 1.5 mL microcentrifuge tubes and centrifuged at 17,949 x g for 10 minutes. DNA from the pellets was purified using a QIAprep Spin Miniprep Kit (Qiagen) following the manufacturer's instructions. One QIAprep spin column was used for each 3 mL culture and columns were left to dry for 10 minutes. The DNA was eluted in 30 µL of nuclease-free distilled water (nH_2O), which was left to stand for 5 minutes before being centrifuged for 1 minute.

To perform a Midiprep, 50 mL overnight cultures were centrifuged at 6000 x g, 4 °C for 15 minutes. Plasmid DNA from the pellets was purified using a QIAprep Spin Midiprep Kit with filter cartridges (Qiagen) following the manufacturer's instructions and the final DNA pellet was dissolved in 50 µL of nH_2O.

The DNA concentrations were measured by the A_{260}/A_{280} ratio using a NanoDrop (ND-1000) Spectrophotometer (Thermo Scientific), which displays concentrations in ng/µL.

2.10 Cloning

Expression constructs for the LifA fragments were created using an Expresso® Rhamnose Cloning and Expression System kit (Lucigen) following the manufacturer's instructions. Primers were designed according to the manufacturer's instructions for both N- and C-terminal 6 x His tagged variants of the proteins (see Table 2.3), with the exception of F1, which we predicted may undergo N-terminal processing in *E. coli*. Polymerase chain reaction (PCR) was used to amplify the desired fragments of *lifA*, using the sequence-validated pRham-LifA-6 x His plasmid containing full-length *lifA* from E2348/69 as a template (Cassady-Cain *et al*., 2016). Three 100 µL PCR reactions were performed for each fragment, with 100 ng of pRham-LifA-6 x His template being mixed with 1 x PCR master mix. The master mix contained 1 x HF buffer (Thermo Scientific), 10 µM of forward and reverse primers for the appropriate fragments (see Table 2.3), 10 mM dNTPs, 2 U/µL long range Phusion Hot Start II High-Fidelity Polymerase (Thermo Scientific) and nH_2O to make up the 100 µL reaction volume. Separate no-template negative control and

parent plasmid DNA pRham-LifA-6 x His positive control reactions were also included. The PCR parameters are listed in Table 2.4. The PCR products were analysed on a 0.8 % (w/v) agarose (Invitrogen) gel against a 1 kb DNA ladder (Promega). Gels were run at 120 V for 20 minutes, stained with SYBR® Safe (Invitrogen) and imaged using a FluorChem® HD2 chemiluminescent imager (Alpha Innotech).

Table 2.4. PCR programme used for amplifying *lifA* fragments for cloning and screening potential recombinants.

Segment	No. of cycles	Temperature (°C)	Time
1	1	98	10 seconds
2	25	98	10 seconds
		55	15 seconds
		72	10 minutes
3	1	72	10 minutes
4	1	4	∞

Amplicons for each fragment were excised and split into two microcentrifuge tubes with ~300 mg of gel in each. The DNA was extracted from the gel by silica-membrane-based purification using a QIAquick® Gel Extraction Kit (Qiagen) following the manufacturer's instructions and the final DNA pellet was dissolved in 30 µL of nH_2O.

E. cloni® 10G chemically-competent cells were thawed on ice and prepared according to the manufacturer's instructions. Reactions for *lifA* amplicons mixed with pRham were added to separate aliquots of cells. Quantities of 50 ng of N-His Positive Control A Insert and 25 ng of C-His Positive Control B Insert were added to aliquots of cells and the corresponding pRham N-His or pRham C-His vector to determine the transformation efficiency. Vector alone was used as a negative control. The transformation reactions were gently swirled and incubated on ice for 30 minutes, followed by heat shock at 42 °C for 30 seconds and incubation on ice for 2 minutes. The cells were suspended in the Recovery Medium provided with the kit and incubated at 37 °C for 1 hour with shaking at 225–250 rpm to allow recovery and expression of plasmid-mediated antibiotic resistance. Transformed cells were

then spread onto LB/Kan agar with 0.5 % (w/v) glucose and incubated at 37 °C overnight. Cloning is ligation-independent and recombination of the vector and *lifA* amplicons occurs within the host cell. Candidate recombinants were screened for the desired inserts as described in Section 2.12.

2.11 Site-directed mutagenesis of the C/H/D motif of lymphostatin

Mutagenesis of the C/H/D motif was performed using a QuikChange II XL Site-Directed Mutagenesis Kit (Agilent Technologies) following the manufacturer's instructions with some modifications. The primers LifA-C1480A-1 (forward) and LifA-C1480A-2 (reverse; see Table 2.3) were designed using the QuikChange Primer Design Program (www.agilent.com/genomics/qcpd), with the aim of replacing the predicted catalytic cysteine at amino acid position 1480 of E2348/69 *lifA* with an alanine residue using a codon that would simultaneously create a *BsrD*I restriction site. PCR was performed using 10 ng of the pRham-LifA-6 x His plasmid as a template, 1 x reaction buffer, 125 ng of each of the forward and reverse primers, 2 % (v/v) dNTP mix, 6 % (v/v) QuikSolution reagent and nH_2O to make up to 50 µl reaction volume. *PfuUltra* High-Fidelity DNA polymerase was added to the reaction mixture at 2.5 U/µL. PCR was used to introduce the alanine residue by complete replication of the plasmid, followed by digestion of the parent plasmid using 10 U/µL *Dpn*I, which digests methylated template DNA but not DNA generated in the PCR reaction. A commercial pWhitescript plasmid was used as a positive mutagenesis control, using primers (sequence not disclosed by manufacturer) that repair a mutation in the β-galactosidase gene, which can be detected by blue-white screening using a chromogenic β-galactosidase substrate. The PCR parameters used are listed in Table 2.5.

Table 2.5. PCR programme used for site-directed mutagenesis of the pRham-LifA-6 x His plasmid.

Segment	No. of cycles	Temperature (°C)	Time
1	1	95	1 minute
2	18	95	50 seconds
		68	50 seconds
		68	13 minutes (1 minute/kb of plasmid)
3	1	68	7 minutes
4	1	15	∞

XL 10-Gold Ultracompetent cells were thawed on ice and prepared according to the manufacturer's instructions. The *Dpn*I-treated DNA samples were added to separate aliquots of cells. A quantity of 0.01 ng of pUC18 plasmid was added to an aliquot of cells to determine the transformation efficiency. The transformation reactions were gently swirled and incubated on ice for 30 minutes to ensure maximum transformation efficiency, heat shocked at 42 °C for 30 seconds and then incubated on ice for 2 minutes. The cells were suspended in NZY^+ broth (see Appendix 1), which was used as a recovery medium before plating, and incubated at 37 °C for 1 hour with shaking at 225–250 rpm. The cells transformed with the mutant plasmid were spread onto LB/Kan agar with 0.5 % (w/v) glucose and cells transformed with the pWhitescript and pUC18 plasmids were spread onto LB/Amp agar. The LB/Amp plates also had 250 µL of 80 µg/mL X-gal (5-bromo-4-chloro-3-indolyl-β-D-galactopyranoside; Promega) and 250 µL of 20 mM IPTG (isopropyl β-D-1-thiogalactopyranoside; Sigma-Aldrich) spread onto the agar before the cells were added to allow for blue-white screening. The plates were incubated at 37 °C for > 16 hours.

2.12 PCR screening of putative recombinants

2.12.1 Screening of whole plasmids

Putative clones of the *lifA* fragments and the cysteine protease mutant were initially screened by PCR to verify that they contained the appropriate inserts.

Glycerol stocks were made from each of the cultures, which were stored at -80 °C for further use and 2 µL of each culture was lysed in 198 µL of nH_2O. The lysed cells were mixed with 1 x PCR master mix, which contained 1 x HF buffer, 10 µM pRham forward primer, 10 µM pETite reverse primer (see Table 2.3), 10 mM dNTPs and 2 U/µL Phusion polymerase to make up 20 µL reaction volume. PCR and agarose gel screening were performed as described previously for cloning.

2.12.2 *BsrD*I digests of plasmids

PCR was used to amplify a region of putative pRham-LifA-6 x His C1480A plasmids containing the cysteine protease domain using primers LifA FL For3 and LifA FL Rev8 (see Table 2.3). *BsrD*I was used to distinguish between mutated *lifA*, which contains an additional *BsrD*I restriction site at the location of the C1480A substitution, and false positives, which contain only two naturally-occurring *BsrD*I restriction sites between the chosen primer sites. Amplicons were mixed with 1 x *BsrD*I master mix, which contained 1 x NEBuffer™ 2.1 (50 mM NaCl, 10 mM Tris-HCl, pH 7.9, 10 mM $MgCl_2$, 100 µg/mL BSA) and 0.5 U/µL *BsrD*I (both from New England BioLabs® Inc.). A negative and positive control of nH_2O and pRham-LifA-6 x His plasmid, amplified with primers LifA FL For3 and LifA FL Rev8, were also treated with *BsrD*I. The DNA was digested at 65 °C for 1 hour and the digestion products were analysed on a 0.8 % (w/v) agarose gel against a 1 kb DNA ladder. Gels were run as previously described. Clones positive for the mutation were archived and plasmid DNA was prepared as described in Section 2.12.3 for sequencing.

2.12.3 Sanger sequencing of plasmids

Plasmids containing fragments of *lifA* or the predicted C1480A substitution were verified by conventional Sanger sequencing by GATC Biotech, Source BioScience and Edinburgh Genomics. The LifA forward primers FL For1–18, the reverse primers FL Rev1–16, the pRham forward primer and the pETite reverse

primer were used to sequence the plasmids, as appropriate to the insert (see Table 2.3).

The sequences were assembled using Lasergene SeqMan Pro (DNASTAR). Briefly, the sequence was clipped using SeqMan Pro to remove any areas of low sequence quality. The complete sequences were constructed by creating contigs of overlapping sequences in SeqMan Pro and differences in the original sequences were resolved by comparison of overlapping sequences with reference to sequencing chromatograms if needed. The complete sequences were compared with the wild-type *E. coli* E2348/69 genome using NCBI Blast (Iguchi *et al*., 2009; reviewed in Madden, 2013) to identify any unintended mutations that may have been introduced to the sequence.

2.13 Pilot-scale protein expression assays

Protein was overexpressed in *E. cloni*® 10G cells transformed with pRham-based plasmids encoding fragments of *lifA*, and XL 10-Gold Ultracompetent cells transformed with the pRham-LifA-6 x His C1480A plasmid. *E. cloni*® 10G with the pRham empty plasmid was used as a negative control. Fresh 10 mL LB subcultures were made from overnight cultures inoculated with single colonies. The subcultures were incubated at 30 °C until they reached an absorbance at 600 nm (A_{600}) between 0.5 and 0.6. Samples of uninduced cultures were collected and held on ice, then 0.2 % (w/v) L-rhamnose was added to cultures to induce protein production. At 3 hours post-induction, the induced and uninduced samples were centrifuged at 17,949 x g, 4 °C for 10 minutes and the pellets were lysed with 100 µL of BugBuster MasterMix (Novagen). The lysates were mixed at room temperature for 10 minutes then centrifuged again at 17,949 x g, 4 °C for 10 minutes. The supernatants were collected and the insoluble pellet was resuspended in 100 µL of BugBuster for analysis by SDS-PAGE.

Protein concentration was quantified using the Direct Detect system (Merck Millipore) according to the manufacturer's instructions using BugBuster as the buffer control. The samples were then denatured in sample reducing agent and LDS sample

buffer as described in Section 2.6. Samples were stored at -20 °C and centrifuged briefly as described previously before SDS-PAGE analysis.

2.14 Optimisation of protein production

Overnight cultures of *E. cloni*® 10G transformed with the various plasmids, grown in LB/Kan broth were separately diluted 10-fold in either LB/Kan or 2 x tryptone/yeast extract (2xTY)/Kan broth and grown at 37 °C to an A_{600} of 0.5. Cultures were either grown normally or stimulated to overproduce chaperones by heat/cold shock. Heat/cold shock cultures were grown to an A_{600} of 0.2, incubated in a 42 °C water bath for 15 minutes then left to recover at room temperature for 20 minutes. These cultures were then incubated in ice water for 15 minutes then left to recover again at room temperature for 20 minutes before resuming growth at 37 °C to an A_{600} of 0.5.

Cultures were cooled to the appropriate induction temperature and induced with the addition of 0.2 % (w/v) L-rhamnose when the A_{600} reached 0.6. The cultures were incubated at either 20 or 30 °C and A_{600} measurements were taken 1, 2, 3 and 4 hours after induction. Aliquots of 1 mL of culture were taken at each time point. The aliquots were centrifuged at 12,500 x g in a benchtop centrifuge for 10 minutes, the supernatant was discarded and the pellets were stored at -20 °C until ready for further processing. The pellets were dissolved in 6 µL of BugBuster for every 0.01 A_{600} unit measured. A volume of 5 µL from each lysate was mixed with 5 µL of 10 x sample reducing agent and 5 µL of 4 x LDS sample buffer then boiled at 100 °C for 2 minutes and run on a 4–12 % Tris-Glycine gel (Bio-Rad) at 250 V for 22 minutes as described in Section 2.4.

Once optimal conditions for induction were defined, large-scale protein production was carried out by first inoculating 3 x 25 mL LB/Kan overnight cultures with a single colony of the appropriate strain. From these overnight cultures, 5 mL was added to each of 12 x 500 mL LB or 2xTY and grown at 30 °C for 3 hours with 0.2 % (w/v) L-rhamnose. The cultures were centrifuged at 6000 x g, 4 °C for 20 minutes, the supernatant was discarded, and the pellets were flash frozen in liquid nitrogen and stored at -80 °C until required for protein purification.

2.15 Purification of recombinant proteins

2.15.1 Four-step purification

Recombinant proteins were purified to varying degrees using a four-step process using ion metal affinity chromatography (IMAC), size exclusion chromatography (SEC), anion exchange chromatography and a desalt column on a fast protein liquid chromatography (FPLC) unit (ÄKTA Explorer 10 UV900 and ÄKTA pure LC systems; GE Healthcare Life Sciences ÄKTA). All buffers used throughout the purification process were filtered and degassed to remove particulate matter (see Appendix 1). The presence of the proteins in samples throughout the purification process was monitored using SDS-PAGE and UV absorbance at 280 nm. The production and purification of the recombinant glycosyltransferase domain (rGT) was performed by Dr Liz Blackburn, Edinburgh Protein Production Facility (EPPF), Centre for Translational and Chemical Biology, University of Edinburgh.

Initially, the protein lysate was subjected to HiTrap nickel-Sepharose® IMAC column chromatography (GE Healthcare Life Sciences). Cell pellets from Section 2.14 were thawed, resuspended in IMAC lysis buffer (IMAC buffer A (see Appendix 1) with 500 mM 3-(1-pyridinio)-1-propansulphonate, 1 protease inhibitor tablet/1 L of cell culture, 0.1 mg/mL benzamidine and 0.1 % (v/v) phenylmethanesulphonylfluoride to prevent protein degradation) and lysed further by cell disruption under pressure (25 kpsi; Constant Cell Disruption Systems). The lysates were centrifuged at 50,000 x g, 4 °C for 1 hour and filtered using a 0.22 µm filter then run over the nickel-Sepharose® column at a flow rate of 1 mL/minute, followed by a wash of 22 column volumes (cv) of 4 % IMAC buffer B (see Appendix 1), equivalent to 20 mM imidazole. The recombinant proteins were eluted with 3 cv of 100 % IMAC buffer B containing 500 mM imidazole and collected in 1 mL fractions.

The fractions of the IMAC filtrates that contained recombinant protein were pooled and applied to a HiLoad 16/600 Superdex 200pg (rF5), Superdex 200pg 10/300 GL (rGT and rF3), Superose 6pg 10/300 GL (rF1) or Superose 6pg XK16/600 SEC column (WT rLifA and rLifA^{C1480A}; all columns from GE Healthcare

Life Sciences), for size exclusion chromatography as appropriate to the protein to be purified, using SEC buffer. The purest IMAC fractions, determined by SDS-PAGE, were run through the column first, followed by the less pure fractions.

The fractions of the SEC filtrates that contained recombinant protein, determined by SDS-PAGE, were run through a HiPrep 26/10 desalt column (GE Healthcare Life Sciences) in a 50 mM NaCl low-salt buffer to remove excess salt that may interfere with binding to the anion exchange chromatography column.

The desalt fractions containing recombinant protein, determined by UV absorbance at 280 nm, were applied to a Mono Q 5/50 GL anion exchange column (GE Healthcare Life Sciences) to separate proteins based on their net charge. The concentration of NaCl in the column was increased from 0 to 500 mM over 30 cv, then sharply to 1 M. The purest fractions of each protein were pooled. Protein concentration was quantified using a NanoDrop Lite Spectrophotometer (Thermo Scientific). Protein for biophysical experiments was stored at 4 °C until required and protein for cellular assays had glycerol added up to 20 % (v/v) then was flash frozen and stored at -80 °C until required. WT rLifA and rLifA^{C1480A} were desalted into either assay buffer or CD buffer (see Appendix 1) before use in the biophysical characterisation experiments.

2.15.2 IMAC optimisation

IMAC was performed in batch to find the optimal conditions for capturing recombinant F1 protein (rF1). HiTrap free resin (GE Healthcare Life Sciences) was charged with either nickel, cobalt, copper or zinc and equilibrated with IMAC buffers A and B with a pH of either 7 or 8. A volume of 1 mL of lysate was added to each resin batch and incubated on ice for 10 minutes. Samples were centrifuged at 500 x g, 4 °C for 5 minutes then washed twice with 4 % IMAC buffer B. Protein was eluted by washing the resin three times with 100 % IMAC buffer B. Samples of unbound lysate, wash steps and elution steps were analysed by SDS-PAGE.

2.16 Matrix assisted laser desorption ionisation time-of-flight (MALDI-TOF) mass spectrometry of purified proteins

A quantity of 2 µg of purified protein was run on a gel in triplicate. Protein species of interest were excised, flash frozen and stored at -80 °C until required. Samples were thawed and incubated at room temperature in 200 mM NH_4HCO_3 (ABC; Sigma-Aldrich) with 50 % (v/v) acetonitrile (ACN; Fisher Scientific) for 30 minutes to remove SDS. This was repeated a further two times. Samples were incubated at 32 °C in 20 mM dithiothreitol (DTT), 200 mM ABC, 50 % ACN for 1 hour to reduce the protein then washed three times with 200 mM ABC, 50 % ACN. Cysteine residues were alkylated by incubating the samples in 50 mM iodacetamide (Sigma-Aldrich), 200 mM ABC, 50 % ACN at room temperature for 20 minutes in the dark. Samples were washed three times with 20 mM ABC, 50 % ACN then centrifuged at 12,500 x g in a benchtop centrifuge for 2 minutes. Gel pieces were covered with ACN until they turned white then the ACN was decanted and the gel pieces were air dried. Gel pieces were rehydrated in 20 µg/mL Trypsin Gold (Promega) at 4 °C then incubated at 32 °C for 16–24 hours to digest the protein.

Before mass spectrometry, samples were sonicated for 1 minute then spotted onto a MALDI plate and covered with an α-cyano-4-hydoxycinnamic acid matrix (see Appendix 1). Peptide fragments were identified by an ultrafleXtreme™ MALDI-TOF mass spectrometer (Bruker). The spectral data were processed using Data Explorer software (Applied Biosystems) and peptide mass lists were searched against the Mascot NCBIprot database (Matrix Science). The parameters used in each search were: taxonomy – *Escherichia coli*; missed cut = 1; fixed cysteine carbamidomethylation modification; variable methionine oxidation modification; and a peptide mass tolerance of 20 ppm.

2.17 Dynamic light scattering (DLS)

DLS was used to determine the size distribution and extent of aggregation of purified proteins. Assay buffer with 1.1 µM of either WT rLifA or rLifA^{C1480A} was passed through a 0.22 µm Ultrafree-MC filter (Merck Millipore) and centrifuged at

12,000 x g, 4 °C for 15 minutes. The mean hydrodynamic radius of both proteins was measured using a Zetasizer Automated Plate Sampler (Malvern Instruments, UK) equipped with a 50 mW laser light source, with a wavelength of 830 nm. DLS data were collected at a scattering angle of 90° for 10 seconds at 25 °C. This was repeated 13 times in triplicate and the values were averaged. Autocorrelation data were fitted to a model of a multiple-exponential form suitable for polydisperse solutions using the protein-specific software supplied with the instrument. This generated a distribution of particles by size (Maslon *et al*., 2010). Assay buffer was used as a background control.

2.18 Circular dichroism (CD)

CD spectra of purified proteins were collected to define aspects of their secondary structure. Samples of 0.11 µM WT rLifA and rLifA^{C1480A} in CD buffer (see Appendix 1) were centrifuged at 12,000 x g, 4 °C for 15 minutes. The mean residue ellipticity ([θ]) for each protein was measured using a J-810 Spectropolarimeter (Jasco; Kelly *et al*., 2005) between wavelengths of 185 and 285 nm. The [θ] for each protein was plotted against wavelength using Microsoft Excel 2013. The percentages of different secondary structure motifs were determined using DichroWeb (http://dichroweb.cryst.bbk.ac.uk/html/home.shtml; Lobley *et al*., 2002).

2.19 Thermal denaturation assays (TDAs)

The thermal denaturation characteristics of rLifA and rLifA^{C1480A} were measured to assess their folding. Each protein was used at a concentration of 0.1 µM in assay buffer and mixed with 5 x SYPRO Orange in a 96 well plate, with a buffer only control in parallel. The plate was sealed and centrifuged at 3220 x g for 2 minutes to remove air bubbles then put into an IQ5 Multicolor Real-Time PCR Detection System (Bio-Rad). The temperature was increased from 15 to 70 °C in 0.5 °C increments every 30 seconds and the fluorescence was recorded at each increment. Normalised relative fluorescence units (RFU) for each sample were

plotted against temperature using Microsoft Excel 2013. The unfolding transition temperature (T_m) of each protein was calculated from the steepest part of the melting curve. To find the steepest part of the melting curve, the curves were differentiated with respect to temperature (T; -dRFU/dT), therefore the T_m of each protein was the average of the lowest -dRFU/dT values.

2.20 Fluorescent labelling of proteins

In order to study binding and uptake of purified proteins upon interaction with T cells, proteins were directly labelled with a tetrafluorophenyl (TFP) ester using an Alexa Fluor® 488 Microscale Protein Labelling Kit (Invitrogen) according to the manufacturer's instructions. A volume equal to 100 µg of protein in NaH_2PO_4, pH 7.6 buffer was mixed with a 1/10 volume of 1 M $NaHCO_3$. The volume of TFP ester dye added to the protein was calculated using the following formula, where the molar ratio of dye:protein was based on that required for the optimal degree of labelling of a 150 kDa protein (Invitrogen, 2006) and 11.3 nmol/µL was the concentration of the dye:

Volume of dye = ((µg of protein/protein molecular mass) x 1000 x molar ratio)/11.3

The protein/dye mixture was incubated at room temperature for 15 minutes and excess dye was removed by spin filtering the mixture at 16,000 x g for 1 minute through the Bio-Gel P-6 fine resin provided with the kit.

2.21 Protein transfection

2.21.1 Transfection of T cells with recombinant LifA fragments

Proteins were transfected into bovine T cells using Xfect™ Protein Transfection Reagent (Clontech Laboratories Inc.) according to the manufacturer's instructions with some modifications. PBS was used to dilute 1 x Xfect Protein Transfection Reagent rather than deionised water (dH_2O) to reduce osmotic stress on

the cells. An appropriate volume of Xfect Protein Buffer was added to 5 µg of the tested proteins in a volume of 100 µL. The protein/buffer mix was added to 100 µL of diluted transfection reagent and incubated at room temperature for 30 minutes. T cells at a density of 8 x 10^6 cells/mL in serum-free RPMI were added in a volume of 400 µL to each transfection reaction then incubated at 37 °C, 5 % CO_2 for 1 hour. Cells were then centrifuged at 425 x g for 10 minutes then washed with PBS. Cells were resuspended in 400 µL of RPMI-CT, counted as described in Section 2.1, then diluted to a density of 4 x 10^6 cells/mL and seeded in 50 µL in a 96 well plate. A volume of 50 µL of RPMI-CT or 2 µg/mL ConA in RPMI-CT was added to the appropriate wells and the assay was continued as for standard T cell proliferation assays to determine if the transfected fragments were able to inhibit mitogen-stimulated proliferation. Negative controls with the transfection reagent but no proteins were used to determine the effects of the transfection reagent on ConA-stimulated proliferation and WT rLifA was used as a positive control. As a control to demonstrate that the transfection reagent was active, β-galactosidase supplied with the reagent was used as a positive control to determine transfection efficiency by blue-white screening as below.

2.21.2 X-gal staining of transfected cells

Blue-white screening for the presence of β-galactosidase in transfected T cells was performed using a Beta-Galactosidase Staining Kit (Clontech Laboratories Inc.) following the manufacturer's instructions. Cells were centrifuged at 425 x g for 10 minutes then washed with 1 x PBS. Cells were incubated in Fixing Buffer at room temperature for 10 minutes then washed twice with 1 x PBS. Cells were then incubated in X-Gal Staining Mix (see Appendix 1) overnight at 37 °C, 5 % CO_2.

Cells were washed and resuspended in PBS then attached to poly-L-lysine coated slides (BD Biosciences) by centrifugation at 300 rpm for 5 minutes in a Cytospin 3 centrifuge (Shandon). Coverslips were mounted using ProLong® Gold Antifade Mountant (Life Technologies) and left to cure overnight. Cells were examined for the presence of intracellular β-galactosidase (blue staining) by light microscopy and images were analysed in Zen 2011 (Carl Zeiss). Transfection

efficiency was determined by counting both the total number of cells and number of blue-stained cells.

2.21.3 Confocal microscopy

T cells treated with fluorescently-labelled lymphostatin, or fragments thereof, were prepared as described in Section 2.6 and imaged by confocal laser scanning microscopy. After incubation with the labelled protein, cells were centrifuged at 425 x g for 10 minutes then washed three times with PBS. Cells were fixed by incubating them with 4 % (w/v) PFA on ice for 30 minutes, centrifuged at 425 x g for 10 minutes then washed three times with PBS. Cells were counter-stained with DAPI (4′,6-diamidino-2-phenylindole) at a dilution of 1/10,000 then washed with dH_2O. Cells were attached to poly-L-lysine coated coverslips as described for X-gal staining. Images were obtained using a Nikon EC-1 inverted confocal microscope and analysed using ImageJ (National Institutes of Health).

2.22 Analysis of lymphostatin processing in cells

2.22.1 Culture of J774A.1 cells

J774A.1 murine macrophage-like cells were cultured at 37 °C, 5 % CO_2 in RPMI-1640 medium (Gibco) with 10 % (v/v) FCS (Gibco), 2mM L-glutamine (Gibco) and 100µg/mL penicillin/streptomycin (Sigma-Aldrich; RPMI-CJ). The cells were grown to a confluence of 80–90 % then passaged into fresh medium as follows. The cell monolayer was dislodged from the flask with a cell scraper then centrifuged at 290 x g for 10 minutes at room temperature. Cells were resuspended in fresh medium, counted by trypan blue exclusion (0.4 % (w/v) trypan blue; HyClone) using disposable haemocytometer grids (Kova International) and re-seeded at a density of 0.5×10^6 cells/mL in a T175 filter cap flask (Fisher Scientific). For long-term storage at -150 ºC, cells were spun down and resuspended in 90 % (v/v) FCS/10 % (v/v) dimethyl sulphoxide (DMSO; Sigma-Aldrich) at a density of 1×10^7 cells/mL, frozen in a cell freezer at -80 ºC overnight, followed by transfer to -150 ºC.

2.22.2 Detection of lymphostatin cleavage in J774A.1 cells

J774A.1 cells were seeded at a density of 1 x 10^6 cells/mL in a 12 well plate and cultured for 24 hours at 37 °C, 5 % CO_2 in RPMI-CJ. Cells were serum starved in serum-free DMEM for 1 hour. The medium was removed from the cells and WT rLifA or rLifA^{C1480A} was added to the medium at a final concentration of 1 µg/mL. The medium was mixed by vortexing and reapplied to the cells. Buffer treated cells were used as a negative control. After 1 hour of incubation, treated cells were lysed with 120 µL of NP-40 lysis buffer and incubated on ice for 30 minutes. Lysates were transferred to microcentrifuge tubes then centrifuged at 17,949 x g, 4 °C for 10 minutes and the supernatants were transferred into clean microcentrifuge tubes. Lysates were processed as described for T cells in Section 2.6.

Western blots used rabbit polyclonal anti-LifA antibody at a dilution of 1/20,000 or mouse monoclonal anti-6 x His antibody (BioLegend) at a dilution of 1/1000. Primary antibodies were detected using DyLight™ 800 4X PEG-conjugated goat anti-rabbit IgG (1/30,000 dilution) and DyLight™ 800-conjugated goat anti-mouse IgG (1/10,000 dilution) antibodies respectively (both from Cell Signaling Technology).

2.23 Treatment of T lymphocytes with inhibitors of endosome acidification

These experiments were carried out as described for T lymphocyte protein association assays (Section 2.6) but T cells were incubated with either bafilomycin A1 (at a final concentration of 0.0005–50 µM; LC Laboratories) or chloroquine diphosphate (over a range of 0.0125–1250 µM; Sigma-Aldrich) during the serum starving step. DMSO and PBS were used as carrier controls for bafilomycin A1 and chloroquine respectively.

Western blots used rabbit polyclonal anti-LifA antibody at a dilution of 1/20,000 and mouse monoclonal anti-β-actin as a protein loading control (GeneTex) at a dilution of 1/5000. Primary antibodies were detected using DyLight™ 800 4X PEG-conjugated goat anti-rabbit IgG (1/30,000 dilution) and DyLight™

680-conjugated goat anti-mouse IgG (1/15,000 dilution) antibodies respectively (both from Cell Signaling Technology).

Densitometry was performed on the putative N-terminal cleavage product of rLifA and β-actin signal using Image Studio Lite v5.2 and Microsoft Excel 2013. Linear regression analysis was carried out using Minitab 17. Average regression slopes were tested for statistical significance using a one-sample T-test. *P* values ≤ 0.05 were taken to be statistically significant.

2.24 Detection of GlcNAcylated proteins in bovine T lymphocytes in the presence or absence of lymphostatin

2.24.1 Western blotting for detection of O-GlcNAc-modified proteins

These experiments were carried out as described for T lymphocyte protein association assays (Section 2.6), with T cells being treated with a final concentration of 2 µg/mL WT rLifA or rLifA$^{DTD/AAA}$. Buffer-treated cells were used as a negative control. SDS-PAGE was carried out using three different gel systems with different molecular weight resolutions: 3–8 % Tris-Acetate gels (Novex) for proteins in the range of 71–460 kDa; 4–12 % Tris-Glycine gels (Novex) for proteins of 25–250 kDa; and 4–12 % Tris-Glycine gels (BioRad) for proteins of 10–150 kDa. Western blots were performed using mouse monoclonal anti-O-GlcNAc antibody (Novus Biologicals) at a dilution of 1/1000, which was detected using DyLight^{TM} 800-conjugated goat anti-mouse IgG antibody (Cell Signaling Technology) at a dilution of 1/10,000.

2.24.2 Shotgun mass spectrometry

T cells were treated as described above for western blot analysis and lysed with 8 M urea. Protein concentrations were determined using Bradford reagent (BioRad) according to the manufacturer's instructions. Samples were incubated for 30 minutes at room temperature in 2 M urea, 25 mM ABC and 5 mM DTT to denature and reduce the protein. Cysteine residues were alkylated by incubating the

samples at room temperature with 12.5 mM iodacetamide (Sigma-Aldrich) for 1 hour in the dark. Trypsin (0.4 µg; Worthington Biochemical Corporation) digestion was performed overnight at room temperature. Peptide extracts were cleaned on Omix reverse stage phase tips (Agilent Technologies). Samples were dried by Speedvac and stored a -20 °C until required. Samples were reconstituted in 0.05 % (v/v) trifluoroacetic acid (Fisher Scientific) and filtered using a 0.45 µm Millex® filter (Merck Millipore).

Shotgun mass spectrometry was performed using an online system of a nano-HPLC (Dionex™ UltiMate™ 3000 RSLC; Fisher Scientific) coupled to a QExactive mass spectrometer (Fisher Scientific) with a 300 µm internal diameter (I.D.) x 5 mm pre-column (5 µm particle size; Acclaim Pepmap) joined with a 75 µm I.D. x 50 cm column (3 µm particle size; Acclaim Pepmap). Peptides were separated using a multi-step gradient of 2–98 % buffer B (80 % (v/v) ACN and 0.1 % (v/v) formic acid (Merck Millipore)) at a flow rate of 300 nL/minute over 90 minutes. Buffer A was 2 % ACN and 0.1 % formic acid. Data from mass spectrometry spectra were searched against a *Bos taurus* protein database using Mascot. The parameters used in each search were: missed cut = 2; fixed cysteine carbamidomethylation modification; variable methionine oxidation and N- and O-linked GlcNAc modifications; peptide mass tolerance of 10 ppm; and a fragment mass tolerance of 0.05 Da. Search results were exported using a significance threshold (*P* value) of less than 0.05 and a peptide score cutoff of 20. Mascot searches were able to detect either one or two GlcNAc modifications to either Asn, Ser or Thr residues within a single peptide.

This experiment was repeated a second time using 3.6 x 10^8 cells/sample for WT rLifA and buffer-treated cells. In-solution protein digestion and data collection and analysis were performed by Lisa Imrie, Kinetic Parameter Facility (KPF), Centre for Synthetic and Systems Biology, University of Edinburgh.

2.24.3 Glycoprotein enrichment

T cells were treated with WT rLifA or buffer as described in Section 2.24.1. Glycoprotein enrichment was performed using a wheat germ agglutinin (WGA)

Glycoprotein Isolation Kit (Thermo Scientific) according to the manufacturer's instructions. T cell lysates containing 1–1.5 mg of total protein were diluted 1/4 with 5 x Binding/Wash Buffer stock solution. Lysates were added to WGA resin columns pre-equilibrated with 1 x Binding/Wash Buffer and incubated for 10 minutes at room temperature on a rocking platform. The columns were centrifuged at 1000 x g for 1 minute and the flowthrough was discarded. Columns were then washed twice with 1 x Binding/Wash Buffer, incubated at room temperature for 5 minutes on a rocking platform and then centrifuged at 1000 x g for 1 minute. Glycoproteins were eluted from the columns into clean microcentrifuge tubes by twice incubating the columns with Elution Buffer at room temperature for 10 minutes on a rocking platform, followed by centrifugation at 1000 x g for 1 minute. The protein concentration of pre- and post-enrichment lysates was measured using Bradford reagent (Sigma-Aldrich) according to the manufacturer's instructions. Equal concentrations of pre- and post-enrichment lysates were examined by western blotting using mouse monoclonal anti-O-GlcNAc antibody (Novus Biologicals) at a dilution of 1/1000, which was detected by HRP-conjugated goat anti-mouse IgG antibody (AbD Serotec) at a dilution of 1/10,000 in TBS-T/2 % (w/v) skimmed milk powder (Chem Cruz).

To remove detergent, glycoprotein enriched lysates were run on a Bolt™ 4–12 % Bis-Tris Plus gel (Invitrogen) at 200 V until all of the sample had run into the gel. Gel pieces were excised and destained by three 15 minute washes with 50 mM ABC, 50 % ACN then shrunk in methanol for 10 minutes. SDS was removed by alternate 10 minute washes with 50 mM ABC and methanol. Proteins were reduced by incubation at 60 °C with 20 mM DTT, 50 mM ABC. Gels pieces were washed with methanol for 10 minutes then incubated with 50 mM iodacetamide, 50 mM ABC at room temperature for 1 hour in the dark to alkylate cysteine residues. Gel pieces were covered with methanol until they turned white then the methanol was decanted and the gel pieces were air dried. Gel pieces were rehydrated in 20 µg/mL trypsin (Worthington Biochemical Corporation) at 4 °C then incubated at room temperature overnight to digest the protein. Digest solutions were transferred to clean tubes and additional peptides were extracted from the gel pieces by 15 minute incubations with 1 % (v/v) formic acid followed by 1 % (v/v) formic acid, 50 % (v/v)

methanol then methanol alone. Peptide extracts were added to the digest solutions, dried by Speedvac, resuspended in 0.05 % (v/v) trifluoroacetic acid and filtered before shotgun mass spectrometry as described in Section 2.24.2. In-gel trypsin digests and shotgun mass spectrometry data collection and analysis were performed by Lisa Imrie, KPF.

2.25 Protein pull-downs to detect LifA-interacting partners in T cells

2.25.1 Anti-His protein pull-downs

Anti-His protein pull-downs were performed using a Pierce™ Pull-Down PolyHis Protein:Protein Interaction Kit (Thermo Scientific) according to the manufacturer's instructions. A quantity of 150 µg of rLifA, or the equivalent volume of buffer, was added to a HisPur™ cobalt resin column pre-equilibrated with wash solution (1:1 ratio of BupH™ TBS and Pierce Lysis Buffer with 10 mM imidazole) and incubated for 30 minutes at 4 °C on a rocking platform. Columns were centrifuged at 1250 x g, 4 °C for 1 minute then washed four times with wash solution. T cells (2 x 10^8 cells) from three independent donors were centrifuged at 500 x g for 5 minutes, washed and resuspended in 2.5 mL/g wet weight of cells in ice cold TBS with 1 x Halt™ protease inhibitor cocktail (Thermo Scientific). Cells were lysed in an equal volume of Pierce Lysis Buffer and incubated for 30 minutes on ice with periodic inversions. Lysates were centrifuged at 12,000 x g, 4 °C for 5 minutes and 4 M Imidazole Stock Solution was added to the supernatant to make final concentration of 10 mM. Clarified lysate or wash solution was added to the appropriate columns and incubated for 30 minutes at 4 °C on a rocking platform. Columns were centrifuged at 1250 x g, 4 °C for 1 minute then washed a further five times. Proteins were eluted from the columns three times by the addition of 290 mM imidazole elution buffer, incubation for 5 minutes at 4 °C on a rocking platform followed by centrifugation at 1250 x g, 4 °C for 1 minute. Protein samples were denatured by the addition of an appropriate volume of 1 x sample reducing agent and 1 x LDS sample buffer and heated at 70 °C for 10 minutes. Samples were stored at -20 °C until analysis.

2.25.2 Silver staining

Pull-down eluates were subjected to SDS-PAGE using three different gel systems with different molecular weight resolutions: 3–8 % Tris-Acetate gels (Novex) for 71–460 kDa; 4–12 % Tris-Glycine gels (Novex) for 25–250 kDa; and 4–12 % Tris-Glycine gels (BioRad) for 10–250 kDa. Gels were stained using a Pierce™ Silver Stain Kit (Thermo Scientific) according to the manufacturer's instructions. Gels were washed twice in dH_2O for 5 minutes then fixed for 30 minutes with 30 % (v/v) ethanol (Fisher Scientific), 10 % (v/v) acetic acid (Fisher Scientific). Gels were washed twice in 10 % (v/v) ethanol followed by a further two washes with dH_2O before incubation with Silver Stain Sensitizer (1/500 dilution) for 1 minute. Gels were washed twice with dH_2O then incubated for 30 minutes with 1 part Silver Stain Enhancer, 50 parts Silver stain. Gels were washed twice with dH_2O for 20 seconds then incubated with 1 part Silver Stain Enhancer, 50 parts Silver Stain Developer for 2.5 minutes. Development was stopped with 5 % (v/v) acetic acid.

2.25.3 Liquid chromatography mass spectrometry (LC-MS) to identify candidate interacting partners

The maximum possible volumes of pull-down eluates were run in triplicate on a gel. Protein species of interest were excised from silver stained gels, cut into pieces of ~1 x 1 mm and processed according to Shevchenko *et al*. (2006). Gel pieces were destained by three 15 minute washes with 50 mM ABC, 50 % ACN then shrunk in neat ACN for 10 minutes. Proteins were reduced by incubation at 56 °C with 10 mM DTT, 100 mM ABC for 1 hour. Gels pieces were washed with ACN for 10 minutes then incubated with 55 mM iodacetamide, 100 mM ABC at room temperature for 20 minutes in the dark to alkylate cysteine residues. Gel pieces were covered with ACN until they turned white then the ACN was decanted and the gel pieces were air dried. Gel pieces were rehydrated in 13 µg/mL trypsin (Promega), 10 mM ABC, 10 % ACN at 4 °C then incubated at 37 °C overnight to digest the protein. Digest solutions were transferred to clean tubes and additional peptides were

extracted from the gel pieces by 15 minute incubations with 1 % (v/v) formic acid, 2 % ACN then ACN alone. Digested peptide extracts were purified using StageTips (Rappsilber *et al*., 2007).

Nanoflow LC-MS/MS was performed using an online system of a nano-HPLC (UltiMate^{TM} 3000 RSLC; Fisher Scientific) coupled to a micrOTOF-II mass spectrometer (Bruker). Tryptic digests were delivered to a 100 μm I.D. × 2 cm trap column (5 μm particle size; Acclaim PepMap100) at a flow rate of 20 μL/minute in 100 % buffer A (0.1 % (v/v) formic acid in LCMS grade water). Following a brief washing step, peptides were transferred to a 75 μm I.D. × 25 cm analytical column (3 μm particle size; Acclaim PepMap100) and resolved on a 60 minute gradient of 7–35 % buffer B (0.1 % (v/v) formic acid in ACN) at a flow rate of 300 nL/minute. The eluent from LC was passed onto the nano electrospray source of the micrOTOF-II, which was operated in data-dependent mode, automatically switching between MS and MS/MS mode. The m/z values of tryptic peptides were measured from an MS scan (300–2000 m/z), followed by MS/MS scans of the six most intense peaks. Rolling collision energy for fragmentation was selected based on the precursor ion mass and a dynamic exclusion was applied for 30 seconds.

Raw spectral data were processed using DataAnalysis software (Bruker). Data from mass spectrometry spectra were searched against the Uniprot *B. taurus* protein sequence database, NCBI whole database and the EPEC E2348/69 LifA sequence using Mascot. The parameters used in each search were: missed cut = 1; fixed cysteine carbamidomethylation modification; variable methionine oxidation and deamidation modifications; peptide mass tolerance of 25 ppm; fragment mass tolerance of 0.08 Da; and peptide charges were set to 2+ and 3+. In-gel digestion and LC mass spectrometry data collection and analysis were performed by Dr Dominic Kurian, Proteomics and Metabolomics Facility, The Roslin Institute.

2.25.4 Immunoprecipitation of putative LifA-protein complexes

T cells were serum starved in serum-free RPMI for 1 hour. A total of 1 x 10^7 cells, at a density of 4 x 10^6 cells/mL, were incubated with a final concentration of 1 μg/mL rLifA or the equivalent volume of buffer at 37 °C for 1 hour. Cells were washed with

ice-cold PBS and transferred to clean microcentrifuge tubes as described for protein association assays (Section 2.6). Cells were lysed in 500 µL of NP-40 lysis buffer and incubated on ice for 30 minutes. Lysates were centrifuged at 17,949 x g, 4 °C for 10 minutes and the supernatants were transferred into clean microcentrifuge tubes. Lysates were incubated with 25 µL of Pierce™ Protein A Plus agarose beads (Thermo Scientific), pre-equilibrated with NP-40 lysis buffer, at 4 °C for 1 hour on a rotator to remove proteins that may bind non-specifically to the beads. Samples were centrifuged at 2500 x g, 4 °C for 3 minutes and the supernatants were transferred to clean microcentrifuge tubes. Samples were then incubated with either rabbit polyclonal anti-INPP5E antibody (Proteintech) at a dilution of 1/500 or rabbit polyclonal anti-glutathione peroxidase 1 antibody (Abcam) at a dilution of 1/10 at 4 °C overnight on a rotator.

Samples were centrifuged at 2500 x g, 4 °C for 3 minutes and the supernatants were discarded. Beads were resuspended in 12.5 µL of NP-40 lysis buffer. Protein samples were denatured by the addition of 12.5 µL of 10 x sample reducing agent and 12.5 µL of 4 x LDS sample buffer and heated at 70 °C for 10 minutes. Samples were stored at -20 °C until analysis. Immunoprecipitated material was run alongside protein pull-down eluates on a 4–12 % Tris-Glycine gel. Anti-INPP5E and anti-glutathione peroxidase 1 antibodies bound to Pierce™ Protein A Plus agarose beads alone were included as antibody controls. Western blots were performed using rabbit polyclonal anti-INPP5E antibody at a dilution of 1/500 and rabbit polyclonal anti-glutathione peroxidase 1 antibody at a dilution of 1/1000. Primary antibodies were detected using DyLight™ 800 4X PEG-conjugated goat anti-rabbit IgG antibody at a dilution of 1/30,000.

2.26 Analysis of Akt phosphorylation

2.26.1 Incubation with rLifA proteins prior to mitogen stimulation

T cells were serum starved in serum-free RPMI for 1 hour then 6 x 10^6 cells, at a density of 4 x 10^6 cells/mL, were incubated with a final concentration of 1 µg/mL WT rLifA, rLifA$^{DTD/AAA}$, rLifA^{C1480A} or the equivalent volume of buffer at

37 °C for 1 hour. Cells were then stimulated with ConA at a final concentration of 5 µg/mL for the indicated times then processed as described for protein association assays (Section 2.6). Unstimulated cells were used as a negative control. Western blots were performed using rabbit monoclonal anti-pan Akt antibody (Cell Signaling Technology) at a dilution of 1/1000 in TBS-T/5 % (w/v) BSA or rabbit polyclonal anti-phospho-Akt (Ser^{473}) antibody (Cell Signaling Technology) at a dilution of 1/1000 in TBS-T/5 % (w/v) BSA. As a protein loading control, blots treated with anti-phospho-Akt (Ser^{473}) antibody were also probed with mouse monoclonal anti-β-actin antibody at a dilution of 1/5000. Primary antibodies were detected using DyLight™ 800 4X PEG-conjugated goat anti-rabbit IgG antibody at a dilution of 1/30,000 and DyLight™ 680-conjugated goat anti-mouse IgG antibody at a dilution of 1/15,000.

Densitometry was performed using Image Studio Lite v5.2 and Microsoft Excel 2013. Phospho-Akt1 (Ser^{473}) signals for each sample were normalised against their respective actin protein-loading controls. Data were then further normalised against the 'cells alone' samples at each stimulation time point to provide fold changes in normalised phospho-Akt1 (Ser^{473}) signal in comparison to cells alone. Data were transformed using $\log_{10}$ and one-way ANOVAs were used to determine statistically significant differences between samples at each time point using Minitab 17. Post hoc Dunnett tests were used to calculate 95 % confidence intervals and confirm significance. Densitometry values derive from three independent biological replicates. *P* values ≤ 0.05 were taken to be statistically significant.

2.26.2 Incubation with rLifA proteins after mitogen stimulation

T cells were serum starved in serum-free RPMI for 1 hour then 6 x 10^6 cells, at a density of 4 x 10^6 cells/mL, were stimulated with 5 µg/mL ConA for 15 minutes as above. Cells were then incubated with 1 µg/mL rLifA or the equivalent volume of buffer at 37 °C for the indicated times. Unstimulated cells and cells stimulated with ConA but without rLifA/buffer treatment were used as negative and positive controls respectively. Cells were processed for western blotting and as described in Section 2.26.1. Densitometry data from each replicate were normalised to the protein

loading control as described in Section 2.26.1, then the fold change to the positive control of ConA-stimulated buffer-treated T cells was calculated. Data were transformed using $\log_{10}$ and two-sample T-tests were used to determine statistically significant differences between samples at each time point using Minitab 17. Densitometry values derive from four independent biological replicates. *P* values ≤ 0.05 were taken to be statistically significant.

2.26.3 Infection of T cells with EPEC strains

EPEC E2348/69 wild-type bacteria, and isogenic mutant strains with single or double mutations in *lifA* and *lifA-like* genes or *escN* (Table 2.1) were grown in static DMEM cultures at 37 °C for ~5 hours to induce Type III secretion. The A_{600} of each culture was measured, with an A_{600} of 1 taken to reflect ~1 x 10^9 bacteria/mL based on prior analysis of the relationship between culture absorbance and viable counts detected by direct plating. T cells were serum starved in serum-free RPMI for 1 hour then 6 x 10^6 cells, at a density of 4 x 10^6 cells/mL, were incubated with bacteria at a multiplicity of infection (MOI) of 200:1 (bacteria:T cells) at 37 °C for the indicated times. Cells were stimulated with a final concentration of 5 µg/mL ConA for 15 minutes where indicated and processed as described previously. Unstimulated cells and cells stimulated with ConA, but without EPEC infection, were used as negative and positive controls respectively. Cells were processed for the detection of pan-Akt, Ser^{473}-phosphorylated Akt and β-actin as described previously.

Densitometry was performed as described previously and data from each replicate were normalised first to the β-actin loading control and the fold change was calculated relative to the positive control. Statistical analysis was performed as described in Section 2.26.1. Experiments involving EPEC E2348/69 Nal^R strains used post hoc Fisher tests in addition to Dunnett tests to calculate 95 % confidence intervals and confirm significance. Densitometry values derive from three independent biological replicates. *P* values ≤ 0.05 were taken to be statistically significant.

2.26.4 Immunoprecipitation of Akt and analysis of its post-translational modifications

T cells were serum starved in serum-free RPMI for 1 hour. A total of 1 x 10^7 cells, at a density of 4 x 10^6 cells/mL, were incubated at 37 °C with either 1 µg/mL rLifA/buffer for the indicated times or EPEC E2348/69 strains at an MOI of 200:1 for 1 hour. Cells were stimulated with 5 µg/mL ConA for 15 minutes. Unstimulated cells and cells stimulated with ConA, but without rLifA/buffer treatment or EPEC infection, were used as negative and positive controls respectively. Immunoprecipitation of Akt was performed as described previously using rabbit monoclonal anti-pan Akt at a dilution of 1/50. Beads were resuspended in 25 µL of NP-40 lysis buffer. Protein samples were denatured by the addition of 25 µL of 10 x sample reducing agent and 25 µL of 4 x LDS sample buffer and heated at 70 °C for 10 minutes. Whole cell lysate samples in 500 µL of NP-40 lysis buffer were also made for each immunoprecipitation condition. Samples were stored at -20 °C until analysis. Rabbit monoclonal anti-pan Akt antibody bound to Pierce™ Protein A Plus agarose beads alone were included as antibody controls. Western blots were performed using rabbit monoclonal anti-pan Akt antibody at a dilution of 1/1000 in TBS-T/5 % (w/v) BSA, rabbit polyclonal anti-phospho-Akt (Ser^{473}) antibody at a dilution of 1/1000 in TBS-T/5 % (w/v) BSA and mouse monoclonal anti-O-GlcNAc antibody at a dilution of 1/1000. Primary antibodies were detected using DyLight™ 800 4X PEG-conjugated goat anti-rabbit IgG antibody at a dilution of 1/30,000 and DyLight™ 800-conjugated goat anti-mouse IgG antibody at a dilution of 1/10,000.

3 Activity of lymphostatin fragments

3.1 Introduction

In silico analysis of the lymphostatin (LifA) protein from the prototype EPEC O127:H6 strain E2348/69 reveals several Pfam domains with homology to other proteins (Figure 3.1). The N-terminal amino acids (aa) 20–1144 are homologous to the nucleotide-binding domain of reticulocyte binding/rhoptry proteins expressed by *Plasmodium* species (22 % identity and 39 % similarity over 1124 amino acids). These proteins are involved in adhesion to reticulocytes (Galinski *et al*., 1992; Triglia *et al*., 2001), which may potentially be significant as lymphostatin is near identical in sequence to EHEC factor for adherence (Efa1), which has been reported to influence adherence of EHEC O111:H- to Chinese hamster ovary (CHO) cells (Nicholls *et al*., 2000). Located within this region is also a glycosyltransferase (GT) domain (aa 314–754) that shares homology with the large clostridial toxins (LCTs) TcdA and B (as described in Section 1.3.5.1) and a TcdB N-terminal helical domain (aa 219–280), thought to be involved in substrate recognition. Between amino acid residues 1465–1646 lies a YopT-like cysteine protease (CP) domain, described in Section 1.3.5.2, and at the C-terminal end of the protein (aa 2181–3107) is a conserved domain that belongs to the DUF3491 superfamily that has no known function.

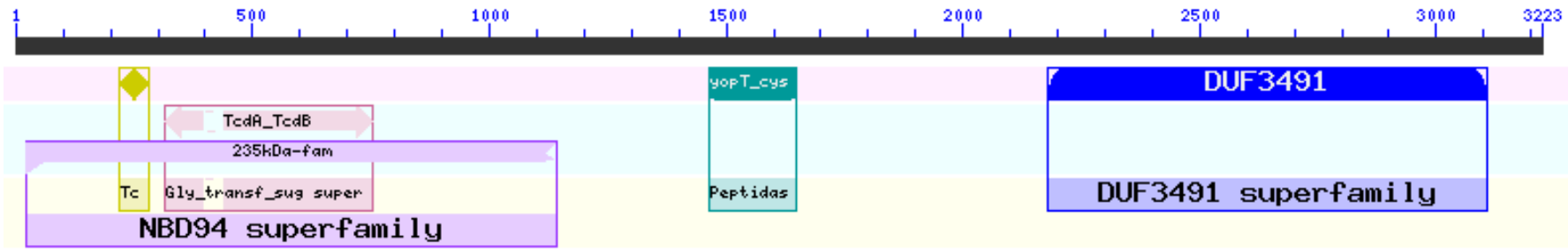

Figure 3.1. *In silico* predicted domains of lymphostatin from EPEC O127:H6 strain E2348/69. NCBI Blast identified five domains with homology to other known proteins including reticulocyte binding/rhoptry protein (NBD94 superfamily, aa 20–1144), a glycosyltransferase domain (GT, aa 314–754), a TcdB N-terminal helical domain (Tc, aa 219–280), a YopT-like cysteine protease domain (aa 1465–1646) and a domain of unknown function (DUF3491 superfamily, aa 2181–3107).

Other domains and motifs of lymphostatin have also been previously reported. Klapproth *et al*. (2005) described an aminotransferase II motif in LifA from *C. rodentium* that is also present in EPEC E2348/69 LifA between amino acid residues 1947–1956. Nicholls *et al*. (2000) identified a number of predicted motifs in Efa1 from EHEC O111:H- (which is 99 % identical to E2348/69 lymphostatin) including two potential prepilin peptidase processing sites between residues 15–16 and 772–773 that are homologous to EPEC BfpA and *V. cholerae* TcpB respectively, both of which are Type IV pilus precursors (Donnenberg *et al*., 1992; Ng *et al*., 2016). A predicted transmembrane domain was also identified by Nicholls *et al*. (2000) between residues 2001–2033 of Efa1, however, this region of LifA has no homology to the transmembrane domain from LCTs that is required for the translocation of the LCT glycosyltransferase domain into the cytoplasm from the endosome (Nicholls *et al*., 2000; Qa'dan *et al*., 2000; Barth *et al*., 2001). In contrast to the NBCI Blast analysis, Nicholls *et al*. (2000) reported that only the initial 500 amino acids of LifA had 36 % homology to reticulocyte binding protein 2 from *Plasmodium vivax*. Other reported proteins with homologous regions to LifA include interaptin from *Dictyostelium discoideum* (21 % identity, 43 % similarity, aa 850–1150), *Mycoplasma pneumoniae* cytadherence high molecular weight protein 2 (HMW2; 32 % identity, 48 % similarity, aa 1766–1806) and *Streptococcus pyogenes* M5 protein (32 % identity, 65 % similarity, aa 1052–1095; Nicholls *et al*., 2000).

In our previous research, limited tryptic proteolysis of recombinant LifA (rLifA) from EPEC E2348/69 produced five major fragments (Figure 3.2A), which were identified by matrix-assisted laser desorption ionisation time-of-flight (MALDI-TOF) mass spectrometry (Figure 3.2B; Cassady-Cain *et al*., 2016). However, the contribution of these fragments to the overall function and activity of LifA is unknown. The largest fragment, designated F1, which encompasses the putative GT and CP domains, is richer in basic amino acids over the first 100 aa than full-length lymphostatin, which enabled us to separate F1 from other digest products by anion exchange chromatography (Cassady-Cain *et al*., 2016). The F1 fragment, purified in this way, did not inhibit the concanavalin A (ConA)-stimulated proliferation of bovine T lymphocytes (Cassady-Cain *et al*., 2016). Interestingly, several LifA fragments derived by limited trypsin proteolysis were eluted in the same

fractions from a size exclusion chromatography column (Walkinshaw Laboratory, unpublished data), suggesting that they may be capable of associating with each other despite not being covalently bonded.

It was hypothesised that predicted globular domains released by limited proteolysis may represent functional domains, and that if these fragments were capable of associating with each other, the resulting complexes may retain lymphostatin activity against T cells. In this chapter, I cloned, expressed and purified a selection of LifA fragments and assayed their ability to bind to T lymphocytes and inhibit their mitogen-activated proliferation.

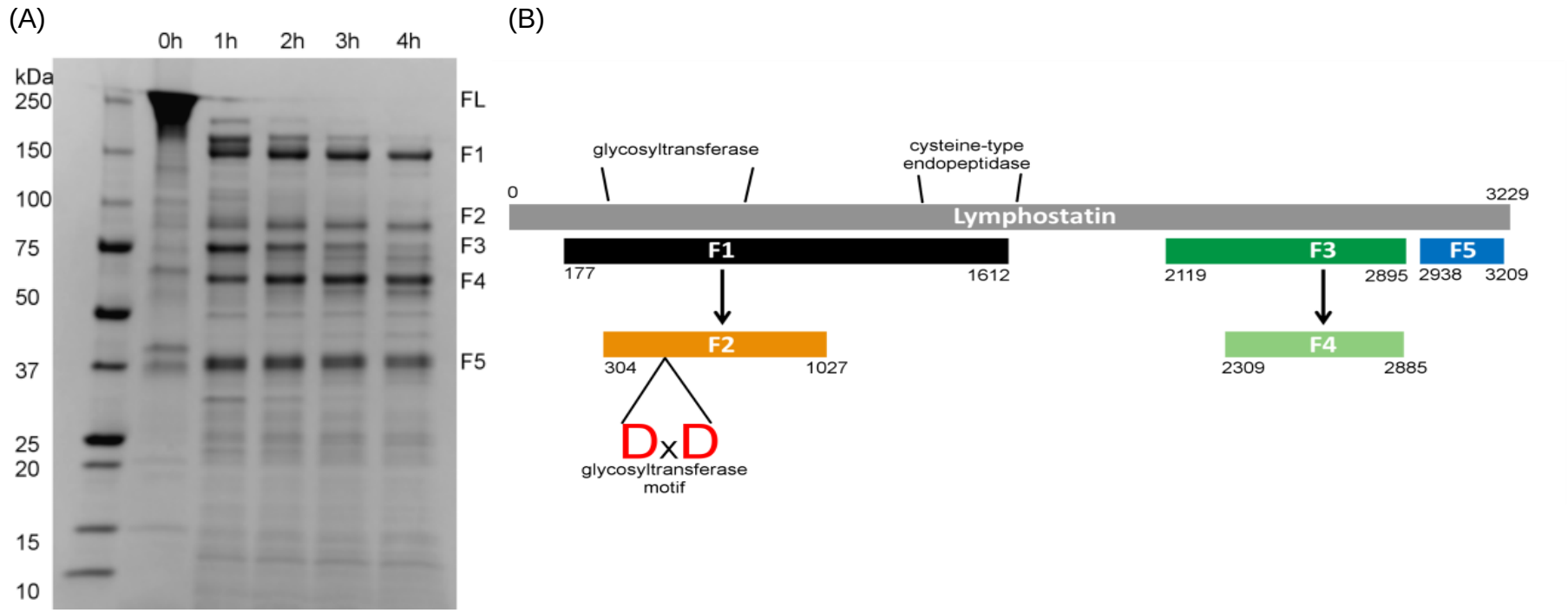

Figure 3.2. Tryptic digests revealed predicted globular domains of lymphostatin. (A) Limited trypsin proteolysis of rLifA produced five major fragments, designated F1–5. (B) The approximate amino acid boundaries of the five fragments were determined by MALDI-TOF mass spectrometry, which revealed that fragments F2 and F4 were sub-fragments of F1 and F3 respectively (from Cassady-Cain *et al.*, 2016).

3.2 Development of a robust assay for lymphocyte proliferation

Early experiments studying lymphostatin activity used bulk peripheral blood mononuclear cells (PBMCs) treated with crude bacterial lysates to examine the effects of LifA on mitogen-stimulated proliferation as no stable expression clone existed (Klapproth *et al*., 1995, 1996 and 2000; Malstrom and James, 1998; Stevens *et al*., 2002; Abu-Median *et al*., 2006; Deacon *et al*., 2010). Cassady-Cain *et al*. (2016) were the first to use highly-purified recombinant lymphostatin in proliferation assays. In order to establish whether enriching T cells was necessary for testing the activity of LifA fragments, I first compared the activity of wild-type (WT) rLifA against ConA-stimulated bulk PBMCs and enriched T cells from three independent donors using a colorimetric plate-based assay. The assay measured the conversion of MTS (3-(4, 5-dimethylthiazol-2-yl)-5-(3-carboxymethoxyphenyl)-2-(4-sulphophenyl)-2H-tetrazolium) into a coloured formazan product by metabolically active cells, the absorbance of which was detected at around 490 nm. The quantity of formazan produced was directly proportional to the metabolic activity of dividing cells in the culture (Cory *et al*., 1991; Promega, 2012).

In both cell populations, rLifA inhibited ConA-stimulated proliferation in a concentration-dependent manner, producing typical sigmoidal curves where at high concentrations inhibitory activity was saturated and at low concentrations the activity was titrated away (Figure 3.3). The proliferation index (the ratio of proliferation of cells treated with rLifA + ConA/ConA alone), with standard deviation, of PBMCs decreased gradually from 0.99 ± 0.06 at 0.001 ng/mL of rLifA to 0.51 ± 0.06 at 0.1 ng/mL, then the curve leveled out to 0.56 ± 0.03 at 100 ng/mL. T cells produced a curve that was level between 0.001 and 0.01 ng/mL of rLifA, decreased sharply from 0.95 ± 0.24 at 0.01 ng/mL to 0.47 ± 0.12 at 0.1 ng/mL, then leveled out to 0.43 ± 0.13 at 100 ng/mL. The effective dose at which 50 % of cell proliferation was inhibited by rLifA (ED_{50}), with standard error of the mean, was 0.01 ± 0.001 ng/mL for PBMCs and 0.04 ± 0.02 ng/mL for T cells (W = 8, P = 0.3827). Despite there being no statistically significant difference between the ED_{50}s, enriched T cells were used in all further experiments as the PBMCs did not consistently produce a fold induction of proliferation ≥ 2, which was used as a quality control for each

proliferation assay. The buffer that rLifA was dissolved in was used as a carrier control. The volumes of buffer added to cells were equal to those of the different concentrations of rLifA. The buffer did not affect cell proliferation.

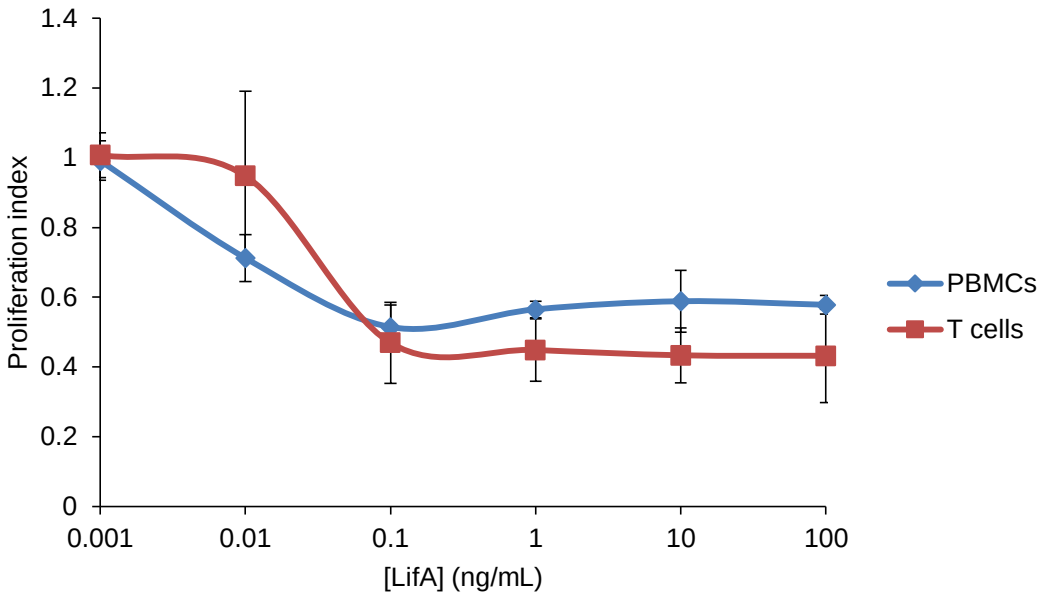

Figure 3.3. Concentration-dependent inhibition of proliferation of ConA-stimulated peripheral bovine PBMCs and T lymphocytes by recombinant LifA. An absolute number of 200,000 cells were seeded into the wells of a 96 well plate. Titrations were carried out in triplicate and the results are the average obtained from 3 independent experiments using separate donors. Data were normalised against cells with ConA alone to produce a proliferation index. Error bars indicate the standard deviation of the average proliferation indices from across the 3 experiments.

3.3 Development of an assay to detect the association of LifA with T cells

In order to detect interactions between LifA and T lymphocytes, whether by binding of the protein to the plasma membrane or uptake into the cells, bovine T cells were incubated in the presence of rLifA for various time points and the cell lysates were analysed using a polyclonal anti-LifA antibody (Stevens Laboratory, clone 45). Despite some reactivity of the antiserum to T cell proteins, it recognised a protein of the expected size for rLifA (365 kDa). Initially, it appeared that rLifA was

associated with the T cells at all time points between 5 minutes and 2 hours (Figure 3.4A) However, through investigation of additional controls, it was subsequently found that rLifA was bound to the microcentrifuge tubes when no cells were present (Figure 3.4B). Attempts to remove this non-specific binding by repeated washing with PBS or transferring the cells to a clean tube once failed (Figure 3.4C), as did using Eppendorf® LoBind or bovine serum albumin-coated microcentrifuge tubes (data not shown). It was found that washing the cells and transferring them to clean tubes twice was sufficient to remove the non-specifically bound rLifA (Figure 3.4D).

Once the assay method had been optimised, bulk PBMCs and enriched T cells were incubated with rLifA from 5 minutes up to 24 hours (Figure 3.5). As with the pilot experiments, rLifA was observed to associate with PBMCs/T cells at all time points. This provided a useful assay for detecting interactions between T cells and WT rLifA, or mutated forms or fragments thereof, under different conditions.

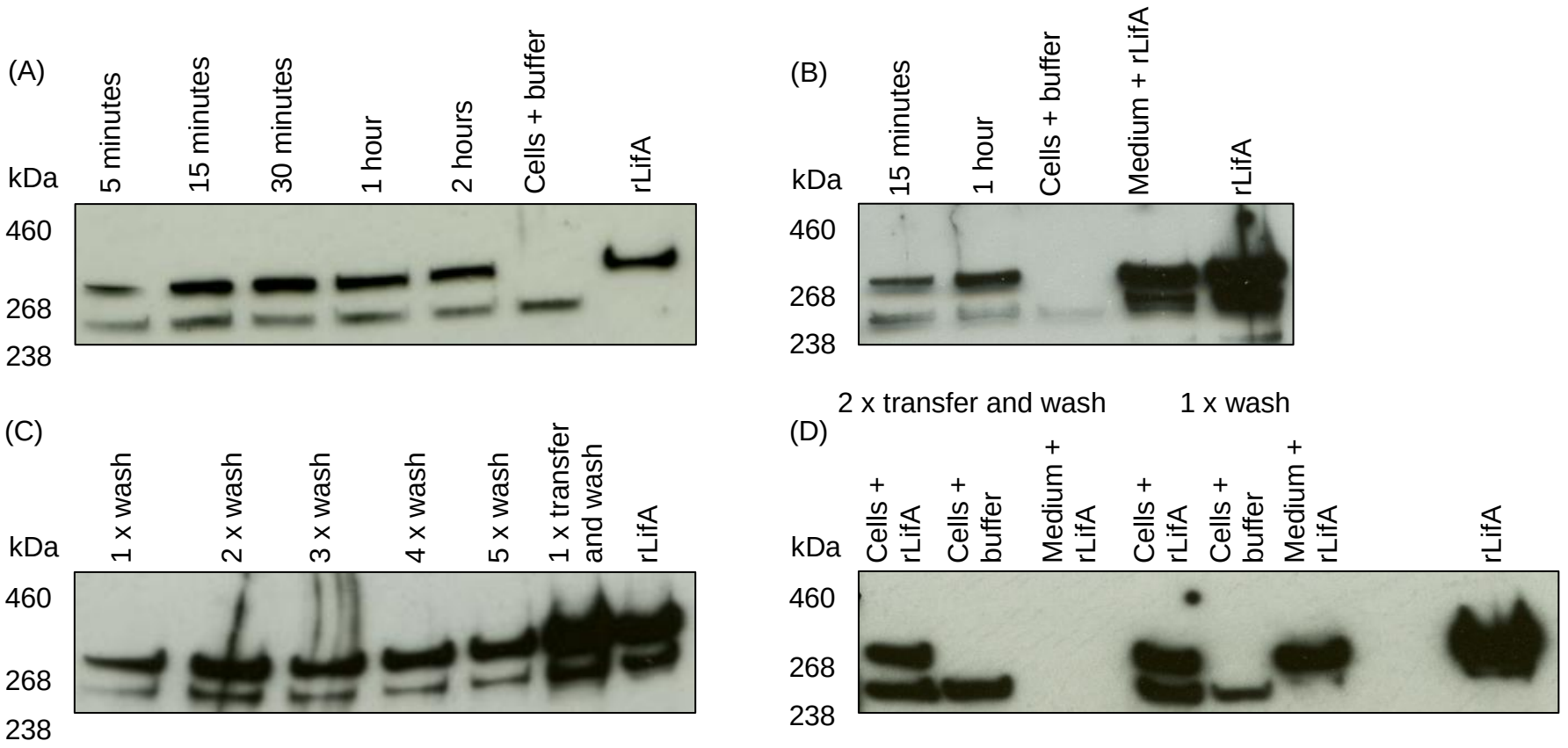

Figure 3.4. The development of an assay to detect the association of rLifA with T lymphocytes. (A) Lysates from T cells treated with rLifA for varying time points appeared to show that rLifA associated with T cells from as little as 5 minutes to at least 2 hours. (B) A medium + rLifA control with no T cells revealed that rLifA non-specifically bound to the microcentrifuge tubes. (C) Washing tubes with PBS or transferring the cells to a clean tube once did not remove non-specific binding. (D) Washing and transferring the cells to a clean tube twice was sufficient to remove non-specifically bound rLifA. A quantity of 2 ng of rLifA was used a positive control. Proteins were detected using a polyclonal anti-LifA antibody (Stevens Laboratory, clone 45).

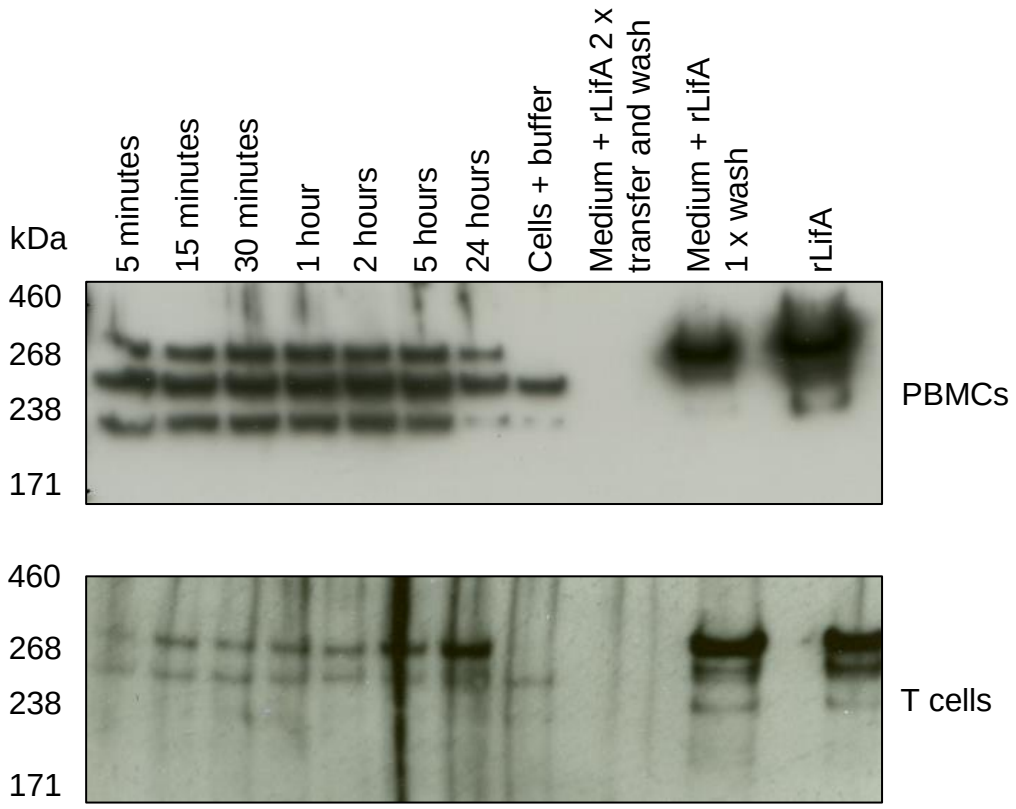

Figure 3.5. Association of rLifA with PBMCs/T cells. rLifA associated with bulk PBMCs and enriched T cells from as little as 5 minutes to at least 24 hours. A quantity of 2 ng of rLifA was used a positive control. Proteins were detected using a polyclonal anti-LifA antibody (Stevens Laboratory, clone 45).

3.4 Generation of pRham-LifA-6 x His fragment clones

As noted in Section 3.1, three putative structural fragments of LifA (F1, F3 and F5) and two smaller subfragments (F2 and F4) were identified by limited proteolysis (Cassady-Cain *et al*., 2016) but the contribution of these fragments to the overall function and activity of lymphostatin is unknown. Expression clones were therefore made for modified versions of the three largest fragments that span the majority of the LifA protein (Figure 3.6). These subunits were the N-terminal putative catalytic fragment (F1, aa 1–1620), which contains the predicted putative GT and CP domains, the C-terminal large fragment (F3, aa 2111–2900) and C-terminal small fragment (F5, aa 2901–3223). The regions cloned in this study were

longer than the tryptic fragments for which the boundaries had been mapped by MALDI-TOF in order to preserve predicted secondary structure at the boundary and fully encompass predicted catalytic domains (secondary structure analysis performed by Dr Liz Blackburn, Edinburgh Protein Production Facility (EPPF), Centre for Translational & Chemical Biology). The N-terminal fragment was extended to the beginning of the protein to account for any possible processing events. An expression clone was also made for the glycosyltransferase domain (aa 221–1033) based on the predicted structural alignment of LifA with LCTs and the known boundaries of the GT domain of LCTs (Cassady-Cain *et al*., 2016). In all cases, the predicted open reading frame for LifA fragments was cloned in-frame to both N- and C-terminal six histidine (6 x His) tags for affinity purification of the proteins. In the case of the F1 fragment, this was cloned with only a C-terminal tag to ensure that the affinity tag would not be lost if a predicted N-terminal signal peptide was cleaved.

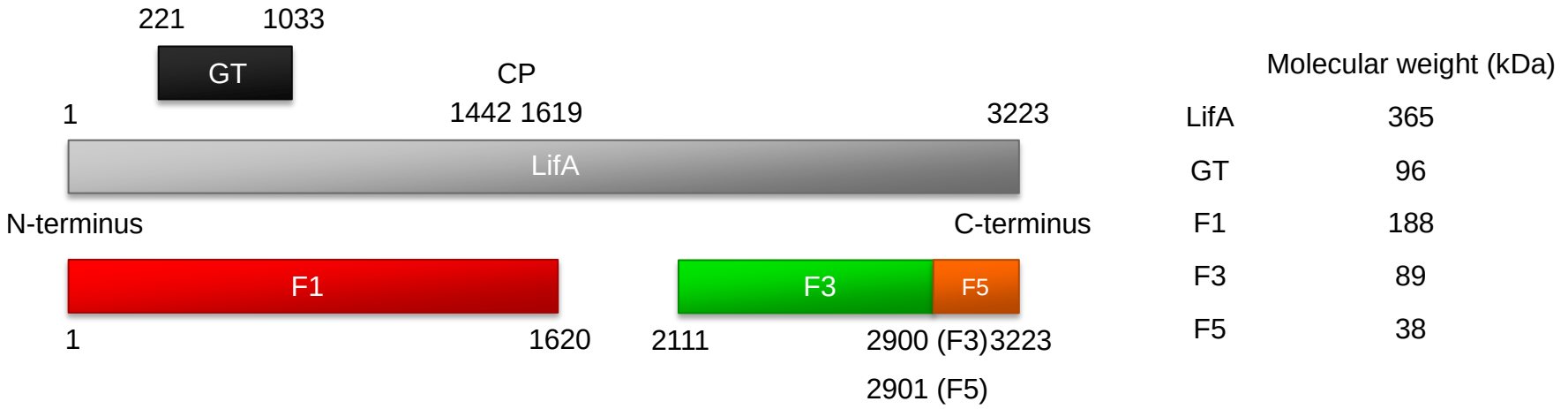

Figure 3.6. Schematic of the full-length LifA protein and the relative positions of fragment proteins. F1 – N-terminal fragment encompassing GT and CP domains; GT – glycosyltransferase domain; F3 – C-terminal large fragment; F5 – C-terminal small fragment. Numbers indicate amino acid positions within the full-length protein. CP – cysteine protease domain (aa 1442–1619) as defined by homology with other C58 cysteine proteases (Walkinshaw Laboratoty, unpublished data), which was encompassed by F1 but was not made into a recombinant protein itself.

PCR amplicons encoding the LifA fragments, which were confirmed to be of the expected size by gel electrophoresis, were fused to N- or C-terminal 6 x His tags using the Expresso™ Rhamnose Cloning and Expression System. All of the cloned fragments were under the control of a rhamnose-inducible glucose-repressible promoter that we previously established affords tight control of rLifA expression (Cassady-Cain *et al*., 2016) and adopted due to concerns from published studies regarding the instability of *lifA* clones (Klapproth *et al*., 2000; Nicholls *et al*., 2000). Putative recombinants for each expression clone were screened by colony PCR to determine if they contained the expected fragments. Positive colonies were validated by double-stranded sequencing of the inserts (see Appendix 2) and one validated clone for each LifA fragment was taken forward for protein production experiments (Figure 3.7).

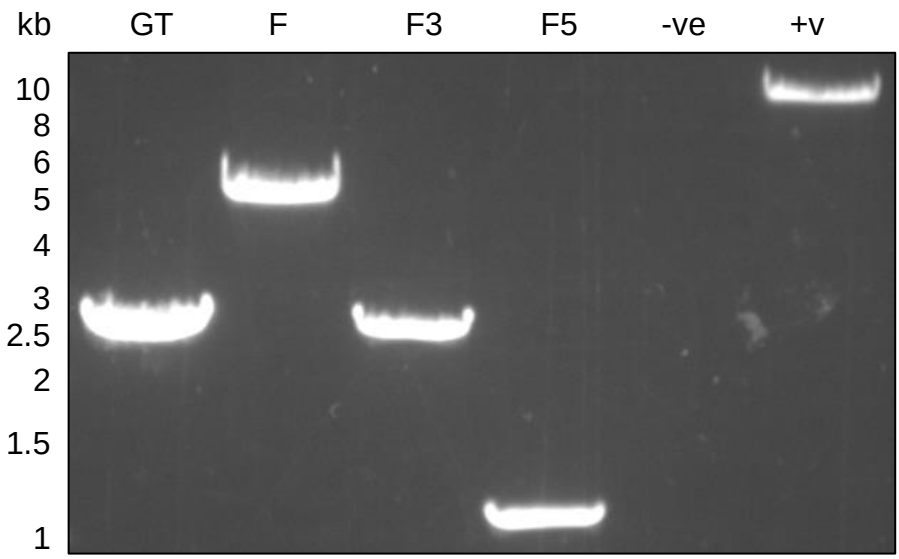

Figure 3.7. PCR screen of the expression clones chosen for further experiments. All expression clones contained gene inserts of the appropriate sizes (GT – 2460 bp; F1 – 4878 bp; F3 – 2391 bp; F5 – 990 bp; plus 150 bp to each insert from the vector amplified by the pRham Forward and pETite Reverse primers). Nuclease-free distilled water was used as a negative control. The full-length LifA insert (9687 bp + 150 bp) was used as a positive control.

3.5 Production of LifA fragment proteins

Pilot-scale protein production used one expression clone for each LifA fragment to determine whether recombinant fragments could be expressed at the optimal conditions known for rLifA production as previously described (Cassady-Cain *et al*., 2016). Recombinant LifA fragments of the expected sizes were observed in the soluble and insoluble bacterial lysate fractions of each expression clone (Figure 3.8). The rF1 expression clone produced not only the expected ~188 kDa fragment but also a unique ~150 kDa protein that was also reactive to the polyclonal anti-LifA antibody. rF5 was not observed in the soluble lysate fraction by western blotting, possibly due to its small size (~38 kDa).

Protein expression was optimised before large-scale production by examining the effects of growth medium (LB or 2xTY), post-induction temperature (20 or 30 °C), time (1, 2, 3 or 4 hours) and the pre-induction over-expression of chaperones by heat/cold shock. The optimal expression conditions for each fragment are listed in Table 3.1.

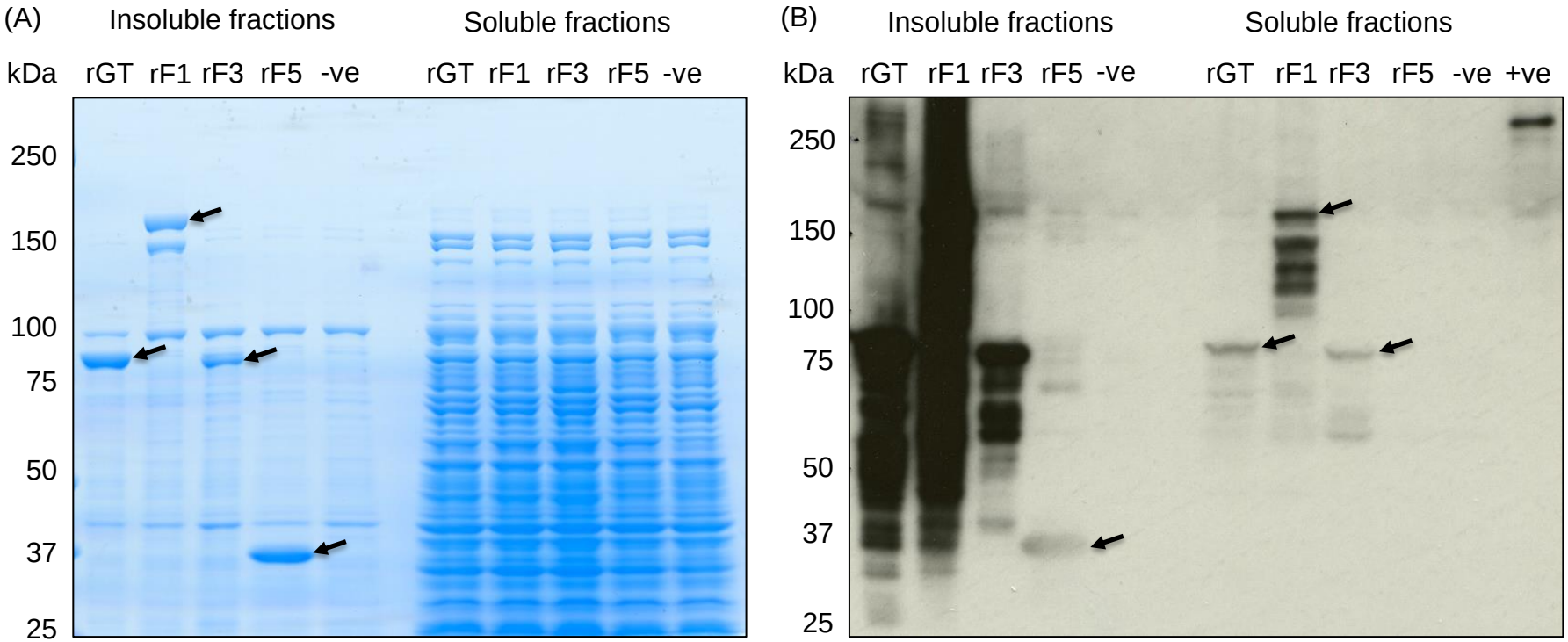

Figure 3.8. *E. cloni*® 10G chemically competent cells produced LifA fragments when induced with 0.2 % L-rhamnose. Soluble and insoluble fractions of bacterial cell lysates were examined by (A) Coomassie staining and (B) western blotting using a polyclonal anti-LifA antibody (Stevens Laboratory, clone 45). Soluble rGT (~96 kDa), rF1 (~188 kDa) and rF3 (~89 kDa) were observed in the western blot. rF5 (~38 kDa) was observed in the insoluble fraction but not the soluble fraction, possibly due to its small size. A protein of ~150 kDa was observed only in cells producing rF1, suggesting that this protein may be derived from rF1, for example by processing, internal initiation of translation or premature termination. Cells transformed with the pRham empty plasmid were used as a negative control and 2 ng of rLifA was used as a positive control in the western blot. Proteins of the expected sizes are marked with arrows.

Table 3.1. The optimal expression conditions for each recombinant LifA fragment.

Protein	Growth medium	Post-induction temperature (°C)	Post-induction time (hours)	Heat/cold shock required
rGT	LB	30	3	No
rF1	2xTY	30	3	No
rF3	LB	30	3	No
rF5	LB	30	3	Yes

3.6 Protein purification

3.6.1 LifA fragment purification

Large-scale production of the recombinant LifA fragments was carried out once the optimal expression conditions had been determined. Prior to purification, the optimal IMAC capture conditions for rF1 were determined to be the use of a nickel-Sepharose® column and IMAC buffers at pH 8. rF1, rF3 and rF5 were purified using only a two-step process of ion metal affinity chromatography (IMAC) and size exclusion chromatography (SEC). Figures for the purification of rF1 are shown as an example (Figures 3.9 and 3.10). rF1 could not be further purified by anion exchange chromatography using the same conditions as for F1 released by tryptic digestion (Cassady-Cain *et al*., 2016; data not shown). The recombinant GT domain was purified to a higher degree using anion exchange by Dr Liz Blackburn, EPPF.

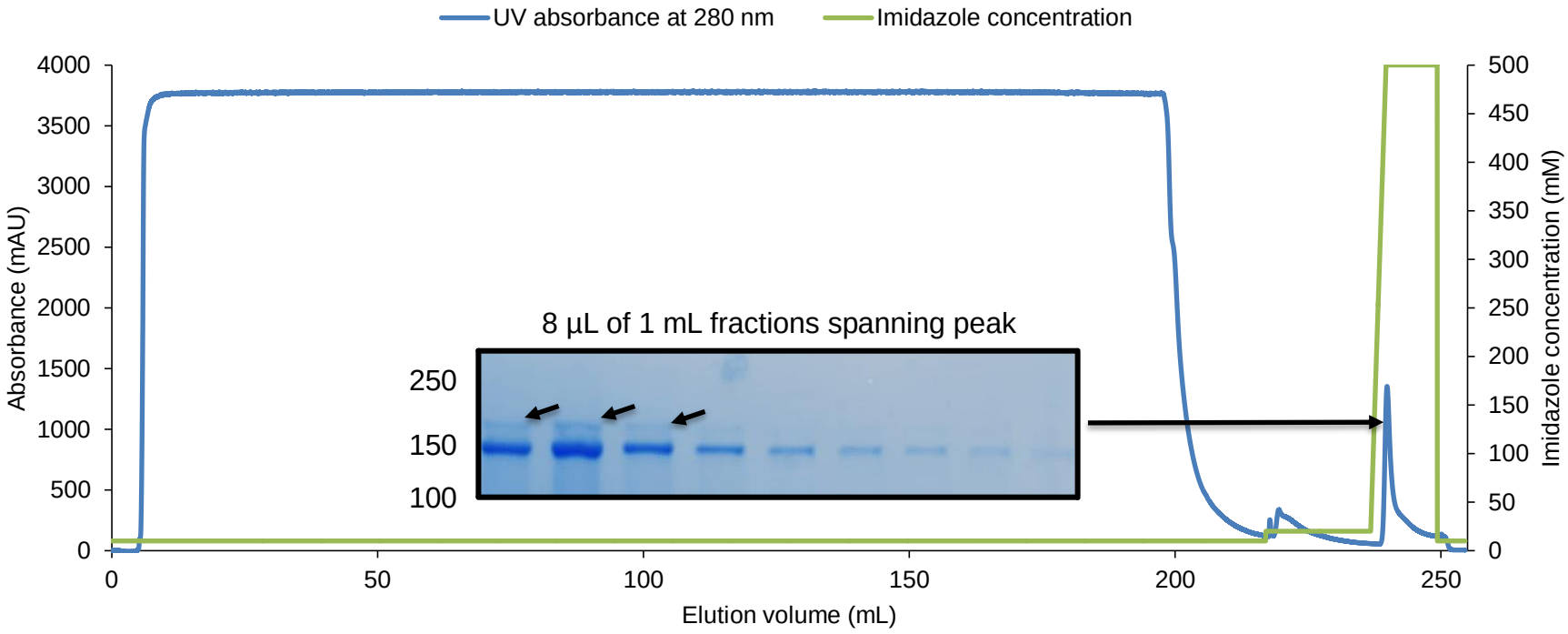

Figure 3.9. IMAC purification of rF1 protein using Ni^{2+}-Sepharose®. The absorbance of elution buffer at 280 nm shows the presence of rF1 where the concentration of imidazole was increased from 20 to 500 mM (marked with an arrow) to elute the protein from the nickel-Sepharose® beads. The large absorbance peak between ~0 and 200 mL corresponds to large cell debris that did not bind the column. The small peak before 230 mL corresponds to non-specifically bound proteins washed off by the increase in imidazole concentration from 10 to 20 mM. Inset: Coomassie stain of 8 µL from 1 mL IMAC filtrate fractions showing the rF1 protein eluted. The dominant protein species was ~150 kDa but the 188 kDa rF1 could be seen above it, indicated by arrows.

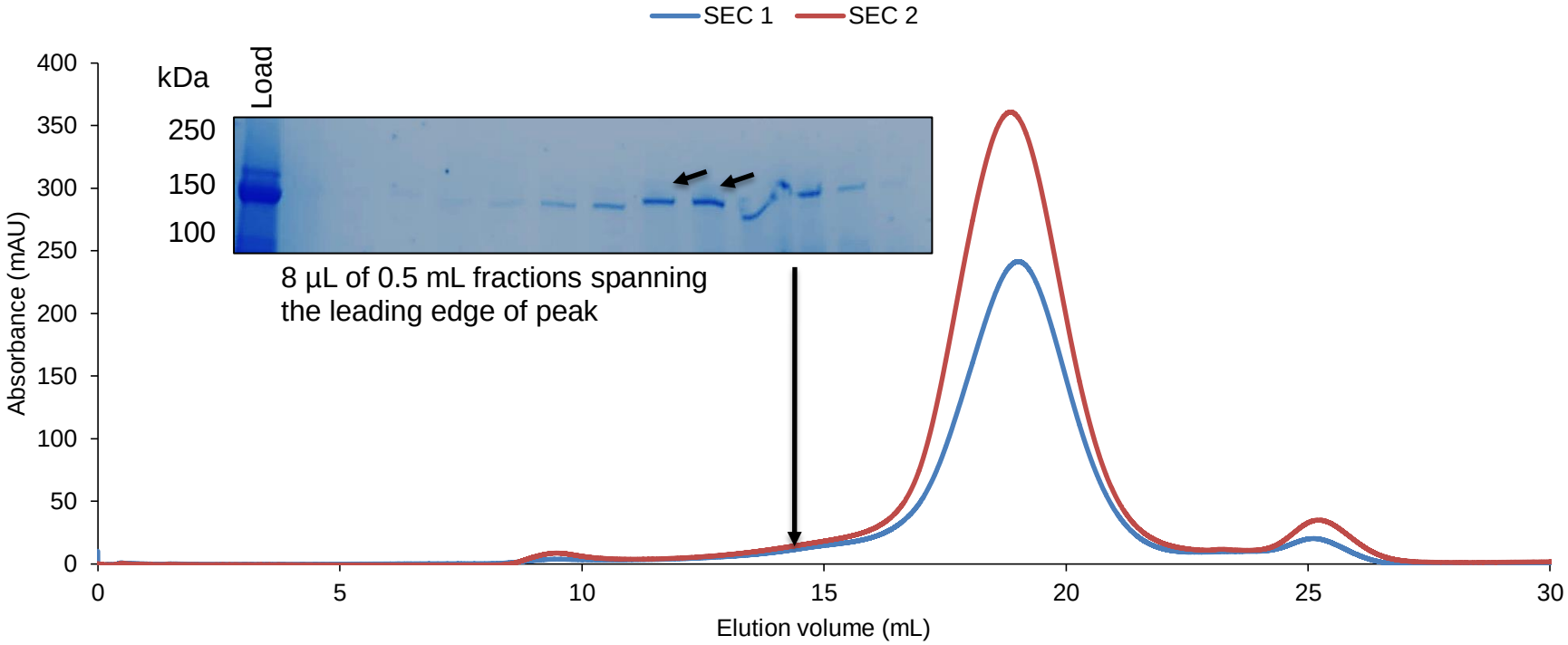

Figure 3.10. Purification of rF1 protein by size exclusion chromatography (SEC). The leading edges of the large absorbance peaks (marked with an arrow) correspond to the presence of rF1 in the filtrates of the Superose 6pg 10/300 SEC column used to filter the pooled IMAC fractions. SEC 1 – less pure IMAC fractions. SEC 2 – purest IMAC fractions. Inset: Coomassie stains of 8 µL from 0.5 mL SEC filtrate fractions showing the rF1 protein eluted. The rF1 protein of 188 kDa (expected size indicated by arrows) was no longer visible above the dominant ~150 kDa protein. rF1 was eluted earlier than it should for a globular protein of the same size, suggesting it could be linear, but this was likely caused by shortening of the protein. The large peaks correspond to proteins of lower molecular masses.

The recombinant LifA fragments were found to be eluted from the SEC columns in multiple forms. A protein of ~150 kDa was the dominant protein in the rF1 preparation after purification, while the presence of full-length rF1 was reduced, suggesting that full-length rF1 may be processed into a lower molecular mass product (Figure 3.11). rGT and anion exchange purified rF3 (made by Dr Liz Blackburn, EPPF) were analysed by size exclusion chromatography-multi-angle light scattering (SEC-MALS) and found to contain not only the monomeric proteins but also heptamer and trimer forms respectively. This suggests that these proteins are capable of associating into multimeric forms under normal buffer conditions. rF5 was eluted as a large aggregate protein, with a mass between 75–440 kDa, across 70 mL of SEC column eluate. Despite a large absorbance peak at the expected monomeric size of rF5, the protein was only observed in the multimer-containing elution fractions by western blotting. The size, purity and reactivity of rF1, rF3, rF5 and rGT proteins to anti-LifA antibody is shown in Figure 3.12. The identity of each recombinant fragment was confirmed by MALDI-TOF mass spectrometry of tryptic digests of the proteins. Details of the identified peptides are listed in Table 3.2 and mapped peptides are illustrated in Appendix 3. Mass spectrometry data for rGT was collected by Dr Liz Blackburn, EPPF.

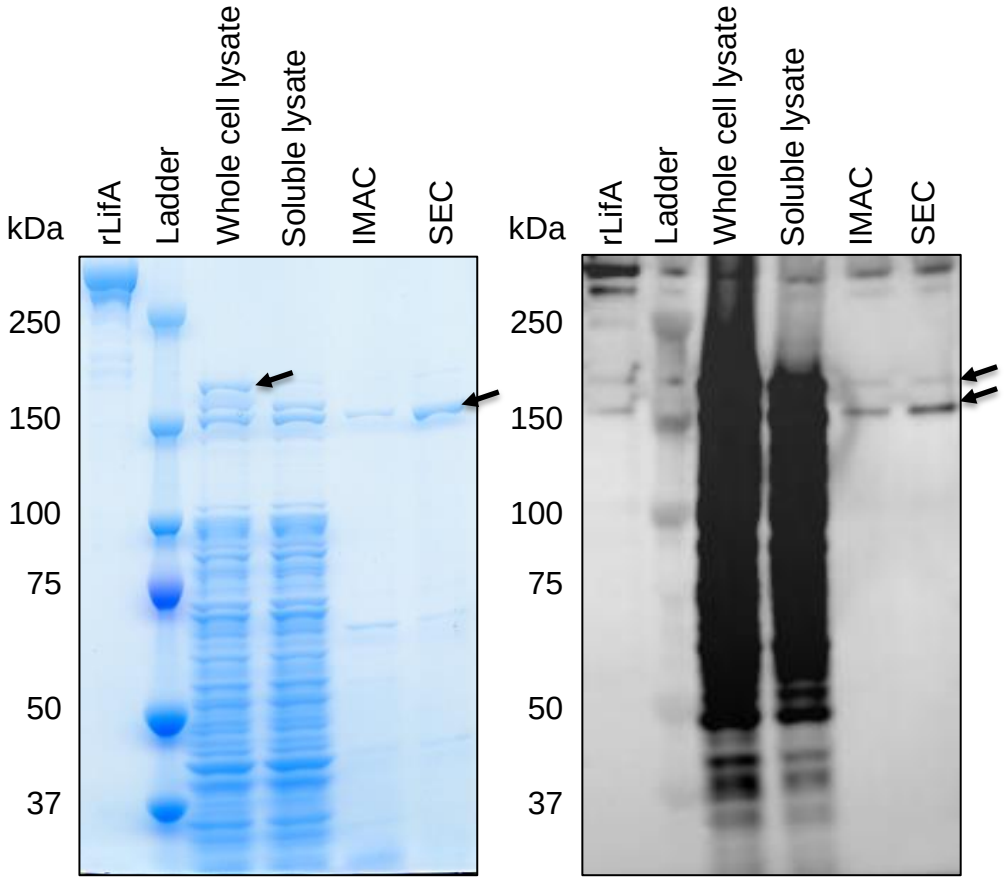

Figure 3.11. Coomassie stain (left) and western blot (right) of recombinant F1 purification steps. Full-length rF1 (~188 kDa) was observed in the whole cell lysate but after purification the ~150 kDa variant of rF1 became the dominant protein in the eluate. Full-length rF1 was still observed after SEC purification by western blotting. Quantities of 200 ng and 2 ng of rLifA were used as positive controls in the Coomassie stain and western blot respectively. The position of the ~188 kDa and ~150 kDa variants of rF1 are marked with arrows.

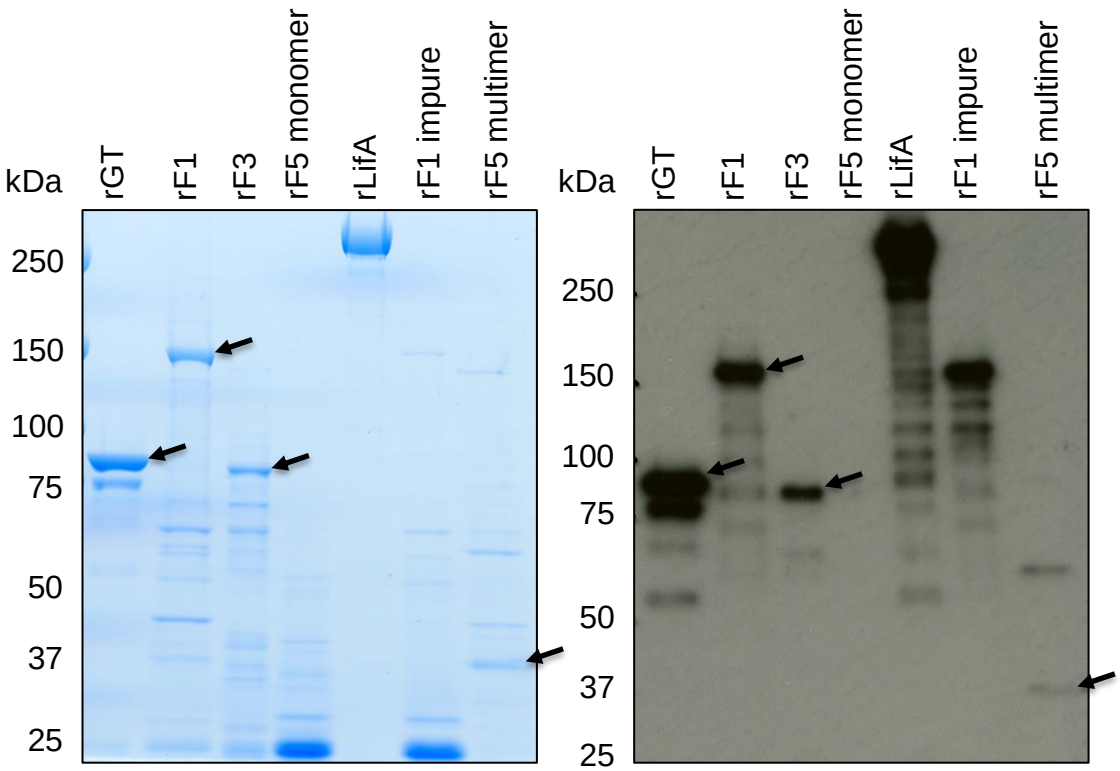

Figure 3.12. Coomassie stain (left) and western blot (right) of recombinant LifA fragments. rGT (~96 kDa), rF3 (~89 kDa) and full-length LifA (~365 kDa) were observed at the expected positions. The pure and impure fractions of rF1 (~188 kDa) showed almost only the ~150 kDa form of rF1 after purification. rF5 (~38 kDa) was not observed in the fractions suspected to contain monomeric rF5 but was seen in fractions suspected to contain a multimeric form. Proteins of the expected sizes and ~150 kDa rF1 are marked with arrows.

Table 3.2. Summary of the MALDI-TOF mass spectrometry results for the recombinant LifA fragments.

Protein	Mascot score	Peptide matches	Amino acid range	Coverage (%)
rGT	318	49	18–804	58
rF1	279	30	251–1017	23
rF3	135	19	241–286	22
rF5	77	13	45–310	22

3.6.2 LifA fragment co-purification

In order to determine whether the recombinant LifA fragments could associate with each other as observed previously with fragments from limited proteolysis (Walkinshaw Laboratory, unpublished data), rF1, rF3 and rF5 were produced and purified together. Bacterial lysates of the three expression clones were pooled then purified by IMAC and SEC. Proteins of the expected sizes appeared in some of the same SEC elution fractions (Figure 3.13). However, the presence of rF5 was not as clear as the other fragments, and given that both rF3 and rF5 are known to form multimers it could not be concluded that a genuine association was observed.

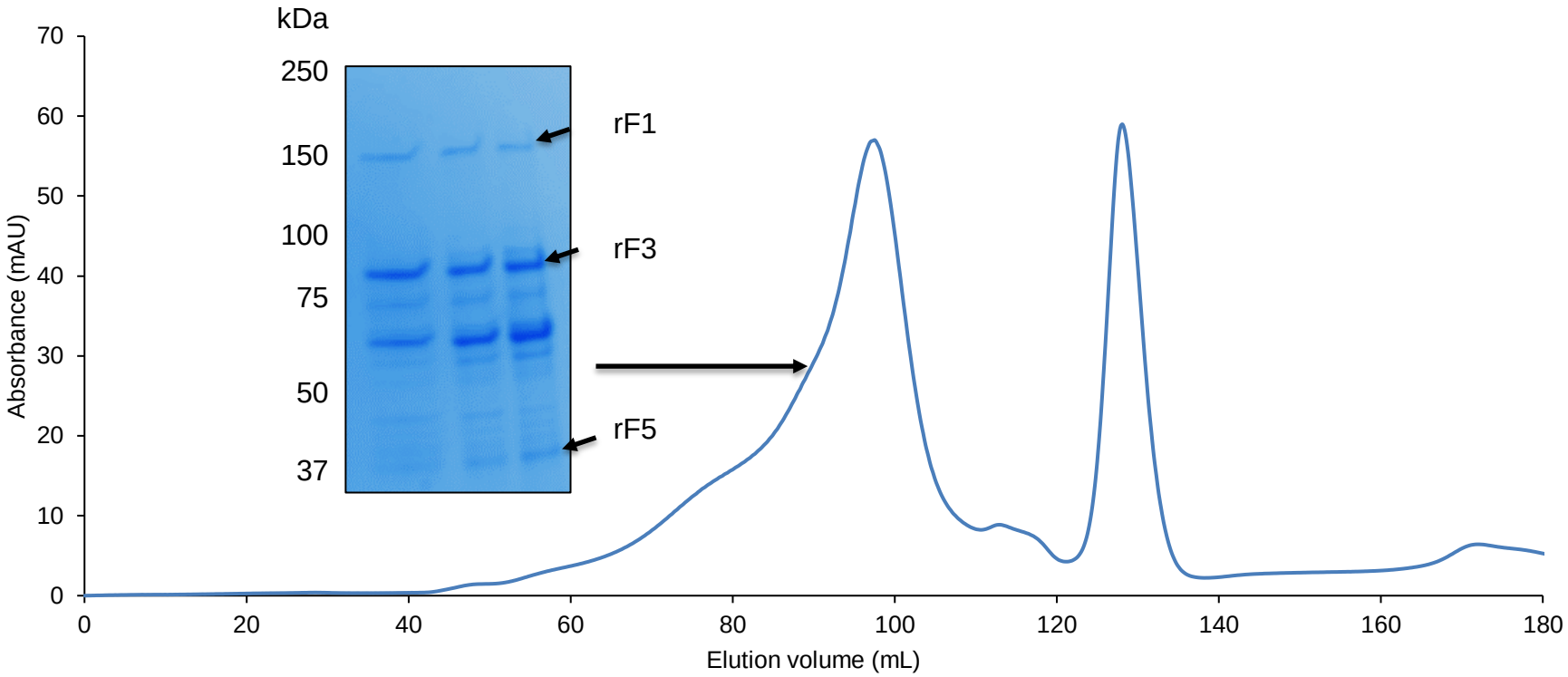

Figure 3.13. SEC co-purification of rF1, rF3 and rF5. The recombinant fragments were co-purified using a Superose 6pg XK16/600 SEC column to determine whether they were capable of associating. Proteins of the expected sizes (rF1 – 150 kDa form; rF3 – ~89 kDa; rF5 – ~38 kDa) were observed in elution fractions at the expected elution volume for an ~277 kDa protein (~90 mL; rLifA elutes at ~80 mL). However, rF5 appeared just under the 37 kDa ladder on previous gels/blots and given that rF3 and rF5 are known to form a trimer (~267 kDa) and an aggregate (~74–440 kDa) respectively, it could not be concluded that the apparent observed association was genuine.

3.7 T cell proliferation assays using rLifA fragments

rLifA and the recombinant fragments were added to cells at a concentration of 2.73 nM, equivalent to 1 µg/mL of rLifA. None of the fragments exhibited lymphostatin activity when exogenously applied to T cells in either isolation or in combination (Figure 3.14). The proliferation indices, with standard deviations, for cells treated with each protein were 0.19 ± 0.03 (rLifA), 1.06 ± 0.1 (rGT), 0.96 ± 0.04 (rF1), 0.96 ± 0.08 (rF3), 1.01 ± 0.13 (rF5) and 0.86 ± 0.03 (rF1, rF3 and rF5 in combination). Although the proliferation index of the fragments in combination was found to be statistically significantly different from cells with ConA alone ($W = 120$, $P = 0.0027$), the fragments clearly did not inhibit proliferation to a similar degree as rLifA. This significance was not observed in experiments where the quantity of rF5 was increased or when uridine diphosphate-N-acetylglucosamine (UDP-GlcNAc) was mixed with the fragments (data not shown).

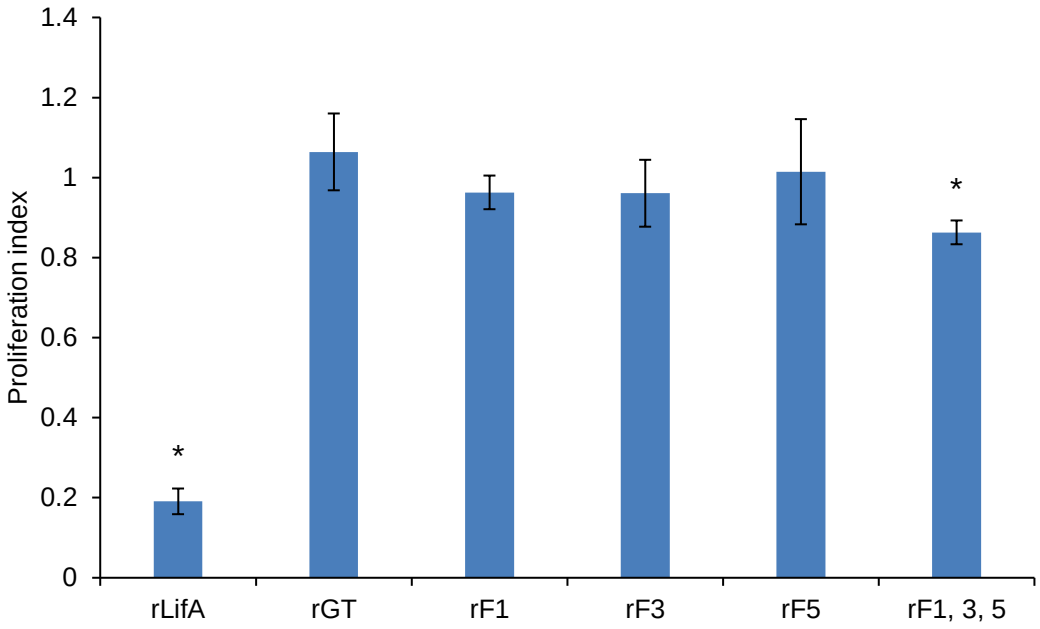

Figure 3.14. The recombinant LifA fragments do not exhibit lymphostatin activity in isolation or in combination against bovine T lymphocytes. An absolute number of 200,000 cells were seeded into the wells of a 96 well plate. Equimolar concentrations of protein were added to cells in triplicate and the results are the average obtained from 3 independent experiments using separate donors. Data were normalised against cells with ConA alone to produce a proliferation index. Error bars indicate the standard deviation of the average proliferation indices from across the 3 experiments. rF1, 3, 5 represents rF1, rF3 and rF5 combined in a molar ratio of 1:1:1. Asterisks indicate proliferation indices that were statistically significantly different from cells with ConA alone.

3.8 Protein transfection

Although the recombinant LifA fragments lacked lymphostatin activity when applied exogenously to T cells, it was hypothesised that rGT and rF1 may retain their activity when introduced into cells by protein transfection. This hypothesis reflects previous studies with LCTs, which established that the N-terminal GT region is sufficient to cause the collapse of the actin cytoskeleton when introduced into epithelial cells by microinjection or fusion to anthrax toxin lethal factor, which can

penetrate the plasma membrane of eukaryotic cells when combined with anthrax toxin protective antigen (Hofmann *et al*., 1997; Busch *et al*., 2000; Rupnik *et al*., 2005; Spyres *et al*., 2001).

3.8.1 X-gal staining

The commercially available Xfect^{TM} Protein Transfection Reagent was tested on bovine T cells using purified β-galactosidase as a control. All imaged cells treated with both transfection reagent and β-galactosidase were heavily stained blue by the X-gal (5-bromo-4-chloro-3-indolyl-β-D-galactopyranoside) substrate of β-galactosidase (Figure 3.15), indicating that β-galactosidase had been transfected into the cells. Cells without transfection reagent or β-galactosidase and cells with transfection reagent alone appeared clear. Cells treated with β-galactosidase alone exhibited staining that was far less intense, which may have been due to β-galactosidase binding to the cell surface.

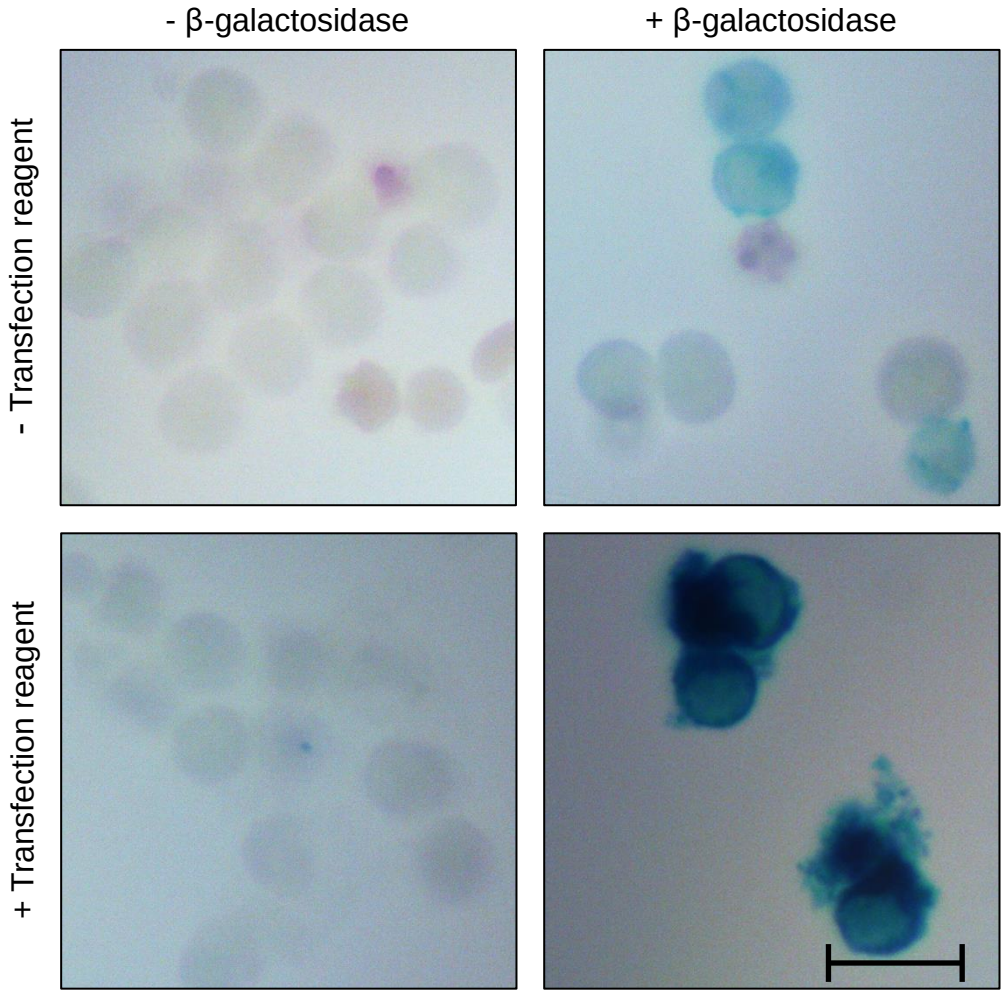

Figure 3.15. β-galactosidase can be transfected into bovine T lymphocytes. As a positive control for the Xfect™ Protein Transfection Reagent, β-galactosidase was transfected into T cells and detected by X-gal staining. Low level staining was observed in some cells treated with β-galactosidase but without transfection reagent, possibly caused by the protein sticking to the cell surface. All cells observed that were treated with both β-galactosidase and transfection reagent were heavily stained by comparison, demonstrating that the transfection reagent functioned as expected. Scale bar = 10 µm. All light microscopy images are of the same scale.

3.8.2 Confocal microscopy of T cells treated with rLifA fragments

To establish if the transfection reagent was capable of transfecting rF1 into T cells, cells were treated with fluorescently labelled rF1 and the Xfect™ Protein

Transfection Reagent and examined by confocal microscopy. Labelled rF1 was observed inside T cells, which had been optically sectioned at 1 μm (Figure 3.16), indicating that it had been introduced into the cells. Labelled rF1 was not visible in T cells that were not treated with transfection reagent.

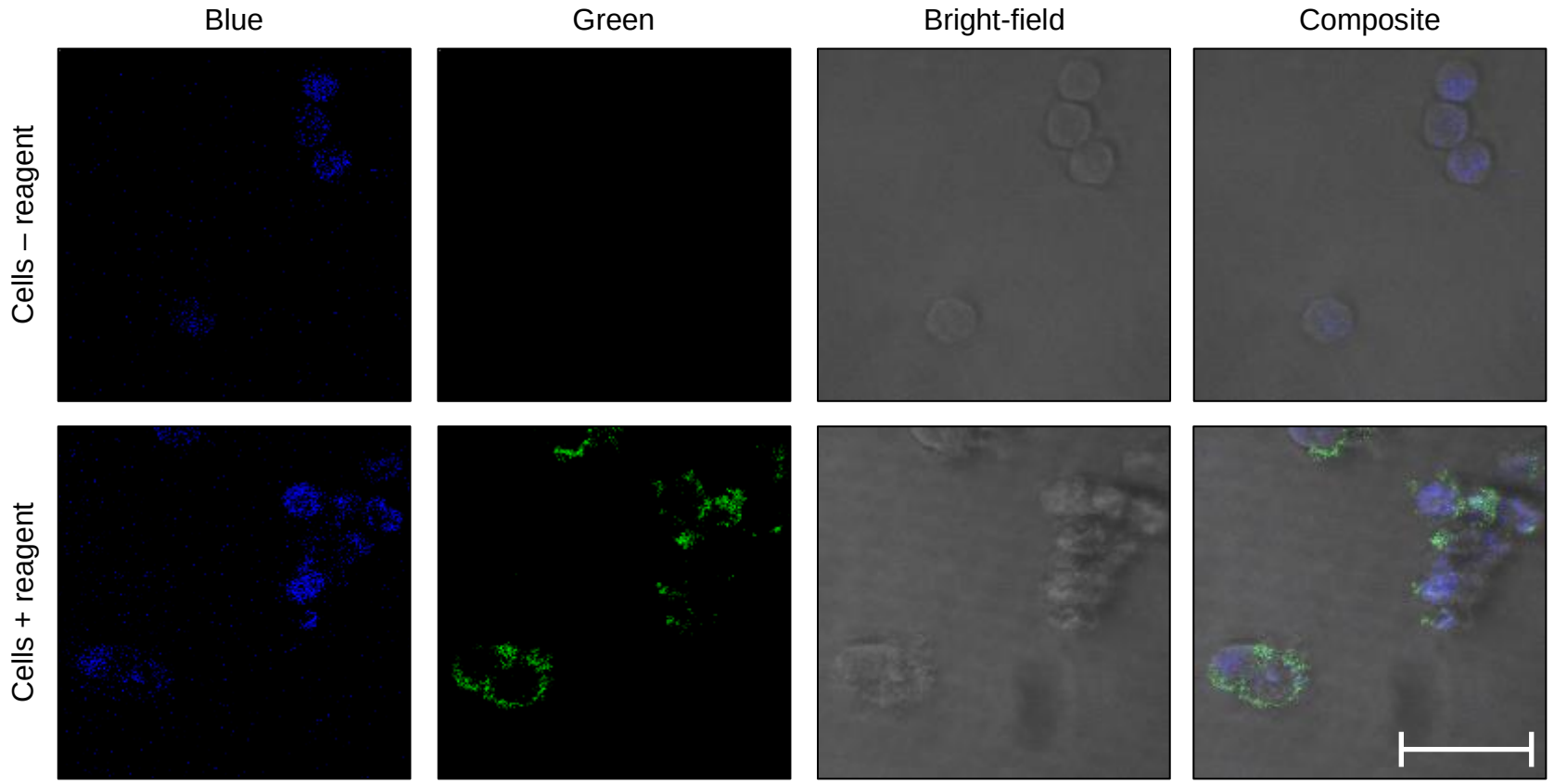

Figure 3.16. rF1 was transfected into bovine T lymphocytes. Fluorescently labelled rF1 (green channel) was transfected into T cells (bright-field channel) using the Xfect^{TM} Protein Transfection Reagent. The nuclei of lymphocytes (blue channel; stained with DAPI (4′,6-diamidino-2-phenylindole)) occupies most of the cells but labelled rF1 can be seen within the area of the plasma membrane (composite), indicating the reagent is capable of inserting rF1 into the cells. rF1 is not observed in cells without transfection reagent. Scale bar = 10 µm. All confocal microscopy images are of the same scale.

3.8.3 Transfection assays

T cell proliferation assays were performed using cells treated with transfection reagent and rF1. The assay required optimising due to cytotoxic effects of the transfection reagent and did not yield consistent results. Ultimately, an assay performed by Dr Robin Cassady-Cain at The Roslin Institute using rGT revealed that the transfection reagent was capable of stimulating T cells without the addition of ConA (Figure 3.17). Despite the transfection reagent being able to insert protein into T cells, the proliferation assay was not a suitable system for measuring the potential inhibitory activity of transfected recombinant LifA fragments.

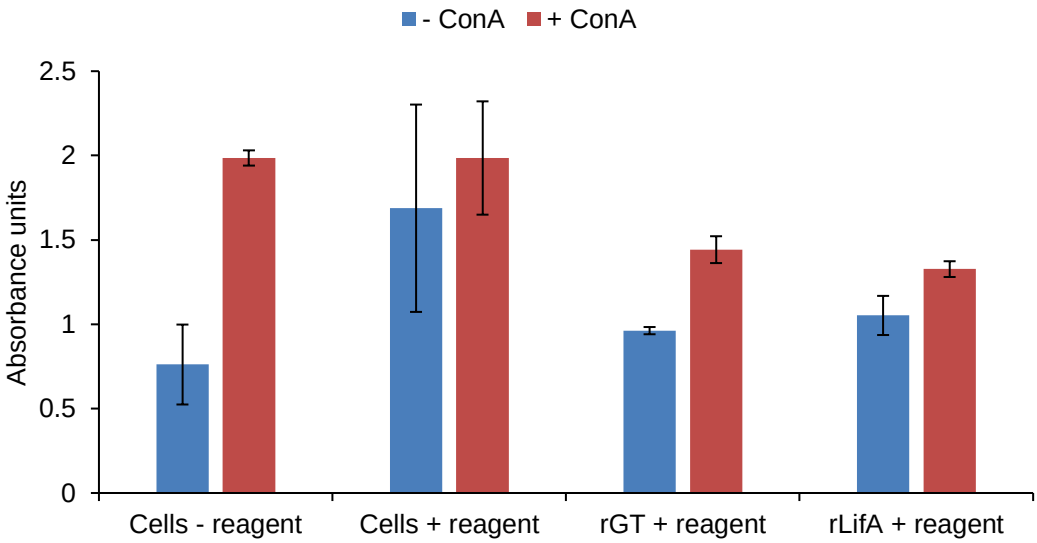

Figure 3.17. Xfect™ Protein Transfection Reagent interfered with T cell proliferation. An absolute number of 200,000 cells, treated with transfection reagent and protein, were seeded into the wells of a 96 well plate. Titrations were carried out in triplicate. The absorbance at 492 nm revealed that the transfection reagent appeared to stimulate T cells that had not been treated with ConA, making the assay unsuitable for measuring proliferation. Error bars indicate the standard deviation of the triplicate wells from one donor. Absorbance units are shown rather than proliferation indices as they show how the proliferation of cells – reagent and cells + reagent compares in the presence/absence of ConA separately. Data were collected by Dr Robin Cassady-Cain, The Roslin Institute.

3.9 Association of LifA fragments with T cells

Association assays were performed to determine whether the recombinant LifA fragments were capable of associating with T cells, similar to full-length rLifA. Proteins species of the expected sizes for rGT and rF1 (~150 kDa variant) were observed in lysates of T cells treated using the optimised protocol from Section 3.3 but rF3 and rF5 could not be detected, even after a long exposure in the chemiluminescent detection method used (Figure 3.18). It is possible that the regions of LifA encompassed by rF3 and rF5 are not capable of associating with T cells unless they are part of an intact protein, or that these two fragments were below the limit of detection for the antibody. A protein species between 100 and 150 kDa that is reactive to anti-LifA antibody was observed only in rLifA treated T cells, suggesting that it is a processed or degraded form of rLifA.

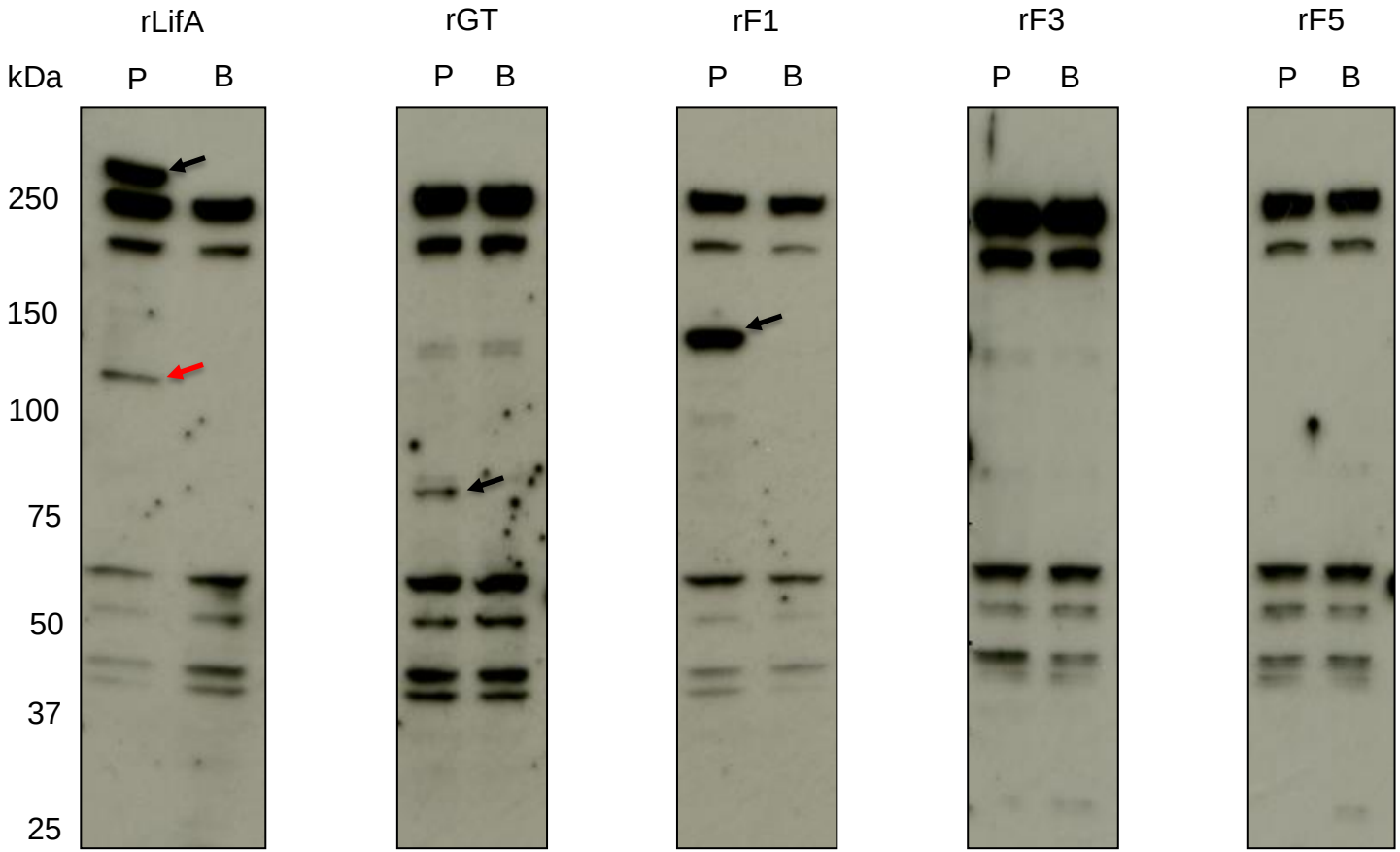

Figure 3.18. rGT and rF1 associated with T cells. T cells were treated with molar equivalents of protein (P)/buffer (B) and incubated at 37 °C for 1 hour. Assays were performed using the same donor on the same day but films were exposed to the membranes for either 5 minutes (rLifA and rF1) or 15 minutes (rGT, rF3 and rF5) to achieve the clearest blots. Full-length rLifA (~365 kDa), rGT (~96 kDa) and rF1 (~150 kDa; marked with arrows) were observed in treated T cell lysates but rF3 (~89 kDa) and rF5 (~38 kDa) could not be detected. A quantity of 2 ng of rLifA was used as a positive control (not shown on blot). The red arrow indicates a putative processed form of rLifA. Experiments were performed using 2 separate donors and representative blots are shown.

3.10 Association of LifA fragments with T cells in the presence of UDP-GlcNAc

As our previous research established that WT rLifA can bind to UDP-GlcNAc (Cassady-Cain *et al*., 2016) and GlcNAc moieties are abundant on cellular glycosaminoglycans and surface glycoproteins, we sought to determine if binding of rGT or rF1 to T cells may be competitively inhibited by free UDP-GlcNAc. We hypothesised that increasing the concentration of exogenous UDP-GlcNAc would competitively inhibit the interaction between the fragments and cell surface-bound GlcNAc. To investigate this, rGT and rF1 as well as rLifA were pre-incubated with different concentrations of UDP-GlcNAc before being exposed to T cells from three independent donors.

The concentrations of UDP-GlcNAc used were based around the dissociation constant (K_d) of UDP-GlcNAc with rLifA (120 ± 30 µM; Cassady-Cain *et al*., 2016), the concentration at which 50 % of the UDP-GlcNAc is bound to rLifA. The highest concentration (1 mM) was chosen, as at ~10 times the K_d, > 90 % of the UDP-GlcNAc should be bound to the proteins (reviewed in Price *et al*., 2007). The concentrations of 50 and 250 µM were chosen so that concentrations above and below the K_d were included.

The association of rLifA with T cells was not affected by exogenous UPD-GlcNAc. rGT and rF1 associated with T cells in a manner independent of UDP-GlcNAc concentration (Figure 3.19), suggesting that the fragments did not bind to GlcNAc moieties on the T cell surface, or that insufficient exogenous UDP-GlcNAc was used to competitively inhibit binding.

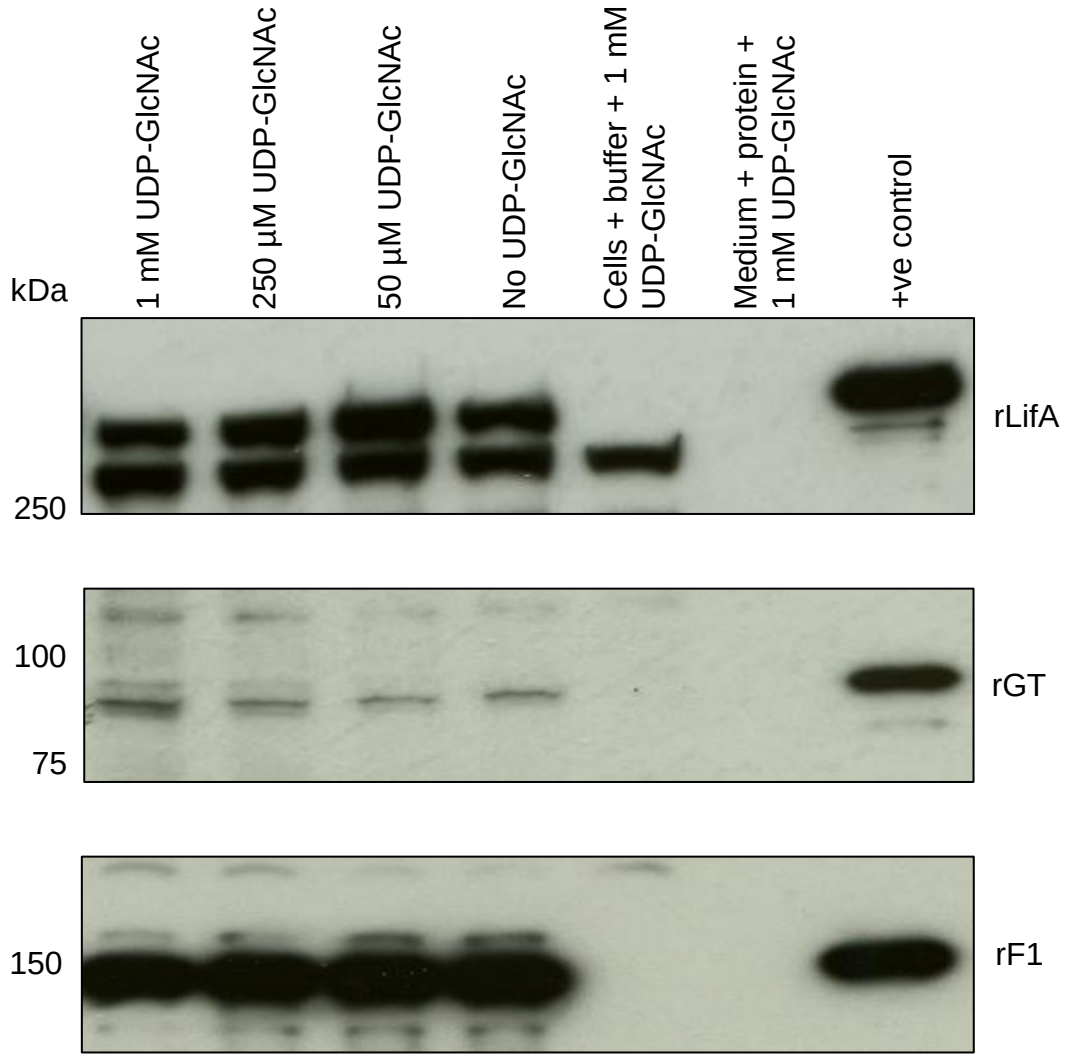

Figure 3.19. The association of rGT and rF1 with T cells was not inhibited by exogenous UDP-GlcNAc. Equimolar concentrations of protein were pre-incubated with different concentrations of UDP-GlcNAc before incubation with T cells. Experiments were performed using 3 separate donors and representative blots are shown. Even at 1 mM, ~10 times the K_d of UDP-GlcNAc with rLifA (Cassady-Cain *et al*., 2016), the fragments associated with T cells, suggesting that the association was not caused by the fragments binding to GlcNAc on the T cell surface.

3.11 Discussion

Toward an understanding of the structure and function of lymphostatin, domains predicted by limited proteolysis were cloned, expressed and purified. The

recombinant LifA fragments did not reconstitue lymphostatin activity when applied exogenously to bovine T cells, either in isolation or in combination. Based on our knowledge of large clostridial toxins homologous to LifA, it is possible that this is a consequence of having separated the putative catalytic domain(s) of LifA from the region(s) involved in cell binding and intracellular processing. To address this, we sought to introduce the predicted glycosyltransferase domain (rGT and rF1) directly into T cells, mindful that a similar strategy for LCTs could rescue the cytotoxic activity of the native toxin (Hofmann *et al*., 1997; Busch *et al*., 2000; Rupnik *et al*., 2005; Spyres *et al*., 2001). Despite rF1 being successfully transfected into T cells, the transfection reagent used interfered with the proliferation of the lymphocytes, rendering the T cell proliferation assay unsuitable for measuring lymphostatin activity. Microinjection was suitable for experiments with LCTs as these measured morphological changes in cells (Hofmann *et al*., 1997; Busch *et al*., 2000; Rupnik *et al*., 2005), however, the number of T cells required for a proliferation assay make this an unsuitable delivery system for the recombinant fragments. Creating a fusion protein of the fragments and the N-terminal 255 amino acids of anthrax toxin lethal factor, then combining them with anthrax toxin protective antigen may be a more effective way of transfecting the proteins into large numbers of T cells. Protective antigen facilitates the translocation of lethal factor and the adjoined protein across the endosomal membrane (Arora and Leppla, 1993; Milne *et al*., 1995). This method has been shown to be effective at delivering the N-terminal 556 amino acids of TcdB into CHO cells (Spyres *et al*., 2001), suggesting that it can be used for large proteins such as rGT and rF1.

There are also a number of methods that could be used to transfect genetic material into cells, which will then express the gene product. A plasmid encoding rGT or rF1 could be transiently transfected into T cells for short-term expression, or alternatively, stable transfection, in which the plasmid is inserted into the host cell genome, could be used (reviewed in Kim and Eberwine, 2010). However, stable transfection is not suitable for primary T cells as it requires an immortalised cell line that can be cultured and selected for using an additional selection marker, such as neomycin resistance (reviewed in Stepanenko and Heng, 2017). Jurkat cells could be used as a T cell model for stable transfection but they could not be used in

proliferation assays as they are immortal and therefore proliferate continuously. However, there is evidence that rLifA inhibits interleukin expression in Jurkat cells, which could be used as a method for examining the activity of the fragments (Malstrom and James, 1998; Stevens Laboratory, unpublished data). One major drawback of stable transfection is that the DNA vector is inserted randomly into the host cell genome, which can disrupt host cell genes and cause non-specific effects (reviewed in Stepanenko and Heng, 2017). Viruses such as herpes simplex virus and adenovirus can be used for stable transfection but are limited by size of the DNA package (reviewed in Kim and Eberwine, 2010). Recombinant, replication deficient adenovirus has been used to efficiently transfect *lacZ* into both primary T cells and Jurkat cells. It is unclear what effect this had on proliferation but phorbol myristate acetate (PMA)/ionomycin-stimulated cytokine production was not affected (Chen *et al*., 2002b). While no evidence could be found of herpes simplex virus being used for transfection of T cells, the viral protein Us3 is known to inhibit T cell activation and increase expression of the anti-inflammatory cytokine IL-10 (Sloan and Jerome, 2007; Yang *et al*., 2015). Therefore, any viral vectors used for transfection would have to be screened for potential effects on lymphocyte proliferation.

Alternatively, chemical reagents, such as calcium phosphate, DEAE-dextran or lipofectin can be used for transient transfection. These are not limited by DNA size but have a lower transfection efficiency than viral vectors and can be cytotoxic (reviewed in Kim and Eberwine, 2010; reviewed in Stepanenko and Heng, 2017). The transient transfection of RNA is another possible transfection method. RNA of rF1 and rGT could be produced using a commercially available *in vitro* transcription kit, which would allow for rapid expression of the encoded proteins since transcription is not required (reviewed in Kim and Eberwine, 2010). However, there are certain elements of mRNA that are not present in DNA, such as the 5′ cap and poly-A tail, as well as nucleoside modifications that must be taken into account when a plasmid is designed for *in vitro* transcription (Elango *et al*., 2005; Rozenski *et al*., 1999).

Rather than measuring the effect of transfected proteins on T cell proliferation, an alternative read-out could be used. LifA has been reported to inhibit the expression of multiple cytokines in T cells including IL-2, IL-4 and IFN-γ

(Klapproth *et al*., 1995, 1996 and 2000; Malstrom and James, 1998; Cassady-Cain *et al*., 2017). Therefore, measuring cytokine expression could be used to detect effects of transfected rGT and rF1 using an enzyme-linked immunosorbent assay. Appropriate controls could be included to ensure that the transfection reagent does not affect cytokine expression.

The lack of lymphostatin activity with the rF1 fragment is consistent with previous observations using F1 released by limited trypsin proteolysis and purified by anion exchange chromatography (Cassady-Cain *et al*., 2016). Previously, and in these studies, protein species of the expected sizes for rF1, rF3 and rF5 were observed in the same elution fractions of a size exclusion column, suggesting that they may be able to associate. However, no lymphostatin activity was detected on T cells treated with a mixture of the fragments and since rF3 and rF5 are known to form multimers it could not be concluded that the fragments were genuinely associating with each other under the assay conditions. It is possible that co-transformation of the expression strain with each fragment plasmid, so that all fragments are present at genesis, may be required for the recombinant fragment to associate.

rGT and rF1 were capable of associating with T cells and did so in a GlcNAc-independent manner. LCTs bind host cell receptors via multiple domains located in C-terminal portion of the proteins (von Eichel-Streiber and Sauerborn, 1990; Schorch *et al*., 2014; LaFrance *et al*., 2015; Manse and Baldwin, 2015; Tao *et al*., 2016; Lambert and Baldwin, 2016) and therefore I hypothesised that the C-terminus may be required for LifA binding and cell entry. If the C-terminus is required for receptor binding in LifA, it is unclear why rGT and rF1 were observed to associate with T cells while the two C-terminal fragments did not. Using a fluorescent secondary antibody in these assays may reveal low concentrations of bound rF3 and rF5 however. It is possible that, just as multiple domains are required for LCT binding, the N-terminus of LifA may also play a role in cell binding. *In silico* analysis of LifA has shown that the N-terminus shares homology with the nucleotide binding domain of reticulocyte binding proteins from *Plasmodium*, which are responsible for adherence to reticulocytes (Galinski *et al*., 1992; Triglia *et al*., 2001; Grüber *et al*., 2011). The N-terminal amino acid residues 1052–1095 of LifA

also share 32 % homology with M5 protein from *S. pyogenes*, which is thought to bind CD46 on keratinocytes (Courtney *et al*., 2002). However, LifA is only homologous to the N-terminal amino acids 86–126 of M5 protein, whereas it is the conserved C-terminal end of M proteins that is implicated in the adhesion of *S. pyogenes* to keratinocytes (Okada *et al*., 1995; Perez-Casal *et al*., 1995). LifA also exhibits homology to HMW2, which is required for adherence of *M. pneumoniae* to cells, however, the role of HMW2 may be indirect as it is part of the *Mycoplasma* cytoskeleton (reviewed in Balish, 2014). Similarly, interaptin plays a role in the cytoskeleton of *D. discoideum*, linking actin to intracellular membrane compartments (Rivero *et al*., 1998). Therefore, the significance of the homology between LifA and the proteins HMW2 and interaptin is unclear. It is also possible that rGT and rF1 are able to bind to T cells via regions of the proteins that are not normally exposed in full-length LifA.

The association assay is limited in that it cannot distinguish proteins bound to the outer membrane of T cells with those that have been taken up by the cells. Therefore, it is unclear whether rGT and rF1 are adhering to the surface of the T cells or are being endocytosed. Fixing T cells before treating them with the recombinant LifA fragments could be used but carries the risk that receptors may be denatured by the fixative. Similarly, future binding experiments could be conducted at low temperature or in the presence of specific inhibitors of uptake pathways. Alternatively, quenching reagents such as trypan blue could be used to distinguish between surface-bound and internalised fragments (Loike and Silverstein, 1983; Sahlin *et al*., 1983). T cells could be treated with FITC-labelled rGT or rF1 for varying durations then quenched with trypan blue. Flow cytometry could then be used to quantitatively determine whether the fragments are internalised over time (Vranic *et al*., 2013). Had rGT and rF1 associated with T cells in a GlcNAc-dependent manner, it could be inferred that they are still capable of binding the sugar. However, as this is not the case, no conclusions can be made about the sugar binding ability of rGT and rF1. The possibility of these proteins binding to other sugars besides GlcNAc on the T cell surface cannot be ruled out, as the sugar binding ability of rLifA has only been tested using UDP-GlcNAc and UDP-Glc (Cassady-Cain *et al*., 2016). Future studies could examine the ability of the rF1 and

GT fragments to bind UDP-GlcNAc by measuring changes in tryptophan fluorescence, as we previously described (Bease, 2015; Cassady-Cain *et al*., 2016).

There were a number of limitations with the experiments using the recombinant LifA fragments, one of which was the purity of the proteins. With the exception of rGT, all of the fragments used in these experiments were only purified by IMAC and SEC, whereas full-length rLifA is purified with an additional anion exchange step. This lower purity affects the concentration measurement, which is used to determine the quantity of protein required for each experiment. Therefore, negative results may have been the consequence of less protein being used and failure to achieve equimolar amounts to rLifA. Additionally, contaminating proteins may affect T cell proliferation. The low purity of the fragments also prevented any structural data from being gathered. rLifA and the DXD mutant variant rLifA$^{DTD/AAA}$ were biophysically characterised by a number of experiments when they were originally produced (Bease, 2015; Cassady-Cain *et al*., 2016). These biophysical characterisation experiments require the tested proteins to be of a high purity, which could not be achieved with rF1 and rF5. Despite rGT and rF3 being purified to a higher degree using anion exchange chromatography by Dr Liz Blackburn, no biophysical measurements were made for these proteins. Therefore, the only data regarding whether the fragments were correctly folded is derived from the SEC purification traces, which provides an approximate size for the proteins. However, the SEC purification of rF5 demonstrates that the protein likely forms aggregates. Additionally, an attempt to purify rF1 by anion exchange chromatography shows that the recombinant protein has different properties from the fragment released by the tryptic digest of full-length rLifA, which was purified using the same method (Cassady-Cain *et al*., 2016).

If the purification of the recombinant fragments could be optimised, the proteins could be subjected to the same biophysical experiments performed with rLifA and rLifA$^{DTD/AAA}$. Dynamic light scattering could be used to determine whether the proteins had aggregated and circular dichroism could provide information on the secondary structure of the proteins. It would be particularly useful to compare the circular dichroism spectra of rF1 and tryptic digest F1 to determine how these two fragments differ. Thermal denaturation assays would allow for the

examination of the thermal stability of the recombinant fragments, giving an indication as to whether they were correctly folded.

The apparent shortening of rF1 from ~188 to ~150 kDa was an unexpected result that may have unintended consequences for the protein as the part of the protein that is lost may be required for activity. It is not clear what portion of the protein is lost, or by which process this happens, but it was hypothesised that the CP domain may be involved. MALDI-TOF analysis of tryptic fragments of the ~150 kDa species of rF1 may help to delineate which region is absent. In LCTs, a CP domain mediates autocatalytic cleavage of the proteins between the GT and CP domains (Egerer *et al*., 2007; Pruitt *et al*., 2009; Guttenberg *et al*., 2011; Rupnik *et al*., 2005; Kreimeyer *et al*., 2011) and a similar process could occur in LifA (see Chapter 4). This process occurs after a conformational change in LCTs inside cells (Qa'dan *et al*., 2000 and 2001; Barth *et al*., 2001) and can be challenging to reproduce *in vitro* owing to the potential requirement for low pH-induced structural changes and a co-factor. Although there were concerns that rF1 may be cleaved at the potential prepilin peptidase sites identified by Nicholls *et al*. (2000), the products produced by cleavage at these sites would be shorter than the observed ~150 kDa form of rF1.

Other structural abnormalities may also account for the inactivity of the recombinant LifA fragments. The additional methionine residues at the N-terminus of rF3 and rF5 as well as the C-terminal polyhistidine tags on rF1 and rF3 interrupt the normal amino acid sequence of LifA. In particular, since the sequences for rF3 and rF5 are joined in the full-length protein, the extra amino acids inserted between them could disrupt interactions necessary for the fragments to associate. Such issues could be resolved by using cleavable tags. N-terminal His-tags can be cleaved using a number of enzymes such as the TAGZyme system, which uses dipeptidyl peptidase I, glutamyl cyclotransferase and pyroglutamyl aminopeptidase (Pedersen *et al*., 1999; Schäfer *et al*., 2002; reviewed in Waugh, 2011). Alternatively, where it is unsuitable to use an N-terminal His-tag, C-terminal His-tags with tobacco etch virus or tobacco vein mottling virus protease cleavage sites can be used (Eschenfeldt *et al*., 2010). It is also possible to remove the methionine residues attached to the N-termini of rF3 and rF5. A modified form of methionine aminopeptidase has been reported to

remove the N-terminal methionine from bulky and acidic penultimate residues, as well as from small residues such as the penultimate glycine and proline found in rF3 and rF5 respectively (Liao *et al*., 2004). The main drawback of these techniques is that they require separation of the recombinant proteins from the proteases, which would likely dilute the proteins.

Although the recombinant fragments represent the three main tryptic digest fragments of rLifA, they do not cover the whole amino acid sequence of LifA. No recombinant fragment was made for aa 1621–2110. Given that this region is predicted to contain an aminotransferase II motif and a transmembrane domain (Klapproth *et al*., 2005; Nicholls *et al*., 2000), it may be required for the function of the full-length protein. Producing and purifying this sequence could be useful in order to determine whether this region can rescue lymphostatin activity when mixed with the other fragments. A lack of lymphostatin activity, even when fragments representing the whole sequence of the full-length protein are combined, would likely be indicative that these recombinant fragments do not associate. Alternatively, if the tryptic digest LifA fragments could be produced in sufficient quantities, they could be tested for inhibitory activity against T cells since there is evidence that these fragments actually associate.

Lastly, there appeared to be a lack of epitope affinity of anti-LifA antibody for rF5. This may be due to the small size of rF5 or that the F5 sequence is normally buried within the full-length protein, which may explain the apparent low solubility of rF5 and why it forms aggregates. This is consistent with previous attempts to detect the C-terminal end (aa 1897–3223) of Efa1 from EHEC O111:H- cloned into *E. coli* K-12 with an anti-6 x His (Abu-Median *et al*., 2006).

In conclusion, while the recombinant fragments of lymphostatin may yet prove useful for structural studies, their use in cellular assays is limited. Future studies of functional domains of lymphostatin will require the adoption of either more sophisticated approaches to using these recombinant fragments or alternative strategies.

4 The role of the cysteine protease motif in processing and activity of lymphostatin

4.1 Introduction

Lymphostatin contains a cysteine protease (CP) domain that is homologous to the CP domain of *Yersinia* YopT and other C58 family proteases (Shao *et al*., 2002). The protease activity of these proteins is dependent on a catalytic triad consisting of Cys, His and Asp residues. Such residues are present in LifA at amino acid positions 1480, 1581 and 1596 respectively (Shao *et al*., 2002). Some C58 proteases, such as *Yersinia* YopT and LopT from *Photorhabdus luminescens*, cleave Rho GTPases within target cells and act as cytotoxins (Shao *et al*., 2002; Brugirard-Ricaud *et al*., 2005). LifA, however, has not been reported to exhibit cytotoxicity in studies using diverse cell types (Klapproth *et al*., 1995 and 2000; Malstrom and James, 1998; Nicholls *et al*., 2000; Bease, 2015; Cassady-Cain *et al*., 2016). Other C58 proteases, such as *Pseudomonas syringae* AvrPphB and *Rhizobium* NopT, undergo CP domain-mediated autoproteolysis (Shao *et al*., 2002; Dai *et al*., 2008).

Large clostridial toxins (LCTs), which have N-terminal homology to LifA, also possess a CP domain with a D/H/C orientated catalytic triad (reviewed in Chandrasekaran and Lacy, 2017). After entering host cells by receptor-mediated endocytosis (Papatheodorou *et al*., 2010), LCTs undergo a pH-induced conformational change in the endosome resulting in pore formation in the membrane and insertion of the N-terminus into the host cell cytosol (Qa'dan *et al*., 2000 and 2001; Barth *et al*., 2001; Figure 4.1). The CP domain of LCTs then autocatalytically cleaves the protein to release the glucosyltransferase domain, which targets Rho GTPases (Pfeifer *et al*., 2003; Egerer *et al*., 2007; Guttenberg *et al*., 2011; reviewed in Chandrasekaran and Lacy, 2017). The autocatalytic cleavage of LCTs is dependent on the cellular co-factor inositol hexakisphosphate ($InsP_6$; Reineke *et al*., 2007), but previous attempts to induce autocatalytic cleavage of rLifA using $InsP_6$ *in vitro* showed no evidence of effect (Cassady-Cain *et al*., 2016).

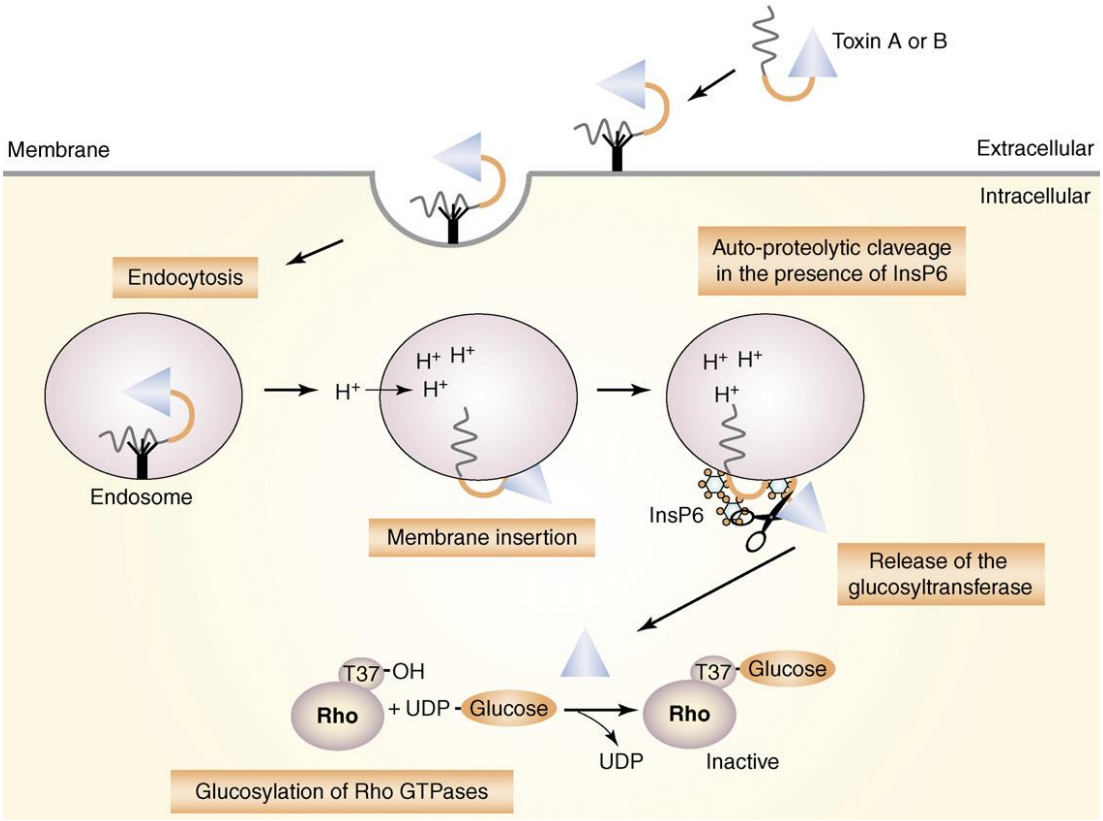

Figure 4.1. Schematic representation of the uptake and processing of large clostridial toxins (LCTs) in host cells. LCTs are taken up by receptor-mediated endocytosis. Acidification of the endosome results in a conformational change in the proteins and insertion through the membrane. The proteins are autocatalytically cleaved by the cysteine protease domain, an event that requires the co-factor inositol hexakisphosphate, and the N-terminal glucosyltransferase domain is released into the cytoplasm where it glucosylates Rho GTPases resulting in the collapse of the actin cytoskeleton (from Jank and Aktories, 2008).

Few studies have been carried out to investigate the role of the CP domain of LifA and those that have were limited by a lack of precise mutagenesis and structural information on the mutant protein. For example, the CP domain of LifA was previously reported to be required for the colonisation of mice by *C. rodentium* (Klapproth *et al*., 2005). However, the method used to generate a CP domain mutant introduced a stop codon to the *lifA* gene resulting in protein truncation rather than an in-frame deletion as claimed by the authors. This was corrected in a second study by

the same laboratory, which implicated the CP domain in LifA-mediated redistribution of β-catenin and E-cadherin at enterocyte apical junctions and the activation of RhoA during *C. rodentium* infection (Babbin *et al*., 2009). The relevance of such events to pathogenesis is unclear and the study did not investigate the impact of the CP domain mutation on intestinal colonisation or lymphostatin activity. In another study, it was independently reported that a deletion of over 100 amino acids, encompassing the entire C/H/D motif, marked by a triple alanine sequence in EPEC E2348/69 abolished the inhibitory activity of LifA against ConA-stimulated PBMCs (Deacon *et al*., 2010). However, since no biophysical information was obtained for this protein, it cannot be ruled out that loss of lymphostatin activity was caused by structural changes to the protein.

Given that CP domains homologous to that of LifA are known to be required for autoproteolysis in a number of bacterial virulence factors, it was hypothesised that LifA is taken up by cells and undergoes CP domain-mediated processing to release the glycosyltransferase domain into the cytosol, similar to LCTs. The detection of a circa (c.) 140 kDa protein in the lysates of rLifA-treated T cells that was reactive to anti-LifA antibody (see Section 3.9) suggests that this may happen. To test this hypothesis, I substituted the predicted catalytic Cys^{1480} residue for an alanine residue using the existing pRham-LifA-6 x His plasmid by site-directed mutagenesis, then expressed and purified the protein. The mutant protein was assayed for its ability to inhibit mitogen-stimulated T cell proliferation and to be processed within different cell types. Biophysical properties of the protein were also analysed relative to wild-type (WT) lymphostatin. It was predicted that the mutation would abolish lymphostatin activity against T cells and prevent the appearance of the suspected cleavage product.

4.2 Generation of the pRham-LifA-6 x His C1480A clone

QuikChange site-directed mutagenesis was performed using the existing pRham-LifA-6 x His plasmid as a template to create the C1480A substitution in the *lifA* gene (Figure 4.2). An alanine substitution was chosen because alanine residues are small, non-polar and unreactive, which should allow the mutant protein to fold

correctly and be structurally similar to the WT protein. Previous experiments using this method were successful in substituting the DXD motif of the glycosyltransferase domain with a triple alanine sequence, which abolished UDP-GlcNAc binding and lymphostatin activity without affecting the structure of the protein (Bease, 2015; Cassady-Cain *et al.*, 2016). Primers were designed to create a C1480A substitution and introduce a *BsrD*I restriction site at the same location in the plasmid (Figure 4.2A; see Section 2.8). Template plasmid with no primers and primers with no template plasmid were used as negative controls for the PCR. The pWhitescript plasmid and oligonucleotide control primers were used as a positive mutagenesis control. The oligonucleotide control primers repair a mutation in the β-galactosidase gene, which can be detected by blue-white screening using a chromogenic β-galactosidase substrate. The pUC18 plasmid was used as a positive transformation control because it contains part of the *E. coli lac* operon, which complements the host cell's defective *lac*^{q}*ZΔM15* gene, and can also be detected by blue-white screening using a chromogenic β-galactosidase substrate.

Sixty-four transformants were obtained with *Dpn*I digested DNA derived from the PCR reaction to introduce the C1480A substitution into the pRham-LifA-6 x His plasmid. This was within the expected range of 10–1000 colonies per plate. The transformants were cultured overnight to make glycerol stocks. Two colonies grew on the plate with cells transformed with the 'no template' control. The pWhitescript control had a mutagenesis efficiency of 95.4 %.

Ten of the putative C1480A substitution clones were screened by colony PCR, using primers to amplify the full-length *lifA* gene and vector, and analysed by agarose gel electrophoresis. All 10 tested positive for the presence of the full-length *lifA* gene and plasmid (data not shown). The colonies were screened against purified parental plasmid as a positive control and a no template negative control. To test whether these transformed colonies contained the C1480A mutation and were not simply derived from the template, they were screened by *BsrD*I digestion.

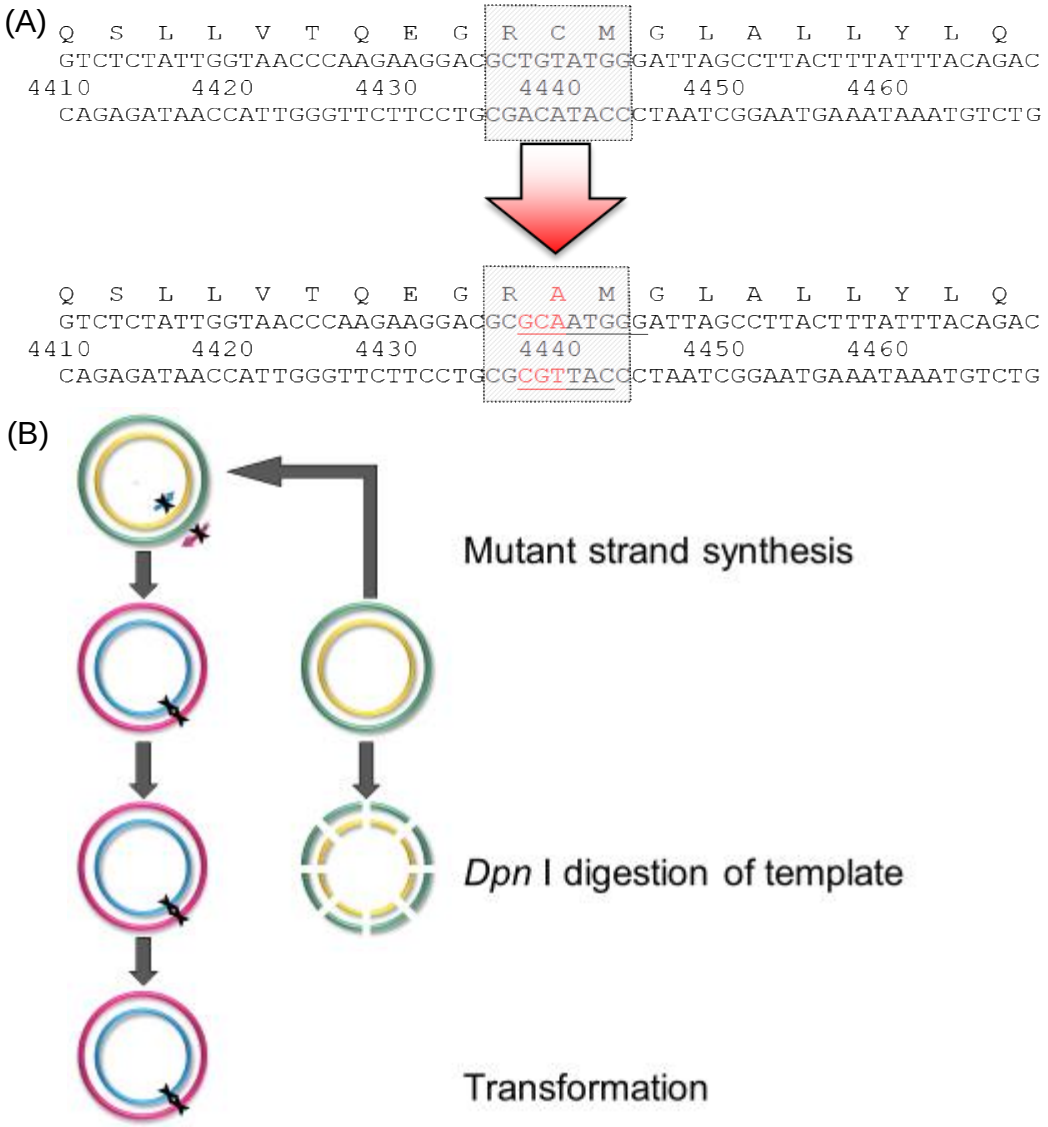

Figure 4.2. The process of creating the C1480A substitution mutant of LifA. (A) Nucleotide and amino acid sequence of the part of the catalytic C/H/D motif within the putative cysteine protease domain of LifA, highlighting the codon that was targeted for site-directed mutagenesis in order to create an alanine substitution mutant. It was also possible to incorporate a new *BsrD*I restriction site (GCAATGGG) at this location. (B) Schematic of the procedure for QuikChange Mutagenesis. Mutant strand synthesis is carried out using the mutagenic primers to replicate the entire plasmid using PCR. This is followed by *Dpn*I digestion of methylated and hemimethylated template DNA to remove the parental plasmid DNA. Finally, the mutated plasmid is transformed into chemically competent cells (adapted from Agilent Technologies, 2015).

In the WT *lifA* sequence amplified by primers LifA FL For3 and LifA FL Rev8, there are two *BsrD*I restriction sites, whereas an additional *BsrD*I site was expected to be introduced within this amplicon with the C1480A substitution (Figure 4.3), thereby providing a rapid screen to identify putative mutant clones. Digestion of amplicons generated by PCR with LifA FL For3 and LifA FL Rev8 was expected to give fragments of ~1686, 1258, 1051 and 174 bp on a gel if the plasmid was mutated successfully (Figure 4.3). If the mutant insert was not present, bands of ~2735, 1258 and 174 bp would be expected. All but one of the clones tested were found to contain the mutant insert. The clones were screened against *BsrD*I digested template plasmid, amplified with primers LifA FL For3 and LifA FL Rev8, and a 'no template' negative control. The two colonies that grew on the 'no template' control plate were also screened and found not to contain the pRham-LifA-6 x His plasmid. Excess plasmid from the PCR reaction was observed at ~10 kb.

From the putative mutant clones identified, three clones were verified by sequencing, initially at the site of mutation using primers LifA FL For7, LifA FL For8, LifA FL Rev10 and LifA FL Rev11 to confirm that the expected sequence was present. Once this was confirmed, the entire *lifA* gene of two clones was sequenced to verify that no additional mutations were introduced during the mutagenesis process. Both clones were verified to contain the appropriate mutation, however, one clone was found to contain a G-T substitution at position 6999 of the gene sequence, resulting in a glycine-cysteine substitution. The other clone contained the expected sequence of the mutated EPEC E2348/69 *lifA* gene and was carried forward for further characterisation (see Appendix 4 for full sequence).

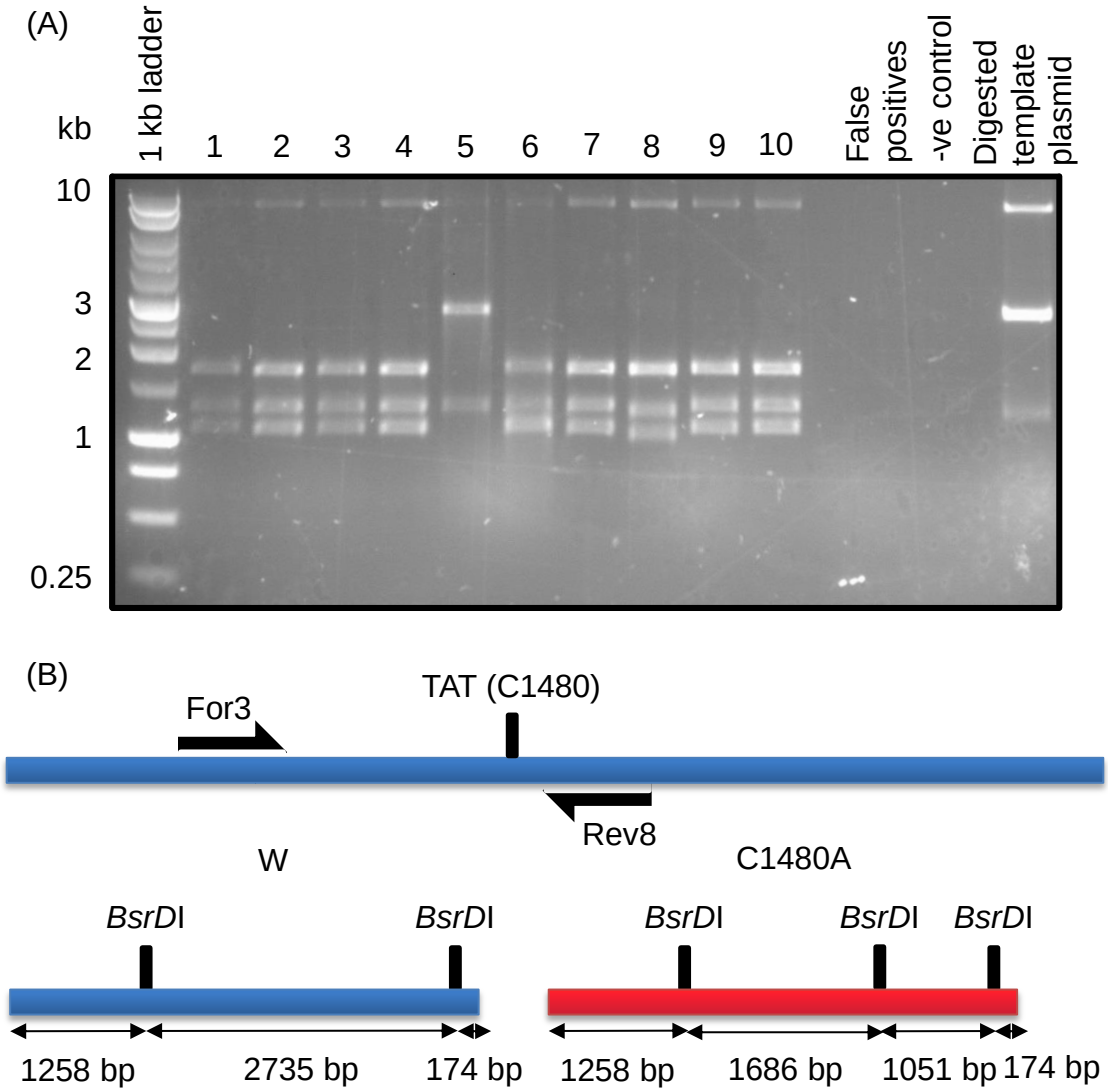

Figure 4.3. *BsrD*I digestion of amplicons from putative pRham-LifA-6 x His C1480A plasmid clones. (A) Of the 64 colonies that grew on a kanamycin plate, 10 were selected to be screened by *BsrD*I digestion of amplicons generated by PCR using primers LifA FL For3 and LifA FL Rev8. Two colonies that grew on a negative control plate were tested to confirm that they were false positives. Nuclease-free water was used as a negative control. Digested parent plasmid was included as a control. Excess plasmid from the PCR reaction can be seen at ~10 kb. Out of the 10 putative C1480A substitution clones selected, all but one tested positive for the presence of the C1480A mutation. (B) Schematic showing the expected sizes of amplified *lifA* gene products of *BsrD*I digestion. The 174 bp fragment produced by positive and negative clones is too faint to be visualised on the gel and so the image has been cropped to the limit of the lowest marker.

4.3 Production of recombinant LifA^{C1480A} protein

Pilot protein expression assays were performed in parallel to the sequencing analysis using the three clones that were verified for the C1480A substitution. The pRham-LifA-6 x His C1480A plasmids were examined for their ability to produce recombinant LifA^{C1480A} (rLifA^{C1480A}) when induced by rhamnose. Clones were grown under the conditions previously identified as optimal for the production of WT rLifA and rLifA$^{DTD/AAA}$ (Bease, 2015; Cassady-Cain *et al*., 2016). Uninduced samples from the mutant plasmid-containing cells were used to ensure that the rLifA^{C1480A} was not produced without rhamnose induction.

In pilot experiments, cells transformed with the mutant plasmids were capable of producing a protein of the expected size of full-length rLifA^{C1480A} (~365 kDa) when induced by the addition of rhamnose to the culture, and the rLifA^{C1480A} protein could be found in the soluble and insoluble cell lysate fractions by western blotting (Figure 4.4). rLifA^{C1480A} was not present in the uninduced mutant plasmid-containing cells. While the size of the main reactive species in insoluble fractions of clones 1 and 2 appeared to be lower than that produced by clone 3, this was not evident upon analysis of the soluble fractions and is inferred to be a gel artefact (Figure 4.4).

The pRham-LifA-6 x His C1480A plasmid from clone 1 was transformed into *E. cloni*® 10G cells. These cells were found to express more protein than XL-10 Gold Ultracompetent cells and have been used previously for the expression of WT rLifA and derived proteins (Bease, 2015; Cassady-Cain *et al*., 2016; see Chapter 3). They have also previously been shown to be the best expresser of full-length rLifA in comparison to other expression strains tested (Walkinshaw Laboratory, unpublished data). *E. cloni*® 10G cells were examined to determine the optimal post-induction time for rLifA^{C1480A} production. It was found that 3 hours was the optimal post-induction time for rLifA^{C1480A} production (data not shown), the same as for WT rLifA and rLifA$^{DTD/AAA}$ (Bease, 2015; Cassady-Cain *et al*., 2016).

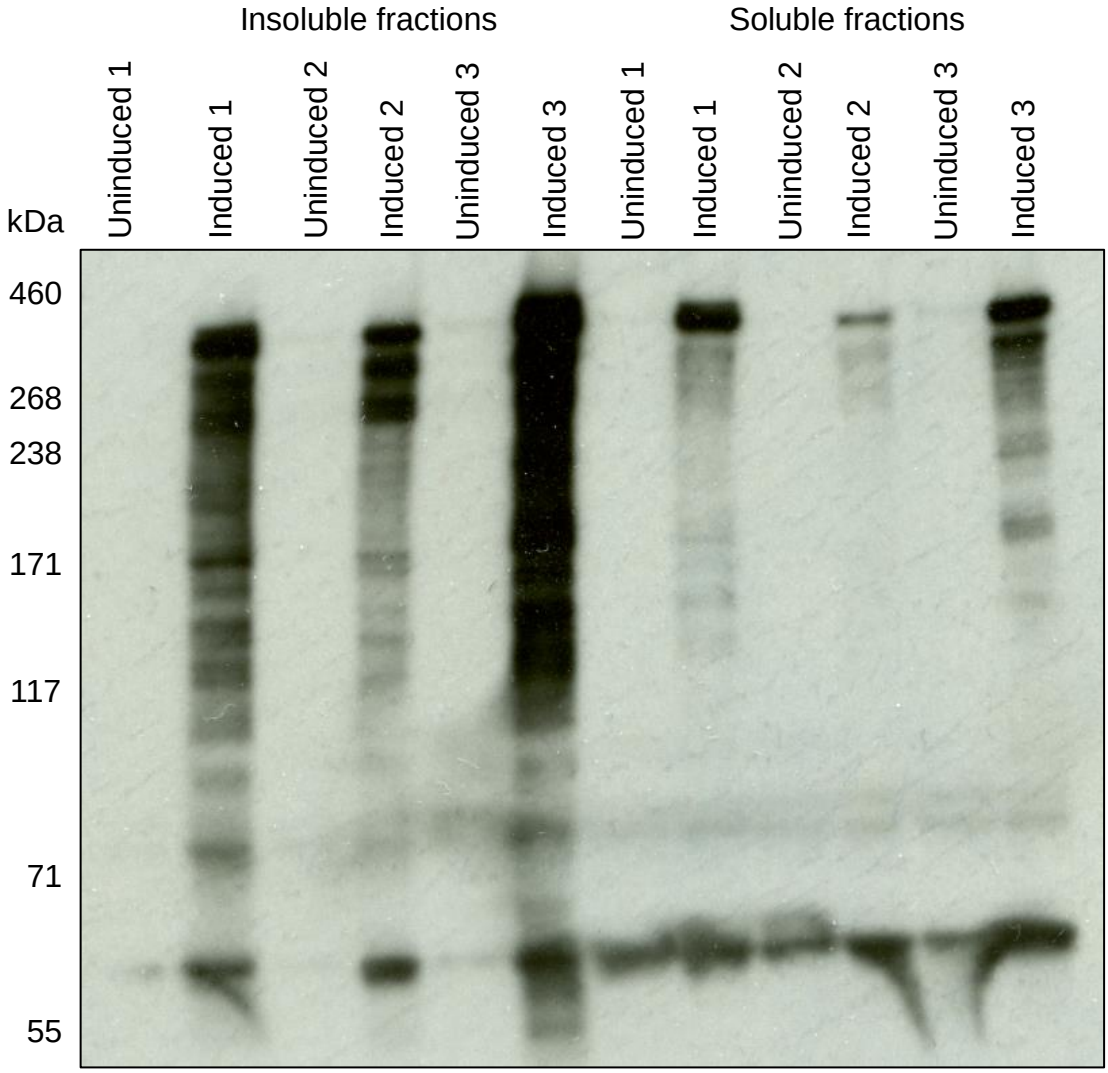

Figure 4.4. Pilot protein expression assay of LifA^{C1480A}. Three clones that tested positive for the C1480A mutation by *BsrD*I digestion were grown at 30 °C until the A_{600} was between 0.5 and 0.6. Protein expression was induced by the addition of 0.2 % L-rhamnose and samples were taken from each clone at 3 hours post-induction. The insoluble and soluble fractions of lysates from the clones were analysed by western blotting using polyclonal anti-LifA antiserum. Uninduced samples were used as negative controls. All three clones were shown to produce full-length LifA^{C1480A}.

4.4 rLifA^{C1480A} purification

Large-scale production of rLifA^{C1480A} was carried out using the previously described conditions for WT rLifA production (Cassady-Cain *et al*., 2016) and the protein was isolated to a high purity via a four-step process, which was monitored at each step. WT rLifA was also produced and purified in parallel so that it could be compared with rLifA^{C1480A} in biophysical experiments. rLifA^{C1480A} was eluted from the IMAC, SEC and anion exchange chromatography columns in a single absorbance peak (Figures 4.5–4.7). The multiple peaks observed between 120 and 160 mL on the IMAC trace are likely to have been caused by air passing over the column. rLifA^{C1480A} was eluted from the SEC column at the same volume as WT rLifA, indicating that the two proteins are of similar size and are folded in a similar manner. Anion exchange chromatography was able to separate full-length rLifA^{C1480A} from truncated versions of the protein. Only the fractions of highest purity after anion exchange were taken forward for biophysical characterisation. After purification, the rLifA^{C1480A} protein was estimated to be > 90 % pure (Figure 4.8).

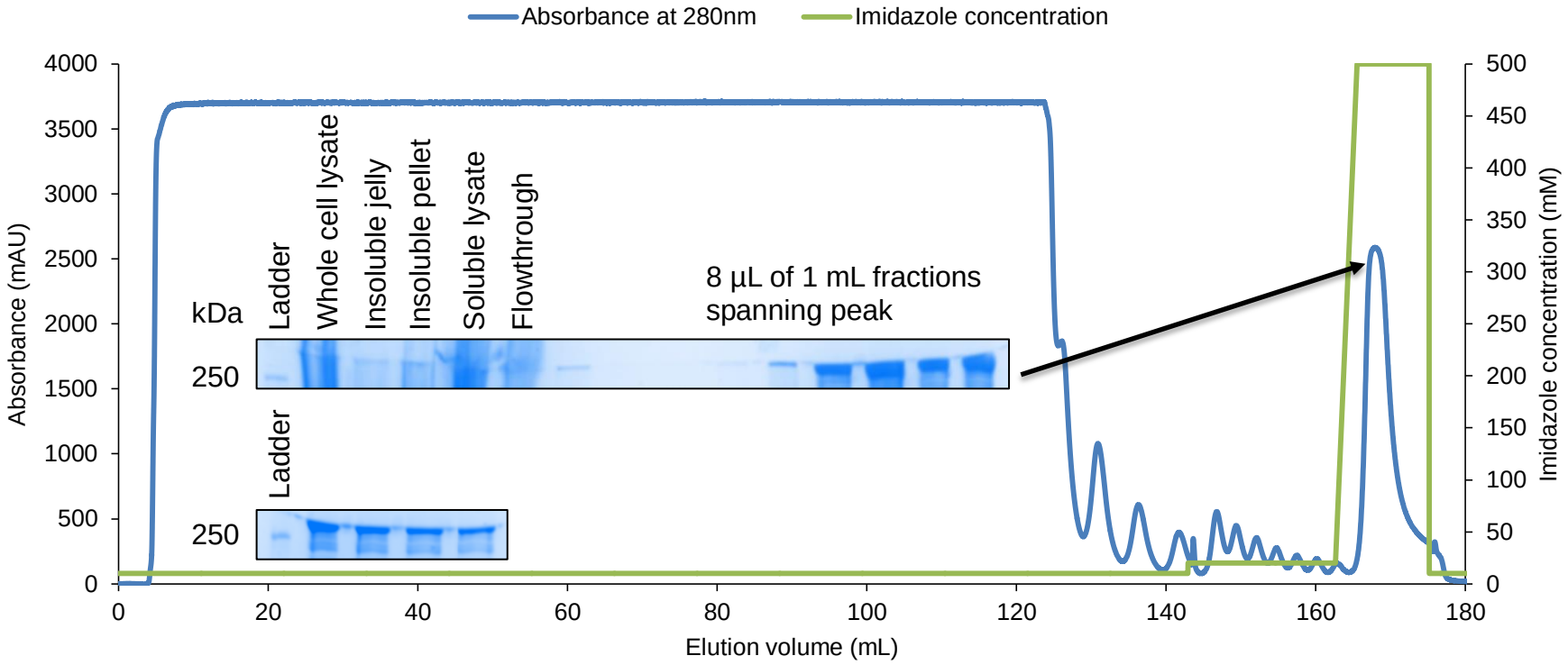

Figure 4.5. Ion metal affinity chromatography (IMAC) purification of rLifA^{C1480A} using Ni^{2+}-Sepharose®. The absorbance of elution buffer at 280 nm shows the presence of rLifA^{C1480A} where the concentration of imidazole was increased from 20 to 500 mM (marked with an arrow) to elute the protein from the nickel-Sepharose® beads. The large absorbance peak between ~0 and 130 mL corresponds to large cell debris that did not bind the column. Inset: Coomassie stain of 8 µL from 1 mL IMAC filtrate fractions analysed by SDS-PAGE showing the rLifA^{C1480A} eluted. The protein appeared to have a lower molecular weight than expected due to being run on a Tris-Glycine gel rather than a Tris-Acetate gel. The second inset (bottom) is a continuation of the first (top).

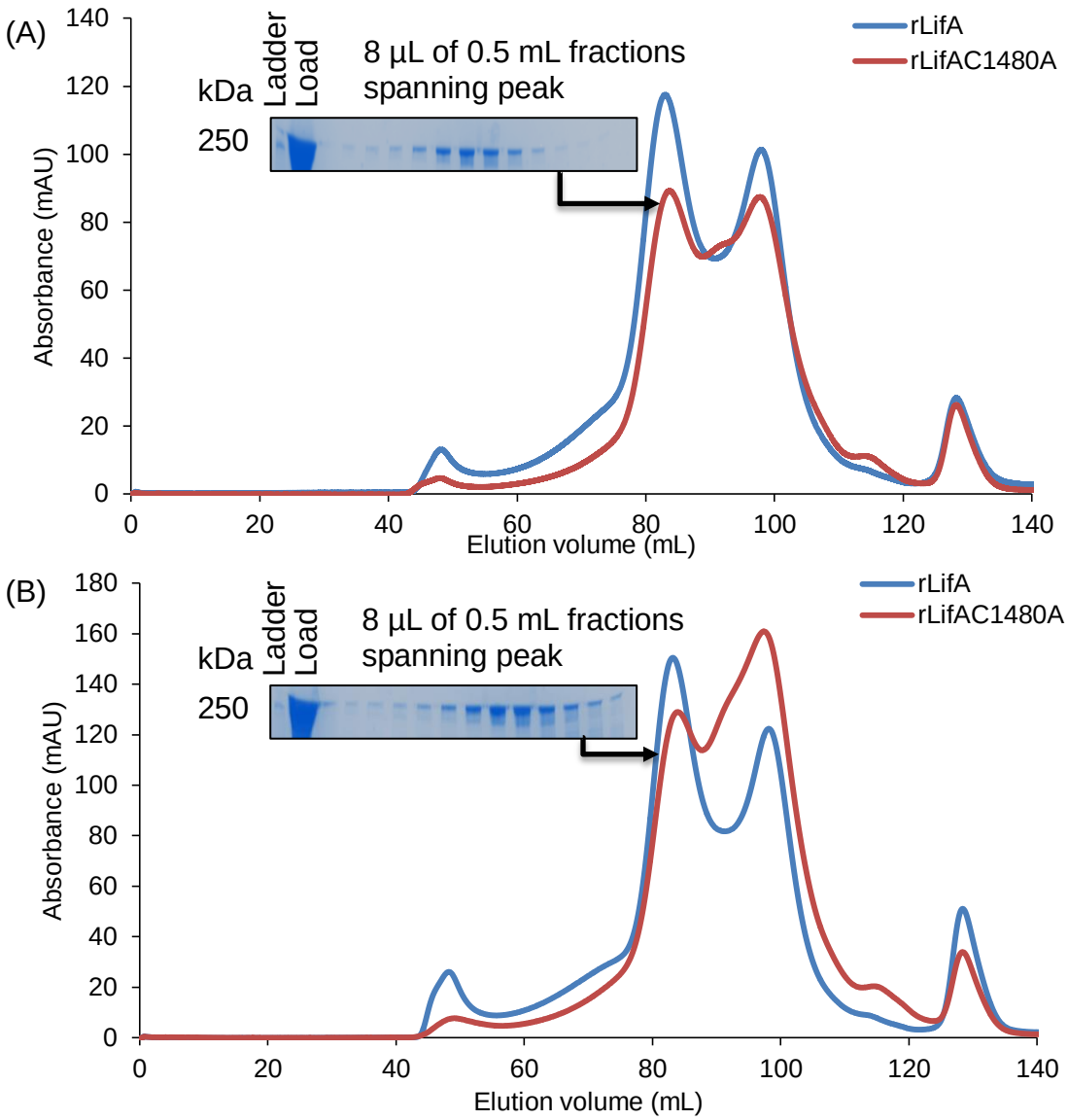

Figure 4.6. Purification of rLifA^{C1480A} by size exclusion chromatography (SEC). The absorbance peaks marked with arrows correspond to the presence of rLifA^{C1480A} in the filtrates of the Superose 6pg XK16/600 SEC columns used to filter (A) the purest IMAC fractions and (B) the less pure IMAC fractions. rLifA^{C1480A} was eluted from the columns at the same volume as WT rLifA, giving confidence that the mutant protein was the same size as the WT. Inset: Coomassie stains of 8 µL from 0.5 mL SEC filtrate fractions analysed by SDS-PAGE showing the rLifA^{C1480A} eluted. The protein appeared to have a lower molecular weight than expected due to being run on a Tris-Glycine gel rather than a Tris-Acetate gel.

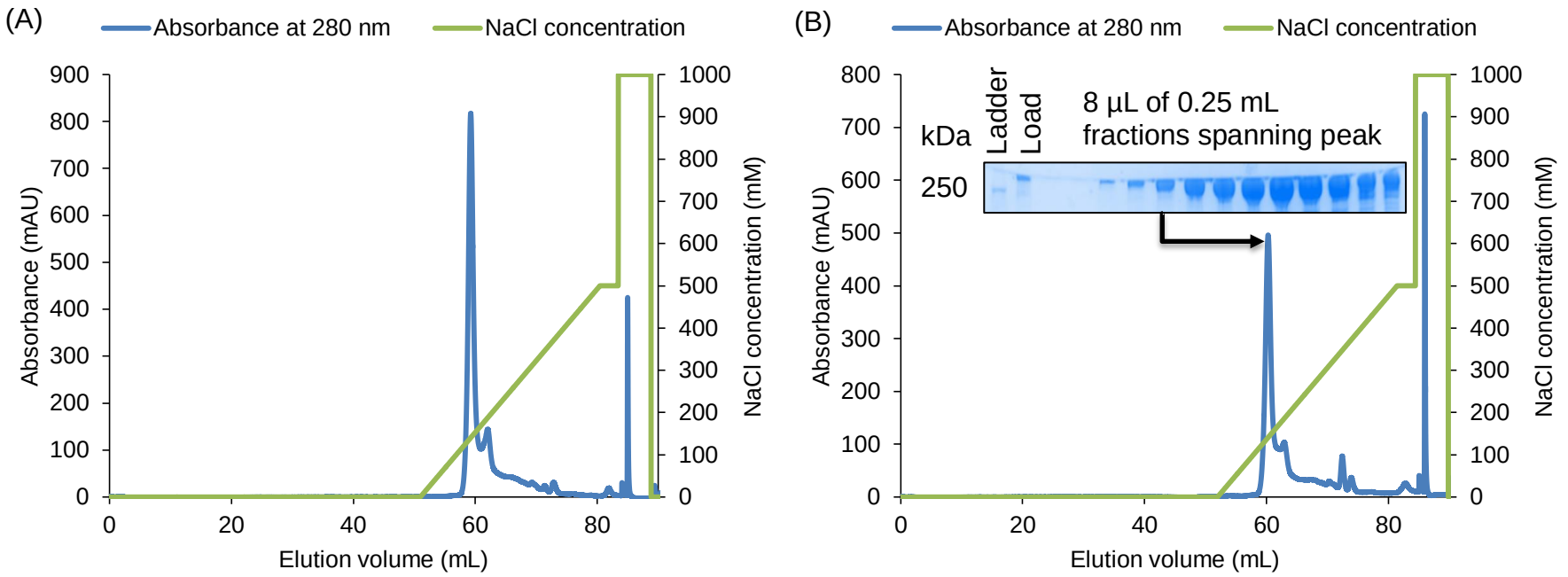

Figure 4.7. Purification of rLifA^{C1480A} by anion exchange chromatography. (A) The elution profile of WT rLifA. (B) The elution profile of rLifA^{C1480A}. The absorbance peak marked with an arrow corresponds to the presence of rLifA^{C1480A} in the filtrate of the Mono Q 5/50GL column used to filter the SEC fractions. The purest and less pure fractions were pooled into separate aliquots after the anion exchange chromatography but only the purest aliquot was used for further experiments. Both the WT and mutant proteins were eluted with ~140 mM NaCl. The small absorbance peak to the right of the marked peak corresponds to truncated rLifA^{C1480A}. Inset: Coomassie stains of 8 µL from 0.25 mL anion exchange filtrate fractions analysed by SDS-PAGE showing the rLifA^{C1480A} eluted. The protein appeared to have a lower molecular weight than expected due to being run on a Tris-Glycine gel rather than a Tris-Acetate gel.

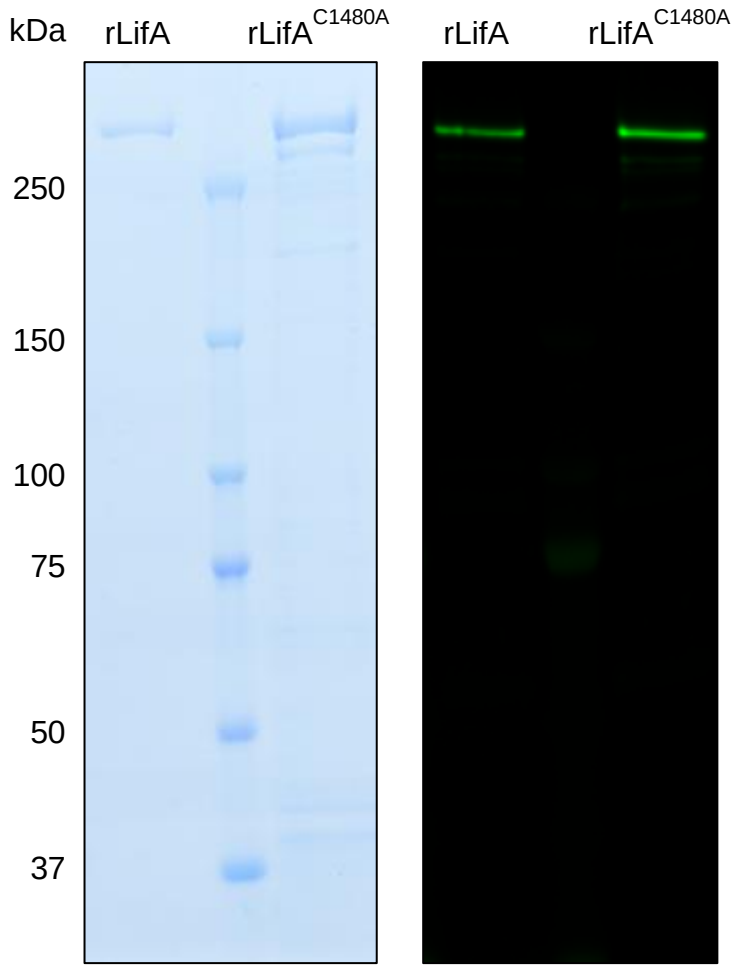

Figure 4.8. Coomassie stain (left) and western blot (right) of purified WT rLifA and rLifA^{C1480A} analysed by SDS-PAGE. Quantities of 2 µg and 2 ng of anion exchange purified protein were used for the Coomassie stain and western blot respectively. The estimated purity of rLifA^{C1480A} was > 90 %.

4.5 Biophysical characterisation

In order to determine whether the rLifA^{C1480A} protein was folded and behaved in the same manner as the WT rLifA protein, a number of biophysical measurements were made, including analysis of dynamic light scattering (DLS), circular dichroism (CD) and thermal denaturation assays (TDAs). All biophysical measurements were made using the same batches of WT rLifA and rLifA^{C1480A}.

4.5.1 DLS showed that rLifA^{C1480A} was of a similar size to WT rLifA

DLS was used to determine the size and state of the rLifA^{C1480A} protein. DLS works by measuring the different intensities of laser scattering caused by the Brownian motion of particles in suspension. This allows protein-specific software supplied with the Zetasizer Auto Plate Sampler to calculate the velocity of the Brownian motion and therefore the size of the particles by using the Stokes-Einstein relationship (Malvern, 2015; Folta-Stogniew and Williams, 1999). This allows an approximate size determination and gives some insight into whether the protein is aggregated or multimeric.

Thirteen scans of WT rLifA and rLifA^{C1480A} were performed in triplicate. The size distribution of the proteins was measured by the intensity of light scattering and by volume (Figure 4.9). The distribution by volume provides a more accurate size of the protein and distribution by the intensity of light scattering was used to detect large aggregates, which scatter light at much higher intensity than monomeric protein. Both distribution graphs had tight peaks between 9 and 30 nm. The mode hydrodynamic radius of rLifA^{C1480A} as measured by intensity and volume was 15.78 and 11.94 nm respectively, compared to 17.3 and 11.63 nm for WT rLifA. DLS also provided approximate molecular weights for rLifA and rLifA^{C1480A} based on their size, 308.7 ± 48 and 301.7 ± 15.6 kDa respectively, but these measurements are less accurate than measuring the molecular weight by SEC-MALS. rLifA^{C1480A} appeared to have some aggregation but the peak between 100 and 1000 nm may have been caused by dust as subsequent DLS experiments performed with rLifA^{C1480A} by Dr Liz Blackburn, EPPF, did not show any sign of aggregation (data not shown). A small peak was observed at ~5 nm on the rLifA^{C1480A} distribution by volume trace, which was considered to be an artefact in one of the samples.

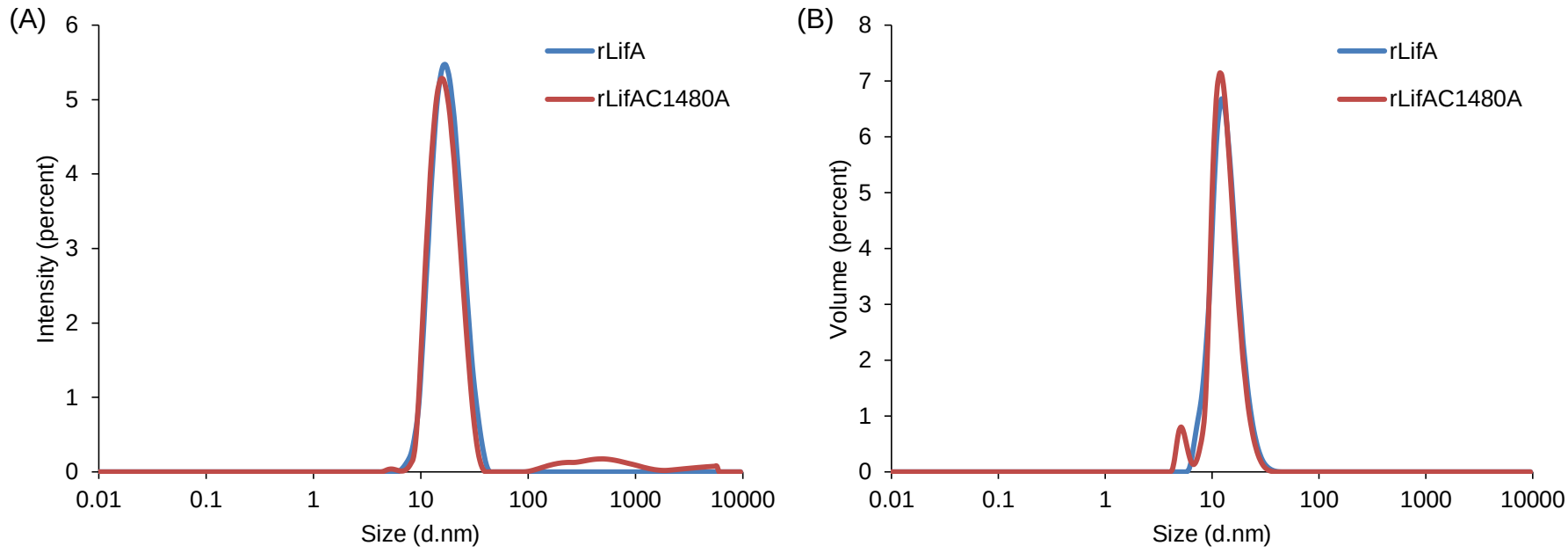

Figure 4.9. The size distribution by intensity and by volume of rLifA^{C1480A} compared to WT rLifA, measured by dynamic light scattering (DLS). rLifA and rLifA^{C1480A} at a concentration of 1.1 µM were measured by DLS to determine the size of the mutant protein and ensure that any loss of function was not caused by the protein forming large aggregates. (A) The distribution by the intensity of light scattering is used to detect aggregation. (B) The distribution by volume provided a more accurate size of the protein. Slight aggregation of LifA^{C1480A} was observed but the majority of the protein was monomeric. The proteins were scanned 13 times and the measurements were averaged. This was repeated in triplicate.

4.5.2 CD showed that rLifA^{C1480A} had a similar secondary structure to WT rLifA

CD was used to determine if the rLifA^{C1480A} protein had folded correctly on a secondary structure level and to observe whether it deviated significantly from the profile for the WT protein. CD works by detecting the difference in absorption between clockwise and anti-clockwise polarised light. CD signals only arise where the absorption of radiation occurs and therefore spectral bands can be assigned to distinct structural features of a molecule. The different secondary structures of a protein can be detected because they give rise to characteristic CD spectra in the far UV (Kelly *et al*., 2005). NaF was used in the CD buffer instead of NaCl as chloride ions interfere with CD at short wavelengths.

The CD profile confirmed that rLifA^{C1480A} had folded in a manner not significantly different from WT rLifA (Figure 4.10). The mean residue ellipticity peak and trough on the graph were indicative of a protein with a high α-helix content. The percentage of α-helices and β-sheets in rLifA^{C1480A} were 46 ± 5 % and 13 ± 2 % respectively, compared with 44 ± 5 % and 16 ± 2 % in WT rLifA. The percentage of turns and unstructured amino acids in rLifA^{C1480A} were 13 ± 6 % and 28 ± 7 % respectively, compared with 13 ± 6 % and 27 ± 3 % in WT rLifA. Overall, it can be concluded that rLifA^{C1480A} was folded and had a very similar structural profile to that of the WT protein.

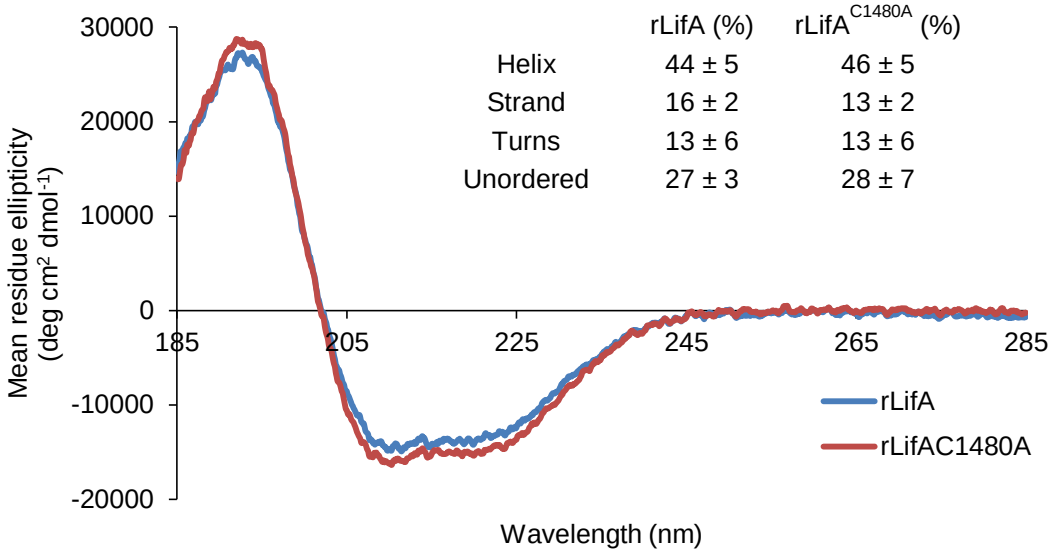

Figure 4.10. Far UV spectrum of rLifA^{C1480A} compared to WT rLifA. rLifA and LifA^{C1480A} at a concentration of 0.11 μM were measured by CD to compare the secondary structure of the proteins. The mean residue ellipticity peak and trough indicated that both proteins had a high α-helix content. Each protein was scanned 5 times and the measurements were averaged. The data were analysed using DichroWeb (http://dichroweb.cryst.bbk.ac.uk/html/home.shtml; Lobley *et al*., 2002). The mutant protein had a similar spectrum to that of the WT protein.

4.5.3 TDAs showed that rLifA^{C1480} had a similar mid-point melting temperature to WT rLifA

TDAs were used to measure the thermal stability of rLifA^{C1480A} in comparison to the WT protein. This was carried out by using a fluorescence-based assay with the fluorophore SYPRO Orange, which fluoresces weakly in hydrophilic conditions and strongly in hydrophobic conditions, across a range of temperatures. As the temperature increases and the target protein unfolds it reveals hydrophobic amino acid chains that cause the SYPRO Orange to increase its fluorescence. The fluorescence intensity is proportional to the degree of protein unfolding (Lo *et al*., 2004; Pantoliano *et al*., 2001).

The mid-point melting temperatures (T_m) of WT rLifA and rLifA^{C1480A} were 41.3 and 41 °C respectively (Figure 4.11). The slight decrease in T_m may have been

the result of minor structural instability caused by the C1480A substitution and was consistent with the reduction in T_m observed with the rLifA$^{DTD/AAA}$ mutant protein (Bease, 2015; Cassady-Cain *et al.*, 2016). Overall, the thermal stability of rLifA^{C1480A} was largely unaffected by the substitution.

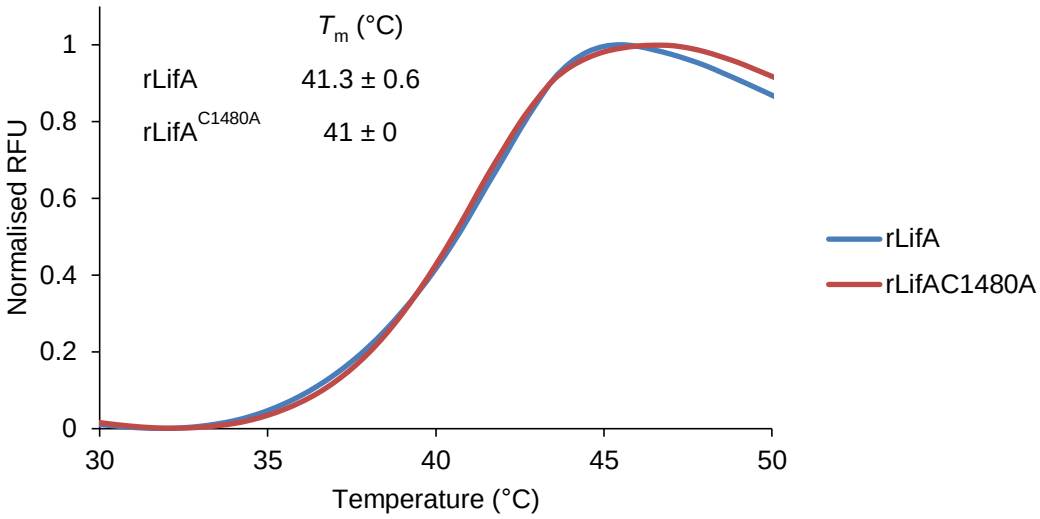

Figure 4.11. Thermal denaturation assays to evaluate the mid-point melting temperature (T_m) of WT rLifA and rLifA^{C1480A}. The fluorescence of SYPRO Orange dye mixed with 0.1 µM rLifA and rLifA^{C1480A} was measured over a temperature range of 15–70 °C to determine the T_m of each protein. Each fluorescence measurement was performed in triplicate. A reproducible T_m of ~41 °C was observed in both proteins. These results are from a single experiment.

4.6 Analysis of the ability of rLifA^{C1480A} to inhibit mitogen-stimulated T cell proliferation

Peripheral blood T lymphocytes from five independent donors were used to test the activity of purified rLifA^{C1480A} against ConA-stimulated T cells in comparison to the WT rLifA. Titration of WT LifA produced a sigmoid curve, with higher concentrations of LifA causing an increase in inhibition (Figure 4.12). The proliferation index, with standard deviation, decreased sharply from 0.91 ± 0.08 at 0.001 ng/mL of rLifA to 0.27 ± 0.15 at 0.1 ng/mL, then the curve leveled out and

decreased to a proliferation index of 0.23 ± 0.17 at 100 ng/mL. rLifA^{C1480A} produced a curve that saw the proliferation index, with standard deviation, gradually decrease from 0.95 ± 0.05 at 0.1 ng/mL to 0.48 ± 0.14 at 10 µg/mL. It required an ~100,000-fold increase in concentration for rLifA^{C1480A} to have the same inhibitory effect as that of the WT protein, which was comparable to the glycosyltransferase mutant rLifA$^{DTD/AAA}$ (Bease, 2015; Cassady-Cain *et al.*, 2016). The ED_{50}s, with standard errors, for WT rLifA and rLifA^{C1480A} were 0.013 ± 0.004 ng/mL and 1215.3 ± 684.1 ng/mL respectively (W = 15, P = 0.0097). This experiment combined with the biophysical data showed that the predicted catalytic Cys^{1480} of the CP domain was required for the inhibitory activity of LifA and that loss of activity was not associated with major structural abnormalities relative to the WT protein.

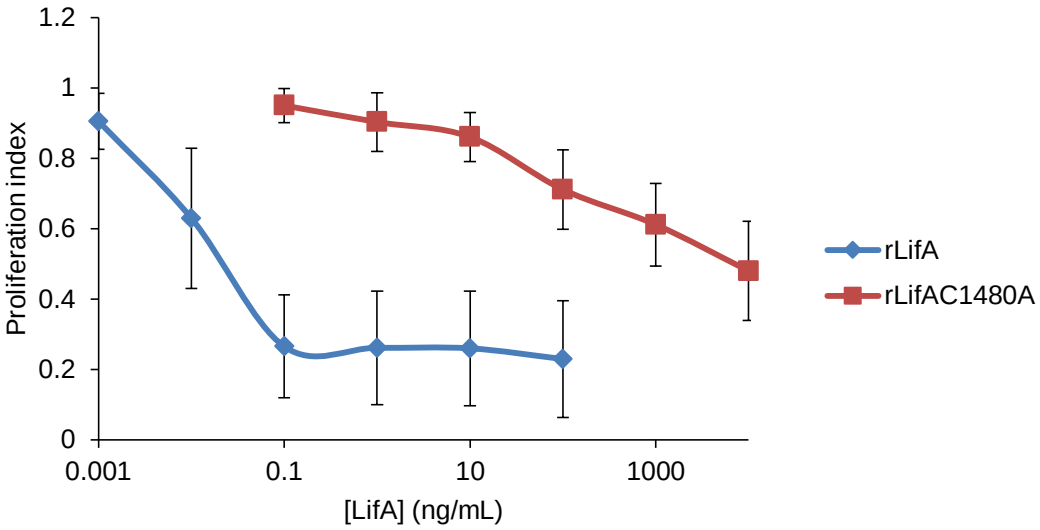

Figure 4.12. Concentration titration of recombinant WT rLifA and rLifA^{C1480A} against ConA-stimulated peripheral bovine T lymphocytes. An absolute number of 200,000 cells were seeded into the wells of a 96 well plate. Titrations were carried out in triplicate and the results are the average obtained from 5 independent experiments using separate donors. Data were normalised against cells with ConA alone to produce a proliferation index. Error bars indicate the standard deviation of the average proliferation indices from across the 5 experiments.

4.7 Detection of putative autocatalytic cleavage of LifA

4.7.1 Detection of LifA cleavage in bovine T lymphocytes

A protein species reactive to anti-LifA antibody of ~140 kDa was previously observed in lysates of bovine T cells treated with rLifA but not buffer or recombinant LifA fragments (see Section 3.9, Figure 3.18). This same protein was also observed in lysates of T cells treated with the glycosyltransferase mutant rLifA$^{DTD/AAA}$ (data not shown). It was suspected that this c. 140 kDa species was produced by a cleavage event within the T cells that required the CP motif. To determine if this protein was produced by C1480-mediated cleavage, T cells from two independent donors were treated with either WT rLifA or rLifA^{C1480A} for various durations. For cells treated with rLifA^{C1480A}, the 15 minute time point was replaced with a 2 hour time point to determine whether putative cleavage occurred at a slower rate than for the WT protein.

The putative cleavage product was observed at ~140 kDa in T cells treated with WT rLifA from 15 minutes and appeared to increase in concentration up to 1 hour (Figure 4.13). No proteins of this size were detected in lysates from T cells treated with rLifA^{C1480A}, even after 2 hours. This suggests that the detected protein of ~140 kDa was a processed form of LifA, the production of which required an intact CP motif. A second protein fragment of ~225 kDa, corresponding to the other half of LifA, was expected but never observed in T cell lysates. Attempts to identify the C-terminal portion of the protein using anti-6 x His antibodies and InVision^{TM} His-Tag In-Gel Stain were unsuccessful.

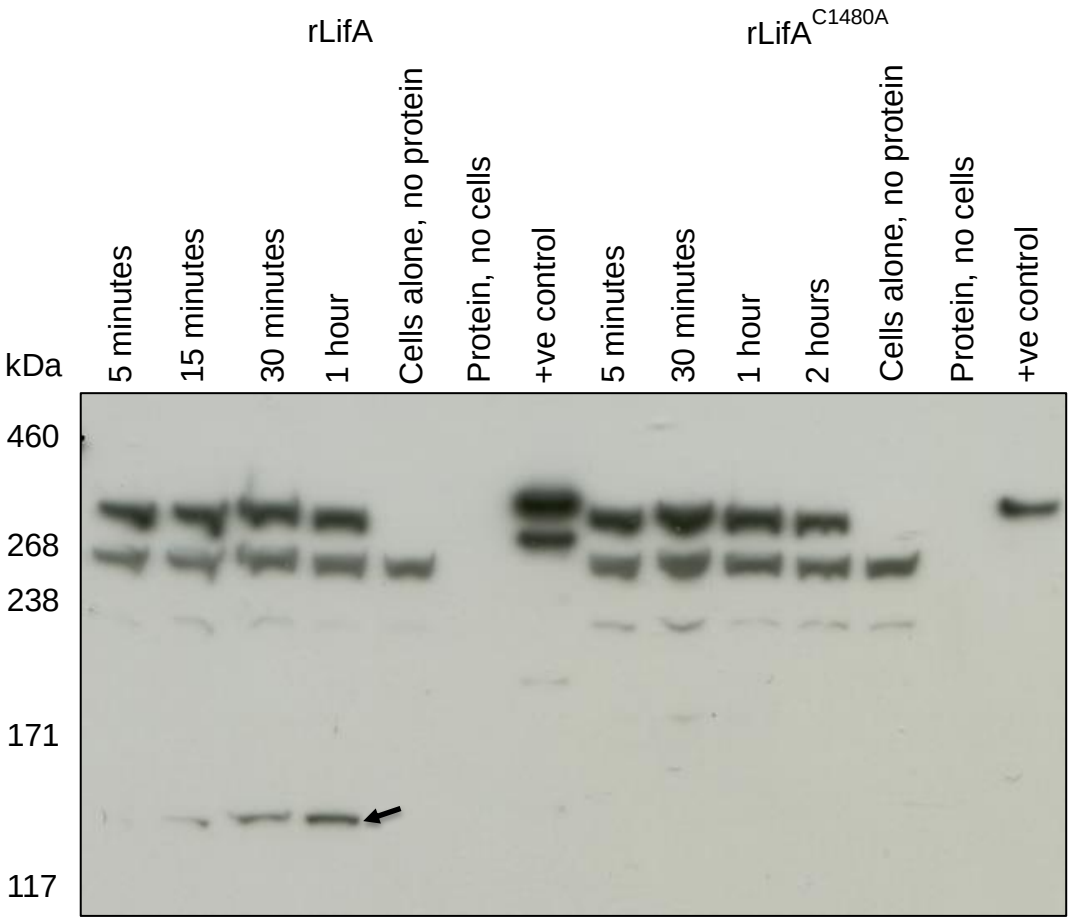

Figure 4.13. Cleavage of lymphostatin in T cells was dependent on the cysteine protease motif. Western blot of lysates from T cells (1.2 x 10^7 cells) treated with 2 µg/mL WT rLifA or rLifA^{C1480A} for the times indicated. A volume equivalent to 2 x 10^6 cells was run in each well. A predicted c. 140 kDa cleavage product of WT rLifA was visible at 15 minutes post-incubation and increased in concentration up to 1 hour after treatment (marked with an arrow), while no cleavage product was observed in rLifA^{C1480A}-treated T cells even after 2 hours. This experiment was performed with 2 separate donors and a representative blot is shown.

4.7.2 Detection of LifA cleavage in J774A.1 murine macrophage-like cells

Cell types other than primary T lymphocytes have previously been used in experiments to test the effects of LifA. EPEC E2348/69 lysates have been reported to inhibit IL-2 secretion by mitogen-stimulated Jurkat cells (Malstrom and James, 1998)

and WT rLifA has been shown to inhibit the IL-4-induced proliferation of bovine B lymphocytes (Cassady-Cain *et al*., 2017). EPEC lysates did not inhibit the proliferation of epithelial cells in a LifA-dependent manner (Klapproth *et al*., 2000). However, EPEC E2348/69 has been reported to modulate signalling in epithelial and J774A.1 macrophage-like cells in a manner dependent on Type III secretion but independent of LEE-encoded and several non-LEE-encoded effectors (Ruchaud-Sparagano *et al*., 2007; Amin, 2017), suggesting a possible role for LifA. Therefore, I sought to determine whether cell types other than bovine T lymphocytes could be used to detect processed forms of LifA.

Jurkat cells were used initially, and although a protein of ~140 kDa was observed in the lysates of rLifA-treated Jurkats, full-length rLifA was not observed as it is in T cells (data not shown). J774A.1 murine macrophage-like cells were used subsequently. Cleavage products of ~140 and 225 kDa were detected in the lysates of J774A.1 cells treated with WT rLifA but not rLifA^{C1480A} for 1 hour (Figure 4.14A). The product of ~225 kDa was also detected with anti-6 x His antibody, indicating that it was the C-terminal portion of the protein (Figure 4.14B). The quantity of full-length WT rLifA in the lysates was reduced in comparison to rLifA^{C1480A}, most likely due the protein being processed into the observed cleavage products. Full-length rLifA^{C1480A} was not detected by the anti-6 x His antibody in J774A.1 cells despite being visible on the anti-LifA blot, possibly due to there being less epitopes on rLifA proteins for monoclonal anti-6 x His antibodies than for polyclonal anti-LifA antibodies.

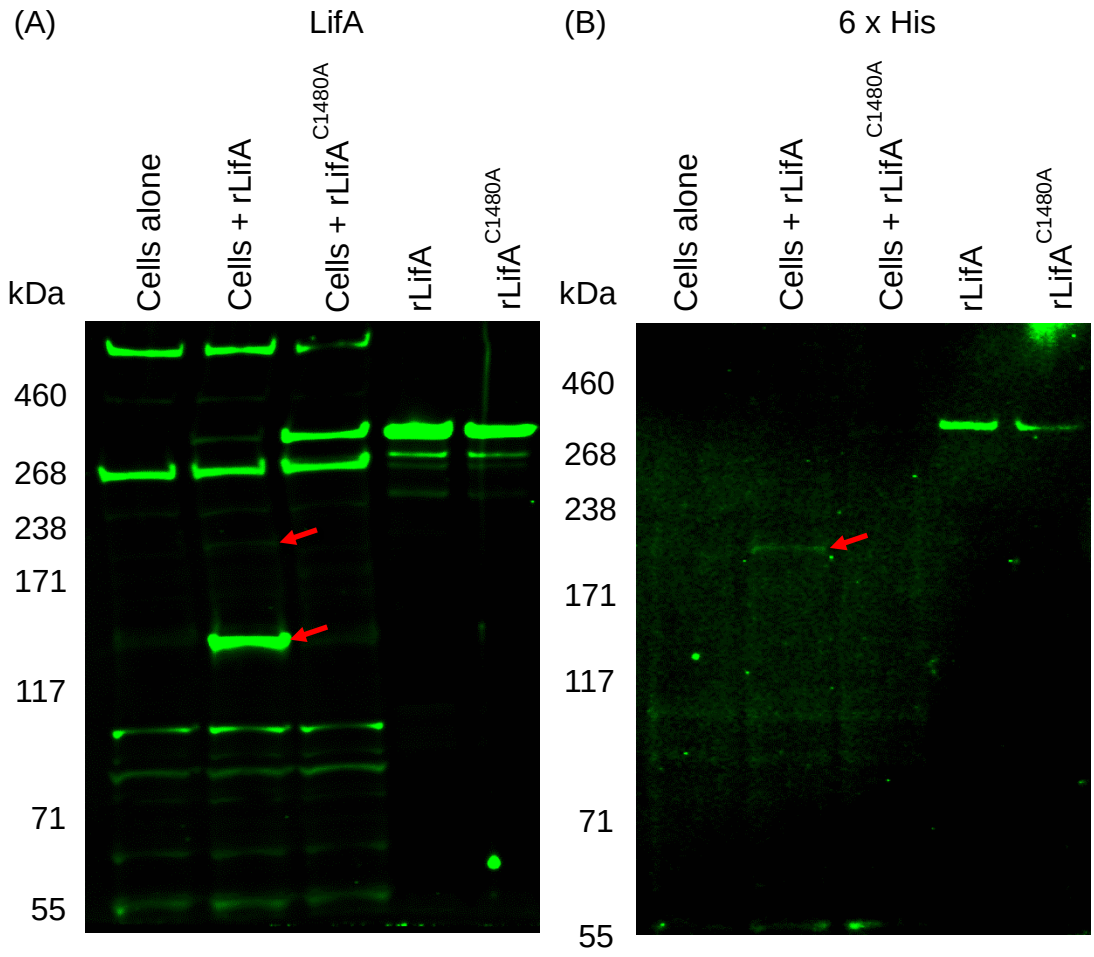

Figure 4.14. Lymphostatin was processed by J774A.1 cells into N- and C-terminal forms of ~140 and 225 kDa respectively. Western blots of lysates from J774A.1 macrophage-like cells (1 x 10^6 cells) treated separately with rLifA or rLifA^{C1480A} for 1 hour. A volume equivalent to 2.5 x 10^5 cells was run in each well. (A) An anti-LifA blot revealed the fragment of ~140 kDa previously observed in T cells as well as the predicted fragment of ~225 kDa (marked with arrows), the presence of which were dependent on an intact cysteine protease motif. The quantity of full-length rLifA in the cell lysate was reduced in comparison to rLifA^{C1480A}, likely due to the processing of rLifA into the lower molecular weight forms. (B) The c. 225 kDa fragment was reactive to anti-6 x His antibody (marked by arrow), indicating that it was the C-terminal portion of rLifA. Quantities of 2 ng of WT rLifA and rLifA^{C1480A} were used as positive controls. Western blots are from a single experiment.

4.8 Impact of inhibitors of endosome acidification on predicted autocatalytic cleavage

Given that LifA underwent CP domain-mediated cleavage in T and J774A.1 cells, it was thought that this process may have required endosome acidification to initiate a conformational change in the protein, as with LCTs (Qa'dan *et al*., 2000 and 2001; Barth *et al*., 2001). To test this, T cells were pre-treated with two different inhibitors of endosomal acidification, bafilomycin A1 and chloroquine, before treatment with rLifA.

4.8.1 Bafilomycin A1

Bafilomycin A1 is an inhibitor of V-ATPases, which acts by binding to and preventing the rotation of V-ATPase C subunits (Bowman *et al*., 1988 and 2004). Bafilomycin A1 concentrations were informed by previous studies and pilot western blots. Qa'dan *et al*. (2000) and Wu *et al*. (2015) used 0.5 and 5 nM bafilomycin A1 respectively, however, a western blot revealed that production of the c. 140 kDa cleavage product was not inhibited at 5 nM. Partial and total inhibition was observed at 0.5 and 50 µM bafilomycin A1 respectively (data not shown), therefore bafilomycin A1 was titrated from 50 µM down to 0.0005 µM.

Western blot analysis showed that the appearance of the c. 140 kDa cleavage product remained constant with increasing bafilomycin A1 concentration from 0.0005 to 0.5 µM but was reduced at concentrations of 5 and 50 µM (Figure 4.15). Densitometry from five independent donors showed that the fold change in normalised fluorescent signal of the cleavage product in comparison to the DMSO control, with standard deviation, decreased gradually from 1.21 ± 0.19 at 0.0005 µM bafilomycin A1 to 1.07 ± 0.23 at 0.05 µM, then decreased sharply to 0.19 ± 0.14 at 50 µM (Figure 4.16). The overall loss of protein at 50 µM, indicated by the actin control, suggested that bafilomycin A1 became toxic to T cells at this concentration. The average linear regression slope was found to be statistically significantly different from a horizontal line representing no change in normalised fluorescent signal as the concentration of bafilomycin A1 increases ($T(4) = -13.77$, $P < 0.001$).

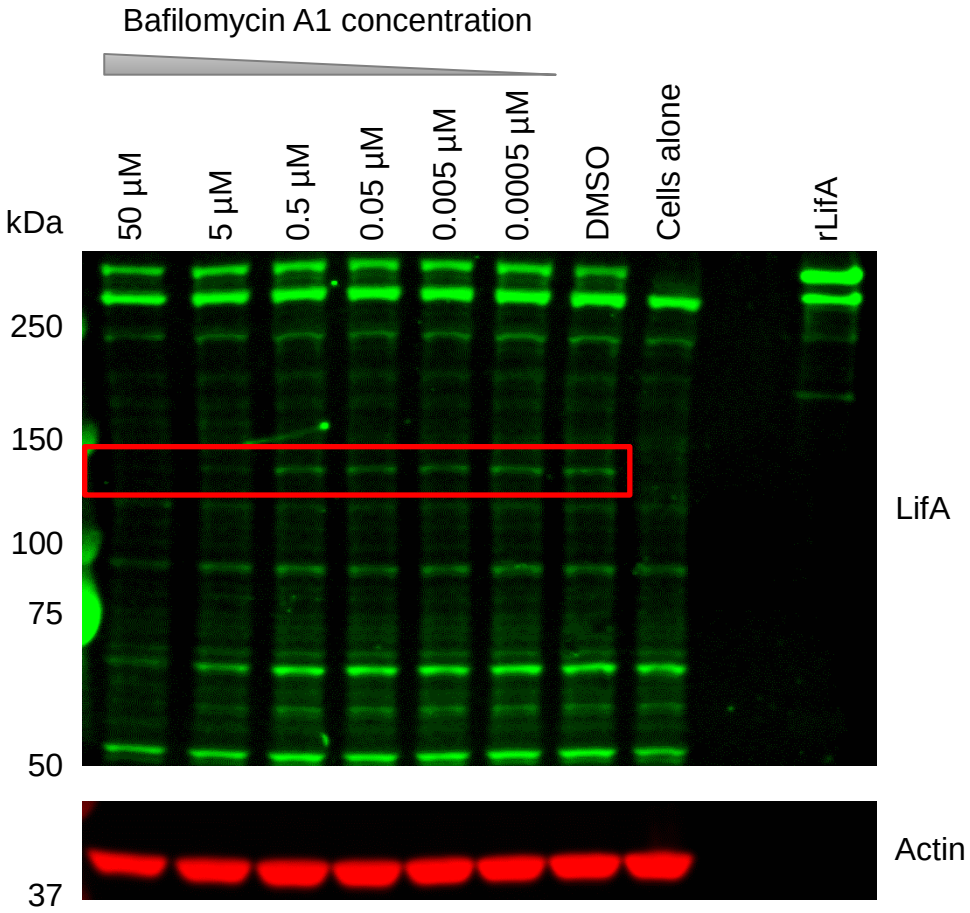

Figure 4.15. Bafilomycin A1 inhibited lymphostatin cleavage in a concentration-dependent manner (western blot). An absolute number of 1.2 x 10^7 cells were incubated with the indicated concentrations of bafilomycin A1 then treated with rLifA for 1 hour. A volume equivalent to 2 x 10^6 cells was run in each well. Western blot analysis of bafilomycin A1-treated T cells showed that the appearance of the cleavage product (red box) was reduced with increasing inhibitor concentration. DMSO was used as a diluent only control. A quantity of 2 ng of rLifA was used as a positive control for the anti-LifA antibody. Actin was used as a loading control. Data were generated from 5 independent donors and blots are shown from a representative donor.

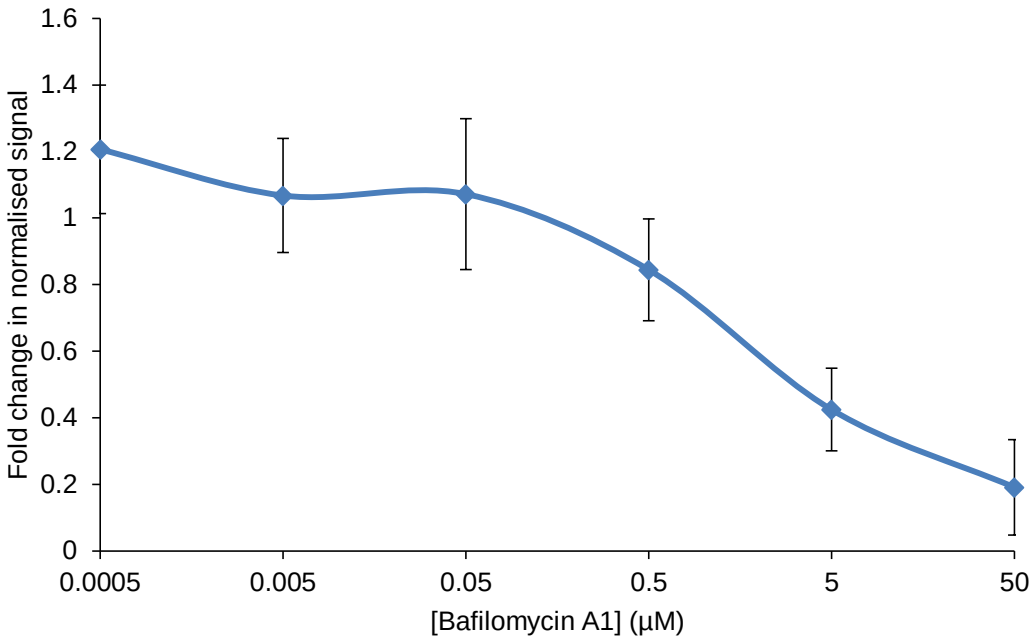

Figure 4.16. Bafilomycin A1 inhibited lymphostatin cleavage in a concentration-dependent manner (densitometry). Densitometry was performed on the western blots and the cleavage product signal at each inhibitor concentration was normalised against its respective actin signal to account for overall loss of protein. Data were normalised again against the DMSO control to give a fold change in normalised signal compared to untreated cells. The average fold change in normalised signal of bafilomycin A1-treated T cells decreased as the concentration increased. Error bars indicate the standard deviation of the average fold changes from across 5 experiments.

4.8.2 Chloroquine

Chloroquine is a lysosomotropic agent that can freely diffuse across cytoplasmic vesicles in its unprotonated form. Once inside acidic vesicles, chloroquine becomes protonated and is trapped, thereby raising the pH of the vesicle (reviewed in Al-Bari, 2015). The concentrations of chloroquine used were informed by a study using PK-15 (porcine kidney) cells in which 125 µM chloroquine was reported to be the maximum concentration that did not affect cell viability (Misinzo *et al*., 2008). As such, chloroquine was titrated from 1250 µM down to 0.0125 µM.

Western blot analysis showed that the appearance of the c. 140 kDa cleavage product remained constant when increasing the chloroquine concentration from 0.0125 to 1.25 µM and was reduced at 12.5 µM. The c. 140 kDa cleavage product appeared to be absent in T cells treated with 125 and 1250 µM chloroquine (Figure 4.17). Densitometry from five independent donors showed that the fold change in normalised fluorescent signal of the cleavage product in comparison to the PBS control, with standard deviation, decreased gradually from 1.19 ± 0.19 at 0.0125 µM chloroquine to 1.08 ± 0.24 at 12.5 µM, then decreased sharply to 0.09 ± 0.15 at 1250 µM (Figure 4.18). The overall loss of protein at 1250 µM, indicated by the actin control suggested that chloroquine became toxic to T cells at this concentration. The average linear regression slope was found to be statistically significantly different from a horizontal line representing no change in normalised fluorescent signal as the concentration of chloroquine increases ($T(4) = -13.71$, $P < 0.001$).

Taken together with the results from experiments using bafilomycin A1, these data suggested that LifA required endosome acidification to undergo CP domain-mediated cleavage.

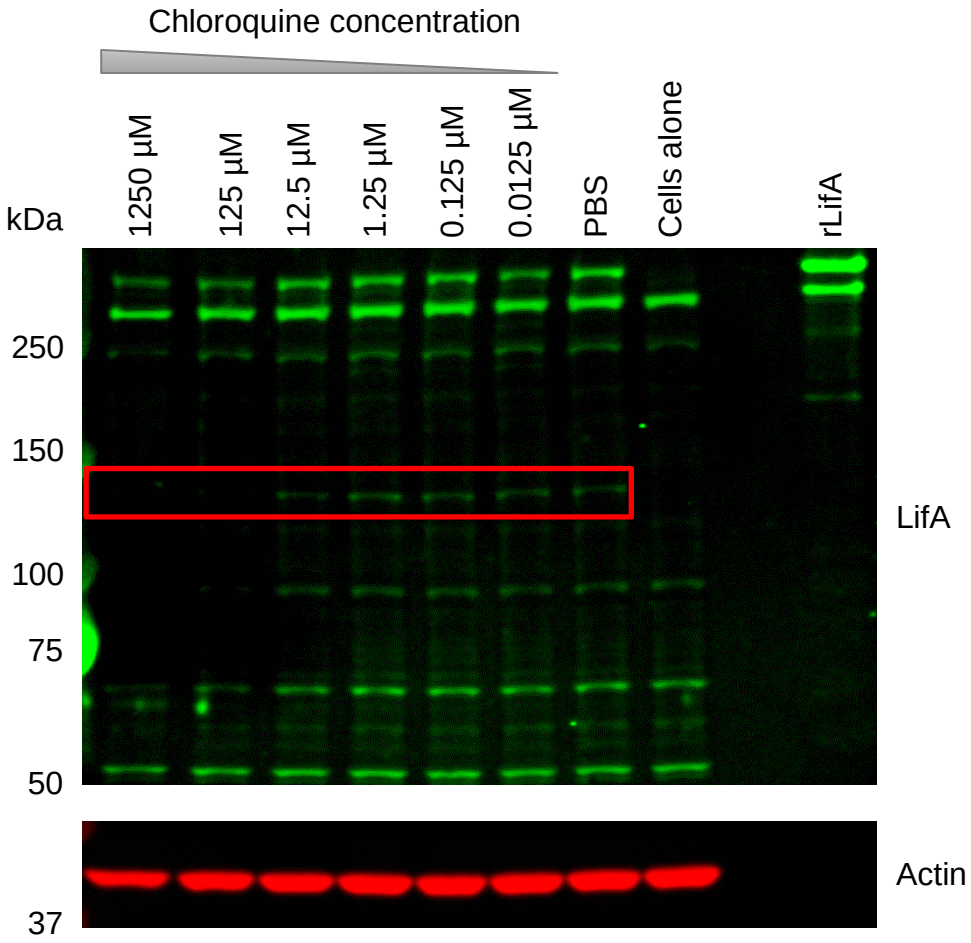

Figure 4.17. Chloroquine inhibited lymphostatin cleavage in a concentration-dependent manner (western blot). An absolute number of 1.2 x 10^7 cells were incubated with the indicated concentrations of chloroquine then treated with rLifA for 1 hour. A volume equivalent to 2 x 10^6 cells was run in each well. Western blot analysis of chloroquine-treated T cells showed that presence of cleavage product (red box) remained constant between 0.0125–12.5 µM but was reduced at higher concentrations. PBS was used a diluent only control. A quantity of 2 ng of rLifA was used as a positive control for the anti-LifA antibody. Actin was used as a loading control. Data were generated from 5 independent donors and blots are shown from a representative donor.

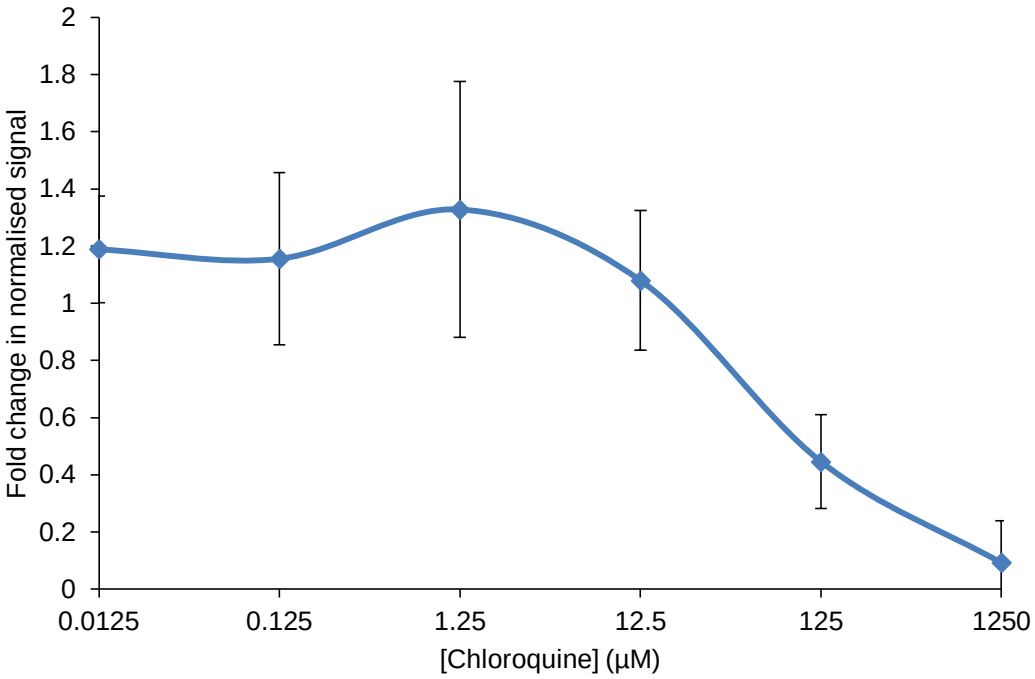

Figure 4.18. Chloroquine inhibited lymphostatin cleavage in a concentration-dependent manner (densitometry). Densitometry was performed on the western blots and the cleavage product signal at each inhibitor concentration was normalised against its respective actin signal to account for overall loss of protein. Data were normalised again against the PBS control to give a fold change in normalised signal compared to untreated cells. The average fold change in normalised signal of chloroquine-treated T cells remained constant between 0.0125–12.5 µM but decreased at higher concentrations. Error bars indicate the standard deviation of the average fold changes from across 5 experiments.

4.8.3 Proliferation assays using inhibitor-treated bovine T cells

To determine whether inhibitors of endosome acidification could block lymphostatin activity against mitogen-stimulated T cells, cells were pre-treated with bafilomycin A1 or chloroquine at the concentrations described previously and used in proliferation assays. T cells were treated with buffer or 1 µg/mL of rLifA for an hour then washed with PBS to remove the inhibitors before ConA stimulation. It was expected that the proliferation indices of rLifA treated cells would increase as the concentration of inhibitor increased.

In contrast to what was expected, the proliferation indices of rLifA-treated cells remained constant at all inhibitor concentrations and became highly variable at the highest concentrations (data not shown). To determine whether these results were due to toxicity, the absorbance values of buffer-treated cells with and without the addition of ConA were examined (Figure 4.19). Proliferation was normal from 0.0005–0.5 µM bafilomycin A1 and 0.0125–12.5 µM chloroquine but reduced at higher concentrations. The concentrations at which proliferation was inhibited were the same concentrations at which the c. 140 kDa cleavage product was absent in the western blots of T cell lysates. Therefore, proliferation assays are not a suitable system for measuring the effect of endosome acidification inhibitors on lymphostatin activity.

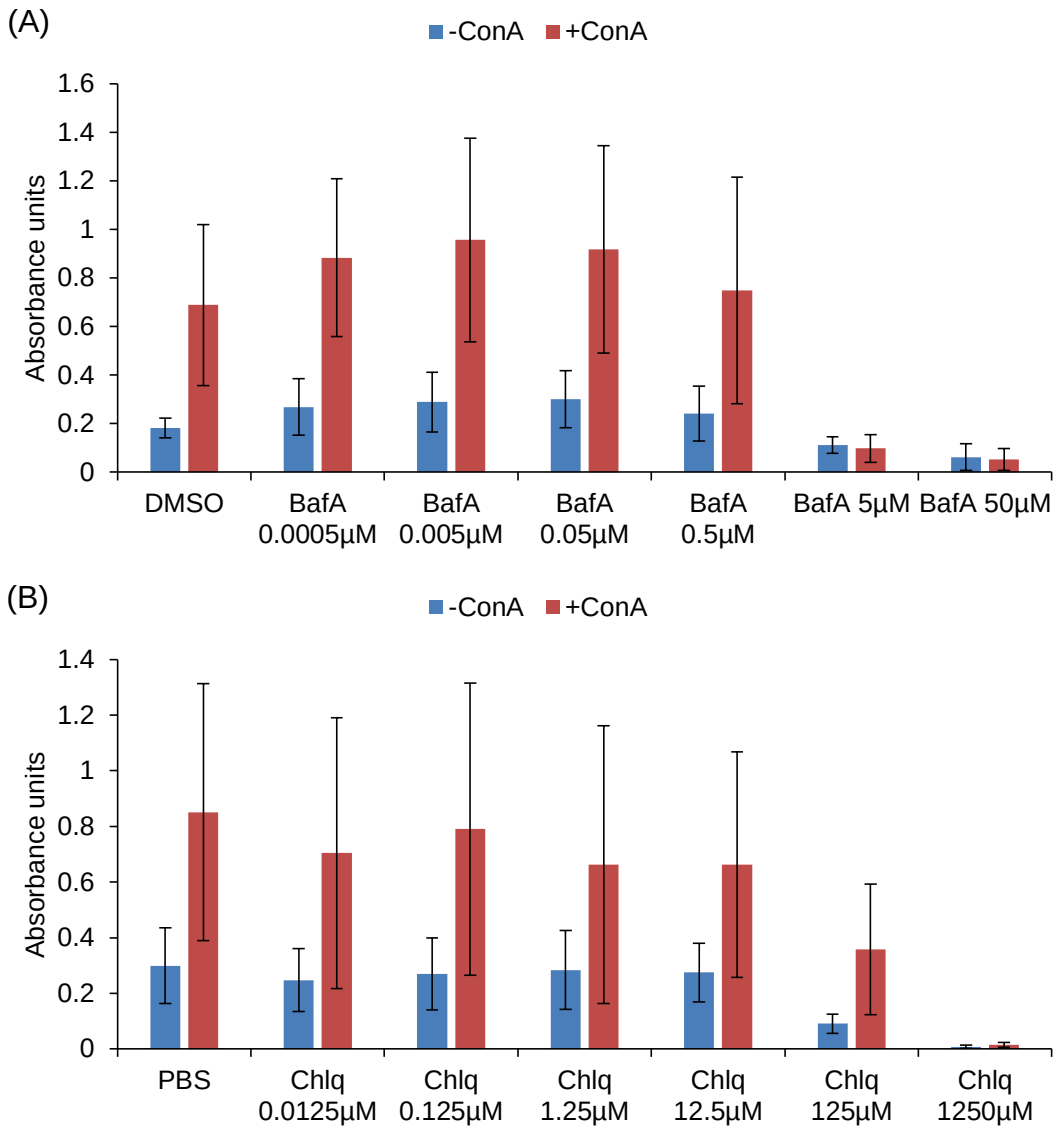

Figure 4.19. Concentration titration of bafilomycin A1 and chloroquine against ConA-stimulated peripheral bovine T lymphocytes. An absolute number of 200,000 cells were seeded into the wells of a 96 well plate. T cells were pre-treated with 10-fold dilutions of (A) bafilomycin A1 (BafA) or (B) chloroquine (Chlq) before incubation in the presence/absence of ConA. DMSO and PBS were used as carrier controls for bafilomycin A1 and chloroquine respectively. Comparing the absorbance values of stimulated and unstimulated cells revealed that high concentrations of the inhibitors appeared to be toxic to the cells. Titrations were carried out in triplicate and the results are the average obtained from 3 independent experiments using separate donors. Error bars indicate the standard deviation of the absorbance values from across the 3 experiments.

4.9 Discussion

The putative YopT-like CP domain of lymphostatin, including a conserved C/H/D catalytic triad, was hypothesised to be required for autoproteolysis and activity of the protein. To investigate this, a C1480A substitution mutant was created, expressed and purified. The mutant protein was found to be structurally identical to WT rLifA by the methods used for biophysical characterisation but was substantially impaired in its ability to inhibit ConA-stimulated lymphocyte proliferation. The inhibition observed at high concentrations may have been due to residual activity or contaminants, as even lysates of *E. coli* K-12 with empty plasmids can inhibit the ConA-stimulated proliferation of PBMCs at high concentrations (Klapproth *et al*., 2000; Deacon *et al*., 2010). Within T cells, rLifA is cleaved into N- and C-terminal products of ~140 and 225 kDa respectively in a processing event that requires both the predicted catalytic Cys^{1480} and endosome acidification. These observations are consistent with the notion that LifA enters cells and is processed in a manner akin to the LCTs.

Unfortunately, attempts to confirm whether $rLifA^{C1480A}$ retained its ability to bind UDP-GlcNAc using the previously described method of measuring changes in intrinsic tryptophan fluorescence (Bease, 2015; Cassady-Cain *et al*., 2016) were inconclusive. The fluorescence of intrinsic Trp residues can either decrease via quenching (reviewed in Price and Nairn, 2009) or increase (Weljie and Vogel, 2000), which is detected by a spectrophotometer. Fluorescence quenching occurs when an excited Trp residue loses energy by either colliding with molecules in the solvent (collisional quenching) or by forming long-lasting interactions with molecules (static quenching; reviewed in Price and Nairn, 2009). The exposure of each Trp residue to the quenching molecule determines how easily it is quenched (Eftink and Ghiron, 1976). Intrinsic Trp fluorescence increases when a protein undergoes a conformational change that exposes Trp residues to the solvent, but is stabilised by the binding of another molecule, such as UDP-GlcNAc, that prevents quenching (Weljie and Vogel, 2000). An increase in fluorescence has previously been observed when UDP-GlcNAc was added to WT rLifA (Bease, 2015; Cassady-Cain *et al*., 2016). The assay is technically difficult, however, since lymphostatin contains

36 Trp residues, which can mask the subtle change in fluorescence of a single residue. Due to the difficulty of detecting UDP-GlcNAc binding with WT rLifA and the reagent intensive nature of the assay, this experiment was ultimately abandoned. Given that WT rLifA and rLifA^{C1480A} were found to be structurally identical by the various methods of biophysical characterisation, it was thought that the C1480A substitution was unlikely to affect UDP-GlcNAc binding.

Only the N-terminal cleavage product was observed in T cell lysates, possibly due to the C-terminal end being retained in the endosome and degraded or being centrifuged out of the lysate with the insoluble material. T cells were treated with WT rLifA and rLifA^{C1480A} in parallel to the J774A.1 cells and a volume equivalent to 4 x 10^6 cells was run the same gel as the J774A.1 cells. There appeared to be a protein species in the lysate of rLifA-treated T cells on the anti-LifA blot at ~225 kDa but it was too faint to be conclusive (data not shown). Given that some transmembrane proteins, such as the growth factor receptor ErbB-1, are known to be degraded by the ubiquitin-proteasome pathway from the endosome, treating T cells with proteasome inhibitors, such as β-lactone or MG-132, may reveal more of the LifA C-terminus (Levkowitz *et al*., 1998; van Kerkhof *et al*., 2001). Using these two different inhibitors would be useful, as peptide aldehydes like MG-132 can also inhibit lysosomal degradation (Rock *et al*., 1994; Craiu *et al*., 1997). Double the quantity of rLifA was applied to eight times the number of T cells compared to J774A.1 cells, with a volume equivalent to 16 times more T cells then J774A.1 cells being loaded into the gel. Despite this, more of each cleavage product and less full-length rLifA was observed in the lysates of J774A.1 cells compared to T cells. Although densitometry would be required to make a definite conclusion regarding this, the blot suggests that J774A.1 cells uptake more rLifA than T cells, which could provide a useful model for future studies of LifA cleavage. Full-length rLifA^{C1480A} was detected by anti-LifA antibodies in J774A.1 cells but not anti-6 x His antibodies, likely as there are more epitopes for anti-LifA binding present on rLifA proteins than for anti-6 x His binding. However, given that the C-terminal portion of WT rLifA could be detected with anti-6 x His, this suggestes that there was either less full-length rLifA^{C1480A} present in the lysates compared to WT rLifA C-terminus or there was inconsistent staining with this antibody. Detection of proteins with

anti-6 x His antibody was generally poor when attempted, hence it was not used more extensively.

In parallel to the experiments investigating LifA cleavage, experiments were conducted to determine whether LifA might cleave host cell proteins like other virulence factors containing C58 protease domains (Shao *et al*., 2002 and 2003a; Brugirard-Ricaud *et al*., 2005). The detection of LifA protease activity was attempted using a commercially available Protease Fluorescent Detection Kit (Sigma-Aldrich), which uses a protocol modified from Twining (1984). Proteins exhibiting protease activity cleave the FITC-labelled casein substrate. After incubation, trichloroacetic acid is used to precipitate undigested casein, which is centrifuged out. The supernatant is neutralised and small fragments of labelled casein that are not precipitated can be detected by measuring the fluorescence intensity with excitation and emission wavelengths of 485 and 535 nm respectively (Sigma-Aldrich, 2019). A trypsin control was provided with the kit and papain was used as a cysteine protease control. Protease activity was not detected at any concentration of rLifA, however, the trypsin control failed to produce the expected standard curve, even after trouble shooting, and the assay was deemed unsuitable. Even if LifA does exhibit protease activity against a host protein(s), it cannot be guaranteed that it would act on the casein substrate. The C58 proteases YopT and AvrPphB require specific recognition sequences at their respective cleavage sites and such a sequence may be required for LifA protease activity (Shao *et al*., 2003a and 2003b). Although western blots suggest that the CP domain of LifA is required for autoproteolysis, AvrPphB uses its CP domain for both autocatalytic cleavage and cleavage of the host cell protein PBS1 (Shao *et al*., 2002 and 2003a). This could mean a dual role for the CP domain of LifA but this would likely require cleavage to occur to the C-terminal end of the C/H/D motif rather than between the CP and glycosyltransferase domains as it does in LCTs (Rupnik *et al*., 2005; Kreimeyer *et al*., 2011; Guttenberg *et al*., 2011). The sizes of the cleavage products, however, suggest that cleavage of LifA occurs between these two domains, similar to the LCTs.

Autocatalytic cleavage of LCTs requires the co-factor $InsP_6$ and occurs optimally between pH 7 and 8, although they have also been reported to cleave in the presence of DTT and β-mercaptoethanol (Reinke *et al*., 2007; Egerer *et al*., 2007;

Rupnik *et al*., 2005). Attempts to initiate the autocatalytic cleavage of rLifA *in vitro*, however, have been unsuccessful despite the range of conditions used, including different pHs, incubation times, and the presence or absence of $InsP_6$ and DTT (Cassady-Cain *et al*., 2016; Walkinshaw Laboratory, unpublished data). An experiment was performed to determine whether the putative co-factor of LifA was proteinaceous. T cell lysates without protease inhibitors were either incubated at 70 °C for 10 minutes, the same conditions used to denature protein for SDS-PAGE, or prepared immediately before the addition of rLifA and incubation at 37 °C for 1 hour. However, western blots revealed a complex ladder of protein species reactive to the anti-LifA antibody from lysates with and without heat treatment, making the c. 140 kDa cleavage product impossible to detect (data not shown). This may have been due to active proteases that survived the heat treatment cleaving rLifA, or host cell proteins that contain anti-LifA antibody reactive peptides, as experiments of this nature using LCTs heated lysates at 96 °C for 30 minutes (Reinke *et al*., 2007).

To confirm the requirement of endosome acidification for LifA cleavage, a number of approaches could be used. T cells could be pre-incubated with inhibitors, incubated with rLifA for 1 hour then acid pulsed, which may allow the protein to translocate across the plasma membrane (Qa'dan *et al*., 2000 and 2001). An alternative method would be to allow rLifA to bind T cells at 4 °C, briefly incubate the cells with inhibitor then replace the medium with fresh medium at a lower pH (Barth *et al*., 2001). Additional experiments performed by Qa'dan *et al*. (2000 and 2001) with the LCTs TcdB and TcsL could be used to obtain data relating to pH-induced conformational changes in LifA. Tryptophan fluorescence assays, used previously to detect UDP-GlcNAc binding with LifA (Bease, 2015; Cassady-Cain *et al*., 2016), can be used to detect changes in tryptophan fluorescence if differences in pH cause structural changes to the protein (Qa'dan *et al*., 2000 and 2001). rLifA could also be subjected to TNS (2-(*p*-Toluidinyl) naphthalene-6-sulphonate) fluorescence analysis to identify pH-induced changes in hydrophobicity. Similar to SYPRO Orange used in TDAs, TNS fluoresces at a greater intensity in hydrophobic environments, which can be measured between 380 and 500 nm (McClure and Edelman, 1966; Qa'dan *et al*., 2000). This method or TDAs could reveal structural changes that make rLifA more hydrophobic. The pH-induced structural changes in

TcdB and TcsL were also found to be reversible, as protein shifted from pH 4 to 7 exhibited normal background fluorescence (Qa'dan *et al*., 2000 and 2001). Membrane insertion of LifA could be studied using the acid pulse method described above from Barth *et al*. (2001). Cells could be pre-loaded with $^{86}Rb^{+}$, the release of which would be measured after protein treatment, indicating whether LifA forms a pore in the endosomal membrane like LCTs (Barth *et al*., 2001). Lastly, digestion of rLifA at different pHs with the pH stable *Staphylococcus aureus* V8 protease may reveal different digest profiles, confirming that previously unavailable digestion sites become exposed under acidic conditions (Qa'dan *et al*., 2000).

Attempts to determine the effects of endosome acidification inhibition on the biological activity of LifA were unsuccessful, as the concentrations of bafilomycin A1 or chloroquine required to inhibit LifA cleavage also inhibited T cell proliferation. An experiment using two-fold dilutions of bafilomycin A1 (0.15625–5 µM) or chloroquine (3.90625–125 µM) was carried out to look for subtle changes in proliferation that may have been missed in previous experiments. The proliferation index of rLifA treated T cells increased as the concentration of bafilomycin A1 increased but toxicity was observed at as low as 1.25 µM (data not shown). Toxicity caused by chloroquine did not become apparent until a concentration of 62.5 µM but the proliferation index remained constant as the concentration of chloroquine increased (data not shown). Although the effects of bafilomycin A1 on T cell proliferation have not been previously reported, the effects of chloroquine have. Schmidt *et al*. (2017) reported that 0.6 µM chloroquine reduced the proliferative capacity of human $CD4^{+}$ T cells to ~80 % of that of untreated cells, and by 10 µM it was reduced to ~30 %. It was also reported that the relative viability of activated T cells was not affected up to a concentration of 10 µM chloroquine but decreased to ~30 % at 100 µM (Schmidt *et al*., 2017).

Taken together, the work presented in this chapter identified a key role for the Cys^{1480} residue in intracellular processing and activity of lymphostatin in the absence of obvious effects on the biophysical properties of the protein relative to WT rLifA. However, it cannot be concluded if the loss of activity reflects a requirement for autocatalytic cleavage to release the catalytic domain from endosomal membranes, allowing it to reach its cellular target (as for LCTs), or a direct role for cysteine

protease activity against a cellular target that results in inhibition of T cell proliferation.

5 Identifying interacting partners of lymphostatin

5.1 Introduction

Although the inhibitory effects of lymphostatin on T cells were first observed over two decades ago, before the protein responsible was formally identified (Klapproth *et al*., 1995), the target(s) of lymphostatin activity remains unknown. Given that LifA binds UDP-GlcNAc and that mutation of the DXD motif within the glycosyltransferase (GT) domain abolishes this binding, as well as inhibitory activity, it was hypothesised that LifA acts as a glycosyltransferase (Bease, 2015; Cassady-Cain *et al*., 2016). Given the N-terminal homology between LifA and large clostridial toxins (LCTs), Rho GTPases that regulate the cytoskeleton may seem like a plausible target for LifA. However, LifA does not exhibit direct cytotoxicity or alter the morphology of treated cells (Klapproth *et al*., 1995 and 2000; Stevens *et al*., 2002; Bease, 2015; Cassady-Cain *et al*., 2016), which is associated with the glycosylation of Rho GTPases by LCTs (Just *et al*., 1994 and 1995a; Selzer *et al*., 1996). There is only limited evidence to suggest that LifA targets Rho GTPases (Babbin *et al*., 2009), which could not be confirmed by subsequent studies (Deacon *et al*., 2010). These experiments only examined well studied Rho GTPases however, and so LifA may target lesser studied Rho GTPases that have functions aside from regulating cell morphology.

As LifA inhibits the mitogen- and antigen-stimulated proliferation of T cells (Cassady-Cain *et al*., 2016 and 2017), it is possible that it targets part of the T cell signalling cascade. T cell signalling begins at the T cell receptor (TCR). T lymphocytes can be classed as either αβ or γδ depending on the class of proteins that make up the TCR (reviewed in Alcover *et al*., 2018). αβ T cells are activated against antigens by the interaction of the TCR with peptide-MHC complexes and co-stimulation from other cells, particularly antigen-presenting cells (APCs; reviewed in Courtney *et al*., 2017; reviewed in Attanasio and Wherry, 2016). The TCR of γδ T cells however, either interacts with antigens directly or MHC proteins that do not belong to either MHC class I or II (Adams *et al*., 2005; reviewed in Vermijlen *et al*., 2018). The TCR forms a complex with CD3, which itself is formed

from γε, δε and ζζ subunits (Brenner *et al*., 1985; Samelson *et al*., 1985; Sussman *et al*., 1988), which acts as the intracellular signalling portion of the receptor. In αβ T cells, when the TCR interacts with a peptide-MHC complex the TCR co-receptors CD4 and CD8 bring the Src kinase Lck into contact with its substrates, which are the immunoreceptor tyrosine-based activation motifs (ITAMs) of the CD3 γ-, δ-, ε- and ζ-chains (Rudd *et al*., 1988; Veillette *et al*., 1988; Baniyash *et al*., 1988; Barber *et al*., 1989). The Src kinase Fyn also phosphorylates CD3 ITAMs but to a lesser extent than Lck (Denny *et al*., 2000). The phosphorylation of CD3 ITAMs results in the recruitment and Lck-dependent phosphorylation of ZAP70 (Iwashima *et al*., 1994; Neumeister *et al*., 1995; Chan *et al*., 1995). This in turn triggers a complex series of phosphorylation/dephosphorylation events in the linker for activation of T cells (LAT) signalosome that results in the remodelling of the cell cytoskeleton, signal transduction to the nucleus and binding to APCs (Figure 5.1; reviewed in Huse, 2009). A brief description of these events is given below highlighting the main processes involved.

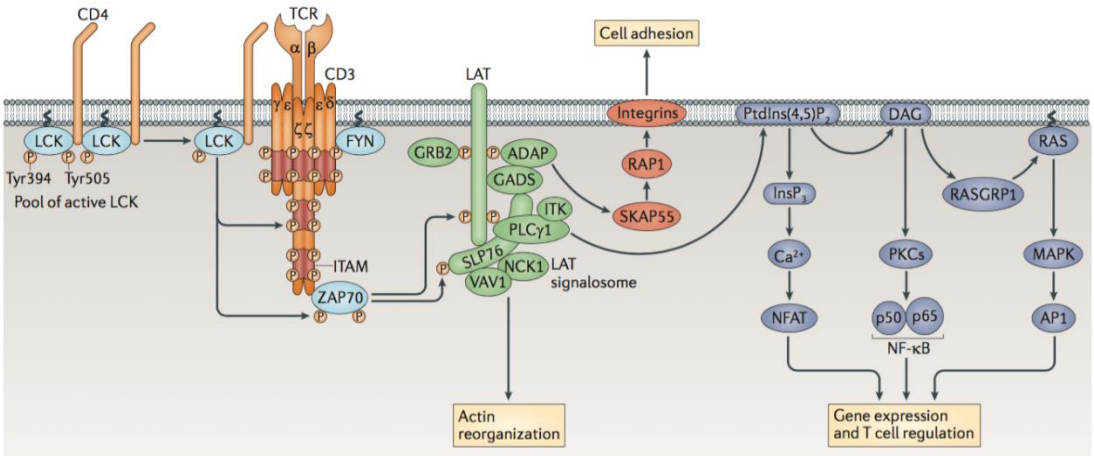

Figure 5.1. The early TCR signalling pathway. The interaction of the TCR with peptide-MHC complexes results in the recruitment and activation of various proteins that are responsible for cytoskeleton remodelling, APC binding and co-stimulation and changes in gene expression (from Brownlie and Zamoyska, 2013).

Remodelling of the actin cytoskeleton occurs when the TCR is activated by an APC and results in areas of the T cell plasma membrane spreading across the

surface of the APC (reviewed in Kumari *et al*., 2014). Wiskott-Aldrich syndrome protein (WASP) is recruited to the LAT signalosome by Nck, where it is activated by the Rho GTPase Cdc42, which itself is activated first by Vav1 (Zeng *et al*., 2003). Vav1 also activates a second Rho GTPase, Rac1, which in turn activates WASP family veprolin homologous protein (Wave2; Crespo *et al*., 1996 and 1997; Nolz *et al*., 2006). WASP and Wave2 then recruit the actin-related protein 2/3 complex, which triggers actin polymerisation (reviewed in Kumari *et al*., 2014).

While cytoskeletal remodelling provides a large surface area for T cell-APC interaction, the upregulation of integrins, particularly lymphocyte function-associated antigen 1, results in the adhesion of the two cells (Bachmann *et al*., 1997). This allows for the co-stimulation of the T cell, which is necessary for effective stimulation. Typically, the T cell co-stimulatory receptor CD28 binds with the ligands CD80 or CD86 on APCs, which promotes proliferation, cell survival and cytokine production (reviewed in Esensten *et al*., 2016).

Gene expression after TCR activation is influenced by the protein PLCγ1, which controls the calcium ion, NF-κB and MAPK signalling pathways (reviewed in Cantrell, 2015). These three pathways respectively result in the transcription factors NF-AT, NF-κB and AP-1 upregulating the expression of IL-2, which is responsible for proliferation as well as the differentiation of naïve T cells into memory or effector T cells (reviewed in Cantrell, 2015; reviewed in Ross and Cantrell, 2018). The TCR is also capable of activating the mammalian target of rapamycin (mTOR) pathway through phosphoinositide 3-kinase (PI3K), which promotes cell survival and proliferation (Gorentla *et al*., 2011; Sinclair *et al*., 2008).

Recent studies provide some insight into the action of LifA on the T cell activation pathway. rLifA inhibits the proliferation of T cells that have been stimulated by the mitogen ConA (Cassady-Cain *et al*., 2016 and 2017), which activates T cells by interacting with the T3/antigen receptor complex, initiating the calcium ion signalling pathway (Kanellopoulos *et al*, 1985; Weiss *et al*, 1987; reviewed in Weiss *et al*, 1986). However, rLifA does not block the stimulation of T cells by phorbol myristate acetate (PMA) and ionomycin (Cassady-Cain *et al*., 2017). PMA activates protein kinase C (PKC) and ionomycin is a Ca^{2+} ionophore that activates both PKC and calmodulin (CaM; Castagna *et al*., 1982; Chatila *et al*.,

1989). This suggests that the target of LifA may lie downstream of the TCR but upstream of PKC and CaM (Figure 5.2). Cassady-Cain *et al*. (2017) also found that rLifA inhibited the IL-2 stimulated proliferation of T cells. IL-2 signalling has some downstream effects in common with TCR signalling, such as the activation of mTOR and the activation of Ras through the phosphorylation of SHC1, which associates with growth factor receptor-bound protein 2 (Grb2; reviewed in Ross and Cantrell, 2018). rLifA also inhibits the IL-4-stimulated proliferation of B cells but to a lesser degree than T cells (Cassady-Cain *et al*., 2017). It does not, however, inhibit the IL-12/IL-18-stimulated production of IFN-γ by NK cells, suggesting that the target(s) of LifA may be expressed in different quantities in different cell types, and/or that uptake and processing of LifA may vary between cell types in a way that dictates how much of the protein reaches the cellular target(s). The target(s) of LifA may also only be important in certain cell types. Additionally, LifA may not affect NK cells if its target(s) is not involved in IL-12/IL-18 signalling.

In this chapter, I sought to identify potential targets of glycosylation in rLifA-treated T cells. Since there were no suspected targets of LifA, a broad approach was employed to identify unique glycosylation events using western blotting and shotgun mass spectrometry. In addition, protein pull-downs were used to identify potential interacting partners and targets of LifA, including receptors and adaptor proteins that may traffic the GT domain-containing N-terminus to its target.

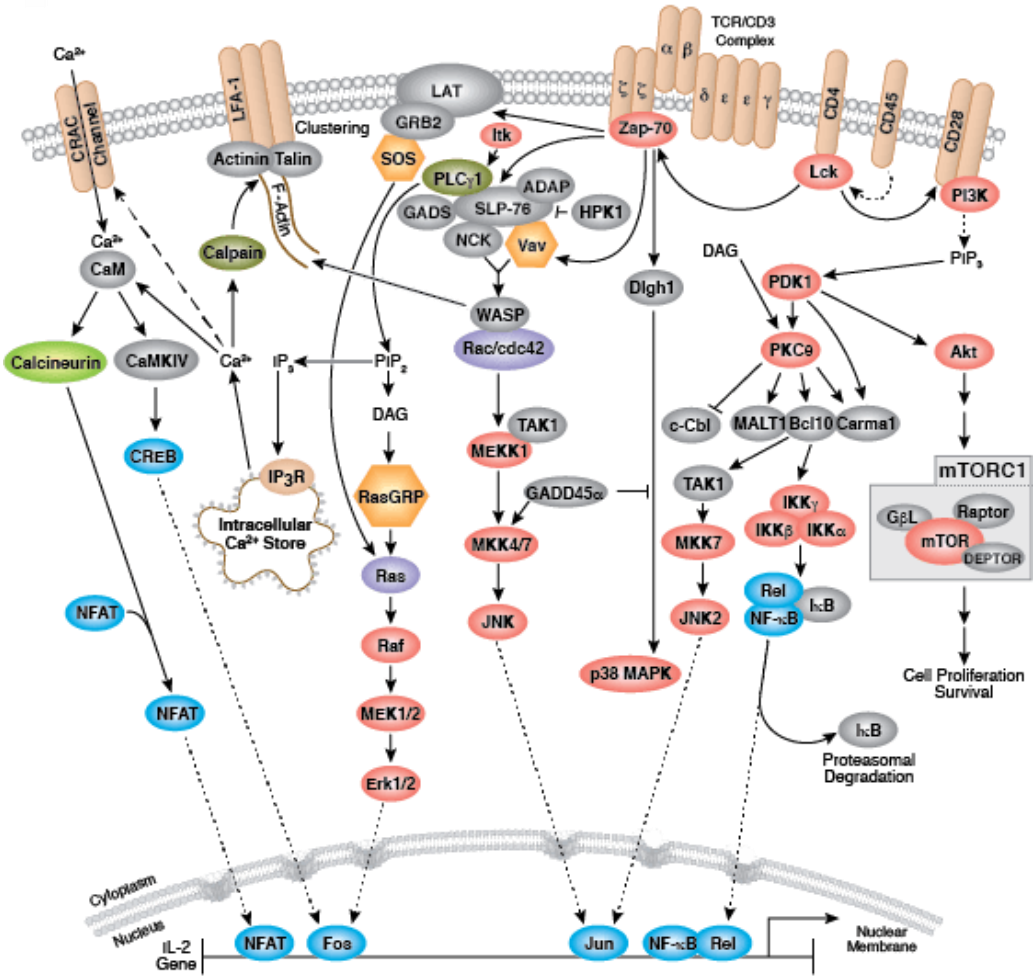

Figure 5.2. Overview of T cell signalling. ConA stimulates the T cell receptor (TCR) while PMA activates protein kinase C (PKC), which normally requires calcium for activation. The Ca^{2+} ionophore ionomycin activates PKC and calmodulin (CaM). It may be hypothesised that LifA acts by glycosylating a protein in the signalling pathway somewhere between the TCR and PKC and CaM, allowing to it to inhibit proliferation stimulated by ConA but not PMA and ionomycin (from Cell Signaling Technology®, 2014).

5.2 The bovine T lymphocyte O-GlcNAc profile

5.2.1 Western blotting

Initially, to identify possible targets of glycosylation and observe changes in the O-GlcNAcome, western blots were performed using the lysates of either T cells alone, rLifA-treated T cells, or T cells treated with the GT mutant rLifA$^{DTD/AAA}$. T cells were treated with protein at a final concentration of 2 μg/mL, as this concentration of rLifA achieves inhibition of ConA-stimulated proliferation at saturation. Lysates were run on three different gel systems to provide the best resolution at different molecular weights, with ranges of 10–150 kDa, 25–250 kDa and 71–460 kDa. Blots were probed with an anti-O-GlcNAc antibody, which detects O-linked GlcNAc. As there are currently no antibodies available that can detect N-linked GlcNAc, an examination of this modification by western blotting was not possible. No obvious changes were detected in the O-GlcNAc profile of rLifA-treated T cells in comparison to untreated or rLifA$^{DTD/AAA}$-treated T cells (Figure 5.3). Additionally, no O-GlcNAcylated proteins were detected below 50 kDa, even when the brightness and contrast of the image were increased.

Since no changes were detected in the O-GlcNAc profile of rLifA-treated T cells, untreated and rLifA-treated T cell lysates were subjected to glycoprotein enrichment using a commercially available kit. Wheat germ agglutinin (WGA) beads were used to isolate glycoproteins from the lysates with the intention of enhancing the detection of O-GlcNAcylated proteins and removing proteins that might bind to the anti-O-GlcNAc antibody non-specifically. It was also predicted that the glycoprotein enrichment would aid the identification of GlcNAcylated peptides by shotgun mass spectrometry (see Section 5.2.2). Despite a modest enrichment of some proteins in enriched lysates there was still no detectable change in the O-GlcNAc profile of rLifA-treated cells in comparison to untreated cells (Figure 5.4). Again, no O-GlcNAcylated proteins were detected below 50 kDa.

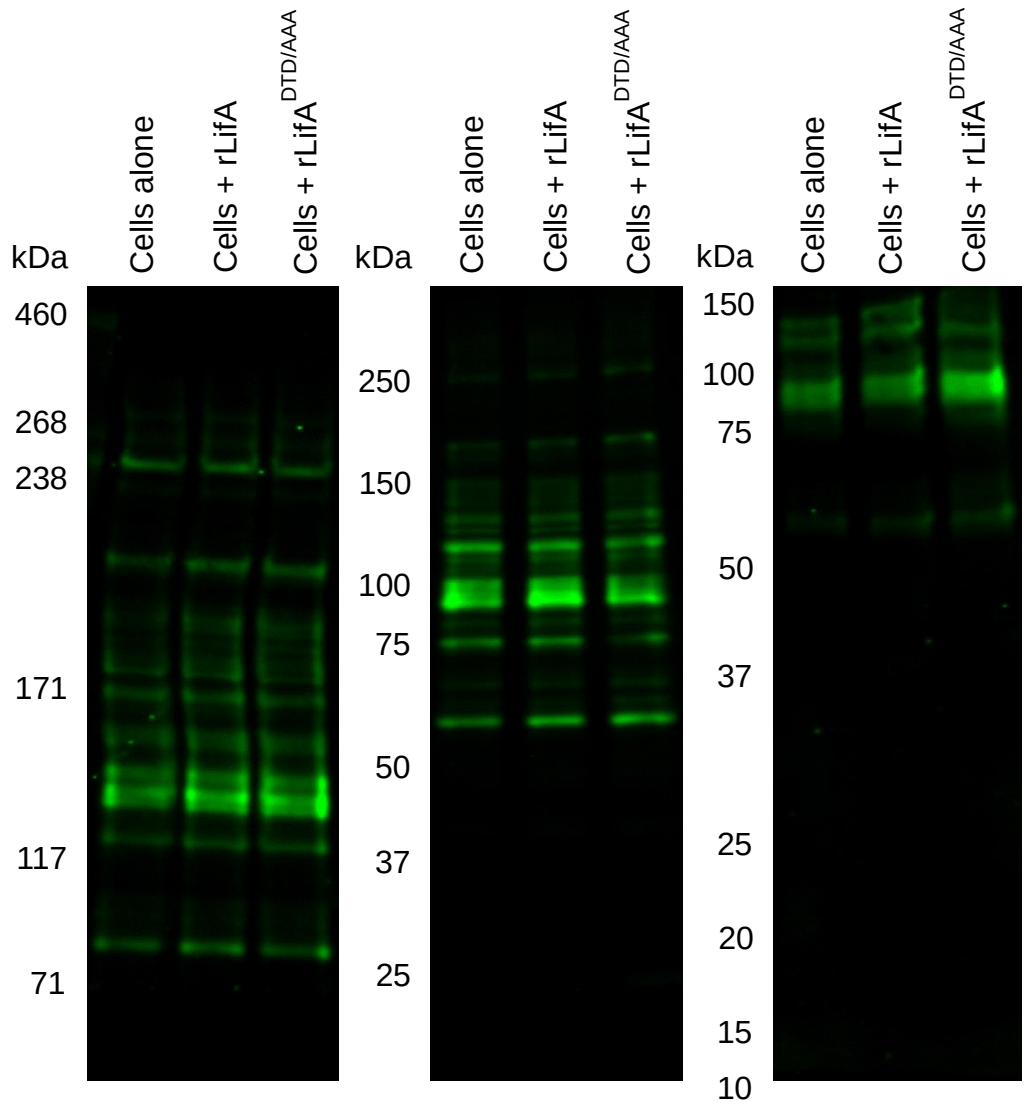

Figure 5.3. The O-GlcNAc profile of bovine T lymphocytes in the presence or absence of rLifA. T cells were treated with buffer, rLifA or rLifA$^{DTD/AAA}$ at a final concentration of 2 μg/mL and the lysates were probed with an anti-O-GlcNAc antibody to identify changes in the O-GlcNAc profile. Lysates were run on three different gel systems to provide the best resolution at different molecular masses. No obvious changes in the O-GlcNAc profile were detected in cells treated with rLifA compared to cells alone or treatment with rLifA$^{DTD/AAA}$, and no O-GlcNAcylated proteins were detected below 50 kDa.

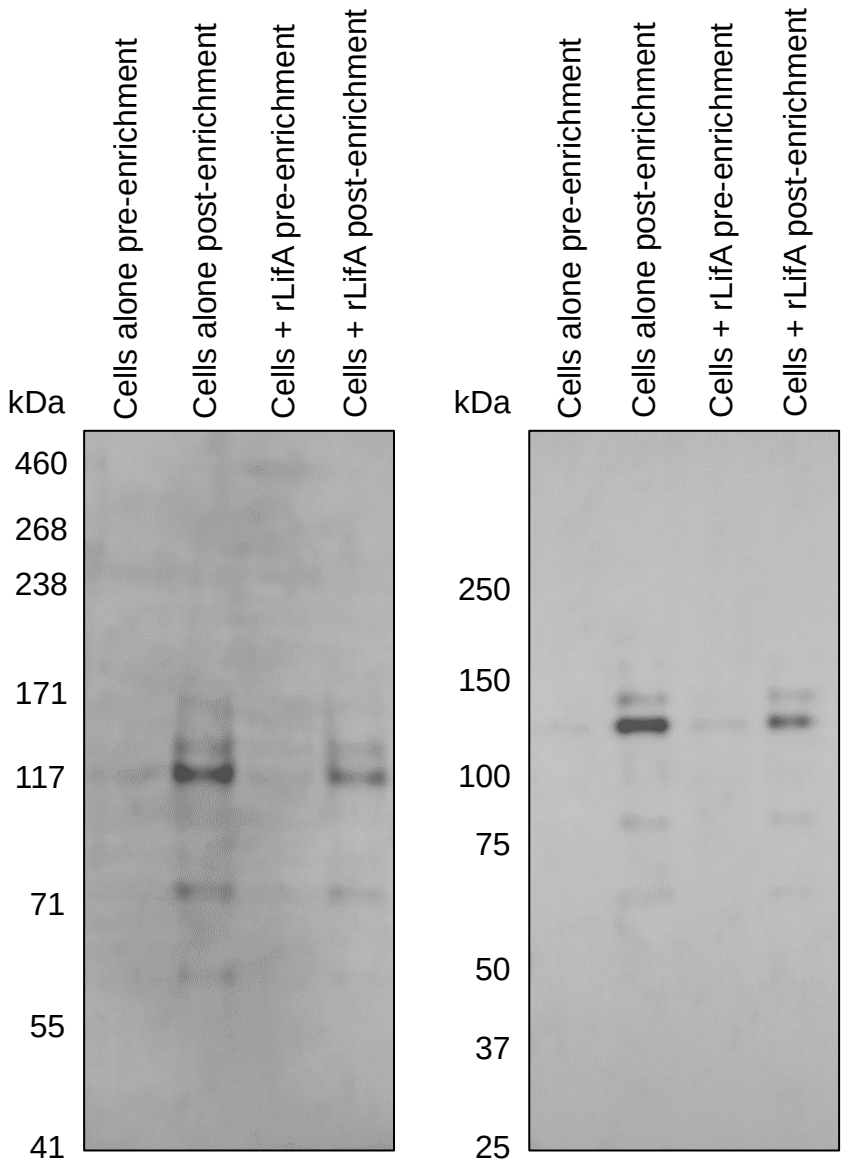

Figure 5.4. The O-GlcNAc profile of enriched T cell lysates in the presence or absence of rLifA. T cells were treated with buffer or rLifA at a final concentration of 2 μg/mL. Lysates were enriched for O-GlcNAcylated proteins using wheat germ agglutinin beads. Equal quantities of total protein from pre- and post-enriched lysates were run on two different gel systems to look for changes in the O-GlcNAc profile at different molecular mass ranges. While some glycoproteins were modestly enriched, there was an overall loss of protein diversity during the enrichment process. Again, there were no obvious differences in the O-GlcNAc profiles of cells treated with rLifA and those without.

5.2.2 Shotgun mass spectrometry

Published research to identify the target of LCT activity used electrospray mass spectrometry to determine both the sugar substrate and the particular amino acid that is glycosylated on RhoA (Just *et al*., 1995b and 1995c; Selzer *et al*., 1996). However, at the time of these experiments, RhoA was suspected of being a target since the toxins TcdA and B were known to cause actin depolymerisation similar to that observed in cells treated with *C. botulinum* C3 toxin, which ADP-ribosylates Rho GTPases (Quilliam *et al*., 1989). Additionally, treatment of cells with TcdA and B inhibited the ADP-ribosylation of RhoA by C3 toxin (Just *et al*., 1994 and 1995a). Unlike these experiments, there is currently no putative target protein of lymphostatin activity, as LifA treatment does not cause morphological changes and is not known to interfere with other effectors. Therefore, I used shotgun mass spectrometry to examine lysates of T cells treated, or not, with rLifA to detect peptides modified with GlcNAc, allowing for different types of linkage and multiple GlcNAc moieties.

Three independent sets of samples were sent to the Kinetic Parameter Facility (KPF) at the University of Edinburgh for analysis by Lisa Imrie: pellets of 1.2 x 10^7 T cells treated with buffer, rLifA or rLifA$^{DTD/AAA}$ at a final concentration of 2 μg/mL for 1 hour; pellets of 3.6 x 10^7 T cells treated with buffer or rLifA at a final concentration of 2 μg/mL for 1 hour; and T cell lysates subjected to glycoprotein enrichment from Section 5.2.1 (Tables 5.1–5.3). Peptides were searched for modifications with one or two GlcNAc molecules on either N-linkages, which occur on Asn residues, or O-linkages, which occur on Ser and Thr residues. The overall number of unique proteins and peptides detected in the two sets of cell pellets was between 399–744 and 1565–3259 respectively, but the number of unique GlcNAcylated peptides detected was much lower than expected. Shotgun mass spectrometry was expected to detect > 700 proteins from eukaryotic cell pellets of the sizes used (Lisa Imrie, personal communications). Only one unique N-linked modified peptide was detected that possessed the consensus sequence of Asn-Xaa-Ser/Thr/Cys, where Xaa is any amino acid other than proline, which is required for N-linked glycosylation (Pless and Lennarz, 1977; Bause and Legler,

1981). This peptide was detected in T cells treated with rLifA$^{DTD/AAA}$, however, meaning that it could not have been modified in a GT domain-dependent manner. From the two sets of cell pellets a total of four peptides were detected with O-linked GlcNAc on Ser residues and two peptides had O-linked GlcNAc on Thr residues. No GlcNAc modified peptides were detected in the glycoprotein enriched samples, which also had lower numbers of unique proteins and peptides detected. A quality control sample of *Ostreococcus tauri* proteins was run on the spectrometer before each experimental sample, which tracked the retention times, intensities of the base peaks and number of proteins identified. All quality control samples performed as expected (Lisa Imrie, personal communications). Detailed information on the proteins/peptides identified can be found in Appendix 5.

Table 5.1. Proteins and peptides detected in pellets of 1.2 x 10^7 T cells by shotgun mass spectrometry. Data were collected and analysed by Lisa Imrie, KPF.

Sample	No. of unique proteins	Total No. of peptides	No. of unique peptides	No. of unique glycosylated peptides
Cells alone	686	119839	2965	4 N-linked modified peptides (none have correct linkage site)
Cells + rLifA	598	143953	2649	7 N-linked modified peptides (none have correct linkage site), 2 O-linked (S) peptides, 1 O-linked (S & T) peptide
Cells + rLifA$^{DTD/AAA}$	697	161510	3012	8 N-linked modified peptides (none have correct linkage site), 1 O-linked (S) peptide, 1 N-linked & O-linked (T) peptide

Table 5.2. Proteins and peptides detected in pellets of 3.6 x 10^8 T cells by shotgun mass spectrometry. Data were collected and analysed by Lisa Imrie, KPF.

Sample	No. of unique proteins	Total No. of peptides	No. of unique peptides	No. of unique glycosylated peptides
Cells alone	744	45067	3259	2 N-linked modified peptides (none have correct linkage site), 1 O-linked (S) peptide
Cells + rLifA	399	18315	1565	0

Table 5.3. Proteins and peptides detected in glycoprotein enriched T cell lysates by shotgun mass spectrometry. Data were collected and analysed by Lisa Imrie, KPF.

Sample	No. of unique proteins	Total No. of peptides	No. of unique peptides	No. of unique glycosylated peptides
Cells alone	85	21366	322	0
Cells + rLifA	80	4087	303	0

Only three GlcNAcylated peptides were detected that were unique to T cells treated with WT rLifA but these were not repeatedly detected in independent replicates. Eukaryotic initiation factor 4A-III (EIF4A3) and histone H2B were found to have O-GlcNAc modifications on Ser^{368} and Ser^{20} respectively. EIF4A3 is an RNA helicase that is involved in RNA splicing (Chan *et al.*, 2004) but no evidence could be found in the literature that it can be regulated by O-GlcNAcylation. Histone H2B is known to be O-GlcNAcylated in a manner that regulates transcription, but this occurs on Ser^{112} (Fujiki *et al.*, 2011). Although both of these proteins have the potential to affect T cell proliferation, they act at a transcriptional level and would therefore likely be affected by PMA/ionomycin stimulation, which is not inhibited by rLifA (Cassady-Cain *et al.*, 2017).

The third GlcNAc modified peptide was derived from glyceraldehyde 3-phosphate dehydrogenase (GAPDH). In pellets of 1.2 x 10^7 cells treated with WT rLifA, there is an O-linked GlcNAc on one of three possible Thr residues (Thr^{141}, Thr^{151} or Thr^{152}) and another on either Ser^{146} or Ser^{149}. However, this peptide was not

consistently detected in pellets of 3.6 x 10^8 cells treated with rLifA. This peptide sequence was detected in rLifA$^{DTD/AAA}$-treated T cells but with different modifications. Again, there was an O-linked GlcNAc on one of three Thr residues, but there was also an N-linked modification on either Asn^{139} or Asn ^{147}, rather than a Ser modification. GAPDH exists in a tetrameric form in the cytoplasm and has been shown to regulate calcium flux in kidney cells by interacting with IP_3R and delivering NADH, which stimulates IP_3R-mediated intracellular Ca^{2+} release (Patterson *et al*., 2005). O-GlcNAcylation of GAPDH disrupts its tetrameric form, allowing it to be translocated to the nucleus, however, this modification is known to occur on Thr^{227} (Park *et al*., 2009). It is possible that LifA may GlcNAcylate GAPDH at a unique site however. It is also not clear whether GAPDH plays a major role in calcium flux caused by T cell activation. GAPDH is an attractive candidate for lymphostatin activity given its potential role in calcium flux and that it is targeted by the glycosyltransferase NleB as an innate immune evasion strategy (Gao *et al*., 2013; El Qaidi *et al*., 2017). Inhibiting GAPDH expression in macrophages has been shown to reduce IFN-γ production (Yamaguchi *et al*., 2016) but in T cells, GAPDH binds to and inhibits the translation of IFN-γ transcripts unless it is recruited for glycolysis (Chang *et al*., 2013). Calcium flux is also important for NK cell signalling (Bryceson *et al*., 2006) yet expression of IFN-γ by these cells did not appear to be affected by LifA treatment (Cassady-Cain *et al*., 2017). It is therefore unclear as to whether GAPDH is targeted by LifA.

Given the small number of GlcNAcylated peptides detected using shotgun mass spectrometry, it was decided that this method (or the equipment available) may not be sufficiently sensitive to identify potential targets of LifA activity and that other approaches should be pursued.

5.3 Protein pull-downs

5.3.1 Identifying candidate LifA interacting partners by silver staining and liquid chromatography mass spectrometry (LC-MS)

To detect proteins that interact with LifA, lysates of T cells were passed through a column on which His-tagged rLifA was immobilised on Co^{2+}-agarose beads (Thermo Fisher Scientific Inc., 2013a; reviewed in Puckett, 2015). Control columns on which rLifA alone was immobilised, or where T cell lysate was passed with no rLifA loaded on the column, were respectively used to distinguish putative interacting proteins from degraded forms of rLifA and proteins that bind non-specifically to the beads. Eluted proteins were analysed on three different gel systems to provide the best resolution at different molecular weights, with ranges of 10–250 kDa, 25–250 kDa and 55–460 kDa. Silver staining revealed potential interacting partners of rLifA at ~70, 100 and 180 kDa (Figures 5.5 and 5.6). The c. 180 kDa protein was consistently observed using T cells from three independent donors while the other proteins were not. In Figures 5.5 and 5.6, the c. 180 kDa appeared at the same size as a protein species in the rLifA alone control but appeared slightly below this species on other silver-stained gels. The presence of the c. 180 kDa protein appeared to remain consistent at each elution step, whereas very little of the rLifA species was eluted after the first elution step. No putative interacting partners of rLifA were detected below 50 kDa (Figure 5.7).

The c. 180 kDa protein and the corresponding area from the T cells alone control were excised and analysed by LC-MS by Dr Dominic Kurian, Proteomics and Metabolomics Facility, The Roslin Institute. Most of the peptides identified were from various forms of keratin, which is a common contaminant, or other proteins that are not involved in T cell signalling. Peptides from lymphostatin were detected when the c. 180 kDa protein was searched against the whole NCBI database and the EPEC E2348/69 LifA sequence, indicating that some of the protein at this position in the gel is derived from rLifA. Two proteins detected by searching the Uniprot *B. taurus* database were unique to the c. 180 kDa gel band from the rLifA pull-down but not the T cell only control. These were found to be involved directly in lymphocyte

signalling, however, only a single peptide was detected for each protein and both proteins are smaller than 180 kDa. One was derived from Calpain 7, an ~93 kDa protein that is activated by calcium and has been reported to be required for T cell proliferation, the expression of proinflammatory cytokines and lymphocyte function-associated antigen-1-mediated adhesion (Smith *et al*., 2011; Stewart *et al*., 1998). However, further examination of the peptide ion fragmentation pattern gave little confidence that this peptide was genuine.

The second protein located at c. 180 kDa in the rLifA pull-down but not the T cell only control was inositol polyphosphate-5-phosphatase E (INPP5E), also known as pharbin, which is predicted to be ~72 kDa. INPP5E regulates protein kinase B (Akt) phosphorylation by hydrolysing phosphatidylinositol (3,4,5)-triphosphate (PIP_3), $PI(3,5)P_2$ and $PI(4,5)P_2$, which is converted into PIP_3 by PI3K (reviewed in Eramo and Mitchell, 2016). PIP_3 is required for the Ser^{473} phosphorylation of Akt1 by mTORC2 (Sarbassov *et al*., 2005; Gan *et al*., 2011), and given that Akt1 Ser^{473} phosphorylation was found to be reduced in rLifA-treated T cells in independent studies (Stevens Laboratory, unpublished data; see Chapter 6), this made INPP5E an attractive candidate for future work. INPP5E has been reported to be phosphorylated by aurora kinase A, which increased its phosphatase activity (Plotnikova *et al*., 2015). It can also be O-GlcNAcylated by O-GlcNAc transferase but the effect of this on its activity is not known (Tian and Qin, 2019). Analysis of the peptide ion fragmentation also gave confidence that the peptide detected by LC-MS was genuine, despite the difference in molecular weight. Therefore, further experiments with INPP5E were carried out as described in Section 5.3.3. Detailed information on the proteins/peptides identified can be found in Appendix 5.

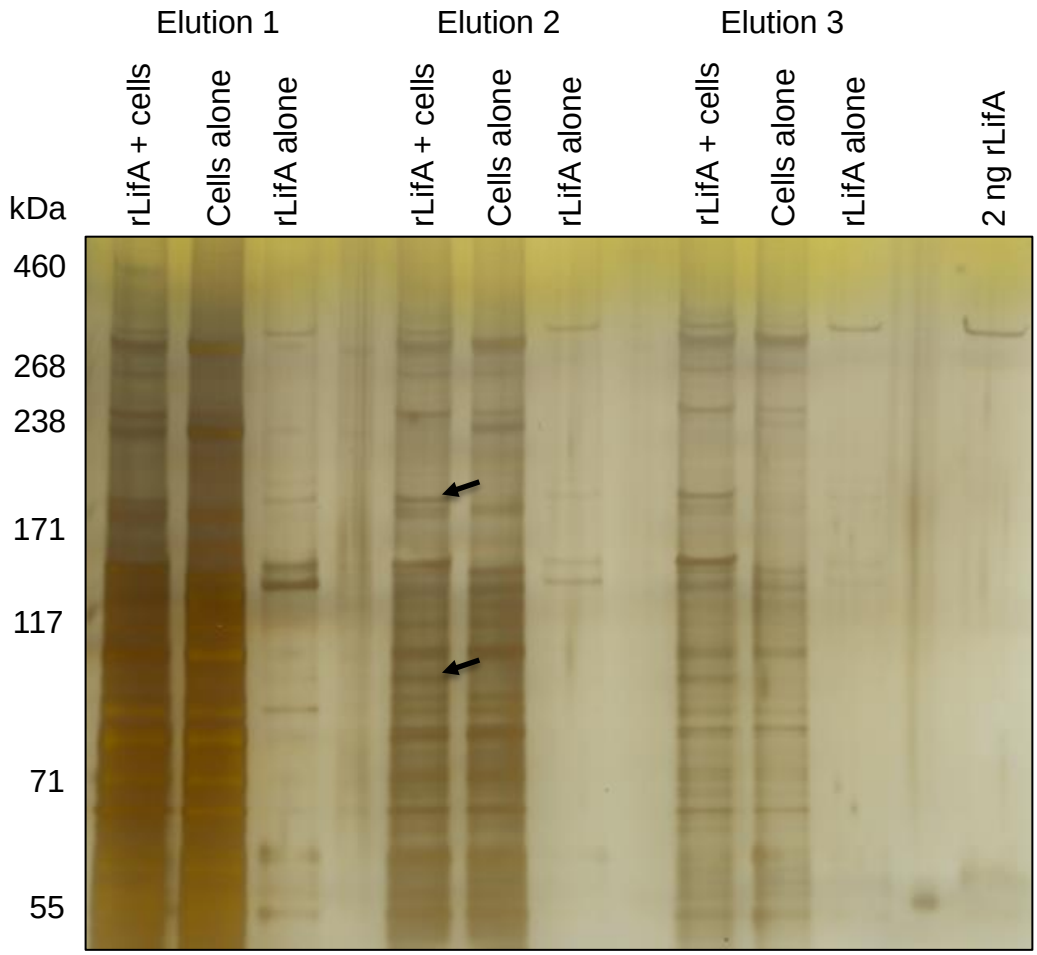

Figure 5.5. Pull-down assays using rLifA immobilised on columns to capture T cell proteins (55–460 kDa). rLifA or buffer was captured on cobalt resin beads and T cell lysate was then mixed with the resin. Proteins were eluted from the resin three times and silver staining was used to detect protein species that were unique to rLifA with T cell lysate or found in greater quantities than in lysate alone. rLifA was captured and mixed with lysis buffer to determine which protein species were products of rLifA. Two unique protein species were detected at ~100 and 180 kDa (marked with arrows). Although the c. 180 kDa protein appears at roughly the same position as a protein from the rLifA alone control, this protein was seen consistently in multiple replicates below the rLifA alone band. A quantity of 2 ng of rLifA was used to show the position of full-length rLifA. This experiment was performed with 3 independent donors and a representative gel is shown.

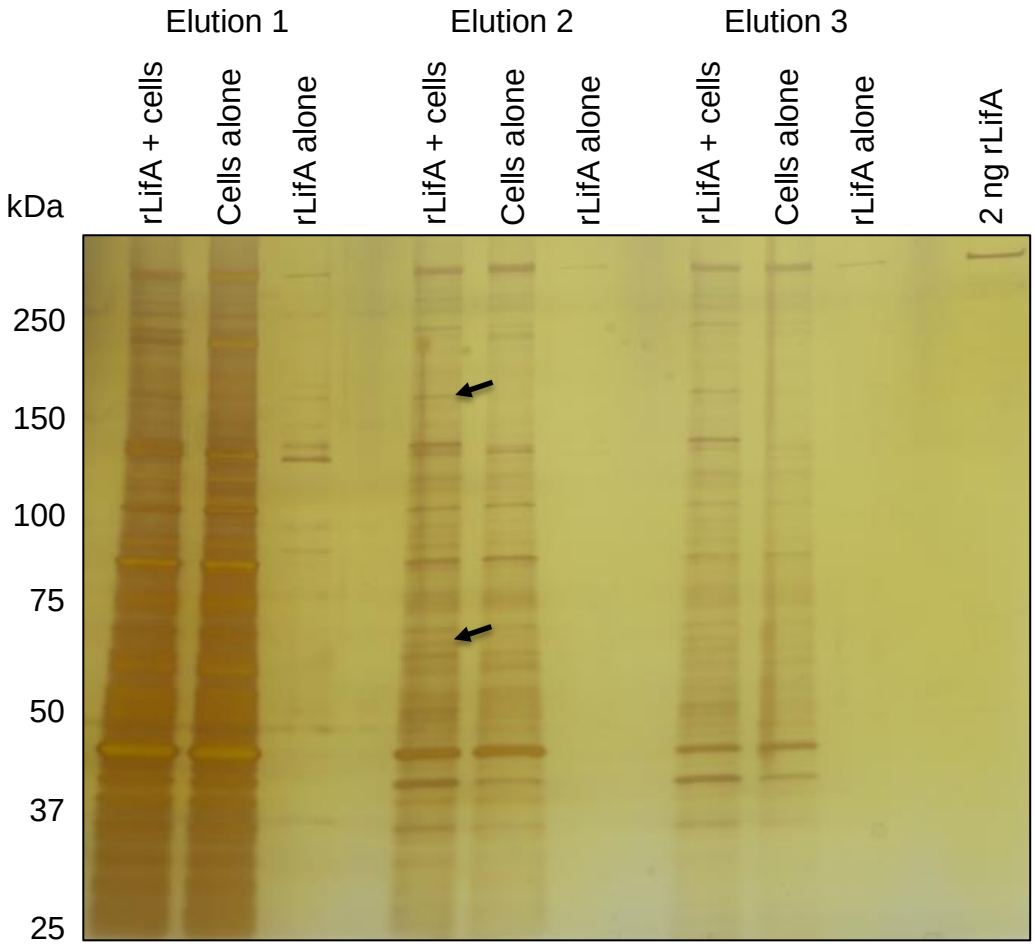

Figure 5.6. Pull-down assays using rLifA immobilised on columns to capture T cell proteins (25–250 kDa). The c. 180 kDa protein species detected on the previous gel was also observed on this gel type. The c. 100 kDa protein could not be seen using this gel system but another protein species was detected at ~70 kDa. Unique protein species are marked with arrows. A quantity of 2 ng of rLifA was used to show the position of full-length rLifA. This experiment was performed with 3 independent donors and a representative gel is shown.

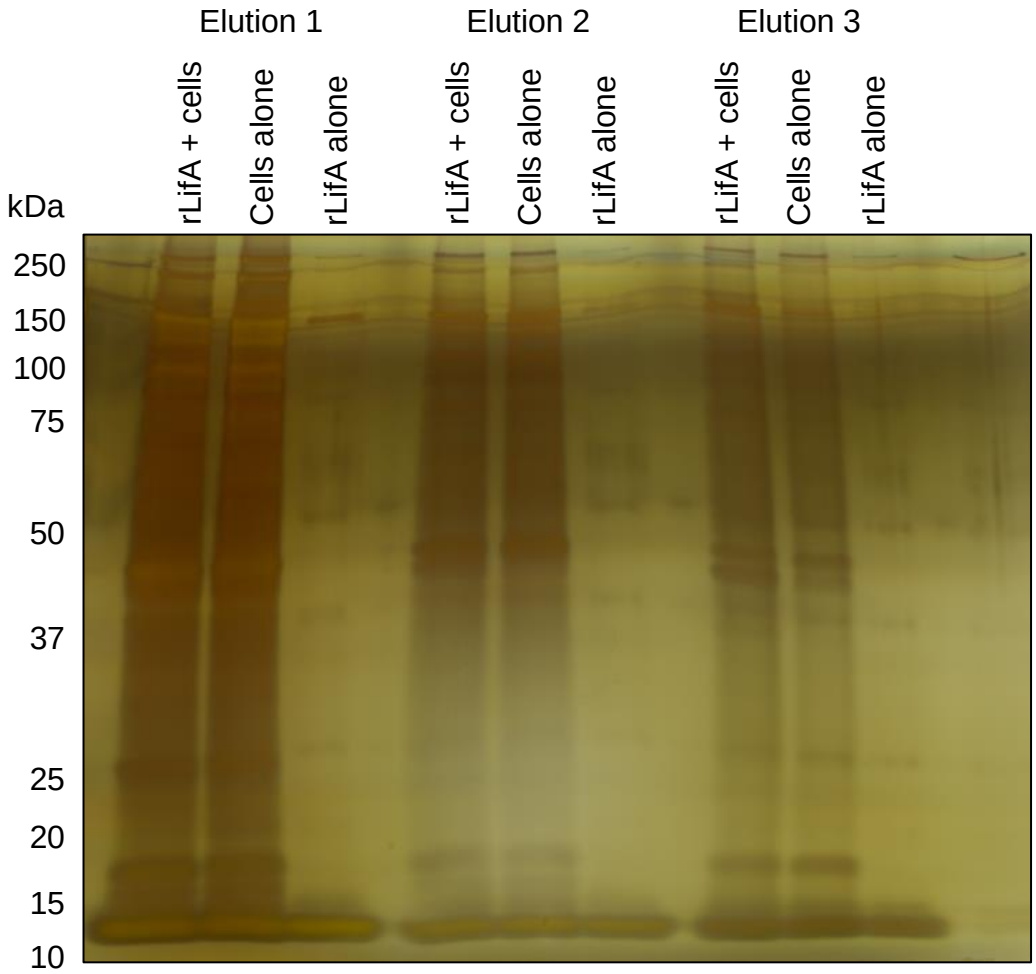

Figure 5.7. Pull-down assays using rLifA immobilised on columns to capture T cell proteins (10–250 kDa). Using a gel to achieve resolution at the lowest molecular weights did not reveal any unique protein species below 25 kDa (the limit of the gel system used in Figure 5.6). Even the proteins of higher molecular weights observed using other gel types could not be seen. This experiment was performed with 3 independent donors and a representative gel is shown.

5.3.2 Shotgun mass spectrometry of pull-down eluates

Whole eluates from the same donor used in the experiments shown in Figures 5.5–5.7 were used for shotgun mass spectrometry, performed by Lisa Imrie, KPF. Eluates from the first elution step were used as these contained the most protein. However, the number of proteins/peptides detected was far lower than previously

observed when searching for GlcNAc modified peptides (Tables 5.4 and 5.5). The same quality controls were applied to these analyses as described in Section 5.2.2. Detailed information on the proteins/peptides identified can be found in Appendix 5.

Table 5.4. Proteins and peptides detected in protein pull-down eluates by shotgun mass spectrometry. Data were collected and analysed by Lisa Imrie, KPF.

Sample	No. of unique proteins	Total No. of peptides	No. of unique peptides
Cells alone	12	43	12
rLifA + cells	8	24	8

Table 5.5. Identities of proteins and peptide sequences detected in protein pull-down eluates by shotgun mass spectrometry. Green cells highlight proteins unique to the 'rLifA + cells' sample. Most proteins were detected in both samples but some were identified by different peptide sequences. Data were collected and analysed by Lisa Imrie, KPF.

Sample	Protein name	Peptide sequence
Cells alone	Actin, alpha cardiac muscle 1	AGFAGDDAPR
	Antithrombin-III	RVWELSK
	Apolipoprotein A-I	VQPYLDEFQKK
	Cationic trypsin	SSGTSYPDVLK
	Complement C3	LPYSVVR
	Epidermal growth factor receptor (Fragment)	IPLENLQIIR
	Fibronectin	STTPDITGYR
	Gelsolin	AALKTASDFISK
	Inter-alpha-trypsin inhibitor heavy chain H3	GHVSFKPSLDQQR
	ITIH2 protein	TILDDLR
	Lumican	ILGPLSYSK
	Serum albumin	LGEYGFQNALIVR
rLifA + cells	Antithrombin-III	EVALNTIIFMGR
	Cationic trypsin	SSGTSYPDVLK
	Complement C3	LPYSVVR
	Fibronectin	STTPDITGYR
	Gelsolin	AGKEPGLQIWR
	Glutathione peroxidase	FLVGPDGIPVMR
	ITIH2 protein	FYNQVSTPLLR
	Serotransferrin	DLLFRDDTK

Despite the low number of proteins/peptides detected, two proteins were unique to the sample where T cell lysate was mixed with rLifA bound to Co^{2+}-agarose beads. The first was serotransferrin, which is an ~77 kDa protein that is N-glycosylated. It transports Fe^{3+} ions, which are required for cell replication, but it is unlikely to interact with LifA in T cells as it is a blood plasma glycoprotein (reviewed in Clerc *et al.*, 2016). The second is glutathione peroxidase (GPx), which is ~24 kDa and is known to protect cells from reactive oxygen species (ROS)-induced oxidative stress as well as regulate various signalling pathways (reviewed in Brigelius-Flohé and Maiorino, 2013). ROS promote T cell proliferation and GPx deficient $CD4^+$ T cells exhibit increased proliferation and are driven

towards a Th1 response (Won *et al*., 2010). Human GPx activity can be regulated by phosphorylation of Tyr^{96} by the non-receptor tyrosine kinases ABL1 and 2 (Cao *et al*., 2003), but this residue is not present in the bovine homologue. GPx can also be O-GlcNAcylated within the C-terminal 100 amino acids, which increases binding with ABL1 and 2 and therefore phosphorylation (Yang *et al*., 2010). If LifA O-GlcNAcylates GPx at this known site, thereby increasing its activity and lowering proliferation, this would coincide with the observations made in Chapter 6, where rLifA inhibited Akt1 Ser^{473} phosphorylation. This is because overexpression of GPx has been reported to suppress Akt1 Ser^{473} phosphorylation (McClung *et al*., 2004; Handy *et al*., 2009). In contrast, however, Akt1 Ser^{473} phosphorylation has also been reported to be downregulated in GPx deficient cells (Taylor *et al*., 2004; Taylor *et al*., 2005).

Since GPx was the only plausible candidate identified by shotgun mass spectrometry, further experiments were carried out with this protein as described in Section 5.3.3.

5.3.3 INPP5E and GPx do not appear to specifically interact with rLifA

Given that it was uncertain whether rLifA targeted or interacted with INPP5E or GPx, western blotting using polyclonal antibodies against these proteins was used to determine whether they were specifically pulled down from T cell lysates by rLifA. Eluates from the first elution step were used as these contained the most protein. However, reactivity at the expected positions was not obvious (Figure 5.8A), except for INPP5E when the brightness was increased (Figure 5.8B). This suggested that INPP5E was present in both the eluate from the column with rLifA plus T cell lysate, as well as the column with T cell lysate alone.

Whole T cell lysates were originally used as positive controls for the antibodies but INPP5E and GPx could not be detected (data not shown). To resolve this, immunoprecipitation (IP) was used to isolate both proteins from T cell lysates and concentrate them prior to western blot analysis. IP was performed on T cells treated with buffer or rLifA to determine whether rLifA caused any changes in protein expression. At the expected positions in the gel for INPP5E, similar reactivity

was observed for the IP sample of rLifA-treated T cells relative to the IP sample of T cells alone (red box in Figure 5.8A), however, reactivity to GPx was neither clear nor specific. The bulk of reactivity observed was due to detection of the antibodies used for immunoprecipitation. A protein species was detected at ~180 kDa with the anti-INPP5E antibody, however, this was also detected in the IP controls, making it unclear as to whether a peptide from INPP5E was at that position. No proteins were detected below 20 kDa. Given that full-length INPP5E was detected in both pull-down eluates, that GPx was not convincingly detected in either, and that the presence of the INPP5E peptide at ~180 kDa could not be confirmed, it was decided that no further experiments would be carried out with these proteins.

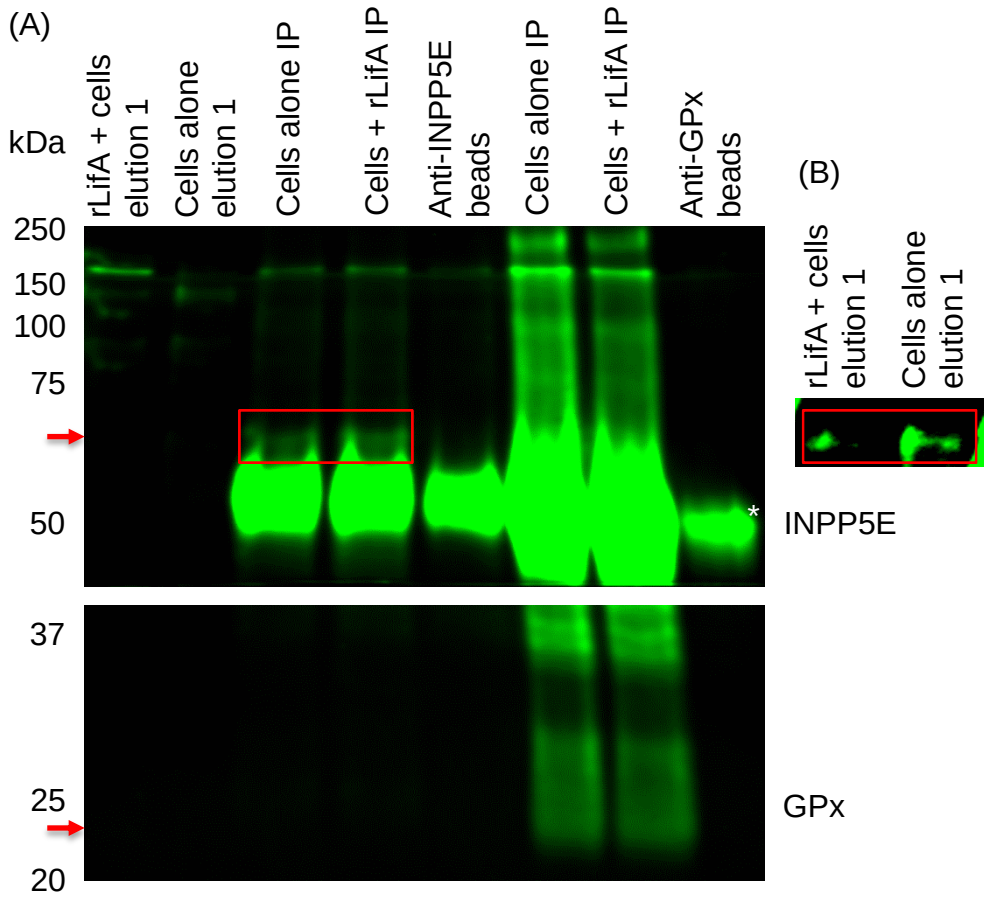

Figure 5.8. Detection of inositol polyphosphate 5 phosphatase E (INPP5E) and glutathione peroxidase (GPx) in eluates from columns loaded with rLifA (or diluent) and used to capture T cell proteins. (A) Protein pull-down eluates were probed for INPP5E (43–250 kDa) and GPx (20–43 kDa). Immunoprecipitation (IP) was performed on the lysates of T cells treated with buffer/rLifA to provide positive controls for INPP5E (~72 kDa; marked with box) and GPx (~24 kDa; no clear band). IP was performed using polyclonal anti-INPP5E and anti-GPx1 antiodies. INPP5E and GPx could not be detected at the expected sizes initially, although a band was observed at ~180 kDa on the anti-INPP5E blot, around the same size as the protein species used for mass spectrometry that identified a peptide belonging to INPP5E. Anti-INPP5E and anti-GPx antibodies bound to protein A beads were used to show the position of the antibody heavy chains at ~50 kDa. Arrows indicate the expected sizes of INPP5E and GPx. Asterisk indicates the antibody heavy chain. (B) Increasing the brightness of the western blot revealed protein species at the expected size for INPP5E in both pull-down eluates, suggesting it is not unique to rLifA with T cell lysate (marked with box). Even at this brightness, GPx could not be detected.

5.4 Discussion

Despite previous studies providing an insight into where LifA is likely to act in the T cell signalling cascade, a target of LifA glycosyltransferase activity has yet to be identified. Various methods were employed to detect putative targets of GlcNAc modification and other proteins that LifA may interact with. However, inconsistent results meant that the few proteins identified could not be confirmed as genuine targets/interacting partners.

Anti-O-GlcNAc western blotting detected far fewer O-GlcNAc modified proteins than anticipated, as mammalian cells have been reported to contain over 1000 O-GlcNAcylated proteins (Trinidad *et al*., 2012; Qin *et al*., 2017). However, western blots performed on murine T cells with the same antibody used in this study (Swamy *et al*., 2016) detected a number of proteins comparable to that in Section 5.2.1. This suggests that many of the predicted O-GlcNAcylated proteins in mammalian cell lysates may be present at concentrations below the limit of detection for this antibody or are only transiently modified. Additionally, anti-O-GlcNAc antibodies recognise specific peptide sequences with O-GlcNAc modifications, not solely the O-linked sugar moiety, meaning that other proteins may have been identified if several different antibodies had been used (reviewed in Ma and Hart, 2014). Swamy *et al*. (2016) reported that O-GlcNAcylated proteins were upregulated after CD3/CD28 activation for 24 hours. However, in experiments using ConA-stimulated T cells, no changes to the O-GlcNAc profile were detected and the overall protein concentration was reduced by 1 hour post-incubation and completely absent by 24 hours post-incubation (data not shown). This may have been caused by incubating the cells in serum-free medium for the entire duration of the experiment. Detecting GlcNAc modified peptides by western blotting is limited by the lack of antibodies against N-linked GlcNAc. The anti-O-GlcNAc IgM clone CTD110.6, however, has been reported to cross-react with N-GlcNAc (Isono, 2011), which could be used to identify previously undetected modifications. N-GlcNAc modifications could then be distinguished from O-GlcNAc by treating T cell lysates with PNGase F, which cleaves between N-GlcNAc and the adjoined Asn residue (Plummer Jr *et al*., 1984).

Like the western blot approach, shotgun mass spectrometry identified far fewer GlcNAcylated proteins than expected. Given that mass spectrometry approaches have previously identified over 1000 O-GlcNAcylated proteins (Trinidad *et al*., 2012; Qin *et al*., 2017), it is possible that the mass spectrometer used in this study may not have been sensitive enough to detect all of the modified peptides. A study using human primary T cells identified 214 O-GlcNAcylated proteins, which is still far more than detected in this study (Lund *et al*., 2016). The digestion of the samples with trypsin may also be responsible for the lack of detected GlcNAcylated peptides. Some O-GlcNAcylation sites are located in sequences with clustered Ser/Thr residues and few Arg and Lys residues, which trypsin cleaves between, resulting in long peptides that are not easily detected. Proteolysis using chemicals, such as cyanogen bromide, or digestion with other enzymes such as Asp-N or Glu-C may improve the detection of such sequences (reviewed in Ma and Hart, 2014). A method that may improve the detection of O-GlcNAcylated peptides would be to subject T cell lysates to β-elimination followed by Michael addition of dithiothreitol (DTT). This method enzymatically removes O-GlcNAc moieties and replaces them with DTT. The bond between DTT and Ser/Thr residues is more stable than the glycosidic bond and does not break during peptide fragmentation, allowing for detection of the modified peptide (Nika *et al*., 2013; Lund *et al*., 2016). This technique would be particularly useful as the form of shotgun mass spectrometry used at the KPF (electrospray ionisation-collision induced dissociation (higher energy collisional dissociation)-quadropole time-of-flight tandem mass spectrometry) is known to break glycosydic bonds during peptide fragmentation (reviewed in Ma and Hart, 2014). The use of this form of mass spectrometry may explain the low the number of O-GlcNAcylated peptides detected. Other GlcNAcylated residues may be missed since all proteins in the sample do not exhibit 100 % peptide coverage. Top-down proteomics is an approach that could be taken to overcome this. Top-down proteomics allows for the analysis of whole proteins by mass spectrometry, provides 100 % coverage and does not cause the loss of post-translational modifications (reviewed in Cui *et al*., 2011; reviewed in Catherman *et al*., 2014). However, top-down proteomics does have some limitations, such as the inability to detect insoluble proteins, a lack of robust methods for protein

separation and difficulty analysing proteins > 70 kDa (reviewed in Gregorich and Ge, 2014).

Isolating GlcNAc modified proteins using WGA enrichment did not allow for the detection of a greater number of GlcNAcylated proteins using shotgun mass spectrometry. This may be due to the method of enrichment. WGA preferentially binds GlcNAc but also has affinity for sialic acid, which is commonly found at terminal positions of glycans (Thermo Fisher Scientific Inc., 2013b; reviewed in Varki *et al*., 2017). Therefore, GlcNAc modified proteins may have been competitively inhibited from binding to the WGA beads due a large number of glycoproteins with terminal sialic acid moieties. This could be rectified by using succinylated WGA, which is an acidic form of WGA that binds normally to GlcNAc but not sialic acid (Monsigny *et al*., 1980). Greater enrichment of GlcNAcylated proteins may also be achieved by using combined antibody/lectin enrichment. Lee *et al*. (2016) developed this method, which uses WGA and multiple anti-O-GlcNAc antibodies attached to resin beads, and were able to identify 990 O-GlcNAcylated proteins alone. Given that O-GlcNAc modifications are a common signalling mechanism in mammalian cells and can be removed by O-GlcNAcase, pre-treating cells with O-GlcNAcase inhibitors, such as PUGNAc or thiamet-G, may prevent the removal of putative LifA-mediated O-GlcNAc modifications (Horsch *et al*., 1991; Yuzwa *et al*., 2008). However, many of these inhibitors are analogues of GlcNAc (reviewed in Gloster and Vocadlo, 2010) and so should be tested to determine whether they might bind to LifA and inhibit its activity. Considering the long-lasting effects of LifA on T cells (Cassady-Cain *et al*., 2017), however, it is likely that predicted GlcNAc modifications made by LifA are not removed by O-GlcNAcase.

It is also possible that proteins modified by LifA were not detected using western blotting or shotgun mass spectrometry approaches because only N- and O-linked GlcNAcylation was investigated. These are the most common forms of glycosylation but sugars can bond to other amino acids. NleB has been shown to GlcNAcylate arginine residues in GAPDH (El Qaidi *et al*., 2017). S-linked GlcNAc is attached to the sulphur atom in cysteine residues and has recently been identified in mammals (Maynard *et al*., 2016). GlcNAc has also been shown to be transferred onto hydroxyproline and phosphate groups attached to serine residues in *D.*

discoideum (Teng-umnuay *et al*., 1999; Mehta *et al*., 1996) but this is not known to occur in mammalian cells. It should also be noted that while LifA has been shown to bind UDP-GlcNAc (Cassady-Cain et al., 2016), we cannot preclude the possibility that it binds other sugar donors, and that transfer of a different sugar is responsible for lymphostatin activity.

Further evidence of issues with the sensitivity of the shotgun mass spectrometry conducted herein is the low number of proteins/peptides identified in protein pull-down eluates. Originally, eluates were fractionated by SDS-PAGE and gel sections of whole wells were sent for analysis by shotgun mass spectrometry. However, no peptides were detected using this method despite protein species being visible on silver stained gels. This led to the analysis of whole eluates, which contained a larger quantity of protein. Given that the 'rLifA + cells' and 'cells alone' samples contained ~39 and 49 µg of protein respectively, it is unlikely that the quantity of protein was too low to detect. This can be assumed because the glycoprotein enriched samples contained as little as 10 µg of protein yet still allowed for the detection of hundreds of unique peptides. Both shotgun mass spectrometry and LC-MS can be further complicated by the fact that bands on a silver stained gel may not all represent proteins. Silver stain is known to also bind nucleic acids, proteolipids and lipopolysaccharide that cannot be matched to the protein databases used to analyse mass spectra (Somerville and Wang, 1981; Cochary *et al*., 1990; Tsai and Frasch, 1982). Silver staining is also not sensitive to all types of proteins (Friedman, 1982), which suggests that interacting partners of LifA could remain unseen using this staining method. Negative stains or fluorescent dyes could potentially be used to search for proteins not detected by silver staining (reviewed in Gauci *et al*., 2011). Another drawback of silver staining is that glutaraldehyde in the sensitising reagent cross-links proteins (Shevchenko *et al*., 1996) meaning that the mass of cross-linked peptides will not be accurately matched to protein databases. It is unclear why a peptide unique to bovine INPP5E was detected ~100 kDa above its expected position in the gel. This may have been due to a degraded peptide binding to another protein or it may simply not have been a genuine result.

The detection of GPx in pull-down eluates was complicated by the fact that there are eight GPx isoforms (reviewed in Brigelius-Flohé and Maiorino, 2013), and

that Uniprot did not state which of these was detected. The polyclonal antibody used to detect GPx was raised against GPx1, which is ubiquitously expressed and is the most studied isoform (reviewed in Brigelius-Flohé and Maiorino, 2013). However, later *in silico* analysis of the protein identified by shotgun mass spectrometry revealed that the isoform was actually GPx5. This protein has only ~47 % identity and~59 % similarity to GPx1 between amino acids 18–201, which may explain why GPx was not detected in the pull-down eluates. However, GPx5 would not be expected to be found in T cells as previous studies using mice, rats, pigs, humans, macaques and cattle have shown that it is expressed specifically in the male reproductive tract (Rejraji *et al*., 2002; Williams *et al*., 1998; Barranco *et al*., 2016; Hall *et al*., 1998; Légaré *et al*., 2017).

Interactions between LifA and other proteins, especially targets of GlcNAc modification, may be transient and therefore difficult to detect using standard protein pull-downs. The detection of interacting partners is also dependent on the strength of the interaction and whether the buffer used disrupts these interactions. Chemical cross-linking could be used in conjunction with protein pull-downs to capture transient interactions (reviewed in Leitner, 2016). A cross-linking reagent could be used to label rLifA at specific surface bound amino acid residues before performing protein pull-downs, which should then be permanently bound to interacting partners from T cell lysates (Thermo Fisher Scientific Inc., 2010). Selecting an appropriate cross-linking reagent is dependent on the desired amino acid target and the spatial proximity of potential interacting proteins (reviewed in Leitner, 2016). A compromise is often required between selecting a large cross-linking reagent, which is more likely to form a cross-link with another protein but is less specific, and a smaller reagent, which is less likely to form a cross-link but be more likely to bind a true interacting partner (reviewed in Leitner, 2016). Not all cross-linked interacting proteins can be isolated by SDS-PAGE as their size prevents them from entering the gel (reviewed in Leitner, 2016), however, some cross-linking reagents contain tags, such as biotin, to facilitate the isolation of protein complexes (Trester-Zedlitz *et al*., 2003). Isolated protein complexes could then be subjected to LC-MS (reviewed in Leitner, 2016).

The approaches used in this chapter were unable to conclusively identify putative targets/interacting partners of lymphostatin. Unlike studies that identified the targets of the LCTs and NleB, where targets of glycosylation were already suspected, no proteins were confidently predicted to interact with LifA at the beginning of this study. As such, methods were used that had the potential to identify interacting partners from complex T cell lysates. However, since no interacting partners were identified this way, I decided to pursue a candidate approach and investigate a protein that was independently shown to be affected by LifA (see Chapter 6).

6 Analysis of the impact of lymphostatin on phosphorylation of the cellular protein kinase Akt

6.1 Introduction

Due to the inconclusive results obtained in the previous chapter, a candidate approach to investigating putative targets of LifA was taken. Initially, Vav1 was considered for investigation as it plays an important role in both T and B cell signalling (reviewed in Bustelo, 2014). Vav1 is a guanine nucleotide exchange factor for Rho GTPases and affects the calcium flux, ERK and NF-κB signalling pathways in T cells (Costello *et al*., 1999). Its activity is regulated by phosphorylation of three tyrosine residues (López-Lago *et al*., 2000). Vav1 deficient Jurkat and murine T cells exhibit reduced IL-2 expression and proliferation, which is observed in LifA-treated T cells (Costello *et al*., 1999; Cao *et al*., 2002; Klapproth *et al*., 1995, 1996 and 2000; Malstrom and James, 1998; Stevens *et al*., 2002; Deacon *et al*., 2010; Cassady-Cain *et al*., 2016 and 2017). Costello *et al*. (1999) also found that ionomycin partially rescues the proliferative capacity of Vav1 deficient T cells and similarly rLifA does not inhibit the proliferation of PMA/ionomycin-stimulated bovine T cells (Cassady-Cain *et al*., 2017). Experiments by Dr Robin Cassady-Cain, The Roslin Institute, revealed that Vav1 was O-GlcNAcylated in both rLifA-treated and untreated bovine T cells (data not shown). While the possibility that lymphostatin modifies Vav1 by addition of a sugar moiety on other linkages (for which antibodies are lacking) cannot be precluded, it was elected not to pursue Vav1 further.

Further experiments by Dr Robin Cassady-Cain using a Proteome Profiler Human Phospho-Kinase Array Kit (R&D systems) with highly purified bovine γδ T cells, highlighted a number of signalling proteins with reduced phosphorylation in ConA-stimulated cells treated with rLifA (Figures 6.1 and 6.2; Stevens Laboratory, unpublished data). One protein of particular interest was protein kinase B (PKB), also known as Akt. Akt has three isoforms that act on a variety of substrates to regulate metabolism and promote cell survival, growth and proliferation (Figure 6.3; reviewed in Manning and Toker, 2017). In T cells, Akt can be activated by the TCR

and Lck kinase through PI3K and Rac1, which causes the nuclear translocation of NF-κB and inhibits NF-AT dephosphorylation by glycogen-synthase kinase 3 (GSK3; Genot *et al*., 2000; Prasad *et al*., 1993; Jones *et al*., 2000; Reif *et al*., 1997; Lafont *et al*., 2000). Akt can also be activated through CD8 co-stimulation, which has the same down-stream effects as TCR-induced activation and is known to result in increased IL-2 expression (Okkenhaug *et al*., 2001; Burr *et al*., 2001; Coudronniere *et al*., 2000; Kane *et al*., 2001; Cross *et al*., 1995; Beals *et al*., 1997).

The kinase activity of Akt1 is regulated by phosphorylation at multiple sites, with the major two being Thr^{308} and Ser^{473} (Alessi *et al*., 1996; Hart and Vogt, 2011; reviewed in Manning and Toker, 2017). Phosphorylation occurs on the homologous residues Thr^{309} and Ser^{474} of Akt2 and on Thr^{305} and Ser^{472} of Akt3 (Meier *et al*., 1997; Brodbeck *et al*., 1999; Nakatani *et al*., 1999). Chemical inhibitors against PI3K and mTORC2, which are required for the phosphorylation of Akt1 Thr^{308} and Ser^{473} (Alessi *et al*., 1996; Tsuchiya *et al*., 2014; Sarbassov *et al*., 2005; Gan *et al*., 2011), have been shown to inhibit the CD3/CD8-stimulated proliferation of human T cells in a dose dependent manner (Herrero-Sánchez *et al*., 2016). This was not the result of increased apoptosis and the inhibition of proliferation produced sigmoid curves akin to those from rLifA-treated bovine T cells (Herrero-Sánchez *et al*., 2016; Cassady-Cain *et al*., 2016 and 2017). Blocking Akt phosphorylation also inhibited the secretion of IL-2, -4 and -10, and IFN-γ, similar to observations by Cassady-Cain *et al*. (2017), as well as IL-6 and TNF-α (Herrero-Sánchez *et al*., 2016).

Akt1 activation is also regulated by O-GlcNAcylation. Akt1 is O-GlcNAcylated at multiple sites, some of which inhibit the phosphorylation of Thr^{308} and Ser^{473}, while others inhibit phosphorylation of other amino acids (Wang *et al*., 2012; Gandy *et al*., 2006). O-GlcNAcylation of the residues Thr^{305} and Thr^{312} disrupts the interaction between Akt1 and 3-phosphoinositide-dependent protein kinase-1 (PDPK1), which inhibits Thr^{308} phosphorylation (Wang *et al*., 2012). O-GlcNAcylation of Ser^{473} inhibits phosphorylation of this residue and has been found to cause apoptosis in murine pancreatic β cells (Kang *et al*., 2008). Shi *et al*. (2015) also claimed that both Thr^{308} and Ser^{473} are O-GlcNacylated, resulting in apoptosis of multiple cell types, but did not explicitly identify the GlcNAcylated residues as was done by Kang *et al*. (2008) and Wang *et al*. (2012).

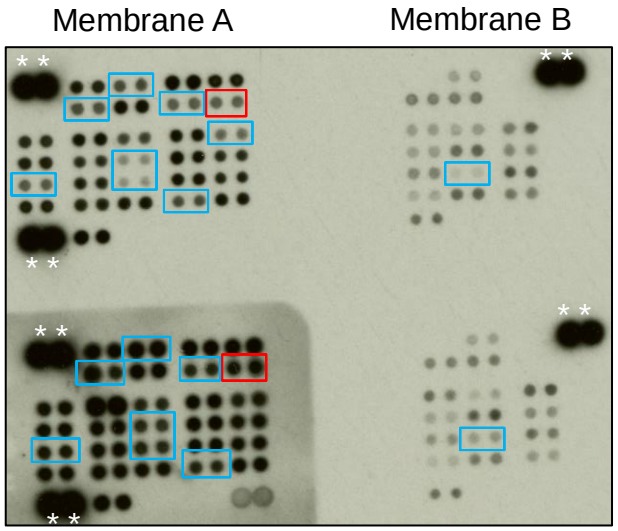

	Membrane A									
	1	2	3	4	5	6	7	8	9	10
A	Reference		p38-α		ERK1/2		JNK1/2/3		GSK3-α/β	
B			EGF R		MSK1/2		AMPKα1		AKT1/2/3 S	
C	TOR		CREB		HSP27		AMPKα2		β-catenin	
D	Src		Lyn		Lck		STAT2		STAT5a	
E	Fyn		Yes		Fgr		STAT6		STAT5b	
F	Hck		Chk-2		FAK		PDGF Rβ		STAT5a/b	
G	Reference		PRAS40						PBS	

	Membrane B							
	11	12	13	14	15	16	17	18
A			p53 S392				Reference	
B	AKT1/2/3 T		p53 S46					
C	p70 S6 K T389		p53 S15		c-Jun			
D	p70 S6 K T421/S424		RSK1/2/3		eNOS			
E	STAT3 Y705		p27		PLCγ1			
F	STAT3 S727		WNK1		PYK2			
G	HSP60						PBS	

Figure 6.1. rLifA inhibited the phosphorylation of various kinases in bovine γδ T cells. γδ T cells were incubated with buffer or 1 μg/mL rLifA for 1 hour at 37 °C, washed twice then stimulated with 5 μg/mL ConA for 15 minutes. T cell lysates were used in experiments with the Proteome Profiler Human Phospho-Kinase Array Kit according to the manufacturer's instructions. The array comprises immobilised antibodies specific for phosphorylated variants of the kinases shown on the right, which capture the proteins from cell lysates. Once unbound proteins have been removed, captured proteins are then detected with a cocktail of biotinylated detection antibodies, streptavidin-horse radish peroxidase and chemiluminescent detection reagents. A representative set of western blots of the kinase array from 1 of 3 independent donors is shown. Red boxes – duplicate spots of Akt1 Ser^{473} (also reacts with Akt2 Ser^{474} and Akt3 Ser^{472}). Blue boxes – duplicate spots of other proteins with noticeably reduced phosphorylation in rLifA-treated cells relative to control cells. White asterisks – reference spots. Data were collected by Dr Robin Cassady-Cain, The Roslin Institute.

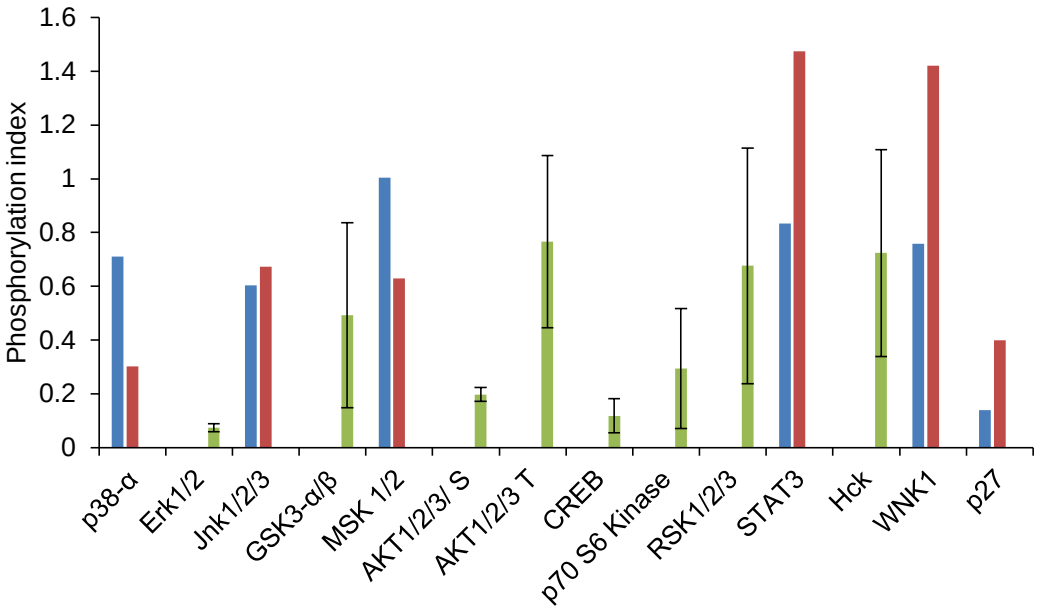

Figure 6.2. Densitometry analysis of the phosphorylation level of proteins detected using the Proteome Profiler Human Phospho-Kinase Array Kit. Pixel density data from duplicate spots of western blots was detected using Image Studio Lite v5.2. Data from cells + rLifA + ConA were normalised against cells + ConA to produce a phosphorylation index. Data is from at least 2 independent donors and shown for a subset of kinases detected by the array where reliable detection was possible. Blue and red bars denote the phosphorylation indices of individual replicates where data were collected from only 2 donors. Green bars denote the mean phosphorylation index where data were collected from 3 independent donors. Error bars indicate the standard deviation of indices across these donors. Data were collected by Dr Robin Cassady-Cain, The Roslin Institute.

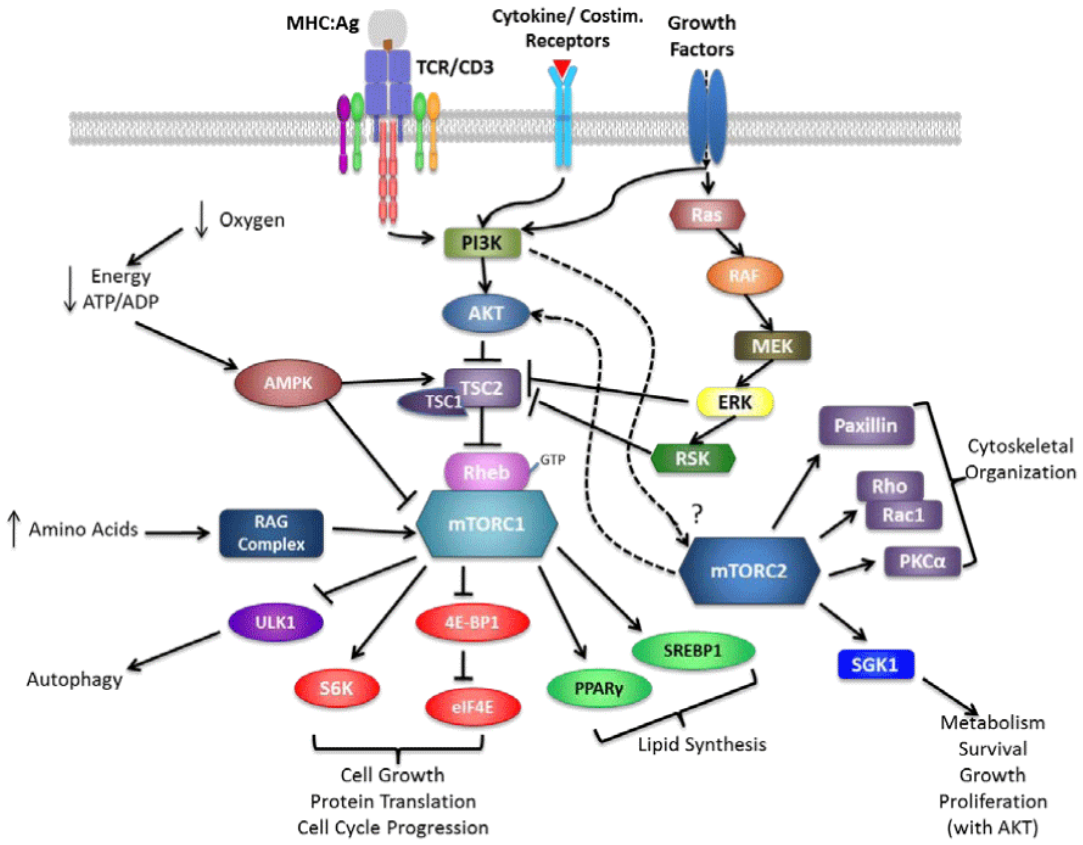

Figure 6.3. Overview of Akt signalling in T cells showing its downstream effects. PI3K can also be activated by Lck kinase in T cells. PI3K activates both PDPK1 (not seen in diagram) and mTORC2, which phosphorylate Akt1 Thr^{308} and Ser^{473} (and corresponding Akt2/3 residues) respectively (from Coquillard *et al*., 2015).

EPEC have been known to modulate the PI3K/Akt pathway in phagocytes for some time with effectors such as EspF, but this protein was not responsible for the observed inhibition of Akt1 Ser^{473} phosphorylation (Celli *et al*., 2001; Quitard *et al*., 2006). Quitard *et al*. (2006) also reported that the inhibition of Akt1 Ser^{473} phosphorylation was dependent on the bacterial T3SS. Ruchaud-Sparagano *et al*. (2007) reported that EPEC inhibited the TNF-α-stimulated phosphorylation of Akt1 Ser^{473} in Caco-2 cells in a manner dependent on EspA but not intimin. A more detailed study found that EPEC suppressed Akt1 Ser^{473} phosphorylation in both HeLa cells and J774A.1 murine macrophage-like cells in a manner dependent on the T3SS but not intimin, six LEE effectors or 14 non-LEE encoded effectors (Amin,

2017). Recent personal communications with Professor Brendan Kenny, Institute for Cell and Molecular Biosciences, Newcastle University, appear to confirm the T3SS-dependent inhibition of Akt1 Ser^{473} phosphorylation in J774A.1 cells. Preliminary evidence from experiments in the Kenny Laboratory using EPEC mutant strains lacking various effector proteins (Cepeda-Molero *et al*., 2017) also suggested that this inhibition was dependent on LifA and the homologous LifA-like protein (data not shown). It was also reported by Professor Kenny that the inhibition of Akt1 Ser^{473} phosphorylation in this manner coincided with the O-GlcNAcylation of the protein (data not shown).

Given the apparent effects of LifA on Akt1 Ser^{473} phosphorylation and the reported LifA dependent O-GlcNAcylation of the protein in J774A.1 cells, it was hypothesised that lymphostatin inhibits Akt1 Ser^{473} phosphorylation by O-GlcNAcylation of this residue. Western blot analysis was used in a number of experiments to investigate the role of rLifA and live EPEC in the inhibition of Akt1 Ser^{473} phosphorylation and putative O-GlcNAcylation. Since the anti-phospho-Akt1 Ser^{473} antibody used in the following experiments also reacts with Akt2 Ser^{474} and Akt3 Ser^{472}, the general term Akt Ser is used to refer to this phosphorylation site for the purposes of this study. It should be noted that Akt possesses a number of other Ser residues that can be phosphorylated (reviewed in Manning and Toker, 2017), which are not relevant to this study.

6.2 Effect of recombinant lymphostatin on Akt Ser phosphorylation

6.2.1 Pre-treatment of bovine T lymphocytes with rLifA inhibited ConA-stimulated phosphorylation of Akt Ser in a manner dependent on catalytic motifs

Highly purified γδ T cells from bovine peripheral blood were used for the kinase array experiments, but the method was costly and reagent intensive. Therefore, I first investigated whether this form of enrichment was necessary to detect Akt Ser phosphorylation by western blot analysis. ConA-treated γδ T cells did not show any greater level of Akt phosphorylation than ConA-treated T cells

enriched using a nylon wool column, nor any greater suppression of phosphorylation when treated with rLifA (data not shown).

T cells from three independent donors were pre-treated with either buffer, wild-type (WT) rLifA, rLifA$^{DTD/AAA}$ or rLifA^{C1480A}, at final concentrations of 1 μg/mL, then stimulated with ConA for various times. The cell lysates were probed by western blotting, using a polyclonal antibody, which although raised against murine Akt1 phospho-Ser^{473}, was also known to recognise Akt2 phospho-Ser^{474} and Akt3 phospho-Ser^{472}. Western blot analysis showed that while Akt Ser phosphorylation was markedly increased upon ConA stimulation of buffer-treated cells, it was reduced to levels only slightly above unstimulated cells in rLifA-treated cells (Figure 6.4). In cells treated with rLifA$^{DTD/AAA}$ or rLifA^{C1480A}, Akt Ser phosphorylation was comparable to that of ConA-stimulated controls when T cells were stimulated for 5 minutes but appeared to decrease gradually with time. Densitometry showed that the fold change in normalised Akt phospho-Ser (pAkt) signal, with standard deviation, from WT rLifA-treated cells was consistently lower than buffer-treated T cells at all time points after ConA stimulation (0.61 ± 0.05 at 5 minutes; 0.13 ± 0.02 at 15 minutes; 0.17 ± 0.12 at 30 minutes) in comparison to untreated cells (Figure 6.5). The fold change in normalised pAkt signal, with standard deviation, from rLifA$^{DTD/AAA}$-treated cells decreased gradually (0.99 ± 0.29 at 5 minutes; 0.86 ± 0.35 at 15 minutes; 0.86 ± 0.03 at 30 minutes) and was more variable in rLifA^{C1480A}-treated cells (0.83 ± 0.05 at 5 minutes; 0.57 ± 0.12 at 15 minutes; 1.05 ± 0.9 at 30 minutes). The fold change in normalised pAkt signal was found to be statistically significantly different from buffer-treated cells in cells treated with WT rLifA ($F(3, 8) = 49.16$, $P < 0.001$ at 5 minutes post-stimulation; $F(3, 8) = 33.76$, $P < 0.001$ 15 minutes; $F(3, 8) = 5.49$, $P = 0.021$ at 30 minutes) but not with the mutant proteins.

These experiments confirmed observations made using the Proteome Profiler Human Phospho-Kinase Array that lymphostatin could inhibit the phosphorylation of Akt Ser in bovine T cells and indicated that this event was dependent on the predicted glycosyltransferase and cysteine protease motifs of LifA.

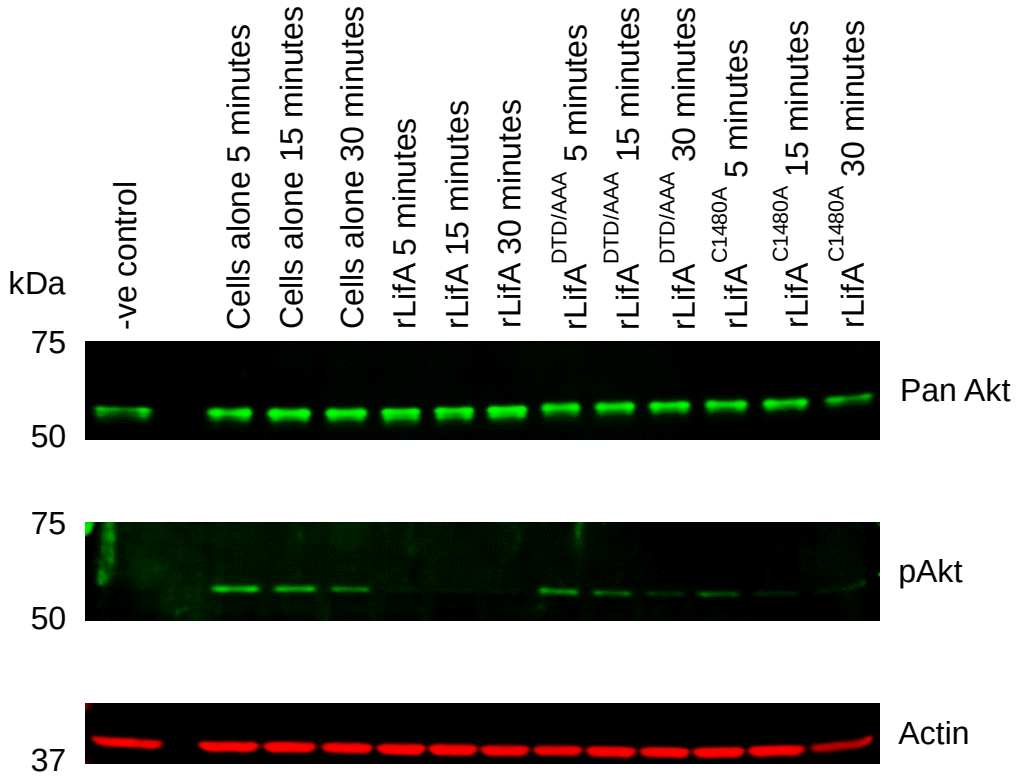

Figure 6.4. The ConA-stimulated phosphorylation of Ser of Akt in bovine T cells was inhibited by rLifA in a manner dependent on the DXD motif and C1480 (western blot). An absolute number of 6 x 10^6 T cells were treated with 1µg/mL rLifA, rLifA$^{DTD/AAA}$, rLifA^{C1480A} or buffer for 1 hour then stimulated with ConA for the times indicated. A volume equivalent to 1 x 10^6 cells was analysed by SDS-PAGE in each well. The phospho-Akt (pAkt) signal was greatly reduced after stimulation at all times in cells pre-treated with rLifA in comparison to untreated cells. The pAkt signal from cells treated with rLifA$^{DTD/AAA}$ and rLifA^{C1480A} decreased with time following ConA stimulation but not to the same extent as with rLifA. Unstimulated cells were used as a negative control. Pan Akt and actin signals were used as loading controls. Data were generated from 3 independent donors and blots are shown from a representative donor.

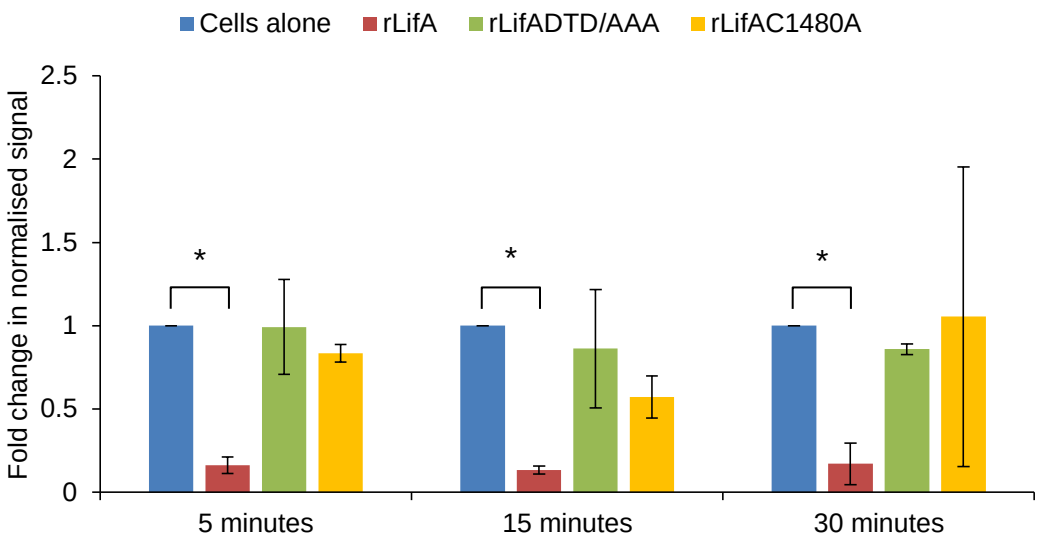

Figure 6.5. The ConA-stimulated phosphorylation of Ser of Akt in bovine T cells was inhibited by rLifA in a manner dependent on the DXD motif and C1480 (densitometry). Densitometry was performed on the western blots and the pAkt signal from each sample was normalised against its respective actin signal to account for overall loss of protein. Data were then normalised against the appropriate cells alone controls to give a fold change in normalised signal compared to untreated cells. The average fold change in normalised signal of rLifA-treated cells was reduced at all time points while there was no significant difference between the normalised signal of cells alone and cells treated with rLifA$^{DTD/AAA}$ or rLifA^{C1480A}. Error bars denote the standard deviation of the average fold changes from across 3 experiments. Asterisks indicate fold changes in normalised signal that were statistically significantly different from ConA-stimulated cells alone.

6.2.2 Treatment of bovine T lymphocytes with rLifA after ConA stimulation did not suppress Akt Ser phosphorylation

To determine whether LifA could suppress Akt phosphorylation in T cells that had already been activated by ConA, akin to phenotypes observed in J774A.1 cells (Professor Brendan Kenny, personal communications), T cells from four independent donors were stimulated with ConA then incubated with buffer or

1 μg/mL rLifA for various time points. rLifA did not suppress Akt Ser phosphorylation at a faster rate than the natural loss of phosphorylation observed in buffer-treated cells (Figure 6.6). The fold change in normalised pAkt signal, with standard deviation, increased slightly from 1.46 ± 0.43 at 0 minutes post-treatment to 1.52 ± 0.47 at 5 minutes in buffer-treated cells and from 1.58 ± 0.58 at 0 minutes to 1.65 ± 0.65 at 5 minutes in rLifA-treated cells (Figure 6.7). It then gradually decreased to 0.58 ± 0.23 at 60 minutes in buffer-treated cells and 0.33 ± 0.26 at 60 minutes in rLifA-treated cells. The fold change in normalised pAkt signal in rLifA-treated cells was not statistically significantly different at any time point from that in buffer-treated cells ($T(5) = -0.18$, $P = 0.862$ at 0 minutes post-incubation; $T(5) = -0.26$, $P = 0.808$ at 5 minutes; $T(5) = 0.55$, $P = 0.605$ at 15 minutes; $T(4) = 2.47$, $P = 0.069$ at 30 minutes; $T(3) = 1.52$, $P = 0.225$ at 60 minutes).

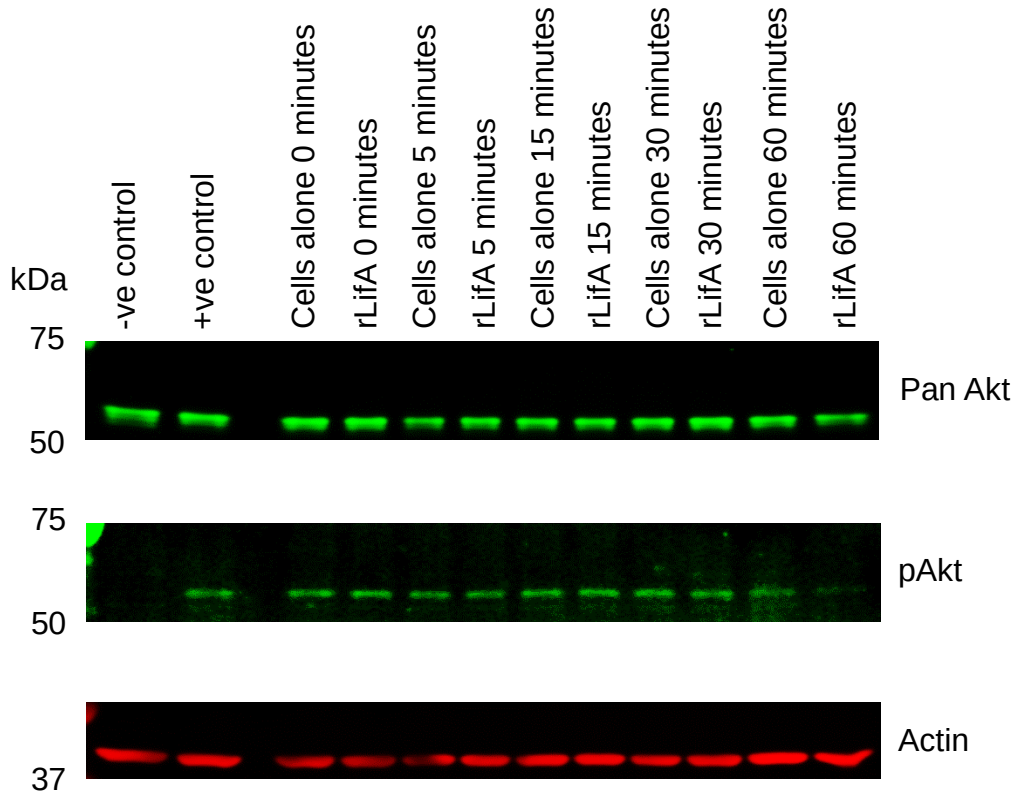

Figure 6.6. rLifA did not inhibit Akt Ser phosphorylation in bovine T cells pre-stimulated with ConA (western blot). An absolute number of 6 x 10^6 T cells were stimulated with ConA for 15 minutes then treated with buffer or 1µg/mL rLifA for the times indicated. A volume equivalent to 1 x 10^6 cells was analysed by SDS-PAGE in each well. The pAkt signal decreased over time and the addition of rLifA did not appear to reduce the pAkt signal at a faster rate than in buffer-treated cells. Unstimulated cells were used as a negative control and cells stimulated with ConA for 15 minutes, but without buffer/rLifA treatment, were used as a positive control. Pan Akt and actin signals were used as loading controls. Data were generated from 4 independent donors and blots are shown from a representative donor.

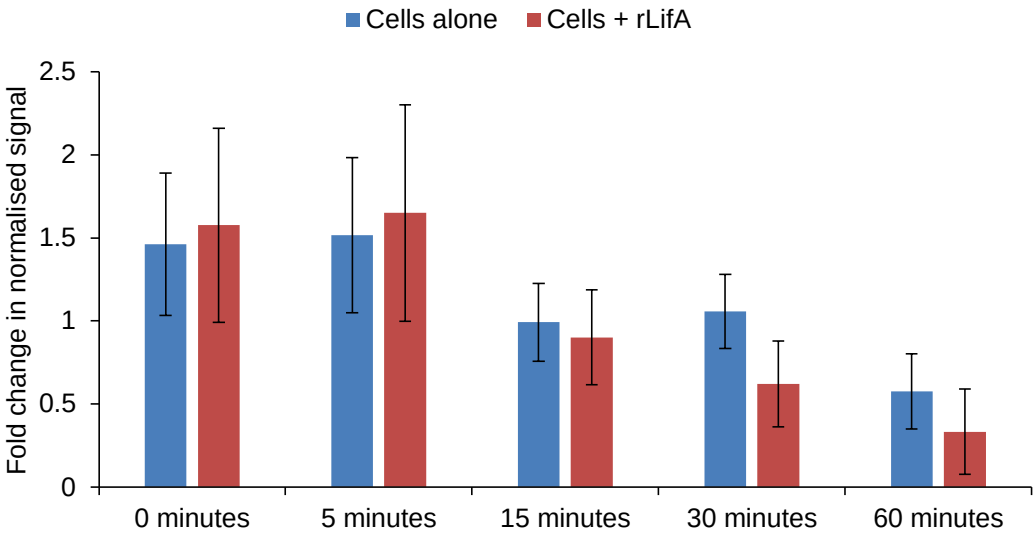

Figure 6.7. rLifA did not inhibit Akt Ser phosphorylation in bovine T cells pre-stimulated with ConA (densitometry). Densitometry was performed on the western blots and the pAkt signal from each sample was normalised against its respective actin signal to account for overall loss of protein. Data were then normalised against the positive control to give a fold change in normalised signal compared to buffer-treated cells. Error bars denote the standard deviation of the average fold changes from across 4 experiments.

6.2.3 rLifA did not appear to O-GlcNAcylate Akt in bovine T lymphocytes

Given that Akt was observed to be O-GlcNAcylated in J774A.1 cells by EPEC in a LifA-dependent manner (Professor Brendan Kenny, personal communications), I sought to determine whether this could be detected in bovine T cells using recombinant protein. Cells from two independent donors were treated with buffer or 1 μg/mL rLifA for various times then stimulated with ConA. Immunoprecipitation (IP) was performed on the lysates using the anti-pan Akt antibody. Western blot analysis revealed that at times when Akt Ser phosphorylation was inhibited by rLifA, no proteins of the expected size of Akt (~56 kDa) could be detected with the anti-O-GlcNAc antibody (Figure 6.8). Protein species detected at ~50 kDa in the IP samples correspond to the heavy chain of the anti-pan Akt antibody. Phosphorylation appeared stronger in the IP samples due to the protein

being concentrated during the IP procedure. Contrary to the hypothesis, these experiments suggested that Akt was not O-GlcNAcylated in bovine T cells as a result of LifA treatment.

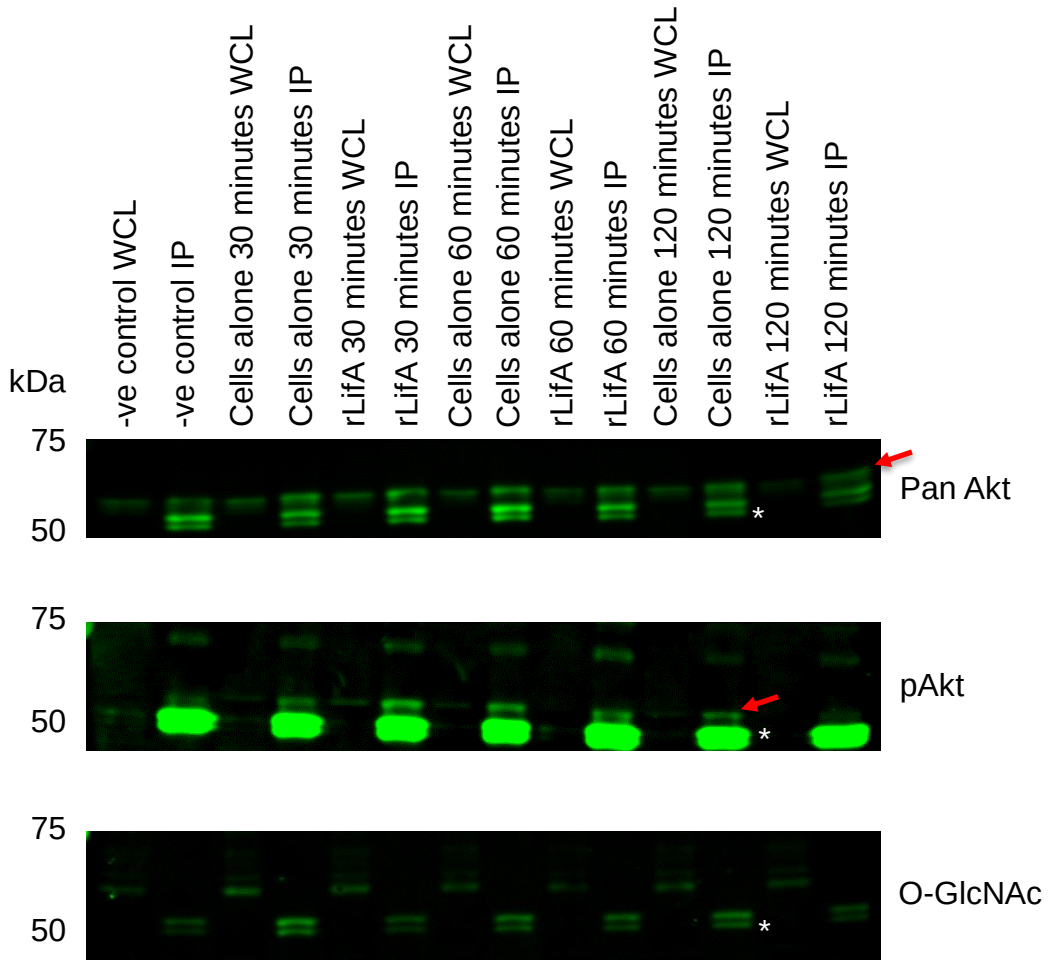

Figure 6.8. rLifA did not appear to O-GlcNAcylate Akt in bovine T lymphocytes. An absolute number of 1 x 10^7 T cells were treated with buffer or rLifA for the times indicated then stimulated with ConA for 15 minutes. IP was performed using the pan Akt antibody and these samples were compared with whole cells lysates (WCL). At 60 and 120 minutes, when the pAkt signal was reduced in cells treated with rLifA, no O-GlcNAcylated proteins could be detected at the expected size for Akt (~56 kDa). Unstimulated cells were used as a negative control. The heavy chain of the anti-pan Akt antibody was observed at ~50 kDa in the IP samples (indicated by asterisks). Arrows indicate Akt. This experiment was performed with 2 independent donors and a representative blot is shown.

6.3 Effects of live EPEC on Akt phosphorylation

6.3.1 Pre-incubation of bovine T lymphocytes with EPEC inhibited ConA-stimulated phosphorylation of Akt Ser in a T3SS-dependent manner

Although LifA did not appear to O-GlcNAcylate Akt it was clear that it inhibited ConA-induced Ser phosphorylation (see Section 6.2). However, the concentration of rLifA applied to T cells in these experiments was likely far in excess of what would be encountered during an infection. Therefore, live EPEC E2348/69 Nal^R (Levine *et al*., 1978 and 1985) and derived mutant strains constructed by the Stevens Laboratory were used to infect T cells at a multiplicity of infection (MOI) of 200:1, akin to experiments by Amin (2017). EPEC E2348/69 Δ*lifA* (Stevens *et al*., 2002) was used to assess the role of lymphostatin, while E2348/69 Δ*escN*::Kan^R, which cannot produce the T3SS-associated ATPase EscN (Garmendia *et al*., 2004), was used as a T3SS-deficient control. Initially, T cells were incubated with bacteria cultured under T3S-inducing conditions for various time points but not stimulated to determine whether EPEC caused an initial activation of Akt followed by inhibition, as seen in J774A.1 cells (Amin, 2017). However, the EPEC strains did not cause an initial activation of Akt in T cells (data not shown).

In further experiments, T cells from three independent donors were stimulated with ConA after incubation with the bacteria at an MOI of 200:1 for 0, 15, 30 or 60 minutes, as was done with rLifA-treated cells. The pAkt signal from both cells infected with WT and Δ*lifA* EPEC decreased rapidly from 0–60 minutes post-infection (Figure 6.9). The pAkt signal from cells infected with the Δ*escN*::Kan^R strain decreased at a slower rate. This was likely due to the decreasing pan Akt signal, which may have been caused by cell death as a result of the bacteria acidifying the medium. The fold change in normalised pAkt signal, with standard deviation, of cells treated with the WT, Δ*lifA* and Δ*escN*::Kan^R strains decreased from 0.62 ± 0.43, 0.73 ± 0.42 and 2.03 ± 1.12 respectively at 0 minutes post-infection to 0.08 ± 0.05, 0.14 ± 0.23 and 0.29 ± 0.28 respectively at 60 minutes (Figure 6.10). The fold change in normalised pAkt signal from E2348/69 Δ*lifA*-infected cells was not statistically significantly different from WT

E2348/69-infected cells at any time ($F(2, 6) = 3.9$, $P = 0.673$ at 0 minutes post-infection; $F(2, 6) = 3.43$, $P = 0.798$ at 15 minutes; $F(2, 6) = 4.38$, $P = 0.73$ at 30 minutes; $F(2, 6) = 0.93$, $P = 0.584$ at 60 minutes). The fold change in normalised pAkt signal from E2348/69 Δ*escN*-infected cells was statistically significantly different from WT E2348/69-infected cells at 0 and 30 minutes post-infection but not at 15 or 60 minutes ($F(2, 6) = 3.9$, $P = 0.04$ at 0 minutes post-infection; $F(2, 6) = 3.43$, $P = 0.054$ at 15 minutes; $F(2, 6) = 4.38$, $P = 0.034$ at 30 minutes; $F(2, 6) = 0.93$, $P = 0.463$ at 60 minutes). These experiments showed that the inhibition of Akt Ser phosphorylation by EPEC in bovine T cells was dependent on the T3SS but not LifA alone.

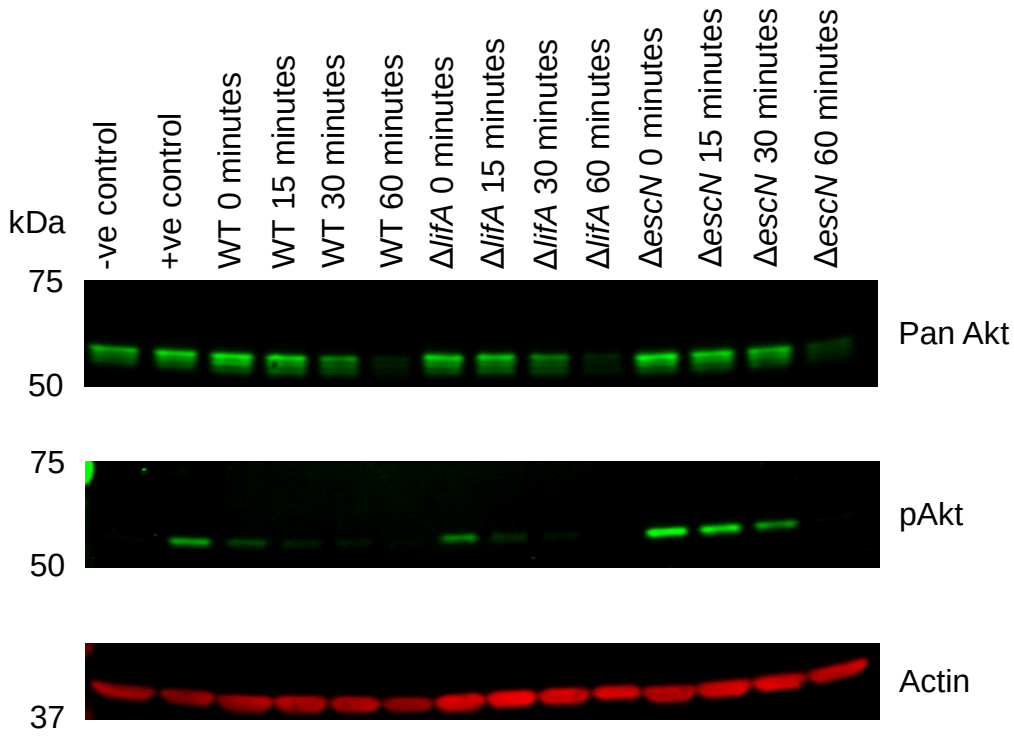

Figure 6.9. Akt Ser phosphorylation induced by ConA was inhibited by prior incubation with live EPEC in a manner dependent on the Type III secretion system but not LifA (western blot). An absolute number of 6 x 10^6 T cells were incubated with EPEC E2348/69 Nal^R strains at an MOI of 200:1 for the times indicated then stimulated with ConA for 15 minutes. A volume equivalent to 1 x 10^6 cells was analysed by SDS-PAGE in each well. The pAkt signal decreased with time with both the wild-type (WT) and Δ*lifA* strains but remained elevated with the Δ*escN*::Kan^R (Δ*escN*) strain until 60 minutes, at which point the pan Akt signal also decreased. Unstimulated cells were used as a negative control and cells stimulated with ConA for 15 minutes, but without EPEC treatment, were used as a positive control. Pan Akt and actin signals were used as loading controls. Data were generated from 3 independent donors and blots are shown from a representative donor.

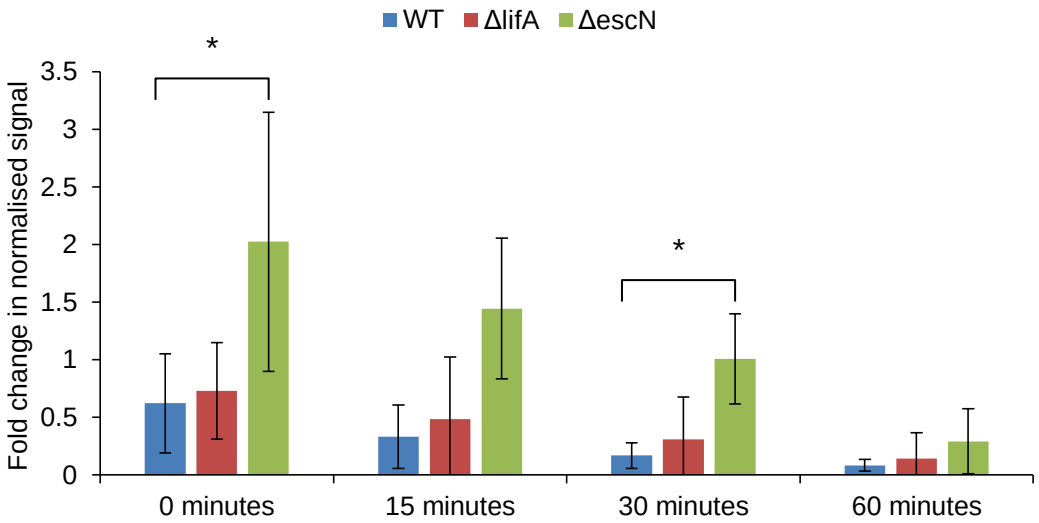

Figure 6.10. Akt Ser phosphorylation induced by ConA was inhibited by prior incubation with live EPEC in a manner dependent on the Type III secretion system but not LifA (densitometry). Densitometry was performed on the western blots and the pAkt signal from each sample was normalised against its respective actin signal to account for overall loss of protein. Data were then normalised against the positive control to give a fold change in normalised signal compared to uninfected cells. Error bars denote the standard deviation of the average fold changes from across 3 experiments. Asterisks indicate fold changes in normalised signal that were statistically significantly different from cells treated with wild-type (WT) EPEC E2348/69.

6.3.2 Inhibition of Akt Ser phosphorylation in bovine T lymphocytes by EPEC was not dependent on LifA or LifA-like protein

Due to claims of functional redundancy between LifA and LifA-like protein in respect of their ability to modulate Akt activation (Professor Brendan Kenny, personal communications), experiments from Section 6.3.1 were repeated using the original EPEC E2348/69 Str^R strain (Taylor, 1970) and derived mutants (Cepeda-Molero *et al.*, 2017) provided by Professor Brendan Kenny, Newcastle University. WT, Δ*lifA* and Δ*escN* strains in the E2348/69 Str^R background were used as described previously for their Nal^R counterparts and compared to Δ*lifA-like* and

Δ*lifA* Δ*lifA-like* strains in the E2348/69 Str^R background. Each strain was incubated with T cells from three independent donors at an MOI of 200:1 for 0, 15 or 30 minutes. The 60 minute incubation was omitted since Akt Ser phosphorylation was previously observed to be reduced at this time even with the T3SS-deficient mutant.

In contrast to observations made by the Kenny Laboratory with J774A.1 cells, the Δ*lifA* Δ*lifA-like* double mutant inhibited ConA-stimulated Akt Ser phosphorylation in bovine T cells (Figure 6.11). The fold change in normalised pAkt signal, with standard deviation, from cells infected with the WT strain decreased from 0.16 ± 0.08 at 0 minutes post-infection to 0.02 ± 0.02 at 30 minutes (Figure 6.12). The fold change in normalised pAkt signal, with standard deviation, from cells infected with the Δ*lifA*, Δ*lifA-like* and Δ*lifA* Δ*lifA-like* strains decreased from 0.24 ± 0.09, 0.22 ± 0.08 and 0.18 ± 0.07 respectively at 0 minutes to 0.1 ± 0.02, 0.09 ± 0.03 and 0.08 ± 0.02 respectively at 15 minutes, then increased slightly to 0.12 ± 0.07, 0.13 ± 0.14 and 0.1 ± 0.1 respectively at 30 minutes. The fold change in normalised pAkt signal, with standard deviation, from E2348/69 Δ*escN*-infected cells also decreased from 0.64 ± 0.13 at 0 minutes post-infection to 0.59 ± 0.27 at 15 minutes, then increased again to 0.76 ± 0.79 at 30 minutes. The fold change in normalised pAkt signal from E2348/69 Δ*lifA*-, Δ*lifA-like*- or Δ*lifA* Δ*lifA-like*-infected cells was not statistically significantly different from WT E2348/69-infected cells at any time. The fold change in normalised pAkt signal from E2348/69 Δ*escN*-infected cells was statistically significantly different from WT E2348/69-infected cells at all time points ($F(4, 10) = 6.18$, $P = 0.004$ at 0 minutes post-incubation; $F(4, 10) = 18.73$, $P < 0.001$ at 15 minutes; $F(4, 10) = 4.75$, $P = 0.005$ at 30 minutes).

These results suggested that while recombinant lymphostatin can inhibit ConA-stimulated Akt Ser phosphorylation, this effect was not obvious when T cells were pre-incubated with EPEC prior to stimulation. However, T3SS-dependent inhibition of Akt Ser phosphorylation upon ConA stimulation could be observed and other Type III secreted effectors may contribute to this activity.

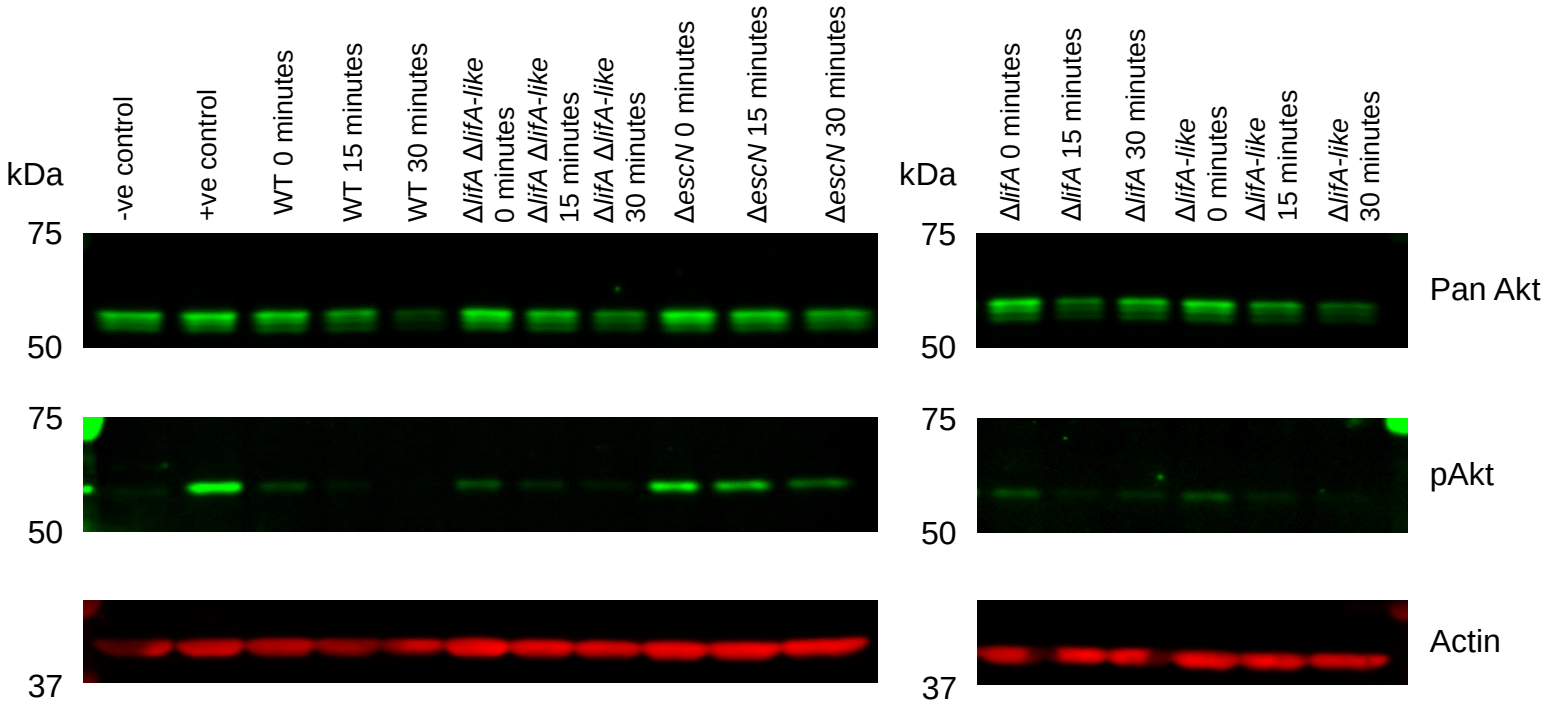

Figure 6.11. The inhibition of ConA-stimulated Akt Ser phosphorylation by prior incubation with live EPEC was independent of LifA and LifA-like protein (western blot). An absolute number of 6 x 10^6 T cells were incubated with EPEC E2348/69 Str^R strains at an MOI of 200:1 for the times indicated then stimulated with ConA for 15 minutes. A volume equivalent to 1 x 10^6 cells was analysed by SDS-PAGE in each well. The pAkt signal decreased with time with all strains except the Δ*escN* strain, where the signal only began to decrease at 30 minutes, at which point the pan Akt signal also decreased. Unstimulated cells were used as a negative control and cells stimulated with ConA for 15 minutes, but without EPEC treatment, were used as a positive control. Pan Akt and actin signals were used as loading controls. Data were generated from 3 independent donors and blots are shown from a representative donor.

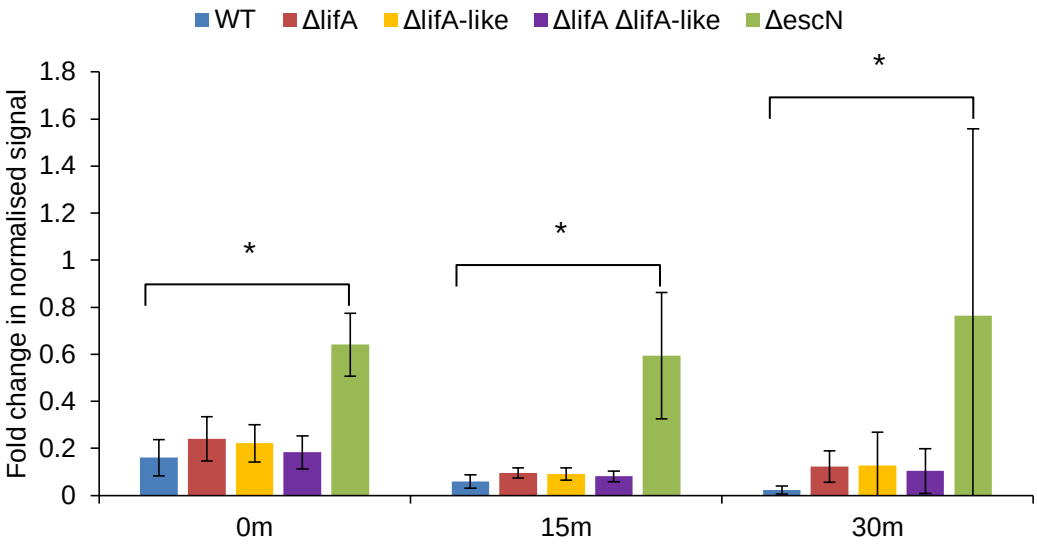

Figure 6.12. The inhibition of ConA-stimulated Akt Ser phosphorylation by prior incubation with live EPEC was independent of LifA and LifA-like protein (densitometry). Densitometry was performed on the western blots and the pAkt signal from each sample was normalised against its respective actin signal to account for overall loss of protein. Data were then normalised against the positive control to give a fold change in normalised signal compared to uninfected cells. Error bars denote the standard deviation of the average fold changes from across 3 experiments. Asterisks indicate fold changes in normalised signal that were statistically significantly different from cells treated with wild-type (WT) EPEC E2348/69.

6.3.3 EPEC did not appear to O-GlcNAcylate Akt in bovine T lymphocytes

Since recombinant LifA did not appear to O-GlcNAcylate Akt, I sought to determine whether another putative effector protein was responsible for the observations made by the Kenny Laboratory. Given that EPEC appeared to cause inhibition of Akt Ser phosphorylation independently of LifA/LifA-like, it was hypothesised that the protein responsible for this may O-GlcNAcylate Akt.

Bacteria were incubated with T cells from a single donor at an MOI of 200:1 for 1 hour (the time at which O-GlcNAcylation was detected by the Kenny Laboratory) and IP was performed as described in Section 6.2.3. Similar to

observations made with rLifA, live EPEC did not appear to O-GlcNAcylate Akt (Figure 6.13). As observed previously, the phospho-Akt signal was reduced by WT and *lifA* mutant strains relative to the ConA-stimulated control.

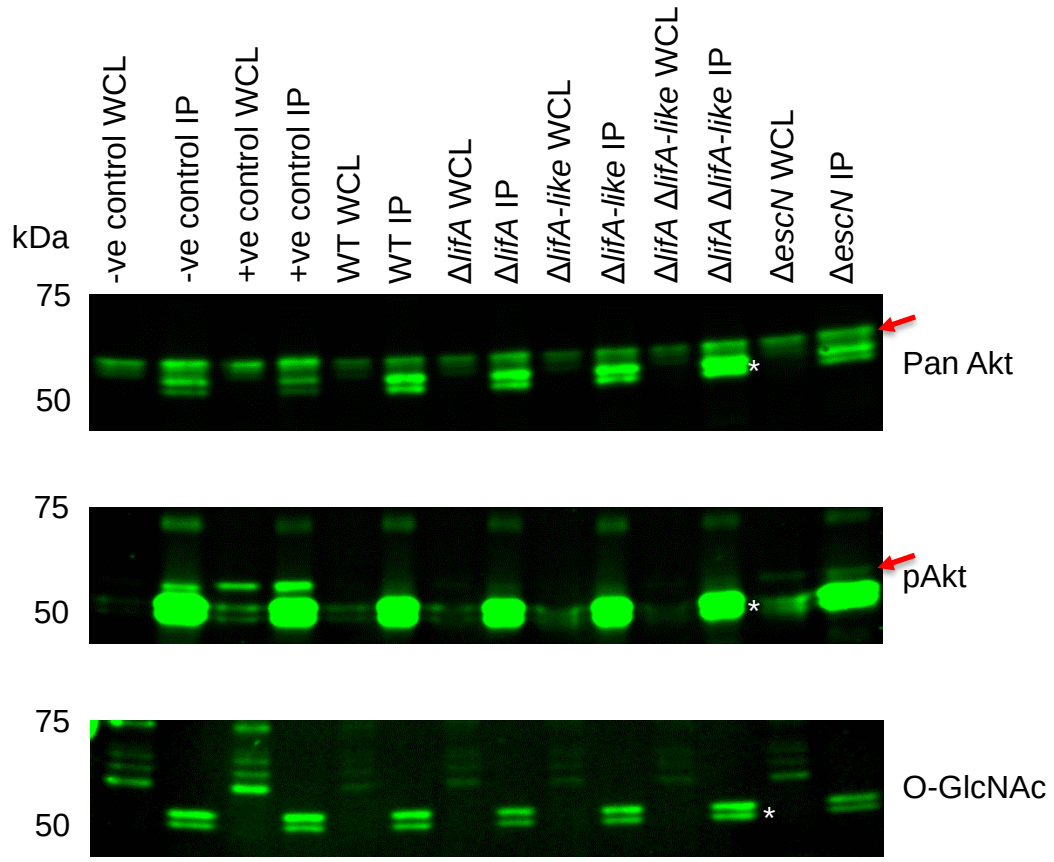

Figure 6.13. EPEC did not appear to O-GlcNAcylate Akt in bovine T lymphocytes. An absolute number of 1 x 10^7 T cells were incubated with EPEC E2348/69 Str^R strains at an MOI of 200:1 for 1 hour then stimulated with ConA for 15 minutes. No O-GlcNAcylated proteins at the expected size of Akt could be detected in IP samples from T cells infected with EPEC strains at the same time as they inhibited Akt phosphorylation. Unstimulated cells were used as a negative control. The heavy chain of the anti-pan Akt antibody was observed at ~50 kDa in the IP samples (indicated by asterisks). Arrows indicate Akt.

6.4 Discussion

Evidence from several previous studies suggested that lymphostatin inhibits the phosphorylation of Akt1 at Ser^{473} and corresponding residues in Akt2/3. To test the hypothesis that Akt is a cellular target of lymphostatin, directly or indirectly, recombinant lymphostatin and live EPEC were assessed for their ability to inhibit Akt Ser phosphorylation and O-GlcNAcylate Akt in primary bovine T cells. rLifA was found to inhibit Akt Ser phosphorylation in a manner dependent on its catalytic DXD motif and C1480 residue. This inhibition was only detected when T cells were treated with rLifA before stimulation with ConA and not after, which contrasts with the findings of the Kenny Laboratory. They found that EPEC suppressed Akt Ser phosphorylation in J774A.1 cells after an initial activation caused by the bacteria (Amin, 2017; Professor Brendan Kenny, personal communications), however, this may have been the result of different signalling pathways that act on Akt in T cells and macrophages. J774A.1 cells are also an immortalised cell line, which do not necessarily reflect the cellular biology of their progenitor cells. It should also be noted that although T cell enrichment using nylon wool columns was more efficient than using anti-γδ TCR antibodies, this would result in some contamination from B cells and monocytes/macrophages, which may have affected the results. In further contrast to the findings of the Kenny Laboratory, recombinant LifA did not appear to O-GlcNAcylate Akt in bovine T cells at a time and concentration previously shown to inhibit ConA-stimulated proliferation and suppress Akt Ser phosphorylation. This study used the RL2 anti-O-GlcNAc antibody clone, as did the Kenny Laboratory, however, antibodies were sourced from different suppliers with different maximum recommended dilutions. As such, this study used an antibody dilution of 1/1000, whereas the Kenny Laboratory used 1/500, which may have been responsible for the difference in results. The concentration of protein applied to the T cells was also not reflective of the quantity of protein that is taken up by cells. Therefore, an apparent lack of O-GlcNAcylation may have been due to low quantities of the LifA N-terminus acting within cells.

I then sought to replicate the experiments of the Kenny Laboratory using bovine T cells and live EPEC strains to determine whether the concentrations of LifA

produced by the bacteria were sufficient to inhibit Akt Ser phosphorylation. Although the T3SS-dependent inhibition of Akt Ser phosphorylation could be confirmed using this model, the inhibition observed was independent of LifA and LifA-like protein. It is possible that another Type III secreted effector(s) was responsible for the inhibition observed, as other effectors from EPEC are known to modulate Akt phosphorylation. Both Tir and EspZ have been reported to indirectly enhance Akt Ser phosphorylation and thus promote the survival of kidney and epithelial cells respectively (Sason *et al*., 2009; Shames *et al*., 2010). However, with the exception of Stx (Gobert *et al*., 2007), which is not produced by EPEC, no other effector proteins from A/E *E. coli* have been identified that inhibit Akt Ser phosphorylation. LifA and its homologues ToxB and Efa1′ have been shown to affect the expression and secretion of Type III secreted proteins in some strains (Stevens *et al*., 2002 and 2004), which raises the possibility that the effect of *lifA* during EPEC infection may be indirect. One method of studying any direct effects of LifA in EPEC on Akt would be to re-insert the *lifA* gene into the EPEC0 strain, which possesses a functional T3SS but lacks all Type III secreted effectors (Cepeda-Molero *et al*., 2017).

In order to determine whether the disparities between this study and the observations of the Kenny Laboratory were caused by the difference in cell types used, EPEC infections of J774A.1 cells were attempted. EPEC appeared to inhibit the phosphorylation of Akt Ser in a manner dependent on the T3SS but not LifA/LifA-like (data not shown). However, Akt Ser phosphorylation was also decreased by 30 minutes post-infection with an *E. coli* K-12 strain that lacks LifA (HB101) to a level similar to that of the EPEC E2348/69 strains. It is possible that changes to the experimental procedures used by our laboratories could be responsible for this, including in the number of J774A.1 cells used and the extent to which they were serum starved. Akt Ser phosphorylation was not reduced at 1 hour post-infection in E2348/69 Δ*escN*-infected cells, which is consistent with previous observations. An alternative explanation for this observation may be that E2348/69 Δ*escN* causes sustained activation of Akt by an unknown mechanism, rather than fail to inhibit it. Putative O-GlcNAcylation of Akt was not observed in EPEC-infected

J774A.1 cells either (data not shown) and the reasons for the discordance between studies remain unclear.

Proliferation assays in which T cells were incubated with EPEC E2348/69 strains for 1 hour before ConA stimulation were attempted to determine whether live bacteria could inhibit T cell proliferation. Previous assays have used either bacterial lysates or recombinant protein (Klapproth *et al*., 1995, 1996 and 2000; Malstrom and James, 1998; Stevens *et al*., 2002; Deacon *et al*., 2010; Bease, 2015; Cassady-Cain *et al*., 2016 and 2017). After incubation with the bacteria, T cells were washed and resuspended in fresh medium with antibiotics. However, despite streptomycin being the only antibiotic known that these strains were resistant to, the bacteria were found to be capable of surviving in 100 μg/mL gentamicin when 80 μg/mL has been reported to be sufficient kill *E. coli* (Marchès *et al*., 2003). It was thought that the bacteria may have been capable of invading the T cells and re-emerging as they have been reported to invade epithelial cells (Donnenberg *et al*., 1989). However, high concentrations of kanamycin, which penetrates cells, also did not kill the bacteria. They survived in 250 μg/mL kanamycin as well as combinations of antibiotics including chloramphenicol and ceftazidime. It is unclear how the bacteria were able to survive multiple classes of antibiotics, but this prevented the measurement of proliferation as the T cells were killed by the acidified medium due to bacterial outgrowth.

Other experiments were also attempted to assess the potential role of Akt as a target for LifA during this study. An *in vitro* glycosylation assay was attempted using recombinant 6 x His-tagged human Akt1 (rAkt1; Novus Biologicals) and conditions based in on the *in vitro* glucosylation assay described by Donald *et al*. (2013) for RhoA and the large clostridial toxins (LCTs) TcdA and B. Conditions were designed to mimic the host cell cytoplasm and UDP-GlcNAc was used in place of UDP-Glc. However, on western blots rAkt1 appeared as a complex ladder of proteins instead of a single band at ~56 kDa. This may have been the result of a poor quality batch, as the supplier's website showed the protein to be of the expected size. Alternatively, it is possible that this was due to rAkt1 being produced in *E. coli* rather than mammalian or insect cells as may be required for the proper folding of a mammalian protein. Even if rAkt1 was biophysically normal and was a target for LifA, there are

a number of other potential reasons why *in vitro* glycosylation may not occur. Although full-length rLifA is known to bind UDP-GlcNAc (Bease, 2015; Cassady-Cain *et al*., 2016) it is unclear whether it can transfer the sugar in this form. The homologous LCTs can transfer their sugar substrates in their full-length form (Just *et al*., 1995b and 1995c; Selzer *et al*., 1996; Busch *et al*., 1998; Nagahama *et al*., 2011), but given that rLifA is processed within T cells (see Section 4.7), it may require cleavage for the N-terminal glcosyltransferase domain to become active. Other co-factors, such as ATP or metal ions, may also be required for the glycosylation reaction. The reaction was attempted in T cell lysates, as done by Selzer *et al*. (1996), to ensure that the necessary co-factors were present but again, rAkt did not appear at the expected size (data not shown).

Another experiment was performed to determine whether the LifA-mediated inhibition of T cell proliferation was caused by the inhibition of Akt Ser phosphorylation. T cells were treated with titrations of either rLifA or the inhibitor OSU-03012 (AR-12; APExBIO) for 1 hour. AR-12 prevents the phosphorylation of Akt Thr and Ser by inhibiting PDPK1 activity (Zhu *et al*., 2004; Cen *et al*., 2007). However, AR-12 may also target p21-activated kinases and aurora kinase A (Porchia *et al*., 2007; Silva *et al*., 2014), meaning that the effects of this inhibitor may not be specific to Akt. AR-12 at a concentration of 2.5 μM inhibited Akt Ser phosphorylation to a level comparible with 1 μg/mL rLifA in a single donor (data not shown). AR-12 concentrations lower than 2.5 μM (0.1–1 μM) did not appear to inhibit Akt Ser phosphorylation, while higher concentrations (5–10 μM) were toxic. However, this observation could not be confirmed in additional donors due to toxicity issues at 2.5 μM. Toxicity at 5 μM and above was not unexpected as this has previously been reported in human macrophages (Hoang *et al*., 2014), however, this was after a 72 hour incubation. Cytotoxicity was < 10 % at 2.5 μM AR-12 in this same study. It is possible that the toxicity observed at 2.5 μM in bovine T cells was due to differences in the sensitivities of different cell types, species or donors to AR-12. A proliferation assay was performed with a different single donor in which T cells were treated with titrations of either rLifA or AR-12. AR-12 at 2.5 μM was not cytotoxic in the proliferation assay but the effect on Akt Ser phosphorylation was not measured. However, at this concentration the proliferation index was only reduced to

0.71, comparible to 0.01 ng/mL rLifA (data not shown). Although caveats existed, these experiments suggested that LifA does not act by solely inhibiting Akt Ser phosphorylation.

Taken together, the observations made in this study suggest that lymphostatin does not directly target Akt in bovine T cells, at least not via O-GlcNAcylation. rLifA did not reduce Akt Thr phosphorylation to the same degree as Ser phosphorylation in experiments by Dr Robin Cassady-Cain. It is possible that the cellular target of LifA lies upstream of Akt Thr and Ser phosphorylation but has a greater effect on Ser phosphorylation. No kinases from the subset identified with reliable detection (Figure 6.2) lie directly upstream of Akt. GSK3, WNK1 and p27 are all possible substrates for Akt (reviewed in Manning and Toker, 2017) but have variable levels of phosphorylation. There is potentially cross-talk between the TCR and PI3K/Akt signalling pathways however (see Section 7.2.4), which may make determining the upstream effects on Akt and the downstream effects of Akt difficult.

7 Discussion

Lymphostatin is a large protein produced by A/E *E. coli* that inhibits the mitogen- and antigen-stimulated proliferation of T lymphocytes. In this study, I sought to better understand the mode of action of lymphostatin by attempting to identify functional domains and possible targets of the protein, as well as investigating the role of the putative cysteine protease domain.

7.1 Analysis of lymphostatin structure and function

Recombinant fragments of lymphostatin representing putative structural domains did not possess inhibitory activity when applied exogenously to T cells in isolation or in combination. Direct transfection of T cells with the predicted catalytic N-terminal proteins rGT and rF1 did not produce conclusive results with regards to the inhibition of mitogen-activated proliferation. However, these two proteins were found to interact with T cells in a manner insensitive to exogenous GlcNAc, while the C-terminal proteins rF3 and rF5 did not. Experiments seeking to define the roles of structural domains of lymphostatin were limited by several factors. rF3 and rF5 formed multimers, making it difficult to determine using SEC whether or not they associated with each other. Further, rF1 and rF5 could not be purified to a higher degree using anion exchange chromatography, which prevented biophysical measurements from being taken. We cannot preclude the possibility that the absence of activity was a consequence of improper folding of the proteins.

7.1.1 Structural analysis

Currently, there is only limited experimental structural information on the N-terminal portion of LifA, which was gathered by Cassady-Cain *et al.* (2016). The N-terminal half of lymphostatin was predicted by PSIPRED (Buchan *et al*., 2013) to contain the majority of the α-helix content of the protein. PSIPRED predicted that the F1 fragment released by limited trypsin proteolysis was composed of 52 % α-helix, 5 % β-sheet and 43 % coil (Cassady-Cain *et al*., 2016). CD analysis of F1 yielded

similar results to the PSIPRED predictions but with a higher β-sheet content (51 ± 5 % α-helix, 13 ± 3 % β-sheet, 37 ± 7 % coil) and confirmed that the α-helix content was higher in F1 than in full-length LifA (37 ± 3 % α-helix). Cassady-Cain *et al*. (2016) also made structural predictions about the GT domain of LifA. Through alignment of the LifA primary sequence with that of various LCTs it was predicted that the GT domain of LifA consists of a catalytic core with α-helical/unordered insertions. The catalytic core is thought to be involved in substrate binding and the insertions involved in target recognition (Figure 7.1). An XNX motif at the base of the β-hairpin in the substrate binding site is thought to confer sugar specificity (Figure 7.2). The LCTs TcdA and B and TcsL have an INQ sequence at this position, allowing them to bind UDP-Glc but not UDP-GlcNAc. The LNG sequence at this position in LifA has more similarity to the sequences of the UDP-GlcNAc binding LCTs TcnA and TpeL, and it is hypothesised that this sequence is what allows for the accommodation of the acetyl group of GlcNAc (Cassady-Cain *et al*., 2016).

If time and resources were invested in optimising the purification conditions for the recombinant LifA fragments, there are a number of methods, besides those described in Section 3.11, which could be used to gather structural information on lymphostatin. X-ray crystallography could be used to determine the structure of LifA or domains within. X-rays are diffracted by protein crystals to produce a series of spots, which can be used to determine the original crystal structure using Bragg's Law (reviewed in Wang and Wang, 2017). To complete the structural model, further information is obtained by computational methods or by molecular replacement, which uses information from homologous proteins to make inferences about the structure of the protein under investigation (reviewed in Taylor, 2010). This technique has been used to determine the structure of the TcdA glucosyltransferase domain (Pruitt *et al*., 2012), the cysteine protease domain of PaTox (Bogdanović *et al*., 2018), and TcdA lacking the receptor binding domain (Chumbler *et al*., 2016). However, X-ray crystallography requires highly ordered protein crystals and so far attempts to produce crystals of full-length rLifA and rGT have been unsuccessful despite testing diverse conditions (Walkinshaw Laboratory, unpublished data). Producing crystals of rLifA is technically difficult due the size of the protein.

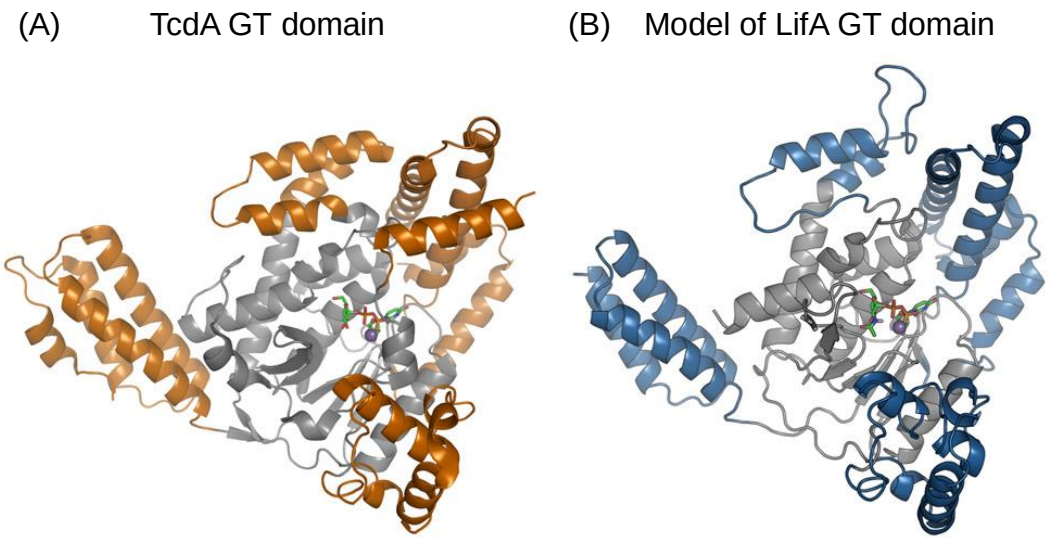

Figure 7.1. The glycosyltransferase (GT) domains of the large clostridial toxin TcdA and lymphostatin. (A) Representation of the crystal structure of the GT domain of *C. difficile* TcdA (Pruitt *et al*., 2012) bound to UDP-Glc. (B) Model of the GT domain of LifA from *E. coli* O127:H6 strain E2348/69 bound to UDP-GlcNAc based on homology with TcdA. The catalytic core (grey) is thought to be involved in substrate binding and the α-helical/unordered insertions (orange/blue) are thought to be involved in target recognition. Purple spheres represent Mn^{2+} ions (from Cassady-Cain *et al*., 2016).

(A) TcdA:UDP-Glc (B) Model of LifA:UDP-

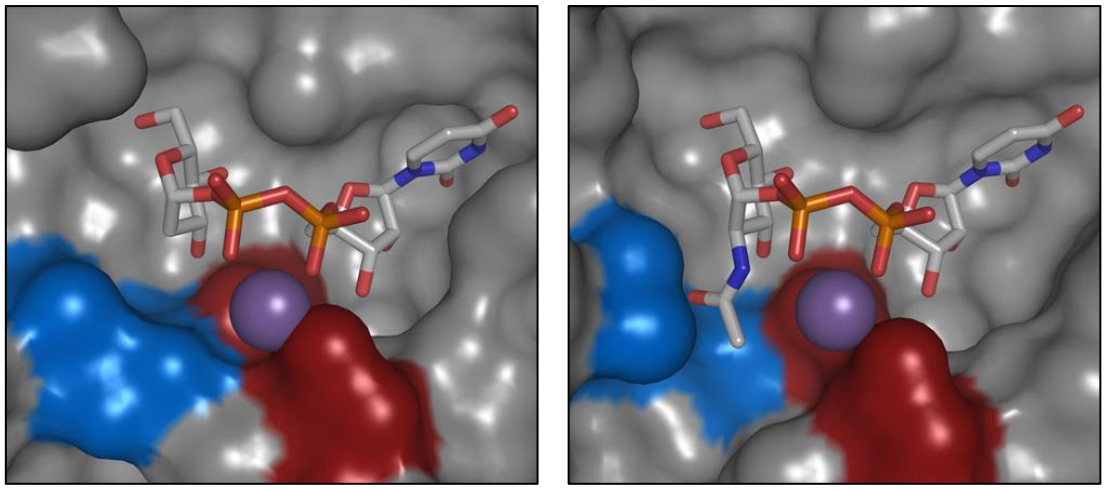

Figure 7.2. The predicted binding sites of the large clostridial toxin TcdA and lymphostatin GT domains, illustrating sugar substrate specificity. (A) Model of the TcdA binding site in complex with UDP-Glc. Asp^{285} and Asp^{287} are shown in red. Ile^{382} and Gln^{384} of the XNX motif are shown in blue. (B) Model of the LifA binding site in complex with UDP-GlcNAc based on homology with TcdA. Asp^{557} and Asp^{559} are shown in red. Lue^{667} and Gly^{669} of the XNX motif are shown in blue and are predicted to allow for the accommodation of the GlcNAc acetyl group. Purple spheres represent Mn^{2+} ions (from Cassady-Cain *et al*., 2016).

Cryo-electron microscopy (EM) is another technique that could be used to produce three-dimensional models of the recombinant fragments. Cryo-EM uses thin sections of molecules frozen at low temperatures on a porous carbon grid, which are visualised by EM, and has the advantage over X-ray crystallography of requiring less material (reviewed in Murata and Wolf, 2018). This technique is predicted to be feasible for lymphostatin, as rLifA appears soluble and monodispersed by negative staining and transmission electron microscopy (Cassady-Cain *et al*., 2016). It is difficult to visualise proteins smaller than 50 kDa using standard cryo-EM, with the current smallest protein visualised being ~43 kDa (Herzik *et al*., 2019), which would be problematic for studying rF5 (~38 kDa). This could be overcome by fusing rF5 to a modular, self-assembling protein scaffold, which can hold an attached protein in symmetric and rigidly defined orientations (Liu *et al*., 2018b). However, given that

rF5 appeared to aggregate, this method may not be possible as proteins that naturally self-associate prevent the assembly of the scaffold protein (Liu *et al*., 2018b). Cryo-EM has previously been used to visualise pH-dependent conformational changes in TcdA (Pruitt *et al*., 2010), and given that rLifA requires endosome acidification for cleavage, a similar experiment could be performed to detect pH-dependent structural changes in lymphostatin.

Small angle X-ray scattering (SAXS) can also be used to provide lower resolution information on the structure of proteins. SAXS measures the intensity of X-rays scattered by a solution of particles to provide information on the size, shape and molecular weight of a protein of interest (reviewed in Kikhney and Svergun, 2015). Although SAXS provides less detailed information than X-ray crystallography, it can be combined with this technique, as well as nuclear magnetic resonance, to provide information on protein flexibility that detailed structural measurements do not detect (Schulte *et al*., 2014; Grishaev *et al*., 2005). Further, it has the advantage that we have successfully used this technique to gain structural insights into lymphostatin. SAXS was combined with transmission electron microscopy of negatively stained rLifA to estimate the surface envelope and volume of the protein (Cassady-Cain *et al*., 2016) and has also been used to detect pH-dependent changes in rLifA and the mutant proteins rLifA$^{DTD/AAA}$ and rLifA^{C1480A} (Walkinshaw Laboratory, unpublished data). Highly purified rGT and rF3, produced by Dr Liz Blackburn, EPPF, have also been subjected to SAXS but the results were confounded by the self-association of these fragments (Walkinshaw Laboratory, unpublished data).

7.1.2 Investigating the role of functional domains

Other methods could also be used to study the roles of predicted functional domains. Given that the N-terminus of lymphostatin contains the GT and CP domains, it was hypothesised that the C-terminus is involved in cell binding and uptake. Immunocytochemistry and confocal microscopy using the polyclonal anti-LifA antibody against rF3 and rF5 could be used to assess the location of these proteins within T cells. However, since these proteins could not be detected in T cell

lysates (see Section 3.9), despite being reactive to anti-LifA antibodies in isolation, they may not be detectible using this method. It is possible that these proteins are incapable of entering cells due to missing amino acids, therefore an alternative would be to produce recombinant LifA C-terminus (aa 1621–3223). Another alternative is splicing by overlap extension (SOEing) PCR. SOEing PCR uses primers for two different genes that overlap, thereby allowing for the creation of fusion proteins (Higuchi *et al*., 1988; Bryksin and Matsumura, 2010). SOEing PCR could be used to create a fusion protein of a reporter such as enhanced green fluorescent protein and the C-terminal end of LifA. After treating T cells with the purified fusion protein, confocal microscopy could then be used to assess the location of the protein. This method would not be limited by antibody sensitivity but may be limited by the quantity of protein that is taken up by cells.

Another method that could be used to study functional domains is the use of nested truncations. A number of methods have been developed to create nested truncations in various genes but all rely on the same underlying principle (Frischauf *et al*., 1980; Poncz *et al*., 1982; Henikoff, 1990). A series of truncations could be made from the N- or C-terminus of LifA and the resulting proteins could be assessed for inhibitory activity to determine which regions of the protein are required for activity. However, when producing truncations from the N-terminus, the possibility of deleting a signal sequence for protein secretion should be considered. Alternatively, a series of in-frame deletions could be created within the coding sequence of *lifA*, for example using restriction and re-ligation (McKnight and Kingsbury, 1982), SOEing PCR or by *de novo* synthesis of the desired *lifA* sequences. It should be noted however, that truncated proteins may not fold properly unless the correct boundaries for structure are chosen (Stevens Laboratory, unpublished data).

Alanine scanning mutagenesis could be used for fine-scale mapping of residues required for activity and involves the sequential substitution of each amino acid in a specific region with Ala residues (Cunningham and Wells, 1989). Since alanine scanning mutagenesis cannot be used to investigate the role of Ala residues within these regions, serine scanning mutagenesis could potentially be used for these particular residues (Pál *et al*., 2005; Follis *et al*., 2005). With a protein the size of

lymphostatin, such a time- and resource-intensive strategy would be optimally focused on predicted catalytic domains or to test structure predictions.

Error-prone PCR could be used to randomly insert mutations into the *lifA* gene. This is performed using a low-fidelity polymerase, such as Taq, and modified PCR conditions, such as increasing the concentration of $MgCl_2$, adding $MnCl_2$ and unbalancing the concentrations of dNTPs (Leung *et al*., 1989; Cadwell and Joyce, 1992). However, not all nucleotide changes will introduce coding changes and some may alter the reading frame, meaning that large numbers of cloned amplicons would likely need to be sequenced. Lastly, mutagenesis using transposons such as Tn5, which inserts at near-random could be used (Ruvkun and Ausubel, 1981). Transposons can also include reporter genes that can provide information regarding the location of proteins within the bacterial cell, such as Tn*phoA* or Tn*lacZ* which can create translational fusions to alkaline phosphatase or β-galactosidase and respectively identify domains located outside or inside the cytoplasmic membrane (Manoil and Beckwith, 1985; Manoil, 1990). A Tn*phoA* insertion in *lifA* from EHEC E45035 confirmed that at least part of the protein is located outside the bacterial cytoplasmic membrane (Nicholls *et al*., 2000). The main drawback of all of these methods is that there is currently no high throughput system for producing and screening the large number of mutant proteins that could be made. Lysates of the mutant strains could be used in assays of lymphostatin activity, however, lysates are known to be less sensitive than recombinant protein for this purpose and biophysical experiments could not be performed to ensure the mutant proteins are folded and stable.

7.2 Mode of action of lymphostatin on T lymphocytes

Due to the N-terminal homology between LifA and the LCTs, it was hypothesised that LifA may similarly enter cells by receptor-mediated endocytosis, undergo a pH-dependent conformational change in the endosome and insert the N-terminus through the endosomal membrane prior to CP domain-mediated cleavage of the protein and release of the GT domain-containing N-terminus into the cytoplasm. In this study, CP domain-mediated cleavage of recombinant lymphostatin

was observed in both primary bovine T cells and J774A.1 murine macrophage-like cells. The cleavage event was found to produce N- and C-terminal cleavage products of ~140 and 225 kDa respectively, but attempts to determine if a co-factor(s) is required for cleavage have been unsuccessful (Cassady-Cain *et al.*, 2016). Lymphostatin does not self-cleave in isolation, which suggests a co-factor of some form is required for this event. Using the inhibitors bafilomycin A1 and chloroquine, endosome acidification was also found to be required for rLifA cleavage in T cells, consistent with the prediction of a low pH-dependent membrane insertion event akin to LCTs.

Attempts to identify targets or other interacting partners of lymphostatin were less successful. Shotgun mass spectrometry appeared to be limited by the sensitivity of the spectrometer, as very few GlcNAcylated proteins were detected, even after using a method to enrich GlcNAcylated proteins from T cell lysates. Two possible candidate targets were identified from the eluates of protein pull-downs, however, follow-up experiments could not confirm that these proteins specifically interacted with rLifA. A candidate target approach with the protein kinase Akt revealed that pre-incubating T cells with rLifA or live EPEC inhibits Akt1 Ser^{473} phosphorylation. However, this inhibition does not appear to be caused by O-GlcNAcylation of Akt as suggested by the laboratory of Professor Brendan Kenny (unpublished observations). The LifA/LifA-like-independent inhibition of Akt1 Ser^{473} phosphorylation by EPEC also suggests that the bacteria possess another virulence factor that may target Akt.

There are a number of experiments based on previous studies with LCTs that could be performed to further the understanding of the mode of action of lymphostatin, which are described in Sections 7.2.1–7.2.4.

7.2.1 Mechanism of cell entry

Lymphostatin is known to be secreted via the LEE-encoded T3SS (Deng *et al.*, 2012; Bease, 2015), but this is not necessary for activity as lysates and recombinant protein can inhibit mitogen-activated lymphocyte proliferation (Klapproth *et al.*, 1995, 1996 and 2000; Malstrom and James, 1998; Stevens *et al.*, 2002; Bease, 2015; Cassady-Cain *et al.*, 2016 and 2017). This, and the requirement

for endosome acidification for rLifA cleavage, suggests that LifA enters cells to reach its target rather than targeting a protein on the host cell surface. However, the exact mechanism by which LifA is taken up has yet to be identified. LCTs are taken up by clathrin-mediated endocytosis (Papatheodorou *et al*., 2010), but given the lack of homology between LifA and LCTs at the C-terminus uptake of LifA by the same pathway cannot be predicted with confidence.

To determine which endocytic pathway LifA is taken up by, experiments could be performed using inhibitors of different pathways. During this study, I attempted to carry out proliferation assays in which T cells were treated with inhibitors before incubation with buffer/rLifA and ConA stimulation. The following inhibitors were used: chlorpromazine, which inhibits clathrin-mediated endocytosis by preventing the formation of clathrin coated pits at the plasma membrane (Wang *et al*., 1993); methyl-β-cyclodextrin, which inhibits cholesterol-dependent endocytosis by forming soluble inclusion complexes with cholesterol and thus depleting it from cell membranes (Vieth *et al*., 2010; Ohtani *et al*., 1989; Kilsdonk *et al*., 1995); and cytochalasin D, which inhibits actin polymerisation and induces depolymerisation, thereby preventing phagocytosis and macropinocytosis (Casella *et al*., 1981; Sakr *et al*., 2001). It was hypothesised that ConA-stimulated T cell proliferation would not be suppressed if the inhibitors used blocked the uptake of rLifA, however, the concentrations of inhibitors used in these experiments proved to be cytotoxic. A more effective method for examining the mechanism of cell entry may be to pre-incubate T cells with a titration of each inhibitor, similar to the experiments performed with bafilomycin A1 and chloroquine. The presence/absence of the c. 140 kDa cleavage product at different inhibitor concentrations could then be used as an indicator for the effects of each inhibitor on rLifA uptake, before loss of cell viability occurs. Other inhibitors could also be tested, such as a combination of PMA and filipin, which inhibits caveolae-mediated endocytosis (Smart *et al*., 1994; Schnitzer *et al*., 1994), and nocodazole, which inhibits microtubule formation (Hoebeke *et al*., 1976; Samson *et al*., 1979). It should be noted, however, that some of these inhibitors have overlapping functions and are not specific to one form of endocytosis (reviewed in Ivanov, 2008). This could prove useful in that two inhibitors with overlapping functions that block rLifA entry could indicate which

mechanism lymphostatin is taken up by. It is unlikely that data exist on the inhibitor concentrations required to specifically block uptake pathways in bovine T cells, therefore significant pilot work and use of control ligands or pathogens would be required.

Chondroitin sulphate proteoglycan 4, polio virus receptor-like 3 and frizzled proteins have all been identified as receptors for TcdB (Yuan *et al*., 2015; LaFrance *et al*., 2015; Tao *et al*., 2016), while lipoprotein receptor-related protein 1 has been identified as a receptor for TpeL (Schorch *et al*., 2014). These LCT receptors were identified by various library screening methods, including gene traps and haploid genetic screens, which screened for toxin resistance. Gene trapping is a form of insertional mutagenesis that uses random integration of a reporter gene with a selectable marker throughout the genome of a host cell. This disrupts gene function and produces a dominant expression phenotype, allowing the products of disrupted genes that would normally interact with a protein of interest to be identified (reviewed in Kumari *et al*., 2018). Haploid genetic screening is a similar method but uses haploid cell lines so that the effects of gene disruption are not masked a second copy of the gene (reviewed in Elling and Penninger, 2014). It may be possible to use such screens to identify the receptor for lymphostatin using Jurkat cells and measuring IL-2 secretion by enzyme-linked immunosorbent assay, which has been reported to be inhibited by LifA (Malstrom and James, 1998).

7.2.2 Translocation

Little is known about LCT pore formation and translocation through the endosomal membrane, but knowledge thus far may be useful for understanding how the N-terminus of LifA escapes the endosome and mostly derives from structural studies and mutagenesis of particular sequences (Genisyuerek *et al*., 2011; Zhang *et al*., 2013b; Chen *et al*., 2016; Chumbler *et al*., 2016). Computational methods could be used to predict regions with particular secondary structures that may be of interest to investigate (Zhang *et al*., 2014; Chen *et al*., 2016). Zhang *et al*. (2014) used TMHMM v2.0 (Krogh *et al*., 2001), which uses a hidden Markov model to predict amino acid sequences that form transmembrane helices in the translocation domain

of TcdB. This programme does not predict EPEC E2348/69 LifA to contain any transmembrane helices, but the complimentary probability plot reveals several regions of hydrophobicity that are more likely to form these structures than the rest of the protein. Similar results are obtained when analysing LCTs, therefore it is likely that transmembrane helices are not predicted because LifA and LCTs are not true transmembrane proteins. Eight small hydrophobic regions were identified in LifA using TMHMM v2.0 at positions 96–113, 1362–1377, 1674–1697, 1901–1927, 2053–2069, 2330–2353, 2571–2590 and 2957–2971. Five larger distinct peaks were identified at positions 1850–1883, 1947–1988, 1988–2038, 2119–2138 and 2235–2264 (Figure 7.3). Interestingly, the largest of these peaks spans the transmembrane domain predicted by Nicholls *et al*. (2000) and the smaller preceding peak encompasses the aminotransferase II motif predicted by Klapproth *et al*. (2005). The overall size of the protein also affects the probability score, as separately analysing the region containing the five peaks provides a higher score for each peak. This suggests that a region of LifA may be inserted into the endosomal membrane of host cells to facilitate translocation of the catalytic N-terminus into the cytoplasm.

Zhang *et al*. (2014) mutated amino acids within the hydrophobic regions that were highly conserved between LCTs. Amino acids were substituted for either polar lysine residues, which would disrupt hydrophobic interactions, or less polar cysteine residues. A similar approach could be taken with LifA, however, choosing highly conserved amino acids may be problematic as LifA homologues do not exhibit as high similarity at the primary sequence level as LCTs. If defective LifA mutants were identified using this method, which would likely be performed by screening lysates, mutant proteins could be purified and biophysically characterised. Mutant proteins that were structurally stable could then be assayed for activity and the ability to form pores as described in Section 4.9 (Qa'dan *et al*., 2000; Barth *et al*., 2001).

Amino acids involved in the predicted pH-dependent conformational change of LifA could be identified by performing similar experiments to Genisyuerek *et al*. (2011). This study first used nested deletions to identify a region of TcdB that was required for pore-forming activity. Two glutamic acid residues located between hydrophobic clusters were substituted for lysine residues, which are not neutralised upon acidification. These amino acids were chosen because similar residues are

required for pore formation by diphtheria toxin (Silverman *et al*., 1994). Mutant TcdB proteins were then assayed for cytotoxicity and pore-forming activity (Genisyuerek *et al*., 2011). Acidic amino acids are found between predicted transmembrane helices in EPEC E2348/69 LifA at the following positions: 1886, 1887, 1898, 1904, 1922, 1930, 1935, 1988, 2040, 2041, 2048, 2055, 2066, 2071, 2084, 2095, 2101, 2109, 2112, 2117, 2151, 2153, 2168, 2170, 2180, 2184, 2195, 2207, 2220, 2224, 2227, and 2234. These may warrant investigation in future studies.

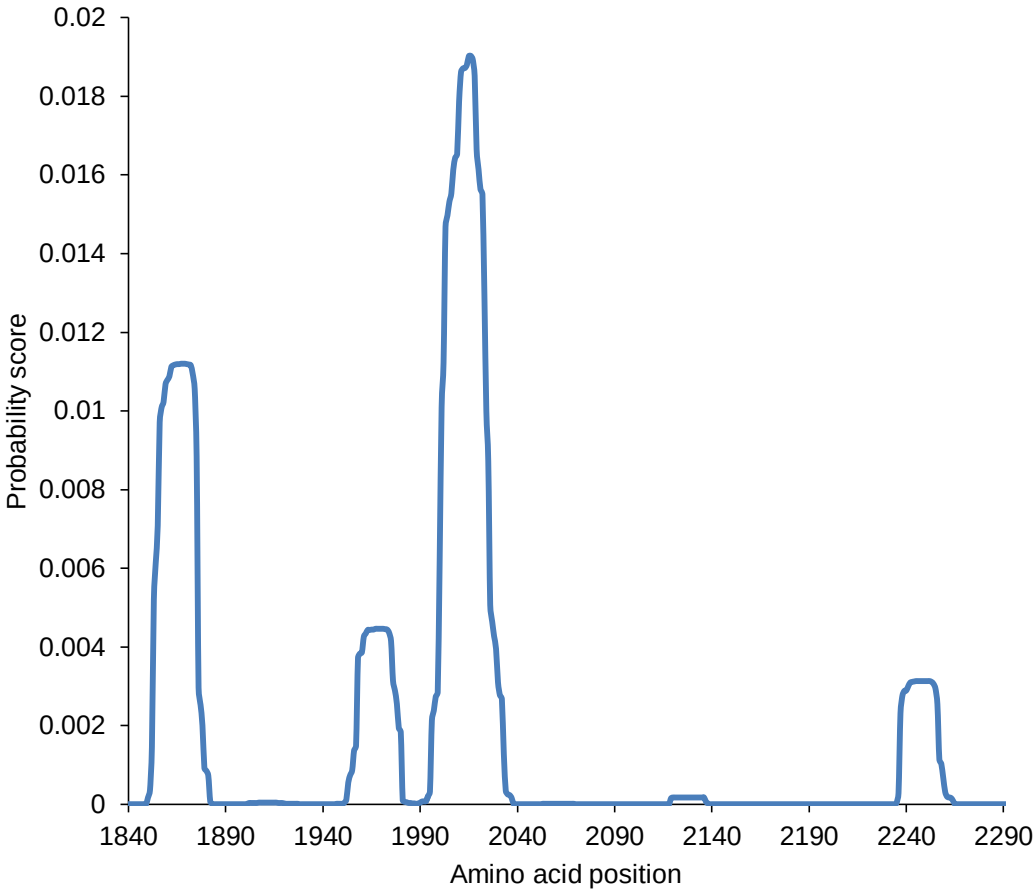

Figure 7.3. Probability plot of transmembrane helices as predicted by TMHMM v2.0 for EPEC E2348/69 LifA. Five distinct peaks located within the 'hinge' (aa 1621–2110) and F3 (aa 2111–2900) regions of LifA indicate amino acids with higher probabilities of forming transmembrane helices than the rest of the protein. Two smaller hydrophobic regions (aa 1901–1927 and 2053–2069) are located between these peaks but are barely visible on the plot. The largest peak and the preceding smaller peak span the predicted transmembrane domain and aminotransferase II motif respectively.

The requirement of cholesterol for pore formation could also be tested as it has been for TcdA and B (Giesemann *et al*., 2006). Methyl-β-cyclodextrin could be used to deplete T cell membranes of cholesterol, and since the acid pulse method used to detect pore formation (see Section 4.9) allows the protein to translocate through the plasma membrane, the potential effects of methyl-β-cyclodextrin on endocytosis would be irrelevant. Rescuing pore formation by restoring cholesterol levels with water-soluble cholesterol could then be attempted. The biggest limitation for studying the translocation of LifA is that any mutant proteins that are made cannot be easily tested for effects of the mutation on other predicted functional domains. Tryptophan fluorescence assays could be used to confirm UDP-GlcNAc binding and directly labelling the protein with a fluorophore could be used to assess uptake. However, unlike LCTs, there is currently no *in vitro* cleavage assay for LifA. As such, using T cells or J774A.1 cells to detect the presence of cleavage products would be prevented if the mutant protein cannot form a pore in the endosomal membrane.

7.2.3 Cleavage of lymphostatin

Although this study found that lymphostatin was cleaved within T cells and J774A.1 cells, autocatalytic cleavage has not been proven as it has with LCTs. Although LifA likely requires a co-factor for cleavage, it unclear whether or not said co-factor is proteinaceous. It was thought that the apparent shortening of rF1 may be the result of autoproteolysis caused by the missing C-terminus acting as a conformational change, which triggers cleavage (see Section 3.11). However, the shortened form of rF1 was ~150 kDa, which is slightly larger than the N-terminal cleavage product detected in cells (c. 140 kDa). If the shortening of rF1 is caused by autoproteolysis it is unclear why cleavage would occur at a different site *in vitro* than in cells. Possible evidence for the autocatalytic cleavage of LifA comes from SAXS experiments. rLifA was reported to shorten after the buffer was acidified by X-ray ionisation, whereas proteins would normally appear larger due to being denatured (Walkinshaw Laboratory, unpublished data). However, this may simply be the result of pH-induced structural changes that cause the protein to adopt a conformation with

a smaller volume. This theory is supported by the fact that rLifA in acidic buffer was observed to elute at a later point than normal on a SAXS-SEC column, and the protein did not appear to fragment (Walkinshaw Laboratory, unpublished data).

The present study only examined the effects of mutating the predicted catalytic Cys^{1480}, but the His and Asp residues of the C/H/D catalytic triad have been reported to be essential for cleavage in both C58 proteases and LCTs (Shao *et al*., 2002; Dai *et al*., 2008; Egerer *et al*., 2007; Pruitt *et al*., 2009). As such, the predicted catalytic His^{1581} and Asp^{1596} could be substituted for alanine residues by site-directed mutagenesis to determine whether these are also required for LifA cleavage and activity. Additionally, the cleavage site of LifA could be identified using the same method that was used for TcdB (Rupnik *et al*., 2005). First, a suitable quantity of the C-terminal c. 225 kDa cleavage product would need to be generated. This may require using J774A.1 cells and potentially immunoprecipitating the cleavage products from the cell lysates. Western blot analysis using polyclonal anti-LifA antibodies indicates that this should be feasible as rF3 and rF5 were reactive. N-terminal sequencing of the c. 225 kDa cleavage product could then be used to identify the site of cleavage. Alternatively, MALDI-TOF/TOF analysis could be used, as was done to identify the cleavage site of TcdA (Kreimeyer *et al*., 2011). The cleavage site could then be confirmed by substituting the identified residues using site-directed mutagenesis.

Despite the findings of this study, it may be that cleavage of LifA is not strictly necessary for inhibitory activity. CP domain mutants of TcdB still induce toxicity in epithelial cell lines but require a longer incubation (Chumbler *et al*., 2012; Li *et al*., 2013a). It is presumed that the GT domain remains bound to the surface of the endosome and is able to interact with Rho GTPases in close proximity. If the GT domain of $rLifA^{C1480A}$ is capable of interacting with its target, albeit at a reduced capacity, a longer incubation with T cells before ConA stimulation may increase inhibitory activity.

7.2.4 Target of glycosylation

Further work could be done to identify the target(s) of lymphostatin based on its impact on signal transduction pathways. It is hypothesised that the target(s) of lymphostatin is located between the points where ConA and PMA/ionomycin stimulate the T cell signalling cascade. The kinase array experiments performed by Dr Robin Cassady-Cain, The Roslin Institute, revealed several proteins other than Akt, which exhibited a LifA-dependent inhibition of phosphorylation. These included Erk1/2, CREB, p70 S6 kinase and p27. It is therefore possible that LifA targets a protein upstream of these in the T cell signalling cascade. Lck is a plausible candidate as it activates the main T cell signalling cascade through CD3 ITAMs (reviewed in Simeoni, 2017) and Akt through PI3K (von Willebrand *et al*., 1994). There is a potentially complex interplay, however, between T cell signalling through the LAT signalosome and the PI3K/Akt pathways. Studies have shown that Akt can activate PLCγ1 in COS-7 kidney cells (Wang *et al*., 2006), and that both Akt and ERK can inactivate tuberous sclerosis 2 (TSC2) to promote cell growth and cell cycle progression in various cell types, including epithelial, myoblast and bone marrow cells (Inoki *et al*., 2002; Ma *et al*., 2005; Wang *et al*., 2009; Miyazaki and Takemasa, 2017). This is further complicated by the fact that TSC2, in complex with TSC1, regulates Akt phosphorylation by enhancing mTORC2 kinase activity (experiments performed using epithelial cells; Huang *et al*., 2008). However, it is unclear whether these findings apply to T cells. Studies targeting candidate proteins can be limited by the availability of specific antibodies and the time required to test individual proteins. Moreover, only O-GlcNAcylation can be tested for by western blotting as antibodies specific to GlcNAc on N-linkages are presently lacking.

Several other methods exist that could be used to identify the target(s) of lymphostatin. Yeast two-hybrid screening has a variety of forms and is commonly used to detect protein-protein interactions (reviewed in Zhu *et al*., 2016). The simplest method was first described by Fields and Song (1989) and uses blue-white colour screening to detect interactions between two proteins. The gene encoding LifA, or more likely the GT domain owing to size, could be fused to the DNA binding domain of the transcription factor GAL4. This could then be screened

against a library of human proteins fused to the activation domain of GAL4 (or *vice versa*). If LifA/GT and the putative interacting partner have a genuine interaction, and thus bring the GAL4 binding and activation domains into close proximity, a *GAL1-lacZ* fusion gene will be transcribed enabling blue-white screening in the presence of a chromogenic substrate of β-galactosidase. However, the proteins under investigation must be small enough to allow the two domains of GAL4 to come within the required distance of each other for activation. The interaction between the two proteins must also be able to occur in the yeast nucleus. Using a mammalian cell two-hybrid system would allow for experiments to be carried out in a native environment (Dang *et al*., 1991) and using fluorescent reporter fusion proteins would allow the proteins to interact outside the nucleus (Zolghadr *et al*., 2008).

Two-hybrid systems are useful for high throughput screening but can result in high numbers of false positives (Deane *et al*., 2002). To confirm any putative interactions, co-immunoprecipitation could be used. This would involve treating T cells with rLifA then using IP to recover rLifA and any associated interacting partner. Western blotting could then be used to confirm the presence of both proteins in the IP sample (reviewed in Lin and Lai, 2017). A monoclonal antibody to rLifA may be required to improve the specificity of such IPs. An alternative may be to use far western blotting, whereby cellular proteins resolved by SDS-PAGE are transferred to a PVDF membrane, which is then exposed to rLifA. Bound protein is then detected with specific antibody and revealed by an enzyme-conjugated secondary antibody. This is not typically as specific as co-IP and can be sensitive to denaturants in the gel system. Candidate interacting partners can then be identified by mass spectrometry of tryptic fragments of proteins excised from the blot (reviewed in Hall, 2015).

Co-IP and far western blotting cannot detect transient interactions, however. To detect targets of LifA when the interaction may be transient, chemoenzymatic labelling could be employed, as it was with NleB to demonstrate transfer of a labelled GlcNAc moiety onto cellular targets (Li *et al*., 2013b). Firstly, genes encoding LifA or the GT domain and a tagged variant of the putative target protein must be transfected into an immortalised cell line where they can be overexpressed. Cells expressing these proteins are then incubated with tetraacylated

N-azidoacetylgalactosamine (Ac4GalNAz), which is then converted into Ac4GlcNAz via the GlcNAc salvage pathway (Boyce *et al*., 2011). IP could be used against the tag of the target protein, the azide group of which would then be bonded to alkyne-linked biotin via a copper catalysed Huisgen 1,3-cycloaddition 'click reaction' (Nishikaze *et al*., 2013; Li *et al*., 2013b). Western blot analysis of the reaction product using streptavidin-HRP or antibodies against the target protein's tag could then reveal whether the target protein has been GlcNAzylated. This technique could also be performed using native proteins, in which case the 'click reaction' would be performed using cell lysates. This may require proteins to be resolubilised after the reaction (reviewed in Speers and Cravat, 2009), which can then be isolated with streptavidin beads. One problem associated with performing this experiment in cells is that Ac4GlcNAz can be added to other proteins. This can be alleviated by pre-treating cells with tunicamycin, which inhibits N-glycosylation (reviewed in Esko *et al*., 2017), and inhibitors of O-GlcNAc transferase, such as alloxan, L01 or 5SGlcNHex (reviewed in Trapannone *et al*., 2016; Liu *et al*., 2017; Liu *et al*., 2018a). Similar to inhibitors of O-GlcNAcase (see Section 5.4), O-GlcNAc transferase inhibitors that are analogues of GlcNAc should be tested to ensure that they do not bind to and inhibit LifA. Performing the reaction *in vitro* would also prevent the GlcNAzylation of non-target proteins by cellular enzymes.

7.2.5 Cell cycle analysis

If lymphostatin causes T cells to pause in a particular phase of the cell cycle, this could be detected using flow cytometry using DNA-binding fluorescent dyes, such as propidium iodide, DAPI or Hoechst 33342 (Krishan, 1975; Belloc *et al*., 1994). This allows for the distinction between cells in the G_0/G_1, S and G_2/M phases. Since doublets of cells in the G_0/G_1 phase contain the same quantity of DNA as single cells in the G_2/M phase, these must be excluded (Wersto *et al*., 2002). Cells may first have to be synchronised to the G_0 phase, which can be reversibly achieved by serum starvation (Griffin, 1976), although this may not be necessary as is it has been reported that peripheral T cells from humans are predominantly in this phase (Witkowski and Bryl, 2004). Such methods have previously been used to

characterise a number of bacterial toxins and Type III secreted effectors termed cyclomodulins (Marchès *et al*., 2003; reviewed in Taieb *et al*., 2011).

7.3 Lymphostatin homologues

There are a number of homologous proteins to lymphostatin in A/E *E. coli* and other bacteria (reviewed in Klapproth, 2010), but few studies have been carried out with regards to the function of these proteins. Abu-Median *et al*. (2006) did not observe inhibitory activity against PBMCs with lysates of *efa1′* and *toxB* EHEC O157:H7 85-170 Nal^R mutants. However, it has recently been shown that ToxB does in fact possess lymphostatin activity against bovine peripheral T cells (Cassady-Cain *et al*., 2017). This is consistent with earlier observations that showed the EHEC O157:H7 lysates could inhibit IL-2 production by ConA-stimulated human PBMCs in a manner dependent on the c. 92 kb pO157 plasmid that encodes *toxB* (Klapproth *et al*., 2000). A number of LifA homologues were described in *C. trachomatis* that exhibit cytotoxic activity (Belland *et al*., 2001). A LifA homologue from *C. pecorum* has recently been shown to inhibit ConA-stimulated T cell proliferation, without causing direct cytotoxicity (Stevens Laboratory, unpublished data). Given that *Chlamydia* species are obligate intracellular pathogens, it is unclear how such proteins would escape infected cells to target T cells. The extracellular elementary bodies of *Chlamydia* are metabolically active (reviewed in Elwell *et al*., 2016) but are not known to secrete virulence factors. *C. pneumonia* have been shown to infect T cells (Haranaga *et al*., 2001), although they do not possess any LifA homologues. However, if other *Chlamydia* species are capable of infecting lymphocytes, this may allow them to secrete LifA homologues either directly into the host cell cytoplasm via the T3SS or into the phagosome, where the protein may then cross the membrane.

Few studies have so far investigated the role of LifA-like protein from EPEC E2348/69 (Cepeda-Molero *et al*., 2017; see Section 7.4), while the slightly different LifA-like protein from EPEC O111:H- strain B171-8 has never been studied. However, if data from the Kenny Laboratory is correct, and EPEC does inhibit Akt1 Ser^{473} phosphorylation in a LifA-like-dependent manner, this suggests that LifA-like

protein may target the same protein(s) as LifA. It would therefore appear that LifA is merely one protein in a larger lymphostatin family with some redundancy of function. Many of the same experiments used to study LifA could be performed with these homologues and/or of particular interest would be whether they use the same sugar substrates and have the same target(s). The biggest limitation to studying these proteins is likely to be obtaining sufficient quantities of the proteins, as purified rToxB and the recombinant *C. pecorum* homologue were obtained in much lower quantities than rLifA (Stevens/Walkinshaw Laboratory, unpublished data). It may be possible to obtain larger quantities of protein using an alternative expression system, such as *Bacillus megaterium*, which were used to produce LCTs as they are expressed poorly in *E. coli* (Burger *et al*., 2003; Yang *et al*., 2008). Given that the LifA-like proteins from EPEC E2348/69 and B171-8 lack the C-terminal 867 and 668 amino acids of LifA respectively, it would be of interest to determine whether these proteins can enter cells in the same way as LifA. If inhibitory activity against T cells could not be detected with exogenously applied LifA-like proteins, using the acid pulse method (see Section 4.9) may reveal activity, as analysis of these proteins with TMHMM v2.0 predicted that they also contain C-terminal transmembrane helices. It is also possible that the LifA-like proteins may be directly secreted into cells via the T3SS, meaning that phenotypes may only be evident after bacterial infection.

Perhaps the most peculiar of the LifA homologues is Efa1′, as it is unclear whether *efa1′* encodes a functional protein or is merely a pseudogene. Given that a DNA vaccine of *efa1′* has been reported to confer protective immunity against EHEC O157:H7 in mice (Riquelme-Neira *et al*., 2016), this suggests that the protein is functional. However, studies using single and double *efa1′* and *toxB* mutants of *E. coli* O157:H7 in calves did not reveal a significant role for the proteins in intestinal colonisation (Stevens *et al*., 2004). If both open reading frames *z4332* and *z4333* are transcribed via ribosome frameshifting, then the full-length Efa1′ protein would include a portion of the LifA GT domain, including the DXD motif. Abu-Median *et al*. (2006) did not attribute inhibitory activity of lysates of EHEC 85-170Nal^{R} to Efa1′, however, we cannot preclude the possibility that it may require Type III secretion into host cells for activity. Transfection of the Efa1′ protein or the gene

encoding it into cells could be used to determine whether this protein possesses lymphostatin activity. The dedicated study of lymphostatin homologues may reveal insights into how these virulence factors evolved and lead to effective therapies against the pathogens that produce them.

7.4 Other potential activities of lymphostatin

The genes encoding lymphostatin from EPEC E2348/69 (*lifA*) and EHEC factor for adhesion (*efa1*) from EHEC O111:H- E43035N were described in the same year and are almost identical (Klapproth *et al*., 2000; Nicholls *et al*., 2000). A number of studies have reported that *lifA*, *toxB* and *efa1′* mutant EPEC and EHEC strains have reduced adherence to epithelial cells (Nicholls *et al*., 2000; Tatsuno *et al*., 2001; Stevens *et al*., 2002 and 2004; Badea *et al*., 2003; Deacon *et al*., 2010). Immunofluorescence microscopy of EPEC O127:H6 strain JPN15 also reportedly detected LifA associated with the perimeter of the bacterial outer membrane (Badea *et al*., 2003). However, the deletion of these genes in some strains has been reported to affect the expression and secretion of Type III secreted proteins that are required for adherence (Tatsuno *et al*., 2001; Stevens *et al*., 2002 and 2004; Deacon *et al*., 2010). This suggests that the role of LifA and its homologues in adherence may be indirect, at least in some strains. The fact that the effect does not appear to occur at the level of transcription (Stevens *et al*., 2004) leads to the hypothesis that the mutations may affect translation of the proteins while docked at T3SS complexes or the hierarchy of secretion of T3S proteins (Wang *et al*., 2008; Mills *et al*., 2013). This suggests that A/E *E. coli* strains possessing *lifA* or its homologues may be more virulent, as observed with atypical EPEC strains (Afset *et al*., 2006; Narimatsu *et al*., 2010; Slinger *et al*., 2017). To determine whether the role of LifA in adherence is direct, laboratory-adapted strains of *E. coli* could be mixed with rLifA or buffer and applied to epithelial cell lines. A count of the microcolonies would reveal whether LifA can enhance bacterial adhesion independently of other effector proteins, unless another protein is required to interact with LifA, similar to the intimin-Tir interaction (see Section 1.1.3.6). A precedent exists for proteins to bridge an interaction between bacteria and host cells in this way, as the Type I secreted 595 kDa SiiE protein from

Salmonella associates with both the bacterial surface and glycan moieties on host cells (Morgan *et al*., 2007; Gerlach *et al*., 2007; Wagner *et al*., 2014). Alternatively, rLifA could be conjugated to fluorescent carboxylate-modified latex beads and cells with bound beads could be detected by flow cytometry, as was performed with intimin (Gonçalves *et al*., 2003).

Recently, it was reported that LifA and LifA-like protein have an accessory role in A/E lesion formation that is masked by other Type III secreted effectors (Cepeda-Molero *et al*., 2017). This function was independent of effects on other effectors as the secretion of T3S proteins was normal in strains lacking LifA and LifA-like protein. Identifying interacting partners of these proteins from epithelial cells may help to elucidate the underlying mechanism of LifA/LifA-like-mediated pedestal formation. Other studies also suggest a potential role for LifA in non-lymphocyte cells. If observations by the Kenny Laboratory are correct in that EPEC inhibit Akt1 Ser^{473} phosphorylation in a LifA/LifA-like-dependent manner in J774A.1 cells (see Section 6.1), this may indicate a role for LifA in modulating a plethora of Akt-dependent cellular processes. The extent to which LifA and its homologues may modulate innate immune responses in other cell types also merits study, given the number of other Type III secreted effectors that target this.

7.5 Concluding remarks

This study significantly contributes to our understanding of the mode of action and molecular biology of lymphostatin, an important virulence factor of A/E *E. coli*. However, while this research has revealed new insights from rLifA-treated bovine T lymphocytes *in vitro*, it does not demonstrate the relevance of lymphocyte inhibitory activity during the course of A/E *E. coli* infection in cattle or other animals. Various studies have previously shown that LifA is an important colonisation factor (see Section 1.3.4) but none have investigated the effects of LifA on the host immune response. One experiment that could be performed to investigate the effects of LifA on the adaptive immune response of the host would be to generate an *E. coli* strain that overexpresses a model antigen, such as ovalbumin, in the presence or absence of lymphostatin. This may allow the impact of LifA on the

induction of ovalbumin-specific antibody or effector cells to be quantified, however, disentangling the contribution of LifA to the modulation of host immunity from its role in gut colonisation may be challenging. It is possible that this could be overcome by repeatedly reapplying the bacteria, or recombinant proteins, directly to an accessible site of immune priming in cattle, such as follicle-associated epithelium in the terminal rectum. This is a key site of persistence of EHEC O157:H7 in cattle and cellular immune responses can be quantified by studying phenotypes of cells from lymph nodes draining this site (Corbishley *et al*., 2014 and 2016). Given that LifA is also produced by *C. rodentium* and RDEC, mouse or rabbit models of infection could be used as alternatives.

Also worthy of consideration is how lymphostatin reaches its target cells given that the frequency that A/E *E. coli* come into direct contact with lymphocytes *in vivo* may be low (see Section 1.3.3). It may be that LifA is directly injected into intraepithelial lymphocytes or is secreted into the extracellular milieu and diffuses to reach intraepithelial lymphocytes. Alternatively, LifA may be translocated across the epithelial cell layer to gut associated lymphoid tissue or into the bloodstream, where it acts on circulating lymphocytes before they reach the site of infection. Future research could seek to determine whether LifA production and/or translocation could be detected in the gut of infected animals using reporter fusions, as was carried out for *Salmonella* Type III secreted proteins (Geddes *et al*., 2007). Studies could also seek to determine whether LifA might be transported through the blood stream in microvesicles, similar to Stx (Ståhl *et al*., 2015). A ligated intestinal loop model previously failed to detect *lifA*-dependent effects on bovine intraepithelial lymphocytes exposed to EHEC *in situ* (Menge *et al*., 2004b), however, the model is constrained by the relatively short time that the animals were maintained under terminal anaesthesia. A model in which loops of gut formed by end-to-end anastomoses of ileal segments could be inoculated with strains and the animals then recovered to enable longer exposure may be useful (Coombes *et al*., 2005). Similar to experiments with Stx (Kolling and Matthews, 1999), outer membrane vesicles from A/E *E. coli* could also be examined for the presence of LifA protein or nucleic acids encoding LifA and homolgous proteins to determine whether this is a possible method of lymphostatin delivery.

There have been few vaccine studies with LifA and its homologues and these have had mixed results (van Diemen *et al*., 2007; Riquelme-Neira *et al*., 2016). However, a greater understanding of the molecular basis of lymphostatin activity may allow for the creation of novel forms of the protein that act as more potent T and B cell antigens as they do not possess inhibitory activity. This follows a similar strategy to the development of detoxified variants of *E. coli* heat labile toxin or cholera toxin, which are immunogenic but lack the capacity to cause pathology (Holmgren *et al*., 1993; Douce *et al*., 1999; Sánchez *et al*., 2002). Continued studies also have the potential to reveal novel aspects of lymphocyte activation, which may lead to new therapies against lymphocyte cancers and autoimmune diseases.

References

Abe, J., Takeda, T., Watanabe, Y., Nakao, H., Kobayashi, N., Leung, D. Y. M. and Kohsaka, T. (1993). Evidence for Superantigen Production by *Yersinia pseudotuberculosis*. *The Journal of Immunology* 151, 4183–4188.

Abu-Median, A., van Diemen, P. M., Dziva, F., Vlisidou, I., Wallis, T. S. and Stevens, M. P. (2006). Functional Analysis of Lymphostatin Homologues in Enterohaemorrhagic *Escherichia coli*. *Federation of European Microbiological Societies Microbiology Letters* 258, 43–49.

Acheson, D. W., Moore, D., de Breuker, S. Lincicome, L., Jacewicz, M., Skutelsky, E. and Keusch, G. T. (1996). Translocation of Shiga Toxin Across Polarized Intestinal Cells in Tissue Culture. *Infection and Immunity* 64, 3294–3300.

Adams, E. J., Chien, Y. and Garcia, K. C. (2005). Structure of a γδ T Cell Receptor in Complex with the Nonclassical MHC T22. *Science* 308, 227–231.

Afset, J. E., Bruant, G., Brousseau, R., Harel, J., Anderssen, E., Bevanger, L. and Bergh, K. (2006). Identification of Virulence Genes Linked with Diarrhea due to Atypical Enteropathogenic *Escherichia coli* by DNA Microarray Analysis and PCR. *Journal of Clinical Microbiology* 44, 3703–3711.

Agilent Technologies (2015). *QuikChange II XL Site Directed Mutagenesis Kit Instruction Manual*.
URL: https://www.agilent.com/cs/library/usermanuals/public/200521.pdf. Accessed: 17/07/2019.

Al-Bari, M. A. (2015). Cholorquine Analogues in Drug Discovery: New Directions of Uses, Mechanisms of Action and Toxic Manifestations from Malaria to Multifarious Diseases. *Journal of Antimicrobial Chemotherapy* 70, 1608–1621.

Alcover, A., Alarcón, B. and Di Bartolo, V. (2018). Cell Biology of T Cell Receptor Expression and Regulation. *Annual Review of Immunology* 36, 103–125.

Alessi, D. R., Andjelković, M., Caudwell, B., Cron, P., Morrice, N., Cohen, P. and Hemmings, B. A. (1996). Mechanism of Activation of Protein Kinase B by Insulin and IGF-1. *The European Molecular Biology Organization Journal* 15, 6541–6551.

Aliberti, J., Viola, J. P. B., Vieira-de-Abreu, A., Bozza, P. T., Sher, A. and Scharfstein, J. (2003). Cutting Edge: Bradykinin Induces IL-12 Production by Dendritic Cells: A Danger Signal that Drives Th1 Polarization. *The Journal of Immunology* 170, 5349–5353.

Allaire, J. M., Crowley, S. M., Law, H. T., Chang, S., Ko, H. and Vallance, B. A. (2018). The Intestinal Epithelium: Central Coordinator of Mucosal Immunity. *Trends in Immunology* 39, 677–696.

Alonso, A., Bottini, N., Bruckner, S., Rahmouni, S., Williams, S., Schoenberger, S. P. and Mustelin, T. (2004). Lck Dephosphorylation at Tyr-394 and Inhibition of T Cell Antigen Receptor Signaling by *Yersinia* Phosphatase YopH. *The Journal of Biological Chemistry* 279, 4922–4928.

Alto, N. M., Weflen, A. W., Rardin, M. J., Yarar, D., Lazar, C. S., Tonikian, R., Koller, A., Taylor, S. S., Boone, C., Sidhu, S. S., Schmid, S. L., Hecht, G. A. and Dixon, J. E. (2007). The Type III Effector EspF Coordinates Membrane Trafficking by the Spatiotemporal Activation of Two Eukaryotic Signaling Pathways. *Journal of Cell Biology* 178, 1265–1278.

Amarante-Mendes, G. P., Adjemian, S., Branco, L. M., Zanetti, C. L., Weinlich, R. and Bortoluci, K. R. (2018). Pattern Recognition Receptors and the Host Cell Death Molecular Machinery. *Frontiers in Immunology* 9, 2379.

Amimoto, K., Noro, T., Oishi, E. and Shimizu, M. (2007). A Novel Toxin Homologous to Large Clostridial Cytotoxins Found in Culture Supernatant of *Clostridium perfringens* Type C. *Microbiology* 153, 1198–1206.

Amin, E. O. M. (2017). Investigating How Enteropathogenic *Escherichia coli* (EPEC) Subverts Akt Signalling. *Doctor of Philosophy Thesis*, Newcastle University.

Amphlett, A. (2015). Far East Scarlet-Like Fever: A Review of the Epidemiology, Symptomatology, and Role of Superantigenic Toxin: *Yersinia pseudotuberculosis*-Derived Mitogen A. *Open Forum Infectious Diseases* 3, ofv202.

Anderson, C. L., Shen, L., Eicher, D. M., Wewers, M. D. and Gill, J. K. (1990). Phagocytosis Mediated by Three Distinct Fcγ Receptor Classes on Human Leukocytes. *Journal of Experimental Medicine* 171, 1333–1345.

Andrade, A., Pardo J. P., Espinosa, N., Pérez-Hernández, G. and González-Pedrajo, B. (2007). Enzymatic Characterization of the Enteropathogenic *Escherichia coli* Type III Secretion ATPase EscN. *Archives of Biochemistry and Biophysics* 468, 121–127.

Arce, S., Nawar, H. F., Russell, M. W. and Connell, T. D. (2005). Differential Binding of *Escherichia coli* Enterotoxins LT-IIa and LT-IIb and of Cholera Toxin Elicits Differences in Apoptosis, Proliferation, and Activation of Lymphoid Cells. *Infection and Immunity* 73, 2718–2727.

Arencibia, I., Suárez, N. C., Wolf-Watz, H. and Sundqvist, K. G. (1997). *Yersinia* Invasin, a Bacterial Beta1-Integrin Ligand, is a Potent Inducer of Lymphocyte Motility and Migration to Collagen Type IV and Fibronectin. *The Jounal of Immunology* 159, 1853–1859.

Armstrong, G. D., Mulvey, G. L., Marcato, P., Griener, T. P., Kahan, M. C., Tennent, G. A., Sabin, C. A., Chart, H. and Pepys, M. B. (2006). Human Serum Amyloid P Component Protects Against *Escherichia coli* O157:H7 Shiga Toxin 2 *In Vivo*: Therapeutic Implications for Hemolytic-Uremic Syndrome. *The Journal of Infectious Diseases* 193, 1120–1124.

Arora, N. and Leppla, S. H. (1993). Residues 1–254 of Anthrax Toxin Lethal Factor are Sufficient to Cause Cellular Uptake of Fused Polypeptides. *The Journal of Biological Chemistry* 268, 3334–3341.

Artis, D., Wang, M. L., Keilbaugh, S. A., He, W., Brenes, M., Swain, G. P., Knight, P. A., Donaldson, D. D., Lazar, M. A., Miller, H. R. P., Schad, G. A. Scott, P. and Wu, G. D. (2004). RELMβ/FIZZ2 is a Goblet Cell-Specific Immune-Effector Molecule in the Gastrointestinal Tract. *Proceedings of the National Academy of Sciences of the United States of America* 101, 13596–13600.

Attanasio, J. and Wherry, E. J. (2016). Costimulatory and Coinhibitory Receptor Pathways in Infectious Disease. *Immunity* 44, 1052–1068.

Babbin, B. A., Sasaki, M., Gerner-Schmidt, K. W., Nusrat, A. and Klapproth, J. A. (2009). The Bacterial Virulence Factor Lymphostatin Compromises Intestinal Epithelial Barrier Function by Modulating Rho GTPases. *The American Journal of Pathology* 174, 1347–1357.

Bachmann, M. F., McKall-Faienza, K., Schmits, R., Bouchard, D., Beach, J., Speiser, D. E., Mak, T. W. and Ohashi, P. S. (1997). Distinct Roles for LFA-1 and CD28 During Activation of Naive T Cells: Adhesion Versus Costimulation. *Immunity* 7, 549–557.

Badea, L., Doughty, S., Nicholls, L., Sloan, J., Robins-Browne, R. M. and Hartland, E. L. (2003). Contribution of Efa1/LifA to the Adherence of Enteropathogenic *Escherichia coli* to Epithelial Cells. *Microbial Pathogenesis* 34, 205–215.

Bagel, S., Hüllen, V., Wiedemann, B. and Heisig, P. (1999). Impact of *gyrA* and *parC* Mutations on Quinolone Resistance, Doubling Time, and Supercoiling Degree of *Escherichia coli*. *Antimicrobial Agents and Chemotherapy* 43, 868–875.

Baldauf, K. J., Royal, J. M., Hamorsky, K. T. and Matoba, N. (2015). Cholera Toxin B: One Subunit with Many Pharmaceutical Applications. *Toxins (Basel)* 7, 974–996.

Balish, M. F. (2014). *Mycoplasma pneumoniae*, an Underutilized Model for Bacterial Cell Biology. *Journal of Bacteriology* 196, 3675–3682.

Bandeira, A., Mota-Santos, T., Itohara, S., Degermann, S., Heusser, C., Tonegawa, S. and Coutinho, C. (1990). Localization of γ/δ T Cells to the Intestinal Epithelium is Independent of Normal Microbial Colonization. *Journal of Experimental Medicine* 172, 239–244.

Baniyash, M., Garcia-Morales, P., Luong, E., Samelson, L. E. and Klausner, R. D. (1988). The T Cell Antigen Receptor ζ Chain is Tyrosine Phosphorylated upon Activation. *The Journal of Biological Chemistry* 263, 18225–18230.

Barber, E. K., Dasgupta, J. D., Schlossman, S. F., Trevillyan, J. M. and Rudd, C. E. (1989). The CD4 and CD8 Antigens are Coupled to a Protein-Tyrosine Kinase (p561ck) that Phosphorylates the CD3 Complex. *Proceedings of the National Academy of Sciences of the United States of America* 86, 3277–3281.

Barnes, I. H. A., Bagnall, M. C., Browning, D. D., Thompson, S. A., Manning, G. and Newell, D. G. (2007). γ-Glutamyl Transpeptidase has a Role in the Persistent Colonization of the Avian Gut by *Campylobacter jejuni*. *Microbial Pathogenesis* 43, 198–207.

Barranco, I., Tvarijonaviciute, A., Perez-Patiño, C., Vicente-Carrillo, A., Parrilla, I., Ceron, J. J., Martinez, E. A., Rodriuez-Martinez, H. and Roca, J. (2016). Glutathione Peroxidase 5 is Expressed by the Entire Pig Male Genital Tract and Once in the Seminal Plasma Contributes to Sperm Survival and *In Vivo* Fertility. *Public Library of Science ONE* 11, e0162958.

Barth, H., Pfeifer, G., Hofmann, F., Maiers, E., Benz, R. and Aktories, K. (2001). Low pH-Induced Formation of Ion Channels by *Clostridium difficile* Toxin B in Target Cells. *The Journal of Biological Chemistry* 276, 10670–10676.

Baruch, K., Gur-Arie, L., Nadler, C., Koby, S., Yerushalmi, G., Ben-Neriah, Y., Yogev, O., Shaulian, E., Guttman, C., Zarivach, R. and Rosenshine, I. (2011). Metalloprotease Type III Effectors that Specifically Cleave JNK and NF-κB. *The European Molecular Biology Organization Journal* 30, 221–231.

Bause, E. and Legler, G. (1981). The Role of the Hydroxy Amino Acid in the Triplet Sequence Asn-Xaa-Thr(Ser) for the N-Glycosylation Step During Glycoprotein Biosynthesis. *The Biochemical Journal* 195, 639–644.

Beals, C. R., Sheridan, C. M., Turck, C. W., Gardner, P. and Crabtree, G. R. (1997). Nuclear Export of NF-ATc Enhanced by Glycogen Synthase Kinase-3. *Science* 275, 1930–1933.

Bease, A. G. (2015). Mode of Action of Lymphostatin, a Key Virulence Factor of Attaching & Effacing *Escherichia coli*. *Master of Science by Research Thesis*, The University of Edinburgh.

Bekiari, V., Persson, E. K. and Agace, W. W. (2014). Intestinal Dendritic Cells in the Regulation of Mucosal Immunity. *Immunological Reviews* 260, 86–101.

Belland, R. J., Scidmore, M. A., Crane, D. D., Hogan, D. M., Whitmire, W., McClarty, G. and Caldwell, H. D. (2001). *Chlamydia trachomatis* Cytotoxicity Associated with Complete and Partial Cytotoxin Genes. *Proceedings of the National Academy of Sciences of the United States of America* 98, 13984–13989.

Belloc, F., Dumain, P., Boisseau., M. R., Jalloustre, C., Reiffers, J., Bernard, P. and Lacombe, F. (1994). A Flow Cytometric Method Using Hoechst 33342 and Propidium Iodide for Simulataneous Cell Cycle Analysis and Apoptosis Determination in Unfixed Cells. *Cytometry* 17, 59–65.

Bentley, R. and Meganathan, R. (1982). Biosynthesis of Vitamin K (Menaquinone) in Bacteria. *Microbiological Reviews* 46, 241–280.

Berger, C. N., Crepin, V. F., Baruch, K., Mousnier, A., Rosenshine, I., Frankel, G. (2012). EspZ of Enteropathogenic and Enterohemorrhagic *Escherichia coli* Regulates Type III Secretion System Protein Translocation. *mBio* 3, 1–12.

Berger, C. N., Crepin, V. F., Jepson, M. A., Arbeloa, A. and Frankel, G. (2009). The Mechanisms Used by Enteropathogenic *Escherichia coli* to Control Filopodia Dynamics. *Cellular Microbiology* 11, 309–322.

Berin, M. C., Darfeuille-Michaud, A., Egan, L. J., Miyamoto, Y. and Kagnoff, M. F. (2002). Role of EHEC O157:H7 Virulence Factors in the Activation of Intestinal Epithelial Cell NF-κB and MAP Kinase Pathways and the Unregulated Expression of Interleukin 8. *Cellular Microbiology* 4, 635–647.

Berton, G., Bellavite, P., de Nicoloa, G. Dri, P. and Rossi, F. (1982). Plasma Membrane and Phagosome Localisation of the Activated NADPH Oxidase in Elicited Peritoneal Macrophages of the Guinea-Pig. *The Journal of Pathology* 136, 241–252.

Beutin, L., Geier, D., Steinrück, H., Zimmermann, S. and Scheutz, F. (1993). Prevalence and Some Properties of Verotoxin (Shiga-Like Toxin)-Producing *Escherichia coli* in Seven Different Species of Healthy Domestic Animals. *Journal of Clinical Microbiology* 31, 2483–2488.

Bieber, D., Ramer, S. W., Wu, C., Murray, W. J., Tobe, T., Fernandez, R. and Schoolnik G. K. (1998). Type IV Pili, Transient Bacterial Aggregates, and Virulence of Enteropathogenic *Escherichia coli*. *Science* 280, 2114–2118.

Bielaszewska, M., Rüter, C., Bauwens, A., Greune, L., Jarosch, A., Steil, D., Zhang, W., He, X., Lloubes, R., Fruth, A., Kim, K. S., Schmidt, M. A., Dobrindt, U., Mellmann, A. and Karch, H. (2017). Host Cell Interactions of Outer Membrane Vesicle-Associated Virulence Factors of Enterohemorrhagic *Escherichia coli* O157: Intracellular Delivery, Trafficking and Mechanisms of Cell Injury. *Public Library of Science Pathogens* 13, e1006159.

Blasche, S., Mörtl, M., Steuber, H., Siszler, G,. Nisa, S., Schwarz, F., Lavrik, I., Gronewold, T.M.A., Maskos, K., Donnenberg, M.S., Ullman, D., Uetz, P. and Kögl, M. (2013). The *E. coli* Effector Protein NleF is a Caspase Inhibitor. *Public Library of Science ONE* 8, e58937.

Blattner, F., Plunkett III, G., Bloch, C. A., Perna, N. T., Burland, V., Riley, M., Collado-Vides, J., Glasner, J. D, Rode, C. K., Mayhew, G. F., Gregor, J., Davis, N. W., Kirkpatrick, H. A., Goeden, M. A., Rose, D. J., Mua, B. and Shao, Y. (1997). The Complete Genome Sequence of *Escherichia coli* K-12. *Science* 277, 1453–1462.

Blum, J. S., Wearsch, P. A. and Cresswell, P. (2013). Pathways of Antigen Processing. *Annual Review in Immunology* 31, 443–473.

Boerlin, P., McEwen, S. A., Boerlin-Petzold, F., Wilson, J. B., Johnson, R. P. and Gyles, C. L. (1999). Associations between Virulence Factors of Shiga Toxin-Producing *Escherichia coli* and Disease in Humans. *Journal of Clinical Microbiology* 37, 497–503.

Bogdanović, X., Schneider, S., Levanova, N., Wirth, C., Trillhaase, C., Steinemann, M., Hunte, C., Aktories, K. and Jank, T. (2018). A Cysteine Protease-Like Domain Enhances the Cytotoxic Effects of the *Photorhabdus asymbiotica* Toxin PaTox. *The Journal of Biological Chemistry* 294, 1035–1044.

Bole, D. G., Hendershot, L. M. and Kearney, J. F. (1986). Posttranslational Association of Immunoglobulin Heavy Chain Binding Protein with Nascent Heavy Chains in Nonsecreting and Secreting Hybridomas. *The Journal of Cell Biology* 102, 1558–1566.

Boncristiano, M., Paccani, S. R., Barone, S., Ulivieri, C. Patrussi, L., Ilver, D., Amemdei, A., D'Elios, M. M., Telford, J L. and Baldari, C. T. (2003). The *Helicobacter pylori* Vacuolating Toxin Inhibits T Cell Activation by Two Independent Mechanisms. *Journal of Experimental Medicine* 198, 1887–1897.

Borche, L, Lozano, F., Vilella, R. and Vives, J. (1987). CD43 Monoclonal Antibodies Recognize the Large Sialoglycoprotein of Human Leukocytes. *European Journal of Immunology* 17, 1523–1526.

Bowman, E. J., Graham, L. A., Stevens, T. H. and Bowman, B. J. (2004). The Bafilomycin/Concanmycin Binding Site in Subunit C of the V-ATPases from *Neurospora crassa* and *Saccharomyces cerevisiae*. *The Journal of Biological Chemistry* 279, 33131–33138.

Bowman, E. J., Siebers, A. and Altendorf, K. (1988). Bafilomycins: A Class of Inhibitors of Membrane ATPases from Microorganisms, Animal Cells, and Plant Cells. *Proceedings of the National Academy of Sciences of the United States of America* 85, 7972–7976.

Boyce, M., Carrico, I. S., Ganguli, A. S., Yu, S., Hangauer, M. J., Hubbard, S. C., Kohler, J. J. and Bertozzi, C. R. (2011). Metabolic Cross-Talk Allows Labeling of O-linked β-N-Acetylglucosamine-Modified Proteins via the N-Acetylgalactosamine Salvage Pathway. *Proceedings of the National Academy of Sciences of the United States of America* 108, 3141–3146.

Brady, M. J., Campellone, K. G., Ghildiya, M. and Leong, J. M. (2007). Enterohaemorrhagic and Enteropathogenic *Escherichia coli* Tir Proteins Trigger a Common Nck-Independent Actin Assembly Pathway. *Cellular Microbiology* 9, 2242–2253.

Brandelli, J. R., Griener, T. P., Laing, A., Mulvey, G. and Armstrong, G. D. (2015). The Effects of Shiga Toxin 1, 2 and Their Subunits on Cytokine and Chemokine Expression by Human Macrophage-Like THP-1 Cells. *Toxins (Basel)* 7, 4054–4066.

Brenner, M. B., Trowbridge, I. S. and Strominger, J. L. (1985). Cross-Linking of Human T Cell Receptor Proteins: Association between the T Cell Idiotype β Subunit and the T3 Glycoprotein Heavy Subunit. *Cell* 40, 183–190.

Brigelius-Flohé, R. and Maiorino, M. (2013). Glutathione Peroxidases. *Biochimica et Biophysica Acta – General Subjects* 1830, 3289–3303.

Brodbeck, D., Cron, P. and Hemmings, B. A. (1999). A Human Protein Kinase Bγ with Regulatory Phosphorylation Sites in the Activation Loop and in the C-Terminal Hydrophobic Domain. *The Journal of Biological Chemistry* 274, 9133–9136.

Brooks, J. T., Sowers, E. G., Wells, J. G., Greene, K. D., Griffin, P. M., Hoekstra, R. M. and Stockbine, N. A. (2005). Non-O157 Shiga Toxin-Producing *Escherichia coli* Infections in the United States, 1983–2002. *The Journal of Infectious Diseases* 192, 1422–1429.

Brownlie, R. J. and Zamoyska, R. (2013). T Cell Receptor Signalling Networks: Branched, Diversified and Bounded. *Nature Reviews Immunolgy* 13, 257–269.

Brubaker, S. W., Bonham, K. S., Zanoni, I. and Kagan, J. C. (2015). Innate Immune Pattern Recognition: A Cell Biological Perspective. *Annual Review of Immunology* 33, 257–290.

Bruckner, S., Rhamouni, S., Tautz, L., Denault, J., Alonso, A., Becattini, B., Slavesen, G. S. and Mustelin, T. (2005). *Yersinia* Phosphatase Induces Mitochondrially Dependent Apoptosis of T Cells. *The Journal of Biological Chemistry* 280, 10388–10394.

Brugirard-Ricaud, K., Duchaud, E., Givaudan, A., Girard, P. A., Kunst, F., Boemare, N., Brehélin, M. and Zumbihl, R. (2005). Site-Specific Antiphagocytic Function of the *Photorhabdus luminescencs* Type III Secretion System During Insect Colonization. *Cellular Microbiology* 7, 363–371.

Bryceson, Y. T., March, M. E., Ljunggren, H. and Long, E. O. (2006). Synergy Among Receptors on Resting NK Cells for the Activation of Natural Cytotoxicity and Cytokine Secretion. *Blood* 107, 159–166.

Bryksin, A. V. and Matsumura, I. (2010). Overlap Extension PCR Cloning: A Simple and Reliable Way to Create Recombinant Plasmids. *Biotechniques* 48, 463–465.

Buchan, D. W. A., Minneci, F., Nugent, T. C. O., Bryson, K. and Jones, D. T. (2013). Scalable Web Services for the PSIPRED Protein Analysis Workbench. *Nucleic Acids Research* 41, W349–W357.

Burger, S., Tatge, H., Hofmann, F., Genth, H., Just, I. and Gerhard, R. (2003). Expression of Recombinant *Clostridium difficile* Toxin A Using the *Bacillus megaterium* System. *Biochemical and Biophysical Reseach Communications* 307, 584–588.

Burland, V., Shao, Y., Perna, N. T., Plunkett, G., Sofia, H. J. and Blattner, F. R. (1998). The Complete DNA Sequence and Analysis of the Large Virulence Plasmid of *Escherichia coli* O157:H7. *Nucleic Acids Research* 26, 4196–4204.

Burr, J. S., Savage, N. D. L., Messah, G. E., Kimzey, S. L., Shaw, A. S., Arch, R. H. and Green, J. M. (2001). Cutting Edge: Distinct Motifs within CD28 Regulate T Cell Proliferation and Induction of Bcl-X_L. *The Journal of Immunology* 166, 5331–5335.

Busch, C., Hofmann, F., Selzer, J., Munro, S., Jeckel, D. and Aktories, K. (1998). A Common Motif of Eukaryotic Glycosyltransferases is Essential for the Enzyme Activity of Large Clostridial Cytotoxins. *The Journal of Biological Chemistry* 273, 19566–19572.

Busch, C., Schömig, K., Hofmann, F. and Aktories, K. (2000). Characterization of the Catalytic Domain *Clostridium novyi* Alpha-Toxin. *Infection and Immunity* 68, 6378–6383.

Bustelo, X. R. (2014). Vav Family Exchange Factors: An Integrated Regulatory and Functional View. *Small GTPases* 5, e973757.

Cadwell, R. C. and Joyce, G. F. (1992). Randomization of Genes by PCR Mutagenesis. *PCR Methods and Applications* 2, 28–33.

Caliezi, C., Wuillemin, W. A., Zeerleder, S., Redondo, M., Eisele, B. and Hack, C. E. (2000). C1-Esterase Inhibitor: An Anti-Inflammatory Agent and Its Potential Use in the Treatment of Diseases Other than Hereditary Angioedema. *Pharmacoligical Reviews* 52, 91–112.

Campellone, K. G. and Leong, J. M. (2005). Nck-Independent Actin Assembly is Mediated by Two Phosphorylated Tyrosines within Enteropathogenic *Escherichia coli* Tir. *Molecular Microbiology* 56, 416–432.

Campellone, K. G., Robbins, D. and Leong, J. M. (2004). $EspF_U$ is a Translocated EHEC Effector that Interacts with Tir and N-WASP and Promotes Nck-Independent Actin Assembly. *Developmental Cell* 7, 217–228.

Cantrell, D. (2015). Signaling in Lymphocyte Activation. *Cold Spring Harbour Perspectives in Biology* 7, a018788.

Cao, C., Leng, Y., Huang, W., Liu, X. and Kufe, D. (2003). Glutathione Peroxidase 1 is Regulated by the c-Abl and Arg Tyrosine Kinases. *The Journal of Biological Chemistry* 278, 39609–39614.

Cao, Y., Janssen, E. M., Duncan, A. W., Altman, A., Billadeau, D. D. and Abraham, R. T. (2002). Pleiotroptic Defects in TCR Signaling in a Vav-1-Null Jurkat T-Cell Line. *The European Molecular Biology Organization Journal* 21, 4809–4819.

Carnoy, C., Mullet, C., Müller-Alouf, H., Leteurtre, E. and Simonet, M. (2000). Superantigen YPMa Exacerbates the Virulence of *Yersinia pseudotuberculosis* in Mice. *Infection and Immunity* 68, 2553–2559.

Casella, J. F., Flanagan, M. D. and Lin, S. (1981). Cytochalasin D Inhibits Actin Polymerization and Induces Depolymerization of Actin Filaments Formed During Platelet Shape Change. *Nature* 293, 302–305.

Cassady-Cain, R. L., Blackburn, E. A., Alsarraf, H., Dedic, E., Bease, A. G., Böttcher, B., Jørgensen, R., Wear, M. and Stevens, M. P. (2016). Biophysical Characterization and Activity of Lymphostatin, a Multifunctional Virulence Factor of Attaching & Effacing *Escherichia coli*. *The Journal of Biological Chemistry* 291, 5803–5816.

Cassady-Cain, R. L., Blackburn, E. A., Bell, C. R., Elshina, E., Hope, J. C. and Stevens, M. P. (2017). Inhibition of Antigen-Specific and Nonspecific Stimulation of Bovine T and B Cells by Lymphostatin from Attaching and Effacing *Escherichia coli*. *Infection and Immunity* 85, e00845-16.

Cassady-Cain, R. L., Hope, J. C. and Stevens, M. P. (2018). Direct Manipulation of T Lymphocytes by Proteins of Gastrointestinal Bacterial Pathogens. *Infection and Immunity* 86, e00683-17.

Castagna, M., Takai, Y., Kaibuchi, K., Sano, K., Kikkawa, U. and Nishizuka, Y. (1982). Direct Activation of Calcium-Activated, Phospholipid-Dependent Protein Kinase by Tumor-Promoting Phorbol Esters. *The Journal of Biological Chemistry* 257, 7847–7851.

Catherman, A. D., Skinner, O. S. and Kelleher, N. L. (2014). Top Down Proteomics: Facts and Perspectives. *Biochemical and Biophysical Research Communications* 445, 683–693.

Cech, P. and Lehrer, R. I. (1984). Phagolysosomal pH of Human Neutrophils. *Blood* 63, 88–95.

Celli, J., Olivier, M. and Finlay, B. B. (2001). Enteropathogenic *Escherichia coli* Mediates Antiphagocytosis through the Inhibition of PI 3-Kinase-Dependent Pathways. *The European Molecular Biology Organization Journal* 20, 1245–1258.

Cell Signaling Technology®. (2014). T Cell Receptor Signaling Interactive Pathway. URL: https://www.cellsignal.com/contents/science-cst-pathways-immunology-and-inflammation/t-cell-receptor-signaling-interactive-pathway/pathways-tcell. Accessed: 14/08/2019.

Cen, L., Hsieh, F., Lin, H., Chen, S., Qualman, S. J. and Lin, J. (2007). PDK-1/AKT Pathway as a Novel Therapeutic Target in Rhabdomyosarcoma Cells Using OSU-03012 Compound. *British Journal of Cancer* 97, 785–791.

Cepeda-Molero, M., Berger, C. N., Walsham, A. D. S., Ellis, S. J., Wemyss-Holden, S., Schüller, S., Frankel, G. and Fernández, L. Á. (2017). Attaching and Effacing (A/E) Lesion Formation by Enteropathogenic *E. coli* on Human Intestinal Mucosa is Dependent on Non-LEE Effectors. *Public Library of Science Pathogens* 13, e1006706.

Chan, A. C., Dalton, M., Johnson, R., Kong, G. H., Wang, T., Thoma, R. and Kurosaki, T. (1995). Activation of ZAP-70 Kinase Activity by Phosphorylation of Tyrosine 493 is Required for Lymphocyte Antigen Receptor Function. *The European Molecular Biology Organization Journal* 14, 2499–2508.

Chan, C. C., Dostie, J., Diem, M. D., Feng, W., Mann, M., Rappsilber, J. and Dreyfuss, G. (2004). eIF4A3 is a Novel Component of the Exon Junction Complex. *RNA* 10, 200–209.

Chandrasekaran, R. and Lacy, D. B. (2017). The Role of Toxins in *Clostridium difficile* Infection. *Federation of European Microbiological Societies Microbiology Reviews* 41, 723–750.

Chang, C., Curtis, J. D., Maggi Jr, L. B., Faubert, B., Villarino, A. V., O'Sullivan, D., Huang, S. C., van der Windt, G. J. W., Blagih, J., Qiu, J., Weber, J. D., Pearce, E. J., Jones, R. G. and Pearce, E. L. (2013). Posttranscriptional Control of T Cell Effector Function by Aerobic Glycolysis. *Cell* 153, 1239–1251.

Charpentier, X. and Oswald, E. (2004). Identification of the Secretion and Translocation Domain of the Enteropathogenic and Enterohemorrhagic *Escherichia coli* Effector Cif, Using TEM-1 β-Lactamase as a New Fluorescence-Based Reporter. *Journal of Bacteriology* 186, 5486–5495.

Chatila, T., Silverman, L., Miller, R. and Geha, R. (1989). Mechanisms of T Cell Activation by the Calcium Ionophore Ionomycin. *The Journal of Immunology* 143, 1283–1289.

Chaudhuri, R. R., Morgan, E., Peters, S. E., Pleasance, S. J., Hudson, D. L., Davies, H. M., Wang, J., van Diemen, P. M., Buckley, A. M., Bowen, A. J., Pullinger, G. D., Turner, D. J., Langridge, G. C., Turner, A. K., Parkhill, J., Charles, I. G., Maskell, D. J. and Stevens, M. P. (2013). Comprehensive Assignment of Roles for *Salmonella* Typhimurium Genes in Intestinal Colonization of Food-Producing Animals. *Public Library of Science Genetics* 9, e1003456.

Chen, S., Wang, H., Gu, H., Sun, C., Li, S., Feng, H. and Wang, J. (2016). Identification of an Essential Region for Translocation of *Clostridium difficile* Toxin B. *Toxins (Basel)* 8, 241.

Chen, Y., Chou, K., Fuchs, E., Havran, W. L. and Boismenu, R. (2002a). Protection of the Intestinal Mucosa by Intraepithelial γδ T Cells. *Proceedings of the National Academy of Sciences of the United States of America* 99, 14338–14343.

Chen, Z., Ahonen, M., Hämäläinen, H., Bergelson, J. M., Kähäri, V. and Lahesmaa, R. (2002b). High-Efficiency Gene Transfer to Primary T lymphocytes by Recombinant Adenovirus Vectors. *Journal of Immunological Methods* 260, 79–89.

Chevalier, C., Thiberge, J., Ferrero, R. L. and Labigne, A. (1999). Essential Role of *Helicobacter pylori* γ-Glutamyltranspeptidase for the Colonization of the Gastric Mucosa of Mice. *Molecular Microbiology* 31, 1359–1372.

Choi, Y., Kotzin, B., Herron, L., Callahan , J., Marrack, P. and Kappler, J. (1989). Interaction of *Staphylococcus aureus* Toxin 'Superantigens' with Human T Cells. *Proceedings of the National Academy of Sciences of the United States of America* 86, 8941–8945.

Chumbler, N. M., Farrow, M. A., Lapierre, L. A., Franklin, J. L., Haslam, D. B., Goldenring, J. R. and Lacy, D. B. (2012). *Clostridium difficile* Toxin B Causes Epithelial Cell Necrosis through an Autoprocessing-Independent Mechanism. *Public Library of Science Pathogens* 8, e1003072.

Chumbler, N. M., Rutherford, S. A., Zhang, Z., Farrow, M. A., Lisher, J. P., Farquhar, E., Giedroc, D. P., Spiller, B. W., Melnyk, R. A. and Lacy, D. B. (2016). Crystal Structure of *Clostridium difficile* Toxin A. *Nature Microbiology* 1, 15002.

Cleary, J., Lai, L., Shaw, R. K., Straatman-Iwanoska, A., Donnenberg, M. S., Frankel, G. and Knutton, S. (2004). Enteropathogenic *Escherichia coli* (EPEC) Adhesion to Intestinal Epithelial Cells: Role of Bundle-Forming Pili (BFP), EspA Filaments and Intimin. *Microbiology* 150, 527–538.

Clements, A., Smollett, K., Lee, S. F., Hartland, E. L., Lowe, M. and Frankel, G. (2011). EspG of Enteropathogenic and Enterohemorrhagic *E. coli* Binds the Golgi Matrix Protein GM130 and Disrupts the Golgi Structure and Function. *Cellular Microbiology* 13, 1429–1439.

Clerc, F., Reiding, K. R., Jansen, B. C., Kammeijer, G. S. M., Bondt, A. and Wuhrer, M. (2016). Human Plasma Protein *N*-Glycosylation. *Glycoconjugate Journal* 33, 309–343.

Cochary, E. F., Bizzozero, O. A., Sapirstein, V. S., Nolan, C. E. and Fischer, I. (1990). Presence of the Plasma Membrane Proteolipid (Plasmolipin) in Myelin. *Journal of Neurochemistry* 55, 602–610.

Coombes, B. K., Coburn, B. A., Potter, A. A., Gomis, S., Mirakhur, K., Li, Y. and Finlay, B. B. (2005). Analysis of the Contribution of *Salmonella* Pathogenicity Islands 1 and 2 to Enteric Disease Progression Using a Novel Bovine Ileal Loop Model and a Murine Model of Infectious Enterocolitis. *Infection and Immunity* 73, 7161–7169.

Coquillard, C. Vilchez, V. Marti, F. and Gedaly, R. (2015). mTOR Signaling in Regulatory T Cell Differentiation and Expansion. *Symbiosis Open Access Journals Immunology* 3, 1–10.

Corbishley, A., Ahmad, N. I., Hughes, K., Hutchings, M. R., McAteer, S. P., Connelley, T. K., Brown, H., Gally, D. L. and McNeilly, T. N. (2014). Strain-Dependent Cellular Immune Responses in Cattle Following *Escherichia coli* O157:H7 Colonization. *Infection and Immunity* 82, 5117–5131.

Corbishley, A., Connelley, T. K., Wolfson, E. B., Ballingall, K., Beckett, A. E., Gally, D. L. and McNeilly, T. N. (2016). Identification of Epitopes Recognised by Mucosal $CD4^+$ T-Cell Populations from Cattle Experimentally Colonised with *Escherichia coli* O157:H7. *Veterinary Research* 47, 90.

Cornelis, G. R., Biot, T., de Rouvroit, C. L., Michiels, T., Mulder, B., Sluiters, C., Sory, M., Van Bouchaute, M. and Vanooteghem, J. (1989). The *Yersinia yop* Regulon. *Molecular Microbiology* 3, 1455–1459.

Cornelis, G. R., Boland, A., Boyd, A. P., Geuijen, C., Iriarte, M., Neyt, C., Sory, M. and Stainier, I. (1998). The Virulence Plasmid of *Yersinia*, an Antihost Genome. *Microbiology and Molecular Biology Reviews* 62, 1315–1352.

Cory, A. H., Owen, T. C., Barltrop, J. A. and Cory, J. G. (1991). Use of an Aqueous Soluble Tetrazolium/Formazan Assay for Cell Growth Assays in Culture. Cancer Communications 3, 207–212

Costa, T. R. D., Felisberto-Rodrigues, C., Meir, A., Prevost, M. S., Redzej, A., Trokter, M. and Waksman, G. (2015). Secretion Systems in Gram-Negative Bacteria: Structural and Mechanistic Insights. *Nature Reviews Microbiology* 13, 343–359.

Costello, P. S., Walters, A. E., Mee, P. J., Turner, M., Reynolds, L. F., Prisco, A., Sarner, N., Zamoyska, R. and Tybulewicz, V. L. J. (1999). The Rho-Family GTP Exchange Factor Vav is a Critical Transducer of T Cell Receptor Signals to the Calcium, ERK, and NF-κB Pathways. *Proceedings of the National Academy of Sciences of the United States of America* 96, 3035–3040.

Coudronniere, N., Villalba, M., Englund, N. and Altman, A. (2000). NF-κB Activation Induced by T Cell Receptor/CD28 Costimulation is Mediated by Protein Kinase C-θ. *Proceedings of the National Academy of Sciences of the United States of America* 97, 3394–3399.

Courtney, A. H., Lo, W. and Weiss, A. (2017). TCR Signaling: Mechanisms of Initiation and Propagation. *Trends in Biochemical Sciences* 43, 108–123.

Courtney, H. S., Hasty, D. L. and Dale, J. B. (2002). Molecular Mechanisms of Adhesion, Colonization, and Invasion of Group A Streptococci. *Annals of Medicine* 34, 77–87.

Craiu, A., Gaczynska, M., Akopian, T., Gramm, C. F., Fenteany, G., Goldberg, A. L. and Rock, K. L. (1997). Lactacystin and *Clasto*-Lactacystin β-Lactone Modify Multiple Proteasome β-Subunits and Inhibit Intracellular Protein Degradation and Major Histocompatability Complex Class I Antigen Presentation. *The Journal of Biological Chemistry* 272, 13437–13445.

Creasey, E. A., Delaha, R. M., Daniell, S. J and Frankel, G. (2003). Yeast Two-Hybrid System Survey of Interactions between LEE-Encoded Proteins of Enteropathogenic *Escherichia coli*. *Microbiology* 149, 2093–2106.

Crepin, F., Shaw, R., Abe, C. M., Knutton, S. and Frankel, G. (2005). Polarity of Enteropathogenic *Escherichia coli* EspA Filament Assembly and Protein Secretion. *Journal of Bacteriology* 187, 2881–2889.

Crespo, P., Bustelo, X. R., Aaronson, D. S., Coso, O. A., Lopez-Barahona, M., Barbacid, M. and Gutkind, J. S. (1996). Rac-1 Dependent Stimulation of the JNK/SAPK Signaling Pathway by Vav. *Oncogene* 13, 455–460.

Crespo, P., Schuebel, K. E., Ostrom, A. A., Gutkind, J. S. and Bustelo, X. R. (1997). Phosphotyrosine-Dependent Activation of Rac-1 GDP/GTP Exchange by the *vav* Proto-Oncogene Product. *Nature* 385, 169–172.

Creuzburg, K., Giogha, C., Lung, T. W. F., Scott, N. E., Mühlen, S., Hartland, E. L. and Pearson, J. S. (2017). The Type III Effector NleD from Enteropathogenic *Escherichia coli* Differentiates between Host Substrates p38 and JNK. *Infection and Immunity* 85, e00620-16.

Cross, D. A. E., Alessi, D. R., Cohen, P., Andjelković, M. and Hemmings, B. A. (1995). Inhibition of Glycogen Synthase Kinase-3 by Insulin Mediated by Protein Kinase B. *Nature* 378, 785–789.

Cui, W., Rohrs, H. W. and Gross, M. L. (2011). Top-Down Mass Spectrometry: Recent Developments, Applications and Perspectives. *Analyst* 136, 3854–3864.

Cunningham, B. C. and Wells, J. A. (1989). High-Resolution Epitope Mapping of hGH-Receptor Interactions by Alanine-Scanning Mutagenesis. *Science* 244, 1081–1085.

Cunnion, K. M., Hair, P. S., and Buescher, E. S. (2004). Cleavage of Complement C3b to iC3b on the Surface of *Staphyloccus aureus* is Mediated by Serum Complement Factor I. *Infection and Immunity* 72, 2858–2863.

Dai, W., Zeng, Y., Xie, Z. and Staehelin, C. (2008). Symbiosis-Promoting and Deleterious Effects of NopT, a Novel Type 3 effector of *Rhizobium* sp. Strain NGR234. *Journal of Bacteriology* 190, 5101–5110.

Dang, C. V., Barrett, J., Villa-Garcia, M., Resar, L. M. S., Kato, G. J. and Fearon, E. R. (1991). Intracellular Leucine Zipper Interactions Suggest c-Myc Hetero-Oligomerization. *Molecular and Cellular Biology* 11, 954–962.

Daniell, S. J., Koonis, E., Morris, E., Knutton, S., Booy, F. P. and Frankel, G. (2003). 3D Structure of EspA Filaments from Enteropathogenic *Escherichia coli*. *Molecular Microbiology* 49, 301–308.

Davis, W. C., Brown, W. C., Hamilton, M. J., Wyatt, C. R., Orden, J. A., Khalid, A. M. and Naessens, J. (1996). Analysis of Monoclonal Antibodies Specific for the γδ TcR. *Veterinary Immunology and Immunopathology* 52, 275–283.

Deacon, V., Dziva, F., van Diemen, P. M., Frankel, G. and Stevens, M. P. (2010). Efa-1/LifA Mediates Intestinal Colonization of Calves by Enterohaemorrhagic *Escherichia coli* O26:H- in a Manner Independent of Glycosyltransferase and Cysteine Protease Motifs or Effects on Type III Secretion. *Microbiology* 156, 2527–2536.

Dean, P., Maresca, M., Schüller, S., Phillips, A. D. and Kenny, B. (2006). Potent Diarrheagenic Mechanism Mediated by the Cooperative Action of Three Enteropathogenic *Escherichia coli*-Injected Effector Proteins. *Proceedings of the National Academy of Sciences of the United States of America* 103, 1876–1881.

Dean, P. and Kenny, B. (2004). Intestinal Barrier Dysfunction by Enteropathogenic *Escherichia coli* is Mediated by Two Effector Molecules and a Bacterial Surface Protein. *Molecular Microbiology* 54, 665 675.

Deane, C. M., Salwiński, Ł., Xenarios, I. and Eisenberg, D. (2002). Protein Interactions: Two Methods for the Assessment of the Reliability of High Throughput Observations. *Molecular and Cellular Proteomics* 1, 349–356.

Deibel, C., Dersch, P. and Ebel, F. (2001). Intimin from Shiga Toxin-Producing *Escherichia coli* and its Isolated C-Terminal Domain Exhibit Different Binding Properties for Tir and a Eukaryotic Surface Receptor. *International Journal of Medical Microbiology* 290, 683–691.

Deibel, C., Krämer, S., Chakraborty, T. and Ebel, F. (1998). EspE, a Novel Secreted Protein of Attaching and Effacing Bacteria, is Directly Translocated into Infected Host Cells, Where it Appears as a Tyrosine-Phosphorylated 90 kDa Protein. *Molecular Microbiology* 28, 463–474.

de la Puerta, M. L., Trinidad, A. G., Rodríguez, M. d. C., Bogetz, J., Crespo, M. S., Mustelin, T., Alonso, A. and Bayón, Y. (2009). Characterization of New Substrates Targeted by *Yersinia* Tyrosine Phosphatase YopH. *Public Library of Science ONE* 4, e4431.

Deng, W., Marshall, N. C., Rowland, J. L., McCoy, J. M., Worrall, L. J., Santos, A. S., Strynadka, N. C. J. and Finlay, B. B. (2017). Assembly, Structure, Function and Regulation of Type III Secretion Systems. *Nature Reviews Microbiology* 15, 323–337.

Deng, W., Li, Y., Vallance, B. A. and Finlay, B. B. (2001). Locus of Enterocyte Effacement from *Citrobacter rodentium*: Sequence Analysis and Evidence for Horizontal Transfer Among Attaching and Effacing Pathogens. *Infection and Immunity* 69, 6323–6335.

Deng, W., Puente, J. L., Gruenheid, S., Li, Y., Vallance, B. A., Vázquez, A., Barba, J., Ibarra, J. A., O'Donnell, P., Metalnikov, P., Ashman, K., Lee, S., Goode, D., Pawson, T. and Finlay, B. B. (2004). Dissecting Virulence: Systematic and Functional Analyses of a Pathogenicity Island. *Proceedings of the National Academy of Sciences of the United States of America* 101, 3597–3602.

Deng, W., Yu, H. B., de Hoog, C. L., Stoynov, N., Li, Y., Foster, L. J. and Finlay, B. B. (2012). Quantitative Proteomic Analysis of Type III Secretome of Enteropathogenic *Escherichia coli* Reveals an Expanded Effector Repertoire for Attaching/Effacing Bacterial Pathogens. *Molecular & Cellular Proteomics* 11, 692–709.

Denny, M. F., Patai, B. and Straus, D. B. (2000). Differential T-Cell Antigen Receptor Signaling Mediated by the Src Family Kinases Lck and Fyn. *Molecular and Cellular Biology* 20, 1426–1435.

Dettmar, A. K., Binder, E., Greiner, F. R., Liebau, M. C., Kurschat, C. E., Jungraithmayr, T. C., Saleem, M. A., Scmitt, C., Feifel, E., Orth-Höller, D., Kemper, M. J., Pepys, M., Würzner, R. and Oh, J. (2014). Protection of Human Podocytes from Shiga Toxin 2-Induced Phosphorylation of Mitogen-Activated Protein Kinases and Apoptosis by Human Serum Amyloid P Component. *Infection and Immunity* 82, 1872–1879.

DeVinney, R., Puente, J. L., Gauther, A., Gossney, D. and Finlay, B. B. (2001). Enterohaemorrhagic and Enteropathogenic *Escherichia coli* Use a Different Tir-Based Mechanism for Pedestal Formation. *Molecular Microbiology* 41, 1445–1458.

DeVinney, R., Stein, M., Reinscheid, D., Abe, A., Ruschowski, S. and Finlay, B. B. (1999). Enterohemorrhagic *Escherichia coli* O157:H7 Produces Tir, which is Translocated to the Host Cell Membrane but is not Tyrosine Phosphorylated. *Infection and Immunity* 67, 2389–2398.

Dignass, A., Lynch-Devaney, K., Kindon, H., Thim, L. and Podolsky, D. K. (1994). Trefoil Peptides Promote Epithelial Migration through a Transforming Growth Factor β-Independent Pathway. *The Journal of Clinical Investigation* 94, 376–383.

DiScipio, R. G. (1982). The Activation of the Alternative Pathway C3 Convertase by Human Plasma Kallikrein. *Immunology* 45, 587–595.

Donald, R. G. K., Flint, M., Kalyan, N., Johnson, E., Witko, S. E., Kotash, C., Zhao, P., Megati, S., Yurgelonis, I., Lee, P. K., Matsuka, Y. V., Severina, E., Deatly, A., Sidhu, M., Jansen, K. U., Minton, N. P. and Anderson, A. S. (2013). A Novel Approach to Generate a Recombinant Toxoid Vaccine Against *Clostridium difficile*. *Microbiology* 159, 1254–1266.

Dong, N., Liu, L. and Shao, F. (2010). A Bacterial Effector Targets Host DH-PH Domain Rho GEFs and Antagonizes Macrophage Phagocytosis. *The European Molecular Biology Organization Journal* 29, 1363–1376.

Dong, N., Zhu, Y., Lu, Q., Hu, L., Zheng, Y. and Shao, F. (2012). Structurally Distinct Bacterial TBC-like GAPs Link Arf GTPase to Rab1 Inactivation to Counteract Host Defenses. *Cell* 150, 1029–1041.

Donnenberg, M. S., Donohue-Rolfe, A. and Keusch, G. T. (1989). Epithelial Cell Invasion: An Overlooked Property of Enteropathogenic *Escherichia coli* (EPEC) Associated with the EPEC Adherence Factor. *The Journal of Infectious Diseases* 160, 452–459.

Donnenberg, M. S., Girón, J. A., Nataro, J. P. and Kaper, J. B. (1992). A Plasmid-Encoded Type IV Fimbrial Gene of Enteropathogenic *Escherichia coli* Associated with Localized Adherence. *Molecular Microbiology* 6, 3427–3437.

Donnenberg, M. S., Lai, L. and Taylor, K. A. (1997). The Locus of Enterocyte Effacement Pathogenicity Island of Enteropathogenic *Escherichia coli* Encodes Secretion Functions and Remnants of Transposons at its Extreme Right End. *Gene* 184, 107–114.

Douce, G., Giannelli, V., Pizza, M., Lewis, D., Everest, P., Rappuoli, R. and Dougan, G. (1999). Genetically Detoxified Mutants of Heat-Labile Toxin from *Escherichia coli* are Able to Act as Oral Adjuvants. *Infection and Immunity* 67, 4400–4406.

Du Clos, T. W. (2013). Pentraxins: Structure, Function, and Role in Inflammation. *International Scholarly Research Notices Inflammation* 2013, 379040.

Dziva, F., van Diemen P. M., Stevens, M. P., Smith, A. J. and Wallis T. S. (2004). Identification of *Escherichia coli* O157:H7 Genes Influencing Colonization of the Bovine Gastrointestinal Tract Using Signature-Tagged Mutagenesis. *Microbiology* 150, 3631–3645.

Eaton, K. A., Fontaine, C., Friedman, D. I., Conti, N. and Alteri, C. J. (2017). Pathogenesis of Colitis in Germ-Free Mice Infected With EHEC O157:H7. *Veterinary Pathology* 54, 710–719.

Ebel, F., Podzadel, T., Rohde, M., Kresse, A. U., Krämer, S., Deibel, C., Guzmán, C. A. and Chakraborty, T. (1998). Initial Binding of Shiga Toxin-Producing *Escherichia coli* to Host Cells and Subsequent Induction of Actin Rearrangements Depend on Filamentous EspA-Containing Surface Appendages. *Molecular Microbiology* 30, 147–161.

Eckburg, P. B., Bik, E. M., Bernstein, C. N., Purdom, E., Dethlefsen, L., Sargent, M., Gill, S. R., Nelson, K. E. and Relman, D. A. (2005). Diversity of the Human Intestinal Microbial Flora. *Science* 308, 1635–1638.

Eckert, S. E., Dziva, F., Chaudhuri, R. R., Langridge, G. C., Turner, D. J., Pickard, D. J., Maskell, D. J., Thomson, N. R. and Stevens, M. P. (2011). Retrospective Application of Transposon-Directed Insertion Site Sequencing to a Library of Signature-Tagged Mini-Tn*5*Km2 Mutants of *Escherichia coli* O157:H7 Screened in Cattle. *Journal of Bacteriology* 193, 1771–1776.

Eftink, M. R. and Ghiron, C. A. (1976). Exposure of Tryptophanyl Residues in Proteins. Quantitative Determination by Fluorescence Quenching Studies. *Biochemisty* 15, 672–680.

Egerer, M., Giesemann, T., Jank, T., Satchell, K. J. F. and Aktories, K. (2007). Auto-Catalytic Cleavage of *Clostridium difficile* Toxins A and B Depends on Cysteine Protease Activity. *The Journal of Biological Chemisrty* 282, 25341–25321.

Eisen, S. A., Wedner, H. J. and Parker, C. W. (1972). Isolation of Pure Human Peripheral Blood T-Lymphocytes Using Nylon Wool Columns. *Immunological Communications* 1, 571–577.

Elango, N., Elango, S., Shivshankar, P. and Katz, M. S. (2005). Optimized Transfection of mRNA Transcribed from a $d(A/T)_{100}$ Tail-Containing Vector. *Biochemical and Biophysical Research Communications* 330, 958–966.

Elling, U. and Penninger, J. M. (2014). Genome Wide Functional Genetics in Haploid Cells. *Federation of European Biochemical Societies Letters* 588, 2415–2421.

Elliott, S. J., Wainwright, L. A., McDaniel, T. K., Jarvis, K. G., Deng, Y., Lai, L., McNamara, B. P., Donnenberg, M. S. and Kaper, J. B. (1998). The Complete Sequence of the Locus of Enterocyte Effacement (LEE) from Enteropathogenic *Escherichia coli* E2348/69. *Molecular Microbiology* 28, 1–4.

El Qaidi, S., Chen, K., Halim, A., Siukstaite, L., Rueter, C., Hurtado-Guerrero, R., Clausen, H. and Hardwidge, P. R. (2017). NleB/SseK Effectors from *Citrobacter rodentium*, *Escherichia coli*, and *Salmonella enterica* Display Distinct Differences in Host Substrate Specificity. *The Journal of Biological Chemistry* 292, 11423–11430.

Elwell, C., Mirrashidi, K. and Engel, J. (2016). *Chlamydia* Cell Biology and Pathogenesis. *Nature Reviews Microbiology* 14, 385–400.

Endo, Y., Tsurugi, K., Yutsudo, T., Takeda, Y., Ogasawara, T. and Igarashi, K. (1988). Site of Action of a Vero Toxin (VT2) from *Escherichia coli* O157:H7 and of Shiga Toxin on Eukaryotic Ribosomes. *European Journal of Biochemistry* 50, 45–50.

Eramo, M. J. and Mitchell, C. A. (2016). Regulation of PtdIns(3,4,5)P_3/Akt Signalling by Inositol Polyphosphate 5-Phosphatases. *Biochemical Society Transactions* 44, 240–252.

Eschenfeldt, W. H., Maltseva, N., Stols, L., Donnelly, M. I., Gu, M., Nocek, B., Tan, K., Kim, Y. and Joachimiak, A. (2010). Cleavable C-Terminal His-Tag Vectors for Structure Determination. *Journal of Structural and Functional Genomics* 11, 31–39.

Esensten, J. H., Helou, Y. A., Chopra, G., Weiss, A. and Bluestone, J. A. (2016). CD28 Costimulation: From Mechanism to Therapy. *Immunity* 44, 973–988.

Esko, J. D., Bertozzi, C. and Schnaar, R. L. (2017). Chemical Tools for Inhibiting Glycosylation. *Essentials of Glycobiology [Internet] Third Edition*. Cold Spring Harbour Laboratory Press. URL: https://www.ncbi.nlm.nih.gov/books/NBK310274/

Fehniger, T. A., Cooper, M. A., Nuovo, G. J., Cella, M., Facchetti, F., Colonna, M. and Caligiuri, M. A. (2003). $CD56^{bright}$ Natural Killer Cells are Present in Human Lymph Nodes and are Activated by T Cell-Derived IL-2: A Potential New Link between Adaptive and Innate Immunity. *Blood* 101, 3052–3057.

Ferens, W. A. and Hovde, C. J. (2000). Antiviral Activity of Shiga Toxin 1: Suppression of Bovine Leukemia Virus-Related Spontaneous Lymphocyte Proliferation. *Infection and Immunity* 68, 4462–4469.

Fields, S. and Song, O. (1989). A Novel Genetic System to Detect Protein-Protein Interactions. *Nature* 340, 245–246.

Finlay, B. B., Rosenshine, I., Donnenberg, M. S. and Kaper J. B. (1992). Cytoskeletal Composition of Attaching and Effacing Lesions Associated with Enteropathogenic *Escherichia coli* Adherence to HeLa Cells. *Infection and Immunity* 60, 2541–2543.

Fisher, M. L., Castillo, C. and Mecsas, J. (2007). Intranasal Inoculation of Mice with *Yersinia pseudotuberculosis* Causes a Lethal Lung Infection that is Dependent on *Yersinia* Outer Proteins and PhoP. *Infection and Immunity* 75, 429–442.

Flo, T. H., Smith, K. D., Sato, S., Rodriguez, D. J., Holmes, M. A., Strong, R. K., Akira, S. and Aderem, A. (2004). Lipocalin 2 Mediates an Innate Immune Response to Bacterial Infection by Sequestrating Iron. *Nature* 432, 917–921.

Floch, P., Pey, V., Castroviejo, M., Dupuy, J. W., Bonneu, M., de la Guardia, A. H., Pitard, V., Mégraud, F. and Lehours, P. (2014). Role of *Campylobacter jejuni* Gamma-Glutamyl Transpeptidase on Epithelial Cell Apoptosis and Lymphocyte Proliferation. *Gut Pathogens* 6.

Foegeding, N. J., Caston, R. R., McClain, M. S., Ohi, M. D. and Cover, T. L. (2016). An Overview of *Helicobacter pylori* VacA Toxin Biology. *Toxins (Basel)* 8, 173.

Follis, K. E., York, J. and Nunber, J. H. (2005). Serine-Scanning Mutagenesis Studies of the C-Terminal Heptad Repeats in the SARS Coronavirus S Glycoprotein Highlight the Important Role of the Short Helical Region. *Virology* 341, 122–129.

Folta-Stogniew, E. and Williams, K. R. (1999). Determination of Molecular Masses of Proteins in Solution: Implementation of an HPLC Size Exclusion Chromatography and Laser Light Scattering Service in a Core Laboratory. *Journal of Biomolecular Techniques* 10, 51–63.

Foubister, V., Rosenshine, I., Donnenberg, M. S. and Finlay, B. B. (1994). The *eaeB* Gene of Enteropathogenic *Escherichia coli* is Necessary for Signal Transduction in Epithelial Cells. *Infection and Immunity* 62, 3038–3040.

Frank, C., Werber, D., Cramer, J. P., Askar, M., Faber, M., an der Heiden, M., Bernard, H., Fruth, A., Prager, R., Spode, A., Wadl, M., Zoufaly, A., Jordan, S., Kemper, M. J., Follin, P., Müller, L., King, L. A., Rosner, B., Buchholdz, U., Stark, K. and Krause, G. (2011). Epidemic Profile of Shiga-Toxin-Producing *Escherichia coli* O104:H4 Outbreak in Germany. *The New England Journal of Medicine* 365, 1771–1780.

Frankel, G., Candy, D. C. A., Everest, P. and Dougan, G. (1994). Characterization of the C-Terminal Domains of Intimin-Like Proteins of Enteropathogenic and Enterohemorrhagic *Escherichia coli*, *Citrobacter freundii*, and *Hafnia alvei*. *Infection and Immunity* 62, 1835–1842.

Frankel, G., Lider, O., Hershkoviz, R., Mould, A. P., Kachalsky, S. G., Candy, D. C. A., Cahalon, L., Humphries, M. J. and Dougan, G. (1996). The Cell-Binding Domain of Intimin from Enteropathogenic *Escherichia coli* Binds to β_1-Integrins. *The Journal of Biological Chemistry* 271, 20359–20364.

Fraser, M. E., Chernaia M. M., Kozlov, Y. V. and James, M. N. G. (1994). Crystal Structure of the Holotoxin from *Shigella dysenteriae* at 2.5 Å Resolution. *Nature Structural Biology* 1, 59–64.

Fratamico, P. M., DebRoy, C., Lui, Y., Needleman, D. S., Baranzoni, G. M. and Feng, P. (2016). Advances in Molecular Serotyping and Subtyping of *Escherichia coli*. *Frontiers in Microbiology* 7, 644.

Frick, I., Åkesson, P., Herwald, H., Mörgelin, M., Malmsten, M., Nägler, D. K. and Björck, L. (2006). The Contact System – A Novel Branch of Innate Immunity Generating Antimicrobial Peptides. *The European Molecular Biology Organization Journal* 25, 5569–5578.

Friedman, R. D. (1982). Comparison of Four Different Silver-Staining Techniques for Salivary Protein Detection in Alkaline Polyacrylamide Gels. *Analytical Biochemistry* 126, 346–349.

Frischauf, A. M., Garoff, H. and Lehrach, H. (1980). A Subcloning Strategy for DNA Sequence Analysis. *Nucleic Acids Research* 8, 5541–5549.

Fujiki, R., Hashiba, W., Sekine, H., Yokoyama, A., Chikanishi, T., Ito, S., Imai, Y., Kim, J., He, H. H., Igarashi, K., Kanno, J., Ohtake, F., Kitagawa, H., Roeder, R. G., Brown, M. and Kato, S. (2011). GlcNAcylation of Histone H2B Facilitates its Monoubiquitination. *Nature* 480, 557–560.

Fukuda, M. and Carlsson, S. R. (1986). Leukosialin, a Major Sialoglycoprotein on Human Leukocytes as Differentiation Antigens. *Medical Biology* 64, 335–343.

Fukushima, H., Matsuda, Y., Seki, R., Tsubokura, M., Takeda, N., Shubin, F. N., Paik, I. K. and Zheng, X. B. (2001). Geographical Heterogeneity between Far Eastern and Western Countries in Prevalence of the Virulence Plasmid, the Superantigen *Yersinia pseudotuberculosis*-Derived Mitogen, and the High-Pathogenicity Island among *Yersinia pseudotuberculosis* Strains. *Journal of Clinical Microbiology* 39, 3541–3547.

Furniss, R. C. D., Low, W. W., Mavridou, D. A. I., Dagley, L. F., Webb, A. I., Tate, E. W. and Clements, A. (2018). Plasma Membrane Profiling During Enterohemorrhagic *E. coli* Infection Reveals that the Metalloprotease StcE Cleaves CD55 from Host Epithelial Surfaces. *Journal of Biological Chemistry* 293, 17188–17199.

Gabig, T. G., Kipnes, R. S. and Babior, B. M. (1978). Solubilization of the O_2^--Forming Activity Responsible for the Respiratory Burst in Human Neutrophils. *The Journal of Biological Chemistry* 253, 6663–6665.

Galinski, M. R., Medina, C. C., Ingravallo, P. and Barnwell J. W. (1992). A Reticulocyte-Binding Complex of *Plasmodium vivax* Merozoites. *Cell* 69, 1213–1226.

Gallo, R. L. and Hooper, L. V. (2012). Epithelial Antimicrobial Defence of the Skin and Intestine. *Nature Reviews Immunology* 12, 503–516.

Gan, X., Wang, J., Su, B. and Wu, D. (2011). Evidence for Direct Activation of mTORC2 Kinase Activity by Phosphatidylinositol 3,4,5-Trisphosphate. *The Journal of Biological Chemistry* 286, 10998–11002.

Gandy, J. C., Rountree, A. E. and Bijur, G. N. (2006). Akt1 is Dynamically Modified with O-GlcNAc Following Treatments with PUGNAc and Insulin-Like Growth Factor-1. *Federation of European Biochemical Societies Letters* 580, 3051–3058.

Gao, X., Wan, F., Mateo, K., Callegari, E., Wang, D., Deng, W., Puente, J., Li, F., Chaussee, M. S., Finlay, B. B., Lenardo, M. J. and Hardwidge, P. R. (2009). Bacterial Effector Binding to Ribosomal Protein S3 Subverts NF-κB Function. *Public Library of Science Pathogens* 5, e1000708.

Gao, X., Wang, X., Pham, T. H., Feuerbacher, L. A., Lubos, M., Huang, M., Olsen, R., Musheglan, A., Slawson, C. and Hardwidge, P. R. (2013). NleB, a Bacterial Effector with Glycosyltransferase Activity Targets GAPDH Function to Inhibit NF-κB Activation. *Cell Host & Microbe* 13, 87–99.

García-Angulo, V. A., Kalita, A., Kalita, M., Lozano, L. and Torres, A. G. (2014). Comparative Genomics and Immunoinformatics Approach for the Identification of Vaccine Candidates for Enterohemorrhagic *Escherichia coli* O157:H7. *Infection and Immunity* 82, 2016–2026.

García-Angulo, V. A., Kalita, A. and Torres, A. G. (2013). Advances in the Development of Enterohemorrhagic *Escherichia coli* Vaccines Using Murine Models of Infection. *Vaccine* 31, 3229–3235.

Garmendia, J., Phillips, A. D., Carlier, M., Chong, Y., Schüller, S., Marchès, O., Dahan, S., Oswald, E., Shaw, R. K., Knutton, S. and Frankel, G. (2004). TccP is an Enterohaemorrhagic *Escherichia coli* O157:H7 Type III Effector Protein that Couples Tir to the Actin-Cytoskeleton. *Cellular Microbiology* 6, 1167–1183.

Garred, Ø., van Deurs, B. and Sandvig, K. (1995). Furin-Induced Cleavage and Activation of Shiga Toxin. *The Journal of Biological Chemistry* 270, 10817–10821.

Gauci, V. J., Wright, E. P. and Coorssen, J. R. (2011). Quantitative Proteomics: Assessing the Spectrum of In-Gel Protein Detection Methods. *Journal of Chemical Biology* 4, 3–29.

Gauthier, A., Robertson, M. L., Lowden, M., Ibarra, J. A., Puente, J. L. and Finlay, B. B. (2005). Transcriptional Inhibitor of Virulence Factors in Enteropathogenic *Escherichia coli*. *Antimicrobial Agents and Chemotherapy* 49, 4101–4109.

Gaytán, M. O., Martínez-Santos, V. I., Soto, E. and González-Pedrajo, B. (2016). The Type III Secretion System in Attaching and Effacing Pathogens. *Frontiers in Cellular and Infection Microbiology* 6, 129.

Gebert, B., Fischer, W., Weiss, E., Hoffmann, R. and Haas, R. (2003). *Helicobacter pylori* Vacuolating Cytotoxin Inhibits T Lymphocyte Activation. *Science* 301, 1099–1102.

Geddes, K., Cruz III, F. and Heffron, F. (2007). Analysis of Cells Targeted by *Salmonella* Type III Secretion *In Vivo*. *Public Library of Science Pathogens* 3, 2017–2028.

Genisyuerek, S., Papatheodorou, P., Guttenberg, G., Schubert, R., Benz, R. and Aktories, K. (2011). Structural Determinants for Membrane Insertion, Pore Formation and Translocation of *Clostridium difficile* Toxin B. *Molecular Microbiology* 79, 1643–1654.

Genot, E. M., Arrieumerlou, C., Ku, G., Burgering, B. M. T., Weiss, A. and Kramer, I. M. (2000). The T-Cell Receptor Regulates Akt (Protein Kinase B) via a Pathway Involving Rac1 and Phosphatidylinositide 3-Kinase. *Molecular and Cellular Biology* 20, 5469–5478.

Gerlach, R. G., Jäckel, D., Geymeier, N. and Hensel, M. (2007). *Salmonella* Pathogenicity Island 4-Mediated Adhesion is Coregulated with Invasion Genes in *Salmonella enterica*. *Infection and Immunity* 75, 4697–4709.

Germane, K. L. and Spiller, B. W. (2011). Structural and Functional Studies Indicate that the EPEC Effector, EspG, Directly Binds p21 Activated Kinase. *Biochemistry* 50, 917–919.

Ghebrehiwet, B., Silverberg, M. and Kaplan, A. P. (1981). Activation of the Classical Pathway of Complement by Hageman Factor Fragment. *Journal of Experimental Medicine* 153, 665–676.

Giesemann, T., Jank, T., Gerhar, R., Maier, E., Just, I., Benz, R. and Aktories, K. (2006). Cholesterol-Dependent Pore Formation of *Clostridium difficile* Toxin A. *The Journal of Biological Chemistry* 281, 10808–10815.

Gill, D. M., Clements, J. D., Robertson, D. C. and Finkelstein, R. A. (1981). Subunit Number and Arrangement in *Escherichia coli* Heat-Labile Enterotoxin. *Infection and Immunity* 33, 677–682.

Girard, F., Frankel, G., Phillips, A. D., Colley, W., Weyer, U., Dugdale, A. H. A., Woodward, M. J. and La Ragione, R. M. (2008). Interaction of Enterohemorrhagic *Escherichia coli* O157:H7 with Mouse Intestinal Mucosa. *Federation of European Microbiological Societies Microbiology Letters* 283, 196–202.

Girón, J. A., Ho, A. S. Y. and Schoolnik, G. K. (1991). An Inducible Bundle-Forming Pilus of Enteropathogenic *Escherichia coli*. *Science* 254, 710–713.

Gloster, T. M. and Vocadlo, D. J. (2010). Mechanism, Structure, and Inhibition of *O*-GlcNAc Processing Enzymes. *Current Signal Transduciton Therapy* 5, 74–91.

Gobert, A. P., Vareille, M., Glasser, A., Hindré, T., de Sablet, T. and Martin, C. (2007). Shiga Toxin Produced by Enterohemorrhagic *Escherichia coli* Inhibits PI3K/NF-κB Signaling Pathway in Globotriaosylceramide-3-Negative Human Intestinal Epithelial Cells. *The Journal of Immunology* 178, 8168–8174.

Gomes, T. A. T., Elias, W. P., Scaletsky, I. C. A., Guth, B. E. C., Rodrigues, J. F., Piazza, R. M. F., Ferreira, L. C. S. and Martinez, M. B. (2016). Diarrheagenic *Escherichia coli*. *Brazalian Journal of Microbiology* 47, 3–30.

Gomes, T. A. T., Vieira, M. A. M., Wachsmuth, I. K., Blake, P. A. and Trabulsi, L. R. (1989). Serotype-Specific Prevalence of *Escherichia coli* Strains with EPEC Adherence Factor Genes in Infants with and without Diarrhea in São Paulo, Brazil. *The Journal of Infectious Diseases* 160, 131–135.

Gonçalves, N. S., Hale, C., Dougan, G., Frankel, G. and MacDonald, T. T. (2003). Binding of Intimin from Enteropathogenic *Escherichia coli* to Lymphocytes and its Functional Consequences. *Infection and Immunity* 71, 2960–2965.

Goosney, D. L., DeVinney, R. and Finlay, B. B. (2001). Recruitment of Cytoskeletal and Signaling Proteins to Enteropathogenic and Enterohemorrhagic *Escherichia coli* Pedestals. *Infection and Immunity* 69, 3315–3322.

Gorentla, B. K., Wan, C. and Zhong, X. (2011). Negative Regulation of mTOR Activation by Diacylglycerol Kinases. *Blood* 117, 4022–4031.

Goubard, A., Loïez, C., Abe, J., Fichel, C., Herwegh, S., Faveeuw, C., Porte, R., Cayet, D., Sebbane, F., Penet, S., Foligné, B., Desreumaux, P., Saito, H., Sirard, J., Simonet, M. and Carnoy, C. (2015). Superantigenic *Yersinia pseudotuberculosis* Induces the Expression of Granzymes and Perforin by $CD4^+$ T Cells. *Infection and Immunity* 83, 2053–2064.

Gregorich, Z. R. and Ge, Y. (2014). Top-Down Proteomics in Health and Disease: Challenges and Opportunities. *Proteomics* 14, 1195–1210.

Grewal, T., Wason, S. J., Enrich, C. and Rentero, C. (2016). Annexins – Insights from Knockout Mice. *Biological Chemistry* 397, 1031–1053.

Griffin, M. J. (1976). Synchronization of Some Human Cell Strains by Serum and Calcium Starvation. *In Vitro* 12, 393–398.

Grishaev, A., Wu, J., Trewhella, J. and Bax, A. (2005). Refinement of Multidomain Protein Structures by Combination of Solution Small-Angle X-Ray Scattering and NMR Data. *Journal of the American Chemical Society* 127, 16621–16628.

Grüber, A., Gunalan, K., Ramalingam, J. K., Manimekalai, M. S. S., Grüber, G. and Preiser, P. R. (2011). Structural Characterization of the Erythrocyte Binding Domain of the Reticulocyte Binding Protein Homologue Family of *Plasmodium yoelii*. *Infection and Immunity* 79, 2880–2888.

Gruenheid, S., DeVinney, R., Bladt, F., Goosney, D., Gelkop, S., Gish, G. D., Pawson, T. and Finlay, B. B. (2001). Enteropathogenic *E. coli* Tir Binds Nck to Initiate Actin Pedestal Formation in Host Cells. *Nature Cell Biology* 3, 856–859.

Grys, T. E., Siegel, M. B., Lathem, W. W. and Welch, R. A. (2005). The StcE Protease Contributes to Intimate Adherence of Enterohemorrhagic *Escherichia coli* O157:H7 to Host Cells. *Infection and Immunity* 73, 1295–1303.

Grys, T. E., Walters, L. L. and Welch, R. A. (2006). Characterization of the StcE Protease Activity of *Escherichia coli* O157:H7. *Journal of Bacteriology* 188, 4646–4653.

Guan, K. and Dixon, J. E. (1990). Protein Tyrosine Phosphatase Activity of an Essential Virulence Determinant in *Yersinia*. *Science* 249, 553–556.

Guttenberg, G., Hornei, S., Jank, T., Schwan, C., Lü, W., Einsle, O., Papatheodorou, P. and Aktories, K. (2012). Molecular Caracteristics of *Clostridium perfringens* TpeL Toxin and Consequences of Mono-*O*-GlcNAcylation of Ras in Living Cells. *The Journal of Biological Chemistry* 287, 24929–24940.

Guttenberg, G., Papatheodorou, P., Genisyuerek, S., Lü, W., Jank, T., Einsle, O. and Aktories, K. (2011). Inositol Hexakisphosphate-Dependent Processing of *Clostridium sordellii* Lethal Toxin and *Clostridium novyi* α-Toxin. *The Journal of Biological Chemistry* 286, 14779–14786.

Guzman, E., Hope, J., Taylor, G., Smith, A. L., Cubillos-Zapata, C. and Charleston, B. (2014). Bovine γδ T Cells are a Major Regulatory T Cell Subset. *The Journal of Immunology* 193, 208–222.

Hacker, J., Blum-Oehler, G., Mühldorfer, I. and Tschäpe, H. (1997). Pathogenicity Islands of Virulent Bacteria: Structure, Function and Impact on Microbial Evolution. *Molecular Microbiology* 23, 1089–1097.

Hall, L., Williams, K., Perry, A. C., Frayne, J. and Jury, J. A. (1998). The Majority of Human Glutathione Peroxidase Type 5 (GPX5) Transcripts are Incorrectly Spliced: Implications for the Role of GPX5 in the Male Reproductive Tract. *Biochemical Journal* 333, 5–9.

Hall, L. J., Murphy, C. T., Hurley, G., Quinlan, A., Shanahan, F., Nally, K. and Melgar, S. (2013). Natural Killer Cells Protect Against Mucosal and Systemic Infection with the Enteric Pathogen *Citrobacter rodentium*. *Infection and Immunity* 81, 460–469.

Hall, R. A. (2015). Studying Protein-Protein Interactions via Blot Overlay or Far Western Blot. *Methods in Molecular Biology vol. 261: Protein-Protein Interactions, Methods and Applications*, pp. 167–174. Humana Press, Totowa.

Handy, D. E., Lubos, E., Yang, Y., Galbraith, J. D., Kelly, N., Zhang, Y., Leopold, J. A. and Loscalzo, J. (2009). Glutathione Peroxidase-1 Regulates Mitochondrial Function to Modulate Redox-Dependent Cellular Responses. *The Journal of Biological Chemistry* 284, 11913–11921.

Hanford, C. L., Stang, C. T., Raivio, T. L. and Dennis, J. J. (2003). The Contribution of Small Cryptic Plasmids to the Antibiotic Resistance of Enteropathogenic *Escherichia coli* E2348/69. *Canadian Journal of Microbiology* 55, 1229–1239.

Harama, D., Koyama, K., Mikai, M., Shimokawa, M., Miyata, M., Nakamura, Y., Ohnuma, Y., Ogawa, H., Matsuoka, S., Paton, A. W., Paton, J. C., Kitamura, M. and Nakao, A. (2009). A Subcytotoxic Dose of Subtilase Cytotoxin Prevents Lipopolysaccharide-Induced Inflammatory Responses, Depending on its Capacity to Induce the Unfolded Protein Response. *The Journal of Immunology* 183, 1368–1374.

Haranaga, S., Yamaguchi, H., Friedman, H., Izumi, S. and Yamamoto, Y. (2001). *Chlamydia pneumoniae* Infects and Multiplies in Lymphocytes *In Vitro*. *Infection and Immunity* 69, 7753–7759.

Hart, J. R. and Vogt, P. K. (2011). Phosphorylation of AKT: A Mutational Analysis. *Oncotarget* 2, 467–476.

Hathcock, K. S. (2001). T Cell Enrichment by Nonadherence to Nylon. *Current Protocols in Immunology* 30, 3.2.1–3.2.4.

Hauf, N. and Chakraborty, T. (2003). Suppression of NF-κB Activation and Proinflammatory Cytokine Expression by Shiga Toxin-Producing *Escherichia coli*. *The Journal of Immunology* 170, 2074–2082.

Harvath, L., Balke, J. A., Christiansen, N. P., Russell, A. A. and Skubitz, K. M. (1991). Selected Antibodies to Leukocyte Common Antigen (CD45) Inhibit Human Neutrophil Chemotaxis. *The Journal of Immunology* 146, 949–957.

Hayashi, T., Makino, K., Ohnishi, M., Kurowaka, K., Ishii, K., Yokoyama, K., Han, C., Ohtsubo, E., Nakayama, K., Murata, T., Tanaka, M., Tobe, T., Iida, T., Takami, H., Honda, T., Sasakawa, C., Ogasawara, N., Yasunaga, T., Kuhara, S., Shiba, T., Hattori, M. and Shinagawa, H. (2001). Complete Genome Sequence of Enterohemorrhagic *Escherichia coli* O157:H7 and Genomic Comparison with a Laboratory Strain K-12. *DNA Research* 8, 11–22.

Hecht, G., Hodges, K., Gill, R. K., Kear, F., Tyagi, S., Malakooti, J., Ramaswamy, K. and Dudeja, P. K. (2004). Differential Regulation of Na^+/H^+ Exchange Isoform Activities by Enteropathogenic *E. coli* in Human Intestinal Epithelial Cells. *American Journal of Physiology – Gastrointestinal and Liver Physiology* 287, G370–G378.

Hemrajani, C., Berger, C. N., Robinson, K. S., Marchès, O., Mousnier, A. and Frankel, G. (2010). NleH Effectors Interact with Bax Inhibitor-1 to Block Apoptosis During Enteropathogenic *Escherichia coli* Infection. *Proceedings of the National Academy of Sciences of the United States of America* 107, 3129–3134.

Henikoff, S. (1990). Ordered Deletions for DNA Sequencing and *In Vitro* Mutagenesis by Polymerase Extension and Exonuclease III Gapping of Circular Templates. *Nucleic Acids Research* 18, 2961–2966.

Herrero-Sánchez, M. C., Rodríguez-Serrano, C., Almeida, J., San Segundo, L., Inogés, S., Santos-Briz, Á., García-Briñón, J., Corchete, L. A., San Miguel, J. F., del Cañizo, C. and Blanco, B. (2016). Targeting of PI3K/AKT/mTOR Pathway to Inhibit T Cell Activation and Prevent Graft-Versus-Host Disease Development. *Journal of Hematology & Oncology* 9, 113.

Herwald, H., Mörgelin, M., Olsén, A., Rhen, M., Dahlbäck, B., Müller-Esterl, W. and Björck, L. (1998). Activation of the Contact-Phase System on Bacterial Surfaces – A Clue to Serious Complications in Infectious Diseases. *Nature Medicine* 4, 298–302.

Herzik, M. A., Wu, M. and Lander, G. C. (2019). High-Resolution Structure Determination of Sub-100 kDa Complexes Using Conventional Cryo-EM. *Nature Communications* 10, 1032.

Hews, C. L., Tran, S., Wegmann, U., Brett, B., Walsham, A. D. S., Kavanaugh, D., Ward, N. J., Juge, N. and Schüller, S. (2017). The StcE Metalloprotease of Enterohaemorrhagic *Escherichia coli* Reduces the Inner Mucus Layer and Promotes Adherence to Human Colonic Epithelium *Ex Vivo. Cellular Microbiology 19, e12717.*

Higgins, L. M., Frankel, G., Connerton, I., Gonçalves, N. S., Dougan, G. and MacDonald, T. T. (1999a). Role of Bacterial Intimin in Colonic Hyperplasia and Inflammation. *Science* 285, 588–591.

Higgins, L. M., Frankel, G., Douce, G., Dougan, G. and MacDonald, T. T. (1999b). *Citrobacter rodentium* Infection in Mice Elicits a Mucosal Th1 Cytokine Response and Lesions Similar to those in Murine Inflammatory Bowel Disease. *Infection and Immunity* 67, 3031–3039.

Higuchi, R., Krummel, B. and Saiki, R. A. (1988). A General Method of *In Vitro* Preparation and Specific Mutagenesis of DNA Fragments: Study of Protein and DNA Interactions. *Nucleic Acids Research* 16, 7351–7367.

Hirayama, D., Iida, T. and Nakase, H. (2018). The Phagocytic Function of Macrophage-Enforcing Innate Immunity and Tissue Homeostasis. *International Journal of Molecular Sciences* 19, 92.

Ho, N. K., Henry, A. C., Johnson-Henry, K. and Sherman, P. M. (2013). Pathogenicity, Host Responses and Implications for Management of Enterohemorrhagic *Escherichia coli* O157:H7 Infection. *Canadian Journal of Gastroenterology* 27, 281–5.

Hoang, K. V., Borteh, H. M., Rajaram, M. V. S., Peine, K. G., Curry, H., Collier, M. A., Homsy, M. L., Bachelder, E. M., Gunn, J. S., Schlesinger, L. S. and Ainslie, K. M. (2014). Acetalated Dextran Encapsulated AR-12 as a Host-Directed Therapy to Control *Salmonella* Infection. *International Journal of Pharmaceutics* 477, 334–343.

Hoebeke, J., Van Nijen, G. and De Brabander, M. (1976). Interaction of Oncodazole (R 17934), a New Anti-Tumoral Drug, with Rat Brain Tubulin. *Biochemical and Biophysical Research Communications* 69, 319–324.

Hoey, D. E. E., Sharp, L., Currie, C., Lingwood, C. A., Gally, D. L. and Smith D. G. E. (2003). Verotoxin 1 Binding to Intestinal Crypt Epithelial Cells Results in Localization to Lysosomes and Abrogation of Toxicity. *Cellular Microbiology* 5, 85–97.

Hoffman, M. A., Menge, C., Casey, T. A., Laegreid, W., Bosworth, B. T. and Dean-Nystrom, E. A. (2006). Bovine Immune Response to Shiga-Toxigenic *Escherichia coli* O157:H7. *Clinical and Vaccine Immunology* 13, 1322–1327.

Hoffman, W., Lakkis, F. G. and Chalasani, G. (2016). B Cells, Antibodies, and More. *Clinical Journal of the American Society of Nephrology* 11, 137–154.

Hofmann, F., Busch, C., Prepins, U., Just, I. and Aktories, K. (1997). Localization of the Glucosyltransferase Activity of *Clostridium difficile* Toxin B to the N-terminal Part of the Holotoxin. *The Journal of Biological Chemistry* 272, 11074–11078.

Holmgren, J., Lycke, N. and Czerkinsky, C. (1993). Cholera Toxin and Cholera B Subunit as Oral-Mucosal Adjuvent and Antigen Vector Systems. *Vaccine* 11, 1179–1184.

Horsch, M., Hoesch, L., Vasella, A. and Rast, D. M. (1991). *N*-Acetylglucosaminono-1,5-Lactone Oxime and the Corresponding (Phenylcarbamoyl)oxime. Novel and Potent Inhibitors of *β-N*-Acetylglucosaminidase. *European Journal of Biochemistry* 197, 815–818.

Hu, C. A., Dougan, S. K., Winter, S. V., Paton, A. W., Paton, J. C. and Ploegh, H. L. (2009). Subtilase Cytotoxin Cleaves Newly Synthesized BiP and Blocks Antibody Secretion in B Lymphocytes. *Journal of Experimental Medicine* 206, 2429–2440.

Hua, Y., Ju, J., Wang, X., Zhang, B., Zhao, W., Zhang, Q., Feng, Y., Ma, W. and Wan, C. (2017). Screening for Host Proteins Interacting with *Escherichia coli* O157:H7 EspF Using Bimolecular Fluorescence Complementation. *Future Microbiology* 13, 37–58.

Huang, J., Dibble, C. C., Matsuzaki, M. and Manning, B. D. (2008). The TSC1-TSC2 Complex is Required for Proper Activation of mTOR Complex 2. *Molecular and Cellular Biology* 28, 4104–4115.

Huang, Z., Sutton, S. E., Wallenfang, A. J., Orchard, R. C., Wu, X., Feng, Y., Chai, J. and Alto, N. M. (2009). Structural Insights into Host GTPase Isoform Selection by a Family of Bacterial GEF Mimics. *Nature Structural & Molecular Biology* 16, 853–860.

Hudault, S., Guignot, J. and Servin, A. L. (2001). *Escherichia coli* Strains Colonising the Gastrointestinal Tract Protect Germfree Mice Against *Salmonella typhimurium* Infection. *Gut* 49, 47–55.

Huse, M. (2009). The T-Cell-Receptor Signaling Network. *Journal of Cell Science* 122, 1269–1273.

Huys, G., Cnockaert, M., Janda, J. M. and Swings, J. (2003). *Escherichia albertii* sp. nov., a Diarrhoeagenic Species Isolated from Stool Specimens of Bangladeshi Children. *International Journal of Systematic and Evolutionary Microbiology* 53, 807–810.

Hyland, R. M., Sun, J., Griener, T. P., Mulvey, G. L., Klassen, J. S., Donnenberg, M. S. and Armstrong, G. D. (2008). The Bundlin Pilin of Enteropathogenic *Escherichia coli* is an *N*-Acetyllactosamine-Specific Lectin. *Cellular Microbiology* 10, 177–187.

Iguchi, A., Thomson, N. R., Ogura, Y., Saunders, D., Ooka, T., Henderson, I. R., Harris, D., Asadulghani, M., Kurokawa, K., Dean, P., Kenny, B., Quail, M. A., Thurston, S., Dougan, G., Hayashi, T., Parkhill, J. and Frankel, G. (2009). Complete Genome Sequence and Comparative Genome Analysis of Enteropathogenic *Escherichia coli* O127:H6 Strain E2348/69. *Journal of Bacteriology* 91, 347–354.

Iizumi, Y., Sagara, H., Kabe, Y., Azuma, M., Kume, K., Ogawa, M., Nagai, T., Gillespe, P. G., Sasakawa, C. and Handa, H. (2007). The Enteropathogenic *E. coli* Effector EspB Facilitates Microvillus Effacing and Antiphagocytosis by Inhibiting Myosin Function. *Cell Host & Microbe* 2, 383–392.

Inoki, K., Li, Y., Zhu, T., Wu, J. and Guan, K. (2002). TSC2 is Phosphorylated and Inhibited by Akt and Suppresses mTOR Signalling. *Nature Cell Biology* 4, 648–657.

Invitrogen (2006). *Alexa Fluor® 488 Microscale Protein Labeling Kit (A30006) Product Information*.
URL: https://www.thermofisher.com/document-connect/document-connect.html?url=https%3A%2F%2Fassets.thermofisher.com%2FTFS-Assets%2FLSG%2Fmanuals%2Fmp30006.pdf&title=QWxleGEgRmx1b3IgNDg4IE1pY3Jvc2NhbGUgUHJvdGVpbiBMYWJlbGluZyBLaXQ=. Accessed: 17/07/2019.

Isono, T. (2011). *O*-GlcNAc-Specific Antibody CTD110.6 Cross-Reacts with *N*-GlcNAc$_2$-Modified Proteins Induced under Glucose Deprivation. *Public Library of Science ONE* 6, e18959.

Irmscher, S., Döring, N., Halder, L. D., Jo, E. A. H., Kopka, I., Dunker, C., Jacobsen, I. D., Luo, S., Slevogt, H., Lorkowski, S., Beyersdorf, N., Zipfel, P. F. and Skerka, C. (2018). Kallikrein Cleaves C3 and Activates Complement. *Journal of Innate Immunity* 10, 94–105.

Ivanov, A. I. (2008). Pharmacological Inhibition of Endocytic Pathways: Is it Specific Enough to be Useful? *Methods in Molecular Biology vol. 440: Exocytosis and Endocytosis*, pp. 15–33. Humana Press, Totowa.

Iwashima, M., Irving, B. A., van Oers, N. S. C., Chan, A. C. and Weiss, A. (1994). Sequential Interactions of the TCR with Two Distinct Cytoplasmic Tyrosine Kinases. *Science* 263, 1136–1139.

Jacewicz, M., Clausen, H., Nudelman, E., Donohue-Rolfe, A. and Keusch, G.T. (1986). Pathogenesis of Shigella Diarrhea. XI. Isolation of a *Shigella* Toxin-Binding Glycolipid from Rabbit Jejunum and HeLa Cells and its Identification as Globotriaosylceramide. *Journal of Experimental Medicine* 163, 1391–1404.

Jang, J., Hur, H., Sadowsky, M. J., Byappanahalli, M. N., Yan, T. and Ishii, S. (2017). Environmental *Escherichia coli*: Ecology and Public Health Implications – A Review. *Journal of Applied Microbiology* 123, 570–581.

Jank, T. and Aktories, K. (2008). Structure and Mode of Action of Clostridial Glucosylating Toxins: The ABCD Model. *Trends in Microbiology* 16, 222–229.

Jank, T., Bogdanović, X., Wirth, C., Haaf, E., Spoerner, M., Böhmer, K. E., Steinemann, M., Orth, J. H. C., Kalbitzer, H. R., Warscheid, B., Hunte, C. and Aktories, K. (2013). A Bacterial Toxin Catalyzing Tyrosine Glycosylation of Rho and Deamidation of G_q and G_i Proteins. *Nature Structural & Molecular Biology* 20, 1273–1280.

Janka, A., Bielaszewska, M., Dobrindt, U. and Karch, H. (2002). Identification and Distribution of the Enterohemorrhagic *Escherichia coli* Factor for Adherence (*efa1*) Gene in Sorbitol-Fermenting *Escherichia coli* O157: H-. *International Journal of Medical Microbiology* 292, 207–214.

Jankowski, A., Scott, C. C. and Grinstein, S. (2002). Determinants of the Phagosomal pH in Neutrophils. *The Journal of Biological Chemistry* 277, 6059–6066.

Jarvis, K. G., Girón, J. A., Jerse, A. E., McDaniel, T. K., Donnenberg, M. S. and Kaper, J. B. (1995). Enteropathogenic *Escherichia coli* Contains a Putative Type III Secretion System Necessary for the Export of Proteins Involved in Attaching and Effacing Lesion Formation. *Proceedings of the National Academy of Sciences of the United States of America* 92, 7996–8000.

Jerse, A. E., Yu, J., Tall, B. D. and Kaper, J. B. (1990). A Genetic Locus of Enteropathogenic *Escherichia coli* Necessary for the Production of Attaching and Effacing Lesions on Tissue Culture Cells. *Proceedings of the National Academy of Sciences of the United States of America* 87, 7839–7843.

Johansen, B. K., Wasteson, Y., Granum, P. E. and Brynestad, S. (2001). Mosaic Structure of Shiga-Toxin-2-Encoding Phages Isolated from *Escherichia coli* O157:H7 Indicates Frequent Gene Exchange between Lambdoid Phage Genomes. *Microbiology* 147, 1929–1936.

Johansen, F. and Kaetzel, C. (2012). Regulation of the Polymeric Immunoglobulin Receptor and IgA Transport: New Advances in Environmental Factors that Stimulate pIgR Expression and its Role in Mucosal Immunity. *Mucosal Immunology* 4, 598–602.

Johansson, M. E. V., Phillipson, M., Petersson, J., Velcich, A., Holm, L. and Hansson, G. C. (2008). The Inner of the Two Muc2 Mucin-Dependent Mucus Layers in Colon is Devoid of Bacteria. *Proceedings of the National Academy of Sciences of the United States of America* 105, 15064–15069.

Johnson, W. M., Lior, H. and Bezanson, G. S. (1983). Cytotoxic *Escherichia coli* O157:H7 Associated with Haemorrhagic Colitis in Canada. *The Lancet* 312, 76.

Jones, R. G., Parsons, M., Bonnard, M., Chan, V. S. F., Yeh, W., Woodgett, J. R. and Ohashi, P. S. (2000). Protein Kinase B Regulates T Lymphocyte Survival, Nuclear Factor κB Activation, and Bcl-X_L Levels *In Vivo*. *Journal of Experimental Medicine* 191, 1721–1734.

Jung, S., Smith, C. L., Lee, K., Hong, M., Kweon, D., Stephanopolous, G. and Jin, Y. (2010). Restoration of Growth Phenotypes of *Escherichia coli* DH5α in Minimal Media through Reversal of a Point Mutation in *purB*. *Applied and Environmental Microbiology* 76, 6307–6309.

Just, I., Fritz, G. and Aktories, K. (1994). *Clostridium difficile* Toxin B Acts on the GTP-Binding Protein Rho. *The Journal of Biological Chemistry* 269, 10706–10712.

Just, I., Selzer, J., von Eichel-Streibert, C. and Aktories, K. (1995a). The Low Molecular Mass GTP-Binding Protein Rho is Affected by Toxin A from *Clostridium difficile*. *The Journal of Clinical Investigation* 95, 1026–1031.

Just, I., Selzer, J., Wilm, M., von Eichel-Streibert, C., Mann, M. and Aktories, K. (1995b). Glucosylation of Rho Proteins by *Clostridium difficle* Toxin B. *Nature* 375, 500–503.

Just, I., Wilm, M., Selzer, J., Rex, G., von Eichel-Streibert, C., Mann, M. and Aktories, K. (1995c). The Enterotoxin from *Clostridium difficile* (ToxA) Monoglucosylates the Rho Proteins. *The Journal of Biological Chemistry* 270, 13932–13936.

Kägi, D., Ledermann, B., Bürki, K., Seiler, P., Odermatt, B., Olsen, K. J., Podack, E. R., Zinkernagel, R. M. and Hengartner, H. (1994). Cytotoxicity Mediated by T Cells and Natural Killer Cells is Greatly Impaired in Perforin-Deficient Mice. *Nature* 369, 31–37.

Kane, L. P., Andres, P. G., Howland, K. C., Abbas, A. K. and Weiss, A. (2001). Akt Provides the CD28 Costimulatory Signal for Up-Regulation of IL-2 and IFN-γ but not T_H2 Cytokines. *Nature Immunology* 37–44.

Kanellopoulos, J. M., De Petris, S., Leca, G. and Crumpton, M. J. (1985). The Mitogenic Lectin from *Phaseolus vulgaris* does not Recognize the T3 Antigen of Human Lymphocytes. *European Journal of Immunology* 15, 479–486.

Kang, E., Han, D., Park, J., Kwak, T. K., Oh, M., Lee, S., Choi, S., Park, Z. Y., Youngsoo, K. and Lee, J. W. (2008). O-GlcNAc Modulation at Akt1 Ser473 Correlates with Apoptosis of Murine Pancreatic β Cells. *Experimental Cell Research* 314, 2238–2248.

Karmali, M. A., Petric, M., Lim, C., Fleming, P. C. and Steele, B. T. (1983a). *Escherichia coli* Cytotoxin, Haemolytic-Uraemic Syndrome, and Haemorrhagic Colitis. *The Lancet* 322, 1299–1300.

Karmali, M. A., Petric, M., Steele, B. T. and Lim, C. (1983b). Sporadic Cases of Haemolytic-Uraemic Syndrome Associated with Faecal Cytotoxin and Cytotoxin-Producing *Escherichia coli* in Stools. *The Lancet* 321, 619–620.

Kärre, K., Ljunggren, H. G., Piontek, G. and Kiessling, R. (1986). Selective Rejection of H-2-Deficient Lymphoma Variants Suggests Alternative Immune Defence Strategy. *Nature* 319, 675–678.

Kelly, S. M., Jess, T. J. and Price, N. C. (2005). How to Study Proteins by Circular Dichroism. *Biochimica et Biophysica Acta – Proteins and Proteomics* 1751, 119–139.

Kenny, B. (1999). Phosphorylation of Tyrosine 474 of the Enteropathogenic *Escherichia coli* (EPEC) Tir Receptor Molecule is Essential for Actin Nucleating Activity and is Preceded by Additional Host Modifications. *Molecular Microbiology* 31, 1229–1241.

Kenny, B., Abe, A., Stein, M. and Finlay, B. B. (1997a). Enteropathogenic *Escherichia coli* Protein Secretion is Induced in Response to Conditions Similar to those in the Gastrointestinal Tract. *Infection and Immunity* 65, 2606–2612.

Kenny, B. and Jepson, M. (2000). Targeting of an Enteropathogenic *Escherichia coli* (EPEC) Effector Protein to Host Mitochondria. *Cellular Microbiology* 2, 579–590.

Kenny, B., DeVinney, R., Stein, M., Reinscheid, D. J., Frey, E. A. and Finlay, B. B. (1997b). Enteropathogenic *E. coli* (EPEC) Transfers its Receptor for Intimate Adherence into Mammalian Cells. *Cell* 91, 511–520.

Kenny, B., Ellis, S., Leard, A. D., Warawa, J., Mellor, H. and Jepson, M. A. (2002). Co-Ordinate Regulation of Distinct Host Cell Signalling Pathways by Multifunctional Enteropathogenic *Escherichia coli* Effector Molecules. *Molecular Microbiology* 44, 1095–1107.

Kern, B., Jain, U., Utsch, C., Otto, A., Busch, B., Jiménez-Soto, L., Becher, D. and Haas, R. (2015). Characterization of *Helicobacter pylori* VacA-Containing Vacuoles (VCVs), VacA Intracellular Trafficking and Interference with Calcium Signalling in T Lymphocytes. *Cellular Microbiology* 17, 1811–1832.

Khan, M. M., Bradford, H. N., Isordia-Salas, I., Liu, Y., Wu, Y., Espinola, R. G., Ghebrehiwet, B. and Colman, R. W. (2006). High-Molecular-Weight Kininogen Fragments Stimulate the Secretion of Cytokines and Chemokines through uPAR, Mac-1, and gC1qR in Monocytes. *Arteriosclerosis, Thrombosis and Vascular Biology* 26, 2260–2266.

Kihara, A., Akiyama, Y. and Ito, K. (2001). Revisiting the Lysogenization Control of Bacteriophage Lambda. Identification and Characterization of a New Host Component, HflD. *The Journal of Biological Chemistry* 276, 13695–13700.

Kikhney, A. G. and Svergun, D. I. (2015). A Practical Guide to Small Angle X-Ray Scattering (SAXS) of Flexible and Intrinsically Disordered Proteins. *Federation of European Biochemical Societies Letters* 589, 2570–2577.

Kilsdonk, E. P. C., Yancey, P. G., Stoudt, G. W., Bangerter, F. W., Johnson, W. J., Phillips, M. C. and Rothblat, G. H. (1995). Cellular Cholesterol Efflux Mediated by Cyclodextrins. *The Journal of Biological Chemistry* 270, 17250–17256.

Kim, M., Ashida, H., Ogawa, M., Yoshikawa, Y., Mimuro, H. and Sasakawa, C. (2010). Bacterial Interactions with the Host Epithelium. *Cell Host & Microbe* 8, 20–35.

Kim T. K. and Eberwine, J. H. (2010). Mammalian Cell Transfection: The Present and the Future. *Analytical and Bioanalytical Chemistry* 397, 3173–3178.

Kimura, T., Tani, S., Matsumoto, Y., Takeda, T. (2001). Serum Amyloid P Component is the Shiga Toxin 2-Neutralizing Factor in Human Blood. *The Journal of Biological Chemistry* 276, 41576–41579.

Klapproth, J. A. (2010). The Role of Lymphostatin/EHEC Factor for Adherence-1 in the Pathogenesis of Gram Negative Infection. *Toxins (Basel)* 2, 954–962.

Klapproth, J., Donnenberg, M. S., Abraham, J. M. and James, S. P. (1996). Products of Enteropathogenic *E. coli* Inhibit Lymphokine Production by Gastrointestinal Lymphocytes. *The American Journal of Physiology* 271, 841–848.

Klapproth, J., Donnenberg, M. S, Abraham, J. M., Mobley, H. L. T. and James, S. P. (1995). Products of Enteropathogenic *Escherichia coli* Inhibit Lymphocyte Activation and Lymphokine Production. *Infection and Immunity* 63, 2248–2254.

Klapproth, J. A., Sasaki, M., Sherman, M., Babbin, B., Donnenberg, M. S., Fernandes, P. J., Scaletsky, I. C. A., Kalman, D., Nusrat, A. and Williams, I. R. (2005). *Citrobacter rodentium lifA/efa1* is Essential for Colonic Colonization and Crypt Cell Hyperplasia *In Vivo*. *Infection and Immunity* 73, 1441–1451.

Klapproth, J. A., Scaletsky, I. C., McNamara, B., Lai, L., Malstrom, C., James, S. P. and Donnenberg, M. S. (2000). A Large Toxin from Pathogenic *Escherichia coli* Strains that Inhibits Lymphocyte Activation. *Infection and Immunity* 68, 2148–2155.

Knittler M. R. and Haas, I. G. (1992). Interaction of BiP with Newly Synthesized Immunoglobulin Light Chain Molecules: Cycles of Sequential Binding and Release. *The European Molecular Biology Organization Journal* 11, 1573–1581.

Knoop, K. A., Miller, M. J. and Newberry, R. D. (2013). Trans-Epithelial Antigen Delivery in the Small Intestine: Different Paths, Different Outcomes. *Current Opinion in Gastroenterology* 29, 112–118.

Knutton, S., Lloyd, D. R. and McNeish, A. S. (1987). Adhesion of Enteropathogenic *Escherichia coli* to Human Intestinal Enterocytes and Cultured Human Intestinal Mucosa. *Infection and Immunity* 55, 69–77.

Knutton, S., Rosenhine, I., Pallen, M. J., Nisan, I., Neves, B. C., Bain, C., Wolff, C., Dougan, G. and Frankel, G. (1998). A Novel EspA-Associated Surface Organelle of Enteropathogenic *Escherichia coli* Involved in Protein Translocation into Epithelial Cells. *The European Molecular Biology Organization Journal* 17, 2166–2176.

Knutton, S., Shaw, R. K., Anantha, R. P., Donnenberg, M. S. and Zorgani, A. A. (1999). The Type IV Bundle-Forming Pilus of Enteropathogenic *Escherichia coli* Undergoes Dramatic Alterations in Structure Associated with Bacterial Adherence, Aggregation and Dispersal. *Molecular Microbiology* 33, 499–509.

Kolling, G. L. and Matthews, K. R. (1999). Export of Virulence Genes and Shiga Toxin by Membrane Vesicles of *Escherichia coli* O157:H7. *Applied and Environmental Microbiology* 65, 1843–1848.

Konradt, C., Frigimelica, E., Nothelfer, K., Puhar, A., Salgado-Pabón, W., di Bartolo, V., Scott-Algara, D., Rodrigues, C. D., Sansonetti, P. J. and Phalipon, A. (2011). The *Shigella flexneri* Type Three Secretion System Effector IpgD Inhibits T Cell Migration by Manipulating Host Phosphoinositide Metabolism. *Cell Host & Microbe* 9, 263–272.

Kozub-Witkowski, E., Krause, G., Frankel, G., Kramer, D., Appel, B. and Beutin, L. (2008). Serotypes and Virutypes of Enteropathogenic and Enterohaemorrhagic *Escherichia coli* Strains from Stool Samples of Children with Diarrhoea in Germany. *Journal of Applied Microbiology* 104, 403–410.

Krakauer, T. (2013). Update on Staphylococcal Superantigen-Induced Signaling Pathways and Therapeutic Interventions. *Toxins (Basel)* 5, 1629–1654.

Krakauer, T., Pradhan, K. and Stiles, B. G. (2016). Staphylococcal Superantigens Spark Host-Mediated Danger Signals. *Frontiers in Immunology* 7, 23.

Krause, M., Barth, H. and Schmidt, H. (2018). Toxins of Locus of Enterocyte Effacement-Negative Shiga Toxin-Producing Escherichia coli. *Toxins (Basel)* 10, 241.

Kreimeyer, I., Euler, F., Marckscheffel, A., Tatge, H., Pich, A., Olling, A., Schwarz, J., Just, I. and Gerhard, R. (2011). Autoproteolytic Cleavage Mediates Cytotoxicity of *Clostridium difficile* Toxin A. *Naunyn-Schmiedeberg's Archives of Pharmacology* 383, 253–262.

Kresse, A. U., Beltrametti, F., Müller, A., Ebel, F. and Guzmán, C. A. (2000). Characterization of SepL of Enterohemorrhagic *Escherichia coli*. *Journal of Bacteriology* 182, 6490–6498.

Kresse, A. U., Rohde, M. and Guzmán, C. A. (1999). The EspD Protein of Enterohemorrhagic *Escherichia coli* is Required for the Formation of Bacterial Surface Appendages and is Incorporated in the Cytoplasmic Membranes of Target Cells. *Infection and Immunity* 67, 4834–4842.

Krishan, A. (1975). Rapid Flow Cytofluorometric Analysis of Mammalian Cell Cycle by Propidium Iodide Staining. *The Journal of Cell Biology* 66, 188–193.

Krogh, A., Larsson, B., von Heijne, G. and Sonnhammer, E. L. L. (2001). Predicting Protein Transmembrane Topology with a Hidden Markov Model: Application to Complete Genomes. *Journal of Molecular Biology* 305, 567–580.

Kullas, A. L., McClelland, M., Yang, H., Tam, J. W., Torres, A., Porwollik, S., Mena, P., McPhee, J. B., Bogomolnaya, L., Andrews-Polymenis, H. and van der Velden, A. W. M. (2012). L-Asparaginase II Produced by *Salmonella* Typhimurium Inhibits T Cell Responses and Mediates Virulence. *Cell Host & Microbe* 12, 791–798.

Kumari, A., Sharma, V. K. and Kumar, H. (2018). Gene Trapping: A Powerful Tool of Functional Genomics to Identify Novel Genes. *International Journal of Genetics* 10, 325–332.

Kumari, S., Curado, S., Mayya, V. and Dustin, M. L. (2014). T Cell Antigen Receptor Activation and Actin Cytoskeleton Remodeling. *Biochimica et Biophysica Acta - Biomembranes* 1838, 546–556.

Kyle, J. L., Cummings, C. A., Parker, C. T., Quiñones, B., Vatta, P., Newton, E., Huynh, S., Swimley, M., Degoricija, L., Barker, M., Fontanoz, S., Nguyen, K., Patel, R., Fang, R., Tebbs, R., Petrauskene, O., Furtado, M. and Mandrell, R. E. (2012). *Escherichia coli* Serotype O55:H7 Diversity Supports Parallel Acquisition of Bacteriophage at Shiga Toxin Phage Insertion Sites During Evolution of the O157:H7 Lineage. *Journal of Bacteriology* 194, 1885–1896.

Lafont, V., Astoul, E., Laurence, A., Liautard, J. and Cantrell, D. (2000). The T Cell Antigen Receptor Activates Phosphatidylinositol 3-Kinase-Regulated Serine Kinases Protein Kinase B and Ribosomal S6 Kinase 1. *Federation of European Biochemical Societies Letters* 486, 38–42.

LaFrance, M. E., Farrow, M. A., Chandrasekaran, R., Sheng, J., Rubin, D. H. and Lacy, D. B. (2015). Identification of an Epithelial Cell Receptor Responsible for *Clostridium difficile* TcdB-Induced Cytotoxicity. *Proceedings of the National Academy of Sciences of the United States of America* 112, 7073–7078.

Lalmanach, G., Naudin, C., Lecaille, F. and Fritz, H. (2010). Kininogens: More than Cysteine Protease Inhibitors and Kinin Precursors. *Biochimie* 92, 1568–1579.

Lambert, G. S. and Baldwin, M. R. (2016). Evidence for Dual Receptor-Binding Sites in *Clostrdium difficile* Toxin A. *The Federation of European Biochemical Societies Letters* 590, 4550–4563.

Lanier, L. L., Testi, R., Bindi, J. and Phillips, J. H. (1989). Identity of Leu-19 (CD56) Leukocyte Differentiation Antigen and Neural Cell Adhesion Molecule. *Journal of Experimental Medicine* 169, 2233–2238.

Lathem, W. W., Bergsbaken, T. and Welch, R. A. (2004). Potentiation of C1 Esterase Inhibitor by StcE, a Metalloprotease Secreted by *Escherichia coli* O157:H7. *Journal of Experimental Medicine* 199, 1077–1087.

Lathem, W. W., Grys, T. E., Witowski, S. E., Torres, A. G., Kaper, J. B., Tarr, P. I. and Welch, R. A. (2002). StcE, a Metalloprotease Secreted by *Escherichia coli* O157:H7, Specifically Cleaves C1 Esterase Inhibitor. *Molecular Microbiology* 45, 277–288.

Law, H. T., Chua, M., Moon, K., Foster, L. J. and Guttman, J. A. (2015). Mass Spectrometry-Based Proteomics Identification of Enteropathogenic *Escherichia coli* Pedestal Constituents. *Journal of Proteome Research* 14, 2520–2527.

Lawand, M., Déchanet-Merville, J. and Dieu-Nosjean, M. (2017). Key Features of Gamma-Delta T-Cell Subsets in Human Diseases and Their Immunotherapeutic Implications. *Frontiers in Immunology* 8, 761.

Lawrence, D. W., Bruyninckx, W. J., Louis, N. A., Lublin, D. M., Stahl, G. L., Parkos, C. A. and Colgan, S. P. (2003). Antiadhesive Role of Apical Decay-Accelerating Factor (CD55) in Human Neutrophil Transmigration across Mucosal Epithelia. *Journal of Experimental Medicine* 198, 999–1010.

Lea, N., Lord, J. M. and Roberts, L. M. (1999). Proteolytic Cleavage of the A Subunit is Essential for Maximal Cytotoxicity of *Escherichia coli* O157:H7 Shiga-Like Toxin-1. *Microbiology* 145, 999–1004.

Lee, A., Miller, D., Henry, R., Paruchuri, V. D. P., O'Meally, R. N., Boronina, T., Cole, R. N. and Zachara, N. E. (2016). Combined Antibody/Lectin Enrichment Identifies Extensive Changes in the *O*-GlcNAc Sub-Proteome upon Oxidative Stress. *Journal of Proteome Research* 15, 4318–4336.

Lee, M., Kwon, H., Lee, E., Kim, D., Park, J., Tesh, V. L., Oh, T. and Kim, M. H. (2016). Shiga Toxins Activate the NLRP3 Inflammasome Pathway to Promote Both Production of the Proinflammatory Cytokine Interleukin-1β and Apoptotic Cell Death. *Infection and Immunity* 84, 172–186.

Lee, M. and Tesh, V. (2019). Roles of Shiga Toxins in Immunopathology. *Toxins (Basel)* 11, 212.

Légaré, C., Akintayo, A., Blondin, P., Calvo, E. and Sullivan, R. (2017). Impact of Male Fertility Status on the Transcriptome of the Bovine Epididymis. *Molecular Human Reproduction* 23, 355–369.

Leimbach, A., Hacker, J. and Dobrindt, U. (2013). *E. coli* as an All-Rounder: The Thin Line between Commensalism and Pathogenicity. *Current Topics in Microbiology and Immunology vol. 358: Between Pathogenicity and Commensalism*, pp. 3–33. Springer Heildelberg, New York.

Leitner, A. (2016). Cross-Linking and Other Structural Proteomics Techniques: How Chemistry is Enabling Mass Spectrometry Applications in Structural Biology. *Chemical Science* 7, 4792–4803.

Lennon-Duménil, A., Bakker, A. H., Maehr, R., Fiebiger, E., Overkleeft, H. S., Rosemblatt, M., Ploegh, H. L. and Cécile Lagaudrière-Gesbert, C. (2002). Analysis of Protease Activity in Live Antigen-Presenting Cells Shows Regulation of the Phagosomal Proteolytic Contents During Dendritic Cell Activation. *Journal of Experimental Medicine* 196, 529–540.

Leo, J. C., Oberhettinger, P, Schütz, M. and Linke, D. (2015). The Inverse Autotransporter Family: Intimin, Invasin and Related Proteins. *International Journal of Medical Microbiology* 305, 276–282.

Levine, M. M. and Edelman, R. (1984). Enteropathogenic *Escherichia coli* of Classic Serotypes Associated with Infant Diarrhea: Epidemiology and Pathogenesis. *Epidemiological Reviews* 6, 31–51.

Levine, M. M., Bergquist, E. G., Nalin, D. R., Waterman, D. H., Hornick, R. B., Young, C. R. and Stotman, S. (1978). *Escherichia coli* Strains that Cause Diarrhoea but do not Produce Heat-Labile or Heat-Stable Enterotoxins and are Non-Invasive. *The Lancet* 1, 1119–1122.

Levine, M. M., Nataro, J. P., Karch, H., Baldini, M. M., Kaper, J. B., Black, R. E., Clements, M. L. and O'Brien, A. D. (1985). The Diarrheal Response of Humans to Some Classic Serotypes of Enteropathogenic *Escherichia coli* is Dependent on a Plasmid Encoding an Enteroadhesiveness Factor. *The Journal of Infectious Diseases* 152, 550–559.

Levkowitz, G., Waterman, H., Zamir, E., Kam, Z., Oved, S., Langdon, W. Y., Beguinot, L., Geiger, B. and Yarden, Y. (1998). cCbl/Sli-1 Regulates Endocytic Sorting and Ubiquitination of the Epidermal Growth Factor Receptor. *Genes & Development* 12, 3663–3674.

Leung, D. W., Chen, E. and Goeddel, D. V. (1989). A Method for Random Mutagenesis of a Defined DNA Segment Using a Modified Polymerase Chain Reaction. *Technique* 1, 11–15.

Leyva-Illades, D., Cherla, R. P., Lee, M. and Tesh, V. L. (2012). Regulation of Cytokine and Chemokine Expression by the Ribotoxic Stress Response Elicited by Shiga Toxin Type 1 in Human Macrophage-Like THP-1 Cells. *Infection and Immunity* 80, 2109–2120.

Li, S., Shi, L., Yang, Z. and Feng, H. (2013a). Cytotoxicity of *Clostridium difficile* Toxin B does not Require Cysteine Protease-Mediated Autocleavage and Release of the Glucosyltransferase Domain into the Host Cell Cytosol. *Pathogens and Disease* 67, 11–18.

Li, S., Zhang, L., Yoa, Q., Li, L., Dong, N., Rong, J., Gao, W., Ding, X., Sun, L., Chen, X., Chen, S. and Shao, F. (2013b). Pathogen Blocks Host Death Receptor Signalling by Arginine GlcNAcylation of Death Domains. *Nature* 501, 242–246.

Li, Y., Frey, E., Mackenzie, A. M. R. and Finlay, B. B. (2000). Human Response to *Escherichia coli* O157:H7 Infection: Antibodies to Secreted Virulence Factors. *Infection and Immunity* 68, 5090–5095.

Liao, Y., Jeng, J., Wang, C., Wang, S. and Chang, S. (2004). Removal of N-Terminal Methionine from Recombinant Proteins by Engineered *E. coli* Methionine Aminopeptidase. *Protein Science* 13, 1802–1810.

Lim, J. J., Grinstein, S. and Roth, Z. (2017). Diversity and Versatility of Phagocytosis: Roles in Innate Immunity, Tissue Remodeling, and Homeostasis. *Frontiers in Cellular and Infection Microbiology* 7.

Lin, J. and Lai, E. (2017). Protein-Protein Interactions: Co-Immunoprecipitation. *Methods in Molecular Biology vol. 1615: Bacterial Protein Secretion Systems, Methods and Protocols*, pp. 211–219. Humana Press, New York.

Lindberg, A., Brown, J. E, Strömberg, N., Westling-Ryd, M., Schultz J. E. and Karlsson, K. (1987). Identification of the Carbohydrate Receptor for Shiga Toxin Produced by *Shigella dysenteriae* Type 1. *The Journal of Biological Chemistry* 262, 1779–85.

Liu, T., Zandberg, W. F., Gloster, T. M., Deng, L., Murray, K. D., Shan, X. and Vocadlo, D. J. (2018a). Metabolic Inhibitors of O-GlcNAc Transferase that Act *In Vivo* Implicate Decreased O-GlcNAc Levels in Leptin-Mediated Nutrient Sensing. *Angewandte Chemie (International Edition in English)* 57, 7644–7648.

Liu, Y., Gonen, S., Gonen, T. and Yeates, T. O. (2018b). Near-Atomic Cryo-EM Imaging of a Small Protein Displayed on a Designed Scaffolding System. *Proceedings of the National Academy of Sciences of the United States of America* 115, 3362–3367.

Liu, Y., Ren, Y., Cao, Y., Huang, H., Wu, Q., Li, W., Wu, S. and Zhang, J. (2017). Discovery of a Low Toxicity O-GlcNAc Transferase (OGT) Inhibitor by Structure-Based Virtual Screening of Natural Products. *Scientific Reports* 7, 12334.

Lo, M. C., Aulabaugh, A., Jin, G., Cowling, R., Bard, J., Malamas, M. and Ellestad, G. (2004). Evaluation of Fluorescence-Based Thermal Shift Assays for Hit Identification in Drug Discovery. *Analytical Biochemistry* 332, 153–159.

Lobley, A., Whitmore, L. and Wallace, B. A. (2002). DICROWEB: An Interactive Website for the Analysis of Protein Secondary Structure from Circular Dichroism Spectra. *Bioinformatics* 18, 211–212.

Loike, J. D. and Silverstein, S. C. (1983). A Fluorescence Quenching Technique Using Trypan Blue to Differentiate between Attached and Ingested Glutaraldehyde-Fixed Red Blood Cells in Phagocytosing Murine Macrophages. *Journal of Immunological Methods* 57, 373–379.

López-Lago, M., Lee, H., Cruz, C., Movilla, N. and Bustelo, X. R. (2000). Tyrosine Phosphorylation Mediates Both Activation and Downmodulation of the Biological Activity of Vav. *Molecular and Cellular Biology* 20, 1678–1691.

Loukiadis, E., Nobe, R., Herold, S., Tramuta, C., Ogura, Y., Ooka, T., Morabito, S., Kérourédan, M., Brugère, H., Schmidt, H., Hayashi, T. and Oswald, E. (2008). Distribution, Functional Expression, and Genetic Organization of Cif, a Phage-Encoded Type III-Secreted Effector from Enteropathogenic and Enterohemorrhagic *Escherichia coli*. *Journal of Bacteriology* 190, 275–285.

Luckheeram, R. V., Zhou, R., Verma, A. D. and Xia, B. (2012). $CD4^{+}$T Cells: Differentiation and Functions. *Clinical and Developmental Immunology* 2012, 925135.

Lund, P. J., Elias, J. E. and Davis, M. M. (2016). Global Analysis of *O*-GlcNAc Glycoproteins in Activated Human T Cells. *The Journal of Immunology* 197, 3086–3098.

Luppi, A. (2018). Swine Enteric Colibacillosis: Diagnosis, Therapy and Antimicrobial Resistance. *Porcine Health Management* 3, 16.

Ma. C., Wickham, M. E., Guttman, J. A., Deng, W., Walker, J., Madsen, K. L., Jacobson, K., Vogl, W. A., Finlay, B. B. and Vallance, B. A. (2006). *Citrobacter rodentium* Infection Causes Both Mitochondrial Dysfunction and Intestinal Epithelial Barrier Disruption *In Vivo*: Role of Mitochondrial Associated Protein (Map). *Cellular Microbiology* 8, 1669–1686.

Ma, J. and Hart, G. W. (2014). *O*-GlcNAc Profiling: From Proteins to Proteomes. *Clinical Proteomics* 11, 8.

Ma, L., Chen, Z., Erdjument-Bromage, H., Tempst, P. and Pandolfi, P. P. (2005). Phosphorylation and Functional Inactivation of TSC2 by Erk: Implications for Tuberous Sclerosisand Cancer Pathogenesis. *Cell* 121, 179–193.

Ma, Y. J. and Garred, P. (2018). Pentraxins in Complement Activation and Regulation. *Frontiers in Immunology* 9, 3046.

Mabbott, N. A., Donaldson, D. S., Ohno, H., Williams, I. R. and Mahajan, A. (2013). Microfold (M) Cells: Important Immunosurveillance Posts in the Intestinal Epithelium. *Mucosal Immunology* 6, 666–677.

MacIver, N. J., Michalek, R. D. and Rathmell, J. C. (2013). Metabolic Regulation of T Lymphocytes. *Annual Review of Immunology* 31, 259–283.

Mackay, C. R. and Hein, W. R. (1989). A Large Proportion of Bovine T Cells Express the γδ T Cell Receptor and Show a Distinct Tissue Distribution and Surface Phenotype. *International Immunology* 1, 540–545.

Madden, T. (2013). The BLAST Sequence Analysis Tool. *The NCBI Handbook [Internet]*. Bethesda (MD): National Center for Biotechnology Information (US). URL: https://www.ncbi.nlm.nih.gov/books/NBK143764/

Makino, K., Ishii, K., Yasunaga, T., Hattori, M., Yokoyama, K., Yutsudo, C. H., Kubota, Y. Yamaichi, Y., Iida, T., Yamamoto, K., Honda, T., Han, C., Ohtsubo, E., Kasamatsu, M., Hayashi, T., Kuhara, S. and Shinagawa, H. (1998). Complete Nucleotide Sequences of 93-kb and 3.3-kb Plasmids of an Enterohemorrhagic *Escherichia coli* O157:H7 Derived from Sakai Outbreak. *DNA Research* 5, 1–9.

Mallard, F., Antony, C., Tenza, D., Salamero, J., Goud, B. and Johannes, L. (1998). Direct Pathway from Early/Recycling Endosomes to the Golgi Apparatus Revealed Through the Study of Shiga Toxin B-Fragment Transport. *Journal of Cell Biology* 143, 973–990.

Malstrom, C. and James, S. (1998). Inhibition of Murine Splenic and Mucosal Lymphocyte Function by Enteric Bacterial Products. *Infection and Immunity* 66, 3120–3127.

Malvern (2019). Dynamic Light Scattering. URL: https://www.malvernpanalytical.com/en/products/technology/light-scattering/dynamic-light-scattering. Accessed: 17/07/2019.

Malyukova, I., Murray, K. F., Zhu, C., Boedeker, E., Kane, A., Patterson, K., Peterson, J. R., Donowitz, M. and Kovbasnjuk, O. (2009). Macropinocytosis in Shiga Toxin 1 Uptake by Human Intestinal Epithelial Cells and Transcellular Transcytosis. *American Journal of Physiology – Gastrointestinal and Liver Physiology*, 21205, 78–92.

Manda-Handzlik, A. and Demkow, U. (2015). Neutrophils: The Role of Oxidative and Nitrosative Stress in Health and Disease. *Advances in Experimental Medicine and Biology*, *Neuroscience and Respiration vol. 857: Pulmonary Infection*, pp. 51–60. Springer International Publishing, Switzerland.

Mandal, A. and Viswanathan, C. (2015). Natural Killer Cells: In Health and Disease. *Hematology/Oncology and Stem Cell Research* 8, 47–55.

Manjarrez-Hernandez, H. A., Baldwin, T. J., Aitken, A., Knutton, S. and Williams, P. H. (1992). Intestinal Epithelial Cell Protein Phophorylation in Enteropathogenic *Escherichia coli* Diarrhoea. *The Lancet* 339, 521–523.

Manning, B. D. and Toker, A. (2017). AKT/PKB Signaling: Navigating the Network. *Cell* 169, 381–405.

Manoil, C. (1990). Analysis of Protein Localization by Use of Gene Fusions with Complementary Properties. *Journal of Bacteriology* 172, 1035–1042.

Manoil, C. and Beckwith, J. (1985). Tn*phoA*: A Transposon Probe for Protein Export Signals. *Proceedings of the National Academy of Sciences of the United States of America* 82, 8129–8133.

Manoury, B., Hewitt, E. W., Morrice, N., Dando, P. M., Barrett, A. J. and Watts, C. (1998). An Asparaginyl Endopeptidase Processes a Microbial Antigen for Class II MHC Presentation. *Nature* 396, 695–699.

Manse, J. S. and Baldwin, M. R. (2015). Binding and Entry of *Clostridium difficile* Toxin B is Mediated by Multiple Domains. *Federation of European Biochemical Societies Letters* 589, 3945–3951.

Marchès, O., Batchelor, M., Shaw, R. K., Patel, A., Cummings, N., Nagai, T., Sasakawa, C., Carlsson, S. R., Lundmark, R., Cougoule, C., Caron, E., Knutton, S., Connerton, I. and Frankel, G. (2006). EspF of Enteropathogenic *Escherichia coli* Binds Sorting Nexin 9. *Journal of Bacteriology* 188, 3110–3115.

Marchès, O., Covarelli, V., Dahan, S., Cougoule, C., Bhatta, P., Frankel, G. and Caron, E. (2008). EspJ of Enteropathogenic and Enterohaemorrhagic *Escherichia coli* Inhibits Opsono-Phagocytosis. *Cellular Microbiology* 10, 1104–1115.

Marchès, O., Ledger, T. L., Boury, M., Ohara, M., Tu, X., Goffaux, F., Mainil, J., Rosenshine, I., Sugai, M., De Rycke, J. and Oswald, E. (2003). Enteropathogenic and Enterohaemorrhagic *Escherichia coli* Deliver a Novel Effector Called Cif, which Blocks Cell Cycle G_2/M Transition. *Molecular Microbiology* 50, 1553–1567.

Marshall, J. S., Warrington, R., Watson, W. and Kim, H. L. (2018). An Introduction to Immunology and Immunopathology. *Allergy, Asthma & Clinical Immunology* 14, 49.

Martinez, M. B., Taddei, C. R., Ruiz-Tagle, A., Trabulsi, L. R. and Girón, J. A. (1999). Antibody Response of Children with Enteropathogenic *Escherichia coli* Infection to the Bundle-Forming Pilus and Locus of Enterocyte Effacement-Encoded Virulence Determinants. *The Journal of Infectious Diseases* 179, 269–274.

Martinez-Argudo, I., Sands, C. and Jepson, M. A. (2007). Translocation of Enteropathogenic *Escherichia coli* Across an *In Vitro* M Cell Model is Regulated by its Type III Secretion System. *Cellular Microbiology* 9, 1538–1546.

Martinson, J. N. V., Pinkham, N. V., Peters, G. W., Cho, H., Heng, J., Rauch, M., Broadaway, S. C. and Walk, S. T. (2019). Rethinking Gut Microbiome Residency and the *Enterobacteriaceae* in Healthy Human Adults. *The International Society for Microbial Ecology Journal* 13, 2306–2318.

Martorelli, L., Garbaccio, S., Vilte, D. A., Albanese, A. A., Mejías, M. P., Palermo, M. S., Mercado, E. C., Ibarra, C. E. and Cataldi, A. A. (2017). Immune Response in Calves Vaccinated with Type Three Secretion System Antigens and Shiga Toxin 2B Subunit of *Escherichia coli* O157:H7. *Public Library of Science ONE* 12, e0169422.

Maslon, M. M., Hrstka, R., Vojtesek, B. and Hupp, T. R. (2010). A Divergent Substrate-Binding Loop within the Pro-Oncogenic Protein Anterior Gradient-2 Forms a Docking Site for Reptin. *Journal of Molecular Biology* 404, 418–438.

Matsuzawa, T., Kuwae, A. and Abe, A. (2005). Enteropathogenic *Escherichia coli* Type III Effectors EspG and EspG2 Alter Epithelial Paracellular Permeability. *Infection and Immunity* 73, 6283–6289.

Matsuzawa, T., Kuwae, A., Yoshida, S., Sasakawa, C. and Abe, A. (2004). Enteropathogenic *Escherichia coli* Activates the RhoA Signaling Pathway via the Stimulation of GEF-H1. *The European Molecular Biology Organization Journal* 23, 3570–3582.

Maynard, J. C., Burlingame, A. L. and Medzihradszky, K. F. (2016). Cysteine S-linked *N*-acetylglucosamine (S-GlcNAcylation), a New Post-Translational Modification in Mammals. *Molecular & Cellular Proteomics* 15, 3405–3411.

McCarthy, N. E. and Eberl, M. (2018). Human γδ T-Cell Control of Mucosal Immunity and Inflammation. *Frontiers in Immunology* 9, 985.

McClung, J. P., Roneker, C. A., Mu, W., Lisk, D. J., Langlais, P., Liu, F. and Lei, X. G. (2004). Development of Insulin Resistance and Obesity in Mice Overexpressing Cellular Glutathione Peroxidase. *Proceedings of the National Academy of Sciences of the United States of America* 101, 8852–8857.

McClure, W. O. and Edelman, G. M. (1966). Fluorescent Probes for Conformational States of Proteins. I. Mechanism of Fluorescence of 2-*p*-Toluidinylnapthalene-6-sulfonate, a Hydrophobic Probe. *Biochemistry* 5, 1908–1919.

McCormack, J. M., Moore, S. C., Gatewood, J. W. and Walker, W. S. (1992). Mouse Splenic Macrophage Cell Lines with Different Antigen-Presenting Activities for $CD4^+$ Helper T Cell Subsets and Allogeneic $CD8^+$ T Cells. *Cellular Immunology* 145, 359–371.

McDaniel, T. K., Jarvis, K. G., Donnenberg, M. S. and Kaper, J. B. (1995). A Genetic Locus of Enterocyte Effacement Conserved Among Diverse Enterobacterial Pathogens. *Proceedings of the National Academy of Sciences of the United States of America* 92, 1664–1668.

McDaniel, T. K. and Kaper, J. B (1997). A Cloned Pathogenicity Island from Enteropathogenic *Escherichia coli* Confers the Attaching and Effacing Phenotype on *E. coli* K-12. *Molecular Microbiology* 23, 399–407.

McDole, J. R., Wheeler, L. W., McDonald, K. G., Wang, B., Konjufca, V., Knoop, K. A., Newberry, R. D. and Miller, M. J. (2012). Goblet Cells Deliver Luminal Antigen to $CD103^+$ DCs in the Small Intestine. *Nature* 483, 345–349.

McLaughlin, P. A., McClelland, M., Yang, H., Porwollik, S., Bogomolnaya, L., Chen, J., Andrews-Polymenis, H. and van der Velden, A. W. M. (2016). Contribution of Asparagine Catabolism to *Salmonella* Virulence. *Infection and Immunity* 85, e00740-16.

McKay, D. M. (2001). Bacterial Superantigens: Provocateurs of Gut Dysfunction and Inflammation? *Trends in Immunology* 22, 497–501.

McKnight, S. L. and Kingsbury, R. (1982). Transcriptional Control Signals of a Eukaryotic Protein-Coding Gene. *Science* 217, 316–324.

McNeilly, T. N., Mitchell, M. C., Rosser, T., McAteer, S., Low, J. C., Smith, D. G. E., Huntley, J. F., Mahajan, A. and Gally, D. (2010). Immunization of Cattle with a Combination of Purified Intimin-531, EspA and Tir Significantly Reduces Shedding of *Escherichia coli* O157:H7 Following Oral Challenge. *Vaccine* 28, 1422–1428.

Mehta, D. P., Ichikawa, M., Salimath, P. V., Etchison, J. R., Haak, R., Manzi, A. and Freeze H. H. (1996). A Lysosomal Cysteine Proteinase from *Dictyostelium discoideum* Contains *N*-Acetylglucosamine-1-Phosphate Bound to Serine but not Mannose-6-Phosphate on *N*-linked Oligosaccharides. *The Journal of Biological Chemistry* 271, 10897–10903.

Meier, R., Alessi, D. R., Cron, P., Andjelković, M. and Hemmings, B. A. (1997). Mitogenic Activation, Phosphorylation, and Nuclear Translocation of Protein Kinase Bβ. *The Journal of Biological Chemistry* 272, 30491–30497.

Mellies, J. L. and Lorenzen, E. (2014). Enterohemorrhagic *Escherichia coli* Virulence Gene Regulation. *Microbiology Spectrum* 2, 4.

Menge, C., Blessenohl, M., Eisenberg, T., Stamm, I. and Baljer, G. (2004a). Bovine Ileal Intraepithelial Lymphocytes Represent Target Cells for Shiga Toxin 1 from *Escherichia coli*. *Infection and Immunity* 72, 1896–1905.

Menge, C., Stamm, I., van Diemen, P. M., Sopp, P., Baljer, G., Wallis, T. S. and Stevens, M. P. (2004b). Phenotypic and Functional Characterization of Intraepithelial Lymphocytes in a Bovine Ligated Intestinal Loop Model of Enterohaemorrhagic *Escherichia coli* Infection. *Journal of Medical Microbiology* 53, 573–579.

Menge, C., Stamm, I., Blessenohl, M., Wieler, L. H. and Baljer, G. (2003). Verotoxin 1 from *Escherichia coli* Affects $Gb_3/CD77^+$ Bovine Lymphocytes Independent of Interleukin-2, Tumor Necrosis Factor-α, and Interferon-α. *Experimental Biology and Medicine* 228, 377–386.

Menge, C., Wieler, L. H., Schlapp, T. and Baljer, G. (1999). Shiga Toxin 1 from *Escherichia coli* Blocks Activation and Proliferation of Bovine Lymphocyte Subpopulations *In Vitro*. *Infection and Immunity* 67, 2209–2217.

Merle, N. S., Church, S. E., Fremeaux-Bacchi, V. and Roumenina, L. T. (2015a). Complement System Part I – Molecular Mechanisms of Activation and Regulation. *Frontiers in Immunology* 6, 262.

Merle, N. S., Noe, R., Halbwachs-Mecarelli, L., Fremeaux-Bacchi, V. and Roumenina, L. T. (2015b). Complement System Part II – Role in Immunity. *Frontiers in Immunology* 6, 257.

Mirhoseini, A., Amani, J. and Nazarian, S. (2018). Review on Pathogenicity Mechanism of Enterotoxigenic *Escherichia coli* and Vaccines Against it. *Microbial Pathogenesis* 117, 162–169.

Milne, J. C., Blanke, S. R., Hanna, P. C. and Collier, R. J. (1995). Protective Antigen-Binding Domain of Anthrax Lethal Factor Mediates Translocation of a Heterologous Protein Fused to its Amino- or Carboxy-Terminus. *Molecular Microbiology* 15, 661–666.

Mills, E., Baruch, K., Aviv, G., Nitzan, M. and Rosenshine I. (2013). Dynamics of the Type III Secretion System Activity of Enteropathogenic *Escherichia coli*. *mBio* 4, 1–9.

Misinzo, G., Delputte, P. L. and Nauwynck, H. J. (2008). Inhibition of Endosome-Lysomsome System Acidification Enhances Porcine Circovirus 2 Infection of Porcine Epithelial Cells. *Journal of Virology* 82, 1128–1135.

Miyazaki, M. and Takemasa, T. (2017). TSC2/Rheb Signaling Mediates ERK-Dependent Regulation of mTORC1 Activity in C2C12 Myoblasts. *Federation of European Biochemical Societies Open Bio* 7, 424–433.

Moalli, F., Doni, A., Deban, L., Zelante, T., Zagarella, S., Bottazzi, B., Romani, L., Mantovani, A. and Garlanda, C. (2010). Role of Complement and Fcγ Receptors in the Protective Activity of the Long Pentraxin PTX3 Against *Aspergillus fumigatus*. *Blood* 116, 5170–5180.

Mohamadzadeh, M., Mohamadzadeh, H., Brammer, M., Sestak, K. and Luftig, R. B. (2004). Identification of Proteases Employed by Dendritic Cells in the Processing of Protein Purified Derivative (PPD). *Journal of Immune Based Therapies and Vaccines* 2, 8.

Mold, C., Baca, R., Du Clos, T. W. (2002). Serum Amyloid P Component and C-Reactive Protein Opsonize Apoptotic Cells for Phagocytosis through Fc Gamma Receptors. *Journal of Autoimmunity* 19, 147–154.

Mold, C., Gresham, H. D. and Du Clos, T. W. (2001). Serum Amyloid P Component and C-Reactive Protein Mediate Phagocytosis through Murine Fc Gamma Rs. *The Journal of Immunology* 166, 1200–1205.

Monsigny, M., Roche, A., Sene, C., Maget-Dana, R. and Delmotte, F. (1980). Sugar-Lectin Interactions: How Does Wheat-Germ Agglutinin Bind Sialoglycoconjugates? *European Journal of Biochemistry* 104, 147–153.

Moon, H. W., Whipp, S. C., Argenzio, R. A., Levine, M. M. and Giannella, R. A. (1983). Attaching and Effacing Activities of Rabbit and Human Enteropathogenic *Escherichia coli* in Pig and Rabbit Intestines. *Infection and Immunity* 41, 1340–1351.

Morampudi, V., Graef, F. A., Stahl, M., Dalwadi, U., Conlin, V. S., Huang, T., Vallane, B. A., Yu, H. B. and Jacobson, K. (2016). Tricellular Tight Junction Protein Tricellulin is Targeted by the Enteropathogenic *Escherichia coli* Effector EspG1, Leading to Epithelial Barrier Disruption. *Infection and Immunity* 85, e00700-16.

Morgan, E., Bowen, A. J., Carnell, S. C., Wallis, T. S. and Stevens, M. P. (2007). SiiE is Secreted by the *Salmonella enterica* Serovar Typhimurium Pathogenicity Island 4-Encoded Secretion System and Contributes to Intestinal Colonization in Cattle. *Infection and Immunity* 75, 1524–1533.

Mounier, J., Vasselon, T., Hellio, R., Lesourd, M. and Sansonetti, P. J. (1992). *Shigella flexneri* Enters Human Colonic Caco-2 Epithelial Cells through the Basolateral Pole. *Infection and Immunity* 60, 237–248.

Mundy, R., Girard, F., FitzGerald, A. J. and Frankel, G. (2006). Comparison of Colonization Dynamics and Pathology of Mice Infected with Enteropathogenic *Escherichia coli*, Enterohaemorrhagic *E. coli* and *Citrobacter rodentium*. *Federation of European Microbiological Societies Microbiology Letters* 265, 126–132.

Murata, K. and Wolf, M. (2018). Cryo-Electron Microscopy for Structural Analysis of Dynamic Biological Macromolecules. *Biochimica et Biophysica Acta – General Subjects* 1862, 324–334.

Nadler, C., Baruch, K., Kobi, S., Mills, E., Haviv, G., Farago, M., Alkalay, I., Bartfeld, S., Meyer, T. F., Ben-Neriah, Y. and Rosenshine, I. (2010). The Type III Secretion Effector NleE Inhibits NF-κB Activation. *Public Library of Science Pathogens* 6, 1–11.

Nagahama, M., Ohkubo, A., Oda, M., Kobayashi, K., Amimoto, K., Miyamoto, K. and Sakurai, J. (2011). *Clostridium perfringens* TpeL Glycosylates the Rac and Ras Subfamily Proteins. *Infection and Immunity* 79, 905–910.

Nagler, A., Lanier, L. L., Cwirla, S. and Phillips, J. H. (1989). Comparative Studies of Human FcRIII-Positive and Negative Natural Killer Cells. *The Journal of Immunology* 143, 3183–3191.

Nair, M. G., Guild, K. J., Du, Y., Zaph, C., Yancopoulos, G. D., Valenzuela, D. M., Murphy, A., Stevens, S., Karow, M. and Artis, D. (2008). Goblet Cell-Derived Resistin-Like Molecule β Augments $CD4^+$ T Cell Production of INF-γ and Infection-Induced Intestinal Inflammation. *The Journal of Immunology* 181, 4709–4715.

Nakatani, K., Sakaue, H., Thompson, D. A., Weigel, R. J. and Roth, R. A. (1999). Identification of a Human Akt3 (Protein Kinase Bγ) which Contains the Regulatory Serine Phosphorylation Site. *Biomedical and Biophysical Research Communications* 257, 906–910.

Narimatsu, H., Ogata, K., Makino, Y. and Ito, K. (2010). Distribution of Non-Locus of Enterocyte Effacement Pathogenic Island-Related Genes in *Escherichia coli* Carrying *eae* from Patients with Diarrhea and Healthy Individuals in Japan. *Journal of Clinical Microbiology* 48, 4107–4114.

Nart, P., Holden, N., McAteer, S. P., Wang, D., Flockhart, A. F., Naylor, S. W., Low, J. C., Gally, D. L. and Huntley, J. F. (2008a). Mucosal Antibody Responses of Colonized Cattle to *Escherichia coli* O157-Secreted Proteins, Flagellin, Outer Membrane Proteins and Lipopolysaccharide. *Federation of European Microbiological Societies Immunology & Medical Microbiology* 52, 59–68.

Nart, P., Naylor, S. W., Huntley, J. F., McKendrick, I. J., Gally, D. L. and Low, J. C. (2008b). Responses of Cattle to Gastrointestinal Colonization by *Escherichia coli* O157:H7. *Infection and Immunity* 76, 5366–5372.

Nasr, A. B., Olsén, A., Sjöbring, U., Müller-Esterl, W. and Björck, L. (1996). Assembly of Human Contact Phase Proteins and Release of Bradykinin at the Surface of Curli-Expressing *Escherichia coli*. *Molecular Microbiology* 20, 927–935.

Nataro, J. P., Deng, Y., Maneval, D. R., German, A. L., Martin, W. C. and Levine, M. M. (1992). Aggregative Adherence Fimbriae I of Enteroaggregative *Escherichia coli* Mediate Adherence to HEp-2 Cells and Hemagglutination of Human Erythrocytes. *Infection and Immunity* 60, 2297–2304.

Nataro, J. P., Maher, K. O., Mackie, P. and Kaper, J. B. (1987). Characterization of Plasmids Encoding the Adherence Factor of Enteropathogenic *Escherichia coli*. *Infection and Immunity* 55, 2370–2377.

Naylor, S. W., Low, J. C., Besser, T. E., Mahajan, A., Gunn, G. J., Pearce, M. C., McKendrick, I. J., Smith, D. G. E. and Gally, D. L. (2003). Lymphoid Follicle-Dense Mucosa at the Terminal Rectum is the Principal Site of Colonization of Enterohemorrhagic *Escherichia coli* O157:H7 in the Bovine Host. *Infection and Immunity* 71, 1505–1512.

Naylor, S. W., Roe, A. J., Nart, P., Spears, K., Smith, D. G. E., Low, J. C. and Gally, D. L. (2005). *Escherichia coli* O157:H7 Forms Attaching and Effacing Lesions at the Terminal Rectum of Cattle and Colonization Requires the LEE4 operon. *Microbiology* 151, 2773–2781.

Neely, M. N. and Friedman, D. I. (1998). Functional and Genetic Analysis of Regulatory Regions of Coliphage H-19B: Location of Shiga-Like Toxin and Lysis Genes Suggest a Role for Phage Functions in Toxin Release. *Molecular Microbiology* 28, 1255–1267.

Neumeister, E. N., Zhu, Y., Richard, S., Terhorst, C., Chan, A. C. and Shaw, A. S. (1995). Binding of ZAP-70 to Phosphorylated T-Cell Receptor Zeta and Eta Enhances its Autophosphorylation and Generates Specific Binding Sites for SH2 Domain-Containing Proteins. *Molecular and Cellular Biology* 15, 3171–3178.

Ng, D., Harn, T., Altindal, T., Kolappan, S., Marles, J. M., Lala, R., Spielman, I., Gao, Y., Hauke, C. A., Kovacikova, G., Verjee, Z., Taylor, R. K., Biais, N. and Craig, L. (2016). The *Vibrio cholerae* Minor Toxin TcpB Initiates Assembly and Retraction of the Toxin-Coregulated Pilus. *Public Library of Science Pathogens* 12, e1006109.

Nicholls, L., Grant, T. H. and Robins-Browne, R. M. (2000). Identification of a Novel Genetic Locus that is Required for *In Vitro* Adhesion of a Clinical Isolate of Enterohaemorrhagic *Escherichia coli* to Epithelial Cells. *Molecular Microbiology* 35, 275–288.

Nika, H., Nieves, E., Hawke, D. H. and Angeletti, R. H. (2013). Optimization of the β-Elimination/Michael Addition Chemistry on Reversed-Phase Supports for Mass Spectrometry Analysis of *O*-Linked Protein Modifications. *Journal of Biomolecular Techniques* 24, 132–153.

Nisa, S., Hazen, T. H., Assatourian, L., Nougayrède, J., Rasko, D. A. and Donnenberg, M. S. (2013). *In Vitro* Evolution of an Archetypal Enteropathogenic *Escherichia coli* Strain. *Journal of Bacteriology* 195, 4476–4483.

Nishikaze, T., Kawabata, S., Iwamoto, S. and Tanaka, K. (2013). Reversible Hydrazide Chemistry-Based Enrichment for *O*-GlcNAc-Modified Peptides and Glycopeptides Having Non-Reducing GlcNAc Residues. *Analyst* 138, 7224–7232.

Nolz, J. C., Gomez, T. S., Zhu, P., Li, S., Medeiros, R. B., Shimizu, Y., Burkhardt, J. K., Freedman, B. D. and Billadeau, D. D. (2006). The WAVE2 Complex Regulates Actin Cytoskeletal Reorganization and CRAC-Mediated Calcium Entry during T Cell Activation. *Current Biology* 16, 24–34.

Nordahl, E. A., Rydengård, V., Mörgelin, M. and Schmidtchen, A. (2005). Domain 5 of High Molecular Weight Kininogen is Antibacterial. *The Journal of Biological Chemistry* 280, 34832–34839.

O'Brien, A. D., Newland, J. W., Miller, S. F., Holmes, R. K., Smith, H. W. and Formal, S. B. (1984). Shiga-Like Toxin-Converting Phage from *Escherichia coli* Strains that Cause Hemorrhagic Colitis or Infantile Diarrhea. *Science* 226, 694–696.

O'Brien, A. D., Lively, T. A., Chen, M. E., Rothman, S. W. and Formal, S. B. (1983). *Escherichia coli* O157:H7 Strains Associated with Haemorrhagic Colitis in the United States Produce a *Shigella dysenteriae* 1 (Shiga) Like Cytotoxin. *The Lancet* 321, 702.

O'Connell, C. B., Creasey, E. A., Knutton, S., Elliot, S., Crowther, L. J., Luo, W., Albert, M. J., Kaper, J. B., Frankel, G. and Donnenberg, M. S. (2004). SepL, a Protein Required for Enteropathogenic *Escherichia coli* Type III Translocation, Interacts with Secretion Component SepD. *Molecular Microbiology* 52, 1613–1625.

Oehmcke-Hecht, S. and Köhler, J. (2018). Interaction of the Human Contact System with Pathogens – An Update. *Frontiers in Immunology* 9, 312.

Ofek, I., Mirelman, D. and Sharon, N. (1997). Adherence of *Escherichia coli* to Human Mucosal Cells Mediated by Mannose Receptors. *Nature* 265, 623–625.

Ogura, Y., Ooka, T., Iguchi, A., Toh, H., Asadulghani, M., Oshima, K., Kodama, T., Abe, H., Nakayama, K., Kurokawa, K., Tobe, T., Hattori, M. and Hayashi, T. (2009). Comparative Genomics Reveal the Mechanism of the Parallel Evolution of O157 and Non-O157 Enterohemorrhagic *Escherichia coli*. *Proceedings of the National Academy of Sciences of the United States of America* 106, 17939–17944.

Ohtani, Y., Irie, T., Uekama, K., Fukunaga, K. and Pitha, J. (1989). Differential Effects of α-, β- and γ-Cyclodextrins on Human Erythrocytes. *European Journal of Biochemistry* 186, 17–22.

Okada, N., Liszewski, M. K., Atkinson, J. P. and Caparon, M. (1995). Membrane Cofactor Protein (CD46) is a Keratinocyte Receptor for the M Protein of the Group A *Streptococcus*. *Proceedings of the National Academy of Sciences of the United States of America* 92, 2489–2493.

Okkenhaug, K., Wu, L., Garza, K. M., La Rose, J., Khoo, W., Odermatt, B., Mak, T. W., Ohashi, P. S. and Rottapel, R. (2001). A Point Mutation in CD28 Distinguishes Proliferative Signals from Survival Signals. *Nature Immunology* 2, 325–332.

Ostroff, S. M., Tarr, P. I., Neill, M. A., Lewis, J. H., Hargrett-Bean, N. and Kobayashi, J. M. (1989). Toxin Genotypes and Plasmid Profiles as Determinants of Systemic Sequelae in *Escherichia coli* O157:H7 Infections. *The Journal of Infectious Diseases* 160, 994–998.

Pacheco, A. R. and Sperandio, V. (2012). Shiga Toxin in Enterohemorrhagic *E. coli*: Regulation and Novel Anti-Virulence Strategies. *Frontiers in Cellular and Infection Microbiology* 2, 1–12.

Paegelow, I., Trzeczak, S., Böckmann, S. and Vietinghoff, G. (2002). Migratory Responses of Polymorphonuclear Leukocytes to Kinin Peptides. *Pharmacology* 66, 153–161.

Pahl, J. H. W., Cerwenka, A. and Ni, J. (2018). Memory-Like NK Cells: Remembering a Previous Activation by Cytokines and NK Cell Receptors. *Frontiers in Immunology* 9, 2796.

Pál, G., Fong, S., Kossiakoff, A. A. and Sidhu, S. S. (2005). Alternative Views of Functional Protein Binding Epitopes Obtained by Combinatorial Shotgun Scanning Mutagenesis. *Protein Science* 14, 2405–2413.

Pan, Z. K., Zuraw, B. L., Lung, C., Prossnitz, E. R., Browning, D. D. and Ye, R. D. (1996). Bradykinin Stimulates NF-Kappa B Activation and Interleukin 1 Beta Gene Expression in Cultured Human Fibroblasts. *The Journal of Clinical Investigation* 98, 2042–2049.

Pantoliano, M. W., Petrella, E. C., Kwasnoski, J. D., Lobanov, V. S., Myslik, J., Graf, E., Carver, T., Asel, E., Springer, B. A., Lane, P. and Salemme, F. R. (2001). High-Density Miniturized Thermal Shift Assays as a General Strategy for Drug Discovery. *Journal of Biomolecular Screening* 6, 429–440.

Papatheodorou, P., Domańska, G., Öxle, M., Mathieu, J., Selchow, O., Kenny, B. and Rassow, J. (2006). The Enteropathogenic *Escherichia coli* (EPEC) Map Effector is Imported into the Mitochondrial Matrix by the TOM/Hsp70 System and Alters Organelle Morphology. *Cellular Microbiology* 8, 677–689.

Papatheodorou, P., Zambogluo, C., Genisyuerek, S., Guttenberg, G. and Aktories, K. (2010). Clostridial Glucosylating Toxins Enter Cells via Clathrin-Mediated Endocytosis. *Public Library of Science ONE* 5, e10673.

Park, H., Teja, K., O'Shea, J. J. and Siegel, R. M. (2007). The *Yersinia* Effector Protein YpkA Induces Apoptosis Independently of Actin Depolymerization. *The Journal of Immunology* 178, 6426–6434.

Park, J., Han, D., Kim, K., Kang, Y. and Kim, Y. (2009). *O*-GlcNAcylation Disrupts Glyceraldehyde-3-Phosphate Dehydrogenase Homo-Tetramer Formation and Mediates its Nuclear Translocation. *Biochimica et Biophysica Acta – Proteins and Proteomics* 1794, 254–262.

Parsot, C. (2009). *Shigella* Type III Secretion Effectors: How, Where, When, for What Purposes? *Current Opinion in Microbiology* 12, 110–116.

Patel, C. H. and Powell, J. D. (2017). Targeting T Cell Metabolism to Regulate T Cell Activation, Differentiation and Function in Disease. *Current Opinion in Immunology* 46, 82–88.

Patterson, R. L., van Rossum, D. B., Kaplin, A. I., Barrow, R. K. and Snyder, S. H. (2005). Inositol 1,4,5-Trisphosphate Receptor/GAPDH Complex Augments Ca^{2+} Release via Locally Derived NADH. *Proceedings of the National Academy of Sciences of the United States of America* 102, 1357–1359.

Paton, A. W. and Paton, J. C. (2010). *Escherichia coli* Subtilase Cytotoxin. *Toxins (Basel)* 2, 215–228.

Pearson, J. S., Giogha, C., Mühlen, S., Nachbur, U., Pham, C. L. L., Zhang, Y., Hildebrand, J. M., Oates, C. V., Lung, T., Ingle, D., Dagley, L. F., Bankovacki, A., Petrie, E. J., Schroeder, G. N., Crepin, V. F., Frankel, G., Masters, S. L., Vince, J., Murphy, J. M., Sunde, M., Webb, A. I., Silke, J. and Hartland, E. L. (2017). EspL is a Bacterial Cysteine Protease Effector that Cleaves RHIM Proteins to Block Necroptosis and Inflammation. *Nature Microbiology* 2, 16258.

Pearson, J. S., Giogha, C., Ong, S. Y., Kennedy, C. L., Kelly, M., Robinson, K. S., Lung, T., Mansel, A., Riedmaler, P., Oates, C. V. L., Zaid, A., Mühlen, S., Crepin, V. F., Marchès, O., Ang, C., Williamson, N. A., O'Reilly, L. A., Bankovaki, A., Nachbur, U., Infusini, G., Webb, A. I., Silke, J., Strasser, A., Frankel, G. and Hartland, E. L. (2013). A Type III Effector Antagonizes Death Receptor Signalling During Bacterial Gut Infection. *Nature* 501, 247–51.

Pearson, J. S., Riedmaier, P., Marchès, O., Frankel, G. and Hartland, E. L. (2011). A Type III Effector Protease NleC from Enteropathogenic *Escherichia coli* Targets NF-κB for Degradation. *Molecular Microbiology* 80, 219–230.

Pedersen, J., Lauritzen, C., Madsen, M. T. and Dahl, S. W. (1999). Removal of N-Terminal Polyhistidine Tags from Recombinant Proteins Using Engineered Aminopeptidases. *Protein Expression and Purification* 15, 389–400.

Peiser, L., Gough, P. J., Kodama, T. and Gordon S. (2000). Macrophage Class A Scavenger Receptor-Mediated Phagocytosis of *Escherichia coli*: Role of Cell Heterogeneity, Microbial Strain, and Culture Conditions *In Vitro*. *Infection and Immunity* 68, 1953–1963.

Peralta-Ramírez, J., Hernandez, J. M., Manning-Cela, R., Luna-Muñoz, J., Garcia-Tovar, C., Nougayréde, J., Oswald, E. and Navarro-Garcia, F. (2008). EspF Interacts with Nucleation-Promoting Factors to Recruit Junctional Proteins into Pedestals for Pedestal Maturation and Disruption of Paracellular Permeability. *Infection and Immunity* 76, 3854–3868.

Perez-Casal, J., Okada, N., Caparon, M. and Scott, J. R. (1995). Role of the Conserved C-Repeat Region of the M Protein of *Streptococcus pyogenes*. *Molecular Microbiology* 15, 907–916.

Perna, N. T., Mayhew, G. F., Pósfai, G., Elliott, S., Donnenberg, M. S., Kaper, J. B. and Blattner, F. R. (1998). Molecular Evolution of a Pathogenicity Island from Enterohemorrhagic *Escherichia coli* O157:H7. *Infection and Immunity* 66, 3810–3817.

Perna, N. T., Plunkett III, G., Burland, V., Mau, B., Glasner, J. D., Rose, D. J., Mayhew, G. F., Evans, P. S., Gregor, J., Kirkpatrick, H. A., Pósfai, G., Hackett, J., Klink, S., Boutin, A., Shao, Y., Miller, L., Grotbeck, E. J., Davis, N. W., Lim, A., Dimalanta, E. T., Potamousis, K. D., Apodaca, J., Anantharaman, T. S., Lin, J., Yen, G., Schwartz, D. C., Welch, R. A. and Blattner F. R. (2001). Genome Sequence of Enterohaemorrhagic *Escherichia coli* O157:H7. *Nature* 409, 529–533.

Peterson, L. W. and Artis, D. (2014). Intestinal Epithelial Cells: Regulators of Barrier Function and Immune Homeostasis. *Nature Reviews* 14, 141–153.

Pfeifer, G., Schirmer, G., Leemhuis, J., Busch, C., Meyer, D. K., Aktories, K. and Barth, H. (2003). Cellular Uptake of *Clostrdium difficile* Toxin B. *The Journal of Biological Chemistry* 278, 44535–44541.

Pierard, D., Huyghens, L. and Lauwers, S. (1991). Diarrhoea Associated with *Escherichia coli* Producing Porcine Oedema Disease Verotoxin. *The Lancet* 338, 762.

Pinaud, L., Samassa, F., Porat, Z., Ferrari, M. L., Belotserkovsky, I., Parsot, C., Sansonetti, P. J., Campbell-Valois, F. and Phalipon, A. (2017). Injection of T3SS Effectors not Resulting in Invasion is the Main Targeting Mechanism of *Shigella* Toward Human Lymphocytes. *Proceedings of the National Academy of Sciences of the United States of America* 114, 9954–9959.

Pless, D. D. and Lennarz, W. J. (1977). Enzymatic Conversion of Proteins to Glycoproteins. *Proceedings of the National Academy of Sciences of the United States of America* 74, 134–138.

Plotnikova, O. V., Seo, S., Cottle, D. L., Conduit, S., Hakim, S., Dyson, J. M., Mitchell, C. A. and Smyth, I. M. (2015). INPP5E Interacts with AURKA, Linking Phosphoinositide Signaling to Primary Cilium Stability. *Journal of Cell Science* 128, 364–372.

Plummer Jr, T. H., Elder, J. H., Alexander, S., Phelan, A. W. and Tarentino, A. L. (1984). Demonstration of Peptide:N-Glycosidase F Activity in Endo-Beta-N-Acetylglucosaminidase F preparations. *The Journal of Biological Chemistry* 259, 10700–10704.

Pollard, D. J., Berger, C. N., So, E. C., Yu, L., Hadavizadeh, K., Jennings, P., Tate, E. W., Choudhary, J. S. and Frankel, G. (2018). Broad-Spectrum Regulation of Nonreceptor Tyrosine Kinases by the Bacterial ADP-Ribosyltransferase EspJ. *mBio* 9, e00170-18.

Poncz, M., Solowiejczyk, D., Ballantine, M., Schwartz, E. and Surrey, S. (1982). "Nonrandom" DNA Sequence Analysis in Bacteriophage M13 by the Dideoxy Chain-Termination Method. *Proceedings of the National Academy of Sciences of the United States of America* 79, 4298–4302.

Porchia, L. M., Guerra, M., Wang, Y., Zhang, Y., Espinosa, A. V., Shinohara, M., Kulp, S. K., Kirschner, L. S., Saji, M., Chen, C. and Ringel, M. D. (2007). 2-Amino-*N*-{4-[5-(2-Phenanthrenyl)-3-(Trifluoromethyl)-1*H*-Pyrazol-1-yl]-Phenyl} Acetamide (OSU-03012), a Celecoxib Derivative, Directly Targets p21-Activated Kinase. *Molecular Pharmacology* 72, 1124–1131.

Pósfai, G., Koob, M. D., Kirkpatrick, H. A. and Blattner, F. R. (1997). Versatile Insertion Plasmids for Targeted Genome Manipulations in Bacteria: Isolation, Deletion, and Rescue of the Pathogenicity Island LEE of the *Escherichia coli* O157:H7 Genome. *Journal of Bacteriology* 179, 4426–4428.

Prasad, K. V. S., Kapeller, R., Janssen, O., Repke, H., Duke-Cohan, J. S., Cantley, L. C. and Rudd, C. E. (1993). Phosphatidylinositol (PI) 3-Kinase and PI 4-Kinase Binding to the CD4-p56lck Complex: The p56lck SH3 Domain Binds to PI 3-Kinase but not PI 4-Kinase. *Molecular and Cellular Biology* 13, 7708–7717.

Price, N. C., Dwek, R. A., Ratcliffe, R. G and Wormald, M. R. (2007). Binding of Ligands to Macromolecules. *Principles and Problems in Physical Chemistry for Biochemists Third Edition*, pp. 54–73. Oxford University Press, New York.

Price, N. C. and Nairn, J. (2009). Spectroscopic Methods to Study Secondary and Tertiary Structure. *Exploring Proteins*, pp. 358–365. Oxford University Press, New York.

Prokopowicz, Z., Marcinkiewicz, J., Katz, D. R. and Chain, B. M. (2012). Neutrophil Myeloperoxidase: Soldier and Statesman. *Archivum Immunologiae at Therapiae Experimentalis* 60, 43–54.

Promega (2012). *CellTitre 96® AQ$_{ueous}$ One Solution Cell Proliferation Assay Technical Bulletin*. URL: https://www.promega.com/-/media/files/resources/protocols/technical-bulletins/0/celltiter-96-aqueous-one-solution-cell-proliferation-assay-system-protocol.pdf. Accessed: 17/07/2019.

Pruimboom-Brees, I. M., Morgan, T. W., Ackermann, M. R., Nystrom, E. D., Samuel, J. E., Cornick, N. A. and Moon, H. W. (2000). Cattle Lack Vascular Receptors for *Escherichia coli* O157:H7 Shiga Toxins. *Proceedings of the National Academy of Sciences of the United States of America* 97, 10325–10329.

Pruitt, R. N., Chagot, B., Cover, M., Chazin, W. J., Spiller, B. and Lacy, D. B. (2009). Structure-Function Analysis of Inositol Hexakisphosphate-Induced Autoprocessing in *Clostridium difficile* Toxin A. *The Journal of Biological Chemistry* 284, 21934–21940.

Pruitt, R. N., Chambers, M. G., Ng, K. K., Ohi, M. D. and Lacy, D. B. (2010). Structural Organization of the Functional Domains of *Clostridium difficile* Toxins A and B. *Proceedings of the National Academy of Sciences of the United States of America* 107, 13467–13472.

Pruitt, R. N., Chumbler, N. M., Rutherford, S. A., Farrow, M. A., Friedman, D. B., Spiller, B. and Lacy, D. B. (2012). Structural Determinants of *Clostridium difficile* Toxin A Glucosyltransferase Activity. *The Journal of Biological Chemistry* 287, 8013–8020.

Puckett, M. C. (2015). Hexahistidine (6xHis) Fusion-Based Assays for Protein-Protein Interactions. *Methods in Molecular Biology vol. 1278: Protein-Protein Interactions, Methods and Applications Second Edition*, pp. 365–370. Humana Press, New York.

Puente, J. L., Bieber, D., Ramer, S. W., Murray, W. and Schoolnik, G. K. (1996). The Bundle-Forming Pili of Enteropathogenic *Escherichia coli*: Transcriptional Regulation by Environmental signals. *Molecular Microbiology* 20, 87–100.

Qa'dan, M., Sypres, L. M. and Ballard, J. D. (2000). pH-Induced Conformational Changes in *Clostridium difficile* Toxin B. *Infection and Immunity* 68, 2470–2474.

Qa'dan, M., Sypres, L. M. and Ballard, J. D. (2001). pH-Enhanced Cytopathic Effects of *Clostridium sordellii* Lethal Toxin. *Infection and Immunity* 69, 5487–5493.

Qin, W., Lv, P., Fan, X., Quan, B., Zhu, Y., Qin, K., Chen, Y., Wang, C. and Chen, X. (2017). Quantitative Time-Resolved Chemoproteomics Reveals that Stable O-GlcNAc Regulates Box C/D snoRNP Biogenesis. *Proceedings of the National Academy of Sciences of the United States of America* 144, E6749–E6758.

Quilliam, L. A., Lacal, J. and Bokoch, G. M. (1989). Identification of *rho* as a Substrate for Botulinum Toxin C_3-Catalyzed ADP-Ribosylation. *Federation of European Biochemical Societies Letters* 247, 221–226.

Quitard, S., Dean, P., Maresca, M. and Kenny, B. (2006). The Enteropathogenic *Escherichia coli* EspF Effector Molecule Inhibits PI 3-Kinase-Mediated Uptake Independently of Mitochondrial Targeting. *Cellular Microbiology* 8, 972–981.

Rappsilber, J., Mann, M. and Ishihama, Y. (2007). Protocol for Micro-Purification, Enrichment, Pre-Fractionation and Storage of Peptides for Proteomics Using StageTips. *Nature Protocols* 2, 1896–1906.

Rasko, D. A., Moreira, C. G., Li, D. R., Reading, N. C., Ritchie, J. M., Waldor, M. K., William, N., Taussig, R., Wei, S., Roth, M., Hughes, D. T., Huntley, J. F., Fina, M. W., Falck, J. R. and Sperandio, V. (2008). Targeting QseC Signaling and Virulence for Antibiotic Development. *Science* 321, 1078–1080.

Reeves, E. P., Lu, H., Jacobs, H. L., Messina, C. G. M., Bolsover, S., Gabella, G., Potma, E. O., Warley, A., Roes, J. and Segal, A. W. (2002). Killing Activity of Neutrophils is Mediated through Activation of Proteases by K^+ Flux. *Nature* 416, 291–297.

Reif, K., Lucas, S. and Cantrell, D. (1997). A Negative Role for Phosphoinositide 3-Kinase in T-Cell Antigen Receptor Function. *Current Biology* 7, 285–293.

Reineke, J., Tenzer, S., Rupnik, M., Koschinski, A., Hasselmayer, O., Schrattenholz, A., Schild, H. and von Eichel-Streiber, C. (2007). Autocatalytic Cleavage of *Clostridium difficile* Toxin B. *Nature* 446, 415–419.

Rejraji, H., Vernet, P. and Drevet, J. R. (2002). GPX5 is Present in the Mouse Caput and Cauda Epididymidis Lumen at Three Different Locations. *Molecular Reproduction and Development* 63, 96–103.

Rheinländer, A., Schraven, B. and Bommhardt, U. (2018). CD45 in Human Physiology and Clinical Medicine. *Immunology Letters* 196, 22–32.

Riley, L. W., Remis, R. S., Helgerson, S. D., McGee, H. B., Wells, J. G., Davis, B. R., Hebert, R. J., Olcott, E. S., Johnson, L. M., Hargrett, N. T., Blake, P. A. and Cohen, M. L. (1983). Hemorrhagic Colitis Associated with a Rare *Escherichia coli* Serotype. *The New England Journal of Medicine* 308, 681–685.

Riquelme-Neira, R., Rivera, A., Sáez, D., Fernández, P., Osorio, G., del Canto, F., Salazar, J. C., Vidal, R. M. and Oñare, A. (2016). Vaccination with DNA Encoding Truncated Enterohemorrhagic *Escherichia coli* (EHEC) Factor for Adherence-1 Gene (*efa-1'*) Confers Protective Immunity to Mice Infected with *E. coli* O157:H7. *Frontiers in Cellular and Infection Microbiology* 5, 104.

Ritchie, J. M., Thorpe, C. M., Rogers, A. B. and Waldor, M. K. (2003). Critical Roles for *stx2*, *eae*, and *tir* in Enterohemorrhagic *Escherichia coli*-Induced Diarrhea and Intestinal Inflammation in Infant Rabbits. *Infection and Immunity* 81, 7129–7139.

Ritz, C., Baty, F., Streibig, J. C. and Gerhard, D. (2015). Dose-Response Analysis Using R. *Public Library of Science ONE* 10, e0146021.

Rivero, F., Kuspa, A., Brokamp, R., Matzner, M. and Noegel, A. A. (1998). Interaptin, an Actin-Binding Protein of the α-Actinin Superfamily in *Dictyostelium discoides*, Is Developmentally and cAMP-Regulated and Associates with Intracellular Membrane Compartments. *The Journal of Cell Biology* 142, 735–750.

Robinson, C. M., Sinclair, J. F., Smith, M. J. and O'Brien, A. D. (2006). Shiga Toxin of Enterohemorrhagic *Escherichia coli* Type O157:H7 Promotes Intestinal Colonization. *Proceedings of the National Academy of Sciences of the United States of America* 103, 9667–9672.

Rock, K. L., Gramm, C., Rothstein, L., Clark, K., Stein, R., Dick, L., Hwang, D. and Goldberg, A. L. (1994). Inhibitors of the Proteasome Block the Degradation of Most Cell Proteins and the Generation of Peptides Presented on MHC Class I Molecules. *Cell* 78, 761–771.

Römer, W., Berland, L., Chambon, V., Gaus, K., Windschiegl, B., Tenza, D., Aly, M. R. E., Fraisier, V., Florent, J., Perrais, D., Lamaze, C., Raposo, G., Steinem, C., Sens, P., Bassereau, P. and Johannes, L. (2007). Shiga Toxin Induces Tubular Membrane Invaginations for its Uptake into Cells. *Nature* 450, 670–675.

Rosenshine, I., Donnenberg, M. S., Kaper, J. B. and Finlay, B. B. (1992). Signal Transduction between Enteropathogenic *Escherichia coli* (EPEC) and Epithelial Cells: EPEC Induces Tyrosine Phosphorylation of Host Cell Proteins to Initiate Cytoskeletal Rearrangement and Bacterial Uptake. *The European Molecular Biology Organization Journal* 11, 3551–3560.

Rosenshine, I., Ruschkowski, S. and Finlay, B. B. (1996). Expression of Attaching/Effacing Activity by Enteropathogenic *Escherichia coli* Depends on Growth Phase, Temperature, and Protein Synthesis upon Contact with Epithelial Cells. *Infection and Immunity* 64, 966–973.

Rosqvist, R., Magnusson, K. E. and Wolf-Watz, H. (1994). Target Cell Contact Triggers Expression and Polarized Transfer of *Yersinia* YopE Cytotoxin into Mammalian Cells. *The European Molecular Biology Organization Journal* 13, 964–972.

Ross, G. D., Reed, W., Dalzell, J. G., Becker, S. E. and Hogg, N. (1992). Macrophage Cytoskeleton Association with CR3 and CR4 Regulates Mobility and Phagocytosis of iC3b-Opsonized Erythrocytes. *Journal of Leukocyte Biology* 51, 109–117.

Ross, S. H. and Cantrell, D. A. (2018). Signaling and Function of Interleukin-2 in T Lymphocytes. *Annual Review of Immunology* 36, 411–433.

Rossi, M., Bolz, C., Revez, J., Javed, S., El-Najjar, N., Anderl, F., Hyytiäinen, H., Vuorela, P., Gerhard, M. and Hänninen, M. (2012). Evidence for Conserved Function of γ-Glutamyltranspeptidase in *Helicobacter* Genus. *Public Library of Science ONE* 7, e305423.

Rothbaum, R., McAdams, A. J., Giannella, R. and Partin, J. C. (1982). A Clinicopathologic Study of Enteroctye-Adherent *Escherichia coli*: A Cause of Protracted Diarrhea in Infants. *Gastroenterology* 83, 441–454.

Roxas, J. L., Wilbur, J. S., Zhang, X., Martinez, G., Vedantam, G. and Viswanathan, V. W. (2012). The Enteropathogenic *Escherichia coli*-Secreted Protein EspZ Inhibits Host Cell Apoptosis. *Infection and Immunity* 80, 3850–3857.

Royan, S. V., Jones, R. M., Koutsouris, A., Roxas, J. L., Flazari, K., Weflen, A. W., Kim, A., Bellmeyer, A., Turner, J. R., Neish, A. S., Rhee, K., Viswanathan, V. K. and Hecht, G. A. (2010). Enteropathogenic *E. coli* Non-LEE Encoded Effectors NleH1 and NleH2 Attenuate NF-Kb Activation. *Molecular Microbiology* 78, 1232–1245.

Rozenski, J., Crain, P. F. and McCloskey, J. A. (1999). The RNA Modification Database: 1999 Update. *Nucleic Acids Research* 27, 196–197.

Ruchaud-Sparagano, M., Maresca, M. and Kenny, B. (2007). Enteropathogenic *Escherichia coli* (EPEC) Inactivate Innate Immune Responses Prior to Compromising Epithelial Barrier Function. *Cellular Microbiology* 9, 1909–1921.

Rudd, C. E., Trevillyan, J. M., Dasgupta, J. D., Wong, L. L. and Schlossman, S. F. (1988). The CD4 Receptor is Complexed in Detergent Lysates to a Protein-Tyrosine Kinase (pp58) from Human T Lymphocytes. *Proceedings of the National Academy of Sciences of the United States of America* 85, 5190–5194.

Rupnik, M., Pabst, S., Rupnik, M., von Eichel-Streiber, C., Urlaub, H. Söling, H. (2005). Characterization of the Cleavage Site and Function of Resulting Cleavage Fragments after Limited Proteolysis of *Clostridium difficile* Toxin B (TcdB) by Host Cells. *Microbiology* 151, 199–208.

Ruvkun, G. B. and Ausubel, F. M. (1981). A General Method for Site-Directed Mutagenesis in Prokaryotes. *Nature* 289, 85–88.

Sahlin, S., Hed, J. and Runfquist, I. (1983). Differentiation between Attached and Ingested Immune Complexes by a Fluorescence Quenching Cytofluorometric Assay. *Journal of Immunological Methods* 60, 115–124.

Sakaidani, Y., Nomura, T., Matsuura, A., Ito, M., Suzuki, E., Murakami, K., Nadano, D., Matsuda, T., Furukawa, K. and Okajima, T. (2011). O-Linked-N-Acetylglucosamine on Extracellular Protein Domains Mediates Epithelial Cell–Matrix Interactions. *Nature Communications* 2, 583.

Sakr, S. W., Eddy, R. J., Barth, H., Wang, F., Grennberg, S., Maxfield, F. R. and Tabas, I. (2001). The Uptake and Degradation of Matrix-Bound Lipoproteins by Macrophages Require an Intact Actin Cytoskeleton, Rho Family GTPases, and Myosin ATPase Activity. *The Journal of Biological Chemistry* 276, 37649–37658.

Salama, N. R., Otto, G., Tompkins, L. and Falkow, S. (2001). Vacuolating Cytotoxin of *Helicobacter pylori* Plays a Role during Colonization in a Mouse Model of Infection. *Infection and Immunity* 69, 730–736.

Saldaña, Z., Erdem, A. L., Schüller, S., Okeke, I. N., Lucas, M., Sivananthan, A., Phillips, A. D., Kaper, J. B., Puente, J. L. and Girón, J. A. (2009). The *Escherichia coli* Common Pilus and the Bundle-Forming Pilus Act in Concert During the Formation of Localized Adherence by Enteropathogenic *E. coli*. *Journal of Bacteriology* 191, 3451–3461.

Salgado-Pabón, W., Celli, S., Arena, E. T., Nothelfer, K., Roux, P., Sellge, G., Frigimelica, E., Bousso, P., Sansonetti, P. J. and Phalipon, A. (2013). *Shigella* Impairs T Lymphocyte Dynamics *In Vivo*. *Proceedings of the National Academy of Sciences of the United States of America* 110, 4458–4463.

Samba-Louaka, A., Nougayrède, J., Watrin, C., Oswald, E. and Taieb, F. (2009). The Enteropathogenic *Escherichia coli* Effector Cif Induces Delayed Apoptosis in Epithelial Cells. *Infection and Immunity* 77, 5471–5477.

Samelson, L. E., Harford, J. B. and Klausner, R. D. (1985). Identification of the Components of the Murine T Cell Antigen Receptor Complex. *Cell* 43, 223–231.

Samson, F., Donoso, J. A., Heller-Bettinger, I., Watson, D. and Himes, R. H. (1979). Nocodazole Action on Tubulin Assembly, Axonal Ultrastructureand Fast Axoplasmic Transport. *The Journal of Pharmacology and Experimental Therapeutics* 208, 411–417.

Sánchez, J., Wallerström, G., Fredriksson, M., Ångström, J. and Holmgren, J. (2002). Detoxification of Cholera Toxin without Removal of its Immunoadjuvanticity by the Addition of (STa-Related) Peptides to the Catalytic Subunit. *The Journal of Biological Chemistry* 277, 33369–33377.

Sandkvist, M., Michel, L. O., Hough, L. P., Morales, V. M., Bagdasarian, M., Koomey, M., DiRita, V. J. and Bagdasarian, M. (1997). General Secretion Pathway (*eps*) Genes Required for Toxin Secretion and Outer Membrane Biogenesis in *Vibrio cholerae*. *Journal of Bacteriology* 179, 6994–7003.

Sandvig, K., Garred, Ø., Prydz, K., Kozlov, J. V., Hansen, S. T. and van Deurs, B. (1992). Retrograde Transport of Endocytosed Shiga Toxin to the Endoplasmic Reticulum. *Nature* 358, 510–512.

Sandvig, K., Olsnes, S., Brown, J. E., Peterson, O. W. and van Deurs, B. (1989). Endocytosis from Coated Pits of Shiga Toxin: A Glycolipid-Binding Protein from *Shigella dysenteriae* 1. *Journal of Cell Biology* 108, 1331–1343.

Sanger, J. M., Chang, R., Ashton, F., Kaper, J. B. and Sanger, J. W. (1996). Novel Form of Actin-Based Motility Transports Bacteria on the Surface of Infected Cells. *Cell Motilily and the Cytoskeleton* 34, 279–287.

Sansonetti, P. J., Arondel, J., Catley, J. R., Prévost, M. and Huerre, M. (1996). Infection of Rabbit Peyer's Patches by *Shigella flexneri*: Effect of Adhesive or Invasive Bacterial Phenotypes on Follicle-Associated Epithelium. *Infection and Immunity* 64, 2752–2764.

Santos, A. S. and Finlay, B. B. (2015). Bringing Down the Host: Enteropathogenic and Enterohaemorrhagic *Escherichia coli* Effector-Mediated Subversion of Host Innate Immune Pathways. *Cellular Microbiology* 17, 318–332.

Sarbassov, D. D., Guertin, D. A., Ali, S. M. and Sabatini, D. M. (2005). Phosphorylation and Regulation of Akt/PKB by the Rictor-mTOR Complex. *Science* 307, 1098–1101.

Sarowska, J., Futoma-Koloch, B., Jama-Kmiecik, A., Frej-Madrzak, M., Ksiazczyk, M., Bugla-Ploskonska, G. and Choroszy-Krol, I. (2019). Virulence Factors, Prevalence and Potential Transmission of Extraintestinal Pathogenic *Escherichia coli* Isolated from Different Sources: Recent Reports. *Gut Pathogens* 11, 10.

Sason, H., Milgrom, M., Weiss, A. M., Melamed-Book, N., Balla, T., Grinstein, S., Backert, S., Rosenshine, I. and Aroeti, B. (2009). Enteropathogenic *Escherichia coli* Subverts Phosphatidylinositol 4,5-Bisphosphate and Phosphatidylinositol 3,4,5-Trisphosphate upon Epithelial Cell Infection. *Molecular Biology of the Cell* 20, 544–555.

Sato, E., Koyama, S., Nomura, H., Kubo, K. and Sekiguchi, M. (1996). Bradykinin Stimulates Alveolar Macrophages to Release Neutrophil, Monocyte, and Eosinophil Chemotactic Activity. *The Journal of Immunology* 157, 3122–3129.

Sauvonnet, N., Lambermont, I., van der Bruggen, P. and Cornelis, G. R. (2002). YopH Prevents Monocyte Chemoattractant Protein 1 Expression in Macrophages and T-Cell Proliferation through Inactivation of the PhosphatidylinositoI 3-Kinase Pathway. *Molecular Microbiology* 45, 805–815.

Savina, A., Jancic, C., Hugues, S., Guermonprez, P., Vargas, P., Moura, I. C., Lennon-Duménil, A., Seabra, M. C., Raposo, G. and Amigorena, S. (2006). NOX2 Controls Phagosomal pH to Regulate Antigen Processing during Crosspresentation by Dendritic Cells. *Cell* 126, 205–218.

Savkovic, S. D., Koutsouris, A. and Hecht, G. (1996). Attachment of a Noninvasive Enteric Pathogen, Enteropathogenic *Escherichia coli*, to Cultured Human Intestinal Epithelial Monolayers Induces Transmigration of Neutrophils. *Infection and Immunity* 64, 4480–4487.

Savkovic, S. D., Koutsouris, A. and Hecht, G. (1997). Activation of NF-κB in Intestinal Epithelial Cells by Enteropathogenic *Escherichia coli*. *The American Journal of Physiology* 273, 1160–1167.

Scaletsky, I. C. A., Silva, L. M. L. and Trabulsi, L. R. (1984). Distinctive Patterns of Adherence of Enteropathogenic *Escherichia coli* to HeLa Cells. *Infection and Immunity* 45, 534–536.

Schäfer, F., Schäfer, A. and Steinert, K. (2002). A Highly Specific System for Efficient Enzymatic Removal of Tags from Recombinant Proteins. *Journal of Biomolecular Techniques* 13, 158–171.

Schaut, R. G., Boggiatto, P. M., Loving, C. L. and Sharma, V. K. (2019). Cellular and Mucosal Immune Responses Following Vaccination with Inactivated Mutant of *Escherichia coli* O157:H7. *Scientific Reports* 9, 6401.

Schirmer, J. and Aktories, K. (2004). Large Clostridial Cytotoxins: Cellular Biology of Rho/Ras-Glucosylating Toxins. *Biochimica et Biophysica Acta – General Subjects* 1673, 66–74.

Schmees, C., Prinz, C., Treptau, T., Rad, R., Hengst, L., Voland, P., Bauer, S., Brenner, L., Schmid, R. M. and Gerhard, M. (2007). Inhibition of T-Cell Proliferation by *Helicobacter pylori* γ-Glutamyl Transpeptidase. *Gastroenterology* 132, 1820–1833.

Schmidt, R. L. J., Jutz, S., Goldhahn, K., Witzeneder, N., Gerner, M. C., Trapin, D., Greiner, G., Hoermann, G., Steiner, G., Pickl, W. F., Burgmann, H., Steinberger, P., Ratzinger, F. and Schmetterer, K. G. (2017). Chloroquine Inhibits Human $CD4^+$ T-Cell Activation by AP-1 Signaling Modulation. *Scientific Reports* 7, 42191.

Schnitzer, J. E., Oh, P., Pinney, E. and Allard, J. (1994). Filipin-Sensitive Caveolae-Mediated Transport in Endothelium: Reduced Transcytosis, Scavenger Endocytosis, and Capillary Permeability of Select Macromolecules. *The Journal of Cell Biology* 127, 1217–1232.

Schorch, B., Song, S., van Diemen, F. R., Bock, H. H., May, P., Herz, J., Brummelkamp, T. R., Papatheodorou, P. and Aktories, K. (2014). LPR1 is a Receptor for *Clostridium perfringens* TpeL Toxin Indicating a Two-Receptor Model of Clostridial Glycosylating Toxins. *Proceedings of the National Academy of Sciences of the United States of America* 111, 6431–6436.

Schüller, S., Frankel, G. and Phillips, A. D. (2004). Interaction of Shiga Toxin from *Escherichia coli* with Human Intestinal Epithelial Cell Lines and Explants: Stx2 Induces Epithelial Damage in Organ Culture. *Cellular Microbiology* 6, 289–301.

Schulte, T., Löfling, J., Mikaelsson, C., Kikhney, A., Hentrich, K., Diamante, A., Ebel, C., Normark, S., Svergun, D., Henriques-Normark, B. and Achou, A. (2014). The Basic Keratin 10-Binding Domain of the Virulence-Associated Pneumococcal Serine-Rich Protein PsrP Adopts a Novel MSCRAMM Fold. *Open Biology* 4, 130090.

Segal, A. W., Geisow, M., Garcia, R., Harper, A. and Miller, R. (1981). The Respiratory Burst of Phagocytic Cells is Associated with a Rise in Vacuolar pH. *Nature* 290, 406–409.

Selyunin, A. S., Sutton, S. E., Weigele, B. A., Reddick, L. E., Orchard, R. C., Bresson, S. M., Tomchick, D. R. and Alto, N. M. (2011). The Assembly of a GTPase–Kinase Signalling Complex by a Bacterial Catalytic Scaffold. *Nature* 469, 107–111.

Selzer, J., Hofmann, Rex, G., Wilm, M., Mann, M., Just, I. and Aktories, K. (1996). *Clostridium novyi* α-Toxin-Catalyzed Incorporation of GlcNAc into Rho Subfamily Proteins. *The Journal of Biological Chemistry* 271, 25173–25177.

Servin, A. L. (2014). Pathogenesis of Human Diffusely Adhering *Escherichia coli* Expressing Afa/Dr Adhesins (Afa/Dr DAEC): Current Insights and Future Challenges. *Clinical Microbiology Reviews* 27, 823–869.

Seveau, S., Keller, H., Maxfield, F. R., Piller, F. and Halbwachs-Mecarelli, L. (2000). Neutrophil Polarity and Locomotion are Associated with Surface Redistribution of Leukosialin (CD43), an Antiadhesive Membrane Molecule. *Blood* 95, 2462–2470.

Sewald, X., Gebert-Vogl, B., Prassl, S., Barwig, I., Weiss, E., Fabbri, M., Osicka, R., Schiemann, M., Busch, D. H., Semmrich, M., Holzmann, B., Sebo, P. and Haas, R. (2008). Integrin Subunit CD18 is the T-Lymphocyte Receptor for the *Helicobacter pylori* Vacuolating Cytotoxin. *Cell Host & Microbe* 3, 20–29.

Sewald, X., Jiménez-Soto, L. and Haas, R. (2010). PKC-Dependent Endocytosis of the *Helicobacter pylori* Vacuolating Cytotoxin in Primary T Lymphocytes. *Cellular Microbiology* 13, 482–496.

Shames, S. R., Croxen, M. A., Deng, W. and Finlay, B. B. (2011). The Type III System-Secreted Effector EspZ Localizes to Host Mitochondria and Interacts with the Translocase of Inner Mitochondrial Membrane 17b. *Infection and Immunity* 79, 4784–4790.

Shames, S. R., Deng, W., Guttman, J. A., de Hoog, C. L., Li, Y., Hardwidge, P. R., Sham, H. P., Vallance, B. A., Foster, L. J. and Finlay, B. B. (2010). The Pathogenic *E. coli* Type III Effector EspZ Interacts with Host CD98 and Facilitates Host Cell Prosurvival Signalling. *Cellular Microbiology* 12, 1322–1339.

Shao, F., Golstein, C., Ade, J., Stoutemeyer, M., Dixon, J. E. and Innes, R. W. (2003a). Cleavage of *Arabidopsis* PBS1 by a Bacterial Type III Effector. *Science* 301, 1230–1233.

Shao, F., Merritt, P. M., Bao, Z., Innes, R. W. and Dixon, J. E. (2002). A *Yersinia* Effector and a *Pseudomonas* Avirulence Protein Define a Family of Cysteine Proteases Functioning in Bacterial Pathogenesis. *Cell* 109, 575–588.

Shao, F., Vacratsis, P. O., Bao, Z., Bowers, K. E., Fierke, C. A. and Dixon, J. E. (2003b). Biochemical Characterization of the *Yersinia* YopT Protease: Cleavage Site and Recognition Elements in Rho GTPases. *Proceedings of the National Academy of Sciences of the United States of America* 100, 904–909.

Shaw, R. K., Smollett, K., Cleary, J., Garmendia, J., Straatman-Iwanowska, A., Frankel, G. and Knutton, S. (2005). Enteropathogenic *Escherichia coli* Type III Effectors EspG and EspG2 Disrupt the Microtubule Network of Intestinal Epithelial Cells. *Infection and Immunity* 73, 4385–4390.

Sheridan, B. S., Romagnoli, P. A., Pham, Q., Fu, H., Alonzo III, F., Schubert, W., Freitag, N. E. and Lefrançois, L. (2013). γδ T Cells Exhibit Multifunctional and Protective Memory in Intestinal Tissues. *Immunity* 39, 184–195.

Sherman, P., Drumm, B, Karmali, M. and Cutz, E. (1989). Adherence of Bacteria to the Intestine in Sporadic Cases of Enteropathogenic *Escherichia coli*-Associated Diarrhea in Infants and Young Children: A Prospective Study. *Gastroenterology* 96, 86–94.

Shevchenko, A., Tomas, H., Havli, J., Olsen, J. V. and Mann, M. (2006). In-Gel Digestion for Mass Spectrometric Characterization of Proteins and Proteomes. *Nature Protocols* 1, 2856–2860.

Shevchenko, A. Wilm, M., Vorm, O. and Mann, M. (1996). Mass Spectrometric Sequencing of Proteins from Silver-Stained Polyacrylamide Gels. *Analytical Chemistry* 68, 850–858.

Shi, J., Gu, J., Dai, C., Gu, J., Jin, X., Sun, J., Iqbal, K., Liu, F. and Gong, C. (2015). O-GlcNAcylation Regulates Ischemia-Induced Neuronal Apoptosis through AKT Signaling. *Scientific Reports* 5, 14500.

Shibata, K., Yamada, H., Hara, H., Kishihara, K. and Yoshikai, Y. (2007). Resident Vδ1$^+$ γδ T Cells Control Early Infiltration of Neutrophils after *Escherichia coli* Infection via IL-17 Production. *The Journal of Immunology* 178, 4466–4472.

Shishido, S. N., Varahan, S., Yuan, K., Li, X. and Fleming, S. D. (2012). Humoral Innate Immune Response and Disease. *Clinical Immunology* 144, 142–158.

Shivtiel, S., Kollet, O., Lapid, K., Goichberg, P., Kalinkovich, A., Shezen, E., Tesio, M., Netzer, N., Petit, I., Sharir, A. and Lapidot, T. (2008). CD45 Regulates Retention, Motility, and Numbers of Hematopoietic Progenitors, and Affects Osteoclast Remodeling of Metaphyseal Trabecules. *Journal of Experimental Medicine* 205, 2381–2395.

Shresta, S., MacIvor, D. M., Heusel, J. W., Russell, J. H. and Ley, T. J. (1995). Natural Killer and Lymphokine-Activated Killer Cells Require Granzyme B for the Rapid Induction of Apoptosis in Susceptible Target Cells. *Proceedings of the National Academy of Sciences of the United States of America* 92, 5679–5683.

Sigma-Aldrich (2019). *Protease Fluorescent Detection Kit Technical Bulletin*. URL: https://www.sigmaaldrich.com/content/dam/sigma-aldrich/docs/Sigma/Bulletin/1/pf0100bul.pdf. Accessed 17/07/2019.

Silva, A., Wang, J., Lomahan, S., Tran, T., Grenlin, L., Suganami, A., Tamura, Y. and Ikegaki, N. (2014). Aurora Kinase A is a Possible Target of OSU-03012 to Destabilize MYC Family Proteins. *Oncology Reports* 32, 901–905.

Silverman, J. A., Mindell, J. A., Finkelstein, A., Shen, W. H. and Collier, R. J. (1994). Mutational Analysis of the Helical Hairpin Region of Diptheria Toxin Transmembrane Domain. *The Journal of Biological Chemistry* 269, 22524–22532.

Simeoni, L. (2017). Lck Activation: Puzzling the Pieces Together. *Oncotarget* 8, 102761–102762.

Simmons, C. P., Clare, S., Ghaem-Maghami, M., Uren, T. K., Rankin, J., Huett, A., Goldin, R., Lewis, D. J., MacDonald, T. T., Strugnell, R. A., Frankel, G. and Dougan, G. (2003). Central Role for B Lymphocytes and $CD4^+$ T Cells in Immunity to Infection by the Attaching and Effacing Pathogen *Citrobacter rodentium*. *Infection and Immunity* 71, 5077–5086.

Sinclair, J. F. and O'Brien, A. D. (2002). Cell Surface-Localized Nucleolin is a Eukaryotic Receptor for the Adhesin Intimin-γ of Enterohemorrhagic *Escherichia coli* O157:H7. *The Journal of Biological Chemistry* 277, 2876–2885.

Sinclair, J. F. and O'Brien, A. D. (2004). Intimin Types α, β, and γ Bind to Nucleolin with Equivalent Affinity but Lower Avidity than to the Translocated Intimin Receptor. *The Journal of Biological Chemistry* 279, 33751–33758.

Sinclair, L. V., Finlay, D., Feijoo, C., Cornish, G. H., Gray, A., Ager, A., Okkenhaug, K., Hagenbeek, T. J., Spits, H. and Cantrell, D. A. (2008). Phosphoinositide 3-Kinase (PI3K) and Nutrient Sensing mTOR (Mammalian Target of Rapamycin) Pathways Control T Lymphocyte Trafficking. *Nature Immunology* 9, 513–521.

Singh, V., Davidson, A., Hume, P. J. and Koronakis, V. (2019). Pathogenic *Escherichia coli* Hijacks GTPase-Activated p21-Activated Kinase for Actin Pedestal Formation. *mBio* 10, e01876-19.

Slater, S. L., Sågfors, A. M., Pollard, D. J., Ruano-Gallego, D. and Frankel, G. (2018). The Type III Secretion System of Pathogenic *Escherichia coli*. *Current Topics in Microbiology and Immunology vol. 416: Escherichia coli, a Versatile Pathogen*, pp. 51–72. Springer Nature, Cham.

Slinger, R., Lau, K., Slinger, M., Moldovan, I. and Chan, F. (2017). Higher Atypical Enteropathogenic *Escherichia coli* (a-EPEC) Bacterial Loads in Children with Diarrhea are Associated with PCR Detection of the EHEC Factor for Adherence 1/Lymphocyte Inhibitory Factor A (*efa1*/*lifa*) Gene. *Annals of Clinical Microbiology and Antimicrobials* 16, 16.

Sloan, D. D. and Jerome, K. R. (2007). Herpes Simplex Virus Remodels T-Cell Receptor Signaling, Resulting in p38-Dependent Selective Synthesis of Interleukin-10. *Journal of Virology* 81, 12504–12514.

Smart, E., J., Foster, D. C., Ying, Y., Kamen, B. A. and Anderson, R. G. W. (1994). Protein Kinase C Activators Inhibit Receptor-Mediated Potocytosis by Preventing Internalization of Caveolae. *The Journal of Cell Biology* 124, 307–313.

Smith, A. W., Doonan, P. B., Tyor, W. R., Abou-Fayssal, N., Haque, A. and Banik, N. L. (2011). Regulation of Th1/Th17 Cytokines and IDO Gene Expression by Inhibition of Calpain in PBMCs from MS Patients. *Journal of Neuroimmunology* 232, 179–185.

Sohel, I., Puente, J. L., Ramer, S. W., Bieber, D., Wu, C. and Schoolnik, G. K. (1996). Enteropathogenic *Escherichia coli*: Identification of a Gene Cluster Coding for Bundle-Forming Pilus Morphogenesis. *Journal of Bacteriology* 178, 2613–2628.

Somerville, L. L. and Wang, K. (1981). The Ultrasensitive Silver "Protein" Stain also Detects Nanograms of Nucleic Acids. *Biochemical and Biophysical Research Communications* 102, 53–58.

Sonesson, A., Nordahl, E. A., Malmsten, M. and Schmidtchen, A. (2011). Antifungal Activities of Peptides Derived from Domain 5 of High-Molecular-Weight Kininogen. *International Journal of Peptides* 2011, 761037.

Spangler, B. D. (1992). Structure and Function of Cholera Toxin and the Related *Escherichia coli* Heat-Labile Enterotoxin. *Microbiological Reviews* 56, 622–647.

Speers, A. E. and Cravatt, B. F. (2009). Activity-Based Protein Profiling (ABPP) and Click Chemistry (CC)-ABPP by MudPIT Mass Spectrometry. *Current Protocols in Chemical Biology* 1, 29–41.

Spyers, L. M., Qa'dan, M., Meader, A., Tomasek, J. J., Howard, E. W. and Ballard, J. D. (2001). Cytosolic Delivery and Characterization of the TcdB Glucosylating Domain by Using a Heterologous Protein Fusion. *Infection and Immunity* 599–601.

Ståhl, A., Arvidsson, I., Johansson, K. E., Chromek, M., Rebetz, J., Loos, S., Kristoffersson, A., Békássy, Z. D., Mörgelin, M. and Karpman, D. (2015). A Novel Mechanism of Bacterial Toxin Transfer within Host Blood Cell-Derived Microvesicles. *Public Library of Science Pathogens* 11, e1004619.

Stamm, I., Wuhrer, M., Geyer, R., Baljer, G. and Menge, C. (2002). Bovine Lymphocytes Express Functional Receptors for *Escherichia coli* Shiga Toxin 1. *Microbial Pathogenesis* 33, 251–264.

Stein, P. E., Boodhoo, A., Tyrrell, G. J., Brunton, J. L. and Read, R. J. (1992). Crystal Structure of the Cell-Binding B Oligomer of Verotoxin-1 from *E. coli*. *Nature*, 355, 748–750.

Stepanenko, A. A. and Heng, H. H. (2017). Transient and Stable Vector Transfection: Pitfalls, Off-Target Effects, Artifacts. *Mutation Research* 773, 91–103.

Stevens, M. P. and Frankel, G. M. (2014). The Locus of Enterocyte Effacement and Associated Virulence Factors of Enterohemorrhagic *Escherichia coli*. *Microbiology Spectrum* 2, 4.

Stevens, M. P., Roe, A. J., Vlisidou, I., van Diemen, P. M., La Ragione, R. M., Best, A., Woodward, M. J., Gally, D. L. and Wallis, T. S. (2004). Mutation of *toxB* and a Truncated Version of the *efa-1* Gene in *Escherichia coli* O157:H7 Influences the Expression and Secretion of Locus of Enterocyte Effacement-Encoded Proteins but not Intestinal Colonization in Calves. *Infection and Immunity* 72, 5402–5411.

Stevens, M. P., van Diemen, P. M., Frankel, G., Phillips, A. D. and Wallis, T. S. (2002). Efa1 Influences Colonization of the Bovine Intestine by Shiga Toxin-Producing *Escherichia coli* Serotypes O5 and O111. *Infection and Immunity* 70, 5158–5166.

Stewart, M. P., McDowall, A. and Hogg, N. (1998). LFA-1-Mediated Adhesion is Regulated by Cytoskeletal Restraint and by a Ca^{2+}-Dependent Protease, Calpain. *Journal of Cell Biology* 140, 699–707.

Stone, K. D., Zhang, H., Carlson, L. K. and Donnenberg, M. S. (1996). A Cluster of Fourteen Genes from Enteropathogenic *Escherichia coli* is Sufficient for the Biogenesis of a Type IV Pilus. *Molecular Microbiology* 20, 325–337.

Storset, A. K., Kulberg, S., Berg, I., Boysen, P., Hope, J. C. and Dissen, E. (2004). NKp46 Defines a Subset of Bovine Leukocytes with Natural Killer Cell Characteristics. *European Journal of Immunology* 34, 669–676.

Strom, M. S. and Lory, S. (1993). Structure-Function and Biogenesis of the Type IV Pili. *Annual Review of Microbiology* 47, 565–596.

Stuart, P. M. and Goodward, J. G. (1992). *Yersinia enterocolitica* Produces Superantigenic Activity. *The Journal of Immunology* 148, 225–233.

Sundrud, M. S., Torres, V. J., Unutmaz, D. and Cover, T. L. (2004). Inhibition of Primary Human T Cell Proliferation by *Helicobacter pylori* Vacuolating Toxin (VacA) is Independent of VacA Effects on IL-2 Secretion. *Proceedings of the National Academy of Sciences of the United States of America* 101, 7727–7732.

Sussman, J. J., Bonifacino, J. S., Lippincott-Schwartz, J., Weissman, A. M., Saito, T., Klausner, R. D. and Ashwell, J. D. (1988). Failure to Synthesize the T Cell CD3-ζ Chain: Structure and Function of a Partial T Cell Receptor Complex. *Cell* 52, 85–95.

Suzuki, H., Kumagai, H. and Tochikura, T. (1986). γ-Glutamyltranspeptidase from *Escherichia coli* K-12: Purification and Properties. *Journal of Bacteriology* 168, 1325–1331.

Swamy, M., Pathak, S., Grzes, K. M., Damerow, S., Sinclair, L. V., van Aalten, D. M. F. and Cantrell, D. A. (2016). Glucose and Glutamine Fuel Protein O-GlcNAcylation to Control T Cell Self-Renewal and Malignancy. *Nature Immunology* 17, 712–720.

Szabady, R. L., Lokuta, M. A., Walters, K. B., Huttenlocher, A. and Welch R. A. (2009). Modulation of Neutrophil Function by a Secreted Mucinase of *Escherichia coli* O157:H7. *Public Library of Science Pathogens* 5, e1000320.

Taieb F., Nougayrède J. P. and Oswald, E. (2011). Cycle Inhibiting Factors (Cifs): Cyclomodulins that Usurp the Ubiquitin-Dependent Degradation Pathway of Host Cells. *Toxins (Basel)* 3, 356–68.

Talab, F., Allen, J. C., Thompson, V., Lin, K. and Slupsky, J. R. (2013). LCK is an Important Mediator of B-Cell Receptor Signaling in Chronic Lymphocytic Leukemia Cells. *Molecular Cancer Research* 11, 541–554.

Tam, P. J. and Lingwood, C. A. (2007). Membrane-Cytosolic Translocation of Verotoxin A_1 Subunit in Target Cells. *Microbiology* 153, 2700–2710.

Tamayo, E., Merino, R., González-Rojas, Marquina, R., Santiuste, I., Amado, J. A., Rappuoli, R., Del Guidice, G. and Merino, J. (2005). The *Escherichia coli* Heat-Labile Enterotoxin Induces Apoptosis of Immature Lymphocytes *In Vivo* via a Glucocorticoid-Dependent Pathway. *European Journal of Immunology* 35, 3505–3515.

Tamayo, E., Postigo, J., Del Guidice, G., Rappuoli, R., Benito, A., Yagita, H., Merino, R. and Merino, J. (2009). Involvement of the Intrinsic and Extrinsic Cell-Death Pathways in the Induction of Apoptosis of Mature Lymphocytes by the *Escherichia coli* Heat-Labile Enterotoxin. *European Journal of Immunology* 39, 439–446.

Tao, L., Zhang, J., Meraner, P., Tovaglieri, A., Wu, X., Gerhard, R., Zhang, X., Stallcup, W. B., Miao, J., He, X., Hurdle, J. G., Breault, D. T., Brass, A. L. and Dong, M. (2016). Frizzled Proteins are Colonic Epithelial Cell Receptors for *C. difficile* Toxin B. *Nature* 538, 350–355.

Tapia, D., Ross, B. N., Kalita, A., Kalita, M., Hatcher, C. L., Muruato, L. A. and Torres, A. G. (2016). From *In Silico* Protein Epitope Density Prediction to Testing *Escherichia coli* O157:H7 Vaccine Candidates in a Murine Model of Colonization. *Frontiers in Cellular and Infection Microbiology* 6, 94.

Tatsuno, I., Horie, M., Abe, H., Miki, T., Makino, K., Shinagawa, H., Tagucji, H., Kamiya, S., Hayashi, T. and Sasakawa, C. (2001). Gene on pO157 of Enterohemorrhagic *Escherichia coli* O157:H7 is Required for Full Epithelial Cell Adherence Phenotype. *Infection and Immunity* 69, 6660–6669.

Taupin, D. R., Kinoshita, K. and Podolsky, D. K. (2000). Intestinal Trefoil Factor Confers Colonic Epithelial Resistance to Apoptosis. *Proceedings of the National Academy of Sciences of the United States of America* 97, 799–804.

Tauschek, M., Gorrell, J. R., Strugnell, R. A. and Robins-Browne, R. M. (2002). Identification of a Protein Secretory Pathway for the Secretion of Heat-Labile Enterotoxin by an Enterotoxigenic Strain of *Escherichia coli*. *Proceedings of the National Academy of Sciences of the United States of America* 99, 7066–7071.

Taylor, G. L. (2010). Introduction to Phasing. *Acta Cryatallographica Section D Biological Crystallography* 66, 325–338.

Taylor, J. (1970). Infectious Infantile Enteritis, Yesterday and Today. *Section of Epidemiology and Preventitive Medicine* 63, 1297–1301.

Taylor, J. M., Ali, U., Iannello, R. C., Hertzog, P. J. and Crack, P. J. (2005). Diminished Akt Phosphorylation in Neurons Lacking Glutathione Peroxidase-1 (Gpx1) Leads to Increased Susceptibility to Oxidative Stress-Induced Cell Death. *Journal of Neurochemistry* 92, 283–293.

Taylor, J. M., Crack, P. J., Gould, J. A., Ali, U., Hertzog, P. J. and Iannello, R. C. (2004). Akt Phosphorylation and NFκB Activation are Counterregulated Under Conditions of Oxidative Stress. *Experimental Cell Research* 300, 463–475.

Taylor, K. A., O'Connell, C. B., Luther, P. W. and Donnenberg, M. S. (1998). The EspB Protein of Enteropathogenic *Escherichia coli* is Targeted to the Cytoplasm of Infected HeLa Cells. *Infection and Immunity* 66, 5501–5507.

Teng-umnuay, P., van der Wel, H. and West, C. M. (1999). Identification of a UDP-GlcNAc:Skp1-Hydroxyproline GlcNAc-Transferase in the Cytoplasm of *Dictyostelium*. *The Journal of Biological Chemistry* 274, 36392–36402.

Tesh, V. L., Ramegowda, B. and Samuel, J. E. (1994). Purified Shiga-Like Toxins Induce Expression of Proinflammatory Cytokines from Murine Peritoneal Macrophages. *Infection and Immunity* 62, 5085–5094.

Thanabalasuriar, A., Koutsouris, A., Weflen, A., Mimee, M., Hecht, G. and Gruenheid, S. (2011). The Bacterial Virulence Factor NleA is Required for the Disruption of Intestinal Tight Junctions by Enteropathogenic *E. coli*. *Cell* 12, 31–41.

Thermo Fisher Scientific Inc. (2010). *Thermo Scientific Pierce Protein Interaction Technical Handbook Version 2*.
URL: http://tools.thermofisher.com/content/sfs/brochures/1601945-Protein-Interactions-Handbook.pdf. Accessed 14/08/2019.

Thermo Fisher Scientific Inc. (2013a). *Pierce™ Pull-Down PolyHis Protein:Protein Interaction Kit Instructions*.
URL: https://assets.thermofisher.com/TFS-Assets/LSG/manuals/MAN0011443_Pierce_PulDwnPolyHisProtein_ProteinInter_UG.pdf. Accessed 14/08/2019.

Thermo Fisher Scientific Inc. (2013b). *Glycoprotein Isolation Kit, WGA Instructions*. URL: https://assets.thermofisher.com/TFS-Assets/LSG/manuals/MAN0011544_Glycoprotein_Isolat_WGA_UG.pdf. Accessed 14/08/2019.

Tian, J. L. and Qin, H. (2019). O-GlcNAcylation Regulates Primary Ciliary Length by Promoting Microtubule Disassembly. *iScience* 12, 379–391.

Tiffany, C. W. and Burch, R. M. (1989). Bradykinin Stimulates Tumor Necrosis Factor and Interleukin-1 Release from Macrophages. *Federation of European Biochemical Societies* 247, 189–192.

Tobe, T., Beatson, S. A., Taniguchi, H., Abe, H., Bailey, C. M., Fivian, A., Younis R., Matthews, S., Marchès O., Frankel, G., Hayashi, T. and Pallen, M. J. (2006). An Extensive Repertoire of Type III Secretion Effectors in *Escherichia coli* O157 and the Role of Lambdoid Phages in Their Dissemination. *Proceedings of the National Academy of Sciences of the United States of America* 103, 14941–14946.

Tobe, T., Schoolnik, G. K., Sohel, I., Bustamante, V. H. and Puente, J. L. (1996). Cloning and Characterization of *bfpTVW*, Genes Required for the Transcriptional Activation of *bfpA* in Enteropathogenic *Escherichia coli*. *Molecular Microbiology* 21, 963–975.

Torres, A., Luke, J. D., Kullas, A. L., Kapilashrami, K., Botbol, Y., Koller, A., Tonge, P. J., Chen, E. I., Macian, F. and van der Velden. A. W. M. (2016). Asparagine Deprivation Mediated by *Salmonella* Asparaginase Causes Suppression of Activation-Induced T Cell Metabolic Reprogramming. *Journal of Leukocyte Biology* 99, 387–398.

Torres, V. J., Ivie, S. E., McClain, M. S. and Cover, T. L. (2005). Functional Properties of the p33 and p55 Domains of the *Helicobacter pylori* Vacuolating Cytotoxin. *The Journal of Biological Chemistry* 280, 21107–21114.

Toshima, H., Yoshimura, A., Arikawa, K., Hidaka, A., Ogasawara, J., Hase, A., Masaki, H. and Nishikawa, Y. (2007). Enhancement of Shiga Toxin Production in Enterohemorrhagic *Escherichia coli* Serotype O157:H7 by DNase Colicins. *Applied and Environmental Microbiology* 73, 7582–7588.

Tozzoli, R., Caprioli, A. and Morabito, S. (2005). Detection of *toxB*, a Plasmid Virulence Gene of *Escherichia coli* O157, in Enterohemorrhagic and Enteropathogenic *E. coli*. *Journal of Clinical Microbiology* 43, 4052–4056.

Trabulsi, L. R., Keller, R. and Gomes, T. A. T. (2002). Typical and Atypical Enteropathogenic *Escherichia coli*. *Emerging Infectious Diseases* 8, 508–513.

Trapannone, R., Rafie, K. and van Aalten, D. M. F. (2016). O-GlcNAc Transferase Inhibitors: Current Tools and Future Challenges. *Biochemical Society Transactions* 44, 88–93.

Tree, J. J., Wang, D., McInally, C., Mahajan, A., Layton, A., Houghton, I., Elofsson, M., Stevens, M. P., Gally, D. L. and Roe, A. J. (2009). Characterization of the Effects of Salicylidene Acylhydrazide Compounds on Type III Secretion in *Escherichia coli* O157:H7. *Infection and Immunity* 77, 4209–4220.

Trester-Zedlitz, M., Kamada, K., Burley, S. K., Fenyö, D., Chait, B. T. and Muir, T. W. (2003). A Modular Cross-Linking Approach for Exploring Protein Interactions. *Journal of the American Chemical Society* 125, 2416–2425.

Triadafilopoulos, G., Pothoulakis, C., O'Brien, M. J. and LaMont, J. T. (1987). Differential Effects of *Clostridium difficile* Toxins A and B on Rabbit Ileum. *Gastroenterology* 93, 273–279.

Triglia, T., Thompson, J., Caruana, S. R., Delorenzi, M., Speed, T. and Cowman, A. F. (2001). Identification of Proteins from *Plasmodium falciparum* that are Homologous to Reticulocyte Binding Proteins in *Plasmodium vivax*. *Infection and Immunity* 69, 1084–1092.

Trinidad, J. C., Barkan, D. T., Gulledge, B. F., Thalhammer, A., Sali, A., Schoepfer, R. and Burlingame, A. L. (2012). Global Identification and Characterization of Both *O*-GlcNAcylation and Phosphorylation at the Murine Synapse. *Molecular & Cellular Proteomics* 11, 215–229.

Trombetta, E. S., Ebersold, M., Garrett, W., Pypaert, M. and Mellman, I. (2003). Activation of Lysosomal Function During Dendritic Cell Maturation. *Science* 299, 1400–1403.

Trülzsch, K., Sporleder, T., Igwe, E. I., Rüssmann, H. and Heesemann, J. (2004). Contribution of the Major Secreted Yops of *Yersinia enterocolitica* O:8 to Pathogenicity in the Mouse Infection Model. *Infection and Immunity* 72, 5227–5234.

Tsai, C. and Frasch, C. E. (1982). A Sensitive Silver Stain for Detecting Lipopolysaccharides in Polyacrylamide Gels. *Analytical Biochemistry* 119, 115–119.

Tsuchiya, A., Kanno, T. and Nishizaki, T. (2014). PI3 Kinase Directly Phosphorylates Akt1/2 at Ser473/474 in the Insulin Signal Transduction Pathway. *The Journal of Endocrinology* 220, 49–59.

Twining, S. S. (1984). Fluorescein Isothyiocyanate-Labeled Casein Assay for Proteolytic Enzymes. *Analytical Biochemistry* 143, 30–34.

Tzipori, S., Montanaro, J., Robins-Browne, R. M., Vial, P., Gibson, R. and Levine, M. M. (1992). Studies with Enteroaggregative *Escherichia coli* in the Gnotobiotic Piglet Gastroenteritis Model. *Infection and Immunity* 60, 5302–5306.

Tzipori, S., Wachsmuth, I. K., Chapman, C., Birner, R., Brittingham, J., Jackson, C. and Hogg, J. (1986). The Pathogenesis of Hemorrhagic Colitis Caused by *Escherichia coli* O157:H7 in Gnotobiotic Piglets. *The Journal of Infectious Diseases* 154, 712–716.

Utsch, C. and Haas, R. (2016). VacA's Induction of VacA-Containing Vacuoles (VCVs) and Their Immunomodulatory Activities on Human T Cells. *Toxins (Basel)* 8, 190.

Vallance, B. A., Deng, W., Knodler, L. A. and Finlay, B. B. (2002). Mice Lacking T and B Lymphocytes Develop Transient Colitis and Crypt Hyperplasia yet Suffer Impaired Bacterial Clearance During *Citrobacter rodentium* Infection. *Infection and Immunity* 70, 2070–2081.

Valleau, D., Little, D. J., Borek, D., Skarina, T., Quaile, A. T., Leo, R. D., Houliston, S., Lemak, A., Arrowsmith, C. H., Coombes, B. K. and Savchenko, A. (2018). Functional Diversification of the NleG Effector Family in Enterohemorrhagic *Escherichia coli*. *Proceedings of the National Academy of Sciences of the United States of America* 115, 10004–10009.

van der Velden, A. W. M., Copass, M. K. and Starnbach, M. N. (2005). *Salmonella* Inhibit T Cell Proliferation by a Direct, Contact-Dependent Immunosuppressive Effect. *Proceedings of the National Academy of Sciences of the United States of America* 102, 17769–17774.

van der Velden, A. W. M., Dougherty, J. T. and Starnbach, M. N. (2008). Down-Modulation of TCR Expression by *Salmonella enterica* serovar Typhimurium. *The Journal of Immunology* 180, 5569–5574.

van Diemen, P. M., Dziva, F., Abu-Median, A., Wallis, T. S., van den Bosch, H., Dougan, G., Chanter, N., Frankel, G. and Stevens, M. P. (2007). Subunit Vaccines Based on Intimin and Efa-1 Polypeptides Induce Humoral Immunity in Cattle but do not Protect Against Intestinal Colonisation by Enterohaemorrhagic *Escherichia coli* O157:H7 or O26:H-. *Veterinary Immunology and Immunopathology* 116, 47–58.

van Kerkhof, P., Alves dos Santos, C. M., Sachse, M., Klumperman, J., Bu, G. and Strous, G. J. (2001). Proteasome Inhibitors Block a Late Step in Lysosomal Transport of Selected Membrane but not Soluble Proteins. *Molecular Biology of the Cell* 12, 2556–2566.

van Kessel, K. P. M., Bestebroer, J. and van Strijp, J. A. G. (2014). Neutrophil-Mediated Phagocytosis of *Staphylococcus aureus*. *Frontiers in Immunology* 5, 467.

van's Gravesande, K. S., Layne, M. D., Ye, Q., Le, L., Baron, R. M., Perrella, M. A., Santambrogio, L., Silverman, E. S. and Riese, R. J. (2002). IFN Regulatory Factor-1 Regulates IFN-γ-Dependent Cathepsin S Expression. *The Journal of Immunology* 168, 4488–4494.

Varki, A., Schnaar, R. L. and Schauer, R. (2017). Sialic Acids and Other Nonulosonic Acids. *Essentials of Glycobiology [Internet] Third Edition*. Cold Spring Harbour Laboratory Press. URL: https://www.ncbi.nlm.nih.gov/books/NBK310274/

Veenendaal, A. K. J., Sundin, C. and Blocker, A. J. (2009). Small-Molecule Type III Secretion System Inhibitors Block Assembly of the *Shigella* Type III Secreton. *Journal of Bacteriology* 191, 563–570.

Veillette, A., Bookman, M. A., Horak, E. M. and Bolen, J. B. (1988). The CD4 and CD8 T Cell Surface Antigens are Associated with the Internal Membrane Tyrosine-Protein Kinase p56^{lck}. *Cell* 55, 30-308.

Vermijlen, D., Gatti, D., Kouzeli, A., Rus, T. and Eberl, M. (2018). γδ T cell Responses: How Many Ligands Will it Take Till we Know? *Seminars in Cell Developmental Biology* 84, 75–86.

Vieth, J. A., Kim, M., Pan, X. Q., Schreiber, A. D. and Worth, R. J. (2010). Differential Requirement of Lipid Rafts for FcγRIIA Mediated Effector Activities. *Cellular Immunology* 265, 111–119.

Vlisidou, I., Dziva, F., la Ragione, R. M., Best, A., Garmendia, J., Hawes, P., Monaghan, P., Cawthraw, S. A., Frankel, G., Woodward, M. J. and Stevens, M. P. (2006). Role of Intimin-Tir Interactions and the Tir-Cytoskeleton Coupling Protein in the Colonization of Calves and Lambs by *Escherichia coli* O157:H7. *Infection and Immunity* 74, 758–764.

von Eichel-Streiber, C. and Sauerborn, M. (1990). *Clostridium difficile* Toxin A Carries a C-terminal Repetitive Structure Homologous to the Carbohydrate Binding Region of Streptococcal Glycosyltransferases. *Gene* 96, 107–113.

von Willebrand, M., Baier, G., Couture, C., Burn, P. and Mustelin, T. (1994). Activation of Phosphatidylinositol-3-Kinase in Jurkat T Cells Depends on the Presence of the p56^{lck} Tyrosine Kinase. *European Journal of Immunology* 24, 234–238.

Vorlova, S., Koch, M., Manthey, H. D., Cochain, C., Busch, M., Chaudhari, S. M., Stegner, D., Yepes, M., Lorenz, K., Nolte, M. W., Nieswandt, B. and Zernecke, A. (2017). Coagulation Factor XII Induces Pro-Inflammatory Cytokine Responses in Macrophages and Promotes Atherosclerosis in Mice. *Atherosclerosis and Ischaemic Disease* 117, 176–187.

Vranic, S., Boggetto, N., Contremoulins, V., Mornet, S., Reinhardt, N., Marano, F., Baeza-Squiban, A. and Boland, S. (2013). Deciphering the Mechanisms of Cellular Uptake of Engineered Nanoparticles by Accurate Evaluation of Internalization Using Imaging Flow Cytometry. *Particle and Fibre Toxicity* 10, 2.

Wachter, C., Beinke, C., Mattes, M. and Schmidt, M. A. (1999). Insertion of EspD into Epithelial Target Cell Membranes by Infecting Enteropathogenic *Escherichia coli*. *Molecular Microbiology* 31, 1695–1707.

Wachtfogel, Y. T., Kucich, U., James, H. L., Scott, C. F., Schapira, M., Zimmerman, M., Cohen, A. B. and Colman, R. W. (1983). Human Plasma Kallikrein Releases Neutrophil Elastase During Blood Coagulation. *The Journal of Clinical Investigation* 72, 1672–1677.

Wachtfogel, Y. T., Pixley, R. A., Kucich, U., Abrams, W., Weinbaum, G., Schapira, M. and Colman, R. W. (1986). Purified Plasma Factor XIIa Aggregates Human Neutrophils and Causes Degranulation. *Blood* 67, 1731–1737.

Wagner, C., Barlag, B., Gerlach, R. G., Deiwick J. and Hensel, M. (2014). The *Salmonella enterica* Giant Adhesin SiiE Binds to Polarized Epithelial Cells in a Lectin-Like Manner. *Cellular Microbiology* 16, 962–975.

Wan, F., Hu, C., Ma, J., Gao, K., Xiang, L. and Shao, J. (2017). Characterization of γδ T Cells from Zebrafish Provides Insights into Their Important Role in Adaptive Humoral Immunity. *Frontiers in Immunology* 7, 675.

Wan, F., Weaver, A., Goa, X., Bern, M., Hardwidge, P. R. and Lenardo, M. J. (2011). IKKβ Phosphorylation Regulates RPS3 Nuclear Translocation and NF-κB Function During *Escherichia coli* O157:H7 Infection. *Nature Immunology* 12, 335–343.

Wang, D., Roe, A. J., McAteer, S., Shipston, M. J. and Gally, D. L. (2008). Hierarchal Type III Secretion of Translocators and Effectors from *Escherichia coli* O157:H7 Requires the Carboxy Terminus of SepL that Binds to Tir. *Molecular Microbiology* 69, 1499–1512.

Wang, H., Paton, A. W., McColl, S. R. and Paton, J. C. (2011). *In Vivo* Leukocyte Changes Induced by *Escherichia coli* Subtilase Cytotoxin. *Infection and Immunity* 79, 1671–1679.

Wang, H., Paton, J. C. and Paton, A. W. (2007). Pathologic Changes in Mice Induced by Subtilase Cytotoxin, a Potent New *Escherichia coli* AB_5 Toxin that Targets the Endoplasmic Reticulum. *The Journal of Infectious Diseases* 196, 1093–1101.

Wang, H. and Wang, J. (2017). How Cryo-Electron Microscopy and X-ray Crystallography Complement Each Other. *Protein Science* 26, 32–39.

Wang, J., Whiteman, M. W., Lian, H., Wang, G., Singh, A., Huang, D. and Denmark, T. (2009). A Non-Canonical MEK/ERK Signaling Pathway Regulates Autophagy via Regulating Beclin 1. *The Journal of Biological Chemistry* 284, 21412–21424.

Wang, L., Rothberg, K. G. and Anderson, R. G. W. (1993). Mis-Assembly of Clathrin Lattices on Endosomes Reveals a Regulatory Switch for Coated Pit Formation. *Journal of Cell Biology* 123, 1107–1117.

Wang, S., Huang, X., Sun, D., Xin, X., Pan, Q., Peng, S., Liang, Z., Luo, C., Yang, Y., Jiang, H., Huang, M., Chai, W., Ding, J. and Geng, M. (2012). Extensive Crosstalk between O-GlcNAcylation and Phosphorylation Regulates Akt Signaling. *Public Library of Science ONE* 7, e37427.

Wang, Y., Wu, J. and Wang, Z. (2006). Akt Binds to and Phosphorylates Phospholipase C-γ1 in Response to Epidermal Growth Factor. *Molecular Biology of the Cell* 17, 2267–2277.

Warawa, J., Finlay, B. B. and Kenny, B. (1999). Type III Secretion-Dependent Hemolytic Activity of Enteropathogenic *Escherichia coli*. *Infection and Immunity* 67, 5538–5540.

Wassef, J. S., Keren, D. F. and Mailloux, J. L. (1989). Role of M Cells in Initial Antigen Uptake and in Ulcer Formation in the Rabbit Intestinal Loop Model of Shigellosis. *Infection and Immunity* 858–863.

Waugh, D. S. (2011). An Overview of Enzymatic Reagents for the Removal of Affinity Tags. *Protein Expression and Purification* 80, 283–293.

Weiss, A., Imboden, J., Hardy, K., Manger, B., Terhorst, C. and Stobo, J. (1986). The Role of the T3/Antigen Receptor Complex in T-Cell Activation. *Annual Review of Immunology* 4, 593–619.

Weiss, A. Shields, R., Newton, M., Manger, B. and Imboden, J. (1987). Ligand-Receptor Interactions Required for Commitment to the Activation of the Interleukin 2 Gene. *The Journal of Immunology* 138, 2169–2176.

Weljie, A. M. and Vogel, H. J. (2000). Tryptophan Fluorescence of Calmodulin Binding Domain Peptides Interacting with Calmodulin Containing Unnatural Methionine Analogues. *Protein Engineering* 13, 59–66.

Wersto, R. P., Chrest, F. J., Leary, J. F., Morris, C., Stetler-Stevenson, M. and Gabrielson, E. (2002). Doublet Discrimination in DNA Cell-Cycle Analysis. *Cytometry* 46, 296–306.

Whittam, T. S., Wolfe, M. L., Wachsmuth, I. K., Ørskov, F., Ørskov, I. and Wilson, R. A. (1993). Clonal Relationships Among *Escherichia coli* Strains that Cause Hemorrhagic Colitis and Infantile Diarrhea. *Infection and Immunity* 61, 1619–1629.

Wick, L. M., Qi, W., Lacher, D. W. and Whittam, T. S. (2005). Evolution of Genomic Content in the Stepwise Emergence of *Escherichia coli* O157:H7. *Journal of Bacteriology* 187, 1783–1791.

Williams, K., Frayne, J. and Hall, L. (1998). Expression of Extracellular Glutathione Peroxidase Type 5 (GPX5) in the Rat Male Reproductive Tract. *Molecular Human Reproduction* 4, 841–848.

Witkowski, J. M. and Bryl, E. (2004). Paradoxical Age-Related Cell Cycle Quickening of Human $CD4^+$ Lymphocytes: A Role for Cyclin D1 and Calpain. *Experimental Gerontology* 39, 577–585.

Wöchtl, B., Gunzer, F., Gerner, W., Gasse, H., Kock, M., Bagó, Z., Ganter, M., Weissenböck, H., Dinhopl, N., Coldewey, S. M., von, Altrock, A., Waldmann, K., Saalmüller, A., Zimmermann, K., Steinmann, J., Kehrmann, J., Klein-Hitpass, L., Blom, J., Ehricht, R., Engelmann, I. and Hennig-Pauka, I. (2017). Comparison of Clinical and Immunological Findings in Gnotobiotic Piglets Infected with *Escherichia coli* O104:H4 Outbreak Strain and EHEC O157:H7. *Gut Pathogens* 9, 30.

Wolff, C., Nisan, I., Hanski, E., Frankel, G. and Rosenshine, I. (1998). Protein Translocation into host Epithelial Cells by Infecting Enteropathogenic *Escherichia coli*. *Molecular Microbiology* 28, 143–155.

Won, H. Y., Sohn, J. H., Min, H. J., Lee, K., Woo, H. A., Ho, Y., Park, J. W., Rhee, S. and Hwang, E. S. (2010). Glutathione Peroxidase 1 Deficiency Attenuates Allergen-Induced Airway Inflammation by Suppressing Th2 and Th17 Cell Development. *Antioxidants & Redox Signaling* 13, 575–587.

Woodward, M. J., Best, A., Sprigings, K. A., Pearson, G. R., Skuse, A. M., Wales, A., Hayes, C. M., Roe, J. M., Low, J., C. and La Ragione, R. M. (2003). Non-Toxigenic *Escherichia coli* O157:H7 Strain NCTC12900 Causes Attaching-Effacing Lesions and *eae*-Dependent Persistence in Weaned Sheep. *International Journal of Medical Microbiology* 293, 299–308.

Wu, B., Skarina, T., Yee, A., Jobin, M., DiLeo, R., Semesi, A., Fares, C., Lemak, A., Coombes, B. K., Arrowsmith, C. H., Singer, A. U. and Savchenko, A. (2010). NleG Type 3 Effectors from Enterohaemorrhagic *Escherichia coli* are U-Box E3 Ubiquitin Ligases. *Public Library of Science Pathogens* 6, 1–17.

Wu, X., Gowda, N. M. and Gowda, D. C. (2015). Phagosomal Acidification Prevents Macrophage Inflammatory Cytokine Production to Malaria, and Dendritic Cells are the Major Source at the Early Stages of Infection. *The Journal of Biological Chemistry* 290, 23135–23147.

Wu, Y., Wu, W., Wong, W. M., Ward, E., Thrasher, A. J., Goldblatt, D., Osman, M., Digard, P., Canaday, D. H. and Gustafsson, K. (2009). Human γδ T Cells: A Lymphoid Lineage Cell Capable of Professional Phagocytosis. *The Journal of Immunology* 183, 5622–5629.

Wüstner, S., Mejías-Luque, R., Koch, M. F., Rath, E., Vieth, M., Sieber, S. A., Heller, D. and Gerhard, M. (2015). *Helicobacter pylori* γ-Glutamyltranspeptidase Impairs T-Lymphocyte Function by Compromising Metabolic Adaption through Inhibition of cMyc and IRF4 Expression. *Cellular Microbiology* 17, 51–61.

Xie, G., Bonner, C. A. and Jensen, R. A. (2002). Dynamic Diversity of the Tryptophan Pathway in Chlamydiae: Reductive Evolution and a Novel Operon for Tryptophan Recapture. *Genome Biology* 3, 1–17.

Yamaguchi, R., Yamamoto, T., Sakamoto, A., Ishimaru, Y., Narahara, S., Sugiuchi, H. and Yamaguchi, Y. (2016). Roles of Myeloperoxidase and GAPDH in Interferon-Gamma Production of GM-CSF-Dependent Macrophages. *Heliyon* 2, e00080.

Yamaguchi, T. and Kaneda, M. (1988). Presence of Cytochrome *b*-558 in Guinea-Pig Alveolar Macrophages – Subcellular Localization and Relationship with NADPH Oxidase. *Biochimica et Biophysica Acta – Bioenergetics* 933, 450–459.

Yang, G., Zhou, B., Wang, J., He, X., Sun, X., Nie, W., Tzipori, S. and Feng, H. (2008). Expression of Recombinant *Clostridium difficile* Toxin A and B in *Bacillus megaterium*. *BMC Microbiology* 8, 192.

Yang, W. H., Park, S. Y., Ji, S., Kang, J. G., Kim, J., Song, H., Mook-Jung, I., Choe, K. and Cho, J. W. (2010). *O*-GlcNAcylation Regulates Hyperglycemia-Induced GPX1 Activation. *Biochemical and Biophysical Research Communications* 391, 756–761.

Yang, Y., Wu, S., Wang, Y., Pan, S., Lan, B., Liu, Y., Zhang, L., Leng, Q., Chen, D., Zhang, C., He, B. and Cao, Y. (2015). The Us3 Protein of Herpes Simplex Virus 1 Inhibits T Cell Signaling by Confining Linker for Activation of T Cells (LAT) Activation via TRAF6 Protein. *The Journal of Biological Chemistry* 290, 15670–15678.

Yankelevich, B., Soldatenkov, V. A., Hodgson, J., Polotsky, A. J., Creswell, K. and Mazumder, A. (1996). Differential Induction of Programmed Cell Death in $CD8^+$ and $CD4^+$ T Cells by the B Subunit of Cholera Toxin. *Cellular Immunology* 168, 229–234.

Yao, T., Mecsas, J., Healy, J. I., Falkow, S. and Chien, Y. (1999). Suppression of T and B Lymphocyte Activation by a *Yersinia pseudotuberculosis* Virulence Factor, YopH. *Journal of Experimental Medicine* 190, 1343–1350.

Yen, H., Sugimoto, N. and Tobe, T. (2015). Enteropathogenic *Escherichia coli* Uses NleA to Inhibit NLRP3 Inflammasome Activation. *Public Library of Science Pathogens* 11, e1005121.

Young, J. C., Clements, A., Lang, A. E., Garnett, J. A., Munera, D., Arbeloa, A., Pearson, J., Hartland, E. L., Matthews, S. J., Mousnier, A., Barry, D. J., Way, M., Schlosser, A., Aktories, K. and Frankel, G. (2014). The *Escherichia coli* Effector EspJ Blocks Src Kinase Activity via Amidation and ADP Ribosylation. *Nature Communications* 5, 5887.

Yu, J. and Kaper, J. B. (1992). Cloning and Characterization of the *eae* Gene of Enterohaemorrhagic *Escherichia coli* O157:H7. *Molecular Microbiology* 6, 411–417.

Yuan, P., Zhang, H., Cai, C., Zhu, S., Zhou, Y., Yang, X., He, R., Li, C., Guo, S., Li, S., Huang, T., Perez-Cordon, G., Feng, H. and Wei, W. (2015). Chondroitin Sulfate Proteoglycan 4 Functions as the Cellular Receptor for *Clostridium difficile* Toxin B. *Cell Research* 25, 157–168.

Yuzwa, S. A., Macauley, M. S., Heinonen, J. E., Shan, X., Dennis, R. J., He, Y., Whitworth, G. E., Stubbs, K. A., McEachern, E. J., Davies, G. J. and Vocadlo, D. J. (2008). A Potent Mechanism-Inspired O-GlcNAcase Inhibitor that Blocks Phosphorylation of Tau *In Vivo*. *Nature Chemical Biology* 4, 483–490.

Zeng, R., Cannon, J. L., Abraham, R. T., Way, M., Billadeau, D. D., Bubeck-Wardenberg, J. and Burkhardt, J. K. (2003). SLP-76 Coordinates Nck-Dependent Wiskott-Aldrich Syndrome Protein Recruitment with Vav-1/Cdc42-dependent Wiskott-Aldrich Syndrome Protein Activation at the T Cell-APC Contact Site. *The Journal of Immunology* 171, 1360–1368.

Zhang, G., Ducatelle, R., Pasmans, F., D'Herde, K., Huang, L., Smet, A., Haesebrouck, F. and Flahou, B. (2013a). Effects of *Helicobacter suis* γ-Glutamyl Transpeptidase on Lymphocytes: Modulation by Glutamine and Glutathione Supplementation and Outer Membrane Vesicles as a Putative Delivery Route of the Enzyme. *Public Library of Science ONE* 8, e77966.

Zhang, Y., Shi, L., Li, S., Yang, Z., Standley, C., Yang, Z., ZhuGe, R., Savidge, T., Wang, X. and Feng, H. (2013b). A Segment of 97 Amino Acids within the Translocation Domain of *Clostridium difficile* Toxin B is Essential for Toxicity. *Public Library of Science ONE* 8, e58634.

Zhang, H. and Donnenberg, M. S. (1996). DsbA is Required for Stability of the Type IV Pilin of Enteropathogenic *Escherichia coli*. *Molecular Microbiology* 21, 787–797.

Zhang, H., Lory, S. and Donnenberg, M. S. (1994). A Plasmid-Encoded Prepilin Peptidase Gene from Enteropathogenic *Escherichia coli*. *Journal of Bacteriology* 176, 6885–6891.

Zhang, L., Ding, X., Cui, J., Xu, H., Chen, J., Gong, Y., Hu, L., Zhou, Y., Ge, J., Lu, Q., Liu, L., Chen, S. and Shao, F. (2012). Cysteine Methylation Disrupts Ubiquitin-Chain Sensing in NF-κB Activation. *Nature* 481, 204–208.

Zhang, N. and Bevan, M. J. (2011). $CD8^+$ T Cells: Foot Soldiers of the Immune System. *Immunity* 35, 161–168.

Zhang, X., McDaniel, A. D., Wolf, L. E., Keusch, G. T., Waldor, M. K. and Acheson, D. W. K. (2000). Quinolone Antibiotics Induce Shiga Toxin-Encoding Bacteriophages, Toxin Production, and Death in Mice. *The Journal of Infectious Diseases* 181, 664–670.

Zhang, Z., Park, M., Tam, J., Auger, A., Beilhartz, G. L., Lacy, D. B. and Melnyk, R. A. (2014). Translocation Domain Mutations Affecting Cellular Toxicity Identify the *Clostridium difficle* Toxin B Pore. *Proceedings of the National Academy of Sciences of the United States of America* 111, 3721–3726.

Zhou, J., Zhang, Q., Henriquez, J. E., Crawford, R. B. and Kaminski, N. E. (2018). Lymphocyte-Specific Protein Tyrosine Kinase (LCK) is Involved in the Aryl Hydrocarbon Receptor-Mediated Impairment of Immunoglobulin Secretion in Human Primary B Cells. *Toxicological Sciences* 165, 322–334.

Zhou, Z., Li, X., Liu, B., Beutin, L., Xu, J., Ren, Y., Feng, L., Lan, R., Reeves, P. R. and Wang, L. (2010). Derivation of *Escherichia coli* O157:H7 from its O55:H7 Precursor. *Public Library of Science ONE* 5, e8700.

Zhu, J., Huang, J., Tseng, P., Yang, Y., Fowble, J., Shiau, C., Shaw, Y., Kulp, S. K. and Chen, C. (2004). From the Cyclooxygenase-2 Inhibitor Celecoxib to a Novel Class of 3-Phosphoinositide-Dependent Protein Kinase-1 Inhibitors. *Cancer Research* 64, 4309–4318.

Zhu, Z., Yu, Z., Taylor, J. L., Wu, Y. and Ni, J. (2016). The Application of Yeast Hybrid Systems in Protein Interaction Analysis. *Molecular Biology* 50, 663–670.

Zocchi, M. R., Poggi, A., Mariani, S., Gianazza, E. and Rugarli, C. (1989). Identification of a New Surface Molecule Expressed by Human LGL and LAK Cells: Production of a Specific Monoclonal Antibody and Comparison with Other NK/LAK Markers. *Cellular Immunology* 124, 144–157.

Zolghadr, K., Mortusewicz, O., Rothbauer, U., Kleinhans, R., Goehler, H., Wanker, E. E., Cardoso, M. C. and Leonhardt, H. (2008). A Fluorescent Two-Hybrid Assay for Direct Visualization of Protein Interactions in Living Cells. *Molecular and Cellular Proteomics* 7, 2279–2287.

Zychlinsky, A., Prévost, M. C. and Sansonetti, P. J. (1992). *Shigella flexneri* Induces Apoptosis in Infected Macrophages. *Nature* 358, 167–169.

Appendix 1: Composition of buffers and reagents

Red blood cell lysis buffer was composed of 1 L dH_2O with 100 mM $KHCO_3$, 1.5 mM NH_4Cl and 10 mM EDTA. It was made up to pH 8 using NaOH and HCl split into 10 x 100 mL aliquots and autoclaved.

NP-40 lysis buffer was composed of 100 mL dH_2O with 250 mM Tris, pH 7.4, 150 mM NaCl, 2 mM EGTA, 50 mM NaF, 1 mM EDTA, 1 mM Na_3VO_4 and 1 % (v/v) NP-40. One protease inhibitor tablet (Roche) or 100 µL of Halt™ protease inhibitor cocktail (Thermo Scientific) was added fresh to 10 mL of lysis buffer before use.

To make 300 mL of NZY^+ broth, 2 g of NZ amine, 1 g of yeast extract and 1 g of NaCl was dissolved in dH_2O and made up to pH 7.5 using NaOH and HCl. The media was autoclaved then 2.5 mL of sterile 1 M MgCl and 1 M $MgSO_4$ was added along with 0.4 % (w/v) glucose.

IMAC buffer A was composed of 500 mL dH_2O with 20 mM NaH_2PO_4, 300 mM NaCl, 5 % (v/v) glycerol and 0.1 % (v/v) Tween 20. It was made up to pH 7.6 using NaOH and HCl and 1 mM fresh DTT was added before use. It was kept on ice or at 6 °C when not in use.

IMAC buffer B was composed of 200 mL dH_2O with 20 mM NaH_2PO_4, 300 mM NaCl, 5 % (v/v) glycerol, 0.1 % (v/v) Tween 20 and 500 mM imidazole. It was made up to pH 7.6 using NaOH and HCl and 1 mM fresh DTT was added before use. It was kept on ice or at 6 °C when not in use.

SEC buffer was composed of 1 L dH_2O with 10 mM NaH_2PO_4, 50 mM NaCl, 5 % (v/v) glycerol and 0.1 % (v/v) Tween 20. It was made up to pH 7.6 using NaOH and HCl and 1 mM fresh DTT was added before use. It was kept on ice or at 6°C when not in use.

The low salt buffer used for anion exchange chromatography was composed of 1 L dH_2O with 10 mM Tris or 10 mM NaH_2PO_4, 50 mM NaCl, 5 % (v/v) glycerol and 0.05 % (v/v) Tween 20. It was made up to pH 7.6 using NaOH and HCl and 1 mM fresh DTT was added before use. It was kept on ice or at 6 °C when not in use.

The high salt buffer used for anion exchange chromatography was composed of 200mL dH_2O with 10 mM Tris or 10 mM NaH_2PO_4, 1 M NaCl, 5 % (v/v) glycerol and 0.05 % (v/v) Tween 20. It was made up to pH 7.6 using NaOH and HCl and 1 mM fresh DTT was added before use. It was kept on ice or at 6 °C when not in use.

Assay buffer was composed of 200 mL of dH_2O with 15 mM NaH_2PO_4, 150 mM NaCl and 5 % (v/v) glycerol. It was made up to pH 7.6 using NaOH and HCl and 1 mM fresh DTT was added before use. It was kept on ice or at 6 °C when not in use.

CD buffer was composed of 200 mL of dH_2O with 15 mM NaH_2PO_4, 150 mM NaF and 5 % (v/v) glycerol. It was made up to pH 7.6 using NaOH and HCl and 1 mM fresh DTT was added before use. It was kept on ice or at 6 °C when not in use.

The α-cyano-4-hydoxycinnamic acid matrix was composed of 400 µL dH_2O with 10 mg/mL α-cyano-4-hydoxycinnamic acid, 0.3 % (v/v) trifluoroacetic acid and 50 % (v/v) acetonitrile. The solution was mixed thoroughly after the addition of each reagent then centrifuged at 5000 rpm for 1 minute in a benchtop centrifuge. The supernatant was used for spotting with samples on the MALDI plate.

X-Gal staining mix was made from reagents provided in the Beta-Glactosidase Staining Kit (Clonetech Laboratories Inc.). It was composed of 10 µL of X-Gal Solution, 2 µL of each of Staining Solutions 1, 2 and 3 and 184 µL of 1 x PBS.

Appendix 2: Nucleotide sequences of the *lifA* fragment genes

Sequences contain start codons, polyhistidine tags and stop codons.

lifA F1

ATGAGACTGCCAGAGAAAGTTCTTTTTCCTCCTGTCACTAGTGGCCTGTCAGGGCAGGAAAA
ACAAAAAAAACCGAAGAGCATTACCGGATTTCAGGAAAATTATCAACGCAATATCAGGCCAA
TCAAAACAGCATCAGAAGCCCGACTACGCTTCTTTGATAAAATGGTTTCGAAAGAAAACTCT
CTGGAAGATGTTGTTTCTTTAGGTGAAATGATTCAGAAGGAAATTTATGGGCATGAACAAAG
AACATTTTCACCAGTTCATCATACAGGTAACTGGAAATCATCATTGTTACACAACGCGCTCC
TTGGTCTGGCAAATGTTTATAATGGCTTACGGGAAACAGAATACCCTAACACTTTCAACAGA
GATGGTATAAAAAGTACTAACTCTTTTAGAGATAACTTATTGACAAAAACAAGAACTCCCAG
AGATAATTTTGAGGAAGGAATAAAACATCCTGAACATGCAACAATACCATATGACAACGACA
ATGAAAGTAATAAATTGCTAAAAGCAGGAAAGATAGCTGGTAACAATAACGAGCTGTTGATG
GAAATAAAAAAGGAATCCCAAAGCGACCATCAAATCCCCCTGTCAGATAAGTTCCTGAAAAG
GAAAAAACGATCTCCTGTAGCTGAAGATAAAGTTCAAAACTCGTTAACACCAGAAAATTTTG
TTCAGAAAATTTCACTTAGTGATGAGCTTAAAACAAAATATGCAAATGAAATTATAGAGATA
AAAAGAATAATGGGAGAATACAATCTTTTACCGGATAAAAACAGTCGTAATGGTCTAAAACT
TCTACAGAAGCAAGCTGATTTACTAAAAATAATCATGGAGGATACCTCCGTTACAGAAAATA
CCTTTAAAAACATAGAGATAGCTATAACAGATATAAAAAGGGAGTACTATTCGCATACAGTT
GATATTGAGAAAAATATTCATGCCATATGGGTTGCGGGTTCCCCACCTGAAAGCATTTCGGA
CTATATTAAGACTTTTCTCAAAACCTACAAAGAGTTTACTTACTATCTTTGGGTTGATGAAA
AAGCATTTGGAGCCGCGAAATTTACCAGTGTCTTAAAACAAATTGCATTTGATTTAGCATGC
AGAACTATACAGCAGAATACTCCACAAAAAAATATTGATTTTATTAATCTATATAATGAAAT
AAGGAAGAAATACAACAACAACCCATCGGGACAACAAGAGTACTTAAACAAACTCAGAGAGC
TTTATGCTACTTATCAAAAAATATCCACCCCTCTGAAACACATGTTTAATTCATTTTTTTTA
GAAAACATGATTAAACTTCAGGATAATTTCTTCAACTATTGCATTGTCAAAGGTGTTACAGA
GATTAATGATGAGTTACGAATAAACTACCTTAAAAATGTAATAAAACTGTCAGACGATGACA
TTGGTAATTACCAGAAAACAATTAACGACAATAAAGATAGAGTAAAAAAACTAATTCTTGAT
TTACAGAAACAATTTGGTGAAAACCGCATTTCAATTAAAGATGTTAACTCTTTAACCTCTCT
TTCAAAATCAGAAAATAATCACAATTATCAAACTGAAATGTTGCTTCGATGGAACTATCCTG
CCGCCTCAGACCTGCTCAGGATGTATATCCTTAAAGAGCATGGTGGTATTTATACAGACACA
GATATGATGCCTGCATACTCTAAACAAGTAATTTTTAAAATTATGATGCAGACAAACGGAGA
TAATCGTTTCTTGGAAGATTTGAAACTACGTCGTGCAATATCTGATGGTGTATTAAGATATG

TTAATAACCAAAATATTGATGAAGTTAACTATAATGAAATCAGTGATGCAGATAAAAACATT
ATCAAGAAGATATTAACAGAAATATCTAAAATGCCAGAAGATAGTATTTTTACTAAGATCAA
TACAAGGATTCCTCGAGACACAATGCCCATCCTTCGTCGTTATCACCTATGGCCTGATGGAT
GGAATATTCGTGGGCTCAATGGATTCATGCTATCACATAAAGGTAGTGAAGTGATTGATGCT
GTTATCGCAGGCCAGAATCAGGCTTACAGGGAACTAAGAAGAATAAGAGATAATATTCATAG
TGAAATATACTTCAAACAAACTGATGAATTGTCCTCACTTCCAGATACAGACAAAATTGGAG
GGATTCTGGTAAAAAAATACCTTTCAGGAAGTCTTTTTTCAAAATTCAGACAAGATACTATT
ATCCCGGAGGCATTGAGCACCCTCCAGATATCAGGTCCTGACTTGATTCAAAGAAAGATGTT
GCAATTTTTCAGGAGTAGAGGGGTGTTAGGTGAAGAGTTCATTAATGAAAGAAAACTGAGTG
ATAAAGCTTATATTGGTGTCTACAAAACAACTGGCACAGGGAAATATGACTGGTTAACCCCT
GAATCGATCGGCGTTAATGATGTCACGCCCGCAGATGAAAGTACCTGGTGTATAGGAAAAGG
CCGGTGTGTTGATGACTTCCTGTTCAAAGATGTTTCAACACTAAAAACAGAAAATCTTCCAG
AATTATTCTTAACAAAAATAGATACTGATACGTTTTTCTCTCAGTGGTCAACCAAAACCAAG
AAAGATCTGCAAAAAAAAATACAAGACCTTACTGTACGTTATAATGAGCTAATTGACTCGTC
GACTATCGACTTTAAAAATCTATATGAAATAGATCAAATGCTCCATATGATTATGCTAGAGA
TGAATGATGATATAGCCAAAAGGTCATTGTTTTCATTGCAAGTTCAAATAGCCGAAAAAATT
CGGAGGATGACCATTCCTGTAGACAATATAATTAACATCTATCCTGATCTACATAAAAAAAA
TGACAATGATCTGAGTATGTCCATAAAAGGCTTTCTTGCGAGTAATCCACATACAAAAATAA
ATATTCTTTATAGCAATAAGACTGAGCATAATATTTTTATAAAGGATTTATTCTCCTTCGCA
GTTATGGAAAATGAGTTAAGAGACATTATCAATAACATGAGCAAAGATAAGACTCCTGAAAA
CTGGGAAGGGAGGGTAATGTTACAAAGATATCTCGAATTAAAAATGAAAGATCATCTTAGTT
TGCAATCTTCTCAGGAAGCAAATGAGTTTCTTGAAATATCTACTTTTATTTATGAGAATGAT
TTCTTGAGAGAAAAGATTGAAGCAGTAAAAAACAAAATGAATTCTCACGAACTTTATTTTGA
AAAAATAAAAAAAGAACAAAACACATGGCAGGATCTGTCCACAAAAGAACAAAAATTACAGC
TTATTAAAGCATTGAAAGAAATTTCAGGAAATACAGAGAAGGACTCTCATTACGATAGACTT
CTTGATGCTTTTTTTAAAAAACATAATGAAAATATTCATAATAAAATACAAAGAATAAAAGA
CGAGTTCAAGGAATACTCCCGTGTAGCCATTCATAATATAGATAAAGTTATATTTAAAGGGC
AAACACTGGATCGTCTTTATCATGAAGGATATGTATTTTCTGATATCAATACCTTGTCTCGT
TATACACTACACGGACTAGGAATAACTGGTGTACATACTGAAGAAAACCTGCTACCAGCTCC
TTCATCGTCCTTAATTAATATATTGAAAGAACATTATAATGAAGATGAAATTAGTGCGAAAT
TACCACTAGCATATGATTACATTTTAAATAAAAAAGAATCAAGCTCTATTCCTGTTGAAATT
TTGAACAAACTTTCAGAGTTACCACCACATGAACTACTCACACCTGTTCTTGGCCAGAGTGT
TAATCCTCTGGGCATGGGCTACTCATCCGATAATGGAAAAATCACAGAGCAAGTAATAGTCA
GTGGAGCTGATGGATTTGATAATCCCATATCTGGACTTATATATACCTATCTTGAAGATCTA
TATAACATCCATGTAAGGATGCGAGAAGGTACACTAAATTCACAGAATCTTCGTCAGCTTCT
GGAAAACTCTGTTTCTTCATGCTTTTTGACTGAGCAAAGTATTAATAAATTACTTAGTGAGG

CAGAAAAAAGGCCTTATCAGTCTTTAACAGAAATACATCAGCATCTCACAGGATTACCAACT
ATTGCCGATGCAACCCTTTCATTACTTTCTGTTGGATTACCTGGTACGGGAAAACTATTGCG
CAGGGAGCAGGACTATGGGCGTCCACCAGTTACAGCAATTCAGGATTCCACATTTGTACTCC
CTTATAATTTCAAAGGTATTGGTTTTAACGATAACATTATATCCTCTGCACCTGTAGCCTCC
TCATTACATTTTATCGCTGAACATGCGAAATATACTTTATTGTCATGGCCTGAGTTTTATCG
TCATCATGCACAGCGATGGTTCGAAATGGCTAAAGGATATGGAAGCCAGAATATTGATTTTC
ACCCTCAGTCTCTATTGGTAACCCAAGAAGGACGCTGTATGGGATTAGCCTTACTTTATTTA
CAGACTGAAGATACTGCTCATTATAGCATTCTCCAGGAAAACCTAATGACTGTGAGTGCACT
TCATCAGACCAGTAATCGCGATAAGTTGCCACTGTCCAAAGATGATAATTCCTTAATGACAA
GAACTTATAGTCTGATTGAAATGCTACAGTATCAGGGAAACAAATATATTACCAACGAATCG
CTACTACATAAGACCGCATGGAACCAAGAAAGAATAACTTTATTATTCAATGAAAAAGGAGT
TAAGCGAGCCCTGATAAGCACGCCTAATCATACTCTGGTTCTGCAACAACTGGAGGATATTT
ACCGGCTCACTGATCCAAATTTTGGGCATGCAGATTTCCTTTCACCTATAGATGCTCTGAAG
TTTATTGAGGCTATGATACAATTACATCATCACCACCATCACTAA

lifA GT

ATGCATCATCACCACCATCACTCGTTAACACCAGAAAATTTTGTTCAGAAAATTTCACTTAG
TGATGAGCTTAAAACAAAATATGCAAATGAAATTATAGAGATAAAAAGAATAATGGGAGAAT
ACAATCTTTTACCGGATAAAAACAGTCGTAATGGTCTAAAACTTCTACAGAAGCAAGCTGAT
TTACTAAAAATAATCATGGAGGATACCTCCGTTACAGAAAATACCTTTAAAAACATAGAGAT
AGCTATAACAGATATAAAAAGGGAGTACTATTCGCATACAGTTGATATTGAGAAAAATATTC
ATGCCATATGGGTTGCGGGTTCCCCACCTGAAAGCATTTCGGACTATATTAAGACTTTTCTC
AAAACCTACAAAGAGTTTACTTACTATCTTTGGGTTGATGAAAAAGCATTTGGAGCCGCGAA
ATTTACCAGTGTCTTAAAACAAATTGCATTTGATTTAGCATGCAGAACTATACAGCAGAATA
CTCCACAAAAAAATATTGATTTTATTAATCTATATAATGAAATAAGGAAGAAATACAACAAC
AACCCATCGGGACAACAAGAGTACTTAAACAAACTCAGAGAGCTTTATGCTACTTATCAAAA
AATATCCACCCCTCTGAAACACATGTTTAATTCATTTTTTTTAGAAAACATGATTAAACTTC
AGGATAATTTCTTCAACTATTGCATTGTCAAAGGTGTTACAGAGATTAATGATGAGTTACGA
ATAAACTACCTTAAAAATGTAATAAAACTGTCAGACGATGACATTGGTAATTACCAGAAAAC
AATTAACGACAATAAAGATAGAGTAAAAAAACTAATTCTTGATTTACAGAAACAATTTGGTG
AAAACCGCATTTCAATTAAAGATGTTAACTCTTTAACCTCTCTTTCAAAATCAGAAAATAAT
CACAATTATCAAACTGAAATGTTGCTTCGATGGAACTATCCTGCCGCCTCAGACCTGCTCAG
GATGTATATCCTTAAAGAGCATGGTGGTATTTATACAGACACAGATATGATGCCTGCATACT
CTAAACAAGTAATTTTTAAAATTATGATGCAGACAAACGGAGATAATCGTTTCTTGGAAGAT

TTGAAACTACGTCGTGCAATATCTGATGGTGTATTAAGATATGTTAATAACCAAAATATTGA
TGAAGTTAACTATAATGAAATCAGTGATGCAGATAAAAACATTATCAAGAAGATATTAACAG
AAATATCTAAAATGCCAGAAGATAGTATTTTTACTAAGATCAATACAAGGATTCCTCGAGAC
ACAATGCCCATCCTTCGTCGTTATCACCTATGGCCTGATGGATGGAATATTCGTGGGCTCAA
TGGATTCATGCTATCACATAAAGGTAGTGAAGTGATTGATGCTGTTATCGCAGGCCAGAATC
AGGCTTACAGGGAACTAAGAAGAATAAGAGATAATATTCATAGTGAAATATACTTCAAACAA
ACTGATGAATTGTCCTCACTTCCAGATACAGACAAAATTGGAGGGATTCTGGTAAAAAAATA
CCTTTCAGGAAGTCTTTTTTCAAAATTCAGACAAGATACTATTATCCCGGAGGCATTGAGCA
CCCTCCAGATATCAGGTCCTGACTTGATTCAAAGAAAGATGTTGCAATTTTTCAGGAGTAGA
GGGGTGTTAGGTGAAGAGTTCATTAATGAAAGAAAACTGAGTGATAAAGCTTATATTGGTGT
CTACAAAACAACTGGCACAGGGAAATATGACTGGTTAACCCCTGAATCGATCGGCGTTAATG
ATGTCACGCCCGCAGATGAAAGTACCTGGTGTATAGGAAAAGGCCGGTGTGTTGATGACTTC
CTGTTCAAAGATGTTTCAACACTAAAAACAGAAAATCTTCCAGAATTATTCTTAACAAAAAT
AGATACTGATACGTTTTTCTCTCAGTGGTCAACCAAAACCAAGAAAGATCTGCAAAAAAAAA
TACAAGACCTTACTGTACGTTATAATGAGCTAATTGACTCGTCGACTATCGACTTTAAAAAT
CTATATGAAATAGATCAAATGCTCCATATGATTATGCTAGAGATGAATGATGATATAGCCAA
AAGGTCATTGTTTTCATTGCAAGTTCAAATAGCCGAAAAAATTCGGAGGATGACCATTCCTG
TAGACAATATAATTAACATCTATCCTGATCTACATAAAAAAAATGACAATGATCTGAGTATG
TCCATAAAAGGCTTTCTTGCGAGTAATCCACATACAAAAATAAATATTCTTTATAGCAATAA
GACTGAGCATAATATTTTTATAAAGGATTTATTCTCCTTCGCAGTTATGGAAAATGAGTTAA
GAGACATTATCAATAACATGAGCAAAGATAAGACTCCTGAAAACTGGGAAGGGAGGGTAATG
TTACAAAGATATCTCGAATTAAAAATGAAAGATCATCTTAGTTAA

lifA F3

ATGGGGGACTGGCAAATTCGTGAGAAGGTGGGGTATGCCAACAGTATCAGTCCCTACTCTTC
TCTGGCGCACGGTTACGCCAACAGTAAATGGCCACGAACAATACCGAAAATTCCCTCGGGAG
AATATGACACCATAATTCTGGGCTACGGTCACCAGTATCAGGCCAATACGGAAATAGAATAT
CTGTCTAACTGGATTGTATGGCGGGAAGCCGTACCAGACAGTACTTCCCGCCACAAACGTCC
TCCTCTGGAGGTTCTTAATAGTCAGTGTACTGTGATAGCTGGAGAGCGTAAAACCACAGTAC
TTCCCCTGAGAGTGCTCAGCGATCTGACACCGGAATGCACAGAACAGGCTATATCGTTAAAA
GATTATAAATTCATACTGAGAGGGGGAAGCGGTGGGCTGGCTGTTCAGGTCGGTGGCGCGGG
ATATTATGATATTGATGCAAATCTTGTGGCAAAAGAAAATACGCTCTCTTTTCGCGGGCTAC
CGGAAGAGTTTCCGCTCACCTTTGATTTATCAAAACAAACACAGTCGGTCATGCTGAAAACA
CCAGACGATGAGGTGCCGGTAATGACCATTACCCAGAAGGGAATAAACACCCTGGTAGGTAC

AGCCGCCGGTAAAGACCGACTAATCGGTAACGATAAGGACAATACCTTCCATACAAGCTCTG
GCGGCGGTACAGTCATCTCCGGAGGCGGGAATAACCGCTATATTATCCCCCGGGATTTAAAA
ACGCCGTTGACACTGACGCTGTCCAGTAACTCAGTCTCTCACGAAATCTTTCTGCCAGAAAC
AACCCTAGCTGAATTAAAACCTGTCGCCTTTGAGCTGAGTTTGATTTACTGGGCCGGGAACA
ACATAAATGTTCAACCAGAGGATGAAGCAAAACTGAACCACTTTGCCGGAAACTTCAGGGTG
CATACCCGTGATGGCATGACTCTGGAGGCGGTTTCCCGGGAAAATGGTATTCAACTGGCGAT
TTCATTATGTGATGTTCAACGCTGGCAGGCTGTTTATCCGGAAGAAAATAACAGACCGGATG
CCATACTGGACAGGCTGCATGATATGGGCTGGAGTCTGACACCAGAAGTCCGGTTCCAAGGA
GGAGAAACACAAGTCAGCTATGATCCCCTGACTCGTCAGCTCGTTTACCAGCTTCAGGCGCG
TTACTCTGAATTCCAGTTGGCCGGTAGTCGCCACCATACCACGGCTGTAACCGGAACTCCGG
GAAGCCGATACATTATCATGAAGCCAGTTACAACACAGATATTACCGACACAAATCATACTG
GCTGGTGATAATGACCATCCGGAAACGATTGATTTACTGGAAGCTAGTCCTGTTCTGGTTGA
AGGGAAAAAAGACAAAAACAGCGTGATATTAACGATTGCTACGATTCAGTATTCCCTTCAAC
TGACAATATCCGGGATCGAAGAATCGCTGCCCGAGACAACCCGTGTGGCAATTCAGCCTCAG
GATACCCGTTTACTGGGTGACGTACTCCGGATCTTACCAGATAATGGTAACTGGGTGGGGAT
TTTCCGGAGTGGTCATACACCAACGGTAAACCGGCTGGAAAATTTGATGGCACTGAATCAGG
TAATGACGTTCCTGCCCCGGGTATCCGGAAGTGCAGAGCAGGTATTATGCCTCGAAAACCTA
GGTGGCGTAAGGAAAAAAGTGGAGGGGGAGTTACTGTCAGGGAAGCTGAAAGGTGCGTGGAA
AGCCGAAGGTGAACCTACTGTTCCGGTAAATATCTCAGATCTAAGTATCCCACCCTATTCAC
GTCTGTATCTGATTTTTGAAGGGAAAAATAATGTGTTGCTACGCAGTAAAGTACATGCAGCT
CCGTTGAAAATAACATCCGCAGGAGAGATGCAGTTATCTGAAAGGCAGTGGCAACAGCAGGA
ACATATTATTGTCAAGCCCGACAACGAAGCCCCCTCATTAATACTCAGTGAATTTCGTCGTT
TCACTATTTCATCGGATAAAACATTTTCTTTAAAACTGATGTGCCATCAGGGTATGGTCCGC
ATCGACCGCAGATCATTATCGGTCAGATTGTTCTATCTGCGTGAACAGCCAGGTATCGGCAG
TTTACGTCTGACGTTCAGAGATTTTTTCACAGAAGTGATGGATACAACGGACAGGGAAATTC
TGGAGAAAGAGCTGAGACCAATTCTGATAGGAGATACACACCGCTTTATCAACGCTGCATAC
AAAAATCATCTGAATATCCAGTTAGGAGATGGCGTTCTGAATCTGGCAGACATTGTTGCGGA
ATACGCCCGTATTCAAAAGGAAGAAACATCAAAAATATTGTATCAATATCAAGGTGCCATGA
AAAAAAAAACAGATGGACATCATCACCACCATCACTAA

lifA F5

ATGCCATCTGTGGTAGAAGATGCCATTATGACCACTACTGTCACAACAGATTCAGGTGAACT
ATTCCCTACCTTCCACCCGTGGTATACAGATGATTTATCAGGGCGTTATAAGAGCGTACCTA
TGGCAAGAAAAGCAGATACTTTGTATCACCTGACACCAAAAGGTGATCTACAGATAATATAT

CAGGTAGCTACAAAAATGGTGAATCAGGCGATGATTGTATCCCTGCCAAACTACCGACACGA
GTGGGAAAAATATAATTTAAGCATCTTATCCGAAATCCCTCAGAACAATAATACTGTTGTAC
ATTCAATCCTCAGGGTTAATGGCCCCACAATGCAGGTGCGCACAATTGACTACAGAGGAACG
GATGAAAACAATCCCATAGTATCTTTTTCAGATACAACCTTCATCAATGGTGAACAGATGTT
GAGTTATGACTCGCATTCATCAGGGCGAGTCTATTCCAGAGAAGAATATATGATGTGGGAAT
TGCAGCAACGGGTATCAGAAGCTTCCAGTGCCCGGACACAGGATTACTGGCTGATGGATGCA
GCGGTAAGAAACGGAGAATGGAAGATCACACCAGAATTATTACGTCACACACCGGGATATAT
CCGGAGTACGGTATCGAAATGGTCCAGAGGATGGCTGAAAACCGGCACAATACTCCAGACTC
CAGAAGACAGAAATACGGATGTATACCTGACTACCATACAGAACAATGTATTTAGTCGTCAG
GGGGGCGGCTACCAAGTGTATTATCGGATTGATGGAATGGCTGGTGCGGATATAGCGGATAA
TGCACCAGGGGAAACCCGCTGCACCCTCAGGCCCGGAACATGTTTTGAAGTGACAAGTGTGG
ATGAAAGGCATTATGAGTGGAATATCATTTATGTCACGCTGAAAACCTGTGGCTGGAGCCGA
AATGGCCAAAGCAAAACGCCGAATGGTGACAACCTTTTTAACCATCATCACCACCATCACTA
A

Appendix 3: Peptide map of recombinant LifA fragments

Sequences in red denote peptides identified by MALDI-TOF mass spectrometry.

rF1

1 MRLPEKVLFP PVTSGLSGQE KQKKPKSITG FQENYQRNIR PIKTASEARL
51 RFFDKMVSKE NSLEDVVSLG EMIQKEIYGH EQRTFSPVHH TGNWKSSLLH
101 NALLGLANVY NGLRETEYPN TFNRDGIKST NSFRDNLLTK TRTPRDNFEE
151 GIKHPEHATI PYDNDNESNK LLKAGKIAGN NNELLMEIKK ESQSDHQIPL
201 SDKFLKRKKR SPVAEDKVQN SLTPENFVQK ISLSDELKTK YANEIIEIKR
251 IMGEYNLLPD KNSRNGLKLL QKQADLLKII MEDTSVTENT FKNIEIAITD
301 IKREYYSHTV DIEKNIHAIW VAGSPPESIS DYIKTFLKTY KEFTYYLWVD
351 EKAFGAAKFT SVLKQIAFDL ACRTIQQNTP QKNIDFINLY NEIRKKYNNN
401 PSGQQEYLNK LRELYATYQK ISTPLKHMFN SFFLENMIKL QDNFFNYCIV
451 KGVTEINDEL RINYLKNVIK LSDDDIGNYQ KTINDNKDRV KKLILDLQKQ
501 FGENRISIKD VNSLTSLSKS ENNHNYQTEM LLRWNYPAAS DLLRMYILKE
551 HGGIYTDTDM MPAYSKQVIF KIMMQTNGDN RFLEDLKLRR AISDGVLRYV
601 NNQNIDEVNY NEISDADKNI IKKILTEISK MPEDSIFTKI NTRIPRDTMP
651 ILRRYHLWPD GWNIRGLNGF MLSHKGSEVI DAVIAGQNQA YRELRRIRDN
701 IHSEIYFKQT DELSSLPDTD KIGGILVKKY LSGSLFSKFR QDTIIPEALS
751 TLQISGPDLI QRKMLQFFRS RGVLGEEFIN ERKLSDKAYI GVYKTTGTGK
801 YDWLTPESIG VNDVTPADES TWCIGKGRCV DDFLFKDVST LKTENLPELF
851 LTKIDTDTFF SQWSTKTKKD LQKKIQDLTV RYNELIDSST IDFKNLYEID
901 QMLHMIMLEM NDDIAKRSLF SLQVQIAEKI RRMTIPVDNI INIYPDLHKK
951 NDNDLSMSIK GFLASNPHTK INILYSNKTE HNIFIKDLFS FAVMENELRD
1001 IINNMSKDKT PENWEGRVML QRYLELKMKD HLSLQSSQEA NEFLEISTFI
1051 YENDFLREKI EAVKNKMNSH ELYFEKIKKE QNTWQDLSTK EQKLQLIKAL
1101 KEISGNTEKD SHYDRLLDAF FKKHNENIHN KIQRIKDEFK EYSRVAIHNI
1151 DKVIFKGQTL DRLYHEGYVF SDINTLSRYT LHGLGITGVH TEENLLPAPS
1201 SSLINILKEH YNEDEISAKL PLAYDYILNK KESSSIPVEI LNKLSELPPH
1251 ELLTPVLGQS VNPLGMGYSS DNGKITEQVI VSGADGFDNP ISGLIYTYLE
1301 DLYNIHVRMR EGTLNSQNLR QLLENSVSSC FLTEQSINKL LSEAEKRPYQ
1351 SLTEIHQHLT GLPTIADATL SLLSVGLPGT GKLLRREQDY GRPPVTAIQD
1401 STFVLPYNFK GIGFNDNIIS SAPVASSLHF IAEHAKYTLL SWPEFYRHHA
1451 QRWFEMAKGY GSQNIDFHPQ SLLVTQEGRC MGLALLYLQT EDTAHYSILQ
1501 ENLMTVSALH QTSNRDKLPL SKDDNSLMTR TYSLIEMLQY QGNKYITNES
1551 LLHKTAWNQE RITLLFNEKG VKRALISTPN HTLVLQQLED IYRLTDPNFG
1601 HADFLSPIDA LKFIEAMIQL HHHHHH

rGT

```
1   MHHHHHHSLT PENFVQKISL SDELKTKYAN EIIEIKRIMG EYNLLPDKNS
51  RNGLKLLQKQ ADLLKIIMED TSVTENTFKN IEIAITDIKR EYYSHTVDIE
101 KNIHAIWVAG SPPESISDYI KTFLKTYKEF TYYLWVDEKA FGAAKFTSVL
151 KQIAFDLACR TIQQNTPQKN IDFINLYNEI RKKYNNNPSG QQEYLNKLRE
201 LYATYQKIST PLKHMFNSFF LENMIKLQDN FFNYCIVKGV TEINDELRIN
251 YLKNVIKLSD DDIGNYQKTI NDNKDRVKKL ILDLQKQFGE NRISIKDVNS
301 LTSLSKSENN HNYQTEMLLR WNYPAASDLL RMYILKEHGG IYTDTDMMPA
351 YSKQVIFKIM MQTNGDNRFL EDLKLRRAIS DGVLRYVNNQ NIDEVNYNEI
401 SDADKNIIKK ILTEISKMPE DSIFTKINTR IPRDTMPILR RYHLWPDGWN
451 IRGLNGFMLS HKGSEVIDAV IAGQNQAYRE LRRIRDNIHS EIYFKQTDEL
501 SSLPDTDKIG GILVKKYLSG SLFSKFRQDT IIPEALSTLQ ISGPDLIQRK
551 MLQFFRSRGV LGEEFINERK LSDKAYIGVY KTTGTGKYDW LTPESIGVND
601 VTPADESTWC IGKGRCVDDF LFKDVSTLKT ENLPELFLTK IDTDTFFSQW
651 STKTKKDLQK KIQDLTVRYN ELIDSSTIDF KNLYEIDQML HMIMLEMNDD
701 IAKRSLFSLQ VQISEKIRRM TIPVDNIINI YPDLHKKNDN DLSMSIKGFL
751 ASNPHTKINI LYSNKTEHNI FIKDLFSFAV MENELRDIIN NMSKDKTPEN
801 WEGRVMLQRY LELKMKDHLS
```

rF3

```
1   MGDWQIREKV GYANSISPYS SLAHGYANSK WPRTIPKIPS GEYDTIILGY
51  GHQYQANTEI EYLSNWIVWR EAVPDSTSRH KRPPLEVLNS QCTVIAGERK
101 TTVLPLRVLS DLTPECTEQA ISLKDYKFIL RGGSGGLAVQ VGGAGYYDID
151 ANLVAKENTL SFRGLPEEFP LTFDLSKQTQ SVMLKTPDDE VPVMTITQKG
201 INTLVGTAAG KDRLIGNDKD NTFHTSSGGG TVISGGGNNR YIIPRDLKTP
251 LTLTLSSNSV SHEIFLPETT LAELKPVAFE LSLIYWAGNN INVQPEDEAK
301 LNHFAGNFRV HTRDGMTLEA VSRENGIQLA ISLCDVQRWQ AVYPEENNRP
351 DAILDRLHDM GWSLTPEVRF QGGETQVSYD PLTRQLVYQL QARYSEFQLA
401 GSRHHTTAVT GTPGSRYIIM KPVTTQILPT QIILAGDNDH PETIDLLEAS
451 PVLVEGKKDK NSVILTIATI QYSLQLTISG IEESLPETTR VAIQPQDTRL
501 LGDVLRILPD NGNWVGIFRS GHTPTVNRLE NLMALNQVMT FLPRVSGSAE
551 QVLCLENLGG VRKKVEGELL SGKLKGAWKA EGEPTVPVNI SDLSIPPYSR
601 LYLIFEGKNN VLLRSKVHAA PLKITSAGEM QLSERQWQQQ EHIIVKPDNE
651 APSLILSEFR RFTISSDKTF SLKLMCHQGM VRIDRRSLSV RLFYLREQPG
701 IGSLRLTFRD FFTEVMDTTD REILEKELRP ILIGDTHRFI NAAYKNHLNI
751 QLGDGVLNLA DIVAEYARIQ KEETSKILYQ YQGAMKKKTD GHHHHHH
```

rF5

```
1   MPSVVEDAIM TTTVTTDSGE LFPTFHPWYT DDLSGRYKSV PMARKADTLY
51  HLTPKGDLQI IYQVATKMVN QAMIVSLPNY RHEWEKYNLS ILSEIPQNNN
101 TVVHSILRVN GPTMQVRTID YRGTDENNPI VSFSDTTFIN GEQMLSYDSH
151 SSGRVYSREE YMMWELQQRV SEASSARTQD YWLMDAAVRN GEWKITPELL
201 RHTPGYIRST VSKWSRGWLK TGTILQTPED RNTDVYLTTI QNNVFSRQGG
251 GYQVYYRIDG MAGADIADNA PGETRCTLRP GTCFEVTSVD ERHYEWNIIY
301 VTLKTCGWSR NGQSKTPNGD NLFNHHHHHH
```

Appendix 4: Nucleotide sequence of the *lifA*^{C1480A} gene

The sequence contains the polyhistidine tag and stop codon. The substituted C1480-encoding codon is highlighted in yellow.

ATGAGACTGCCAGAGAAAGTTCTTTTTCCTCCTGTCACTAGTGGCCTGTCAGGGCAGGAAAA
ACAAAAAAAACCGAAGAGCATTACCGGATTTCAGGAAAATTATCAACGCAATATCAGGCCAA
TCAAAACAGCATCAGAAGCCCGACTACGCTTCTTTGATAAAATGGTTTCGAAAGAAAACTCT
CTGGAAGATGTTGTTTCTTTAGGTGAAATGATTCAGAAGGAAATTTATGGGCATGAACAAAG
AACATTTTCACCAGTTCATCATACAGGTAACTGGAAATCATCATTGTTACACAACGCGCTCC
TTGGTCTGGCAAATGTTTATAATGGCTTACGGGAAACAGAATACCCTAACACTTTCAACAGA
GATGGTATAAAAAGTACTAACTCTTTTAGAGATAACTTATTGACAAAAACAAGAACTCCCAG
AGATAATTTTGAGGAAGGAATAAAACATCCTGAACATGCAACAATACCATATGACAACGACA
ATGAAAGTAATAAATTGCTAAAAGCAGGAAAGATAGCTGGTAACAATAACGAGCTGTTGATG
GAAATAAAAAAGGAATCCCAAAGCGACCATCAAATCCCCCTGTCAGATAAGTTCCTGAAAAG
GAAAAAACGATCTCCTGTAGCTGAAGATAAAGTTCAAAACTCGTTAACACCAGAAAATTTTG
TTCAGAAAATTTCACTTAGTGATGAGCTTAAAACAAAATATGCAAATGAAATTATAGAGATA
AAAAGAATAATGGGAGAATACAATCTTTTACCGGATAAAAACAGTCGTAATGGTCTAAAACT
TCTACAGAAGCAAGCTGATTTACTAAAAATAATCATGGAGGATACCTCCGTTACAGAAAATA
CCTTTAAAAACATAGAGATAGCTATAACAGATATAAAAAGGGAGTACTATTCGCATACAGTT
GATATTGAGAAAAATATTCATGCCATATGGGTTGCGGGTTCCCCACCTGAAAGCATTTCGGA
CTATATTAAGACTTTTCTCAAAACCTACAAAGAGTTTACTTACTATCTTTGGGTTGATGAAA
AAGCATTTGGAGCCGCGAAATTTACCAGTGTCTTAAAACAAATTGCATTTGATTTAGCATGC
AGAACTATACAGCAGAATACTCCACAAAAAAATATTGATTTTATTAATCTATATAATGAAAT
AAGGAAGAAATACAACAACAACCCATCGGGACAACAAGAGTACTTAAACAAACTCAGAGAGC
TTTATGCTACTTATCAAAAAATATCCACCCCTCTGAAACACATGTTTAATTCATTTTTTTTA
GAAAACATGATTAAACTTCAGGATAATTTCTTCAACTATTGCATTGTCAAAGGTGTTACAGA
GATTAATGATGAGTTACGAATAAACTACCTTAAAAATGTAATAAAACTGTCAGACGATGACA
TTGGTAATTACCAGAAAACAATTAACGACAATAAAGATAGAGTAAAAAAACTAATTCTTGAT
TTACAGAAACAATTTGGTGAAAACCGCATTTCAATTAAAGATGTTAACTCTTTAACCTCTCT
TTCAAAATCAGAAAATAATCACAATTATCAAACTGAAATGTTGCTTCGATGGAACTATCCTG
CCGCCTCAGACCTGCTCAGGATGTATATCCTTAAAGAGCATGGTGGTATTTATACAGACACA
GATATGATGCCTGCATACTCTAAACAAGTAATTTTTAAAATTATGATGCAGACAAACGGAGA
TAATCGTTTCTTGGAAGATTTGAAACTACGTCGTGCAATATCTGATGGTGTATTAAGATATG
TTAATAACCAAAATATTGATGAAGTTAACTATAATGAAATCAGTGATGCAGATAAAAACATT

ATCAAGAAGATATTAACAGAAATATCTAAAATGCCAGAAGATAGTATTTTTACTAAGATCAA
TACAAGGATTCCTCGAGACACAATGCCCATCCTTCGTCGTTATCACCTATGGCCTGATGGAT
GGAATATTCGTGGGCTCAATGGATTCATGCTATCACATAAAGGTAGTGAAGTGATTGATGCT
GTTATCGCAGGCCAGAATCAGGCTTACAGGGAACTAAGAAGAATAAGAGATAATATTCATAG
TGAAATATACTTCAAACAAACTGATGAATTGTCCTCACTTCCAGATACAGACAAAATTGGAG
GGATTCTGGTAAAAAAATACCTTTCAGGAAGTCTTTTTTCAAAATTCAGACAAGATACTATT
ATCCCGGAGGCATTGAGCACCCTCCAGATATCAGGTCCTGACTTGATTCAAAGAAAGATGTT
GCAATTTTTCAGGAGTAGAGGGGTGTTAGGTGAAGAGTTCATTAATGAAAGAAAACTGAGTG
ATAAAGCTTATATTGGTGTCTACAAAACAACTGGCACAGGGAAATATGACTGGTTAACCCCT
GAATCGATCGGCGTTAATGATGTCACGCCCGCAGATGAAAGTACCTGGTGTATAGGAAAAGG
CCGGTGTGTTGATGACTTCCTGTTCAAAGATGTTTCAACACTAAAAACAGAAAATCTTCCAG
AATTATTCTTAACAAAAATAGATACTGATACGTTTTTCTCTCAGTGGTCAACCAAAACCAAG
AAAGATCTGCAAAAAAAAATACAAGACCTTACTGTACGTTATAATGAGCTAATTGACTCGTC
GACTATCGACTTTAAAAATCTATATGAAATAGATCAAATGCTCCATATGATTATGCTAGAGA
TGAATGATGATATAGCCAAAAGGTCATTGTTTTCATTGCAAGTTCAAATAGCCGAAAAAATT
CGGAGGATGACCATTCCTGTAGACAATATAATTAACATCTATCCTGATCTACATAAAAAAAA
TGACAATGATCTGAGTATGTCCATAAAAGGCTTTCTTGCGAGTAATCCACATACAAAAATAA
ATATTCTTTATAGCAATAAGACTGAGCATAATATTTTTATAAAGGATTTATTCTCCTTCGCA
GTTATGGAAAATGAGTTAAGAGACATTATCAATAACATGAGCAAAGATAAGACTCCTGAAAA
CTGGGAAGGGAGGGTAATGTTACAAAGATATCTCGAATTAAAAATGAAAGATCATCTTAGTT
TGCAATCTTCTCAGGAAGCAAATGAGTTTCTTGAAATATCTACTTTTATTTATGAGAATGAT
TTCTTGAGAGAAAAGATTGAAGCAGTAAAAAACAAAATGAATTCTCACGAACTTTATTTTGA
AAAAATAAAAAAAGAACAAAACACATGGCAGGATCTGTCCACAAAAGAACAAAAATTACAGC
TTATTAAAGCATTGAAAGAAATTTCAGGAAATACAGAGAAGGACTCTCATTACGATAGACTT
CTTGATGCTTTTTTTAAAAAACATAATGAAAATATTCATAATAAAATACAAAGAATAAAAGA
CGAGTTCAAGGAATACTCCCGTGTAGCCATTCATAATATAGATAAAGTTATATTTAAAGGGC
AAACACTGGATCGTCTTTATCATGAAGGATATGTATTTTCTGATATCAATACCTTGTCTCGT
TATACACTACACGGACTAGGAATAACTGGTGTACATACTGAAGAAAACCTGCTACCAGCTCC
TTCATCGTCCTTAATTAATATATTGAAAGAACATTATAATGAAGATGAAATTAGTGCGAAAT
TACCACTAGCATATGATTACATTTTAAATAAAAAAGAATCAAGCTCTATTCCTGTTGAAATT
TTGAACAAACTTTCAGAGTTACCACCACATGAACTACTCACACCTGTTCTTGGCCAGAGTGT
TAATCCTCTGGGCATGGGCTACTCATCCGATAATGGAAAAATCACAGAGCAAGTAATAGTCA
GTGGAGCTGATGGATTTGATAATCCCATATCTGGACTTATATATACCTATCTTGAAGATCTA
TATAACATCCATGTAAGGATGCGAGAAGGTACACTAAATTCACAGAATCTTCGTCAGCTTCT
GGAAAACTCTGTTTCTTCATGCTTTTTGACTGAGCAAAGTATTAATAAATTACTTAGTGAGG
CAGAAAAAAGGCCTTATCAGTCTTTAACAGAAATACATCAGCATCTCACAGGATTACCAACT

ATTGCCGATGCAACCCTTTCATTACTTTCTGTTGGATTACCTGGTACGGGAAAACTATTGCG
CAGGGAGCAGGACTATGGGCGTCCACCAGTTACAGCAATTCAGGATTCCACATTTGTACTCC
CTTATAATTTCAAAGGTATTGGTTTTAACGATAACATTATATCCTCTGCACCTGTAGCCTCC
TCATTACATTTTATCGCTGAACATGCGAAATATACTTTATTGTCATGGCCTGAGTTTTATCG
TCATCATGCACAGCGATGGTTCGAAATGGCTAAAGGATATGGAAGCCAGAATATTGATTTTC
ACCCTCAGTCTCTATTGGTAACCCAAGAAGGACGCGCAATGGGATTAGCCTTACTTTATTTA
CAGACTGAAGATACTGCTCATTATAGCATTCTCCAGGAAAACCTAATGACTGTGAGTGCACT
TCATCAGACCAGTAATCGCGATAAGTTGCCACTGTCCAAAGATGATAATTCCTTAATGACAA
GAACTTATAGTCTGATTGAAATGCTACAGTATCAGGGAAACAAATATATTACCAACGAATCG
CTACTACATAAGACCGCATGGAACCAAGAAAGAATAACTTTATTATTCAATGAAAAAGGAGT
TAAGCGAGCCCTGATAAGCACGCCTAATCATACTCTGGTTCTGCAACAACTGGAGGATATTT
ACCGGCTCACTGATCCAAATTTTGGGCATGCAGATTTCCTTTCACCTATAGATGCTCTGAAG
TTTATTGAGGCTATGATACAATTAACTCCAACACTTCAGGAATATTATGGCCTATTAAACAA
AGACATTAATAAACATATACAAGTACATTATGCCGAATCAGATATGGTCTGGAATAAGCTTC
TGCCAGAAAATGATGCTGGACTGAGCACCAGAATTCAGCACACCACCACCGACCGTCTGGCG
AATCTGGCTGAACCAGTCGCTGTTGCAGGTATCTCCCTGCCAGTAAAAACACTTTATGATAT
CGGAGCCACCCTTGACGGTCGGCGCATCACCTCTCCTCCAACATCGGAGCAAATCCCTTCTC
TGCGTCTCAACGGTGATGTTCTGAATGATTATCTGTCCCGCACAGTTCTGACTCCAGAACAG
GCTGATAACATAAGAAAAATACTGCACACTCAGGGAATACGCAGCGGTACCCGTCCCATAGA
TCCGGAGATGATTCGTGGGACGCAGGATGACCTAGTTTCGTCACAGACTCGTCTGCAAAGGC
AAGCAACACGGGTTAAACAGCAACTCGCCGGTGTACTTGATACTCTGCAACAGCACTTCCAG
AACATTCCACGTTCATCCGGTCGTCATCTTTCTGTAGAGAATATTGAGCTGGCTGATATCGG
AAGTGGGCGTTTCAACCTTCAAATTCGAGATGGAGAAACATTGCATACCACTTCTGTGGAAG
TACCGGAAGTTGTGTCCCGTTTTCAGAAACTTTCTACCATGCTTTCAGCCCTGCCTGCCAGT
GGAATCATGGATTTCGACCTCGGCATGAGTGTGGTCGGAGTCGTCCAGTATGCCCGCCTGCT
ACAGCAGGGGCACGAAGACAGTACCCTAGCCAAGATAAATCTAGCTATGGATATCAAGCAAC
TTTCCGAAGCAACTCTCGGCAGCATGATTCAGATTGCCGGGAATAAGTTTCTCAATACAGAA
GGAATCCAGGGGTTCAGACTGGAAAGCGCCGTCGCTGAAGGTATGCGCTCAGTAGCAACCCG
TACCGGAGGCACAATGGGGAAAGCCCTTTCTGCCAGTGCCCGTGTTCTTGAACTGCCTGTAC
TGGAAACAGTTCTGGGGACATGGAACCTGTACAACAGCGTCATTCAGCTCCAGCAAGCTACA
TCTTATTCTGAGACAATGGCTGCCCGGGTACAGATTGCGTTTGATTCCATTTCTCTGGGATT
AACTGCCGCTTCGGTAGCTTTCCCGCCACTAATTATTGCCACTGGCCCCATTGCGGCTATTG
GTATGGGAGCTTCCAGTATTGCACGTAATGTGGCACGGAAAGAAGAACGGCATACACAATGG
CTGGAATATAAAAAATTCCTGACTGATGGCAGTAAACACATTGTTGTGGCCTCTCCGGAAAG
AGGTCTGCTGGATTTCTCCGGAAACAAAGTTTTTGGAAAAATGGTGCTGGATCTGCGTCAGT
CTCCTCCTCTCTTGCATGGAGAAAGCTCTTTTAACGCTGACCGCAAAATCGGTCATCGTCCG

GATCTGGGGGACTGGCAAATTCGTGAGAAGGTGGGGTATGCCAACAGTATCAGTCCCTACTC
TTCTCTGGCGCACGGTTACGCCAACAGTAAATGGCCACGAACAATACCGAAAATTCCCTCGG
GAGAATATGACACCATAATTCTGGGCTACGGTCACCAGTATCAGGCCAATACGGAAATAGAA
TATCTGTCTAACTGGATTGTATGGCGGGAAGCCGTACCAGACAGTACTTCCCGCCACAAACG
TCCTCCTCTGGAGGTTCTTAATAGTCAGTGTACTGTGATAGCTGGAGAGCGTAAAACCACAG
TACTTCCCCTGAGAGTGCTCAGCGATCTGACACCGGAATGCACAGAACAGGCTATATCGTTA
AAAGATTATAAATTCATACTGAGAGGGGGAAGCGGTGGGCTGGCTGTTCAGGTCGGTGGCGC
GGGATATTATGATATTGATGCAAATCTTGTGGCAAAAGAAAATACGCTCTCTTTTCGCGGGC
TACCGGAAGAGTTTCCGCTCACCTTTGATTTATCAAAACAAACACAGTCGGTCATGCTGAAA
ACACCAGACGATGAGGTGCCGGTAATGACCATTACCCAGAAGGGAATAAACACCCTGGTAGG
TACAGCCGCCGGTAAAGACCGACTAATCGGTAACGATAAGGACAATACCTTCCATACAAGCT
CTGGCGGCGGTACAGTCATCTCCGGAGGCGGGAATAACCGCTATATTATCCCCCGGGATTTA
AAAACGCCGTTGACACTGACGCTGTCCAGTAACTCAGTCTCTCACGAAATCTTTCTGCCAGA
AACAACCCTAGCTGAATTAAAACCTGTCGCCTTTGAGCTGAGTTTGATTTACTGGGCCGGGA
ACAACATAAATGTTCAACCAGAGGATGAAGCAAAACTGAACCACTTTGCCGGAAACTTCAGG
GTGCATACCCGTGATGGCATGACTCTGGAGGCGGTTTCCCGGGAAAATGGTATTCAACTGGC
GATTTCATTATGTGATGTTCAACGCTGGCAGGCTGTTTATCCGGAAGAAAATAACAGACCGG
ATGCCATACTGGACAGGCTGCATGATATGGGCTGGAGTCTGACACCAGAAGTCCGGTTCCAA
GGAGGAGAAACACAAGTCAGCTATGATCCCCTGACTCGTCAGCTCGTTTACCAGCTTCAGGC
GCGTTACTCTGAATTCCAGTTGGCCGGTAGTCGCCACCATACCACGGCTGTAACCGGAACTC
CGGGAAGCCGATACATTATCATGAAGCCAGTTACAACACAGATATTACCGACACAAATCATA
CTGGCTGGTGATAATGACCATCCGGAAACGATTGATTTACTGGAAGCTAGTCCTGTTCTGGT
TGAAGGGAAAAAAGACAAAAACAGCGTGATATTAACGATTGCTACGATTCAGTATTCCCTTC
AACTGACAATATCCGGGATCGAAGAATCGCTGCCCGAGACAACCCGTGTGGCAATTCAGCCT
CAGGATACCCGTTTACTGGGTGACGTACTCCGGATCTTACCAGATAATGGTAACTGGGTGGG
GATTTTCCGGAGTGGTCATACACCAACGGTAAACCGGCTGGAAAATTTGATGGCACTGAATC
AGGTAATGACGTTCCTGCCCCGGGTATCCGGAAGTGCAGAGCAGGTATTATGCCTCGAAAAC
CTAGGTGGCGTAAGGAAAAAAGTGGAGGGGGAGTTACTGTCAGGGAAGCTGAAAGGTGCGTG
GAAAGCCGAAGGTGAACCTACTGTTCCGGTAAATATCTCAGATCTAAGTATCCCACCCTATT
CACGTCTGTATCTGATTTTTGAAGGGAAAAATAATGTGTTGCTACGCAGTAAAGTACATGCA
GCTCCGTTGAAAATAACATCCGCAGGAGAGATGCAGTTATCTGAAAGGCAGTGGCAACAGCA
GGAACATATTATTGTCAAGCCCGACAACGAAGCCCCCTCATTAATACTCAGTGAATTTCGTC
GTTTCACTATTTCATCGGATAAAACATTTTCTTTAAAACTGATGTGCCATCAGGGTATGGTC
CGCATCGACCGCAGATCATTATCGGTCAGATTGTTCTATCTGCGTGAACAGCCAGGTATCGG
CAGTTTACGTCTGACGTTCAGAGATTTTTTCACAGAAGTGATGGATACAACGGACAGGGAAA
TTCTGGAGAAAGAGCTGAGACCAATTCTGATAGGAGATACACACCGCTTTATCAACGCTGCA

TACAAAAATCATCTGAATATCCAGTTAGGAGATGGCGTTCTGAATCTGGCAGACATTGTTGC
GGAATACGCCCGTATTCAAAAGGAAGAAACATCAAAAATATTGTATCAATATCAAGGTGCCA
TGAAAAAAAAAACAGATGGACCATCTGTGGTAGAAGATGCCATTATGACCACTACTGTCACA
ACAGATTCAGGTGAACTATTCCCTACCTTCCACCCGTGGTATACAGATGATTTATCAGGGCG
TTATAAGAGCGTACCTATGGCAAGAAAAGCAGATACTTTGTATCACCTGACACCAAAAGGTG
ATCTACAGATAATATATCAGGTAGCTACAAAAATGGTGAATCAGGCGATGATTGTATCCCTG
CCAAACTACCGACACGAGTGGGAAAAATATAATTTAAGCATCTTATCCGAAATCCCTCAGAA
CAATAATACTGTTGTACATTCAATCCTCAGGGTTAATGGCCCCACAATGCAGGTGCGCACAA
TTGACTACAGAGGAACGGATGAAAACAATCCCATAGTATCTTTTTCAGATACAACCTTCATC
AATGGTGAACAGATGTTGAGTTATGACTCGCATTCATCAGGGCGAGTCTATTCCAGAGAAGA
ATATATGATGTGGGAATTGCAGCAACGGGTATCAGAAGCTTCCAGTGCCCGGACACAGGATT
ACTGGCTGATGGATGCAGCGGTAAGAAACGGAGAATGGAAGATCACACCAGAATTATTACGT
CACACACCGGGATATATCCGGAGTACGGTATCGAAATGGTCCAGAGGATGGCTGAAAACCGG
CACAATACTCCAGACTCCAGAAGACAGAAATACGGATGTATACCTGACTACCATACAGAACA
ATGTATTTAGTCGTCAGGGGGGCGGCTACCAAGTGTATTATCGGATTGATGGAATGGCTGGT
GCGGATATAGCGGATAATGCACCAGGGGAAACCCGCTGCACCCTCAGGCCCGGAACATGTTT
TGAAGTGACAAGTGTGGATGAAAGGCATTATGAGTGGAATATCATTTATGTCACGCTGAAAA
CCTGTGGCTGGAGCCGAAATGGCCAAAGCAAAACGCCGAATGGTGACAACCTTTTTAACCAT
CATCACCACCATCACTAA

Appendix 5: Electronic files

The attached CD contains the following:

1. Files with detailed information on the proteins/peptides identified by liquid chromatography mass spectrometry (LC-MS). Note that Calpain 7 is referred to as CAPN7 in the file 'LC-MS_rLifA + cells_Uniprot_Cow'.
2. Files with detailed information on the proteins/peptides identified by shotgun mass spectrometry.
3. A copy of a draft manuscript for publication based on work from Chapter 4.
4. Word document and PDF copies of this thesis.